

Investigation of new pantothenate derivatives to combat the antimicrobial crisis

Jinming Guan

Department of Chemistry

McGill University

Montreal, Quebec, Canada

H3A 0B8

April 2018

A thesis submitted to McGill University in partial fulfillment of the requirements of the degree of Doctor of Philosophy

©Jinming Guan, 2018 All rights reserved

Table of contents

Abstract-----	5
Résumé-----	7
Acknowledgements-----	9
List of figures-----	10
List of schemes-----	13
List of tables-----	15
Abbreviations-----	16
Chapter 1: Introduction	
1.1 Antimicrobials-----	20
1.2 Antimicrobial crisis-----	22
1.3 Strategies to combat the antimicrobial crisis-----	23
1.4 Coenzyme A-----	24
1.5 Current investigation on the CoA pathway towards the discovery of antimicrobials----- -----	31
1.6 Research goals-----	42
Chapter 2: A cross-metathesis approach to novel and stable pantothenamide derivatives	
2.1 Preface-----	45
2.2 Introduction-----	45
2.3 Synthesis-----	47
2.4 Biological studies-----	51

2.5 Closing remarks-----52

Chapter 3: Structure-activity relationships of antiparasitodal pantothenamide analogues reveal a new way by which triazoles mimic amide bonds

3.1 Preface-----54

3.2 Introduction-----54

3.3 1,5-Substituted triazoles-----56

3.4 Pantoyl-to-triazole linker study-----57

3.5 Triazole *N*-substituent study-----61

3.6 Discussion-----63

3.7 Closing remarks-----65

Chapter 4: Pantothenamide analogues with the labile amide group replaced with various heteroaromatic rings

4.1 Preface-----68

4.2 Introduction-----68

4.3 Synthesis-----69

4.4 Antiparasitodal studies-----78

4.5 Discussion-----80

4.6 Closing remarks-----81

Chapter 5: Ligand preference for the three types of bacterial pantothenate kinase

5.1 Preface-----84

5.2 Introduction-----84

5.3 Synthesis-----87

5.4 Enzymatic studies-----91

5.5 Antimicrobial studies-----96

5.6 Closing remarks-----98

Chapter 6: Cellular studies of an aminoglycoside potentiator reveal a new inhibitor of aminoglycoside resistance

6.1 Preface-----100

6.2 Introduction-----100

6.3 Cellular studies with *E. faecium*-----104

6.4 Inhibition of AAC(6')-II by compound **6.3b**-----107

6.5 The aminoglycoside potentiating effect of **P-1b** in Gram-negative bacteria-----108

6.6 Cell toxicity study-----110

6.7 Closing remarks-----110

Chapter 7: Contributions and future directions

7.1 Contributions-----113

7.2 Publications-----114

7.3 Future directions-----115

Chapter 8: Experimental

8.1 Chemistry-----117

8.2 Compound characterization-----135

8.3 Biology-----183

References

Appendix: NMR Spectra

Abstract

Antimicrobial resistance has been an increasing public health threat in the world, due to the rapid evolution and gene transfers by microbes. Various efforts have been taken to combat antimicrobial resistance, spanning from a drive to identify unexploited antimicrobial targets to a renewed push for novel antimicrobial agents. Coenzyme A (CoA) is an essential cofactor for all living organisms. It is generally biosynthesized in five universal enzymatic steps. Although this five-step pathway is conserved in various organisms, the involved enzymes differ significantly between organisms. Therefore, focusing on the CoA biosynthetic pathway, this thesis exploits three strategies that have potential to overcome antimicrobial resistance.

The first strategy used is to revisit an old, unexploited class of antimicrobials: pantothenamides, which are secondary or tertiary amides of pantothenic acid. This class of compounds exerts antimicrobial activity via a new mode of action, interfering the CoA-related pathway. Despite their interesting antimicrobial activity, their clinical use is however hindered due to their instability in human serum. To address the instability issue of pantothenamides, in chapter 2, a cross-metathesis approach to install larger groups at the geminal dimethyl position of pantothenamides was successfully developed, and was demonstrated to be an effective way to impart stability to pantothenamides in human serum. In chapter 3 and 4, a pantothenamide analogue which has the labile amide bond replaced with a stable triazole ring, was used to design a series of new pantothenamide derivatives. Overall, three new nanomolar antiplasmodial heteroaromatic pantothenamide analogues were discovered. The results also revealed a new way by which triazoles mimic amide bonds.

The second strategy seeks novel antimicrobial targets. Pantothenate kinase (Pank), which catalyzes the phosphorylation of pantothenate to 4'-phosphopantothenate, is the first enzyme in the CoA biosynthetic pathway. It can be classified into three types (type I, II and III). Several inhibitors and alternative substrates have been reported for type I and II, whereas only weak inhibitors have been reported for type III. To design better inhibitors and substrates for not only type I and II Pank but also type III Pank, a small series of

pantothenate analogues were synthesized in chapter 5. They were exploited as probes to compare the ligand preference of the three types of bacterial PanK. Overall, several new inhibitors and substrates were identified for each type of bacterial PanK.

The third strategy involves reactivating old antibiotics. Effectiveness of aminoglycosides can be reduced towards bacteria after being acetylated by an aminoglycoside acetyltransferase. As an aminoglycoside potentiator, **P-1b** can effectively restore the effectiveness of aminoglycosides towards resistant bacteria. **P-1b** was suggested to exert its potentiating effect after being transformed by the CoA biosynthetic pathway to a CoA derivative which inhibits the acetyltransferase in resistant bacteria. To better understand the mechanism of action of **P-1b**, a series of *in cellulo* studies was performed and reported in chapter 6. The results revealed a new acetyltransferase inhibitor, and suggested that **P-1b** may be transformed into more than one acetyltransferase inhibitors in bacteria.

Résumé

La résistance aux antimicrobiennes est devenue une menace majeure à la santé publique mondiale, due à l'évolution rapide des microbes et aux transferts de gènes qu'ils effectuent. Des efforts variés ont été effectués pour combattre la résistance bactérienne, allant d'une volonté d'identifier des cibles antibactériennes inexploitées à un effort renouvelé pour le développement de nouveaux agents antibactériens. Le coenzyme A (CoA) est un cofacteur essentiel à tout organisme vivant. Il est généralement biosynthétisé par cinq étapes enzymatiques universelles. Bien que cette cascade de cinq étapes soit conservée, les enzymes impliquées diffèrent de manière significative d'un organisme à l'autre. En conséquence, en se concentrant sur le chemin de biosynthèse du CoA, cette thèse exploite trois stratégies présentant un potentiel pour vaincre la résistance microbienne.

La première stratégie utilisée consiste à revisiter une ancienne classe d'antimicrobiennes non exploitée, des amines secondaires et tertiaires de l'acide pantothénique. Cette classe de composés exerce une activité antimicrobienne par un nouveau mode d'action qui interfère avec la voie de synthèse du CoA. En dépit de leur activité antibactérienne intéressante, leur utilisation clinique est empêchée par leur instabilité dans le sérum humain. Afin de remédier à ce problème d'instabilité des pantothénamides, une approche reposant sur la métathèse croisée a été développée avec succès, dans le chapitre 2, qui installe des groupes encombrants à la position diméthyl géminale des pantothénamides, et qui a fait montre d'efficacité dans la stabilisation de pantothénamides dans le sérum humain. Dans les chapitres 3 et 4, un analogue de pantothénamide, dans lequel la liaison amide labile a été remplacée par un cycle triazole stable, a été utilisé pour concevoir une série de nouveaux pantothénamides. Dans l'ensemble, trois nouveaux analogues hétéroaromatiques de pantothénamides possédant une activité anti-plasmodiale au niveau nanomolaire ont été découverts. Les résultats ont également révélé une nouvelle façon qu'ont les triazoles de mimer les liaisons amides.

La deuxième stratégie identifie de nouvelles cibles antimicrobiennes. La pantothénate kinase (Pank), qui catalyse la phosphorylation du pantothénate en 4'-

phosphopantothénate, est la première enzyme du chemin biosynthétique du CoA. Elle peut être classifiée en trois types (types I, II et III). Plusieurs inhibiteurs et substrats alternatifs ont été reportés pour les types I et II, tandis que seulement de faibles inhibiteurs ont été reportés pour le type III. Afin de concevoir de meilleurs inhibiteurs et substrats pour les PanK, non seulement de type I et II mais également III, une courte série d'analogues du pantothénate ont été synthétisées dans le chapitre 5. Ils ont été utilisés en tant que sondes pour comparer les ligands préférentiels des trois types de PanK. Dans l'ensemble, plusieurs nouveaux inhibiteurs et substrats ont été identifiés pour chaque type de PanK.

La troisième stratégie implique la réactivation de vieux antibiotiques. L'efficacité des aminoglycosides contre les bactéries peut être réduite par leur acétylation par une aminoglycoside transférase. En tant que potentiateur d'aminoglycoside, **P-1b** peut rendre leur efficacité aux aminoglycosides à l'encontre des bactéries résistantes. Il a été suggéré que **P-1b** exerce une action de potentiation après avoir été transformé par le chemin de synthèse du CoA en un dérivé de CoA qui inhibe l'acétyltransférase des bactéries résistantes. Dans le but de mieux comprendre le mécanisme d'action de **P-1b**, une série d'études *in cellulo* ont été effectuées et rapportées dans le chapitre 6. Les résultats ont révélé un nouvel inhibiteur d'acétyltransférase et ont suggéré que **P-1b** est possiblement transformé en plus d'une forme d'inhibiteur d'acétyltransférase au sein des bactéries.

Acknowledgements

It has been a great pleasure to pursue my PhD study at McGill University. During the last five years, I have been very luckily supervised by Prof. Auclair, a beautiful and wisdom madam. As a great mentor, she has not only guided me to be a better researcher, but more importantly, taught me how to be a better person with her patience, tolerance and love. I will appreciate all of these for my whole life.

Also, I would like to express my thanks to all my labmates. They have always been there to offer help and support. I also want to extend my thanks to the faculty and staff at Department of Chemistry: thanks the Moitessier group for their help and nice sharing with lab space; thanks Prof. Tsantrizos, Carlos, Cyrus, Yih-Shyan, Demetrios for their help when I first joined the department; thanks Prof. Moitessier, Prof. Sleiman and Prof. Cosa who have sat in my review committee for the last few years; thanks Chantal for her administrative help; thanks Alexander Wahba and Nadim Saadé for their help related to mass spectrometry; thanks Richard Rossi and Weihua Wang for helping me fix instruments like Combiflash and HPLC; thanks Petr Fiuřasek for his help with MilliQ system; thanks Robin Stein, Fred Morin and Tara Sprules for their help related to NMR; and thanks every lab in our department for lending chemicals.

Besides, I want to thank all my collaborators: Erick and Vanessa from the Saliba lab, Barnard from the Strauss lab, Yun from the Mittermaier lab, Kathleen from CDRD, Johans from the Sleiman lab, and Maryam from the Golshani lab, for their wonderful collaboration.

Furthermore, thanks McGill University for giving me the chance to pursue my PhD study here. Thanks China Scholarship Council for awarding me the scholarship.

Lastly, I want to say thanks to my family and friends for their unconditional love and support, which I really appreciate.

List of figures

Figure 1.1 Structure of Salvorsan

Figure 1.2 Common mechanisms of action of antimicrobials

Figure 1.3 Common mechanisms of antimicrobial resistance

Figure 1.4 CoA biosynthetic enzymes in different kingdoms

Figure 1.5 Various PanK inhibitors

Figure 1.6 The mechanisms of action of N5-Pan in different microorganisms

Figure 1.7 Mechanism of inhibition of CJ-15,801 and various other PPCS/PPCDC inhibitors

Figure 1.8 Various PPAT or DPCK inhibitors

Figure 1.9 Examples of pantothenate analogues

Figure 1.10 Pantothenate-related potentiators

Figure 2.1 Hydrolysis of the pantothenamide by serum pantetheinases

Figure 2.2 Pantothenamide analogues modified at the geminal dimethyl position of pantothenamide

Figure 2.3 Structures of the intermediate allyl derivatives and the two Grubbs' catalysts

Figure 2.4 *In vitro* antiplasmodial activity of compound **2.10** in growth medium containing pantetheinases or in medium in which the pantetheinases have been inactivated

Figure 3.1 Structure of the previously reported compound **3.1**, and design of the molecules reported in chapter 3

Figure 3.2 Current hypothesis for how triazoles act as amide bioisosteres

Figure 3.3 Triazole ring mimics the amide bond as proposed by Tron *et al.* for 1,4-substituted triazoles

Figure 3.4 Two classical pantothenamides and their IC₅₀ values against *P. falciparum* in the presence or absence of pantetheinases

Figure 3.5 Triazoles are proposed to mimic amide in two ways

Figure 4.1 Pantothenamide analogues containing various heteroaromatic rings studied in chapter 4

Figure 4.2 The isoxazole ring of **4.1e,f** and the thiadiazole ring of **4.1i** may mimic the amide bond of **3.15**

Figure 5.1 Pantothenate structure and sites of modification discussed in chapter 5

Figure 5.2 Pantothenamide analogues containing the triazole ring

Figure 5.3 Inhibitory profiles of compounds **5.1a-d** and **5.1f-k**

Figure 5.4 Crystal structures of PanKs

Figure 6.1 Examples of aminoglycosides

Figure 6.2 Susceptible sites for modification by different AACs, shown using tobramycin as an example

Figure 6.3 Proposed transformation of aminoglycoside potentiators **P-1a-e** to the corresponding AAC(6') inhibitors **I-1a-e** by enzymes of the CoA biosynthetic pathway

Figure 6.4 MIC plots reporting the antibacterial activity of tobramycin towards *E. faecium* at different concentrations of **P-1b**

Figure 6.5 Time-kill curves of *E. faecium* in the presence of different concentrations of **P-1b** and tobramycin

Figure 6.6 Transformation of **P-1b** in *E. faecium* measured by LCMS

Figure 6.7 Potentiating effect of **P-1b** (512 µg/mL) on the antibacterial activity of ribostamycin towards *E. coli* strains

Figure 6.8 Effect of **P-1b** on the growth of HeLa cells

Figure 8.1 Calibration curve for quantification of **P-1b** by LCMS using SIM detection at $m/z = 655.3343 \pm 0.01$

Figure 8.2 Calibration curves for **P-1b** as determined by HPLC with UV detection at 214 nm, and for **6.2b** as determined by LCMS using SIM detection at $m/z = 735.2998 \pm 0.01$ and 368.1530 ± 0.01

Figure 8.3 Calibration curves for quantifying CoA by HPLC with UV detection at 260 nm, for quantifying **6.3b** by LCMS using SIM detection at $m/z = 532.6815 \pm 0.01$ and 1064.3530 ± 0.01 , and for quantifying **I-1b** by LCMS using SIM detection at $m/z = 572.6638 \pm 0.02$ and 1144.3190 ± 0.02

List of schemes

Scheme 1.1 Coenzyme A biosynthetic pathway

Scheme 1.2 CoA salvage pathway

Scheme 1.3 4'-Phosphopantothencysteine formation catalyzed by PPCS

Scheme 2.1 Optimal conditions of the cross-metathesis reaction

Scheme 2.2 Synthesis of compound **2.10**

Scheme 3.1 Synthesis of 1,5-disubstituted triazoles **3.2a-b**

Scheme 3.2 Synthesis of compounds **3.7a-d**

Scheme 3.3 Synthesis of compounds **3.9a,b**

Scheme 3.4 Synthesis of compounds **3.13a-c**

Scheme 4.1 Retrosynthetic approach to compounds **4.1a-n**. X₁, X₂, X₃ and X₄ are C, N, O or S atom

Scheme 4.2 Synthesis of compound **4.1a**

Scheme 4.3 Synthesis of compounds **4.1b-d**

Scheme 4.4 Synthesis of compounds **4.1e-f**

Scheme 4.5 Synthesis of compound **4.1g**

Scheme 4.6 Synthesis of compound **4.1h**

Scheme 4.7 Synthesis of compound **4.1i**

Scheme 4.8 Synthesis of compound **4.1j**

Scheme 4.9 Synthesis of compounds **4.1k-l**

Scheme 4.10 Synthesis of compounds **4.1m-n**

Scheme 5.1 Synthesis of compounds **5.1a-l**

Scheme 5.2 Synthesis of compounds **5.2a-f**

Scheme 5.3 Synthesis of compounds **5.2g-l**

Scheme 5.4 Synthesis of compounds **5.9a-f**

Scheme 6.1 Synthesis of compound **6.3b**

List of tables

Table 3.1 Effects of compounds **3.2a-b**, **3.7a-d**, **3.9a-b**, **3.13a-c** on the proliferation of *P. falciparum* in growth medium containing 1 μ M pantothenate and in the presence of pantetheinases

Table 4.1 Effect of compounds **4.1a-n** on the proliferation of erythrocytic *P. falciparum* in growth medium containing 1 μ M pantothenate in the presence of pantetheinases

Table 4.2 *In vitro* antiplasmodial activity of compounds **4.1e-f** and **4.1i** in growth medium containing 1 or 100 μ M pantothenate in the presence of pantetheinases

Table 5.1 Kinetic profiles of compounds **5.1e,i**, **5.9a-f**, **3.1**, **3.7a,b,c**, **3.13a**, and **5.11**

Table 5.2 Antistaphylococcal activity of substrate-type pantothenate analogues **5.9a-f**, **3.1**, **3.7a,b,c**, **3.13a** and **5.11**

Table 6.1 The potentiating effects of **P-1a-e** against different aminoglycosides at the concentration of 512 μ g/mL

Table 8.1 HPLC methods for purifying **P-1b**

Table 8.2 HPLC methods for purifying and analyzing **6.3b**

Table 8.3 LCMS method for studying the four compounds of interest (**P-1b**, **6.2b**, **6.3b**, **I-1b**)

Table 8.4 HPLC methods for generating **P-1b** calibration curve (UV detection at 214 nm), and determining the concentration of **6.2b** in the supernatant (UV detection at 214 nm)

Table 8.5 HPLC method used to generate the CoA calibration curve (UV detection at 260 nm)

Abbreviations

AAC	aminoglycoside <i>N</i> -acetyltransferase
AAC(6')	aminoglycoside <i>N</i> -6'-acetyltransferase
AMP	adenosine monophosphate
ANT	<i>O</i> -nucleotidyltransferase
APH	<i>O</i> -phosphotransferase
ASKHA	acetate and sugar kinase/heat-shock protein 70/actin
ATP	adenosine triphosphate
<i>BaPanK</i>	<i>Bacillus anthracis</i> pantothenate kinase
<i>C. difficile</i>	<i>Clostridium difficile</i>
CoA	coenzyme A
CoA-SPC	coenzyme A-synthesizing protein complex
CMP	cytidine monophosphate
CTP	cytidine triphosphate
CuAAC	Cu(I)-catalyzed azide-alkyne cycloaddition
2-DOS	2-dexoystreptamine
DPCK	dephospho-coenzyme A kinase
<i>E. coli</i>	<i>Escherichia coli</i>
<i>EcPanK</i>	<i>Escherichia coli</i> pantothenate kinase
<i>E. faecium</i>	<i>Enterococcus faecium</i>
<i>H. pylori</i>	<i>Helicobacter pylori</i>
HTS	high-throughput screening

IC ₅₀	the half maximal inhibitory concentration
IPTG	isopropyl β-D-1-thiogalactopyranoside
LDH	lactic dehydrogenase
MIC	minimum inhibitory concentration
<i>M. tuberculosis</i>	<i>Mycobacterium tuberculosis</i>
MtPanK	<i>Mycobacterium tuberculosis</i> pantothenate kinase
NADH	nicotinamide adenine dinucleotide
<i>P. aeruginosa</i>	<i>Pseudomonas aeruginosa</i>
PaPanK	<i>Pseudomonas aeruginosa</i> pantothenate kinase
<i>P. falciparum</i>	<i>Plasmodium falciparum</i>
PanK	pantothenate kinase
PfPanK	<i>Plasmodium falciparum</i> pantothenate kinase
PK	pyruvate kinase
PPAT	phosphopantetheine adenylyltransferase
PPCDC	phosphopantothenoylcysteine decarboxylase
PPCS	phosphopantothenoylcysteine synthetase
PP _i	pyrophosphate
ppm	parts per million
<i>S. aureus</i>	<i>Staphylococcus aureus</i>
SaPanK	<i>Staphylococcus aureus</i> pantothenate kinase
SAR	structural-activity relationship
SEM	standard error of the mean
SIM	selected ion monitoring

VRE vancomycin-resistant *Enterococci*

WHO World Health Organization

Chapter 1

Introduction

1.1 Antimicrobials

Infectious diseases have progressed hand in hand with human evolution.¹ They have remained a significant proportion of all human diseases and a big burden to human survival and development. Although humankind has been fighting with infectious diseases for as long as we can remember,² it was not until the late 1800s that Robert Koch (1843–1910) successfully demonstrated the root of infectious diseases: infectious diseases are caused by pathogenic microorganisms.³ Shortly after, Paul Ehrlich (1854–1915) put forward the concept of a “magic bullet” - selectively targeting only the disease-causing microorganisms to treat infectious diseases.⁴ Based on his concept, Paul Ehrlich together with his colleagues synthesized hundreds of arsenobenzene compounds, performed a screening program and finally came up with the drug Salvarsan (Figure 1.1) for the treatment of syphilis, which is caused by *Treponema pallidum*.⁴ Such use of chemical substances to treat diseases is named chemotherapy.^{2, 4-6}

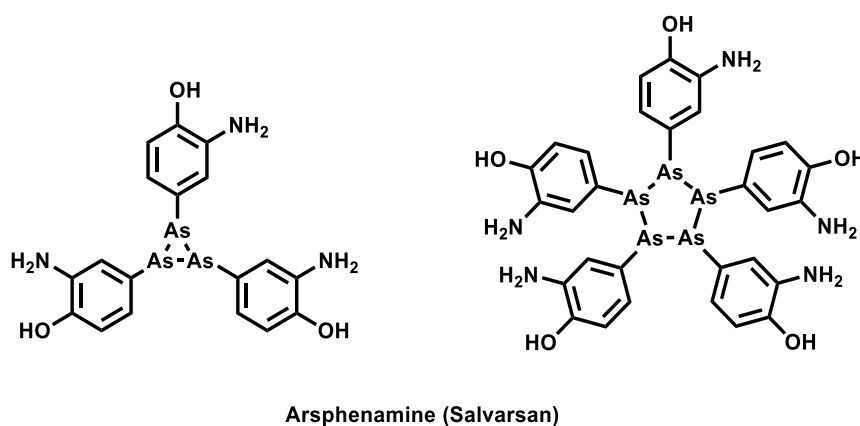
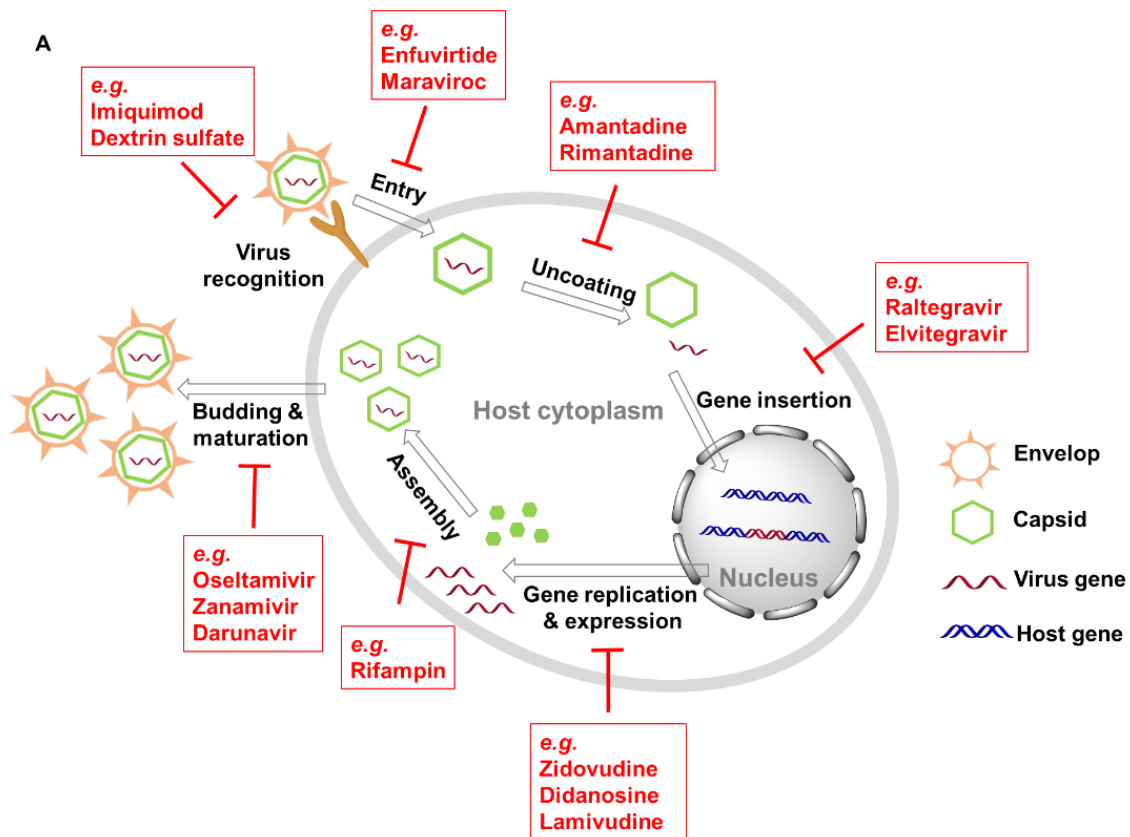


Figure 1.1. The structure of Salvarsan (a mixture of three-membered and five-membered rings).⁵

The discovery of Salvarsan has ushered the era of chemotherapy.⁶ Since then, many drugs and agents that act against microorganisms have been reported. These microorganism-targeting drugs and agents are all coined antimicrobials.⁷ Antimicrobials are classified into four types: antibacterials, antivirals, antifungals and antiparasitics,

according to the microorganisms that they work against.⁸ Antiviral drugs usually work by inhibiting different steps of virus replication (Figure 1.2A).⁹⁻¹² For more complex microorganisms (*i.e.* bacteria, fungi and parasites), antibacterials, antifungals and antiparasitics usually exert their function by interfering with one or multiple microorganism-specific processes, such as cell wall, nucleic acid and/or protein synthesis, or membrane disruption (Figure 1.2B).¹³



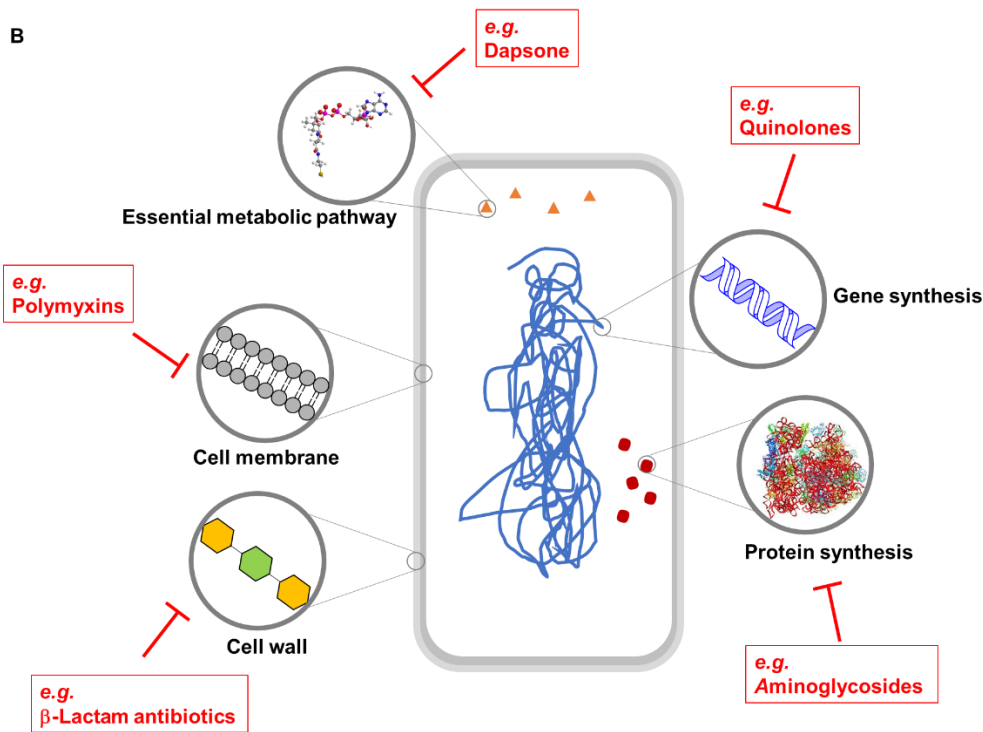


Figure 1.2. Common mechanisms of action of antimicrobials. A) For antivirals; B) for antibacterials, antiparasitics and antifungals.

1.2 Antimicrobial crisis

The prosperous development of antimicrobials has truly revolutionized our healthcare system. For example, small infected wounds seldom worry people nowadays, and the death rates of childbirths and routine surgeries have been largely brought down.¹⁴ However, due to the widespread use of antimicrobials, natural selection of resistant microorganisms has been much accelerated.¹⁵ Consequently, antimicrobial resistance is ubiquitous; microorganisms quickly become resistant to antimicrobials that are used to combat them.

Currently, resistance to many known antimicrobials has been observed. For example, for artemisinin, the core treatment for malaria, resistance has been confirmed in five countries of the Greater Mekong subregion;¹⁶ and even worse, resistance has nearly

been seen to all antibiotics that have been developed so far.¹⁷ Despite resistance to antimicrobials spreading quickly, the introduction of new antimicrobials to market by the pharmaceutical industry has been very slow.¹⁸ As old drugs become ineffective and no new drugs become available, the situation is becoming catastrophic, probably leading humankind to a post-antimicrobial era where the Black Death could return and a small cut could be fatal.¹⁵ It is estimated that drug resistant infections will result in ten million deaths worldwide annually by 2050.¹⁴ Therefore, it is urgent to take actions to combat this antimicrobial crisis.

1.3 Strategies to combat the antimicrobial crisis

The World Health Organization (WHO) has outlined five strategies to help combat the current antimicrobial crisis: 1) improve the general understanding of antimicrobial resistance through effective education and communication; 2) strengthen our knowledge about the antimicrobial crisis through more surveillance and research; 3) improve the hygiene conditions to control and prevent infection; 4) properly regulate the use of the available antimicrobials; 5) develop and encourage new antimicrobials, diagnostic tools and other interventions for infectious diseases.^{15, 19} All these strategies need coordinated efforts.

So far, it has been known that microorganisms usually exploit four ways to protect them from the killing of antimicrobials (Figure 1.3): 1) prevention of antimicrobial access to the target, which includes limiting the entry of antimicrobials and efflux of the entered antimicrobials; 2) modifying the antimicrobials, making them unable to bind with the targets; 3) altering the antimicrobial drug targets, leaving the antimicrobial unrecognized; and 4) bypass of the antimicrobial targets, resulting in the original antimicrobial targets nonessential for microbial growth.²⁰⁻²³

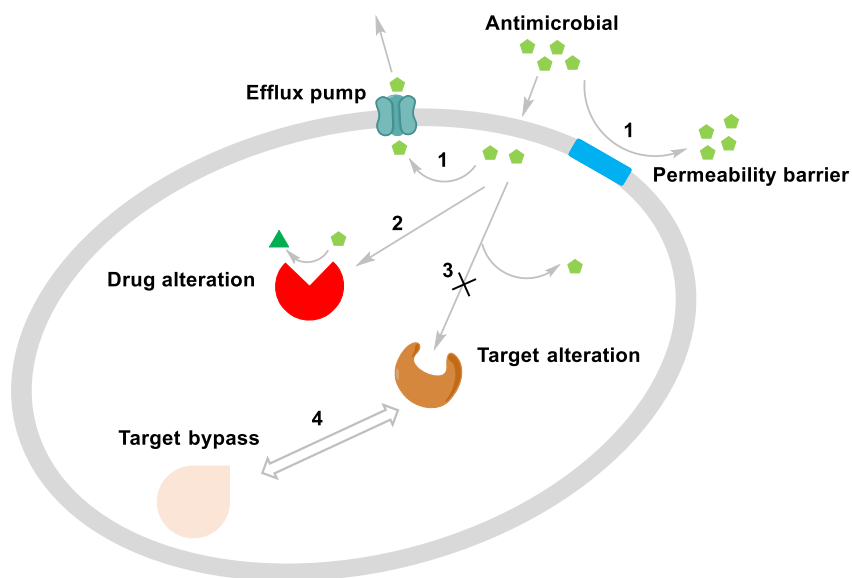


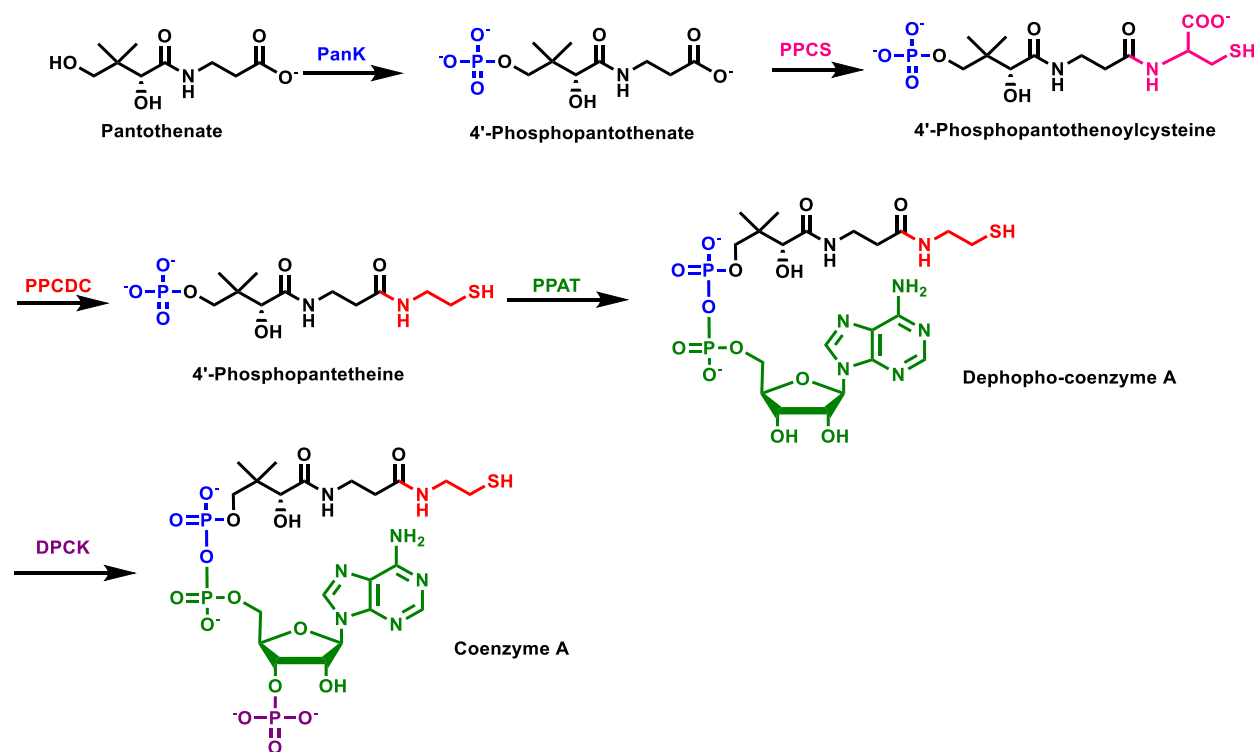
Figure 1.3. Common mechanisms of antimicrobial resistance.

Based on the five strategies suggested by WHO and our current knowledge about how microbes develop resistance, the work presented in this thesis will focus on three ways to make a contribution towards fighting the antimicrobial crisis. Firstly, developing new types of antimicrobials with new targets, which will be discussed in chapters 2, 3 and 4. Secondly, studying novel antimicrobial targets to guide the design of new antimicrobials. This work will be discussed in chapter 5. Lastly, investigating the mechanism of action of a drug candidate, which can reactivate old antibacterial agents – aminoglycosides. This work will be discussed in chapter 6.

1.4 Coenzyme A

Coenzyme A (CoA) (Scheme 1.1) is an acyl group carrier and carbonyl-activating group widely present in living organisms. Since its first discovery by Fritz Lipmann in 1945,²⁴ it has been heavily studied.²⁵ CoA is known to be biosynthesized in five enzymatic steps with pantothenate (also known as vitamin B₅) as the precursor in all eukaryotes, all bacteria, and some archaea (Scheme 1.1).²⁵⁻²⁸ The first step is a phosphorylation reaction

to form 4'-phosphopantothenate catalyzed by pantothenate kinase (PanK). Subsequently, condensation of 4'-phosphopantothenate with cysteine catalyzed by phosphopantothenoylcysteine synthetase (PPCS) yields 4'-phosphopantothenoylcysteine. Followed by a decarboxylation reaction of 4'-phosphopantothenoylcysteine catalyzed by phosphopantothenoylcysteine decarboxylase (PPCDC), 4'-phosphopantetheine is produced. Next, phosphopantetheine adenylyltransferase (PPAT) transfers an adenylyl group to 4'-phosphopantetheine, generating dephospho-CoA. Finally, dephospho-CoA is phosphorylated at the 3'-position of the ribose by dephospho-CoA kinase (DPCK), giving CoA. The formed CoA could participate in over 100 different reactions in metabolic processes, including the tricarboxylic acid cycle, lipid biosynthesis and degradation, and amino acid biosynthesis.^{25, 27} These heavy involvements in biological activities make CoA essential for all living organisms.



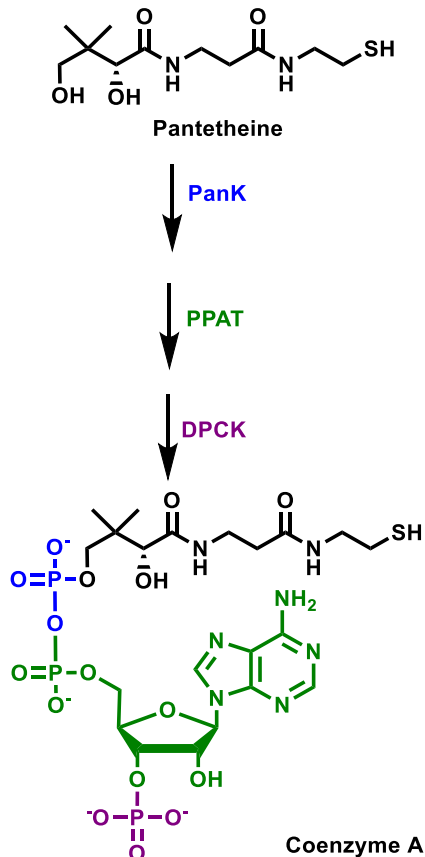
Scheme 1.1. Coenzyme A biosynthetic pathway.

Despite the fact that the five-step CoA biosynthetic pathway is conserved, enzyme structures and mechanisms come in different flavor within different organisms.

1.4.1 Pantothenate kinase (PanK)

PanK (EC 2.7.1.33), also named CoaA, catalyzes the phosphorylation of pantothenate, the first step of the CoA biosynthetic pathway. So far, many PanK enzymes from bacteria, eukaryotes and archaea have been discovered. They can be grouped into three types (type I, II and III) based on sequence analysis and kinetic mechanism.²⁹

Type I PanKs are mostly found in bacteria, such as *Escherichia coli*, *Enterococcus faecium*, *Klebsiella pneumonia* and *Mycobacterium tuberculosis*.³⁰⁻³³ They are usually feedback inhibited by free CoA and CoA thioesters (to a lesser extent) both *in vivo* and *in vitro*.³⁰⁻³² Their pantothenate binding pockets are found being able to tolerate different substrates, such as pantetheine.³⁴⁻³⁶ Thus, bacteria expressing type I PanKs can synthesize CoA from pantetheine, bypassing the PPCS and PPCDC enzymes in the five-step CoA biosynthetic pathway (Scheme 1.2). It is worth noting that a type I PanK has also been found in a thermoacidophilic archaeon, *Picrophilus torridus*.²⁸ Unlike bacterial type I PanKs, the *Picrophilus torridus* type I PanK is refractory to inhibition by CoA or CoA thioesters.



Scheme 1.2. CoA salvage pathway.

Type II PanKs are different from the type I PanKs both from the sequence and 3D structure perspective. Type II PanKs belong to the acetate and sugar kinase/heat-shock protein 70/actin (ASKHA) superfamily of kinase.²⁷ They are mostly found in eukaryotes, including fungi, plants, insects and mammals, although few bacteria, such as *Staphylococcus aureus*, also encode type II PanKs.³⁷⁻³⁹ Like type I PanKs, the pantothenate binding pockets of type II PanKs can also accept different substrates, such as pantetheine (Scheme 1.2).^{27, 40} Eukaryotic type II PanKs also experience feedback inhibition by CoA and CoA thioesters, with the latter typically being more potent.⁴¹⁻⁴⁵ In contrast, *Staphylococcus aureus* pantothenate kinase (SaPanK) diverges from the

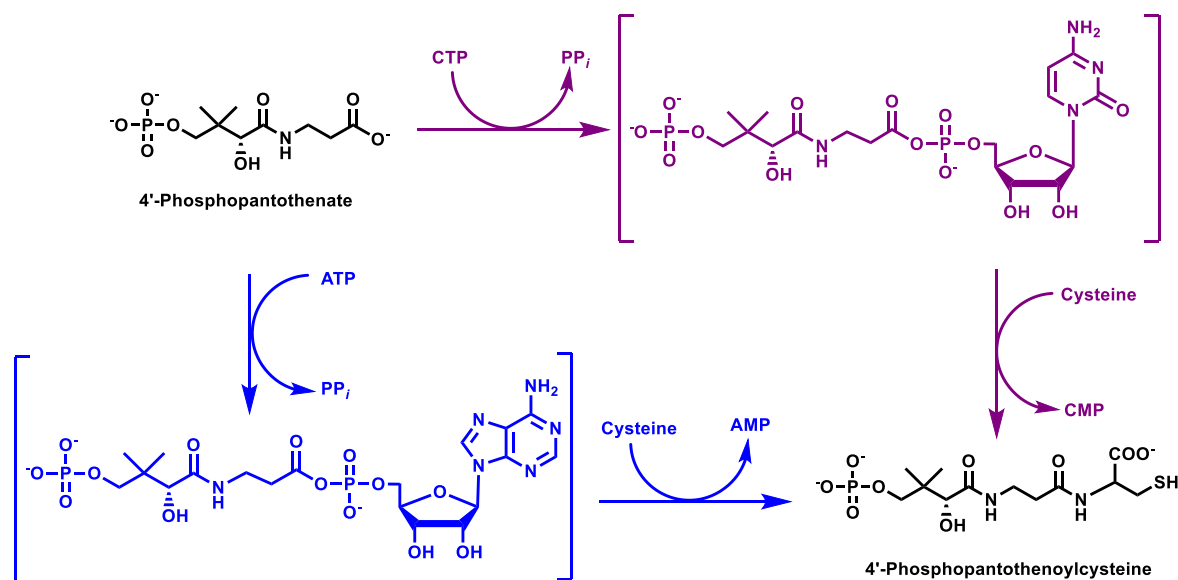
eukaryotic type II PanK profile; it doesn't experience any feedback inhibition by CoA or its thioesters.⁴⁶

So far type III PanKs have only been found in bacteria. They also belong to the ASKHA superfamily of kinases, though sharing only limited sequence identity (~13%) with type II PanKs.^{37, 47-49} Unlike type I and II PanKs, type III PanKs have relatively strict pantothenate binding pockets, and no alternative substrates have been reported yet. Also, most type III PanKs are not feedback inhibited by CoA or its thioesters, except for the *Thermotoga maritima* pantothenate kinase, which is reported to be fully inhibited in the presence of 400 μ M CoA.⁵⁰ Another unique characteristic of type III PanKs is their poor affinity for one of their natural substrates, adenosine triphosphate (ATP); their K_m values are usually ca. 3-10 mM, much higher than those of other PanK types (micromolar range).^{37, 49}

1.4.2 Phosphopantothenoylcysteine synthetase (PPCS) and phosphopantothenoylcysteine decarboxylase (PPCDC)

PPCS (CoaB, EC 6.3.2.5) and PPCDC (CoaC, EC 4.1.1.36) catalyze the second and third steps of the CoA biosynthetic pathway, respectively. In prokaryotes, they are normally fused with each other to form a bifunctional protein (CoaBC), except for the *Streptococci* and *Enterococci* isoforms.^{40, 51-57} In contrast, all eukaryotes have the monofunctional PPCS and PPCDC.⁵⁸⁻⁶¹

A distinct characteristic of CoaBCs in prokaryotes is that their PPCS domain specifically uses cytidine triphosphate (CTP) to activate the carboxylate of 4'-phosphopantothenate through the formation of an acyl-cytidylate intermediate (Scheme 1.3);^{54, 56-57} whereas, eukaryotic PPCS usually utilizes ATP for carboxylate activation.⁵⁸⁻⁶¹



Scheme 1.3. 4'-Phosphopantoenoylcysteine formation catalyzed by PPCS. Purple represents the reaction in prokaryotes. Blue represents the reaction in eukaryotes. Adenosine monophosphate: AMP; cytidine monophosphate: CMP; PP_i: pyrophosphate.

1.4.3 Phosphopantetheine adenylyltransferase (PPAT) and dephospho-CoA kinase (DPCK)

PPAT (EC 2.7.7.3), also known as CoaD, catalyzes the reversible adenylylation of 4'-phosphopantetheine.^{45, 58, 62-66} This step is suggested to be the second rate-limiting step in the CoA biosynthetic pathway, besides the PanK one.^{45, 64-65, 67} DPCK (EC 2.7.1.24), also known as CoaE, catalyzing the phosphorylation of dephospho-CoA to form CoA, is the last enzyme in CoA biosynthetic pathway.

In most eukaryotes, PPAT is fused with DPCK to form a bifunctional PPAT/DPCK protein (CoA synthase);^{58, 65, 68-72} while in plants, archaea and bacteria, PPAT is monofunctional.^{45, 62-64, 66-67, 73-84} Exceptionally, although the PPAT and DPCK of yeasts can function independently, their activities can also be found in a multifunctional CoA-synthesizing protein complex (CoA-SPC) in yeasts, which has the function of PPCS, PPCDC, PPAT and DPCK (Figure 1.4).⁸⁵

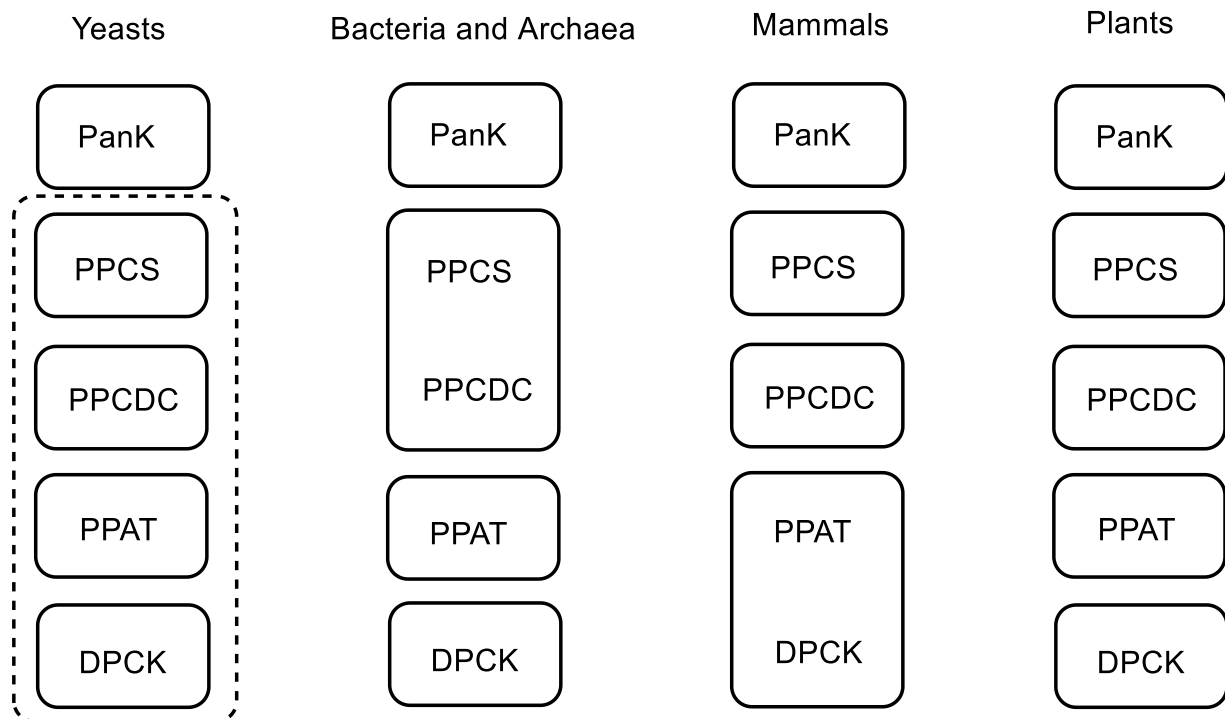


Figure 1.4. CoA biosynthetic enzymes in different kingdoms. Solid-line box refers an individual enzyme. Broken-line box refers the CoA-SPC in yeasts. The figure was adapted from ref. 25.

Regulation of PPAT and DPCK is different between bacteria and mammals. Bacterial PPAT is normally feedback inhibited by CoA and its thioesters, though free CoA is preferred.^{45, 66-67, 75, 81-83} For mammalian CoA synthase, so far three mechanisms of regulation have been reported: 1) inhibition of the DPCK domain by free CoA and by a central scaffold component of processing bodies, enhancer of mRNA-decapping protein 4;^{69, 86} 2) modulation of CoA synthase catalytic activity through its tyrosine phosphorylation status;⁶⁵ and 3) activation of CoA synthase by phosphatidylcholine and phosphatidylethanolamine, the main components of mitochondrial outer membrane.⁷²

1.5 Current investigation on the CoA pathway towards the discovery of antimicrobials

As discussed above, although the CoA biosynthetic steps are highly conserved, the structure and biochemical properties of those CoA biosynthetic enzymes across different kingdoms are different, which allow for the design of antimicrobial agents.⁸⁷⁻⁸⁸

1.5.1 Pantothenate kinase (PanK) inhibitors

Studies on type I PanK inhibitors have mainly focused on *Mycobacterium tuberculosis* pantothenate kinase (*MtPanK*). With a high-throughput assay based on ligand-induced shifts in protein thermal melting temperature, researchers at AstraZeneca identified a range of potent *MtPanK* inhibitors with diverse chemical scaffolds, including triazoles, thiazoles, quinoline carboxamides and biaryl acetic acids (e.g. **1.1** and **1.2** in Figure 1.5).⁸⁹⁻⁹¹ Of these, only the biaryl acetate esters possess interesting minimum inhibitory concentrations (MICs) with wild-type *M. tuberculosis*.⁹¹

As for type II PanK inhibitors, pantothenamides (secondary or tertiary amides of pantothenic acid, Figure 1.5) are probably the most famous one. They were first synthesized by Clifton *et al.* in 1970 and shown to possess antistaphylococcal activity by Choudhry *et al.* in 2003.⁹²⁻⁹³ Since then, many pantothenamide analogues modified at different positions of pantothenamide, such as the β -alanine, geminal dimethyl and the primary hydroxyl group, have been reported.⁹⁴⁻⁹⁷ How pantothenamides and their derivatives take effects in *S. aureus* hasn't been fully deciphered yet.^{46, 93, 95, 97-99} The current accepted mechanism of action in *S. aureus* is that pantothenamides serve as alternative substrates of SaPanK, with the resulting phosphorylated products getting trapped in the active site, and thus reducing enzymatic turnover rate and causing *S. aureus* growth inhibition.^{95, 97, 99} It is worth noting that among all pantothenamides and their derivatives, N7-Pan (Figure 1.5) has the most potent antistaphylococcal activity, yet is not the best SaPanK inhibitor.⁹⁹ This may be explained by different cell permeability.

In addition to *S. aureus*, the eukaryotic malaria parasite, *Plasmodium falciparum* also expresses a type II PanK, *Plasmodium falciparum* pantothenate kinase (*PfPanK*), which

has also been the subject of intensive researches. A class of pantothenate analogues, the *N*-pantoyl-substituted amines (e.g. **1.3a-b** in Figure 1.5) was reported to inhibit the proliferation of asexual intraerythrocytic *P. falciparum* with micromolar the half maximal inhibitory concentrations (IC₅₀s); and these compounds inhibit PfPanK with the nanomolar K_i.¹⁰⁰

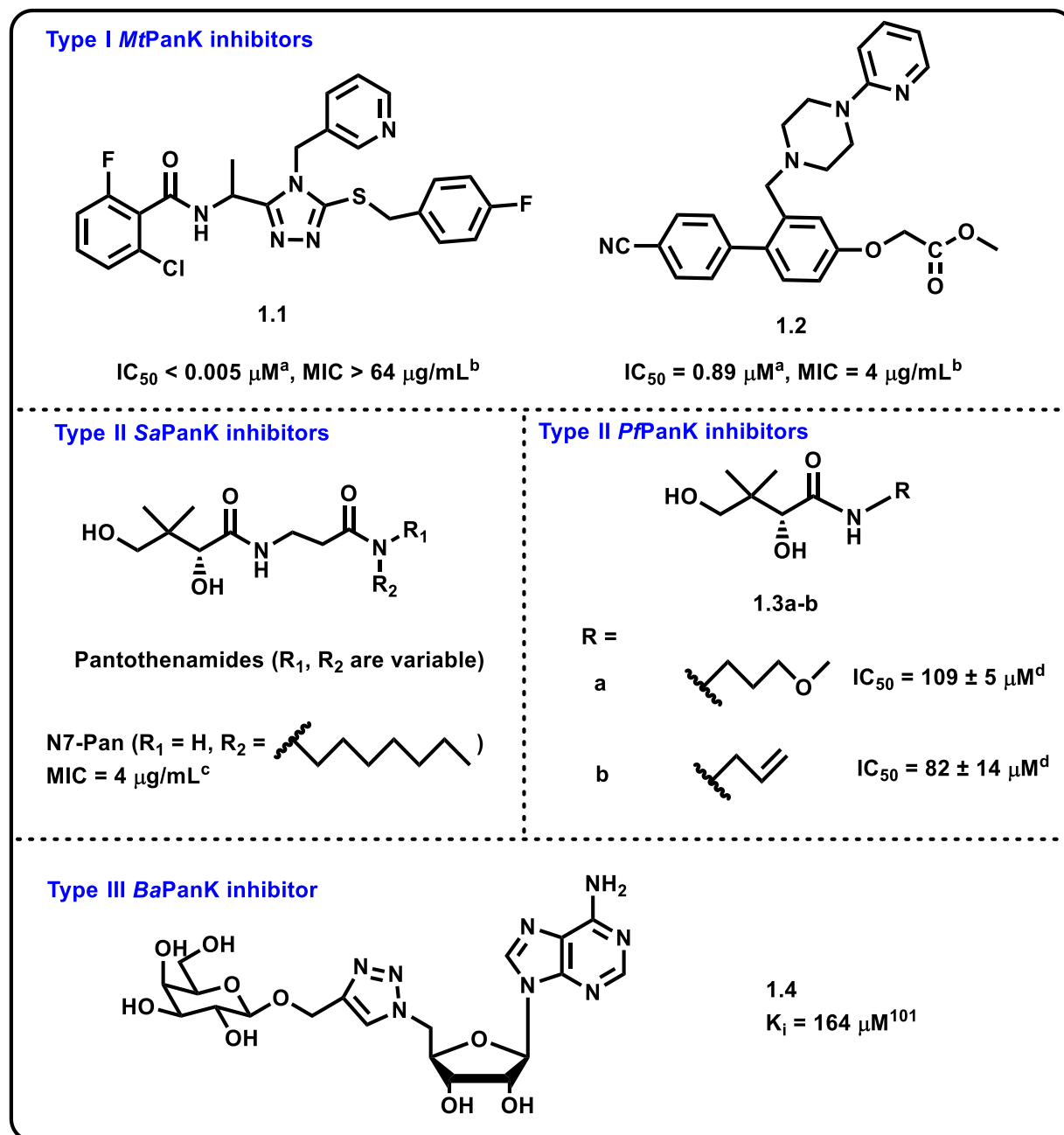


Figure 1.5. Various PanK inhibitors. ^aFrom ref. 91, the IC_{50} shown is towards PanK inhibition. ^bFrom ref. 91, the MIC shown is towards *M. tuberculosis* growth. ^cFrom ref. 93, the MIC shown is towards *S. aureus* growth. ^dFrom ref. 100, the IC_{50} shown is towards *P. falciparum* growth.

To date, the only reported type III PanK inhibitors are nucleoside triphosphate mimics of ATP.¹⁰¹ Of these, the most potent compound **1.4** (Figure 1.5) shows inhibition with a K_i

value of 164 μM (a 3-fold difference compared to the enzyme's K_m value for ATP at 510 μM) towards *Bacillus anthracis* pantothenate kinase (*BaPanK*). However, no bacterial growth inhibition was reported.

1.5.2 Pantothenamides targeting the CoA-related pathways

Pantothenamides inhibit the *S. aureus* growth through the phosphorylated products, as discussed above. However, it is interesting to notice that their mechanism of action can be different in different microorganisms. Studies show that in malaria parasite *P. falciparum* and bacteria containing type I PanK, lethal effects of pantothenamides are not due to inhibition of PanK by 4'-phosphopantothenamides as in *S. aureus*. Instead, the growth inhibition mainly results from the generated CoA antimetabolites (Figure 1.6). In details, pantothenamides can be accepted as alternative substrates of the CoA salvage pathway, forming the CoA antimetabolites. It is the CoA antimetabolites that interfere with various CoA-dependent processes, consequently disturbing normal microbial growth.^{95, 97, 102-109} Although pantothenamides are toxic for microorganisms containing type I or II PanKs, they have no growth inhibitory effect towards bacteria expressing only type III PanKs.

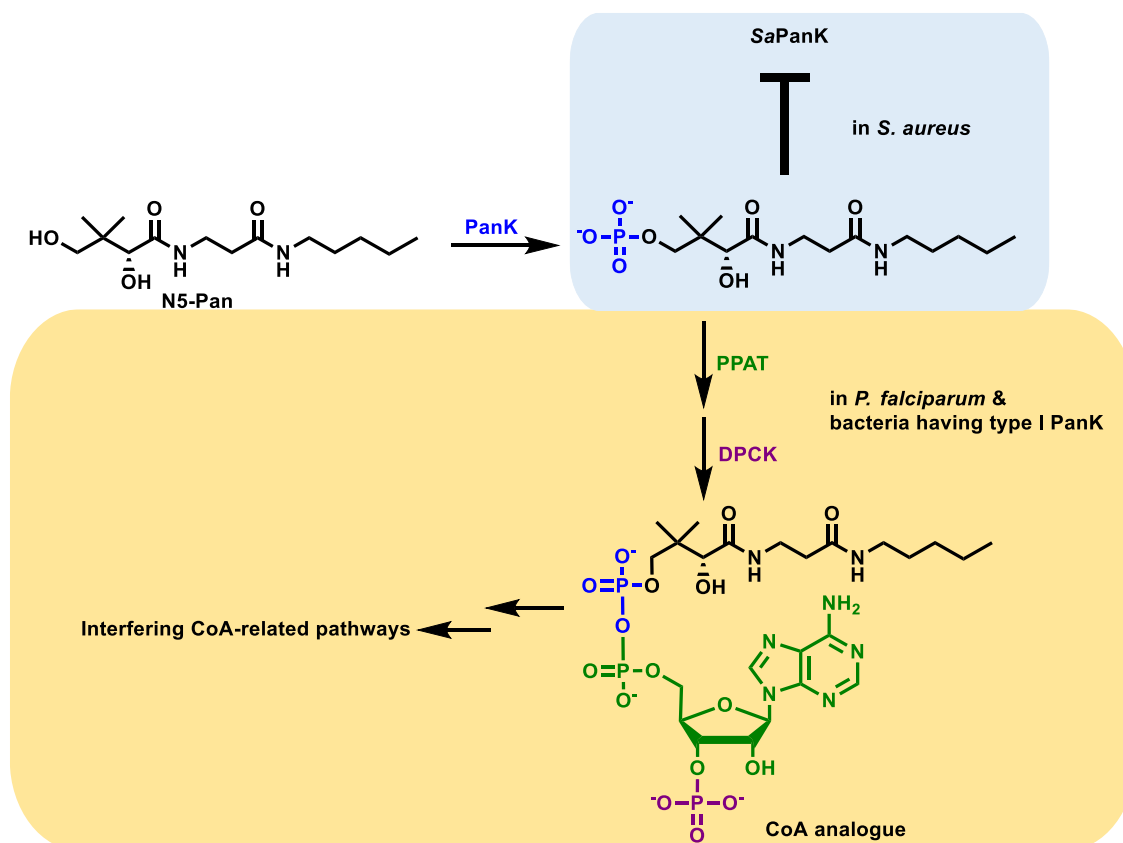


Figure 1.6. The mechanisms of action of N5-Pan (a classical pantothenamide) in different microorganisms.

1.5.3 Phosphopantothenoylcysteine synthetase (PPCS) and phosphopantothenoylcysteine decarboxylase (PPCDC) inhibitors

Diverse chemical structures of PPCS/PPCDC inhibitors have been reported. A natural product CJ-15,801 (Figure 1.7), isolated from fermentation culture of the fungus *Seimatosporium* sp. CL28611 by Pfizer in 2001, was reported to be a growth inhibitor of multi-drug resistant *S. aureus* with MIC value ranging between 6.25-50 $\mu\text{g}/\text{mL}$.¹¹⁰ Although its Michael acceptor moiety suggests that CJ-15,801 might act as a covalent inhibitor, the compound was instead found to be phosphorylated by PanK and then cytidylated by PPCS to give the metabolite **1.5** (Figure 1.7), which tightly binds and inhibits PPCS, resulting in lethal effect.¹¹¹ Later studies found that CJ-15,801 also inhibits the

asexual intraerythrocytic stage of the malaria parasite *P. falciparum*, with an IC₅₀ value of 39 μM.¹¹² The mechanism of action of CJ-15,801 in *P. falciparum* is suggested to be same as the one in *S. aureus*.^{107, 113} Interestingly, Patrone *et al.* reported four bacterial PPCS inhibitors (IC₅₀ values ranging from 10 nM to 279 μM, examples **1.6** and **1.7** shown in Figure 1.7) that are structurally similar to compound **1.5**.¹¹⁴ While very potent against bacterial PPCS, these inhibitors exhibit no whole cell activity, probably due to cell penetration issues.

Pantothenol (also known as provitamin B₅, Figure 1.7), can inhibit the growth of various microorganisms, such as *M. tuberculosis* and *P. falciparum*, although with low potency.^{107, 115-118} In *M. tuberculosis*, pantothenol was reported to be phosphorylated by PanK to afford 4'-phosphopantothenol, which competitively inhibits CoaBC and thus leads to the bactericidal effect.¹¹⁷ In *S. aureus* and *P. falciparum*, the mechanism of action of pantothenol remains disputed.^{107, 116, 118} It is worth noting that although pantothenol has been widely used in cosmetics and personal-care products, it is not useful when used systemically because its terminal alcohol can be oxidized quickly to generate pantothenate (its efficacy is also quite poor, the MIC is higher than 1 mM for *S. aureus*).¹¹⁸

A structurally different nanomolar inhibitor of either *P. falciparum* PPCS or PPCDC, compound **1.8** (Figure 1.7), was identified by Avery *et al.* using a CoA rescue approach from a set of prioritized compounds including the Medicines for Malaria Venture malaria box.¹¹⁹⁻¹²⁰ It is not only active against the asexual stage of *P. falciparum*, but also the parasite in its sexual development stage.

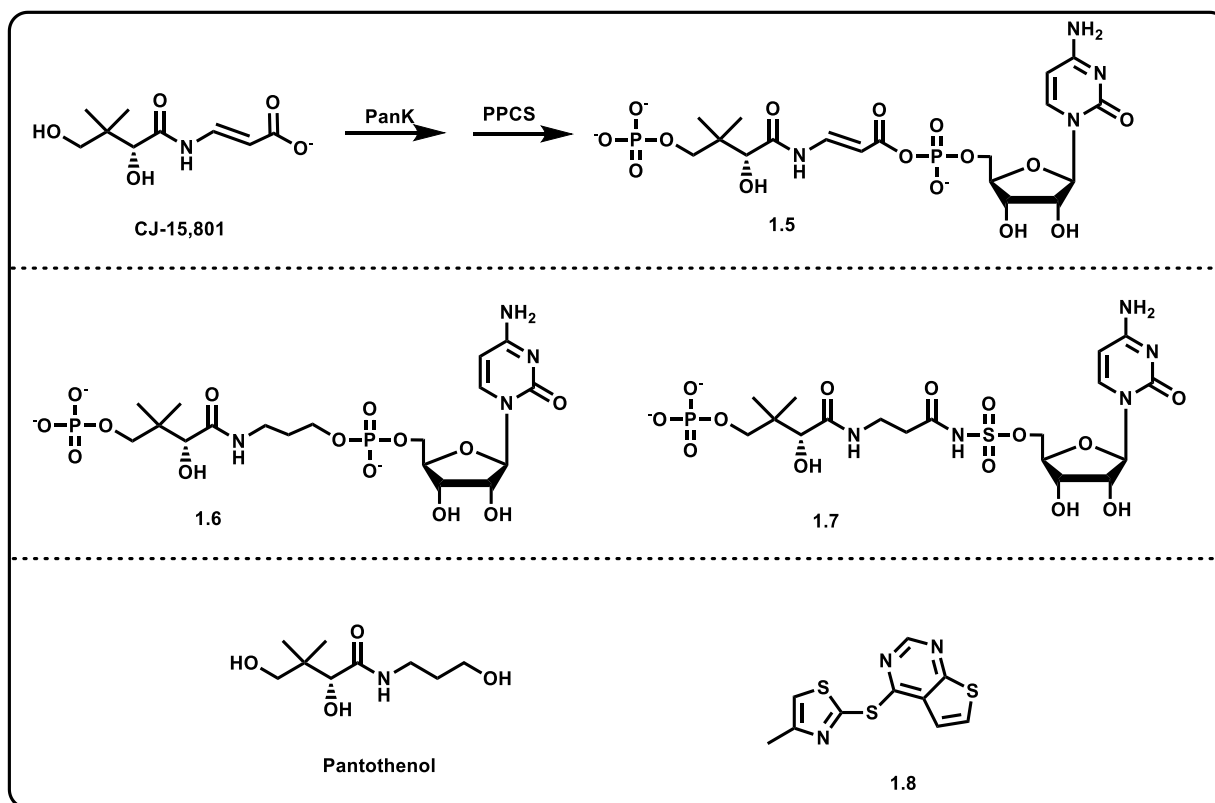


Figure 1.7. Mechanism of inhibition of CJ-15,801 and various other PPCS/PPCDC inhibitors.

1.5.4 Phosphopantetheine adenyltransferase (PPAT) and dephospho-CoA kinase (DPCK) inhibitors

So far, many PPAT inhibitors have been reported (Figure 1.8). As early as 2003, based on the structure of 4'-phosphopantetheine, Zhao *et al.* rationally designed and synthesized a library of dipeptides inhibiting *E. coli* PPAT.¹²¹ Of them, the most potent one, **1.9** (Figure 1.8), has an IC₅₀ of 6 nM. However, these inhibitors lack antibacterial activity. In 2010, a high-throughput screening (HTS) of approximately one million compounds against PPAT was performed.¹²² Several classes of micromolar inhibitors were identified, among which the most promising is a class of ATP-competitive 9-oxo-4,9-dihydropyrazolo[5,1-b]quinazoline-2-carboxylic acids (e.g. **1.10** in Figure 1.8).¹²² Whole-cell activity of these compounds are not reported.

In 2013, Cheng *et al.* virtually screened 407 PubChem listed compounds against the PPAT crystal structure of Gram-negative *Helicobacter pylori* using CDOCKER and LigandFit.¹²³ They identified a molecule, compound **1.11** (Figure 1.8), which not only weakly inhibits *H. pylori* PPAT activity (25% PPAT inhibition at 200 μ M) but also *H. pylori* viability (40% growth inhibition at 10 μ M). The same year, AstraZeneca reported HTS of another library, and the discovery of a series of cycloalkyl pyrimidines with nanomolar inhibition of PPATs from several Gram-positive and Gram-negative bacteria (e.g. **1.12** in Figure 1.8).¹²⁴ These inhibitors were tested against different bacterial strains. They only show growth inhibition towards Gram-positive bacteria with MIC \leq 8 μ g/mL.

Unlike PPAT inhibitory studies as mentioned above, currently, the only inhibitory study that might be related to DPCK is the chemical rescue one by Avery *et al.* discussed earlier.¹¹⁹⁻¹²⁰ In their study, except for compound **1.8**, most of the other compounds identified are either PPAT or DPCK inhibitors with micromolar and sub-micromolar IC₅₀ values towards *Trypanosoma* spp. and *P. falciparum* in different life stages (e.g. **1.13** and **1.14** in Figure 1.8).¹¹⁹⁻¹²⁰

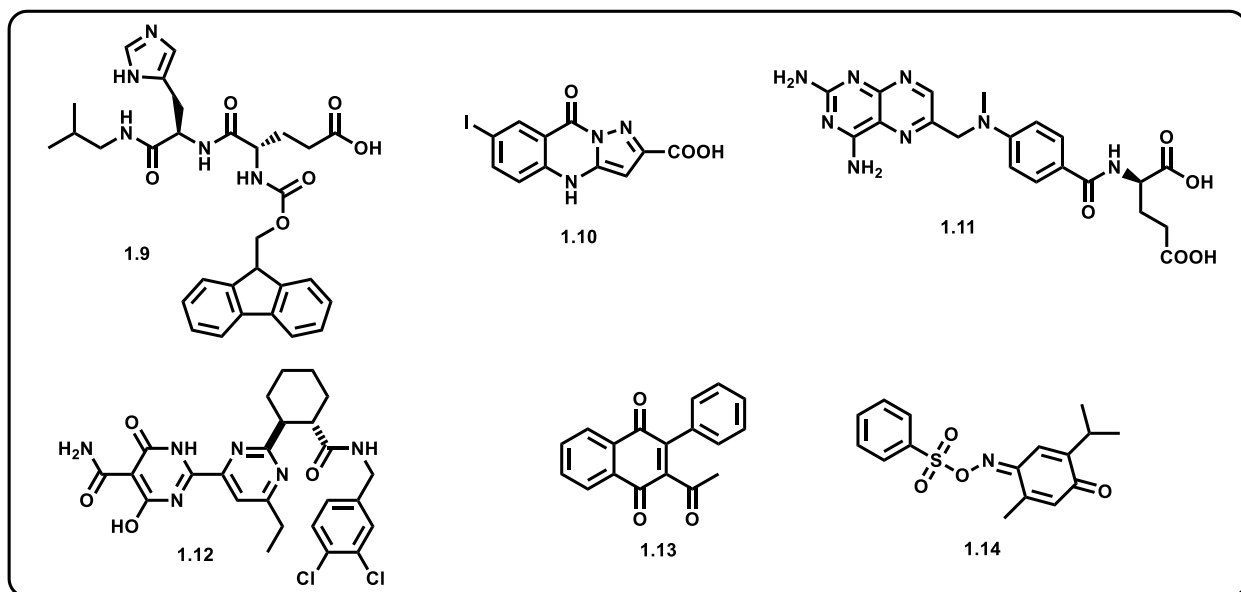


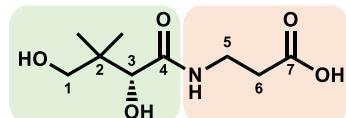
Figure 1.8. Various PPAT or DPCK inhibitors.

1.5.5 Other pantothenate analogues

Since the discovery of pantothenate in 1933 and elucidation of its structure in 1939 by Williams *et al.*,¹²⁵⁻¹²⁶ lots of analogues of this vitamin modified at the pantoyl/ β -alanine moiety (Figure 1.9) have been reported. Among them, some has shown antimicrobial activity, including the aforementioned pantothenamides, *N*-pantoyl-substituted amines, CJ-15,801 and pantothenol. This section summarizes the compounds for which the modes of action are currently unknown, although none of them owns potent antimicrobial activity.

Pantoyltaurine (Figure 1.9) is the first reported growth-inhibitory pantothenate analogue.¹²⁷ It not only inhibits growth of various bacteria such as *Corynebacterium diphtheriae* and *Streptococcus haemolyticus*, but also the yeast *Saccharomyces cerevisiae*, when its concentration is much higher than that of pantothenate in the medium. For example, it can only inhibit the growth of *Lactobacillus arabinosus* completely at a concentration of 1000 times higher than the concentration of pantothenate in medium.⁸⁷ The inhibitory effect of pantoyltaurine can be reversed with the addition of pantothenate, suggesting that pantoyltaurine may compete with pantothenate in important processes.⁸⁷ Additional pantoyltaurine variants, such as replacing the sulphonic acid with either a thiol, a disulphide, a sulphone or a sulphonamide, were also explored. Some of them (e.g. **1.15a-b**) were shown to inhibit the growth of the malarial parasites, in addition of affecting bacterial and/or fungal growth.¹²⁸

Same as the pantoyltaurine series, the pantothenone series (e.g. **1.16a-b**, MIC ranging from 120 μ M to 7200 μ M) modified at the β -alanine moiety of pantothenate, also has the antibacterial, antifungal and antiplasmodial activity.⁸⁷ However, not all of them compete with pantothenate *in cellulo*.¹²⁹



Pantoyl moiety β -Alanine moiety

A. β -Alanine moiety modified

B. Pantoyl moiety modified

C. Both moieties modified

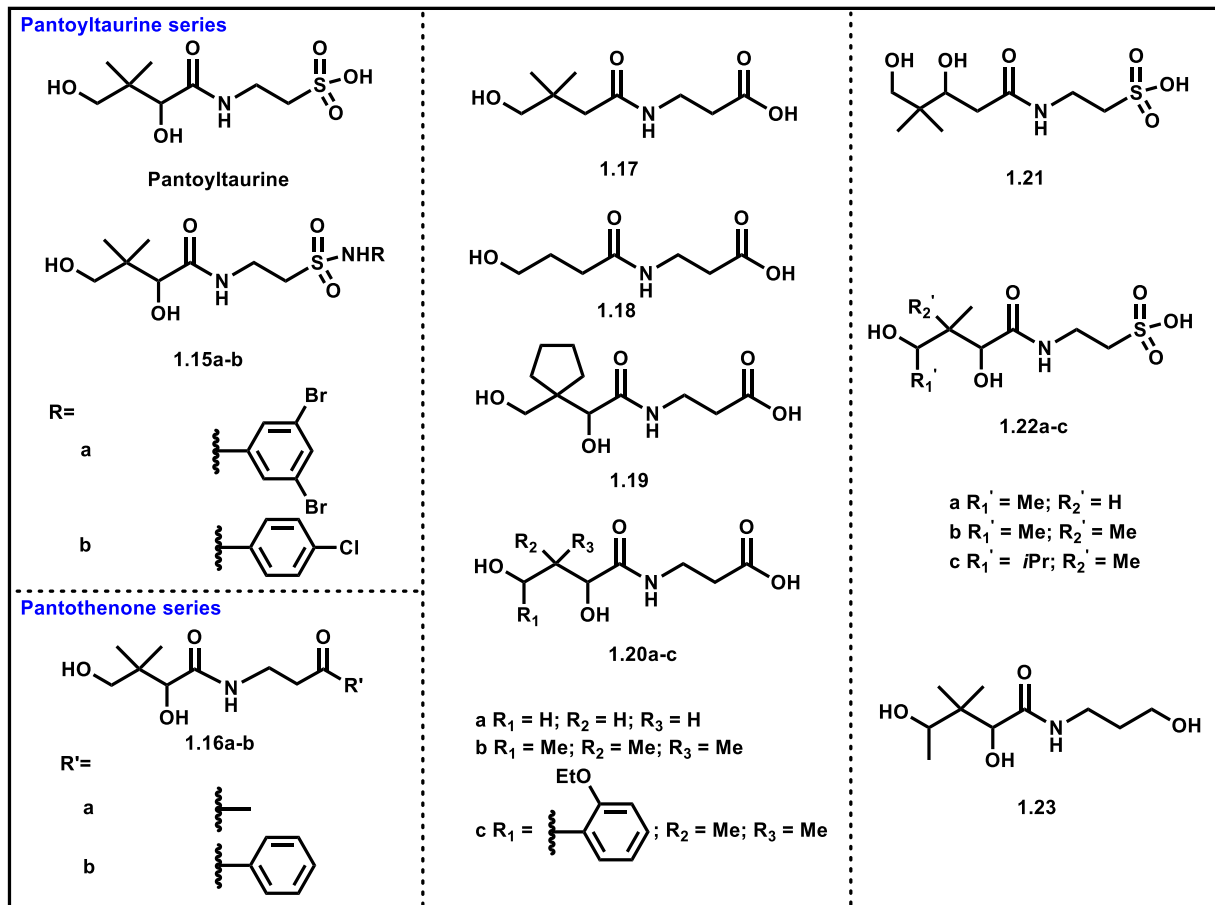


Figure 1.9. Examples of pantothenate analogues (unknown mechanism of action).

Pantothenate analogues modified at the pantoyl moiety have also been reported. Compounds **1.17** and **1.18** which lack the α -hydroxy group only display slight inhibitory activity towards bacteria such as *E. coli*, and this toxic effect is not reversed by addition of pantothenate.^{87, 130} In contrast, the antibacterial activity of compounds **1.19** and **1.20a-c**, in which modifications are introduced on the C-1 and/or C-2 position (Figure 1.9) of

pantothenate, are slightly better, and can be competitively reversed by pantothenate, with the exception of compound **1.20c**.¹³¹

Compounds modified both at the pantooyl and at the β -alanine moieties have also been synthesized (e.g. **1.21**, **1.22a-c** and **1.23**).⁸⁷ However, their activity are not necessarily improved, when compared with their corresponding analogues that are modified only at β -alanine or pantooyl moiety.

1.5.6 Pantothenate-related potentiators

All the antimicrobial agents discussed so far have antimicrobial activity on their own. There is also a class of non-toxic pantothenate-related compounds which do not inhibit the growth of microorganisms by themselves, but Instead help other antimicrobial agents to inhibit growth of microorganisms. These compounds are referred to as pantothenate-related potentiators.

Compounds **P-1a-e** (Figure 1.10A) are a series of pantothenate derivatives reported by the Auclair lab in 2012.¹³²⁻¹³³ Although they structurally belong to the family of pantothenamides, they are not toxic towards *E. faecium*, which possesses the type I PankK. In contrast, when combined with aminoglycosides, **P-1a-e** successfully inhibit the growth of aminoglycoside-resistant *E. faecium*. In other words, they potentiate the activity of aminoglycosides (Figure 1.10A). Compounds **P-1a-e** were suggested to be bioactivated by the CoA salvage pathway in *E. faecium* to produce the active CoA analogues **I-1a-e**, which inhibit the resistance-causing enzyme – aminoglycoside *N*-6'-acetyltransferase (AAC(6')) and consequently resensitize *E. faecium* towards aminoglycosides.

Another pantothenate-related potentiator **1.24** was reported by the Auclair lab in 2016.¹³⁴ Compound **1.24** was used to resensitize *Salmonella enterica* serovar Typhimurium towards itaconate by inhibiting the itaconate degradation pathway (Figure 1.10B).

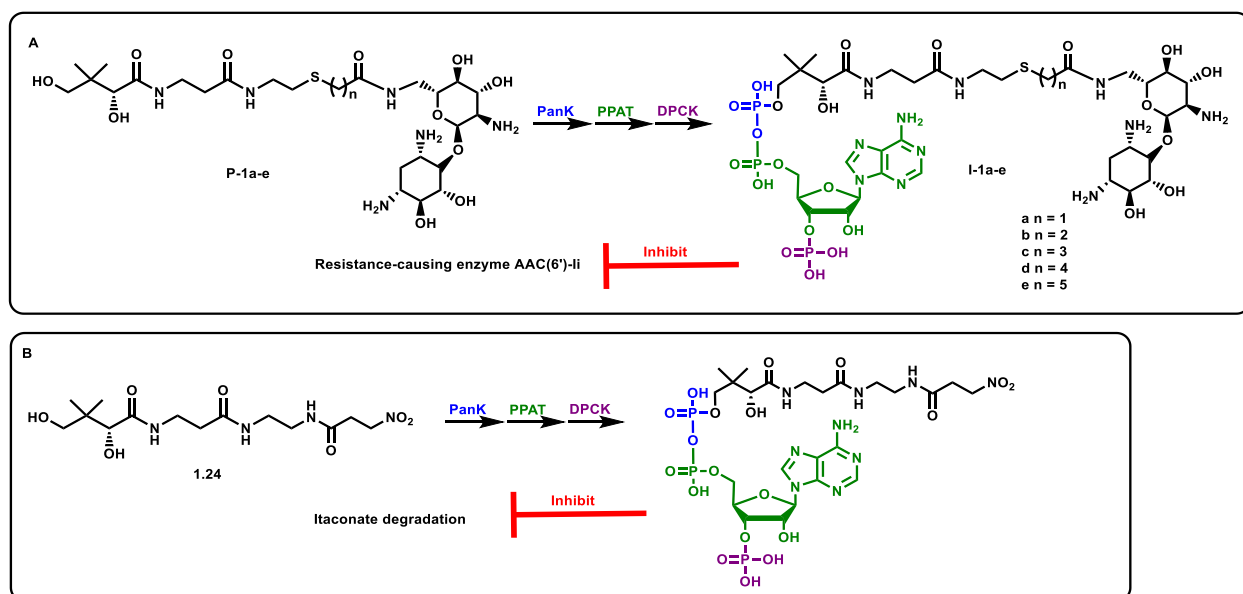


Figure 1.10. Pantothenate-related potentiators. A) Mechanism of action of aminoglycoside potentiation by **P-1a-e**; B) mechanism of action of itaconate potentiation by compound **1.24**.

Overall, the essentiality of the CoA biosynthetic pathway has triggered many research efforts in the field of antimicrobials.

1.6 Research goals

The essentiality and diversity of the CoA biosynthetic pathway across different organisms have made itself an interesting topic in antimicrobial researches. All the work discussed in this thesis will be related to the CoA biosynthetic pathway.

Chapters 2, 3 and 4 are related to pantothenamides. Pantothenamides are potent growth inhibitors of many bacteria, yeasts and parasites, yet show no cytotoxicity towards mammalian cells.⁹³ Their instability in human blood however hinders their clinical use. Chapters 2, 3 and 4 will discuss the efforts in circumventing the instability of pantothenamides in human blood, while maintaining their potency.

The aim of chapter 5 is to study the ligand preference of the three types of PanK. As introduced, various inhibitors, pantothenate antimetabolites and potentiators have been

reported for type I or II PanKs. However, for type III PanKs, only a weak inhibitor of *Ba*PanK, compound **1.4** ($K_i = 164 \mu\text{M}$, Figure 1.5) was reported.¹⁰¹ In order to help design better inhibitors, antimetabolites or potentiators not only for type I or II PanKs, but also for type III PanKs, understanding the ligand preference of the three types of PanK is indispensable. To this end, a series of pantothenate analogues modified at different positions of pantothenate was synthesized in chapter 5 of this thesis.

Chapter 6 is about the pantothenate-related potentiators **P-1a-e**. As suggested, these potentiators exert their potentiating effects after being bioactivated to CoA analogues **I-1a-e** (Figure 1.10A).¹³² It is the **I-1a-e** that actively inhibit the resistance-causing enzyme AAC(6')-Ii. However, the *in vitro* enzymatic data showed that though **P-1c-e** can be transformed into **I-1c-e** with high conversions, **P-1b** was poorly transformed to **I-1b**, and **P-1a** cannot be transformed into **I-1a**. To better understand the mechanism of action of potentiators **P-1a-e**, a series of cellular studies was performed in chapter 6.

Chapter 2

A cross-metathesis approach to novel and stable pantothenamide derivatives

2.1 Preface

In this chapter, a cross-metathesis approach for synthesizing novel and stable pantothenamide derivatives modified at the geminal dimethyl position of pantothenamide has been developed. This work is published as:

Guan, J.; Hachey, M.; Puri, L.; Howieson, V.; Saliba, K. J.; Auclair, K., A cross-metathesis approach to novel pantothenamide derivatives. *Beilstein Journal of Organic Chemistry* **2016**, *12*, 963-968.

Matthew Hachey from the lab of Prof. Auclair proposed and established the synthetic route presented in this chapter (with some technical help from Lekha Puri, an undergraduate student). Mathew Hachey obtained less than a mg of the final product **2.10**, which was too little to characterize. The author of this thesis contributes to synthesizing enough final product **2.10** for characterization and biological studies. Also, the antibacterial studies and the inhibitory assay with *Escherichia coli* pantothenate kinase (EcPanK) were performed by the author. The biological study with *P. falciparum* were performed by Vanessa M. Howieson from the lab of Prof. Saliba at The Australian National University.

2.2 Introduction

Bacteria, fungi, and parasites are all rapidly acquiring resistance to currently applied antimicrobials and as a result, our ability to treat infections effectively is diminishing. Efforts to control infections in this resistance era have taken a variety of paths from a renewed push for novel antimicrobial agents to a drive to study antimicrobial resistance mechanisms.¹³⁵ One successful research direction is to revisit “older” unexploited structural classes of antimicrobials.¹³⁶⁻¹³⁷ First synthesized by Clifton *et al.* in 1970, pantothenamides have attracted interest mostly for their antibacterial activity.⁹² In 2013, Spry *et al.* reported that pantothenamides can also inhibit growth of the malaria parasite *P. falciparum* with submicromolar activity.¹³⁸ Based on their high potency and low cytotoxicity, pantothenamides would be excellent candidates for antimicrobial drug development.^{87-88, 139} Unfortunately however, ubiquitous pantetheinases (also known as

vanins) in human blood rapidly hydrolyze pantothenamides into pantothenate and the corresponding amine (Figure 2.1),¹³⁹ making them unsuitable for therapeutic applications.

To overcome the instability of pantothenamides in human blood, two general strategies have been explored by different labs: 1) the use of pantetheinase inhibitors in combination with pantothenamides;¹⁴⁰⁻¹⁴¹ and 2) chemically modifying pantothenamides to prevent pantetheinase action while maintaining potency.^{94, 96-97, 142-146} Examples of modifications known to slow down or prevent pantothenamide degradation include alterations at the hydroxyl group,^{97, 144} geminal dimethyl group,^{94, 143-144} the β -alanine moiety,^{142, 145} or the labile amide moiety.^{96, 146}

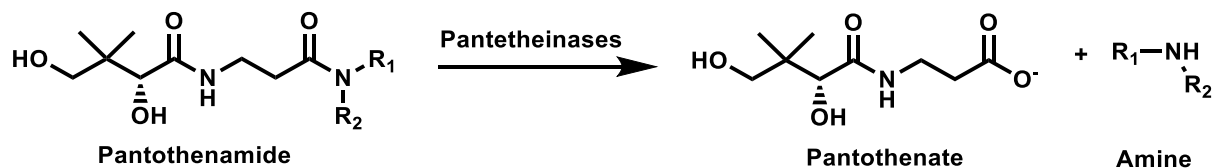
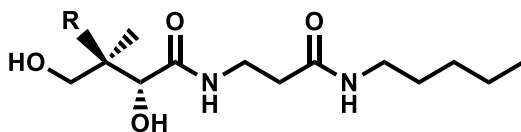


Figure 2.1. Hydrolysis of the pantothenamide by serum pantetheinases (or vanins). R_1 and R_2 are variable chemical groups.

Akinnusi *et al.* from the Auclair lab have previously reported a stereoselective route to access derivatives modified at the geminal dimethyl moiety of pantothenamide.^{94, 143} Those pantothenamide analogues, such as compounds **2.1**, **2.2** and **2.3** (Figure **2.2**), have shown good inhibitory activity against the growth of *P. falciparum* and bacteria like *S. aureus*.⁹⁴ Also, the antiplasmodial activity of those pantothenamide analogues in the presence or absence of pantetheinases indicates that large substituents at the geminal dimethyl position of pantothenamides, as in compounds **2.2** and **2.3**, can help stabilize the labile amide bond without affecting the potency (similar IC_{50} values). Synthesizing more pantothenamide derivatives with larger substituents at the geminal dimethyl position is hence desirable. However, the synthetic route reported by Akinnusi *et al.* fails with larger substituents, which limits the synthetic scope. In this chapter, a new synthetic route

that takes advantage of the reported path and exploits cross-metathesis to install larger groups, is described.



Compound	R =	IC ₅₀ ^a (μM)	IC ₅₀ ^b (μM)
N5-pan		2.0 ± 0.2	124 ± 15
2.1 ¹⁴³		10 ± 1	48 ± 3
2.2 ⁹⁴		11 ± 1	~ 11
2.3 ¹⁴³		25 ± 2	15 ± 2

Figure 2.2. Pantothenamide analogues modified at the geminal dimethyl position of pantothenamides. ^aIC₅₀ values towards *P. falciparum* in the absence of pantetheinases; ^bIC₅₀ values towards *P. falciparum* in the presence of pantetheinases.

2.3 Synthesis

In 2003, Grubbs published a classification system for cross-metathesis catalysts and substrates, defining the substrates by type ranging from I to IV depending on their level of homodimerization observed during metathesis reactions.¹⁴⁷ Type I substrates are defined as resulting in fast homodimerization under the condition of the reaction. Such substrates include terminal alkenes of low steric bulk. Type II and type III substrates, with the latter being bulkier, show slow or no detectable homodimerization, respectively. Type IV is a separate class, including substrates that are spectators to metathesis yet do not inactivate the catalyst. Based on the success of the synthetic route published by Akinnusi *et al.* to generate derivatives modified at the geminal dimethyl moiety of

pantothenamides,⁹⁴ the collaborator of the author, Matthew Hachey, envisaged that the intermediate allyl derivatives **2.4** and **2.5** (Figure 2.3) may present type II and III behavior, respectively. They could be good starting points to add larger moieties via cross-metathesis. Accordingly, Matthew Hachey together with an undergraduate student Lekha Puri, used two commercial cross-metathesis catalysts (Figure 2.3), Grubbs' 2nd generation catalyst (**2.6**) and Hoveyda–Grubbs' 2nd generation catalyst (**2.7**), to optimize the cross-metathesis conditions with compounds **2.4** and **2.5**. Overall, they found that compound **2.5** and catalyst **2.7** give higher yields and provide cleaner reactions. Their optimal conditions are shown in Scheme 2.1, with the scope of coupling partners **2.8a-d**.¹⁴⁸

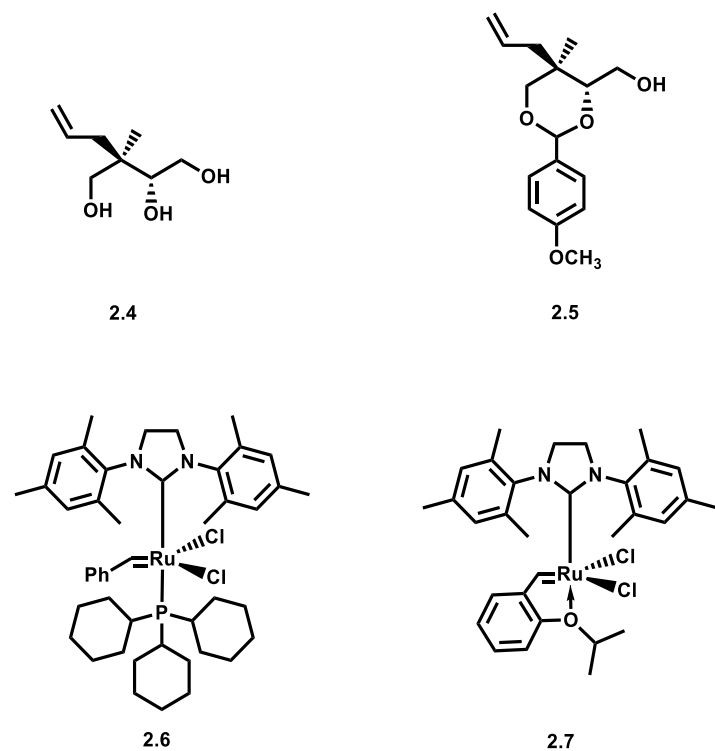
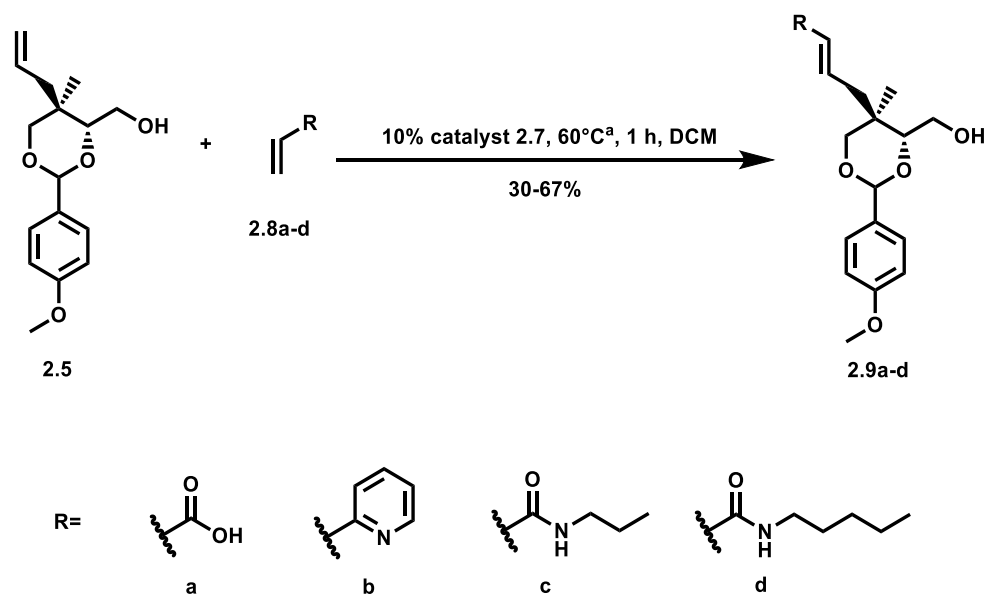


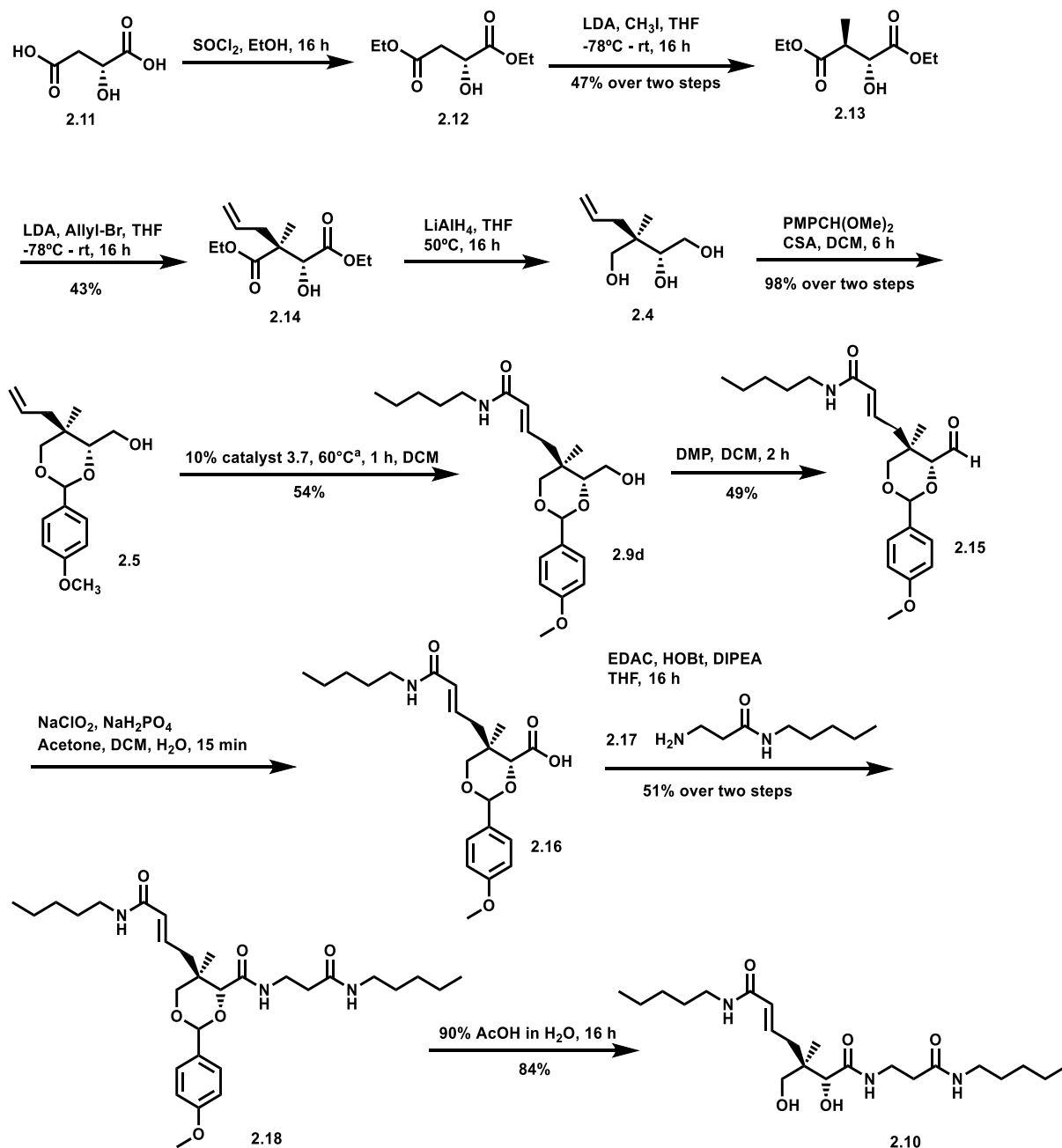
Figure 2.3. Structures of the intermediate allyl derivatives and the two Grubbs' catalysts.



Scheme 2.1. Optimal conditions of the cross-metathesis reaction.^{148 a)}In a microwave reactor.

With the optimization of the metathesis step, compound **2.9d** was next chosen by Matthew Hachey as the molecule to be extended to the final pantothenamide analogue **2.10** (Scheme 2.2), based on docking study with *EcPanK* conducted by Matthew Hachey which suggests that **2.10** might be a good *EcPanK* ligand.¹⁴⁸ Unfortunately, Matthew Hachey didn't get enough compound **2.10** for characterization. In order to demonstrate the viability of the synthetic route designed by Matthew Hachey, the author of the thesis started to synthesize the desired compound **2.10** from compound **2.11** (Scheme 2.2). To this end, the commercial *R*-malic acid (**2.11**) was first ethylated to form compound **2.12**, to which the methyl and allyl group were introduced at the geminal dimethyl position sequentially, producing compounds **2.13** and **2.14** respectively. Compound **2.14** was next reduced to the triol **2.4** using lithium aluminum hydride, the 2- and 4-hydroxyl groups of which were selectively protected using anisaldehyde dimethyl acetal in the presence of camphor sulfonic acid to give compound **2.5**. Compound **2.5** coupled with **2.8d** using the optimal condition developed by Matthew Hachey, producing **2.9d**. Compound **2.9d** was oxidized to the corresponding aldehyde **2.15** using Dess–Martin periodinane.¹⁴⁹ Further oxidation to the carboxylic acid **2.16** was achieved using mild Pinnick oxidation.¹⁵⁰⁻¹⁵³ The

carboxylic acid **2.16** was next coupled to amine **2.17**, which was synthesized from Boc-protected β -alanine and pentylamine using a method reported by Hoegl *et al.*¹⁴⁴ The final step was deprotection of the amide coupling product **2.18** in a 90% aqueous acetic acid solution to give final product **2.10**.



Scheme 2.2. Synthesis of compound **2.10**. LDA: lithium diisopropylamide; CSA: camphor sulfonic acid; DIPEA: *N,N*-diisopropylethylamine; DMP: Dess–Martin periodinane; EDAC: *N*-(3-

dimethylaminopropyl)-*N*'-ethylcarbodiimide hydrochloride; HOBt: hydroxybenzotriazole. ^aIn a microwave reactor.

2.4 Biological studies

2.4.1 Antibacterial studies

Antibacterial activity of compound **2.10** was next studied. Unfortunately, no visible growth inhibition was observed for *Escherichia coli*, *Staphylococcus aureus* and *Pseudomonas aeruginosa* even when concentration of **2.10** was up to 500 μ M. To investigate whether this lack of activity was due to poor target affinity or cell-permeability issues, kinetic study with the purified *EcPank* was performed. Compound **2.10** is neither a good substrate nor inhibitor of this enzyme, hence explaining its lack of antibacterial activity.

2.4.2 Antiplasmodial studies

The antiplasmodial activity and stability of compound **2.10** were next investigated. As shown in Figure 2.4, compound **2.10** has similar IC_{50} values in the presence and absence of pantetheinases: it inhibits the growth of *P. falciparum* with an IC_{50} value of 60 ± 11 μ M in the absence of pantetheinase, and its IC_{50} was unaffected by the presence of pantetheinase (51 ± 7 μ M). This demonstrates that introducing larger substituents at the geminal dimethyl position of pantothenamides is a viable strategy to overcome the blood instability issue of pantothenamides. Besides, in order to verify if compound **2.10** was targeting the CoA biosynthesis as reported for pantothenamides, its antiplasmodial activity was also studied in the presence of excess pantothenate (100 μ M). The dramatic loss of activity observed (Figure 2.4) confirms that compound **2.10** competes with pantothenate and acts on the CoA biosynthesis/utilization pathway, like pantothenamides do.

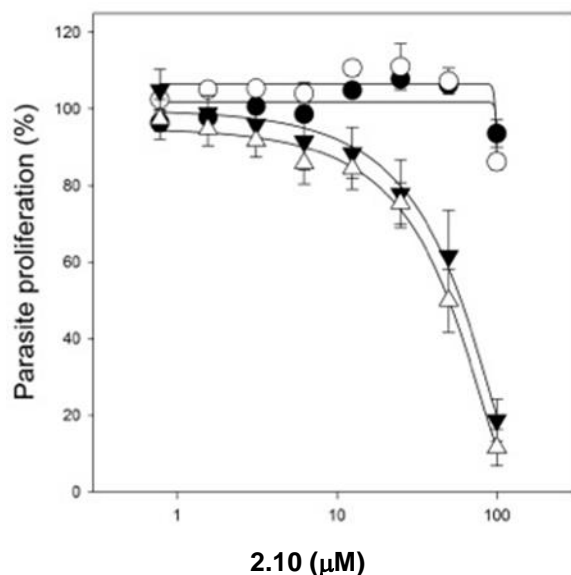


Figure 2.4. *In vitro* antiparasmodial activity of compound **2.10** in growth medium containing pantetheinases (open symbols) or in medium in which the pantetheinases have been inactivated (filled symbols). The antiparasmodial activity of this compound can be antagonized by increasing the extracellular concentration of pantothenate from 1 μM (triangles) to 100 μM (circles).

2.5 Closing remarks

In summary, a new synthetic route that exploits the known allyl derivative **2.5** and allows for the installation of larger groups on pantothenamides via cross-metathesis has been successfully developed. The high stability observed for compound **2.10** demonstrates that introducing larger groups at the geminal dimethyl position of pantothenamides is a viable strategy to solve the instability problem of pantothenamides in blood. Considering the importance of pantothenamides as a potential new class of antimicrobial agents, this stereoselective synthetic route should find utility in accessing novel, potent and stable pantothenamide derivatives.

Chapter 3

Structure-activity relationships of antiplasmodial pantothenamide analogues reveal a new way by which triazoles mimic amide bonds

3.1 Preface

In this chapter, based on a hit compound **3.1** (Figure 3.1) reported by the Auclair lab,¹⁴⁶ 11 novel pantothenamide analogues were synthesized to study its full structural-activity relationships (SARs). This work has been submitted for publication.

Guan, J.; Tjhin, E. T.; Howieson, V. M.; Kittikool, T.; Spry, C.; Saliba, K. J.; Auclair, K., Structure-activity relationships of antiplasmodial pantothenamide analogues reveal a new way by which triazoles mimic amide bonds, submitted for publication.

Of the 11 compounds, 10 were synthesized by the author of the thesis. One compound, **3.7c**, was synthesized by an undergraduate student Tanakorn Kittikool with the help of the author. The biological studies with *P. falciparum* were performed by Erick T. Tjhin and Vanessa M. Howieson from the lab of Prof. Saliba at The Australian National University.

3.2 Introduction

In 2017, the WHO reported that nearly half of the world's population was still at risk of malaria.¹⁶ This is aggravated by the fact that *Plasmodium* parasites are increasingly resistant to antimalarial agents.¹⁵⁴ Even resistance to artemisinin - a core component of modern therapy - has been detected in five countries of the Greater Mekong subregion.^{16,}¹⁵⁵ Development of novel antimalarial agents is necessary to treat an increasing number of drug resistant malaria cases.¹⁵⁶

Pantothenamides are potent growth inhibitors of various microorganisms. Their clinical use is, however, hindered due to the ubiquitous presence of pantetheinases in human serum, which rapidly degrade pantothenamides to pantothenate and the corresponding amine. Besides the method introduced in chapter 2, the Auclair lab also previously reported that replacement of the labile amide bond with a 1,2,3-triazole ring not only imparts stability towards pantetheinases but also improves activity against the malaria parasite, *P. falciparum*.¹⁴⁶ The most potent of those triazoles is compound **3.1** (Figure 3.1), which inhibits the growth of the asexual, erythrocytic stage of *P. falciparum* at nanomolar concentration. With compound **3.1** as the hit, in this chapter, a diversified

series of triazole-containing pantothenamide analogues is described, which allows us to establish important SARs. The synthetic targets were designed based on compound **3.1**, and altered at different positions (Figure 3.1) including: a) the relative position of the two substituents on the triazole ring; b) the pantoyl-to-triazole linker; and c) the triazole *N*-substituent.

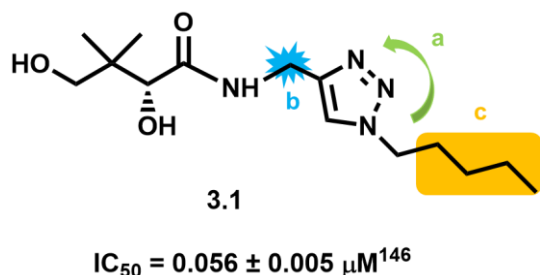


Figure 3.1. Structure of the previously reported compound **3.1** (with its respective inhibitory activity on the growth of intraerythrocytic *P. falciparum* in the presence of pantetheinases), and design of the molecules reported in chapter 3. The synthetic targets were designed based on compound **3.1**, and altered as follows: a) varied the ring substitution pattern (green); b) modified the pantoyl-to-triazole linker (blue); and c) explored further the triazole *N*-substituent (yellow).

As reported for pantothenamides, studies with compound **3.1** suggest that it also exerts its antiparasitic activity after being metabolically activated to a corresponding CoA antimetabolite. It is the CoA antimetabolite that inhibits downstream CoA-related pathways, leading to lethal effect on *P. falciparum*.¹⁰⁷ Therefore, although the bioactivation pathway of compound **3.1** is known,¹⁰⁶⁻¹⁰⁹ its actual targets in the malaria parasite may be numerous, and remain poorly understood. As such, docking studies are impractical. Since 1,2,3-triazoles are known to be good amide bioisosteres,¹⁵⁷⁻¹⁵⁸ and mechanistic studies suggest that compound **3.1** may inhibit the growth of *P. falciparum* by the same mechanism as pantothenamides,¹⁴⁶ the new derivatives presented in this chapter were designed with inspiration from the SARs reported for pantothenamides.

3.3 1,5-Substituted triazoles

Tron *et al.* have suggested that 1,4-disubstituted-1,2,3-triazoles and *Z*-amide bonds may be isosteric, while 1,5-substituted-1,2,3-triazoles may mimic *E*-amide bonds (Figure 3.2).¹⁵⁷ To determine the optimal triazole configuration for antiplasmodial activity, 1,5-substituted triazoles **3.2a,b** were synthesized (Scheme 3.1). To this end, compounds **3.3a,b** were first synthesized from commercially available amine hydrochlorides, and the pentyl azide **3.4** was synthesized from 1-bromopentane. For the subsequent cycloaddition step to produce **3.5a,b**, two different ruthenium catalysts, RuCl(cod)Cp* and RuCl(PPh₃)₂Cp*, were tested.¹⁵⁹ With the former, no reaction was observed at room temperature, and only very little conversion was detected at 100°C. In contrast, RuCl(PPh₃)₂Cp* gave a reasonable yield at 100°C. Finally, the desired products **3.2a,b** were generated after Boc-deprotection of **3.5a,b** and subsequent condensation with D-pantolactone.

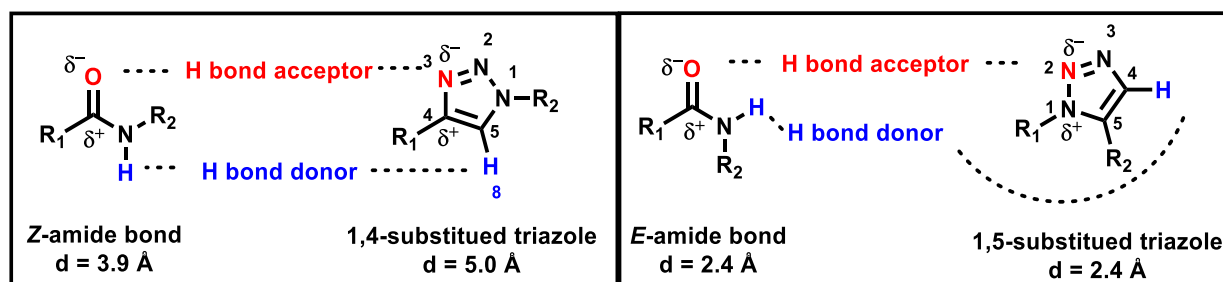
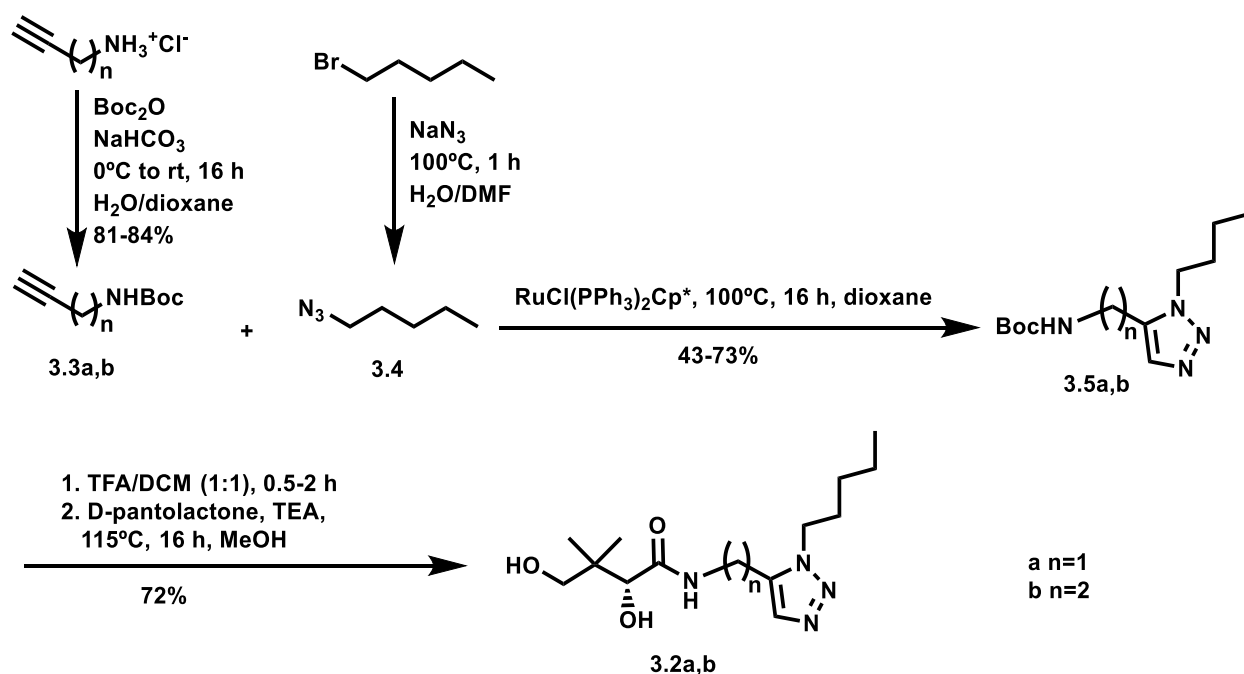


Figure 3.2. Current hypothesis for how triazoles act as amide bioisosteres.¹⁵⁷ The “d” is the distance between the R₁ and R₂ groups.

The antiplasmodial activity of compounds **3.2a-b** was next measured, and the results are shown in Table 3.1. The IC₅₀ values for 1,5-substituted triazole analogues **3.2a,b** are higher than the one of their corresponding 1,4-substituted analogue **3.1**, suggesting that 1,4-substituted triazole is favored over the 1,5-substituted one.



Scheme 3.1. Synthesis of 1,5-disubstituted triazoles **3.2a-b**. TEA: triethylamine; TFA: trifluoroacetic acid.

3.4 Pantoyl-to-triazole linker study

3.4.1 Two-carbon linker

It was next envisaged to study variations in the linker between the pantoyl and the triazole moieties. So far only triazole derivatives with one- or three-carbon linkers have been reported as pantothenamide mimics.¹⁴⁶ Moreover, the currently accepted theory for how triazoles act as amide bioisosteres suggests that compound **3.1** would be isosteric to compound **3.6** (Figure 3.3A), which is short of one carbon in the linker compared to its analogue, N5-Pan (Figure 3.3B). Since N5-Pan is more potent than **3.6** towards *P. falciparum* in the absence of pantetheinases, it was therefore hypothesized that 1,4-substituted triazoles with a two-carbon linker might be optimal, as in compound **3.7a** (Figure 3.3B).

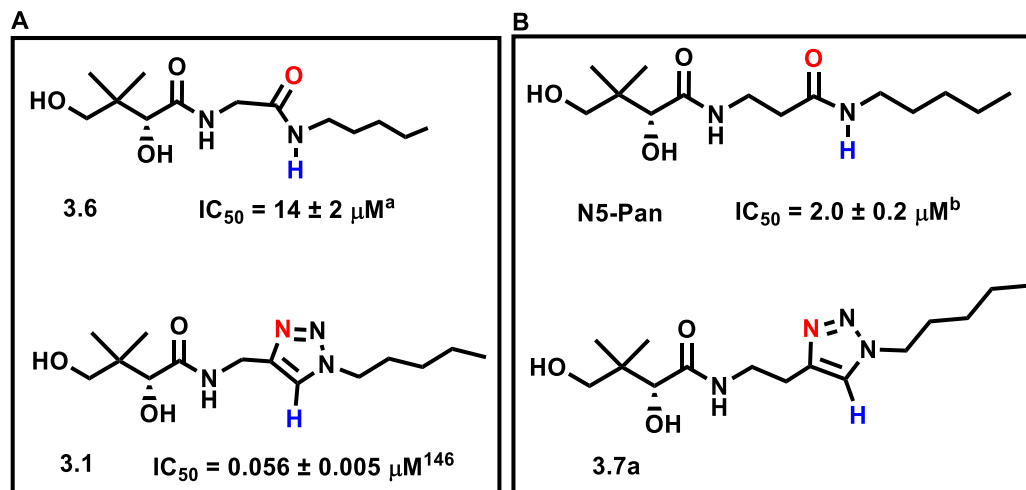
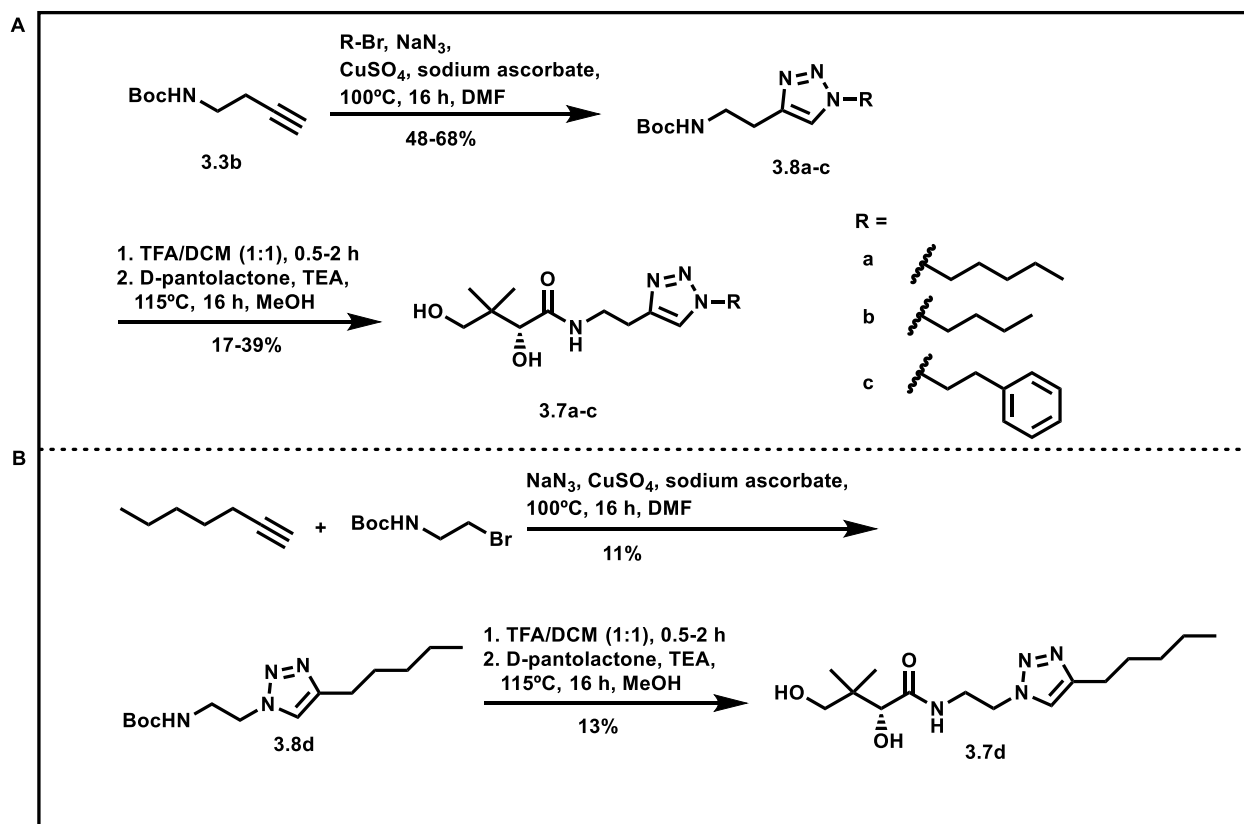


Figure 3.3. The triazole ring mimics the amide bond as proposed by Tron *et al.* for 1,4-substituted triazoles.¹⁵⁷ Unless otherwise noted all IC_{50} values were measured in the presence of pantetheinases. ^aData from ref. 142, in the absence of pantetheinases; ^bdata from ref. 138, in the absence of pantetheinases.

Compounds **3.7a-c** were all prepared from **3.3b**. To get compounds **3.8a-c** (Scheme 3.2A), compound **3.3b** first underwent Cu(I)-catalyzed azide-alkyne cycloaddition (CuAAC) with different commercial alkyl bromides in the presence of sodium azide.¹⁶⁰ It is worth noting that the corresponding alkyl azides were generated in situ by bromide-azide exchange. Compounds **3.8a-c** were then Boc-protected before condensation with D-pantolactone to form the final products **3.7a-c**. Similarly, compound **3.7d** was prepared via CuAAC; however, commercial 1-heptyne and 2-(Boc-amino)ethyl bromide were used as the starting materials (Scheme 3.2B). The low yield for the CuAAC reaction might be due to a slow azide-bromide exchange.

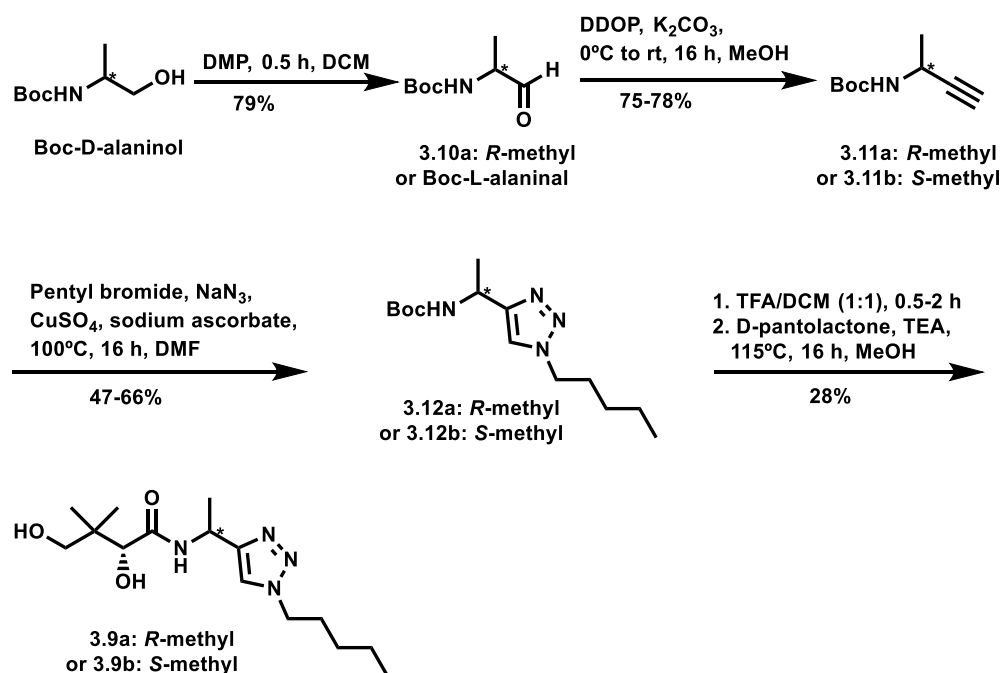


Scheme 3.2. Synthesis of compounds **3.7a-d**. TEA: triethylamine; TFA: trifluoroacetic acid.

As shown in Table 3.1, the IC_{50} values of compounds **3.7a-d** are higher than that of compound **3.1**, demonstrating that a one-carbon linker between the pantoyl and the triazole moieties is optimal. Interestingly, comparing the activity of compound **3.7a** in the presence of pantetheinases to that of N5-Pan in the absence of pantetheinases (Figure 3.3), reveals similar IC_{50} values, suggesting that the triazole moiety in **3.7a** may mimic the amide bond of N5-Pan well. On the other hand, the higher potency of compound **3.1** is consistent with the formation of additional interactions not accessible to N5-Pan or **3.7a**. It is also worth noting that compounds **3.7a** and **3.7d** were designed to have the ring substituents switched relative to one another. The slightly higher potency of **3.7a** over that of **3.7d** is consistent with a nitrogen being preferred over carbon at the attachment point of the alkyl chain.

3.4.2 Branched linker

The effect of branching in the linker was also investigated with a methyl group added to the optimal one-carbon linker (compounds **3.9a,b** in Scheme 3.3). Same as compounds **3.7a-d**, they were synthesized by CuAAC, but from **3.11a,b** and pentyl bromide in the presence of sodium azide. Compound **3.11a** (Scheme 3.3) was prepared from Boc-D-alaninol via Dess-Martin periodinane oxidation to generate the aldehyde **3.10a**, before undergoing the Seyferth-Gilbert homologation to generate the alkyne **3.11a** with the use of dimethyl (1-diazo-2-oxopropyl)phosphonate (Bestmann-Ohira reagent).¹⁶¹ Compound **3.11b** was similarly synthesized but directly from commercial Boc-L-alaninal.



Scheme 3.3. Synthesis of compounds **3.9a,b**. DDOP: dimethyl (1-diazo-2-oxopropyl)phosphonate; DMP: Dess-Martin periodinane; TEA: triethylamine; TFA: trifluoroacetic acid.

Measurement of antiplasmodial activity revealed IC₅₀ values (Table 3.1) above 100 μM for both **3.9a** and **3.9b**, suggesting that branching in the one-carbon linker is detrimental to activity. Since compound **3.1** was reported to be bioactivated to the corresponding CoA derivative in three steps and act as a CoA antimetabolite,¹⁰⁷ its antimicrobial activity is thus affected by multiple factors such as the participation of more than one enzyme during bioactivation, the possible involvement of multiple different targets in the mode of action, as expected for antimetabolites, and of course, cell permeability. The branching modification mentioned above may slow bioactivation and/or negatively impact the interaction with the target(s) and/or reduce cell permeability.

3.5 Triazole *N*-substituent study

The most potent antiplasmodial pantothenamide reported so far is phenethyl-Pan (Figure 3.4), which is not stable in serum as demonstrated by its IC₅₀ value increasing by 3,600-fold in the presence of pantetheinases.¹³⁸ Compared to its analogue, N5-Pan, in the absence of pantetheinases, phenethyl-Pan is 100-fold more active.¹³⁸

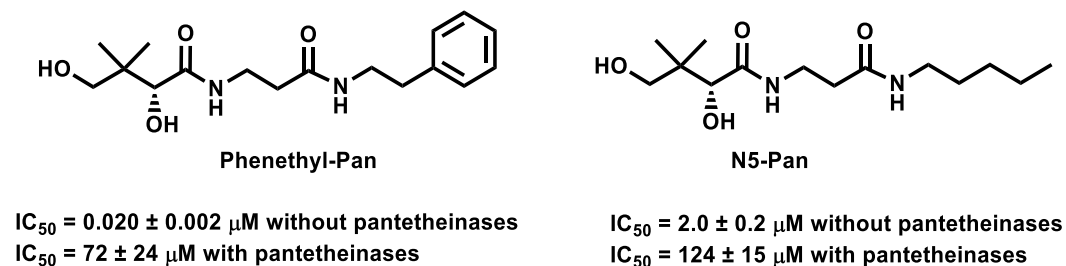
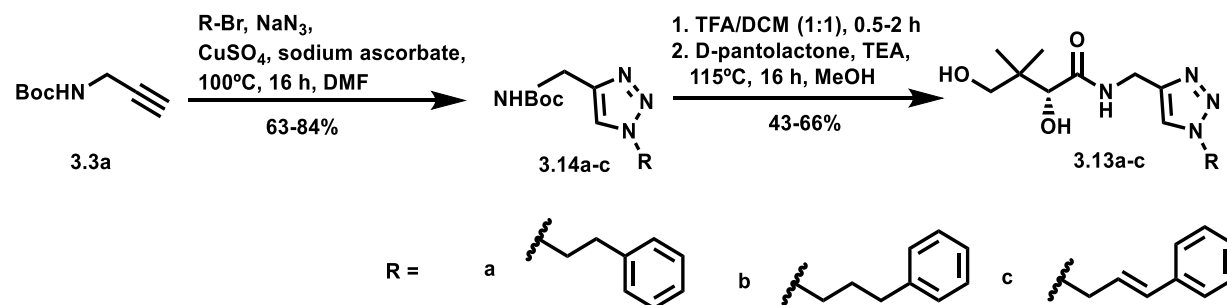


Figure 3.4. Two classical pantothenamides and their IC₅₀ values¹³⁸ against *P. falciparum* in the presence or absence of pantetheinases.

Inspired by this, a small series of 1,4-substituted triazole compounds including a phenyl group in the triazole *N*-substituent, as in compounds **3.13a-c** (Scheme 3.4), were prepared starting from **3.3a** and the corresponding alkyl bromides in the presence of sodium azide. The synthetic route to compounds **3.13a-c** is similar to that of compounds

3.7a-d: CuAAC to generate compounds **3.14a-c**, before Boc-deprotection and condensation with D-pantolactone.



Scheme 3.4. Synthesis of compounds **3.13a-c**. TEA: triethylamine; TFA: trifluoroacetic acid.

Unexpectedly, as shown in Table 3.1, none of compounds **3.13a-c** has a superior antiplasmodial activity when compared to the pentyl analogue, **3.1**. This may be due to reduced cell permeability. However, the possibilities of slow bioactivation and/or negative impact on the interaction with the target(s) cannot be ruled out.

Table 3.1. Effect of compounds **3.2a-b**, **3.7a-d**, **3.9a-b**, **3.13a-c** on the proliferation of erythrocytic *P. falciparum* in growth medium containing 1 μ M pantothenate and *in the presence of pantetheinases*.

Name	Compound	IC ₅₀ (μ M)	Name	Compound	IC ₅₀ (μ M)
3.1		0.056 \pm 0.005 ¹⁴⁶	3.7d		8.5 \pm 3.0
3.2a		36 \pm 10	3.9a		>100
3.2b		>100	3.9b		>100
3.7a		3.3 \pm 0.9	3.13a		25 \pm 9
3.7b		5.3 \pm 1.7	3.13b		16 \pm 4
3.7c		5.4 \pm 0.8	3.13c		55 \pm 10

3.6 Discussion

It is difficult to draw SARs with pantothenamides or their analogues,^{92, 94-95, 99, 106, 138, 142, 146} because their antimicrobial activity is affected by multiple factors such as the participation of more than one enzyme during bioactivation, the possible involvement of multiple different targets in the mode of action, as expected for antimetabolites, and of course, cell permeability. The possibility that these molecules may have multiple targets is nevertheless an advantage as resistance may take longer to be selected for. Our results with triazole derivatives mimicking pantothenamides clearly imply that the 1,4-substitution pattern on the triazole ring, with a simple methylene linker between the triazole and the pantoyl moieties, can overcome all the mechanistic barriers and display antiplasmodial activity at nanomolar concentration.

The results presented herein are consistent with the triazole ring of compound **3.7a** being a good mimic of the amide bond of N5-Pan, while the use of a shorter linker, as in compound **3.1**, may lead to a different binding mode to the target(s) and/or bioactivating enzymes, with enhanced antiplasmodial activity. Furthermore, it is believed that the shorter linker may serendipitously render the triazole in compound **3.1** a bioisostere of the flipped amide in compound **3.15** (Figure 3.5A), a pantothenamide mimic with high nanomolar antiplasmodial activity and stability to pantetheinases.⁹⁶ It is proposed that the triazole N-2 of compound **3.1** may mimic the carbonyl oxygen of the flipped amide bond in compound **3.15** more closely than the triazole N-3 (Figure 3.5A), while the triazole N-3 of **3.7a** is a better mimic of the carbonyl oxygen of the (original orientation) amide bond in N5-Pan (Figure 3.5B). The 10-fold improved activity of **3.1** over that of **3.15**, may be explained by: 1) increased rigidity of compound **3.1** compared to **3.15** leading to lower entropic penalty incurred upon enzyme binding; 2) a larger dipolar moment of the triazole ring compared to amide bond, providing enhanced H bond donor and acceptor properties;¹⁵⁷ 3) interactions between the triazole ring and properly aligned aromatic rings on the target enzyme(s) and/or 4) extra interactions possible via N-1 and/or N-3 of **3.1**. The fact that N-1 may be involved in additional favorable interactions is implied from comparing compounds **3.7a** and **3.7d**, which suggests that a nitrogen atom is preferred over a carbon atom at the site of attachment of the alkyl group. Overall, the proposed arrangement of the triazole to mimic an amide bond is consistent with the similar IC₅₀ values observed for compounds **3.1**, **3.15**, **3.7a** and N5-Pan.

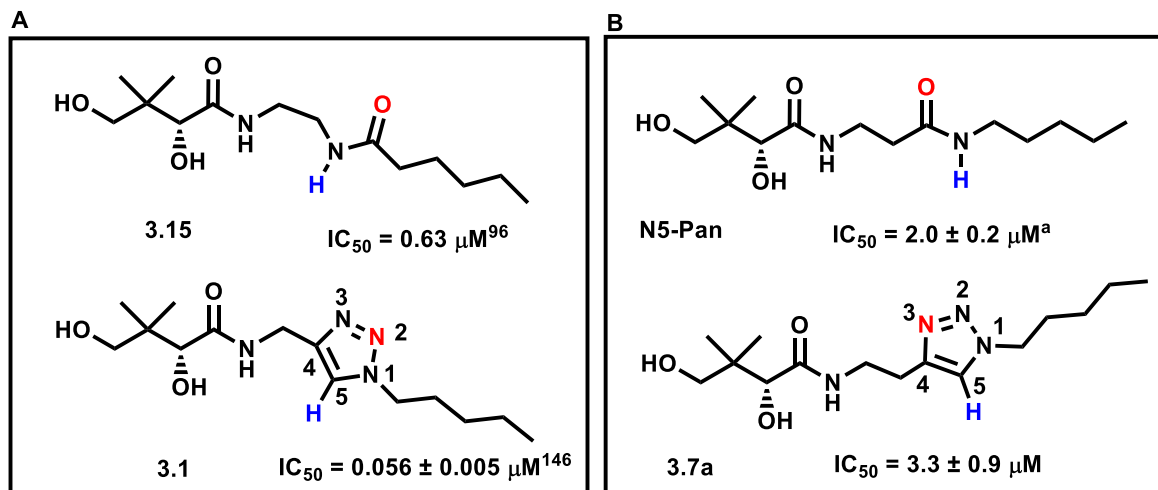


Figure 3.5. Triazoles are proposed to mimic amide in a new way. A) It is proposed that triazoles may mimic amide bonds, with the triazole N-2, instead of N-3, mimicking the C=O H bond accepting capabilities of the amide; B) in compound **3.7a**, the triazole ring is designed to mimic the amide bond of N5-Pan, as proposed by Tron *et al.* for 1,4-substituted triazoles.¹⁵⁷ N-3 of the triazole may mimic the H bond acceptor (C=O) of the amide, and the triazole hydrogen substituent may mimic the amide H bond donor. *Unless otherwise noted all IC_{50} values were measured in the presence of pantetheinases.* Except for N5-Pan, all compounds shown in this figure are stable to pantetheinases. ^aMeasured in the absence of pantetheinases; data from ref. 138. The red highlights the H bond acceptor, and the blue highlights the H bond donor.

3.7 Closing remarks

In conclusion, the results with triazole derivatives mimicking pantothenamides clearly imply that the 1,4-substitution pattern on the triazole ring, with an unbranched methylene linker between the triazole and the pantoyl moieties, is optimal for antiplasmodial activity. This provides important guidance for future SAR studies.

The triazole group is heavily exploited as an amide isostere in drug discovery nowadays. Based on our study, we propose that the triazole ring can mimic amide bonds in different ways, which should all be considered for best results by medicinal chemists. It has been suggested that 1,4-substituted 1,2,3-triazole rings display structural similarity to *Z*-amides, with the lone pair of the triazole N-3 mimicking the carbonyl oxygen of the amide bond,

the triazole H-5 acting as a H bond donor.¹⁵⁷ Our results suggest that in some cases the triazole N-2 (instead of N-3) may mimic the carbonyl oxygen of the amide bond.

The 1,2,3-triazole ring is among the most commonly used scaffolds in drugs. The triazole derivative **3.1** is stable in human blood, shows excellent antiplasmodial activity, is not toxic to human cells,¹⁴⁶ and has a new mode of action compared to clinical drugs, making itself attractive hit for the development of novel antimalarials.

Chapter 4

Pantothenamide analogues with the labile amide group replaced with various heteroaromatic rings

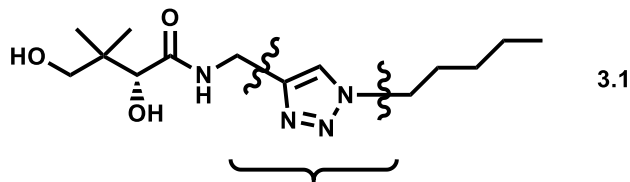
4.1 Preface

In this chapter, based on the triazole compound **3.1** (Figure 4.1) reported by the Auclair lab,¹⁴⁶ 14 novel heteroaromatic ring-containing pantothenamide analogues were synthesized to study the SARs of the heteroaromatic ring. A patent application claiming some of the heteroaromatic compounds is currently being prepared jointly by McGill University and The Australian National University.

Of the 14 compounds, 13 were synthesized by the author of this thesis. One compound, **4.1d**, was synthesized by an undergraduate student, Tanakorn Kittikool, with the help of the author. The antiplasmodial activity of the 14 compounds was tested by Erick T. Tjhin from the lab of Prof. Saliba at The Australian National University.

4.2 Introduction

The SAR study with the triazole compounds reported in chapter 3 suggests that 1,4-substitution pattern on the triazole ring, with a simple methylene linker between the triazole and the pantoyl moieties, is favored for optimal antiplasmodial activity. In order to understand the role of each atom in the triazole ring and look for better amide substituents, synthesizing pantothenamide analogues containing other heteroaromatic rings, as in **4.1a-n** (Figure 4.1), is discussed in this chapter.



Replaced with rings below

Compounds 4.1a-n

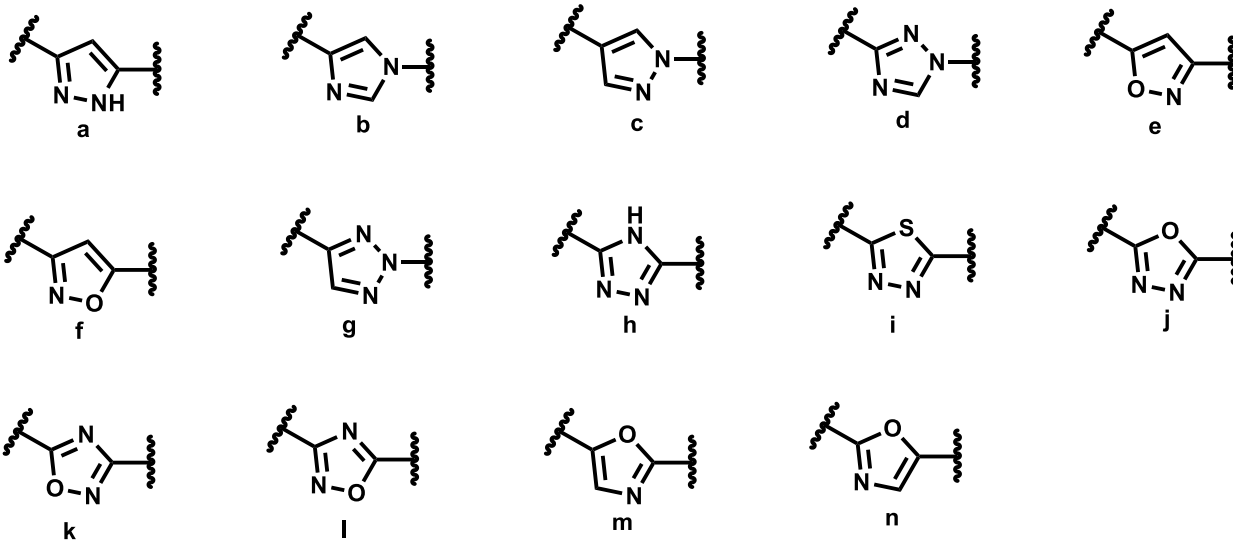
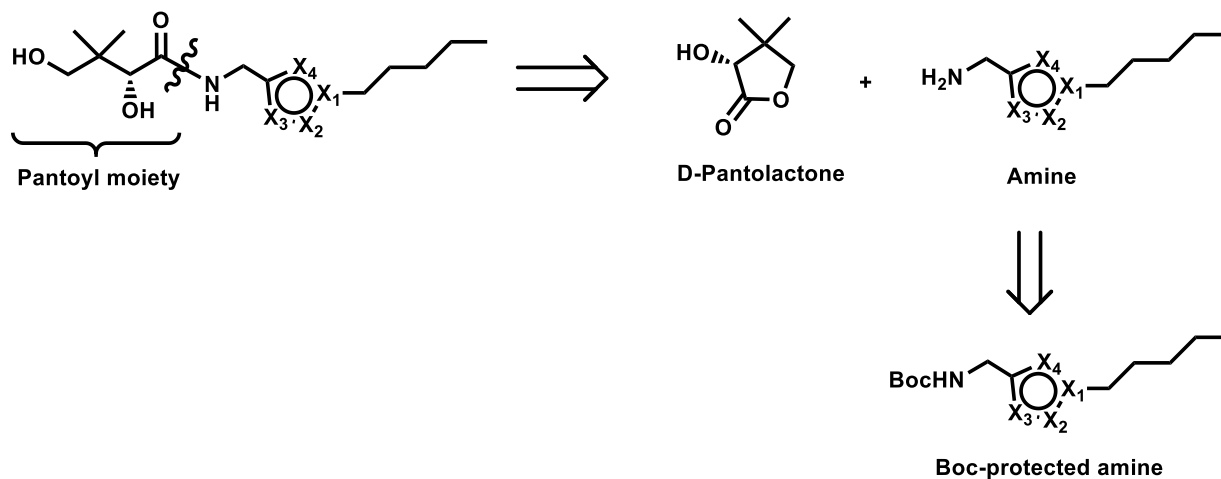


Figure 4.1. Pantothenamide analogues containing various heteroaromatic rings studied in chapter 4.

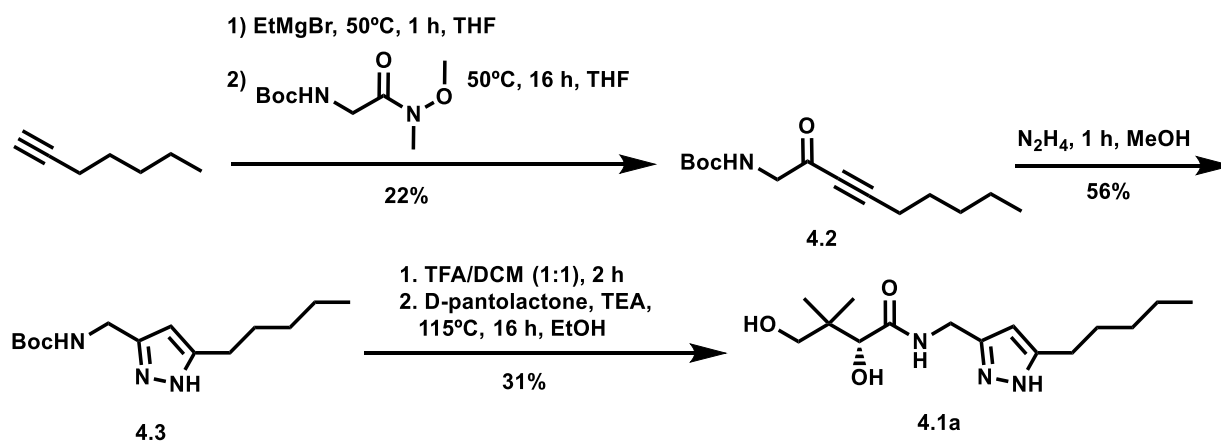
4.3 Synthesis

The common feature of compounds **4.1a-n** is their pantoyl moiety. Therefore, the best strategy to synthesize these compounds is envisaged to be preparing the heteroaromatic ring-containing amines first, and then condensing with D-pantolactone, as shown in Scheme 4.1. Those heteroaromatic ring-containing amines can be synthesized either directly or generated after deprotection of the *tert*-butyloxycarbonyl protecting group. Due to the intrinsic difference of the amines or the protected amines, they have to be synthesized using more than one methodologies.



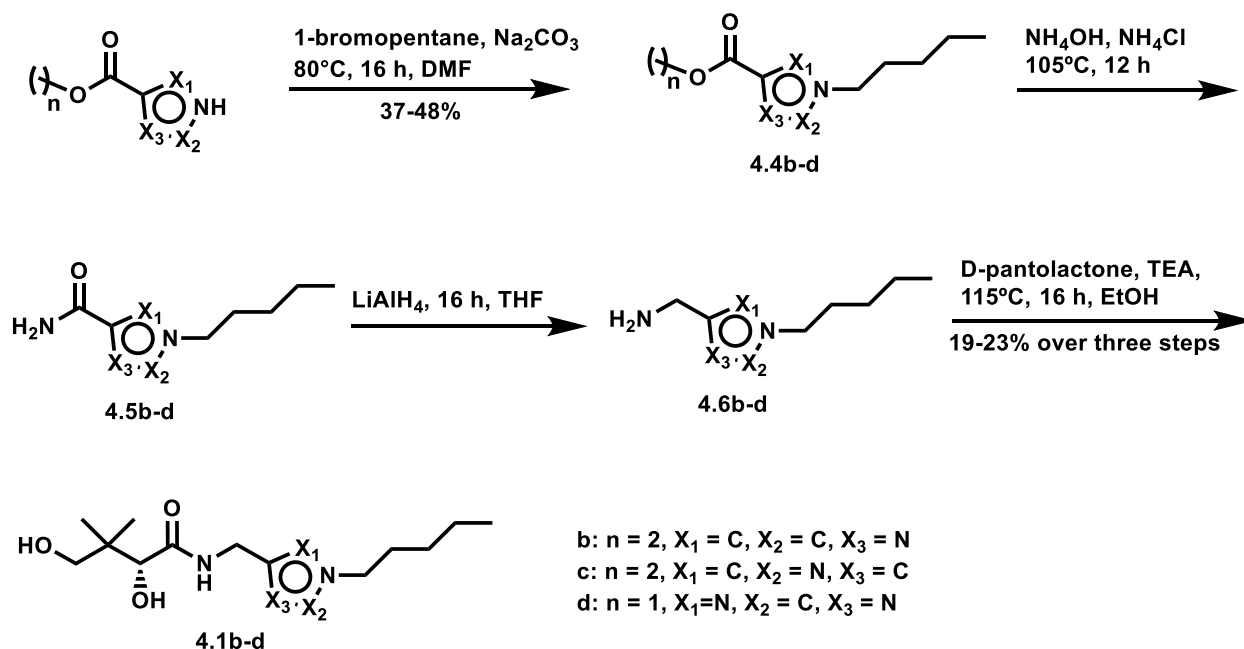
Scheme 4.1. Retrosynthetic approach to compounds **4.1a-n**. X_1 , X_2 , X_3 and X_4 are C, N, O or S atom.

As shown in Scheme 4.2, compound **4.1a** containing the pyrazole moiety was prepared from commercial 1-heptyne and *N*-(*tert*-butoxycarbonyl)glycine *N'*-methoxy-*N'*-methylamide. Firstly, to link the desired Boc-protected amine and the pentyl moieties together, 1-heptyne was deprotonated using the Grignard reagent ethylmagnesium bromide, and allowed to attack the Weinreb amide and yield compound **4.2**. Next, this product was condensed with hydrazine, producing the pyrazole **4.3**. Finally, Boc-deprotection of compound **4.3** by trifluoroacetic acid produced the amine, which subsequently attacked the ring of D-pantolactone, yielding the desired product **4.1a**.



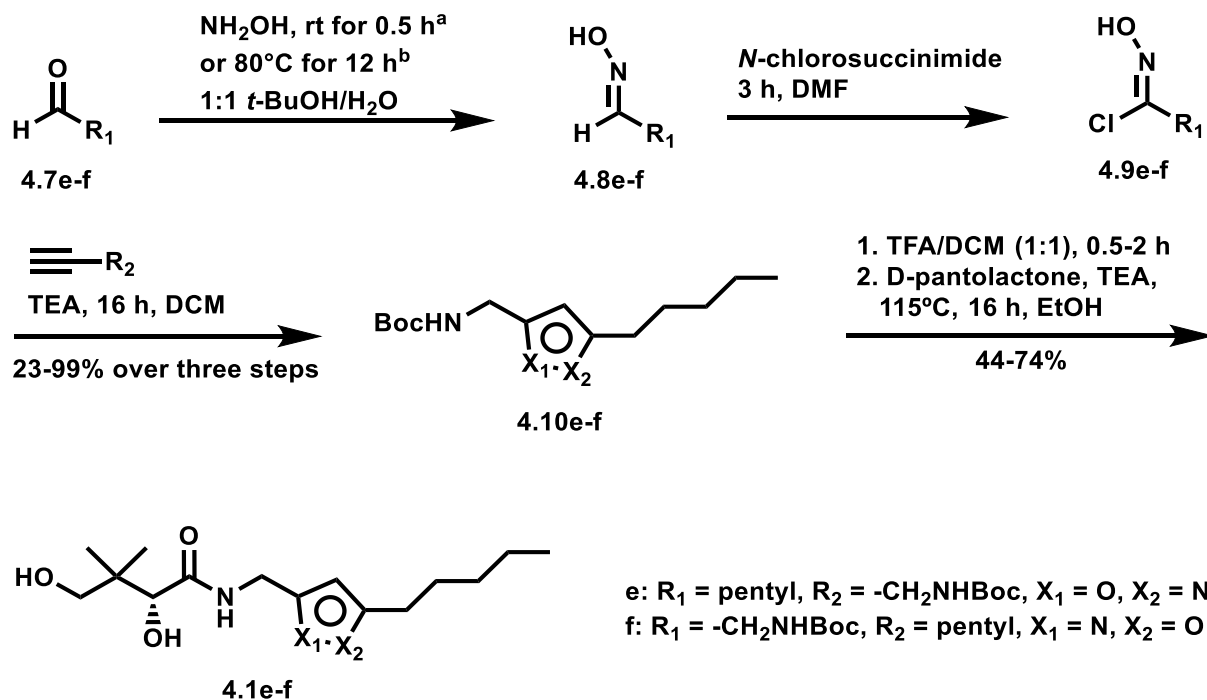
Scheme 4.2. Synthesis of compound **4.1a**. TEA: triethylamine; TFA: trifluoroacetic acid.

Compounds **4.1b-d** were prepared using the general method shown in Scheme 4.3. Instead of constructing the heteroaromatic ring after linking the amine and pentyl moieties, the commercial ester containing the desired ring structure was utilized here. Starting from the desired ester, the pentyl group was first introduced on the ring by deprotonating the ring N-H with sodium carbonate, for substitution on 1-bromopentane. The produced esters **4.4b-d** were then quickly converted to the corresponding amides **4.5b-d** with ammonium hydroxide and ammonium chloride, before further reduction with lithium aluminum hydride to yield amines **4.6b-d**. The amines were next allowed to react with D-pantolactone to generate the final products **4.1b-d**.



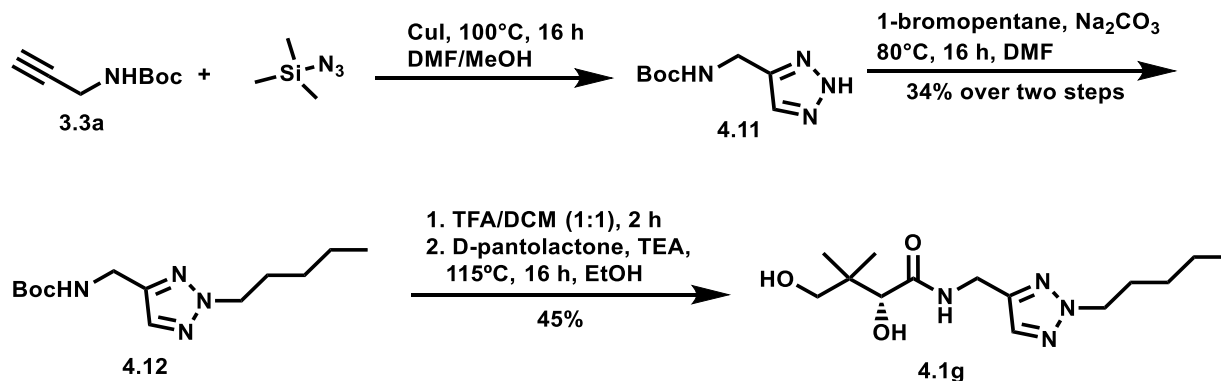
Scheme 4.3. Synthesis of compounds **4.1b-d**. TEA: triethylamine.

Synthesis of compounds **4.1e-f** containing the isoxazole ring was shown in Scheme 4.4. The first step was to produce the desired oximes **4.8e-f** by condensing commercial aldehydes **4.7e-f** with hydroxylamine. The oximes **4.8e-f** were next chlorinated using *N*-chlorosuccinimide to form **4.9e-f**, followed by condensation with the desired alkyne at room temperature. The generated isoxazoles **4.10e-f** were Boc-protected before condensation with D-pantolactone to give the final products **4.1e-f**.



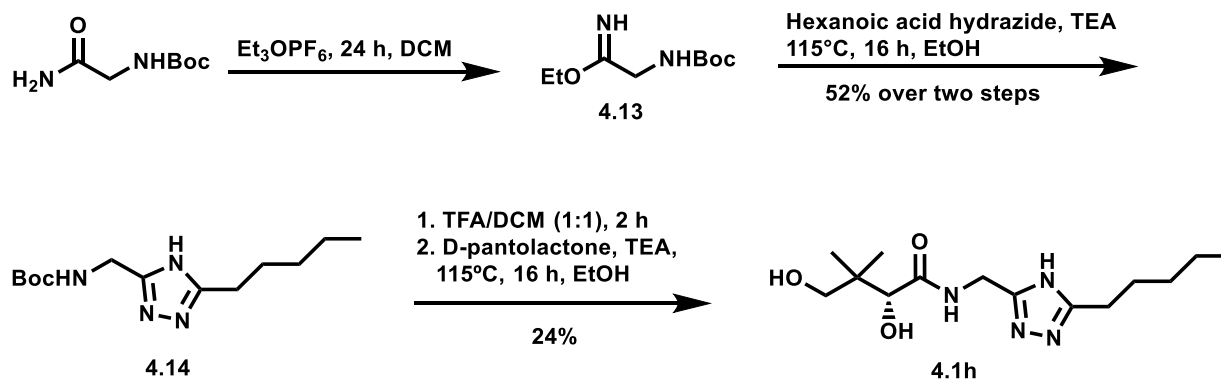
Scheme 4.4. Synthesis of compounds **4.1e-f**. ^aFor compound **4.1e**; ^bfor compound **4.1f**. TEA: triethylamine; TFA: trifluoroacetic acid.

For synthesizing the compound **4.1g** (Scheme 4.5), CuAAC was first exploited, using the alkyne **3.3a** and trimethylsilyl azide to generate the 1,2,3-triazole **4.11**. Triazole **4.11** was next deprotonated using sodium carbonate and allowed to attack 1-bromopentane, giving compound **4.12**. Boc-deprotection of compound **4.12** and condensation with D-pantolactone produced the desired compound **4.1g**.



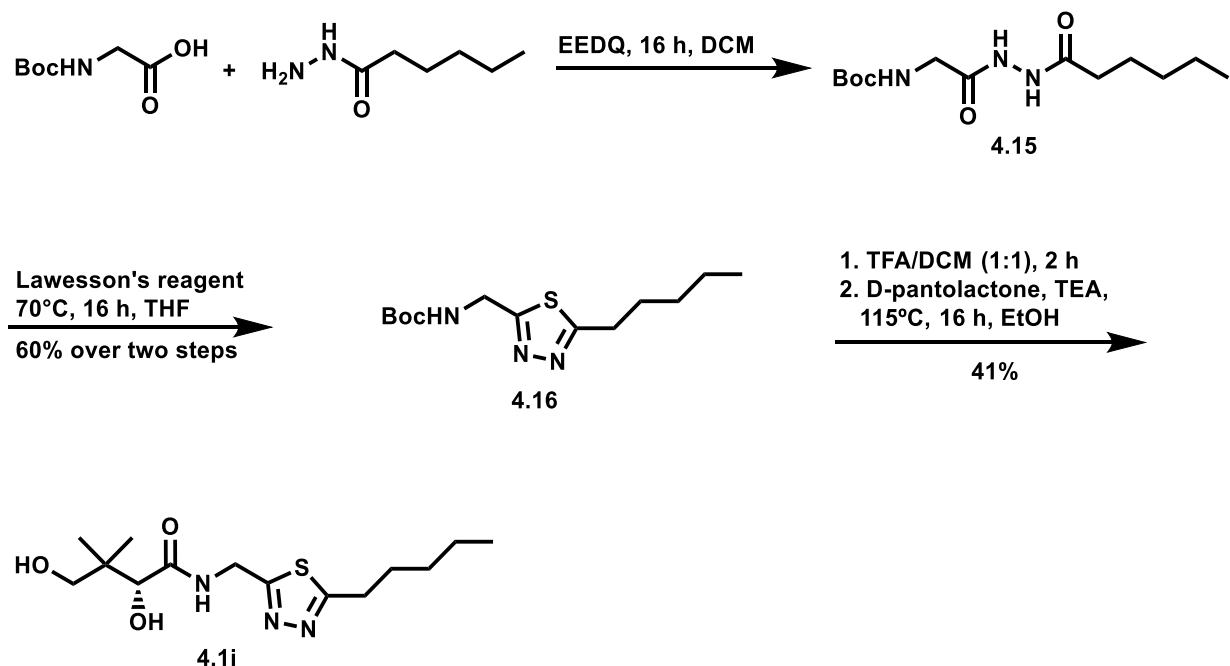
Scheme 4.5. Synthesis of compound **4.1g**. TEA: triethylamine; TFA: trifluoroacetic acid.

To synthesize compound **4.1h** (Scheme 4.6), *N*-Boc-glycinamide was first converted into imidate **4.13** in the presence of triethyloxonium hexafluorophosphate. The imidate **4.13** was next condensed with hexanoic acid hydrazide at 115°C to produce the 1,2,4-triazole **4.14**. Finally, Boc-deprotection followed by D-pantolactone ring-opening afforded the compound **4.1h**.



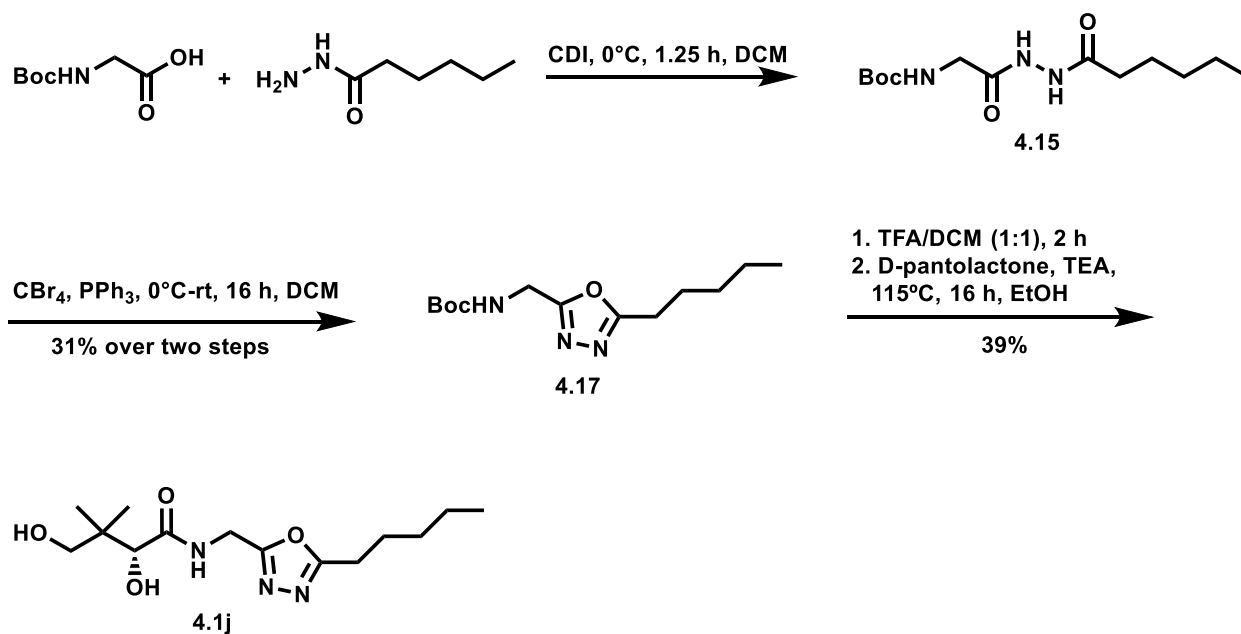
Scheme 4.6. Synthesis of compound **4.1h**. TEA: triethylamine; TFA: trifluoroacetic acid.

1,3,4-Thiadiazole **4.1i** was synthesized in three steps as shown in Scheme 4.7. First, *N*-Boc glycine was coupled to hexanoic acid hydrazide in the presence of 2-ethoxy-1-ethoxycarbonyl-1,2-dihydroquinoline to produce **4.15**. Next, compound **4.15** was thiated by the Lawesson's reagent and cyclized at the same time to generate the 1,3,4-thiadiazole **4.16**.¹⁶² Lastly, Boc-deprotection and D-pantolactone ring opening gave **4.1i**.



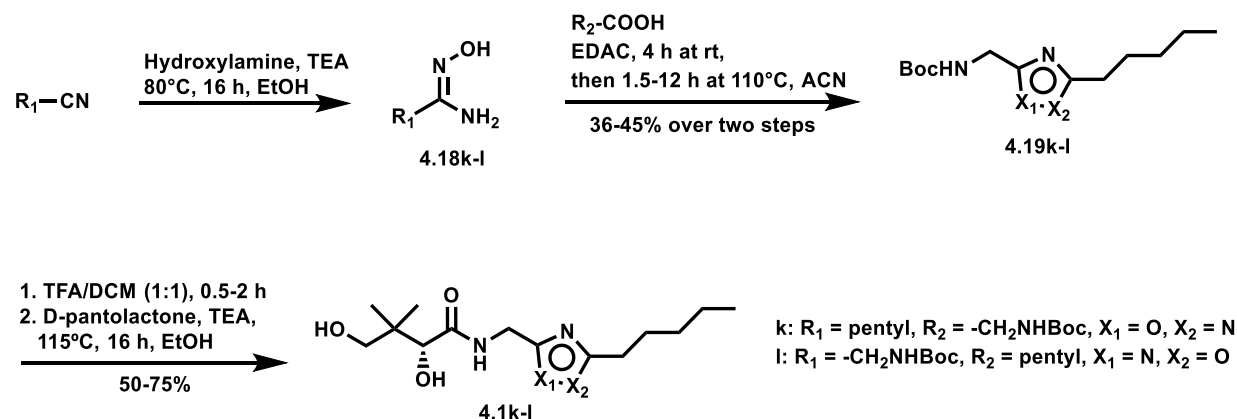
Scheme 4.7. Synthesis of compound **4.1i**. EEDQ: 2-ethoxy-1-ethoxycarbonyl-1,2-dihydroquinoline; TEA: triethylamine; TFA: trifluoroacetic acid.

The synthesis of 1,3,4-oxadiazole **4.1j** (Scheme 4.8) is similar to the one for thiadiazole **4.1i**. The first step was the coupling of *N*-Boc glycine and hexanoic acid hydrazide to yield **4.15**, which was cyclized directly into the 1,3,4-oxadiazole **4.17** in the presence of CBr_4 and PPh_3 . The last step was Boc-deprotection of compound **4.17**, followed by condensation with D-pantolactone.



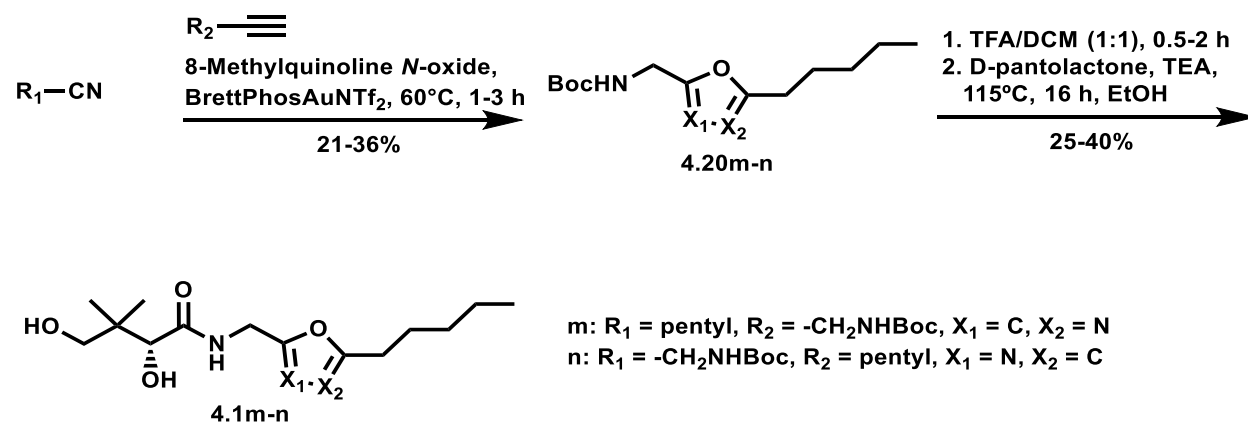
Scheme 4.8. Synthesis of compound **4.1j**. CDI: carbonyldiimidazole; TEA: triethylamine; TFA: trifluoroacetic acid.

Compounds **4.1k-l** have the orientation of the ring reversed compared to each other. They were prepared via a similar synthetic route (Scheme 4.9). The first step involved the generation of **4.18k-l** by reacting the desired nitrile with hydroxylamine. Compounds **4.18k-l** were next condensed with their desired carboxylic acid in the presence of 1-ethyl-3-(3-dimethylaminopropyl)carbodiimide, forming the 1,2,4-oxadiazoles **4.19k-l**. Finally, compounds **4.19k-l** were Boc-protected, followed by D-pantolactone ring-opening to generate the desired products **4.1k-l**.



Scheme 4.9. Synthesis of compounds **4.1k-l**. EDAC: *N*-(3-dimethylaminopropyl)-*N'*-ethylcarbodiimide hydrochloride; TEA: triethylamine; TFA: trifluoroacetic acid.

Oxazoles **4.1m-n** were prepared in three steps (Scheme 4.10). The first step was a [2+2+1] annulation between a terminal alkyne, a nitrile and an oxygen atom from the oxidant 8-methylquinoline *N*-oxide, catalyzed by BrettPhosAuNTf₂.¹⁶³ The last two steps were the Boc-deprotection and D-pantolactone ring-opening.



Scheme 4.10. Synthesis of compounds **4.1m-n**. TEA: triethylamine; TFA: trifluoroacetic acid.

4.4 Antiplasmodial studies

4.4.1 Antiplasmodial activity of compounds 4.1a-n

The synthesized compounds **4.1a-n** were next evaluated for their antiplasmodial activity. As shown in Table 4.1, isoxazoles **4.1e-f** and thiadiazole **4.1i** show IC_{50} values in the nanomolar range, with the most potent **4.1f** only ca. 3-fold less active than the hit compound **3.1**.

Table 4.1. Effect of compounds **4.1a-n** on the proliferation of erythrocytic *P. falciparum* in growth medium containing 1 μ M pantothenate *in the presence of pantetheinases*. IC_{50} s values that are in the nanomolar range are shown in red.

Name	Structure	IC_{50} (μ M)	Name	Structure	IC_{50} (μ M)
3.1		$IC_{50} = 0.056 \pm 0.005 \mu\text{M}^{146}$			
4.1a		7.4 ± 0.3	4.1h		40 ± 3
4.1b		14 ± 1	4.1i		0.95 ± 0.05
4.1c		34 ± 9	4.1j		71 ± 4
4.1d		> 100	4.1k		5.3 ± 0.6
4.1e		0.65 ± 0.05	4.1l		1.8 ± 0.1
4.1f		0.16 ± 0.01	4.1m		80 ± 9
4.1g		28 ± 1	4.1n		23 ± 1

Interestingly, replacing each of the different ring N atoms (positions X₁, X₂ or X₃, Scheme 4.1) of compound **3.1** with a C atom leads to a significant drop in activity, as shown by the IC₅₀ values of compounds **4.1a-c**. This reveals the importance of all these N atoms at the positions of X₁, X₂ or X₃. Besides, based on the comparison between **4.1e-f** and **4.1a**, replacing the N atoms with O atoms at positions X₂ and X₃ is beneficial. This superiority of N or O atom over C atoms at positions X₂ and X₃ is likely explained by they being better H bond acceptors, and suggests important H bond interactions with the target(s).

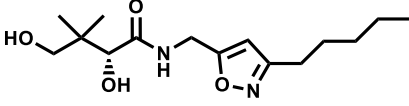
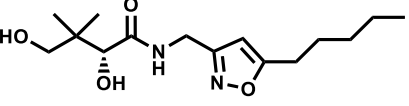
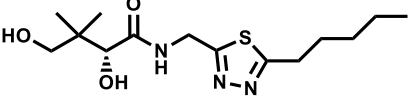
Conversely, at position X₄, a C atom or a S atom is superior over a O atom or N atom (Scheme 4.1). As in compounds **4.1k-l**, switching the C to a N atom, decreased the activity by 10-fold, compared to compounds **4.1e-f**. This preference for a C atom over a N atom at position X₄ is also supported by the better activity of **4.1a** over that of **4.1h**, and of **4.1b** over that of **4.1d**. The preference for a S atom at position X₄ can be drawn by comparing compound **4.1i** with compounds **4.1a,h,j**. It is worth noting that although compounds **4.1a** and **4.1i** have the less electronegative S or C atom at position X₄ and the same N atoms at positions X₂ and X₃, compound **4.1i** is a much better *P. falciparum* growth inhibitor. The poorer antiplasmodial activity of **4.1a** might be due to the extra hydrogen atom at X₂ (or X₃, due to tautomerism) position. In contrast, the larger size of the thiadiazole ring in compound **4.1i**,¹⁶⁴ may force the two N atoms closer to the target(s), leading to stronger H bond interactions and more potent antiplasmodial activity. Besides, the poor tolerance of an O atom at position X₄ can be indicated from the high IC₅₀ values of compounds **4j,m,n**.

4.4.2 Antiplasmodial studies to verify the utilization of CoA biosynthetic pathway by compounds 4.1e,f,i

In order to verify whether compounds **4.1e,f,i** exert their antiplasmodial activity by the same mechanism as that of pantothenamides and compound **3.1**, their antiplasmodial activity were tested in the presence of excess pantothenate (100 μM). As shown in Table 4.2, the dramatic loss of activity (IC₅₀ values increase 10-fold) confirms that as pantothenamides and compound **3.1**, the three new compounds **4.1e,f,i** compete with

pantothenate as the substrates of PanK and may thus be transformed by the CoA biosynthetic enzymes.¹⁴⁶

Table 4.2. *In vitro* antiplasmodial activity of compounds **4.1e-f** and **4.1i** in growth medium containing 1 or 100 μM pantothenate in the presence of pantetheinases.

Name	Structure	IC ₅₀ (μM) with 1 μM pantothenate	IC ₅₀ (μM) with 100 μM pantothenate
4.1e		0.65 \pm 0.05	> 10
4.1f		0.16 \pm 0.01	> 1
4.1i		0.95 \pm 0.05	26 \pm 4

4.5 Discussion

Not all the heteroaromatic rings as presented in compounds **4.1a-n** can be amide bioisosteres, since some of them, such as the oxadiazoles in compounds **4.1j-l**, are apparently missing the hydrogen atom to mimic the N-H of amide bond. However, it is interesting to find that the best three *P. falciparum* growth inhibitors of our 14 compounds, **4.1e,f,i**, are the ones who can better mimic the flipped pantothenamide analogue **3.15**, as shown in Figure 4.2. It is believed that N-2 of **4.1e** and O-1 of **4.1f** may mimic the carbonyl oxygen of **3.15**, while H-4 of both **4.1e** and **4.1f** may mimic the N-H of **3.15**. Compound **4.1i** is a little bit special. Its N-3 may mimic the carbonyl oxygen of **3.15**, while it does not have a hydrogen atom on its thiadiazole ring. However, the low-lying σ^* orbital of the C-S bond is known to interact with electron donors.¹⁶⁵ It is greatly possible that the σ^* orbital of the C-S bond in **4.1i** surrogates the role of a H to mimic the interactions that N-H of **3.15** could have. The preference of the heteroaromatic rings that are probably

good mimics of the flipped pantothenamide analogue **3.15** correlates well with our findings that 1) at position X₁, a N atom is preferred, 2) at positions X₂ and X₃, a N or O atom is preferred, and 3) at position X₄, a C or S atom is preferred. After all, a N or O atom at positions X₂ can mimic the carbonyl oxygen of the amide to be electron donors, and a C or S atom at position X₄ allows for the possibility to mimic the N-H of the amide to be electron acceptors. Moreover, this preference suggests the essentiality of the N or O atom at positions X₂ and of the C or S atom at position X₄, for the optimal antiplasmodial activity.

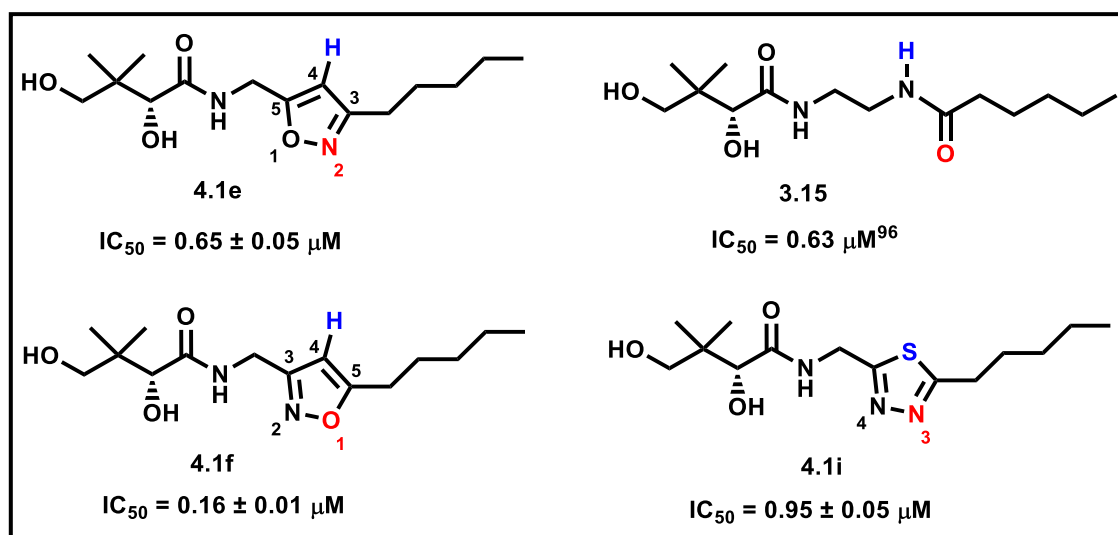


Figure 4.2. The isoxazole ring of **4.1e,f** and the thiadiazole ring of **4.1i** may mimic the amide bond of **3.15**. The red highlights the electron donors, and the blue highlights the electron acceptors.

4.6 Closing remarks

Overall, a detailed SAR study focusing on the heteroaromatic ring was conducted in this chapter. It was observed that the triazole ring in compound **3.1** can be replaced with an appropriately substituted isoxazole or thiadiazole without a large activity loss. Our results suggest that a N atom at position X₁, a N or O atom at positions X₂ and X₃, and a C or S atom at position X₄ are optimal for antiplasmodial activity.

Triazole, isoxazole and thiadiazole rings are among the most commonly used scaffolds in drugs.¹⁶⁶ Although triazoles and isoxazoles have been commonly used as amide bioisosteres in our current drug discovery, thiadiazole is seldom used as an amide bioisostere. Our results revealed the similar antiplasmodial activity of thiadiazole derivative **4.1i** with that of the triazole derivative **3.1**, suggesting that at least in some cases thiadiazole can also be a good amide bioisostere. This helps expand the arsenal of functional groups available to medicinal chemists.

The rapid emergence of antimalarial drug resistance has called for improved malarial treatments, such as novel antimalarials and antimalarial targets. The isoxazole derivatives **4.1e-f** and thiadiazole derivative **4.1i** reported in this chapter all show excellent antiplasmodial activity, and possibly act via interfering with the CoA-utilizing pathways in *P. falciparum* after bioactivation by the CoA biosynthetic pathway.¹⁰⁶⁻¹⁰⁹ It is envisaged that their new mode of action compared to clinical drugs makes them resistant towards the current known mechanisms of resistance. Moreover, since they might have more than one targets in *P. falciparum*, development of resistance may be slow. Thus, coupled with their straightforward synthesis, they should be attractive hits for the development of novel antimalarials. Besides, the potent inhibition of *P. falciparum* growth by compounds **3.1**, **4.1e-f** and **4.1i** demonstrates that the utilization of pantothenate is a valid target for antimalarial drug discovery.

Utilization of the CoA biosynthetic pathway by pantothenamides and their analogues, such as **3.1**, **4.1e-f** and **4.1i**, to generate active inhibitors *in situ* in *P. falciparum* is a unique strategy, which circumvents selectivity and absorption problems that may arise with active inhibitors. Indeed, with several negative charges, CoA derivatives may not enter *P. falciparum*. The demonstration here that one can take advantage of the CoA biosynthetic pathway to generate CoA derivatives *in vivo* suggests that it may be possible to revisit “old” drug candidates from a new perspective. One example will be shown in chapter 6.

Chapter 5

Ligand preference for the three types of bacterial pantothenate kinase

5.1 Preface

In this chapter, a series of pantothenate analogues was synthesized using convenient synthetic methodologies. The compounds were exploited as small organic probes to compare the ligand preference of the three different types of bacterial PanK. Overall, several new inhibitors and substrates were identified for each type of PanK. This work is to be submitted for publication.

Guan, J.; Barnard, L.; Cresson, J.; Hoegl, A.; Chang, J. H.; Strauss, E.; Auclair, K., Ligand preference for the three types of bacterial pantothenate kinase, submitted for publication.

Of the 24 final compounds mentioned in this chapter, 20 compounds were synthesized by the author of this thesis. Four of them, compounds **5.9a,c,d,e** were synthesized by an exchanging student, Jeanne Cresson with the help of the author. One compound, **3.1**, was synthesized by a previous group member of Auclair lab, Annabelle Hoegl. One compound, **5.11**, was synthesized by a previous group member of Auclair lab, Justin H. Chang. The enzyme assays with *P. aeruginosa* pantothenate kinase (*PaPanK*) and *EcPanK*, and the antibacterial study were performed by the author of the thesis. The *SaPanK* assays were performed by Leanne Barnard from the lab of Prof. Strauss at Stellenbosch University.

5.2 Introduction

Antibacterial resistance is growing to become a severe health threat in all parts of the world.^{15, 167} To address this global crisis, identifying new antibacterial targets and developing novel antibacterial agents are indispensable.¹⁵ CoA is an essential cofactor for all living organisms. It participates in over 100 different reactions in metabolic processes such as the tricarboxylic acid cycle, lipid biosynthesis and catabolism, and amino acid biosynthesis.²⁵ Pantothenate, also known as vitamin B₅, is the main precursor for CoA biosynthesis. Its ATP-dependent phosphorylation to produce 4'-phosphopantothenate is catalyzed by PanK, and is the first and committed step of the universal CoA biosynthetic pathway.²⁶ This is followed by four additional steps to finally produce CoA.²⁵⁻²⁶ The CoA biosynthetic steps are conserved across all kingdoms, but the

structure and mechanism of the enzymes involved vary significantly. The utilization of pantothenate has therefore been suggested as a novel target for antimicrobial development.⁸⁷⁻⁸⁸

Since the discovery of pantothenate (Figure 5.1) by Williams *et al.* in 1933,¹²⁵ many pantothenate antimetabolites have been reported to inhibit the growth of *E. coli* and *S. aureus*.⁸⁷ Of these, pantothenamides are arguably the most studied.⁸⁷⁻⁸⁸ It is found that their mechanism of action largely depends on the PanK type found in the bacterium. For bacteria harboring type I PanK, such as *E. coli*, pantothenamides are believed to impede growth after being transformed by the CoA biosynthetic enzymes,^{95, 102-105} and interfering with a series of essential CoA-related pathways. For bacteria expressing a type II PanK, like *S. aureus*, different mechanisms of action of pantothenamides have been suggested.^{46, 93, 95, 97-99} The current accepted one suggests that the inhibitory effects of pantothenamides mainly result from the PanK-catalyzed transformation into 4'-phosphopantothenamides, which in turn inhibit PanK.⁹⁷⁻⁹⁹ Pantothenamides are however not lethal to bacteria producing only a type III PanK such as *Pseudomonas* spp., *Clostridium* spp., *Neisseria* spp., or *Helicobacter* spp, because their longer "tails" compared with pantothenate prevent them from binding to type III PanK either as substrates or inhibitors.

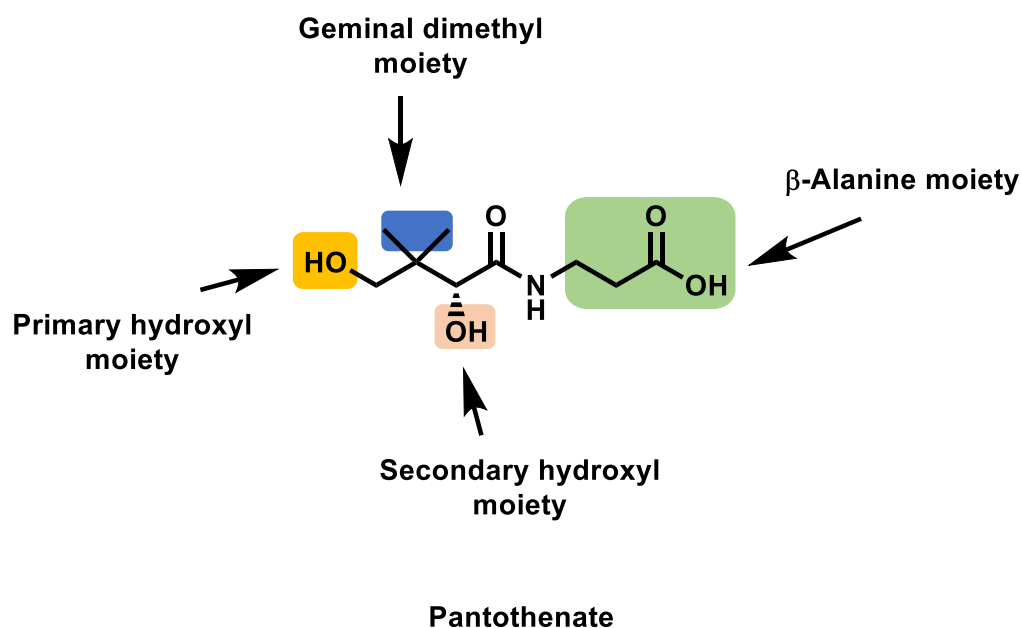


Figure 5.1. Pantothenate structure and sites of modification discussed in chapter 5.

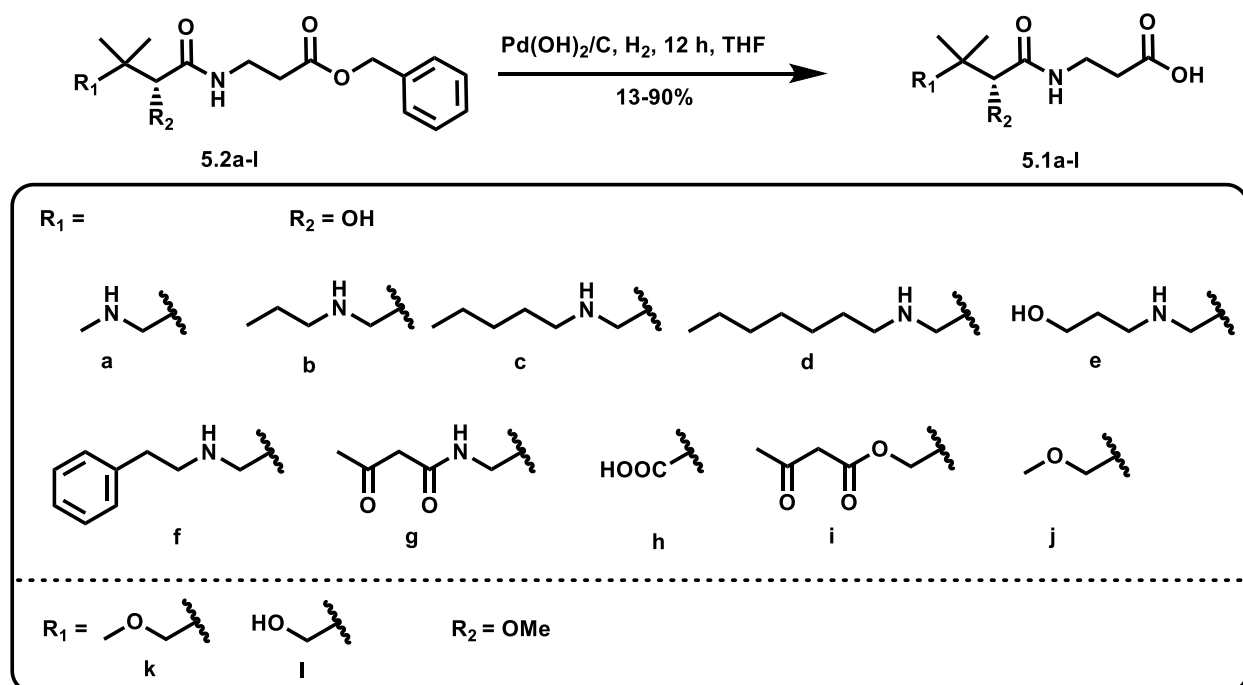
Besides pantothenate antimetabolites, many inhibitors have also been reported for type I and II PanKs.^{89-91, 95, 97, 99} In contrast, only one ATP mimic is published as a type III *BaPanK* inhibitor with a K_i of $164 \pm 3 \mu\text{M}$ (a 3-fold improvement relative to the K_m of ATP which is $510 \mu\text{M}$).¹⁰¹ No bacterial growth inhibition was reported for this compound. The design of novel pantothenate antimetabolites and pantothenate-related PanK inhibitors can benefit from a better understanding of ligand preference for all three types of PanK. Therefore, new pantothenate analogues and their use as probes to study the specificity of the pantothenate binding pockets of the type I, II and III PanKs are discussed in this chapter. Studying the ATP binding pockets is not pursued, because type III PanKs show poor affinity for ATP (K_m is in millimolar range), and the concern of ending up with inhibitors hitting any ATP-dependent enzymes.

It is easy to know how ligands bind and interact with their targets based on crystal structures. However, the contribution of each binding interaction to the total binding affinity of the ligand is usually hard to be accurately predicted, while knowing this is helpful to guide the design/optimization of drug candidates. Therefore, using small molecules to probe the binding pockets of enzymes are good addition of the crystal structures. In our

case, the probes presented in this chapter can be categorized into four classes, depending where the modification is located (Figure 5.1): 1) the primary hydroxyl group; 2) the secondary hydroxyl group; 3) the geminal-dimethyl group; and 4) the β -alanine moiety.

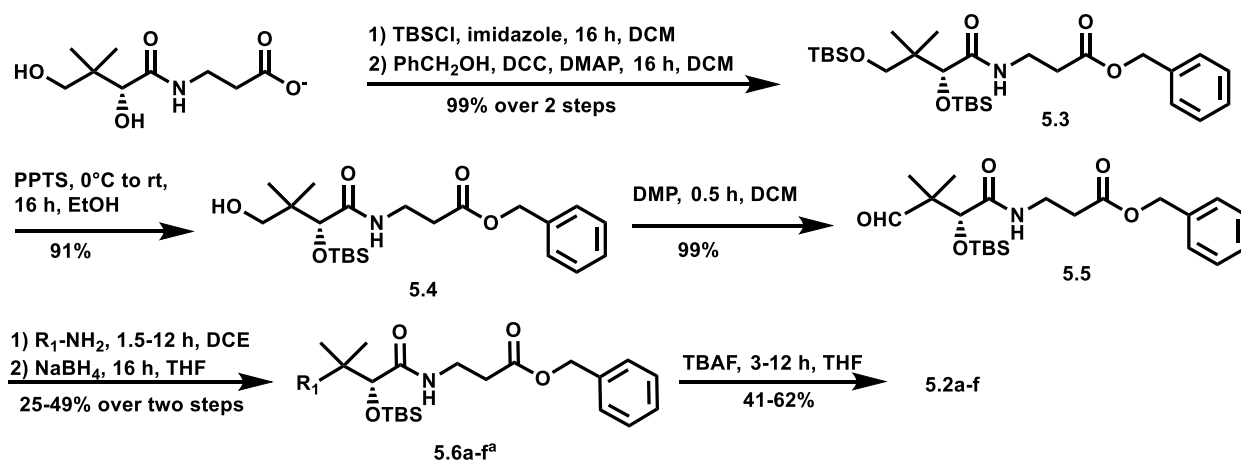
5.3 Synthesis

As shown in Scheme 5.1, pantothenate analogues **5.1a-j** are modified at the primary hydroxyl group of pantothenate. Their different substituents at R_1 including a diversity of hydrophilic, hydrophobic, aliphatic, aromatic, positively charged (e.g. amines), negatively charged (e.g. carboxylate) and neutral (e.g. ether) residues, are to study the nearby binding pocket. Compounds **5.1k-l** have their secondary hydroxyl group blocked with a methyl group, for the purpose of exploring the importance of the hydrogen bond interactions/nearby space. Compounds **5.1a-l** were all prepared from intermediates **5.2a-l** via benzyl deprotection in the presence of $\text{Pd}(\text{OH})_2/\text{C}$.

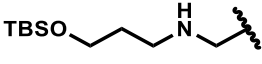


Scheme 5.1. Synthesis of compounds **5.1a-l**.

Commercial D-pantothenate was used as a starting material to synthesize compounds **5.2a-f** (Scheme 5.2). The two hydroxyl groups of pantothenate were first protected each with a TBS group, before protection of the carboxylate as a benzyl ester to generate compound **5.3**. Next, 1.1 equivalent of pyridium *p*-toluenesulfonate was used to selectively deprotect the TBS group on the primary hydroxyl group and yield compound **5.4**. Subsequent oxidation with Dess-Martin periodinane produced aldehyde **5.5**. To produce the amines **5.6a-f**, aldehyde **5.5** was condensed with the desired amine, followed by sodium borohydride reduction. Compounds **5.2a-f** were isolated after tetrabutylammonium fluoride mediated TBS-deprotection of **5.6a-f**.

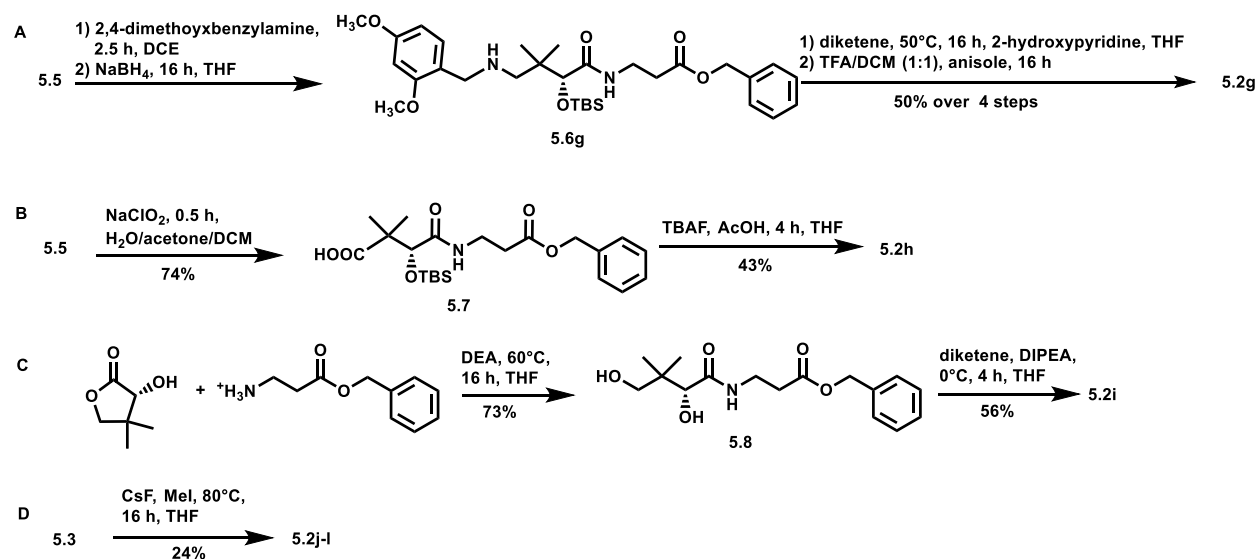


Scheme 5.2. Synthesis of compounds **5.2a-f**. ^aR₁ is same as in Scheme 5.1, except for compound

5.6e, in which R₁ is . DCC: dicyclohexylcarbodiimide; DMAP: 4-(dimethylamino)pyridine; DMP: Dess-Martin periodinane; PPTS: pyridium *p*-toluenesulfonate; TBAF: tetrabutylammonium fluoride; TBSCl: *tert*-butyldimethylsilyl chloride.

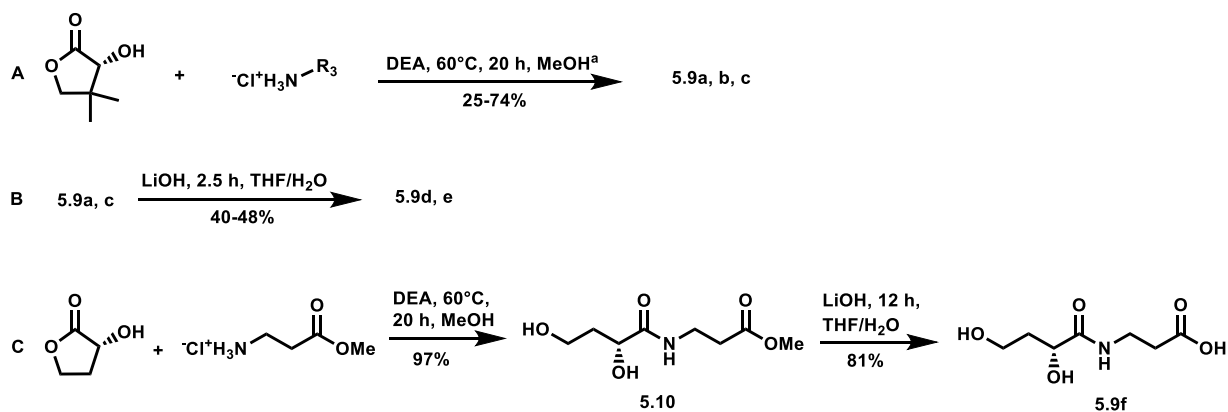
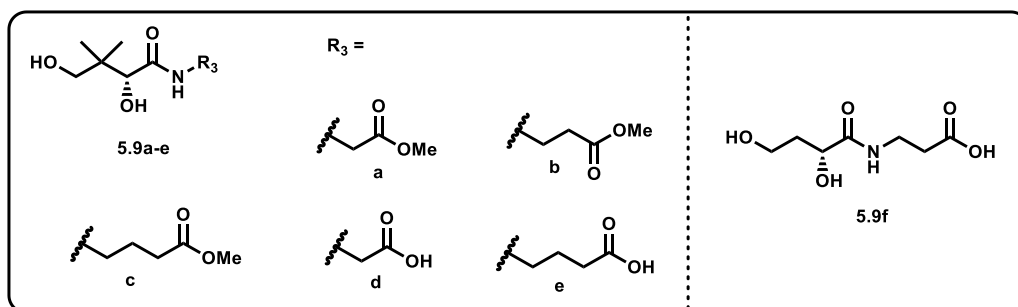
Compound **5.2g** was also generated via reductive amination with aldehyde **5.5**, but followed with ring opening of diketene in the presence of 2-hydroxypyridine, and full deprotection in one pot using trifluoroacetic acid (Scheme 5.3A). To synthesize the carboxylate **5.2h**, aldehyde **5.5** was oxidized to compound **5.7** by Pinnick oxidation (Scheme 5.3B), followed by TBS deprotection using tetrabutylammonium fluoride.

Synthesis of **5.2i** started with the condensation of D-pantolactone and β -alanine benzyl ester 4-toluenesulfonate in the presence of diethylamine at 60°C, to produce compound **5.8** (Scheme 5.3C). This compound was next used as a nucleophile to open the ring of diketene and generate **5.2i**. Compounds **5.2j-i** were prepared from compound **5.3**. Both TBS groups of compound **5.3** were first removed using cesium fluoride, generating the negatively charged alkoxides, to which methyl iodide was added in situ to form **5.2j-i** in one batch (Scheme 5.3D).



Scheme 5.3. Synthesis of compounds **5.2g-i**. ^aR₁ is same as in Scheme 5.1. DEA: diethylamine; DIPEA: *N,N*-diisopropylethylamine; TBAF: tetrabutylammonium fluoride; TFA: trifluoroacetic acid.

Compounds modified at the β -alanine moiety with small substituents (**5.9a-e**) or at the geminal-dimethyl group (**5.9f**) were next synthesized. As shown in Scheme 5.4, methyl esters **5.9a-c** and **5.10** were prepared directly from commercial lactones via ring opening by the desired amine. Hydrolysis of **5.9a,c** and **5.10** separately with lithium hydroxide quickly generated compounds **5.9d,e** and **5.9f**.



Scheme 5.4. Synthesis of compounds **5.9a-f**. ^aOr at 115°C for 2 hours in a microwave reactor. DEA: diethylamine.

Compounds modified at the β -alanine moiety with larger substituents, as in **3.1**, **3.7a,b,c**, **3.13a**, and **5.11** (Figure 5.2) were also prepared, as reported in chapter 3 or as published.¹⁴³ These pantothenamide analogues containing a triazole ring and altering in their pantooyl-to-triazole linkers, were aimed to study the type I and II PanKs, since it is known that type III PanKs can't accept the large "tails" of pantothenamides.

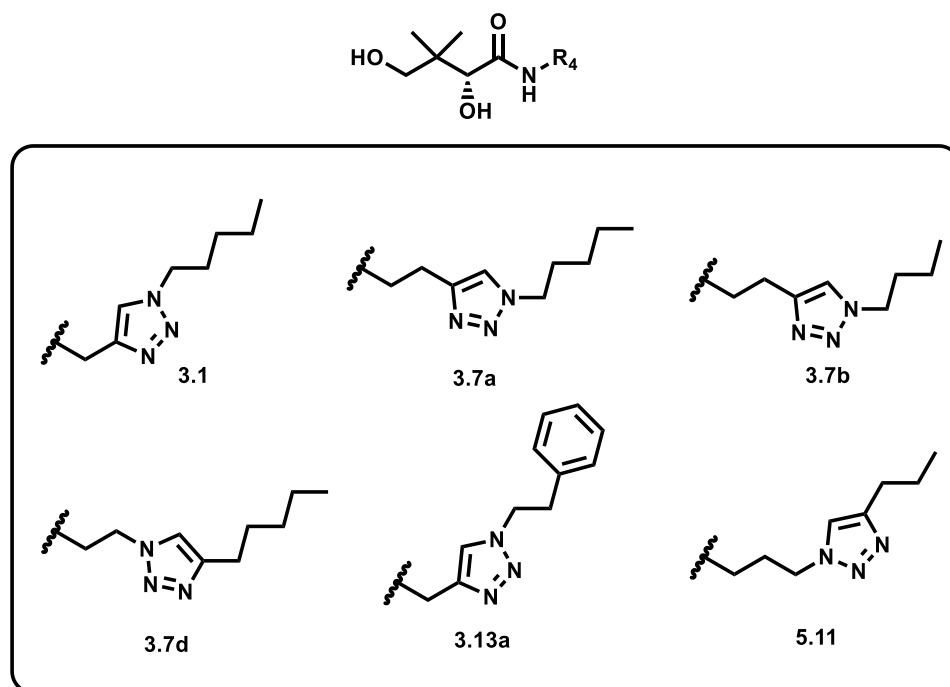


Figure 5.2. Pantothenamides containing the triazole ring.

5.4 Enzymatic studies

For enzymatic studies, *EcPanK* and *PaPanK* were selected as representatives of type I and type III PanKs. *SaPanK*, the only known type II bacterial PanK, was used here as an example of a type II PanK. Compared to pantothenate, the primary hydroxyl group of compounds **5.1a-d**, **5.1f-k** is blocked. It was therefore envisaged that they could only inhibit PanK, but not act as substrates. These compounds were screened for inhibition of the PanK enzymes at 200 μ M. As shown in Figure 5.3, compound **5.1g** exhibits weak inhibition of all three PanK isoforms. We propose that the acetoacetamide moiety of **5.1g** may mimic the polar diphosphate group of ATP, in the ternary complex or the transition state. The acetoacetate group has previously been shown to mimic diphosphate moiety.¹⁶⁸ For *EcPanK*, compounds **5.1c,f,j** also show some inhibition, and **5.1a** to a lesser extent, suggesting that this enzyme can tolerate either N or O at the primary alcohol position. In contrast, *PaPanK* seems to accommodate an amino group at this carbon (e.g. **5.1a**) better than an ether (e.g. **5.1j**). Interestingly, the diacid **5.1h** shows inhibition only for *SaPanK*. The crystal structure of *SaPanK* (PDB: 4M7Y) doesn't reveal any positively

charged residue in the vicinity of this group, hence one or more H bonds may form between this carboxylate and the enzyme (either directly or via water molecules).

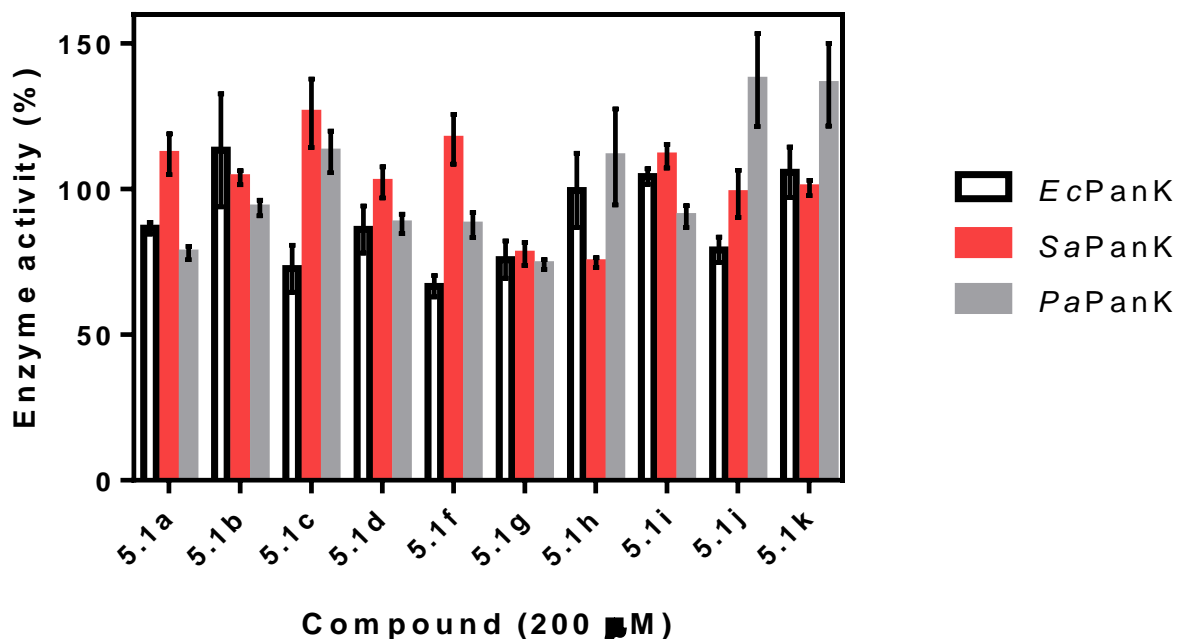


Figure 5.3. Inhibitory profiles of compounds **5.1a-d** and **5.1f-k**.

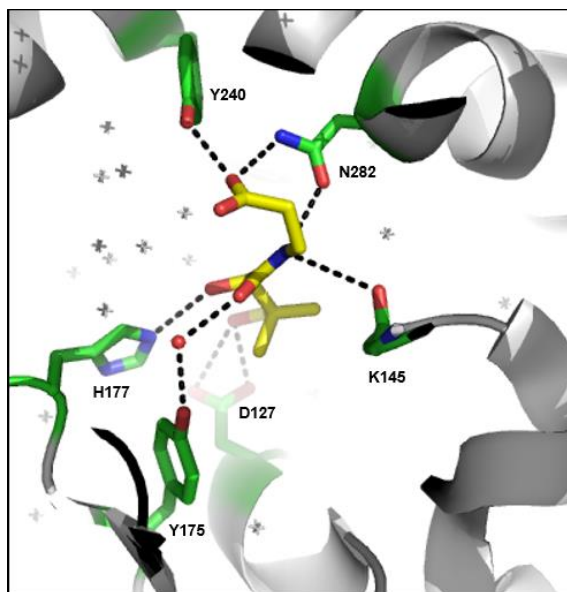
Next, compounds **5.1e,i**, **5.9a-f**, **3.1**, **3.7a,b,c**, **3.13a**, and **5.11** were tested as potential substrates or inhibitors of the PanK enzymes. None of them exhibits obvious inhibition at $\geq 100 \mu\text{M}$, and their activity as PanK substrates is summarized in Table 5.1. As shown, compound **5.1e** is not a substrate for any of the three PanKs. When the secondary hydroxyl group of pantothenate is blocked with a methyl substituent, as in **5.11**, the molecule is only accepted as the *EcPanK* substrate, with a K_m value similar to that of pantothenate, suggesting that the H bond between this hydroxyl group and His-177 (Figure 5.4A) is not contributing significantly to the binding affinity of pantothenate to *EcPanK*. In contrast, compound **5.11** is not a substrate for *SaPanK* or *PaPanK*. Based on the crystal structure of *SaPanK* (Figure 5.4B), there is no any H bond interaction between this secondary hydroxyl group and the *SaPanK*. The loss of activity might be caused by steric hindrance. As for *PaPanK*, since this secondary hydroxyl group forms H bonds with

the Asp-101 (Figure 5.4C), the loss of activity might be caused by the disturbance of the important H bonds and/or by the steric hindrance. Overall, the selectivity at this secondary hydroxyl group may allow the design of pantothenate antimetabolites/inhibitors selective for *EcPanK*.

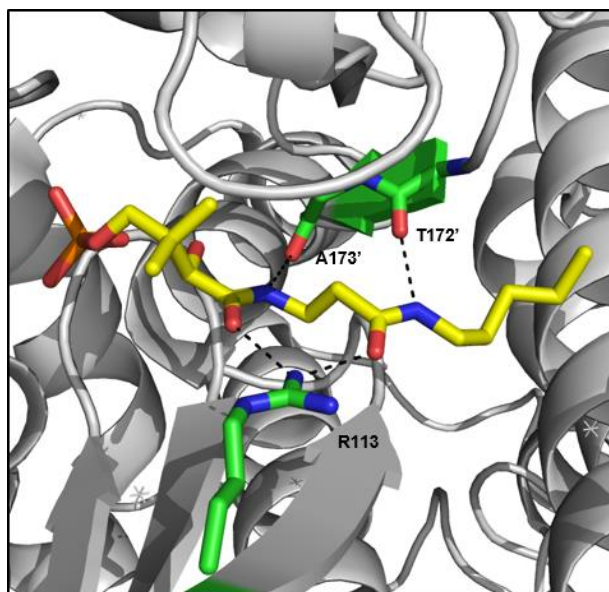
Table 5.1. Kinetic profiles of compounds **5.1e,l**, **5.9a-f**, **3.1**, **3.7a,b,c**, **3.13a**, and **5.11**. *EcPanK* and *PaPanK* data were fitted with the Michaelis-Menten equation, and the *SaPanK* data were fitted with the Hill equation with a floating n. ^aValue of $k_{cat}/K_{0.5}$ estimated from the linear slope ($v = k_{cat}/K_{0.5} \cdot [E] \cdot [S]$ when $[S] \ll K_{0.5}$). ns: not saturated at 200 μM .

Compound	<i>EcPanK</i>			<i>SaPanK</i>			<i>PaPanK</i>		
	K_m (μM)	k_{cat} (s^{-1})	k_{cat}/K_m ($\text{mM}^{-1} \cdot \text{s}^{-1}$)	$K_{0.5}$ (μM)	k_{cat} (s^{-1})	$k_{cat}/K_{0.5}$ ($\text{mM}^{-1} \cdot \text{s}^{-1}$)	K_m (μM)	k_{cat} (s^{-1})	k_{cat}/K_m ($\text{mM}^{-1} \cdot \text{s}^{-1}$)
Pantothenate	17 ± 1	1.29 ± 0.02	76 ± 5	19 ± 1	2.16 ± 0.05	115 ± 10	20 ± 5	0.39 ± 0.01	20 ± 5
N5-Pan	36 ± 3 ¹⁴³	0.93 ± 0.04 ¹⁴³	26 ± 2 ¹⁴³	< 1.58 ⁹⁵	0.44 ± 0.03 ⁹⁵	>290 ⁹⁵			
5.1e									
5.1l	16 ± 3	0.49 ± 0.02	31 ± 6						
5.9a	156 ± 26	0.91 ± 0.04	5.8 ± 1.0	35 ± 2	4.0 ± 0.1	115 ± 12			
5.9b	292 ± 65	0.80 ± 0.06	2.7 ± 0.6	ns	ns	8.3 ± 0.2 ^a			
5.9c				ns	ns	7.1 ± 0.2 ^a			
5.9d	62 ± 12	1.59 ± 0.07	26 ± 5						
5.9e				60 ± 2	3.4 ± 0.1	57 ± 3	683 ± 72	0.98 ± 0.04	1.4 ± 0.2
5.9f							64 ± 14	0.32 ± 0.02	5.0 ± 1.1
3.1	190 ± 20 ¹⁴³	0.96 ± 0.04 ¹⁴³	5.1 ± 0.6 ¹⁴³	64 ± 5	3.4 ± 0.1	54 ± 6			
3.7a	33 ± 5	0.72 ± 0.01	22 ± 3	6.8 ± 0.7	0.73 ± 0.04	107 ± 16			
3.7b	50 ± 8	1.08 ± 0.04	22 ± 4	7.1 ± 0.4	0.82 ± 0.02	115 ± 9			
3.7d	21 ± 5	1.11 ± 0.06	53 ± 13	8.5 ± 1.2	0.82 ± 0.05	97 ± 19			
3.13a	25 ± 3	1.09 ± 0.02	44 ± 5	126 ± 29	4.7 ± 0.5	37 ± 12			
5.11	1000 ± 200 ¹⁴³	0.49 ± 0.06 ¹⁴³	0.49 ± 0.11 ¹⁴³	369 ± 381	7.6 ± 4.3	21 ± 33			

A) *EcPanK*



B) *SaPanK*



C) *PaPanK*

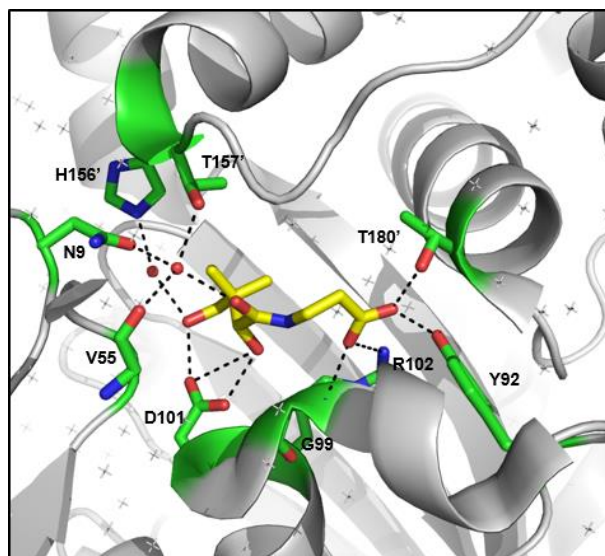


Figure 5.4. Crystal structures of PanKs. A) *EcPanK* in complexed with pantothenate (PDB: 1SQ5);¹⁶⁹ B) *SaPanK* in complexed with phosphorylated N5-Pan (PDB: 4M7Y);⁹⁹ C) *PaPanK* in complexed with pantothenate (PDB: 2F9W).³⁷

When modifications were introduced at the β -alanine moiety (as in compounds **5.9a-f**, **3.1**, **3.7a,b,c**, **3.13a**, and **5.11**), both *EcPanK* and *SaPanK* accept most of these molecules as substrates, while *PaPanK* does not. This was expected based on results with pantothenamides which are often tolerated by *EcPanK* and *SaPanK*, but not by *PaPanK*. A simple methylation of the carboxylate group of pantothenate (as in **5.9b**) is sufficient to decrease its affinity for *PaPanK* below detection, indicating that the H bonds between the terminal carboxylate group of pantothenate and residues Thr-180', Tyr-92, Arg-102 and Gly-99 (Figure 5.3B) contribute a large proportion of the binding affinity of pantothenate. Only the carboxylate **5.9e** is found to be a substrate for *PaPanK*, which might be explained by the flexibility of the three-carbon chain present in compound **5.9e** (compared to the two-carbon chain of pantothenate), allowing accommodation by the binding pocket without radically disturbing the interactions of the carboxylate end of pantothenate with *PaPanK*.

For *EcPanK*, both one- or two-carbon linkers between the amide and the carboxylate or triazole moiety are well tolerated, as demonstrated by compounds **5.9a,b,d**, **3.1**, **3.7a,b,d** and **3.13a**, which are all good *EcPanK* substrates. This is in an agreement with the studies reported earlier.^{95, 169-171} The compounds containing a three-carbon linker (**5.9c,e** and **5.11**) are however poorly or not accepted as substrates by *EcPanK*. This suggests that no matter what the terminal group is (e.g. a methyl ester in **5.9a-c**, a carboxylate in **5.9d-e**, or a triazole substituent in **3.1**, **3.7a,b,d**, **3.13a** and **5.11**), the linker length is determinant for binding affinity with *EcPanK*. Interestingly, *EcPanK*'s tolerance for methyl esters such as **5.9a,b** can be rationalized in light of the crystal structure of the pantothenate-*EcPanK* complex, which shows that only one oxygen in the carboxylate group of pantothenate is involved in the H bonds between this group, and residues Tyr-240 and Asn-282 (Figure 5.4A). In contrast, the crystal structure of the pantothenate-*PaPanK* complex suggests that both oxygen atoms of the carboxylate group of pantothenate participate in H bonds with the *PaPanK* (Figure 5.4C).

As for *SaPanK*, except for compound **5.9d**, the enzyme tolerates substrates with a one-, two-, or three-carbon linker (**5.9a-c**, **5.9e**, **3.1**, **3.7a,b,d**, **3.13a** and **5.11**), which suggests that *SaPanK* owns a relatively large and promiscuous binding pocket near the carboxylate

group of pantothenate. Besides, SaPanK may favor ligands with more hydrophobic moieties at the carboxylate end, as suggested by the fact that compound **5.9a** is a fairly good substrate while compound **5.9d** is not. It is worth noting that although the binding pockets of both *EcPanK* and *SaPanK* are promiscuous, our results demonstrate that it is possible to design pantothenate antimetabolites/inhibitors specific to either enzyme (e.g. compounds **5.9c** is specific for *SaPanK* and **5.9d** is for *EcPanK*).

Interestingly, when both geminal methyl groups of pantothenate were removed, as in compound **5.9f**, only *PaPanK* accepts the molecule as a substrate, although with some loss in affinity (three-fold higher K_m). This is consistent with the binding pocket of *PaPanK* being tight and more dependent on H bonding interactions than hydrophobic ones, while the opposite is observed for *EcPanK* and *SaPanK*. This result also implies that it may be possible to design *PaPanK*-specific pantothenate antimetabolites and/or inhibitors.

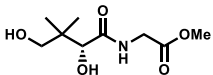
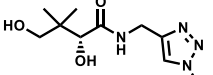
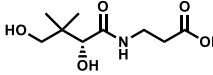
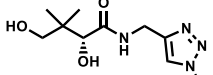
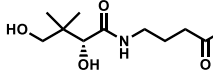
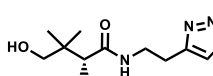
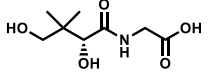
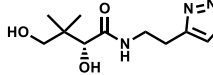
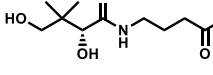
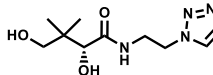
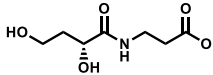
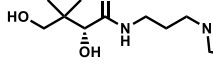
5.5 Antimicrobial studies

The antibacterial activity of compounds **5.1a-l**, **5.9a-f**, **3.1**, **3.7a,b,d**, **3.13a** and **5.11** towards *E. faecium*, *E. coli*, *S. aureus* and *P. aeruginosa* was next measured. Although no potent growth inhibitors were discovered (MIC > 200 μ M), the results with *S. aureus* are interesting.

In chapter 3, we have suggested that the triazole compounds with a two-carbon linker mimic pantothenamides well, while triazoles with a one-carbon linker mimic the flipped pantothenamides. Here, the most potent antistaphylococcal compounds are triazoles **3.7a,b,d** (two-carbon linker). In contrast, the triazoles **3.1** and **3.13a** (one-carbon linker) or **5.11** (three-carbon linker) show minimal growth inhibition (Table 5.2). This is consistent with the fact that pantothenamides have better antistaphylococcal activity than their corresponding flipped pantothenamides,⁹⁷ and hence supports our hypothesis as for how triazoles mimicking amide bonds in chapter 3. Moreover, as shown in Table 5.1, the K_m and k_{cat} of compounds **3.7a,b,d** are similar to those of N5-Pan,⁹⁷ it is possible that these triazoles are inhibiting the growth of *S. aureus* via the same mechanism as N5-Pan. The poorer antibacterial activity of triazoles **3.7a,b,d** compared to that of the corresponding

pantothenamides might be due to poorer inhibition of SaPankK, rapid efflux and/or poorer cell permeability.

Table 5.2. Antistaphylococcal activity of substrate-type pantothenate analogues **5.9a-f**, **3.1**, **3.7a,b,c**, **3.13a** and **5.11**. The values in bracket are the tested concentrations, in μM .

Name	Compound	Inhibition (%)	Name	Compound	Inhibition (%)
5.9a		84 (1000)	3.1		0 (860)
5.9b		15 (1000)	3.13a		2 (1540)
5.9c		16 (1000)	3.7a		86 (550)
5.9d		19 (1000)	3.7b		99 (860)
5.9e		88 (1000)	3.7d		72 (820)
5.9f		9 (1230)	5.11		0 (860)

Besides, compounds **5.9a,e** show better antistaphylococcal activity than **5.9b-d** and **5.9f** (Table 5.2). Since compounds **5.9a,e** are better SaPankK substrates than **5.9b-d** and **5.9f** (Table 5.1), their superior antistaphylococcal activity might be related to their superior ability as SaPankK substrates. It is possible that compounds **5.9a,e** are extended to CoA antimetabolites, which interfere downstream CoA-related pathways, leading to the toxic effects.

5.6 Closing remarks

Overall, a series of pantothenate analogues modified at different positions of pantothenate was synthesized with convenient synthetic methodology. Various substituents were introduced at the primary hydroxyl group, which led to a molecule, **5.1g**, able to inhibit all three PanK isoforms. Inhibitors specific for a single PanK type were also discovered: **5.1c,f,j** for *EcPanK* and **5.1h** for *SaPanK*. The preference for different compounds suggests that when modifications are introduced at the primary hydroxyl group of pantothenate, *SaPanK* might prefer negatively charged moieties. In contrast, *EcPanK* has no preference between nitrogen or oxygen at this position, and *PaPanK* prefers a nitrogen.

Modification at the secondary hydroxyl group of pantothenate allows to design antimetabolites/inhibitors selective for *EcPanK*. When the geminal methyl groups of pantothenate were replaced with hydrogen atoms, the interactions (largely hydrophobic) of the resulting molecule (**5.9f**) with both *EcPanK* and *SaPanK* are greatly affected, while the effect is small for *PaPanK*, allowing selectivity for *PaPanK*. Modification at the β -alanine moiety of pantothenate is a more versatile strategy to diversify activity and produce molecules that are specific for one type of PanK. Consistent with the crystal structures,^{37, 169} the kinetic profiles of these compounds imply that the pocket of *PaPanK* around the terminal carboxylate of pantothenate, is fairly tight, while that of *EcPanK* is somewhat promiscuous, and that of *SaPanK* is even more promiscuous.

In recent years, research has revealed the important role of the gut microbiome in health and disease. It is increasingly recognized that broad-spectrum antibacterial agents lead to severe imbalances of the normal gut microbiome, which is linked to various diseases,¹⁷² and even to secondary infections by *Clostridium difficile* (which harbors a type III PanK).¹⁷³ The advantages of narrow-spectrum antibacterials are evident.¹⁷⁴ The utilization of pantothenate has been suggested as a possible target for the development of new antimicrobials.⁸⁷⁻⁸⁸ As the rate-limiting enzyme in CoA biosynthetic pathway, PanK has attracted increasing interest in recent years. Our use of pantothenate analogues as probes to study the ligand preference of PanK suggests possible paths to design inhibitors or antimetabolites selective for one type of PanK.

Chapter 6

Cellular studies of an aminoglycoside potentiator reveal a new inhibitor of aminoglycoside resistance

6.1 Preface

In this chapter, a series of cellular studies of an aminoglycoside potentiator, **P-1b**, was performed. A new inhibitor of aminoglycoside resistance was discovered, suggesting that **P-1b** can be bioactivated into more than one aminoglycoside resistance inhibitors in *E. faecium*. This work has been submitted for publication.

Guan, J.; Vong, K.; Wee, K.; Fakhoury, J.; Dullaghan, E.; Auclair, K., Cellular studies of an aminoglycoside potentiator reveal a new inhibitor of aminoglycoside resistance, submitted for publication.

All the experiments were performed by the author of the thesis, except for the cytotoxicity study with HeLa cells, which was done by Dr. Johans Fakhoury from the lab of Prof. Sleiman at McGill University.

6.2 Introduction

Aminoglycosides are a group of highly potent, broad-spectrum antibiotics that consist of two or more modified amino-sugars. Since the first aminoglycoside – streptomycin was isolated from *Streptomyces griseus* in 1943, there has been more than 200 kinds of aminoglycosides discovered so far.¹⁷⁶ According to their chemical structures, they can be classified into two types: 1) aminoglycosides containing 2-dexoystreptamine (2-DOS), such as tobramycin; and 2) aminoglycosides without 2-DOS ring, for example, streptomycin (Figure 6.1).¹⁷⁶

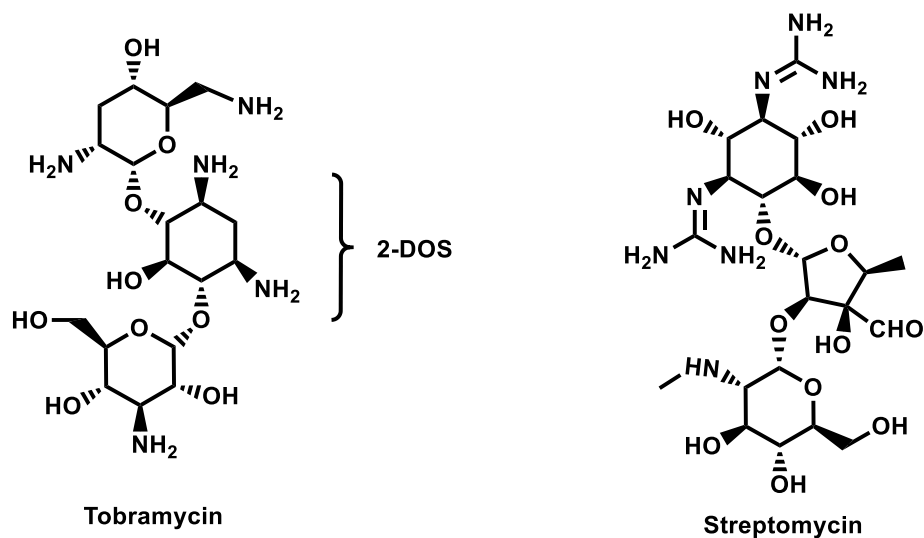


Figure 6.1. Examples of aminoglycosides.

Aminoglycosides have been used to treat serious infections caused by both Gram-positive and Gram-negative bacteria in a hospital setting.¹⁷⁶⁻¹⁷⁷ Their toxic effect on bacteria is mostly attributed to their binding to bacterial ribosomes, and causing infidelity during protein synthesis.¹⁷⁶⁻¹⁷⁷ As with all antibiotics, resistance to aminoglycosides has spread widely.¹⁷⁸ The most common mechanism of aminoglycoside resistance involves the production of aminoglycoside-modifying enzymes such as aminoglycoside *N*-acetyltransferases (AACs), aminoglycoside *O*-phosphotransferases (APHs) and aminoglycoside *O*-nucleotidyltransferases (ANTs).¹⁷⁹ The AAC family of enzymes is the largest one of the three, with over fifty AACs identified in various organisms.^{178, 180} They use acetyl-CoA to acetylate free amines at the 1, 3, 2' or 6' position of aminoglycosides, and are thus further classified as AAC(1), AAC(3), AAC(2') or AAC(6'), respectively (Figure 6.2).¹⁷⁷ Of these, AAC(6') is by far the most prevalent in clinical strains.¹⁷⁸ Some bacteria, such as the important human pathogen *E. faecium*, harbor an ACC(6')-coding gene on the chromosome which renders them intrinsically resistant to aminoglycosides.¹⁸¹

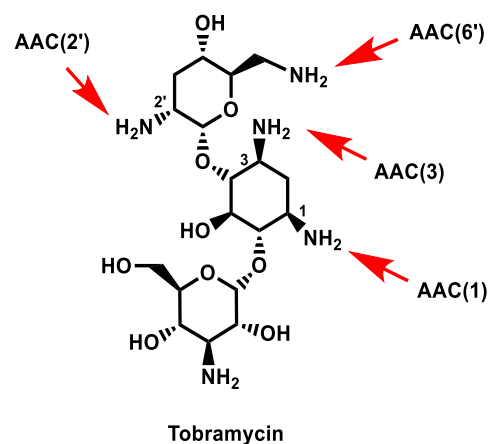


Figure 6.2. Susceptible sites for modification by different AACs, shown using tobramycin as an example.¹⁷⁷

To overcome aminoglycoside resistance, two strategies have been investigated by different labs: 1) modifying aminoglycosides to make them refractory to modification by resistance-causing enzymes while maintaining their potency;¹⁸⁰ and 2) blocking aminoglycoside resistance to give them a second life.¹⁸² Our lab has had interest in the latter,^{132, 168, 183-189} with compounds **I-1a-e** being promising AAC(6') inhibitors (Figure 6.3). In this series, the shorter the linker between the aminoglycoside and CoA moieties, the more potent the inhibitor.^{132, 183} Unfortunately, **I-1a-e** cannot penetrate bacterial cells and have no activity *in cellulo*. To address the permeability issue, a series of prodrugs, **P-1a-e** (Figure 6.3) was next reported.¹³² Prodrugs **P-1a-e** have no antibacterial activity of their own, do not inhibit ACC(6') significantly, but potentiate the activity of aminoglycosides against aminoglycoside-resistant *E. faecium* (due to the chromosomally-encoded *aac(6')*) (Table 6.1).¹³² To exert their potentiating effects, compounds **P-1a-e** were suggested to be bioactivated into compounds **I-1a-e** by three of the CoA biosynthetic enzymes, PanK, PPAT and DPCK. However, the *in vitro* studies using *E. coli* PanK, PPAT and DPCK revealed that although **P-1c-e** can be transformed into **I-1c-e** with high conversion, **P-1b** was poorly transformed into **I-1b**, and **P-1a** was not converted to **I-1a**. Therefore, the suggested mechanism of action for prodrugs **P-1a-e** cannot explain their potentiating effects perfectly. To better understand the mechanism of action of those prodrugs, a series of cellular studies with **P-1b** was performed in this chapter.

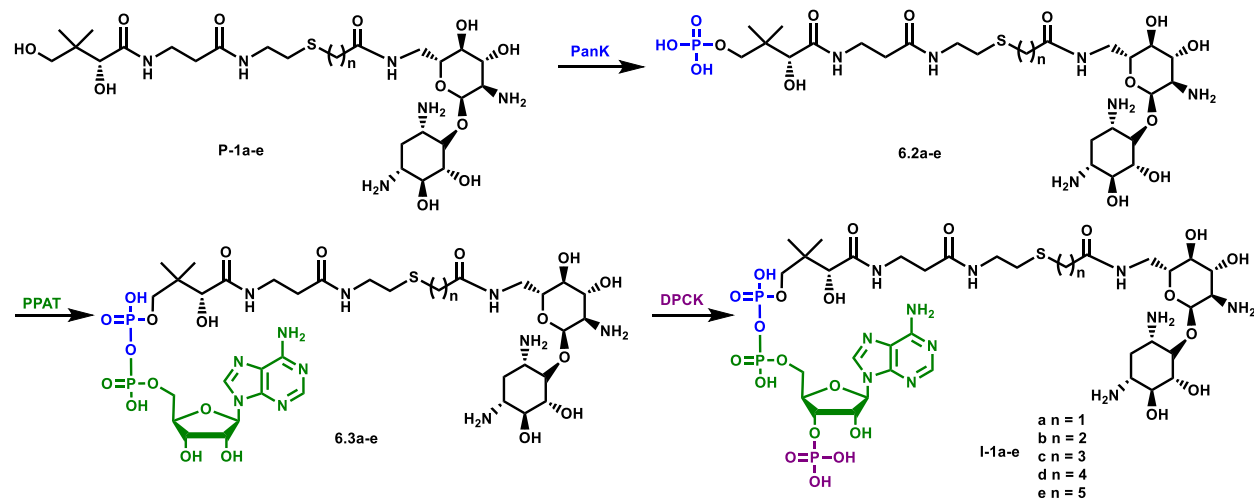


Figure 6.3. Proposed transformation of aminoglycoside potentiators **P-1a-e** to the corresponding AAC(6') inhibitors **I-1a-e** by enzymes of the CoA biosynthetic pathway.

Table 6.1. The potentiating effects of **P-1a-e** against different aminoglycosides at the concentration of 512 $\mu\text{g/mL}$. ^aFor *E. faecium* ATCC 19434, data from ref. 133.

Compound	ΔMIC_{50} ($\mu\text{g/mL}$) ^a		
	Tobramycin	Kanamycin A	Ribostamycin
P-1a	-10 \pm -18	0	-95 \pm -16
P-1b	-169 \pm -7	-51 \pm -5	-198 \pm -15
P-1c	-160 \pm -8	-46 \pm -5	-190 \pm -15
P-1d	-156 \pm -8	-53 \pm -6	-182 \pm -15
P-1e	-146 \pm -8	-54 \pm -6	-191 \pm -15

6.3 Cellular studies with *E. faecium*

6.3.1 Dose-response studies

Dose-response relationship of **P-1b** and tobramycin was first examined. As shown in Figure 6.4, the higher the concentration of **P-1b** used, the less tobramycin was required to inhibit the growth of *E. faecium*; and the higher the concentration of tobramycin, the less **P-1b** was required to achieve the same inhibitory effect. This phenotype is within expectation since more **P-1b** should lead to more AAC(6')-II inhibition in *E. faecium*, leaving the bacteria more sensitive to tobramycin and consequently requiring less tobramycin. Figure 6.4 also reveals that at 15 $\mu\text{g/mL}$ of tobramycin, which is a pharmaceutically-relevant concentration, the minimal concentration of **P-1b** required to obviously inhibit the *E. faecium* growth is 192 $\mu\text{g/mL}$.¹⁹⁰⁻¹⁹²

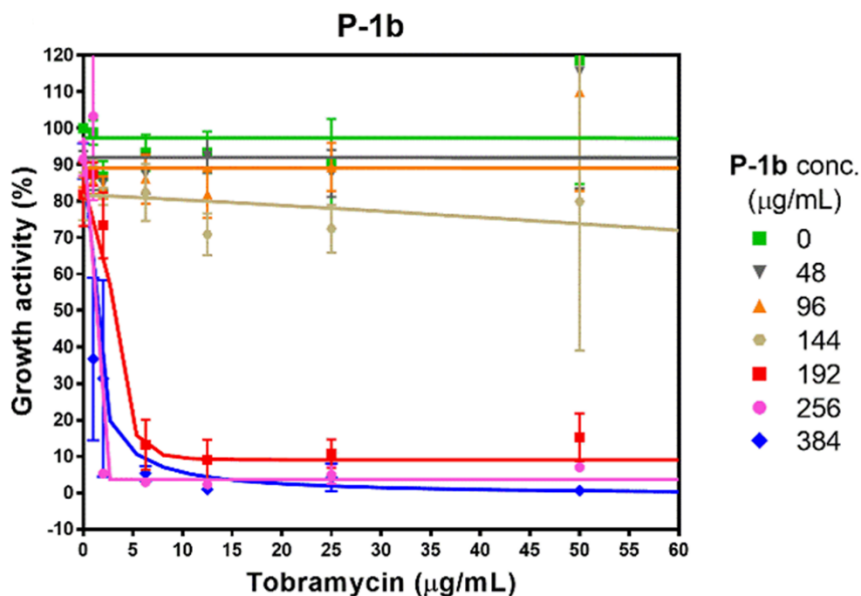


Figure 6.4. MIC plots reporting the antibacterial activity of tobramycin towards *E. faecium* at different concentrations of **P-1b**.

6.3.2 Time-kill studies

Knowing the dose-response relationship of **P-1b** and tobramycin, time-kill studies were next performed with an initial *E. faecium* culture of 10^5 CFU/mL. As shown in Figure 6.5, when no tobramycin nor **P-1b** was added to the growth medium, or only **P-1b** was added, *E. faecium* replicated exponentially and reached a 10^6 CFU/mL concentration within ~2 hours. In the presence of 100 $\mu\text{g/mL}$ tobramycin, *E. faecium* grew slower, taking 4–6 hours to reach the same cell density. In contrast, when both 384 $\mu\text{g/mL}$ **P-1b** and 25 $\mu\text{g/mL}$ tobramycin were added to the growth medium, *E. faecium* remained in static growth for ~8 hours. Finally, when the concentration of tobramycin in the medium was raised to 50 or 100 $\mu\text{g/mL}$ (and **P-1b** was kept at 384 $\mu\text{g/mL}$), the number of *E. faecium* CFU/mL decreased slowly over the first 8 hours. Because the drop in bacterial concentration is only ca. 20-fold, the combination of tobramycin and **P-1b** is considered bacteriostatic (drop less than 1000-fold), not bactericidal (drop more than 1000-fold).¹⁹²⁻¹⁹⁵ Interestingly, in the presence of this pair of molecules, the decrease of *E. faecium* concentration is dependent on the tobramycin concentration but not time, suggesting that the **P-1b**-tobramycin combination is concentration-dependent, as reported for aminoglycosides when used against sensitive bacterial strains.¹⁹⁴ More importantly, when comparing the time-kill curves for tobramycin with or without **P-1b**, it is interesting to note that at time 4 hours, the CFU/mL differs by almost 2 orders of magnitude, indicating that **P-1b** takes effect within four hours. Therefore, the 0-4 hour is a critical time window to study the *in cellulo* bioactivation of **P-1b**.

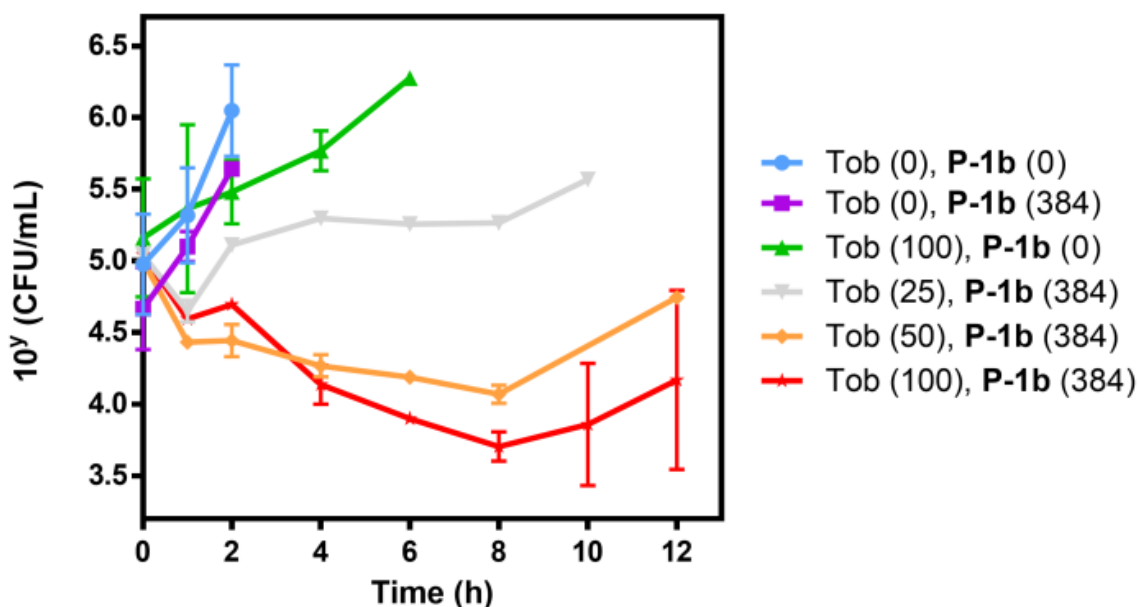


Figure 6.5. Time-kill curves of *E. faecium* in the presence of different concentrations of **P-1b** and tobramycin. Tob: tobramycin. The values in brackets in the legend are concentrations, in $\mu\text{g/mL}$.

6.3.3 Bioactivation of **P-1b** in *E. faecium*

To investigate the bioactivation of **P-1b** in *E. faecium*, 17×10^9 colonies of *E. faecium* were collected every hour after the addition of $384 \mu\text{g/mL}$ **P-1b** into the growth medium. The cells were lysed and the metabolites were extracted at 0°C , before LCMS analysis to quantify the cellular **P-1b**, **6.2b**, **6.3b** and **I-1b**. As shown in Figure 6.6, **P-1b** was quickly transformed by *E. faecium* into **6.2b** and **6.3b** within the first hour. The concentrations of **P-1b** and of **6.3b** were higher than that of **6.2b** for the entire experiment. This phenomenon is consistent with PanK being the rate-limiting enzyme in the CoA biosynthetic pathway. It is worth noting that all over the experiment, no inhibitor **I-1b** was detected (the limit of detection is 0.05 pmol), suggesting little to no **I-1b** was formed. This result is consistent with the previously reported *in vitro* study using purified *E. coli* enzymes (PanK, PPAT and DPCK) where **P-1b** was transformed into 10% **I-1b** + 20% **6.2b** + 70% **6.3b**.¹³² However, if it is the final product of the bioactivation pathway

(compound **I-1b**, Figure 6.3) that is the active molecule to inhibit AAC(6')-li, neither of these sets of data can explain the above-mentioned time-kill results which suggest that **P-1b** has taken effect within four hours, nor the potentiating effect of **P-1a** on the antibacterial activity of tobramycin and ribostamycin. Since **6.3b** was found to rapidly accumulate during the first five hours, it was envisaged that the potentiating effect observed might be attributed in large part to **6.3b**. Besides, no K_i values are reported for the inhibition of AAC(6')-li by **6.2b** or **6.3b**, however, K_i values are known for **P-1a** ($\geq 500 \mu\text{M}$), **6.2a** ($12 \mu\text{M}$), **I-1a** ($0.076 \mu\text{M}$) and **I-1b** ($0.043 \mu\text{M}$).^{132, 168, 183} This trend suggests that the AAC(6')-li inhibitory activity of **6.3a** might be somewhere in between those of **I-1a** and **6.2a**, and considering that the activity of **I-1b** is superior to that of **I-1a**, compound **6.3b** is expected to be a potent inhibitor of *E. faecium* AAC(6')-li.

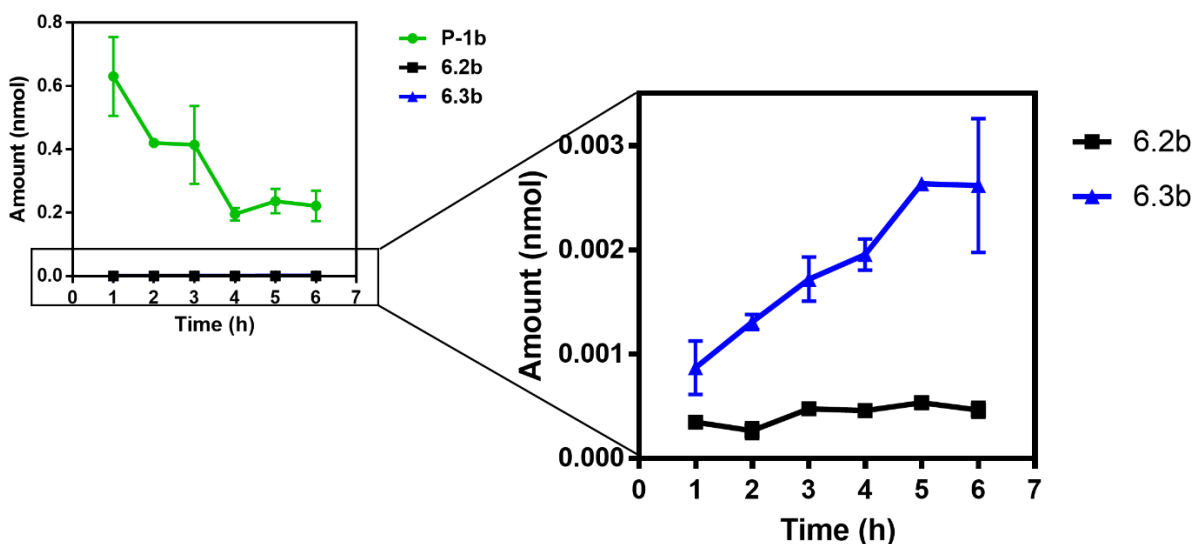
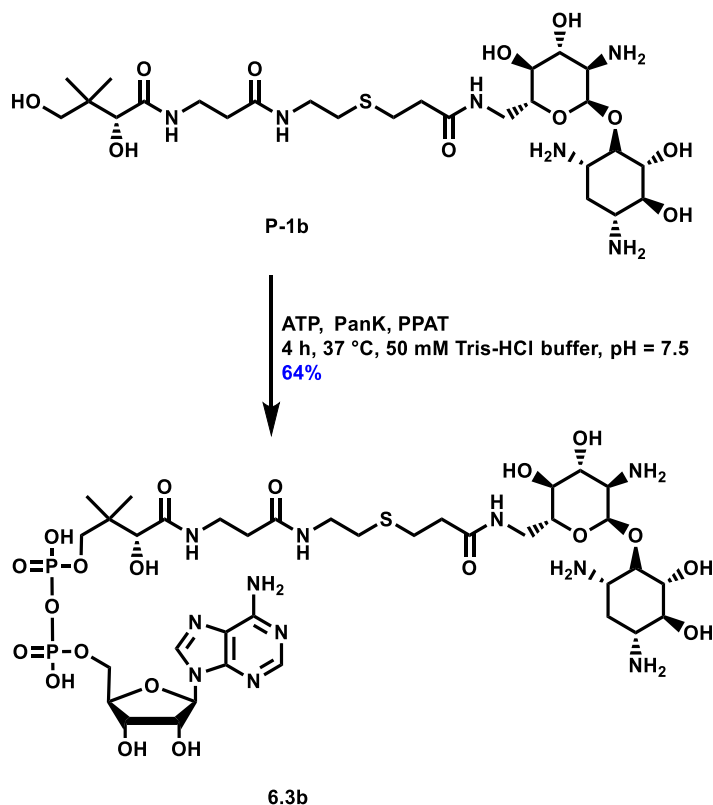


Figure 6.6. Transformation of **P-1b** in *E. faecium* measured by LCMS.

6.4 Inhibition of AAC(6')-li by compound 6.3b

Pure **6.3b** was next prepared enzymatically from **P-1b** and ATP, using purified *E. coli* PanK and PPAT as the catalysts (Scheme 6.1). The K_i of **6.3b** for AAC(6')-li was measured using the previously reported method.^{168, 183} As expected, compound **6.3b** is a

competitive (vs acetyl-CoA), tight-binding inhibitor of AAC(6')-li, with a K_i of $0.12 \pm 0.04 \mu\text{M}$, which is only ~3-fold higher than the K_i of **I-1b** ($0.043 \pm 0.023 \mu\text{M}$).^{168, 183} This provides an explanation for the observed potentiating effect of **P-1b** within the first four hours by time-kill curves. The potentiating effects of **P-1a** on tobramycin and ribostamycin can also be explained, since it is greatly possible that **6.3a**, like **6.3b**, is also a potent AAC(6')-li inhibitor. We therefore propose that the *in cellulo* bioactivation of **P-1b** leads to the formation of at least two AAC(6')-li inhibitors (**6.2b**, **6.3b** and maybe a small amounts of **I-1b**), with **6.3b** contributing the most to the potentiation effect.



Scheme 6.1. Synthesis of compound **6.3b**.

6.5 The aminoglycoside potentiating effect of **P-1b** in Gram-negative bacteria

Compound **P-1b** effectively potentiates the antibacterial activity of aminoglycosides towards the intrinsically resistant Gram-positive bacterium *E. faecium*. Its activity in Gram-

negative bacteria was investigated next. An aminoglycoside-resistant *E. coli* strain was generated by transforming the plasmid pET22b(+)/AAC(6')-li into competent *E. coli* BL21 cells. As expected, the resulting strain (abbreviated BL21-AAC(6')-li) is more resistant towards ribostamycin than the original strain (abbreviated BL21; Figure 6.7A). Besides, in the presence of **P-1b**, the MIC of ribostamycin decreased significantly. This result demonstrates that **P-1b** can also enter Gram-negative bacterial cells and potentiate the activity of aminoglycosides.

To verify whether **P-1b** utilizes the CoA biosynthetic enzymes in *E. coli*, as it does in *E. faecium*, the potentiating effect of compound **P-1b** was studied towards *E. coli* BL21-AAC(6')-li in the excess of pantothenate. As shown in Figure 6.7B, when the minimal growth medium (no pantothenate) was supplemented with 0.1 mM pantothenate, the MIC of ribostamycin for the *E. coli* BL21-AAC(6')-li, in the presence of **P-1b**, increased significantly. This suggests that the activity of **P-1b** in Gram-negative bacteria also requires an input from the CoA biosynthetic enzymes.

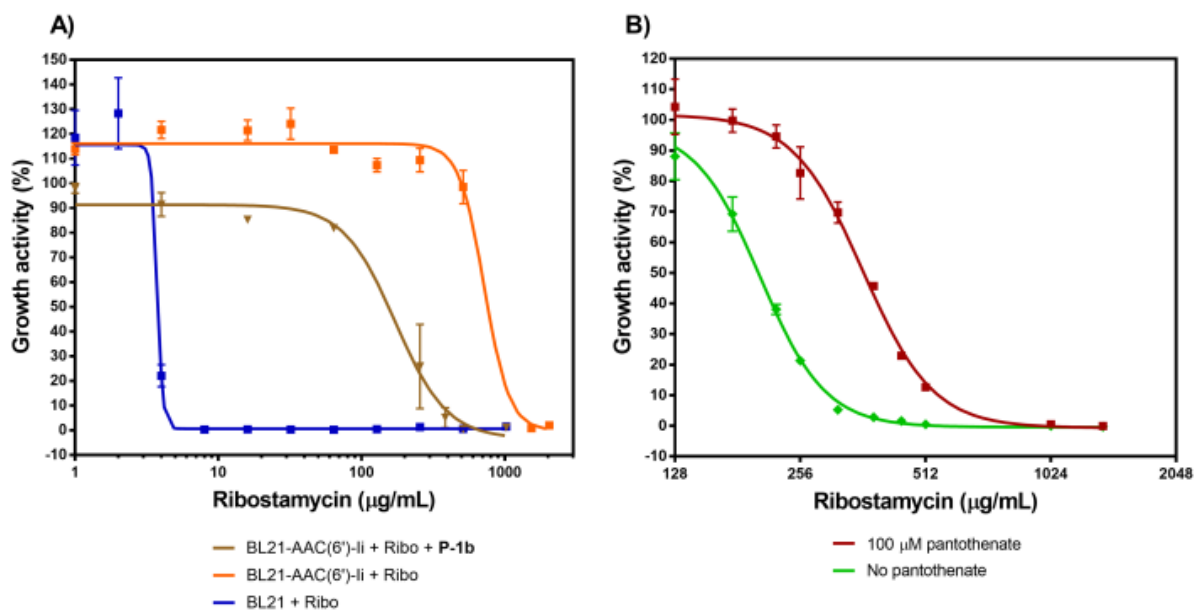


Figure 6.7. Potentiating effect of **P-1b** (512 µg/mL) on the antibacterial activity of ribostamycin towards *E. coli* strains, A) in minimal medium (M9 + 0.2% glycerol) and B) in minimal medium (M9 + 0.2% glycerol) with or without 0.1 mM pantothenate added.

6.6 Cell cytotoxicity study

The cytotoxicity of **P-1b** was also investigated using HeLa cells. As shown in Figure 6.8, even at a concentration of 1024 $\mu\text{g/mL}$, **P-1b** had no effect on the growth of HeLa cells. This is a desirable trait for a drug candidate.

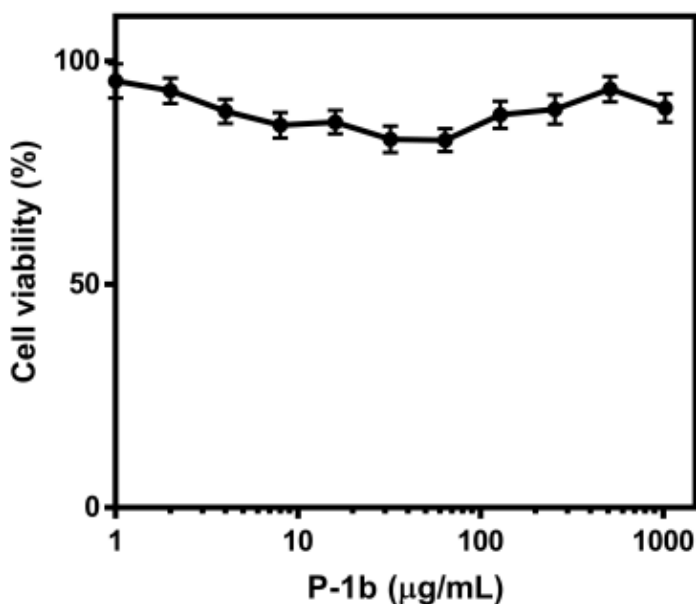


Figure 6.8. Effect of **P-1b** on the growth of HeLa cells.

6.7 Closing remarks

In summary, the cellular studies reported in this chapter reveal that **P-1b** can be bioactivated into more than one active aminoglycoside resistance inhibitors, with the intermediate (**6.3b**) being the most important active molecule. Also, the fast bioactivation of **P-1b** (within one hour), the absence of cell cytotoxicity and the ability to penetrate both Gram-positive and Gram-negative bacteria are all desirable drug traits, suggesting that compound **P-1b** should be a good starting point for the design of drugs to inhibit aminoglycoside resistance. We believe that because the unnatural part of **P-1b** (relative to pantothenate) is expected to lie outside of PanK, PPAT and DPCK, it is improbable that spontaneous mutations lead to resistance to it.

Antibacterial resistance is growing to be a severe health issue around the world.¹⁹⁶ Inhibiting resistance-causing enzymes is a validated approach for the design of new combination drugs to treat resistant infections.¹⁹⁷ While several inhibitors of beta-lactam resistance are used in the clinic, this is not the case for aminoglycoside resistance inhibitors. Our results show that compound **P-1b** is a promising hit for the design of such drugs. In particular, **P-1b** significantly reduces the MIC of different aminoglycosides towards *E. faecium*, an important nosocomial pathogen. Because enterococcal infections are intrinsically resistant to aminoglycosides, beta-lactams, macrolides and clindamycin, their treatment typically requires drug combinations. The treatment of enterococcal infections is further complicated by the rapid spread of plasmids encoding additional resistance-causing genes.¹⁹⁸ As many as 1/3 of all enterococcal infections in intensive care units are vancomycin-resistant (VRE). Compound **P-1b** might find useful for the treatment of VRE infections.

Chapter 7

Contributions and future directions

7.1 Contributions

Antimicrobial resistance is one of the most important threats to health systems around the world. Overcoming this antimicrobial crisis is urgent and indispensable. As an essential cofactor for all living organisms, CoA is usually biosynthesized in five steps starting from pantothenate. Although these five steps are conserved, the structure and mechanism of the enzymes involved vary significantly between different organisms. These differences allow the design of antimicrobial agents. The work described in this thesis has contributed to the current antimicrobial research in at least six ways.

Firstly, in chapter 2, to overcome the low stability of pantothenamides (known antimicrobial agents) in human blood, a synthetic route was developed to introduce larger groups at the geminal dimethyl position of pantothenamides. With the methodology developed, more diversified pantothenamide analogues can be accessed. This synthetic route provides the possibility to enlarge the arsenal of antimicrobial drug candidates.

Secondly, in chapter 3, based on the known antiplasmodial compound **3.1**, a detailed SAR study was performed, focusing on the substitution pattern of the triazole ring, the pantoyl-to-triazole linker and the *N*-substituent of the triazole ring. The results suggest that 1,4-substituted triazole with a simple methylene linker between the pantoyl moiety and the triazole group is favored, providing guideline for future optimization studies. Our results also indicate that the triazole ring can mimic amide bond in different ways. Since triazole is an amide bioisostere used quite often in drug discovery, our discovery may help chemists better take advantage of this bioisostere.

Thirdly, in chapter 4, based on the known antiplasmodial compound **3.1**, various heteroaromatic ring-containing pantothenamide analogues were synthesized. This study reveals three new nanomolar *P. falciparum* growth inhibitors. Since isoxazole and thiadiazole rings are among the most commonly used scaffolds in drugs, the three newly discovered compounds, are attractive hits for the development of novel antiplasmodial agents.

Fourthly, in chapter 5, a small series of pantothenate analogues was synthesized and used to probe the ligand preference of the three types of bacterial PanK. Overall, several

new inhibitors and substrates for each type of PanK were successfully discovered. Since it is increasingly recognized that broad-spectrum antibacterial agents can lead to severe imbalances of the normal gut microbiome, which cause side effects such as diarrhea and secondary *C. difficile* infections. The advantages of narrow-spectrum antibacterials are obvious. The results of our study on the ligand preference for the three types of PanK suggest possible directions for the design of antimicrobial agents selective for some pathogens.

Lastly, in chapter 6, detailed cellular studies of the aminoglycoside potentiator, **P-1b**, were reported. These studies help discover a new aminoglycoside resistance inhibitor, and reveal that **P-1b** is bioactivated into more than one aminoglycoside resistance inhibitors. Antibacterial resistance is growing to be a severe health issue around the world. Inhibiting resistance-causing enzymes is a validated approach for the design of new combination drugs to treat resistant infections. While several inhibitors of beta-lactam resistance are used in the clinic, this is not the case for aminoglycoside resistance inhibitors. Our results show that compound **P-1b** is a promising hit for the design of such drugs.

7.2 Publications

7.2.1 Peer-reviewed publications

- a. **Guan, J.**; Hachey, M.; Puri, L.; Howieson, V.; Saliba, K. J.; Auclair, K., A cross-metathesis approach to novel pantothenamide derivatives. *Beilstein Journal of Organic Chemistry* **2016**, *12*, 963-968.
- b. **Guan, J.**; Tjhin, E. T.; Howieson, V. M.; Kittikool, T.; Spry, C.; Saliba, K. J.; Auclair, K., Structure-activity relationships of antiplasmodial pantothenamide analogues reveal a new way by which triazoles mimic amide bonds, submitted for publication.
- c. **Guan, J.**; Barnard, L.; Cresson, J.; Hoegl, A.; Chang, J. H.; Strauss, E.; Auclair, K., Ligand preference for the three types of bacterial pantothenate kinase, submitted for publication.

- d. **Guan, J.**; Vong, K.; Wee, K.; Fakhoury, J.; Dullaghan, E.; Auclair, K., Cellular studies of an aminoglycoside potentiator reveal a new inhibitor of aminoglycoside resistance, submitted for publication.
- e. Wang, Y.; **Guan, J.**; Di Trani, J.; Auclair, K.; Mittermaier, A., Rapid measurement of product inhibition of kinases by isothermal titration calorimetry. Manuscript in preparation.

7.2.2 Patent in preparation

- a. **Guan, J.**; Auclair, K.; Saliba, K. J.; Spry, C., Heteroaromatic rings that mimic one of the labile amide of pantothenamides, increase their blood stability and lead to molecules with interesting antimicrobial activity, including antiplasmodial. A patent application is currently being prepared for joint filing, by McGill University and The Australian National University.

7.3 Future directions

For the work presented in chapter 2, a future direction would be to apply the developed methodology to synthesize more pantothenamide analogues modified at the geminal dimethyl position of pantothenamides. This may yield more potent, yet stable, new antimicrobial agents.

Secondly, to follow up on the work described in chapters 3 and 4, pre-clinical studies with compounds **3.1**, **4.1e,f,i** are warranted. The targets of these compounds in *P. falciparum* should also be explored.

Thirdly, a future direction of the project discussed in chapter 5 would be to use the knowledge presented in this thesis to design antimicrobial agents selective for one type of PanK. Inhibitors and antimetabolites of type III PanK are of special interest because only a few are reported.

Finally, the results presented in chapter 6 suggest that **P-1b** is a promising drug candidate. Performing pre-clinical studies with **P-1b** should be the next focus.

Chapter 8

Experimental

8.1 Chemistry

8.1.1 Materials

All reagents and solvents were purchased either from Chem Impex International Inc. or Sigma-Aldrich Canada, and used without further purification. Dry solvents were obtained from an Innovative Tech Pure Solve MD-7 Solvent purification system. MilliQ-quality water was used whenever water is mentioned. Unless noted otherwise, all reactions were performed under a nitrogen atmosphere. Flash chromatography was performed on RediSep Rf Gold Silica Flash Chromatography Columns from Teledyne ISCO. TLC analysis (F-254) was performed with 60 Å silica gel TLC plates from Silicycle. HRMS spectra were acquired at the McGill University Mass Spectral Facility on an EXACTIVE™ Plus Orbitrap Mass Spectrometer from Thermo Fisher Scientific or a MaXis Impact HD Mass Spectrometer from Bruker. The NMR chemical shifts (δ) are reported in parts per million (ppm) and are referenced to the internal standard tetramethylsilane. Compound purity was determined by reversed-phase HPLC analyses using an Agilent 6120 Quadrupole LCMS system. Reversed-phase HPLC purification was achieved using an Agilent 1100 series HPLC.

8.1.2 Synthesis of compounds in chapter 2

8.1.2.1 Synthesis of compound 2.10

The synthesis of compound **2.10** followed the previously reported procedure with modifications.⁹⁴ Acetic acid (3 mL, 90% in water) was added to compound **2.18** (0.13 mmol, 1.0 eq) in a round bottom flask (10 mL). The colorless mixture was stirred for 16 hours at room temperature. Next day, the solvent was evaporated *in vacuo* and the residue was loaded on the silica gel directly. Purification was achieved with a gradient of 0-100% EtOAc in hexanes, followed by 0-25% methanol in EtOAc.

8.1.2.2 Synthesis of compound 2.15

The starting material, compound **2.9d**, was prepared as previously reported.⁹⁴ The synthesis of compound **2.15** followed the previously reported procedure with modifications.⁹⁴ To compound **2.9d** (0.61 mmol, 1.0 eq) in DCM (2 mL) was added Dess-

Martin periodinane (1.23 mmol, 2.0 eq). The mixture was stirred at room temperature for 2 hours, and then diluted in diethyl ether (10 mL) and washed with a Na₂S₂O₃/NaHCO₃ solution (4.5 g Na₂S₂O₃ in 15 mL of saturated aqueous NaHCO₃). The combined organic layer was washed with brine (10 mL) and dried over anhydrous magnesium sulfate before evaporation of the solvent *in vacuo* to give the crude product, which was purified by flash chromatography using a gradient of 0-50% EtOAc in hexanes.

8.1.2.3 Synthesis of compound 2.18

The synthesis of compound **2.18** followed the previously reported procedure with modifications.⁹⁴ To a suspension of compound **2.15** (0.28 mmol, 1.0 eq) in a mixture of acetone and CH₂Cl₂ (3:1, v/v, 12 mL) was added a freshly prepared solution of NaH₂PO₄ (2.8 mmol, 10 eq) and NaClO₂ (1.4 mmol, 5.0 eq) in water (4 mL). The mixture was stirred at room temperature for 15 minutes. After evaporation of the solvent *in vacuo*, the residue was dissolved in a saturated solution of sodium sulfite (10 mL). The aqueous solution was extracted with EtOAc (3 × 25 mL). The combined organic layer was dried over magnesium sulfate and concentrated *in vacuo* to give the crude acid **2.16**, which was used without purification.

To compound **2.17** (0.42 mmol, 1.5 eq), prepared with the method of Hoegl *et al.*,¹⁴⁴ were added 1-ethyl-3-(3-dimethylaminopropyl)carbodiimide (0.85 mmol, 3.0 eq), hydroxybenzotriazole (1.02 mmol, 3.6 eq), the crude acid **2.16** in THF (10 mL) and *N,N*-diisopropylethylamine (2.82 mmol, 10 eq) sequentially. The mixture was stirred for 16 hours at room temperature, and next poured into a separatory funnel containing an aqueous solution of saturated ammonium chloride (20 mL), before extraction in EtOAc (3 × 40 mL). The combined organic layer was dried over magnesium sulfate and evaporated to give the crude product, which was purified by flash chromatography using a gradient of 0-100% EtOAc in hexanes, followed by 0-10% methanol in EtOAc.

8.1.3 Synthesis of compounds in chapter 3

8.1.3.1 General protocol 1 for synthesis of compounds (3.2a-b, 3.7a-d, 3.9a-b, 3.13a-c, 4.1a and 4.1e-n)

The synthesis of compounds **3.2a-b**, **3.7a-d**, **3.9a-b**, **3.13a-c**, **4.1a**, **4.1e-n** followed the previously reported procedure with modifications.¹⁴⁶ The Boc-protected heteroaromatic compound (0.19-0.82 mmol, 1 eq) was dissolved in a mixture of DCM and trifluoroacetic acid (1:1, v/v, 2-4 mL). The reaction was stirred at room temperature for 0.5-2 hours, or until completion of the deprotection as judged by TLC. The aqueous NaOH solution (1 M, 10-20 mL) was used to quench the reaction, making sure that the final pH was higher than 9. The product was extracted in EtOAc (4 × 10 mL). The combined organic layers were dried over anhydrous sodium sulfate. The solid was removed by filtration and the solvent was evaporated *in vacuo* to afford the crude free amine, which was used directly in the next step.

In a pressure vessel (5 mL), the free amine dissolved in anhydrous methanol or ethanol (2 mL) was mixed with D-pantolactone (0.75-3.27 mmol, 4 eq) and triethylamine (0.75-3.27 mmol, 4 eq). The reaction was heated to 115°C for 12-16 hours in an oil bath. The reaction mixture was directly loaded on a silica gel column and purification was achieved with a gradient of 0-100% EtOAc in hexanes, followed by 0-50% methanol in EtOAc.

8.1.3.2 General protocol 2 for synthesis of compounds 3.3a,b

The synthesis of compounds **3.3a,b** followed the previously reported procedure with modifications.¹⁴⁶ In a round-bottom flask (100 mL), the desired alkynyl amine hydrochloride (4.74 mmol, 1 eq) was dissolved in H₂O/dioxane (2:1, v/v, 30 mL), before addition of sodium bicarbonate (9.47 mmol, 2 eq). The solution was cooled on ice for 10 minutes. Di-*tert*-butyl dicarbonate (6.16 mmol, 1.3 eq) in dioxane (10 mL) was next slowly added. The mixture was allowed to warm to room temperature and stirred for 16 hours, before water (50 mL) was added to dilute the reaction mixture. The aqueous solution was extracted with EtOAc (4 × 15 mL). The combined organic layers were dried over anhydrous sodium sulfate. The solvent was evaporated *in vacuo* to give the crude product,

which was purified by flash chromatography on silica gel using a gradient of 0-30% EtOAc in hexanes.

8.1.3.3 General protocol 3 for synthesis of Boc-protected 1,5-substituted triazoles (3.5a-b)

In a microwave vial (5 mL), sodium azide (0.97-2.07 mmol, 1.75 eq) dissolved in water (0.4 mL) and 1-bromopentane (0.96-1.77 mmol, 1.5 eq) in DMF (2.1 mL) were mixed and heated to 100°C for 1 hour in a microwave reactor to complete the bromide-azide exchange. After cooled down, the crude reaction mixture was diluted with DCM (5 mL) and dried with anhydrous sodium sulfate. The partially hydrated sodium sulfate was removed by filtration and the filtrate was concentrated to around 1.5 mL under reduced pressure to yield the crude pentyl azide.

In a glove box, RuCl(PPh₃)₂Cp* (0.02-0.08 mmol, 0.07 eq) dissolved in anhydrous dioxane (0.5 mL) was added to a pressure vessel (5 mL), before addition of the desired alkyne (0.50-1.18 mmol, 1 eq) pre-dissolved in dioxane (1 mL) and the crude azide also pre-dissolved in dioxane (1.5 mL). The resulting mixture was allowed to react at 100°C for 16 hours. The reaction mixture was directly purified on the silica gel using a gradient of 0-100% EtOAc in hexanes.

8.1.3.4 General protocol 4 for synthesis of Boc-protected 1,4-substituted triazoles (3.8a-d, 3.12a-b, 3.14a-c)

The synthesis of compounds **3.8a-d**, **3.12a-b**, **3.14a-c** followed the previously reported procedure with modifications.¹⁴⁶ The desired alkyl bromide (0.89-1.93 mmol, 1.5 eq) in DMF (4 mL), the alkyne (0.59-1.29 mmol, 1 eq) in DMF (3 mL), sodium azide (0.89-1.93 mmol, 1.5 eq) in water (1 mL), sodium ascorbate (0.24-0.52 mmol, 0.4 eq) in water (1 mL) and copper sulfate (0.06-0.13 mmol, 0.1 eq) in water (3 mL) were individually added to a pressure vessel (20 mL). The reaction was heated to 100°C in an oil bath for 16 hours. After the reaction mixture had cooled down, the aqueous ammonium hydroxide solution (1 M, 28 mL) was added. The product was extracted in EtOAc (4 × 20 mL). The combined organic layers were dried over anhydrous sodium sulfate. After filtration to remove the

solid and evaporation of the solvent *in vacuo*, the crude product was loaded on silica gel and purified with flash chromatography using a gradient of 0-100% EtOAc in hexanes.

8.1.3.5 Synthesis of compound 3.10a

The synthesis of compound **3.10a** followed the previously reported procedure with modifications.¹⁸⁸ Boc-D-alaninol (5.71 mmol, 1 eq) in wet DCM (10 mL) was added with Dess-martin periodinane (2.86 mmol, 0.5 eq). The mixture was stirred at room temperature for 15 minutes, before another batch of Dess-martin periodinane (2.86 mmol, 0.5 eq) was added and the mixture was stirred for another 15 minutes. The reaction mixture was diluted in EtOAc (30 mL) and washed with aqueous Na₂S₂O₃/NaHCO₃ solution (6 g Na₂S₂O₃ dissolved in 20 mL of aqueous saturated NaHCO₃ solution). The EtOAc layer was dried over anhydrous sodium sulfate and concentrated *in vacuo*. Purification was achieved on silica gel using a gradient of 0-50% EtOAc in hexanes.

8.1.3.6 General protocol 5 for synthesis of compounds 3.11a-b

The synthesis of compounds **3.11a-b** followed the previously reported procedure with modifications.¹⁹⁹ K₂CO₃ (2.60 mmol, 1.5 eq) was added to an ice-cooled methanol solution (3 mL) of Boc-alanine aldehyde (1.73 mmol, 1 eq) and dimethyl (1-diazo-2-oxopropyl)phosphonate (1.99 mmol, 1.15 eq). The mixture was stirred for 16 hours while allowed to warm up to room temperature. The mixture was next filtered through Celite and concentrated under reduced pressure. The crude residue was purified by flash chromatography on silica gel using a gradient of 0-30% EtOAc in hexanes.

8.1.4 Synthesis of compounds in chapter 4

8.1.4.1 General protocol 6 for synthesis of compounds 4.1b-d

The synthesis of compounds **4.1b-d** followed the previously reported procedure with modifications.^{146, 200-201} Compound **4.4b**, **4.4c** or **4.4d** (0.95 mmol, 1.0 eq) was added to an aqueous solution (14 mL) of ammonium hydroxide (100.66 mmol, 105.8 eq), before addition of ammonium chloride (0.26 mmol, 0.3 eq). The mixture was heated to 105°C for 16 hours. The reaction mixture was cooled to room temperature and extracted with EtOAc

(4 × 10 mL). The organic layers were dried over anhydrous sodium sulfate and concentrated *in vacuo* to get the crude amide.

The crude amide was dissolved in THF (10 mL) and lithium aluminum hydride (4.75 mmol, 5.0 eq) in THF (2 mL) was slowly added. The mixture was stirred at room temperature for 16 hours, before quenching with water (0.18 mL), the 15% aqueous NaOH solution (0.18 mL) and water (10 mL) sequentially. The product was extracted with EtOAc (4 × 10 mL). The combined organic layers were dried over anhydrous sodium sulfate and concentrated *in vacuo* to get the crude amine.

To the crude amine were added D-pantolactone (3.80 mmol, 4.0 eq), triethylamine (3.80 mmol, 4.0 eq) and ethanol (2 mL). The reaction was stirred at 115°C for 12 hours. The reaction mixture was purified by flash chromatography on silica gel using a gradient of 0-100% EtOAc in hexanes, followed by 0-50% methanol in EtOAc.

8.1.4.2 Synthesis of compound 4.2

The synthesis of compound **4.2** followed the previously reported procedure with modifications.²⁰²⁻²⁰³ 1-Heptyne (2.75 mmol, 1.2 eq) was added dropwise to a round-bottomed flask, which contained ethylmagnesium bromide (2.75 mmol, 1.2 eq) in THF (4 mL) at 50°C. The reaction mixture was stirred at 50°C for 0.5 hour, before *N*-(*tert*-Butoxycarbonyl)glycine *N'*-methoxy-*N'*-methanamide (2.29 mmol, 1.0 eq) in THF (4 mL) was added. The resulting mixture was stirred at 50°C for 16 hours, before cooled down and poured into water (20 mL). The product was extracted with EtOAc (4 × 20 mL). The combined organic layers were dried over anhydrous sodium sulfate and concentrated *in vacuo*. Purification was achieved on silica gel using a gradient of 0-100% EtOAc in hexanes.

8.1.4.3 Synthesis of compound 4.3

The synthesis of compound **4.3** followed the previously reported procedure with modifications.²⁰⁴ To compound **4.2** (0.87 mmol, 1.0 eq) dissolved in methanol (3 mL) was added hydrazine monohydrate (2.95 mmol, 3.4 eq). The reaction was stirred at room temperature for 1 hour. The product was purified by flash chromatography on silica gel using a gradient of 0-100% EtOAc in hexanes.

8.1.4.4 General protocol 7 for synthesis of compounds 4.4b-d

The synthesis of compounds **4.4b-d** followed the previously reported procedure with modifications.²⁰⁵ To the desired commercial heteroaromatic compound (2.10 mmol, 1.0 eq) in dry DMF (4.5 mL) were added 1-bromopentane (2.31 mmol, 1.1 eq) and Na₂CO₃ (4.20 mmol, 2.0 eq) sequentially. The mixture was stirred at 80°C for 16 hours, before dilution in EtOAc (40 mL) and wash with water (15 mL). The organic layer was dried over anhydrous sodium sulfate and concentrated *in vacuo*. Purification was achieved on silica gel using a gradient of 0-100% EtOAc in hexanes.

8.1.4.5 General protocol 8 for synthesis of compounds 4.10e-f

The synthesis of compounds **4.10e-f** followed the previously reported procedure with modifications.²⁰⁶ The desired commercial aldehyde (1.20-2.00 mmol, 1.0 eq) was added to hydroxylamine (1.25-2.10 mmol, 1.1 eq) in *t*-BuOH/H₂O (1:1, v/v, 4 mL). After stirring for 0.5-12 hours at room temperature or 80°C, TLC analysis indicated that oxime formation was complete. The product was extracted with EtOAc (4 × 10 mL). The combined organic layers were dried over anhydrous sodium sulfate and concentrated *in vacuo* to get the crude oxime.

To a stirred solution of oxime in DMF (2 mL), was added *N*-chlorosuccinimide (1.55-2.60 mmol, 1.3 eq). The reaction mixture was stirred at room temperature for 3 hours. The pale green solution was diluted in brine (10 mL). The product was extracted in diethyl ether (3 × 10 mL). The combined organic layers were dried with anhydrous sodium sulfate and concentrated *in vacuo* to afford the crude **4.9e** or **4.9f**.

To a stirred solution of the desired alkyne (0.90-1.29 mmol, 0.7 eq) in DCM (2 mL), triethylamine (1.10-1.84 mmol, 0.9 eq) was added. A solution of **4.9e** or **4.9f** in DCM (2 mL) was added dropwise. The reaction was stirred at room temperature for 16 hours. The reaction mixture was washed with brine (10 mL), dried over anhydrous sodium sulfate and concentrated *in vacuo*. Purification was achieved on silica gel using a gradient of 0-100% EtOAc in hexanes.

8.1.4.6 Synthesis of compound 4.12

The synthesis of compound **4.12** followed the previously reported procedure with modifications.^{205, 207} To a solution of compound **3.3a** (1.93 mmol, 1.0 eq) in DMF (2 mL) and MeOH (0.45 mL) were added CuI (0.19 mmol, 0.1 eq) and trimethylsilyl azide (2.90 mmol, 1.5 eq). After heating at 100°C for 16 hours, the reaction was cooled to room temperature and filtered through Celite. This crude reaction mixture was used directly in the following step.

To the crude residue were added sodium carbonate (3.87 mmol, 2.0 eq) and 1-bromopentane (2.13 mmol, 1.1 eq) sequentially. The reaction was heated to 80°C for 16 hours. The reaction mixture was cooled to room temperature and filtered through Celite. The mixture was then loaded on silica gel directly and purified with a gradient of 0-100% EtOAc in hexanes.

8.1.4.7 Synthesis of compound 4.14

The synthesis of compound **4.14** followed the previously reported procedure with modifications.²⁰⁸⁻²¹⁰ To *N*-Boc-glycinamide (2.18 mmol, 1.0 eq) in DCM (5 mL) was added triethyloxonium hexafluorophosphate (2.40 mmol, 1.1 eq) in DCM (2 mL). After stirring at room temperature for 24 hours, the reaction mixture was poured into an ice-cold aqueous Na₂CO₃ solution (1 M, 10 mL). The product was extracted in DCM (4 x 10 mL). The combined organic layers were dried over anhydrous sodium sulfate and concentrated *in vacuo*. The crude residue was used directly for the following step.

To hexanoic acid hydrazide (2.18 mmol, 1.0 eq) were added triethylamine (2.18 mmol, 1.0 eq) and an ethanolic solution (2 mL) of the residue from the previous step. The reaction mixture was stirred at 115°C for 16 hours. The mixture was loaded on silica gel directly and purified with a gradient of 0-100% EtOAc in hexanes.

8.1.4.8 Synthesis of compound 4.16

The synthesis of compound **4.16** followed the previously reported procedure with modifications.¹⁶² To *N*-Boc glycine (1.14 mmol, 1.0 eq) dissolved in DCM (3 mL), was added *N*-ethoxycarbonyl-2-ethoxy-1,2-dihydroquinoline (1.14 mmol, 1.0 eq), followed by

hexanoic acid hydrazide (1.37 mmol, 1.2 eq). The mixture was stirred at room temperature for 16 hours. The mixture was filtered and concentrated *in vacuo* to provide the desired coupling product **4.15**, which was used directly in the next step.

To the crude residue of **4.15** in dry THF (5 mL) was added Lawesson's reagent (1.26 mmol, 1.1 eq). The reaction mixture was stirred at 70°C for 16 hours, before concentration *in vacuo*. The concentrated crude product was loaded on silica gel directly. Purification was achieved using a gradient of 0-100% EtOAc in hexanes.

8.1.4.9 Synthesis of compound 4.17

The synthesis of compound **4.17** followed the previously reported procedure with modifications.²¹¹ At 0°C, carbonyldiimidazole (0.92 mmol, 1.1 eq) in DCM (1 mL) was mixed with *N*-Boc glycine (0.88 mmol, 1.0 eq) in DCM (4 mL). The mixture was stirred at 0°C for 30 minutes. Hexanoic acid hydrazide (0.88 mmol, 1.0 eq) in DCM (1 mL) was next added. After stirring at 0°C for 45 minutes, CBr₄ (1.76 mmol, 2.0 eq) and PPh₃ (1.76 mmol, 2.0 eq) in DCM (2 mL) were added at 0°C sequentially. The reaction mixture was stirred for 16 hours while allowing the mixture to warm up to the room temperature. The reaction mixture was loaded on silica gel directly and purified with a gradient of 0-100% EtOAc in hexanes.

8.1.4.10 General protocol 9 for synthesis of compounds 4.19k-l

The synthesis of compounds **4.19k-l** followed the previously reported procedure with modifications.²¹²⁻²¹³ To a stirring solution of the desired commercial nitrile (1.92-2.06 mmol, 1.0 eq) in EtOH (2 mL) were added hydroxylamine (9.60-0.29 mmol, 5.0 eq) and triethylamine (2.11-2.26 mmol, 1.1 eq). The reaction was heated to 80°C for 16 hours. The reaction mixture was diluted in EtOAc (20 mL) and washed with water (10 mL). The organic layer was dried over anhydrous sodium sulfate and concentrated *in vacuo*, which was used directly for the next step.

To a stirring solution of 1-ethyl-3-(3-dimethylaminopropyl)carbodiimide (1.92-2.06 mmol, 1.0 eq) in dry acetonitrile (2-5 mL) was added the desired carboxylic acid (1.92-2.06 mmol, 1.0 eq). The mixture was stirred at room temperature for 20 minutes, before adding the crude product from the first step in DMF (2 mL). The reaction mixture was stirred at room

temperature for 4 hours, and then heated at 110°C for 1.5-12 hours. The reaction residue was loaded on silica gel directly and purified with a gradient of 0-100% EtOAc in hexanes.

8.1.4.11 General protocol 10 for synthesis of compounds 4.20m-n

The synthesis of compounds **4.20m-n** followed the previously reported procedure with modifications.¹⁶³ The desired commercial alkyne (0.38-0.73 mmol, 1.0 eq), nitrile (0.73-2.28 mmol, 1.0-6.0 eq), 8-methylquinoline *N*-oxide (0.49-0.94 mmol, 1.3 eq) and a small scoop of catalyst BrettPhosAuNTf₂ (0.02-0.04 mmol, 0.05 eq) were added to a pressure vessel (5 mL). The reaction was heated at 60°C for 1-3 hour(s) in a microwave reactor. The cloudy mixture was loaded on silica gel directly and purified with a gradient of 0-100% EtOAc in hexanes.

8.1.5 Synthesis of compounds in chapter 5

8.1.5.1 General protocol 11 for the synthesis of 5.1a-l via benzyl deprotection

To the desired benzyl-protected compound (0.09-0.36 mmol) dissolved in dry THF (4 ml) was added a scoop of Pd(OH)₂/C (~5 mol%). The mixture was kept under vacuum and purged with N₂ three times, and then H₂ gas was bubbled in the solution for 12 hours at room temperature. The reaction mixture was next diluted in THF (6 mL), filtered to remove the Pd(OH)₂/C, and purified accordingly.

8.1.5.2 General protocol 12 to produce 5.2a and 5.2h via TBS deprotection

To the desired TBS-protected compound (**5.6a** or **5.7**, 0.24-0.35 mmol, 1.0 eq) in THF (3 mL) were added tetrabutylammonium fluoride (0.27-0.38 mmol, 1.1 eq) and acetic acid (0.61-0.87 mmol, 2.5 eq) sequentially. The mixture was stirred at room temperature for 4 hours until completion of the deprotection as judged by TLC analysis. The reaction mixture was loaded directly on silica gel and purified with a gradient of 0-100% EtOAc in hexanes (both containing 1% TEA), and then 0-50% MeOH in EtOAc (both containing 1% TEA).

8.1.5.3 General protocol 13 to synthesize 5.2b-d via TBS deprotection

To the desired TBS-protected compound (0.36 mmol, 1.0 eq) in THF (3 mL) were added tetrabutylammonium fluoride (0.39 mmol, 1.1 eq) and acetic acid (0.39 mmol, 1.1 eq)

sequentially. The mixture was stirred at room temperature for 12 hours until completion as judged by TLC analysis. The reaction was quenched with brine (10 mL) and the product extracted in EtOAc (4 × 15 mL). The combined organic layers were dried over anhydrous MgSO₄, and concentrated *in vacuo*. Purification was achieved on silica gel with a gradient of 0-100% EtOAc in hexanes both containing 1% TEA, and then 0-50% MeOH in EtOAc, again both containing 1% TEA.

8.1.5.4 Synthesis of compound 5.2e

To compound **5.6e** (0.27 mmol, 1.0 eq) in THF (3 mL) were added tetrabutylammonium fluoride (0.56 mmol, 2.1 eq) and acetic acid (0.56 mmol, 2.1 eq). The mixture was stirred at room temperature for 3 hours until completion as judged by TLC analysis. The reaction mixture was loaded directly on silica gel and purified with a gradient of 0-100% EtOAc in hexanes both containing 1% TEA, and then 0-50% MeOH in EtOAc again both containing 1% TEA.

8.1.5.5 Synthesis of compound 5.2f

To compound **5.6f** (0.23 mmol, 1.0 eq) in THF (3 mL) was added tetrabutylammonium fluoride (0.25 mmol, 1.1 eq). The mixture was stirred at room temperature for 3 hours until completion as judged by TLC analysis. The reaction was quenched with brine (10 mL) and extracted in EtOAc (4 × 15 mL). The combined organic layers were dried over anhydrous MgSO₄, and concentrated *in vacuo*. Purification was achieved on silica gel with a gradient of 0-100% EtOAc in hexanes both containing 1% TEA.

8.1.5.6 Synthesis of compound 5.2g

Following the general protocol 14, crude compound **5.6g** was produced as a yellow oil using aldehyde **5.5** (0.47 mmol, 1.0 eq) and 2,4-dimethoxybenzylamine (0.52 mmol, 1.1 eq). The synthesis of compound **5.2g** followed the previously reported procedure with modifications.¹⁸⁸ To compound **5.6g** dissolved in THF (5 mL), 2-hydroxypyridine (0.47 mmol, 1.0 eq) and diketene (2.46 mmol, 5.2 eq) were added at room temperature. The reaction was then heated up to 50°C and stirred for 16 hours. The reaction mixture was concentrated under reduced pressure and resuspended in DCM (2 mL), to which trifluoroacetic acid (2 mL, 56.0 eq) and anisole (0.25 mL, 4.9 eq) were added. The mixture

was allowed to stir at room temperature for 16 hours, before concentrated *in vacuo* and loaded on the silica gel. Purification was achieved with flash chromatography with a gradient of 0-100% EtOAc in hexanes.

8.1.5.7 Synthesis of compound 5.2i

Compound **5.8** (0.34 mmol, 1.0 eq) dissolved in dry THF (3 mL) was cooled to 0°C on ice, before adding diketene (0.40 mmol, 1.2 eq) and diisopropylethylamine (1.01 mmol, 3.0 eq). The reaction mixture was stirred at 0°C for 4 hours, and next concentrated *in vacuo*. The concentrated residue was loaded directly onto silica gel and purified with a gradient of 0-100% EtOAc in hexanes.

8.1.5.8 Synthesis of compounds 5.2j-l

To compound **5.3** (1.86 mmol, 1.0 eq) dissolved in dry THF (5 mL) was added CsF (9.30 mmol, 5.0 eq). The mixture was stirred at 80°C for 12 hours, before adding methyl iodide (18.59 mmol, 10.0 eq). The mixture was kept stirring at 80°C for another 16 hours. After cooling down to room temperature, the mixture was quenched with a saturated aqueous NH₄Cl solution (20 mL). The product was extracted in EtOAc (4 × 15 mL). The combined organic layers were concentrated *in vacuo* and loaded onto silica gel. Purification was achieved using a gradient of 0-100% EtOAc in hexanes. The overall yield for compounds **5.2j-l** was 24%.

8.1.5.9 Synthesis of compound 5.3

D-Pantothenic acid hemicalcium salt (2.10 mmol, 1.0 eq) dissolved in water (15 mL) was loaded onto a prepacked Amberlite® IR-120 (H⁺) ion-exchange column (1 × 5 cm). The column was flushed continuously with water until the pH of the eluent was neutral. All the eluents were collected, combined and lyophilized, affording pantothenic acid as a yellow oil.

To pantothenic acid dissolved in anhydrous THF (50 mL) were added imidazole (25.18 mmol, 12.0 eq) and *tert*-butyldimethylsilyl chloride (25.18 mmol, 12.0 eq) sequentially. The reaction was stirred at room temperature for 16 hours, before poured into a cold NaHSO₃ solution (1 M, 30 mL). The product was extracted in EtOAc (3 × 30 mL). The

combined organic layers were dried over anhydrous MgSO_4 , and concentrated *in vacuo* to get a colorless oil.

The resulting colorless oil was dissolved in DCM (50 mL) and mixed with benzyl alcohol (6.30 mmol, 3.0 eq). *N,N'*-Dicyclohexylcarbodiimide (4.20 mmol, 2.0 eq) was next added to the mixture, followed by a catalytic amount of 4-dimethylaminopyridine (0.42 mmol, 0.2 eq). The reaction was stirred at room temperature for 16 hours. The generated 1,3-dicyclohexylurea was removed by filtration. The filtrate was concentrated *in vacuo*. Purification was achieved with a gradient of 0-30% EtOAc in hexanes to give the pure product as a colorless oil.

8.1.5.10 Synthesis of compound 5.4

The synthesis of compound **5.4** followed the previously reported procedure with modifications.¹⁸⁸ To compound **5.3** (0.36 mmol, 1.0 eq) dissolved in EtOH (2 mL) at 0°C was added pyridinium *p*-toluenesulfonate (0.37 mmol, 1.1 eq) slowly. The reaction mixture was stirred for 16 hours with the temperature slowly warming up to room temperature. The mixture was concentrated *in vacuo* and then purified by flash column chromatography on silica gel using a gradient of 0-50% EtOAc in hexanes to provide the desired compound as a colorless oil.

8.1.5.11 Synthesis of compound 5.5

The synthesis of compound **5.5** followed the previously reported procedure with modifications.¹⁸⁸ To compound **5.4** (1.42 mmol, 1.0 eq) in wet DCM (10 mL) was added Dess-Martin periodinane (0.71 mmol, 0.5 eq). The mixture was stirred at room temperature for 15 minutes. Another batch of Dess-Martin periodinane (0.71 mmol, 0.5 eq) was added. The reaction was stirred for another 15 minutes. Next, the reaction mixture was diluted with diethyl ether (40 mL) and washed with a solution of $\text{Na}_2\text{S}_2\text{O}_3$ in saturated NaHCO_3 (4.5 g $\text{Na}_2\text{S}_2\text{O}_3$ in 15 mL of aqueous saturated NaHCO_3) and brine (10 mL) sequentially. The organic layer was dried over anhydrous MgSO_4 and concentrated *in vacuo*. Purification was achieved on silica gel with a gradient of 0-30% EtOAc in hexanes to give the product as a colorless oil.

8.1.5.12 General protocol 14 to produce 5.6a-g via reductive amination

The synthesis of compounds **5.6a-g** followed the previously reported procedure with modifications.¹⁸⁸ To aldehyde **5.5** (0.36-1.19 mmol, 1.0 eq) in 1,2-dichloroethane (5 mL) were added anhydrous sodium sulfate (~1.5 g) and the desired commercial amine (0.40-1.30 mmol, 1.1 eq). The reaction mixture was stirred at room temperature until completion as judged by TLC (1.5-12 hours). The reaction mixture was diluted in toluene (10 mL) and filtered over Celite. The filtrate was evaporated to dryness under reduced pressure to yield the crude imine.

The crude imine was dissolved in anhydrous THF (10 mL). Sodium borohydride (1.78-5.93 mmol, 20.0 eq) was added slowly. The reaction was stirred for 16 hours at room temperature, before quenching with saturated aqueous sodium bicarbonate (10 mL) and extracting the product with EtOAc (4 × 20 mL). The combined organic layers were dried over anhydrous MgSO₄, and concentrated under reduced pressure. Purification was achieved on silica gel with a gradient of 0-100% EtOAc in hexanes (both containing 1% TEA), and then 0-30% methanol in EtOAc (both containing 1% TEA).

8.1.5.13 Synthesis of compound 5.6e

Compound **5.6e** was prepared with aldehyde **5.5** (1.19 mmol, 1.0 eq) and the amine obtained from Fmoc-deprotection of compound **5.13**, following the general protocol 14. For the Fmoc-deprotection, compound **5.13** (1.31 mmol, 1.1 eq) dissolved in THF (3 mL) was mixed with piperidine (2 mL). The mixture was stirred at room temperature for 2 hours. Next, the solvent and excess piperidine were removed *in vacuo* to generate the crude amine, which was used directly for synthesizing compound **5.6e**.

8.1.5.14 Synthesis of compound 5.7

The synthesis of compound **5.7** followed the previously reported procedure with modifications.⁹⁴ To a suspension of aldehyde **5.5** (0.47 mmol, 1.0 eq) in a mixture of acetone and DCM (3:1, v/v, 12 mL) was added a freshly prepared aqueous solution (1:3 v/v ratio of water to the total volume of acetone/DCM, 4 mL) of NaH₂PO₄ (4.74 mmol, 10.0 eq) and NaClO₂ (2.37 mmol, 5.0 eq). The mixture was stirred at room temperature for 30 minutes. After concentration *in vacuo*, the residue was quenched with saturated solution

of Na₂SO₃ (15 mL). The product was extracted in EtOAc (4 × 15 mL). The combined organic layers were dried over magnesium sulfate and concentrated *in vacuo* to afford the crude acid. The crude acid was purified on silica gel using a gradient of 0-100% EtOAc in hexanes.

8.1.5.15 Synthesis of compound 5.8

To a pressure vessel (5 mL) were added β-alanine benzyl ester 4-toluenesulfonate salt (1.42 mmol, 1.0 eq) and diethylamine (8.11 mmol, 5.7 eq) dissolved in dry THF (2 mL). D-Pantolactone (3.33 mmol, 2.3 eq) was next added. The reaction mixture was stirred at 60°C for 16 hours, before loaded directly onto silica gel and purified using a gradient of 0-100% EtOAc in hexanes.

8.1.5.16 Synthesis of compound 5.9a

To a pressure vessel (20 mL) were added glycine methyl ester hydrochloride (4.60 mmol, 1.5 eq) and diethylamine (7.70 mmol, 2.5 eq) dissolved in dry DCM (10 mL) and methanol (3 mL). The reaction mixture was stirred at 0°C for 15 minutes, before D-pantolactone (3.1 mmol, 1.0 eq) was added. The mixture was stirred at 60°C for 20 hours, and then loaded directly on silica gel. Purification was achieved using a gradient of 0-100% EtOAc in hexanes, followed by 0-50% MeOH in EtOAc.

8.1.5.17 General protocol 15 for synthesizing compounds 5.9b and 5.10

In a pressure vessel (5 mL), the desired ester (1.08-1.69 mmol, 1.1 eq) and diethylamine (1.47-2.31 mmol, 1.5 eq) dissolved in dry methanol (3 mL) were stirred at 0°C for 15 minutes, before the desired lactone (0.98-1.54 mmol, 1.0 eq) was added. The mixture was stirred at 60°C for 20 hours, and then loaded directly on silica gel. The product was purified using a gradient of 0-100% EtOAc in hexanes, followed by 0-50% MeOH in EtOAc.

8.1.5.18 Synthesis of compound 5.9c

In a pressure vessel (20 mL), methyl aminobutyrate hydrochloride (4.60 mmol, 1.5 eq) and diethylamine (7.70 mmol, 2.5 eq) dissolved in dry DCM (10 mL) and methanol (3 mL) were stirred at 0°C for 15 minutes, before D-pantolactone (3.1 mmol, 1.0 eq) was added. The mixture was stirred at 115°C in a microwave reactor for 2 hours, and then loaded on

silica gel. The product was purified using a gradient of 0-100% EtOAc in hexanes, followed by 0-50% MeOH in EtOAc.

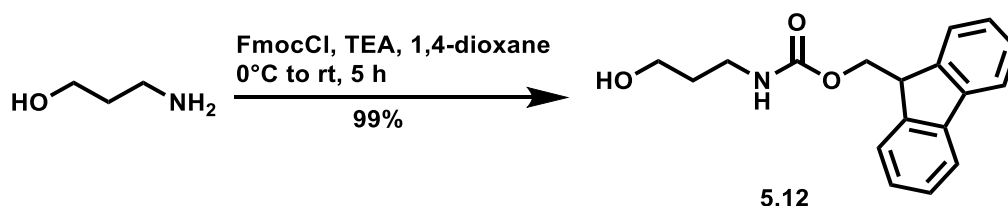
8.1.5.19 General protocol 16 for synthesizing compounds 5.9d and 5.9e

To the desired methyl ester (0.43-0.80 mmol, 1.0 eq) dissolved in THF (5 mL) was added LiOH (0.65-1.20 mmol, 1.5 eq) in water (5 mL). The mixture was stirred at room temperature for 2.5 hours until completion as determined by TLC analysis. The reaction mixture was diluted in brine (10 mL) and acidified to pH ~1. The product was extracted in EtOAc (8 × 25 mL). The combined organic layers were concentrated *in vacuo*. The product was purified using a gradient of 0-100% EtOAc in hexanes, followed by 0-50% MeOH in EtOAc.

8.1.5.20 Synthesis of compound 5.9f

To compound **5.10** (0.49 mmol, 1.0 eq) dissolved in water (2 mL) was added LiOH (0.73 mmol, 1.5 eq) also in water (1 mL). The mixture was stirred at room temperature for 12 hours until completion as determined by TLC analysis. The reaction mixture was next acidified to pH ~3 and purified by reversed-phase HPLC twice. The first purification was achieved using an isocratic elution with 99% water in acetonitrile (both containing 0.05% trifluoroacetic acid) on a 10 × 250 mm, Luna 5 μ CN 100 Å column from Phenomenex, R_t = 8.42 min. The second purification was achieved using an isocratic elution with an aqueous 20 mM NH_4HCO_3 solution on the same column, R_t = 5.63 min.

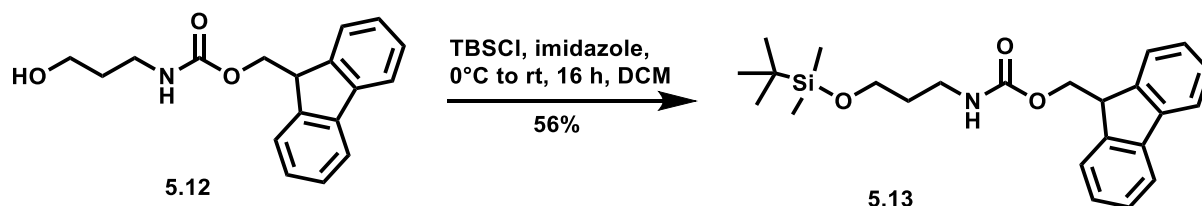
8.1.5.21 Synthesis of compound 5.12



To 3-amino-1-propanol (13.31 mmol, 1.0 eq) dissolved in 1,4-dioxane (40 mL) was added triethylamine (13.31 mmol, 1.0 eq). The mixture was cooled down to 0°C in an ice bath, before dropwise addition of FmocCl (13.31 mmol, 1.0 eq) in 1,4-dioxane (10 mL). The reaction mixture was stirred at 0°C for 1 hour and then at room temperature for another

4 hours. The solvent was removed under reduced pressure. The product was purified on silica gel with 0-100% EtOAc in hexanes.

8.1.5.22 Synthesis of compound 5.13



To compound **5.12** (13.31 mmol, 1.0 eq) in anhydrous DCM (40 mL) at 0°C were added imidazole (13.31 mmol, 1.0 eq) and TBSCl (13.31 mmol, 1.0 eq) sequentially. The reaction mixture was stirred for 16 hours while allowing the temperature to slowly warm up. The salts formed were filtered, and the filtrate was concentrated under reduced pressure. Purification was achieved with a gradient of 0-100% EtOAc in hexanes.

8.1.6 Synthesis of compounds in chapter 6

8.1.6.1 Synthesis of compound P-1b

To a solution of neamine (1.80 mmol, 1.0 eq) in water (6 mL) was added the *endo-N*-hydroxy-5-norbornene-2,3-dicarboximide bromopropanoate (0.92 mmol, 0.5 eq) in acetone (4 mL) dropwise, which was prepared as previously reported.¹³² The solution was stirred for 15 minutes, before dropwise addition of a mixture of D-pantethine (0.48 mmol, 0.3 eq), diisopropylethylamine (23.00 mmol, 12.8 eq), and dithiothreitol (0.52 mmol, 0.3 eq) in water (4 mL). This solution was allowed to stir for 8 hours at room temperature. The acetone was next evaporated *in vacuo* and the residue was redissolved in water (10 mL). Trifluoroacetic acid (1.0 M) was added dropwise until the reaction mixture reached a pH of ~3. The solution was washed with EtOAc (3 × 10 mL). The aqueous layer was concentrated (~1 mL) on a lyophilizer and purified by reversed-phase HPLC. The first purification was achieved using the gradient 1 (Table 8.1) on a reversed-phase 21.20 × 250 mm, Luna 5 μm CN 100 Å column from Phenomenex, $R_t = 25.38$ min. The second purification was achieved using the gradient 2 (Table 8.1) on a reversed-phase 9.4 × 250 mm, Zorbax 300 SB-C8 column from Agilent, $R_t = 9.03$ min.

Table 8.1. HPLC methods for purifying **P-1b**.

Gradient 1			Gradient 2		
Flow rate: 3 mL/min; wavelength: 214 nm			Flow rate: 2 mL/min; wavelength: 214 nm		
Time (min)	Water (%)	Acetonitrile (%)	Time (min)	Water (%)	Acetonitrile (%)
0	99	1	0	99	1
5	99	1	15	50.5	49.5
25	60	40	17	99	1
37	1	99	18	99	1
42	1	99			
50	99	1			
52	99	1			

8.1.6.2 Synthesis of compound 6.3b

To a mixture of ATP (2.5 μmol , 1.0 eq), **P-1b** (2.5 μmol , 1.0 eq), dithiothreitol (1.0 μmol , 0.4 eq), MgCl_2 (10 μmol , 4.0 eq) and KCl (20 μmol , 8.0 eq) dissolved in Tris-HCl buffer (50 mM, pH = 7.6, 960 μL), was added the purified *E. coli* PanK (0.0004 μmol , 20 μL) and purified *E. coli* PPAT (0.0015 μmol , 20 μL). The reaction was incubated for 4 hours at 37°C, before quenching by DCM (-20°C, 1 mL) containing 0.1 M formic acid for 5 minutes. The precipitated protein was removed by centrifugation (14,000 $\times g$) for 2 minutes. The supernatant was purified using gradient 1 with the Agilent 6120 Quadrupole LCMS system (Table 8.2), $R_t = 9.73$ min.

Table 8.2. HPLC methods for purifying and analyzing compound **6.3b**.

Gradient 1		
Flow rate: 0.5 mL/min; wavelength: 214 nm		
Column: ZORBAX RX-C18 5 μm 4.6 x 150 mm from Agilent		
Time (min)	Water with 0.1% formic acid additive (%)	Acetonitrile (%)
0	95	5
3	95	5
10	60	40
12	60	40
14	0	100

Method A

Flow rate: 0.2 mL/min; wavelength: 260 nm

Column: ZORBAX 1.8 μ m SB-C18 2.1 x 50 mm from Agilent

Time (min)	Water with 0.1% formic acid additive (%)	Acetonitrile (%)
0	95	5
1	95	5
8	60	40
10	0	100
12	0	100
12.5	95	5

Method B

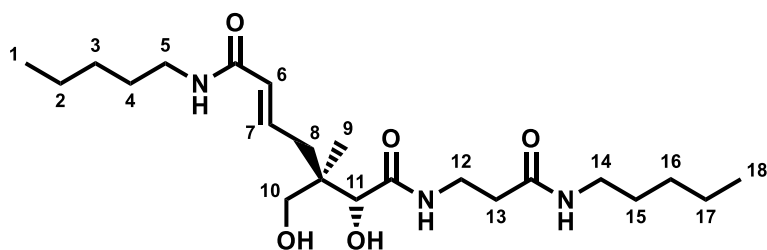
Flow rate: 0.5 mL/min; wavelength: 260 nm

Column: SYNERGI 4 μ Hydro-RP 80 Å from Phenomenex

Time (min)	Water with 20 mM NH ₄ HCO ₃ additive (%)	Acetonitrile (%)
0	99	1
3	99	1
13	90	10
20	60	40
23	60	40
25	99	1

8.2 Compound characterization

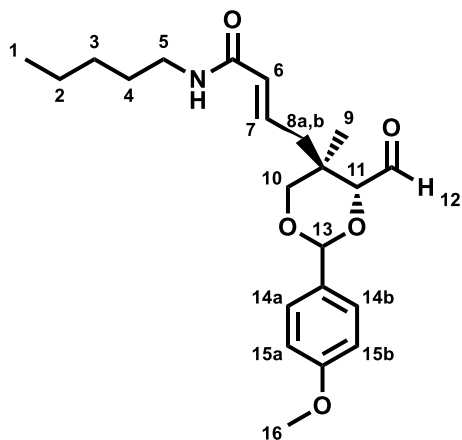
(5*R*,6*R*,*E*)-6-Hydroxy-5-(hydroxymethyl)-5-methyl-*N*'-(3-oxo-3-(pentylamino)propyl)-*N*¹-pentylhept-2-enediamide (2.10)



Compound **2.10** was prepared from compound **2.18** (0.13 mmol) as described in section 8.1.2.1. Yield: 84%, R_f = 0.33 (10% MeOH in EtOAc). ¹H NMR (500 MHz, CDCl₃) δ 7.56 (t, J = 6.1 Hz, 1H, -NH), 6.78 (dt, J = 15.1, 7.8 Hz, 1H, H-7), 6.64 (t, J = 5.4 Hz, 1H, -NH),

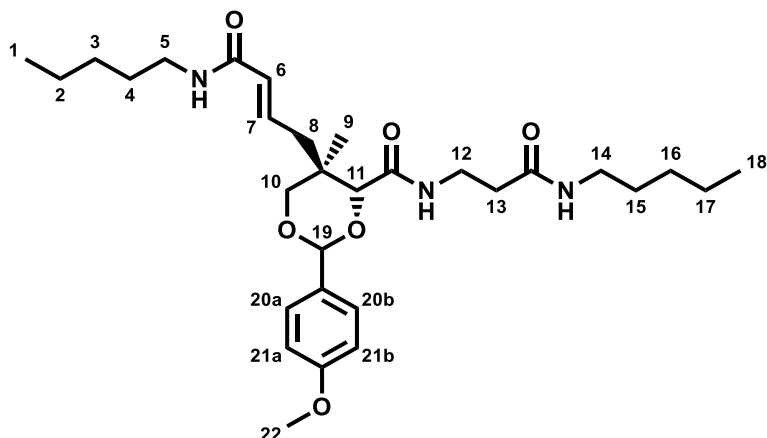
6.01 (t, $J = 5.6$ Hz, 1H, -NH), 5.84 (d, $J = 15.1$ Hz, 1H, H-6), 4.03 (s, 1H, H-11), 3.65–3.49 (m, 4H, H-10, H-12 or H-13), 3.27 (m, 2H, H-5 or H-14), 3.19 (m, 2H, H-5 or H-14), 2.50–2.39 (m, 2H, H-12 or H-13), 2.31 (d, $J = 7.8$ Hz, 2H, H-8), 1.56–1.44 (m, 4H, H-4, H-15), 1.36–1.27 (m, 8H, H-2, H-3, H-16, H-17), 0.99 (s, 3H, H-9), 0.89 (m, 6H, H-1, H-18). ^{13}C NMR (125 MHz, CDCl_3) δ 173.6, 171.4, 166.0, 140.4, 126.4, 76.0, 68.3, 42.6, 39.6, 39.5, 36.5, 35.6, 35.2, 29.1, 29.1, 29.0, 29.0, 22.2, 22.2, 19.5, 13.8, 13.8. HRMS for $\text{C}_{22}\text{H}_{41}\text{N}_3\text{O}_5$ $[\text{M}+\text{H}]^+$ calcd. 428.3119, found 428.3110.

(*E*)-4-((4*R*,5*R*)-4-Formyl-2-(4-methoxyphenyl)-5-methyl-1,3-dioxan-5-yl)-*N*-pentylbut-2-enamide (2.15)



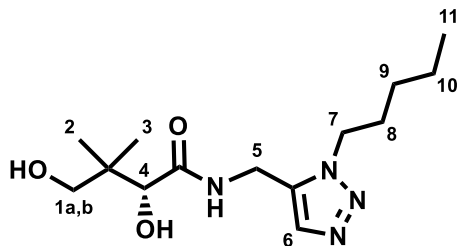
Compound **2.15** was prepared from compound **2.9d** (0.61 mmol) as described in section 8.1.2.2.¹⁴⁸ Yield: 49%, $R_f = 0.75$ (100% EtOAc). The characterization data is in agreement with the previous report. ^1H NMR (500 MHz, CDCl_3) δ 9.65 (s, 1H, H-12), 7.46 (d, $J = 8.7$ Hz, 2H, H-14a,b or H-15a,b), 6.92 (d, $J = 8.7$ Hz, 2H, H-14a,b or H-15a,b), 6.81 (m, 1H, H-7), 5.87 (d, $J = 15.0$ Hz, 1H, H-6), 5.48 (s, 1H, H-13), 5.44 (bs, 1H, -NH), 4.06 (s, 1H, H-11), 3.87–3.77 (m, 5H, H-10, H-16), 3.32 (m, 2H, H-5), 2.39 (dd, $J = 14.3, 8.4$ Hz, 1H, H-8a), 2.31 (dd, $J = 14.2, 7.6$ Hz, 1H, H-8b), 1.53 (m, 2H, H-4), 1.37–1.28 (m, 4H, H-2, H-3), 1.27 (s, 3H, H-9), 0.90 (t, $J = 6.8$ Hz, 3H, H-1). ^{13}C NMR (125 MHz, CDCl_3) δ 202.4, 165.0, 160.4, 137.5, 130.0, 127.9, 127.5, 113.8, 101.5, 85.1, 76.0, 55.4, 39.6, 37.4, 36.7, 29.3, 29.1, 22.4, 18.1, 14.0; HRMS for $\text{C}_{22}\text{H}_{31}\text{NO}_5$ $[\text{M}-\text{H}]^-$ calcd. 388.2130, found 388.2126.

(4*R*,5*R*)-2-(4-Methoxyphenyl)-5-methyl-*N*-(3-oxo-3-(pentylamino)propyl)-5-((*E*)-4-oxo-4-(pentylamino)but-2-en-1-yl)-1,3-dioxane-4-carboxamide (2.18)



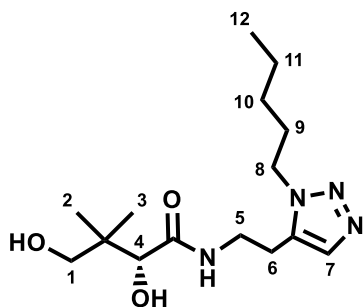
Compound **2.18** was prepared from compound **2.15** (0.28 mmol) as described in section 8.1.2.3. Yield: 51%, $R_f = 0.15$ (100% EtOAc). The characterization data is in agreement with previous report.¹⁴⁸ ^1H NMR (500 MHz, CDCl_3) δ 7.40 (d, $J = 8.7$ Hz, 2H, H-20a,b or H-21a,b), 7.02 (m, 1H, -NH), 6.92 (d, $J = 8.7$ Hz, 2H, H-20a,b or H-21a,b), 6.86 (dt, $J = 15.4, 7.9$ Hz, 1H, H-7), 5.91 (d, $J = 15.3$ Hz, 1H, H-6), 5.86 (m, 1H, -NH), 5.45 (m, 1H, -NH), 5.42 (s, 1H, H-19), 4.20 (s, 1H, H-11), 3.86–3.75 (m, 5H, H-10, H-22), 3.54 (m, 2H, H-12 or H-13), 3.31 (m, 2H, H-5 or H-14), 3.20 (m, 2H, H-5 or H-14), 2.54–2.34 (m, 4H, H-8, H-12 or H-13), 1.55–1.42 (m, 4H, H-4, H-15), 1.37–1.26 (m, 8H, H-2, H-3, H-16, H-17), 1.14 (s, 3H, H-9), 0.89 (m, 6H, H-1, H-18). ^{13}C NMR (125 MHz, CDCl_3) δ 170.6, 169.3, 165.4, 160.3, 138.6, 129.9, 127.5, 127.5, 113.7, 101.3, 81.9, 76.1, 55.3, 39.6, 39.6, 37.9, 36.1, 35.9, 35.1, 29.3, 29.2, 29.1, 29.0, 22.3, 22.3, 17.9, 14.0, 14.0. HRMS for $\text{C}_{30}\text{H}_{47}\text{N}_3\text{O}_6$ $[\text{M}+\text{H}]^+$ calcd. 546.3538, found 546.3535.

(*R*)-2,4-Dihydroxy-3,3-dimethyl-*N*-((1-pentyl-1*H*-1,2,3-triazol-5-yl)methyl)butanamide (3.2a)



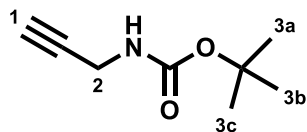
Compound **3.2a** was prepared from **3.5a** (0.19 mmol) using general protocol 1. Yield: 72%, $R_f = 0.62$ (20% MeOH in EtOAc). $^1\text{H NMR}$ (500 MHz, CDCl_3) δ 7.54 (s, 1H, H-6), 7.23 (bs, 1H, -NH), 4.62–4.52 (m, 2H, H-5), 4.33 (m, 2H, H-7), 4.12 (s, 1H, H-4), 3.57 (d, $J = 11.0$ Hz, 1H, H-1a), 3.54 (d, $J = 11.0$ Hz, 1H, H-1b), 1.89 (m, 2H, H-8), 1.39–1.30 (m, 4H, H-9, H-10), 1.03 (s, 3H, H-2 or H-3), 0.96 (s, 3H, H-2 or H-3), 0.90 (t, $J = 7.0$ Hz, 3H, H-11). $^{13}\text{C NMR}$ (126 MHz, CDCl_3) δ 173.24, 133.96, 132.98, 78.07, 71.51, 48.36, 39.20, 31.31, 29.91, 28.66, 22.14, 21.04, 20.67, 13.85. HRMS for $\text{C}_{14}\text{H}_{26}\text{N}_4\text{O}_3\text{Na}$ $[\text{M}+\text{Na}]^+$ calcd. 321.1897, found 321.1890.

(R)-2,4-Dihydroxy-3,3-dimethyl-N-(2-(1-pentyl-1H-1,2,3-triazol-5-yl)ethyl)butanamide (3.2b)



Compound **3.2b** was prepared from **3.5b** (0.35 mmol) using general protocol 1. Yield: 72%, $R_f = 0.56$ (20% MeOH in EtOAc). $^1\text{H NMR}$ (500 MHz, CDCl_3) δ 7.51 (s, 1H, H-7), 7.16 (bs, 1H, -NH), 4.26 (t, $J = 7.4$ Hz, 2H, H-8), 4.05 (s, 1H, H-4), 3.59 (m, 2H, H-5), 3.49 (m, 2H, H-1), 2.93 (m, 2H, H-6), 1.88 (m, 2H, H-9), 1.40–1.28 (m, 4H, H-10, H-11), 0.99 (s, 3H, H-2 or H-3), 0.94–0.86 (m, 6H, H-2 or H-3, H-12). $^{13}\text{C NMR}$ (126 MHz, CDCl_3) δ 173.48, 133.94, 132.19, 77.75, 71.46, 48.01, 39.24, 37.48, 29.82, 28.68, 23.39, 22.15, 21.17, 20.37, 13.86. HRMS for $\text{C}_{15}\text{H}_{29}\text{N}_4\text{O}_3$ $[\text{M}+\text{H}]^+$ calcd. 313.22342, found 313.22281.

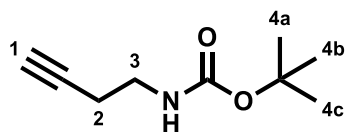
tert-Butyl prop-2-yn-1-ylcarbamate (3.3a)



Compound **3.3a** was prepared from propargylamine (9.08 mmol) using general protocol 2. Yield: 81%, $R_f = 0.65$ (30% EtOAc in hexanes). The characterization data is in

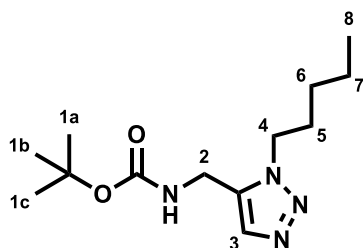
agreement with the previous report.²¹⁴ ¹H NMR (500 MHz, CDCl₃) δ 4.69 (bs, 1H, -NH), 3.92 (s, 2H, H-2), 2.21 (t, *J* = 2.5 Hz, 1H, H-1), 1.45 (s, 9H, H-3a,b,c).

***tert*-Butyl but-3-yn-1-ylcarbamate (3.3b)**



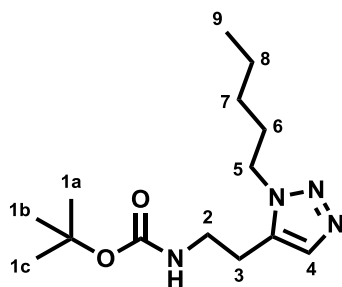
Compound **3.3b** was prepared from 3-butyn-1-amine hydrochloride (4.74 mmol) using general protocol 2. Yield: 84%, *R*_f = 0.22 (10% EtOAc in hexanes). The characterization data is in agreement with a previous report one.²¹⁵ ¹H NMR (400 MHz, CDCl₃) δ 4.84 (bs, 1H, -NH), 3.28 (m, 2H, H-3), 2.38 (td, *J* = 6.4, 2.6 Hz, 2H, H-2), 2.00 (t, *J* = 2.6 Hz, 1H, H-1), 1.45 (s, 9H, H-4a,b,c).

***tert*-Butyl ((1-pentyl-1*H*-1,2,3-triazol-5-yl)methyl)carbamate (3.5a)**



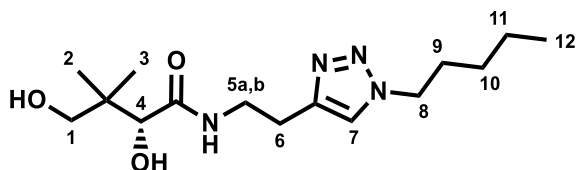
Compound **3.5a** was prepared from **3.3a** (0.64 mmol) using general protocol 3. Yield: 43%, *R*_f = 0.24 (50% EtOAc in hexanes). ¹H NMR (500 MHz, CDCl₃) δ 7.55 (s, 1H, H-3), 4.87 (bs, 1H, -NH), 4.41 (d, *J* = 5.4 Hz, 2H, H-2), 4.31 (t, *J* = 7.4 Hz, 2H, H-4), 1.87 (m, 2H, H-5), 1.45 (s, 9H, H-1a,b,c), 1.36–1.30 (m, 4H, H-6, H-7), 0.89 (t, *J* = 6.8 Hz, 3H, H-8). ¹³C NMR (126 MHz, CDCl₃) δ 155.37, 134.13, 133.11, 80.45, 48.22, 33.25, 29.96, 28.70, 28.29, 22.18, 13.87. HRMS for C₁₃H₂₄N₄O₂Na [M+Na]⁺ calcd. 291.1791, found 291.1800.

tert-Butyl (2-(1-pentyl-1*H*-1,2,3-triazol-5-yl)ethyl)carbamate (3.5b)



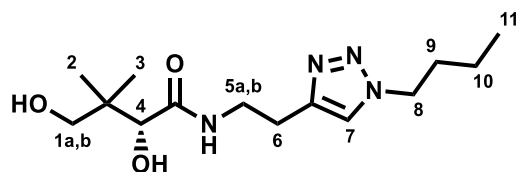
Compound **3.5b** was prepared from **3.3b** (1.18 mmol) using general protocol 3. Yield: 73%, $R_f = 0.17$ (50% EtOAc in hexanes). $^1\text{H NMR}$ (400 MHz, CDCl_3) δ 7.49 (s, 1H, H-4), 4.70 (bs, 1H, -NH), 4.25 (t, $J = 7.4$ Hz, 2H, H-5), 3.40 (m, 2H, H-2), 2.87 (m, 2H, H-3), 1.87 (m, 2H, H-6), 1.44 (s, 9H, H-1a,b,c), 1.39–1.26 (m, 4H, H-7, H-8), 0.90 (t, $J = 7.0$ Hz, 3H, H-9). $^{13}\text{C NMR}$ (126 MHz, CDCl_3) δ 155.76, 134.04, 132.16, 79.85, 47.88, 39.37, 29.87, 28.69, 28.35, 23.92, 22.16, 13.86. HRMS for $\text{C}_{14}\text{H}_{27}\text{N}_4\text{O}_2$ $[\text{M}+\text{H}]^+$ calcd. 283.21285, found 283.21263.

(*R*)-2,4-Dihydroxy-3,3-dimethyl-*N*-(2-(1-pentyl-1*H*-1,2,3-triazol-4-yl)ethyl)butanamide (3.7a)



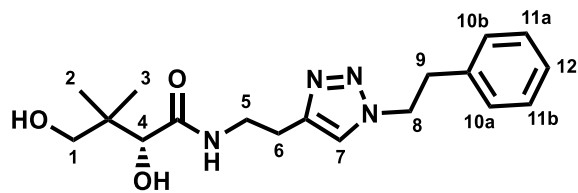
Compound **3.7a** was prepared from **3.8a** (0.28 mmol) using general protocol 1. Yield: 17%, $R_f = 0.65$ (20% MeOH in EtOAc). $^1\text{H NMR}$ (500 MHz, CDCl_3) δ 7.38 (s, 1H, H-7), 7.28 (bs, 1H, -NH), 4.30 (t, $J = 7.3$ Hz, 2H, H-8), 3.98 (s, 1H, H-4), 3.69 (m, 1H, H-5a), 3.59–3.42 (m, 3H, H-1, H-5b), 2.91 (m, 2H, H-6), 1.88 (m, 2H, H-9), 1.38–1.28 (m, 4H, H-10, H-11), 1.01 (s, 3H, H-2 or H-3), 0.94 (s, 3H, H-2 or H-3), 0.89 (t, $J = 7.2$ Hz, 3H, H-12). $^{13}\text{C NMR}$ (126 MHz, CDCl_3) δ 173.40, 145.25, 121.45, 78.12, 70.61, 50.43, 39.20, 38.45, 29.94, 28.58, 25.69, 22.08, 21.93, 20.85, 13.84. HRMS for $\text{C}_{15}\text{H}_{28}\text{N}_4\text{O}_3\text{Na}$ $[\text{M}+\text{Na}]^+$ calcd. 335.2054, found 335.2049.

(R)-N-(2-(1-Butyl-1H-1,2,3-triazol-4-yl)ethyl)-2,4-dihydroxy-3,3-dimethylbutanamide (3.7b)



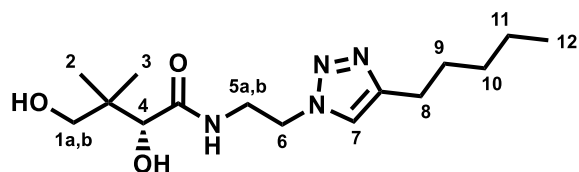
Compound **3.7b** was prepared from **3.8b** (0.37 mmol) using general protocol 1. Yield: 39%, $R_f = 0.61$ (20% MeOH in EtOAc). ^1H NMR (500 MHz, CDCl_3) δ 7.39 (s, 1H, H-7), 7.34 (m, 1H, -NH), 4.30 (t, $J = 7.2$ Hz, 2H, H-8), 3.99 (s, 1H, H-4), 3.65 (m, 1H, H-5a), 3.53 (m, 1H, H-5b), 3.49 (d, $J = 11.2$ Hz, 1H, H-1a), 3.42 (d, $J = 11.2$ Hz, 1H, H-1b), 2.91 (m, 2H, H-6), 1.85 (m, 2H, H-8), 1.33 (m, 2H, H-10), 0.99–0.89 (m, 9H, H-2, H-3, H-11). ^{13}C NMR (126 MHz, CDCl_3) δ 173.68, 145.14, 121.54, 77.72, 70.54, 50.13, 39.20, 38.42, 32.18, 25.67, 21.73, 20.71, 19.68, 13.43. HRMS for $\text{C}_{14}\text{H}_{26}\text{N}_4\text{O}_3\text{Na}$ $[\text{M}+\text{Na}]^+$ calcd. 321.1897, found 321.1887.

(R)-2,4-Dihydroxy-3,3-dimethyl-N-(2-(1-phenethyl-1H-1,2,3-triazol-4-yl)ethyl)butanamide (3.7c)



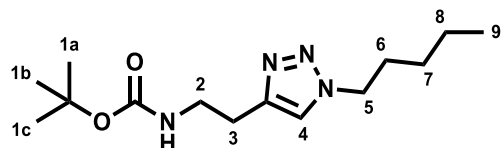
Compound **3.7c** was prepared from **3.8c** (0.38 mmol) using general protocol 1. Yield: 38%, $R_f = 0.57$ (10% MeOH in EtOAc). ^1H NMR (500 MHz, CDCl_3) δ 7.30–7.22 (m, 4H, -NH, H-10a,b or H-11a,b, H-12), 7.14 (s, 1H, H-7), 7.11–7.06 (m, 2H, H-10a,b or H-11a,b), 4.54 (t, $J = 7.3$ Hz, 2H, H-8), 3.98 (s, 1H, H-4), 3.63–3.43 (m, 4H, H-1, H-5), 3.18 (t, $J = 7.3$ Hz, 2H, H-9), 2.86 (t, $J = 6.3$, 2H, H-6), 0.99 (s, 3H, H-2 or H-3), 0.93 (s, 3H, H-2 or H-3). ^{13}C NMR (126 MHz, CDCl_3) δ 173.42, 145.00, 136.87, 128.82, 128.62, 127.16, 121.93, 78.02, 70.65, 51.66, 39.21, 38.48, 36.65, 25.59, 21.87, 20.77. HRMS for $\text{C}_{18}\text{H}_{26}\text{N}_4\text{O}_3\text{Na}$ $[\text{M}+\text{Na}]^+$ calcd. 369.1897, found 369.1883.

(R)-2,4-Dihydroxy-3,3-dimethyl-N-(2-(4-pentyl-1*H*-1,2,3-triazol-1-yl)ethyl)butanamide (3.7d)



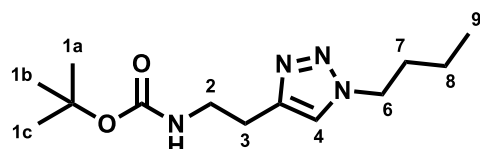
Compound **3.7d** was prepared from **3.8d** (0.23 mmol) using general protocol 1. Yield: 16%, $R_f = 0.37$ (8% MeOH in EtOAc). ^1H NMR (500 MHz, CD_3OD) δ 7.74 (s, 1H, H-7), 4.50 (t, $J = 6.0$ Hz, 2H, H-6), 3.87 (s, 1H, H-4), 3.76 (dt, $J = 14.0, 6.0$ Hz, 1H, H-5a), 3.66 (dt, $J = 14.1, 6.0$ Hz, 1H, H-5b), 3.42 (d, $J = 10.9$ Hz, 1H, H-1a), 3.33 (d, $J = 11.0$ Hz, 1H, H-1b), 2.67 (t, $J = 7.6$, 2H, H-8), 1.67 (m, 2H, H-9), 1.38–1.34 (m, 4H, H-10, H-11), 0.92 (t, $J = 7.0$ Hz, 3H, H-12), 0.84 (s, 6H, H-2, H-3). ^{13}C NMR (126 MHz, CD_3OD) δ 176.52, 149.35, 123.42, 77.26, 70.30, 50.35, 40.32, 39.82, 32.48, 30.28, 26.25, 23.46, 21.29, 20.75, 14.32. HRMS for $\text{C}_{15}\text{H}_{27}\text{N}_4\text{O}_3$ $[\text{M}-\text{H}]^-$ calcd. 311.20886, found 331.20924.

tert-Butyl (2-(1-pentyl-1*H*-1,2,3-triazol-4-yl)ethyl)carbamate (3.8a)



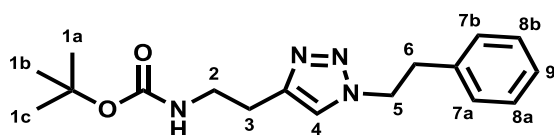
Compound **3.8a** was prepared from **3.3b** (0.59 mmol) using general protocol 4. Yield: 48%, $R_f = 0.18$ (50% EtOAc in hexanes). ^1H NMR (400 MHz, CDCl_3) δ 7.33 (s, 1H, H-4), 5.00 (bs, 1H, -NH), 4.31 (t, $J = 7.3$ Hz, 2H, H-5), 3.46 (m, 2H, H-2), 2.90 (t, $J = 6.6$ Hz, 2H, H-3), 1.88 (m, 2H, H-6), 1.42 (s, 9H, H-1a,b,c), 1.39–1.24 (m, 4H, H-7, H-8), 0.90 (t, $J = 7.0$ Hz, 3H, H-9). ^{13}C NMR (126 MHz, CDCl_3) δ 155.98, 145.32, 121.15, 79.16, 50.26, 39.83, 29.99, 28.61, 28.39, 26.19, 22.08, 13.82. HRMS for $\text{C}_{14}\text{H}_{26}\text{N}_4\text{O}_2\text{Na}$ $[\text{M}+\text{Na}]^+$ calcd. 305.1948, found 305.1950.

tert-Butyl (2-(1-butyl-1*H*-1,2,3-triazol-4-yl)ethyl)carbamate (3.8b)



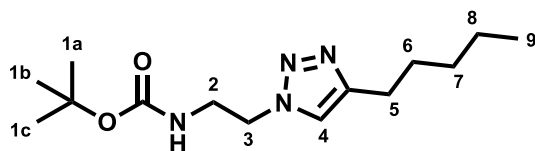
Compound **3.8b** was prepared from **3.3b** (1.18 mmol) using general protocol 4. Yield: 61%, $R_f = 0.14$ (50% EtOAc in hexanes). ^1H NMR (400 MHz, CDCl_3) δ 7.33 (s, 1H, H-4), 5.00 (bs, 1H, -NH), 4.32 (t, $J = 7.2$ Hz, 2H, H-6), 3.46 (m, 2H, H-2), 2.90 (t, $J = 6.6$ Hz, 2H, H-3), 1.87 (m, 2H, H-7), 1.42 (s, 9H, H-1a,b,c), 1.35 (m, 2H, H-8), 0.95 (t, $J = 7.4$ Hz, 3H, H-9). ^{13}C NMR (126 MHz, CDCl_3) δ 155.99, 145.33, 121.18, 79.19, 50.00, 39.82, 32.28, 28.40, 26.20, 19.73, 13.47. HRMS for $\text{C}_{13}\text{H}_{24}\text{N}_4\text{O}_2\text{Na}$ $[\text{M}+\text{Na}]^+$ calcd. 291.1791, found 291.1789.

***tert*-Butyl (2-(1-phenethyl-1*H*-1,2,3-triazol-4-yl)ethyl)carbamate (3.8c)**



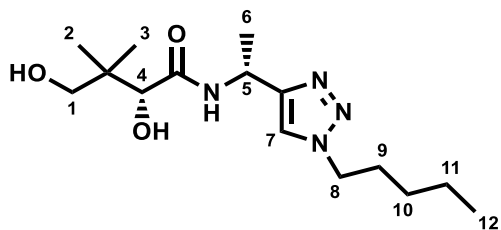
Compound **3.8c** was prepared from **3.3b** (0.59 mmol) using general protocol 4. Yield: 68%, $R_f = 0.39$ (50% EtOAc in hexanes). The characterization data is in agreement with the previous report.²¹⁶ ^1H NMR (500 MHz, CDCl_3) δ 7.31–7.23 (m, 3H, H-4 or H-9, H-7a,b or H-8a,b), 7.10–7.06 (m, 3H, H-4 or H-9, H-7a,b or H-8a,b), 4.90 (bs, 1H, -NH), 4.55 (t, $J = 7.3$ Hz, 2H, H-5), 3.41 (m, 2H, H-2), 3.19 (t, $J = 7.3$ Hz, 2H, H-3), 2.84 (t, $J = 6.5$ Hz, 2H, H-6), 1.43 (s, 9H, H-1a,b,c).

***tert*-Butyl (2-(4-pentyl-1*H*-1,2,3-triazol-1-yl)ethyl)carbamate (3.8d)**



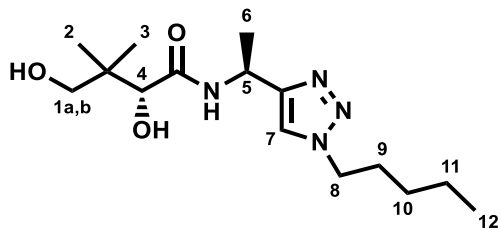
Compound **3.8d** was prepared from 2-(Boc-amino)ethyl bromide (1.21 mmol) using general protocol 4. Yield: 11%, $R_f = 0.21$ (50% EtOAc in hexanes). The characterization data is in agreement with a previous report.²¹⁷ ^1H NMR (500 MHz, CDCl_3) δ 7.28 (s, 1H, H-4), 4.85 (bs, 1H, -NH), 4.43 (m, 2H, H-5), 3.63 (m, 2H, H-2), 2.71 (t, $J = 7.7$ Hz, 2H, H-3), 1.67 (m, 2H, H-6), 1.43 (s, 9H, H-1a,b,c), 1.36–1.33 (m, 4H, H-7, H-8), 0.90 (t, $J = 7.1$ Hz, 3H, H-9).

(R)-2,4-Dihydroxy-3,3-dimethyl-N-((R)-1-(1-pentyl-1*H*-1,2,3-triazol-4-yl)ethyl)butanamide (3.9a)



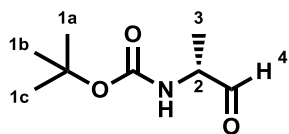
Compound **3.9a** was prepared from **3.12a** (0.50 mmol) using general protocol 1. Yield: 28%, $R_f = 0.49$ (10% MeOH in EtOAc). ^1H NMR (500 MHz, CDCl_3) δ 7.48–7.43 (m, 2H, -NH, H-7), 5.26 (dq, $J = 14.1, 7.0$ Hz, 1H, H-5), 4.30 (t, $J = 7.3$ Hz, 2H, H-8), 4.06 (s, 1H, H-4), 3.50 (m, 2H, H-1), 1.88 (m, 2H, H-9), 1.58 (d, $J = 6.9$ Hz, 3H, H-6), 1.37–1.28 (m, 4H, H-10, H-11), 1.03 (s, 3H, H-2 or H-3), 0.92–0.88 (6H, H-2 or H-3, H-12). ^{13}C NMR (126 MHz, CDCl_3) δ 172.68, 148.95, 120.78, 77.10, 71.07, 50.48, 41.08, 39.57, 29.91, 28.59, 22.06, 21.68, 21.11, 19.96, 13.82. HRMS for $\text{C}_{15}\text{H}_{28}\text{N}_4\text{O}_3\text{Na}$ $[\text{M}+\text{Na}]^+$ calcd. 335.2054, found 335.2059.

(R)-2,4-Dihydroxy-3,3-dimethyl-N-((S)-1-(1-pentyl-1*H*-1,2,3-triazol-4-yl)ethyl)butanamide (3.9b)



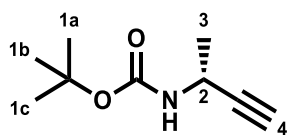
Compound **3.9b** was prepared from **3.12b** (0.50 mmol) using general protocol 1. Yield: 27%, $R_f = 0.17$ (100% EtOAc). ^1H NMR (500 MHz, CDCl_3) δ 7.51 (d, $J = 8.3$ Hz, 1H, -NH), 7.45 (s, 1H, H-7), 5.25 (m, 1H, H-5), 4.29 (t, $J = 7.2$ Hz, 2H, H-8), 4.02 (s, 1H, H-4), 3.50 (d, $J = 11.2$ Hz, 1H, H-1a), 3.42 (d, $J = 11.2$ Hz, 1H, H-1b), 1.88 (m, 2H, H-9), 1.55 (d, $J = 7.0$ Hz, 3H, H-6), 1.38–1.23 (m, 4H, H-10, H-11), 0.95 (s, 3H, H-2 or H-3), 0.92 (s, 3H, H-2 or H-3), 0.87 (t, $J = 7.1$ Hz, 3H, H-12). ^{13}C NMR (126 MHz, CDCl_3) δ 172.80, 149.20, 120.77, 77.65, 70.75, 50.47, 41.02, 39.46, 29.89, 28.54, 22.04, 21.64, 20.89, 20.82, 13.81. HRMS for $\text{C}_{15}\text{H}_{28}\text{N}_4\text{O}_3\text{Na}$ $[\text{M}+\text{Na}]^+$ calcd. 335.20536, found 335.20472.

***tert*-Butyl (*R*)-(1-oxopropan-2-yl)carbamate (3.10a)**



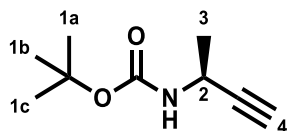
Compound **3.10a** was prepared from Boc-D-alaninol (5.71 mmol) as described in section 8.1.3.5. Yield: 79%, $R_f = 0.33$ (30% EtOAc in hexanes). The characterization data is in agreement with previous report.²¹⁸ ^1H NMR (500 MHz, CDCl_3) δ 9.56 (s, 1H, H-4), 5.09 (bs, 1H, -NH), 4.23 (m, 1H, H-2), 1.45 (s, 9H, H-1a,b,c), 1.33 (d, $J = 7.4$ Hz, 3H, H-3).

***tert*-Butyl (*R*)-but-3-yn-2-ylcarbamate (3.11a)**



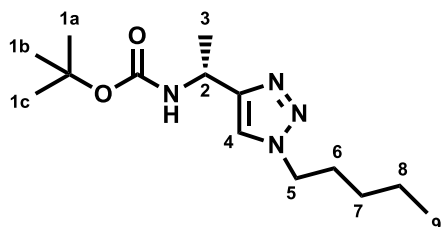
Compound **3.11a** was prepared from **3.10a** (1.73 mmol) using general protocol 5. Yield: 78%, $R_f = 0.56$ (20% EtOAc in hexanes). The characterization data is in agreement with the previous report.²¹⁹ ^1H NMR (400 MHz, CDCl_3) δ 4.71 (bs, 1H, -NH), 4.48 (m, 1H, H-2), 2.25 (d, $J = 2.3$ Hz, 1H, H-4), 1.44 (s, 9H, H-1a,b,c), 1.39 (d, $J = 6.9$ Hz, 3H, H-3).

***tert*-Butyl (*S*)-but-3-yn-2-ylcarbamate (3.11b)**



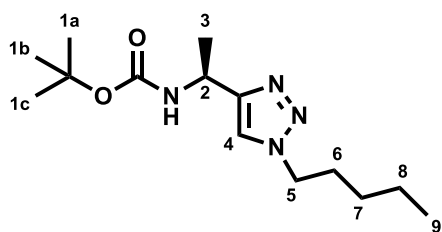
Compound **3.11b** was prepared from Boc-L-alanine aldehyde (1.73 mmol) using general protocol 5. Yield: 75%, $R_f = 0.56$ (20% EtOAc in hexanes). The characterization data is in agreement with the previous report.²²⁰ ^1H NMR (500 MHz, CDCl_3) δ 4.69 (bs, 1H, -NH), 4.49 (m, 1H, H-2), 2.25 (d, $J = 2.3$ Hz, 1H, H-4), 1.45 (s, 9H, H-1a,b,c), 1.40 (d, $J = 6.9$ Hz, 3H, H-3).

***tert*-Butyl (*R*)-(1-(1-pentyl-1*H*-1,2,3-triazol-4-yl)ethyl)carbamate (3.12a)**



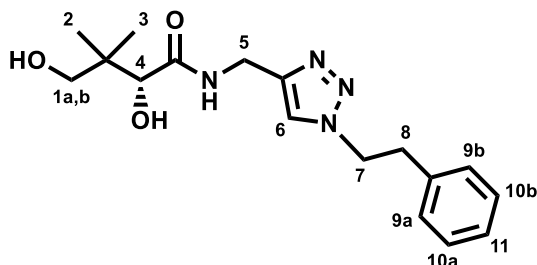
Compound **3.12a** was prepared from **3.11a** (1.18 mmol) using general protocol 4. Yield: 47%, $R_f = 0.25$ (40% EtOAc in hexanes). ^1H NMR (500 MHz, CDCl_3) δ 7.40 (s, 1H, H-4), 5.10 (bs, 1H, -NH), 4.92 (m, 1H, H-2), 4.31 (m, 2H, H-5), 1.87 (m, 2H, H-6), 1.56 (d, $J = 6.7$ Hz, 3H, H-3), 1.43 (s, 9H, H-1a,b,c), 1.37–1.26 (m, 4H, H-7, H-8), 0.90 (t, $J = 7.1$ Hz, 3H, H-9). ^{13}C NMR (126 MHz, CDCl_3) δ 155.15, 149.75, 120.38, 79.51, 50.30, 42.90, 29.97, 28.59, 28.37, 22.07, 21.26, 13.81. HRMS for $\text{C}_{14}\text{H}_{26}\text{N}_4\text{O}_2\text{Na}$ $[\text{M}+\text{Na}]^+$ calcd. 305.19480, found 305.19424.

***tert*-Butyl (*S*)-(1-(1-pentyl-1*H*-1,2,3-triazol-4-yl)ethyl)carbamate (3.12b)**



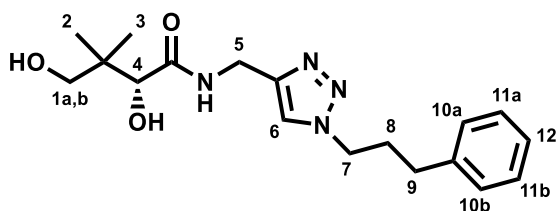
Compound **3.12b** was prepared from **3.11b** (1.18 mmol) using general protocol 4. Yield: 66%, $R_f = 0.42$ (50% EtOAc in hexanes). ^1H NMR (500 MHz, CDCl_3) δ 7.40 (s, 1H, H-4), 5.09 (bs, 1H, -NH), 4.91 (m, 1H, H-2), 4.31 (t, $J = 7.3$ Hz, 2H, H-5), 1.87 (m, 2H, H-6), 1.56 (d, $J = 6.9$ Hz, 3H, H-3), 1.43 (s, 9H, H-1a,b,c), 1.40–1.25 (m, 4H, H-7, H-8), 0.90 (t, $J = 7.1$ Hz, 3H, H-9). ^{13}C NMR (126 MHz, CDCl_3) δ 155.15, 149.76, 120.39, 79.50, 50.30, 42.90, 29.97, 28.59, 28.38, 22.07, 21.26, 13.81. HRMS for $\text{C}_{14}\text{H}_{26}\text{N}_4\text{O}_2\text{Na}$ $[\text{M}+\text{Na}]^+$ calcd. 305.1948, found 305.1954.

(R)-2,4-Dihydroxy-3,3-dimethyl-N-((1-phenethyl-1H-1,2,3-triazol-4-yl)methyl)butanamide (3.13a)



Compound **3.13a** was prepared from **3.14a** (0.40 mmol) using general protocol 1. Yield: 53%, $R_f = 0.29$ (4% MeOH in EtOAc). ^1H NMR (500 MHz, CD_3OD) δ 7.66 (s, 1H, H-6), 7.27–7.18 (m, 3H, H-11, H-9a,b or H-10a,b), 7.15–7.09 (m, 2H, H-9a,b or H-10a,b), 4.62 (t, $J = 7.1$ Hz, 2H, H-7), 4.42 (s, 2H, H-5), 3.91 (s, 1H, H-4), 3.46 (d, $J = 10.9$ Hz, 1H, H-1a), 3.37 (d, $J = 10.9$ Hz, 1H, H-1b), 3.19 (t, $J = 7.1$ Hz, 2H, H-8), 0.89 (m, 6H, H-2, H-3). ^{13}C NMR (126 MHz, CD_3OD) δ 174.61, 144.60, 137.27, 128.35, 128.28, 126.51, 122.98, 75.91, 68.88, 51.23, 39.04, 36.04, 33.58, 19.99, 19.46. HRMS for $\text{C}_{17}\text{H}_{24}\text{N}_4\text{O}_3\text{Na}$ $[\text{M}+\text{Na}]^+$ calcd. 355.17406, found 355.17418.

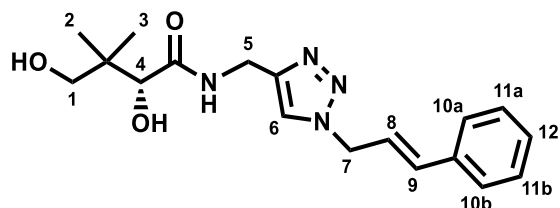
(R)-2,4-Dihydroxy-3,3-dimethyl-N-((1-(3-phenylpropyl)-1H-1,2,3-triazol-4-yl)methyl)butanamide (3.13b)



Compound **3.13b** was prepared from **3.14b** (0.79 mmol) using general protocol 1. Yield: 66%, $R_f = 0.7$ (20% MeOH in EtOAc). ^1H NMR (500 MHz, CDCl_3) δ 7.57 (t, $J = 5.7$ Hz, 1H, -NH), 7.51 (s, 1H, H-6), 7.29 (t, $J = 7.4$ Hz, 2H, H-11a,b), 7.21 (t, $J = 7.4$ Hz, 1H, H-12), 7.15 (d, $J = 7.1$ Hz, 2H, H-10a,b), 4.53 (d, $J = 6.0$ Hz, 2H, H-5), 4.31 (t, $J = 7.1$ Hz, 2H, H-7), 4.06 (s, 1H, H-4), 3.50 (d, $J = 11.2$ Hz, 1H, H-1a), 3.48 (d, $J = 11.2$ Hz, 1H, H-1b), 2.63 (t, $J = 7.5$ Hz, 2H, H-9), 2.24 (m, 2H, H-8), 1.00 (s, 3H, H-2 or H-3), 0.92 (s, 3H, H-2 or H-3). ^{13}C NMR (126 MHz, CDCl_3) δ 173.47, 144.50, 139.96, 128.65, 128.40,

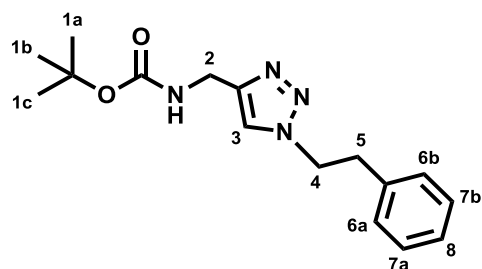
126.41, 122.16, 77.68, 71.04, 49.65, 39.46, 34.31, 32.46, 31.54, 21.56, 20.46. HRMS for $C_{18}H_{26}N_4O_3Na$ $[M+Na]^+$ calcd. 369.1897, found 369.1889.

(R)-N-((1-Cinnamyl-1*H*-1,2,3-triazol-4-yl)methyl)-2,4-dihydroxy-3,3-dimethylbutanamide (3.13c)



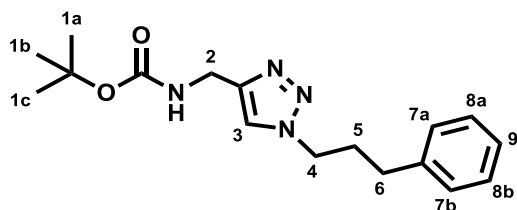
Compound **3.13c** was prepared from **3.14c** (0.72 mmol) using general protocol 1. Yield: 43%, $R_f = 0.45$ (10% MeOH in EtOAc). 1H NMR (500 MHz, $CDCl_3$) δ 7.59 (s, 1H, H-6), 7.49 (t, $J = 5.6$ Hz, 1H, -NH), 7.38–7.27 (m, 5H, H-10a,b, H-11a,b, H-12), 6.67 (d, $J = 15.8$ Hz, 1H, H-9), 6.31 (dt, $J = 15.8, 6.7$ Hz, 1H, H-8), 5.10 (d, $J = 6.7$, 2H, H-7), 4.55 (m, 2H, H-5), 4.05 (s, 1H, H-4), 3.48 (m, 2H, H-1), 1.01 (s, 3H, H-2 or H-3), 0.92 (s, 3H, H-2 or H-3). ^{13}C NMR (126 MHz, $CDCl_3$) δ 173.33, 144.83, 135.73, 135.35, 128.75, 128.65, 126.74, 121.86, 121.50, 77.78, 71.07, 52.50, 39.46, 34.40, 21.61, 20.47. HRMS for $C_{18}H_{24}N_4O_3Na$ $[M+Na]^+$ calcd. 367.17406, found 367.17489.

tert-Butyl ((1-phenethyl-1*H*-1,2,3-triazol-4-yl)methyl)carbamate (3.14a)



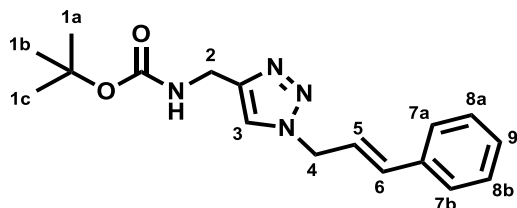
Compound **3.14a** was prepared from **3.3a** (0.64 mmol) using general protocol 4. Yield: 63%, $R_f = 0.18$ (50% EtOAc in hexanes). The characterization data is in agreement with the previous report.²¹⁶ 1H NMR (500 MHz, $CDCl_3$) δ 7.31–7.23 (m, 4H, H-4, H-8, H-6a,b or H-7a,b), 7.13–7.08 (m, 2H, H-6a,b or H-7a,b), 5.08 (bs, 1H, -NH), 4.56 (t, $J = 7.4$ Hz, 2H, H-4), 4.34 (d, $J = 6.0$ Hz, 2H, H-2), 3.19 (t, $J = 7.4$ Hz, 2H, H-5), 1.43 (s, 9H, H-1a,b,c).

***tert*-Butyl ((1-(3-phenylpropyl)-1*H*-1,2,3-triazol-4-yl)methyl)carbamate (3.14b)**



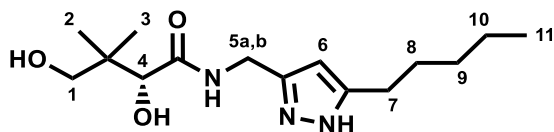
Compound **3.14b** was prepared from **3.3a** (1.29 mmol) using general protocol 4. Yield: 68%, $R_f = 0.24$ (50% EtOAc in hexanes). $^1\text{H NMR}$ (500 MHz, CDCl_3) δ 7.48 (s, 1H, H-3), 7.31–7.28 (m, 2H, H-8a,b), 7.21 (m, 1H, H-9), 7.17–7.15 (m, 2H, H-7a,b), 5.12 (bs, 1H, -NH), 4.38 (d, $J = 6.0$ Hz, 2H, H-2), 4.32 (t, $J = 7.1$ Hz, 2H, H-4), 2.64 (t, $J = 7.5$ Hz, 2H, H-6), 2.25 (m, 2H, H-5), 1.44 (s, 9H, H-1a,b,c). $^{13}\text{C NMR}$ (126 MHz, CDCl_3) δ 155.87, 145.42, 140.09, 128.62, 128.42, 126.36, 121.86, 79.68, 49.51, 36.13, 32.49, 31.60, 28.39. HRMS for $\text{C}_{17}\text{H}_{25}\text{N}_4\text{O}_2$ $[\text{M}+\text{H}]^+$ calcd. 317.19720, found 317.19594.

***tert*-Butyl ((1-cinnamyl)-1*H*-1,2,3-triazol-4-yl)methyl)carbamate (3.14c)**



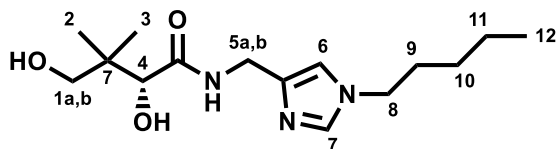
Compound **3.14c** was prepared from **3.3a** (1.29 mmol) using general protocol 4. Yield: 84%, $R_f = 0.20$ (50% EtOAc in hexanes). $^1\text{H NMR}$ (500 MHz, CDCl_3) δ 7.59 (s, 1H, H-3), 7.43–7.29 (m, 5H, H-7a,b, H-8a,b, H-9), 6.69 (d, $J = 15.8$ Hz, 1H, H-6), 6.35 (dt, $J = 15.8$, 6.7 Hz, 1H, H-5), 5.15–5.11 (m, 3H, H-4, -NH), 4.42 (d, $J = 6.0$ Hz, 2H, H-2), 1.45 (s, 9H, H-1a,b,c). $^{13}\text{C NMR}$ (126 MHz, CDCl_3) δ 155.87, 145.79, 135.46, 135.38, 128.72, 128.54, 126.70, 121.86, 121.64, 79.64, 52.33, 36.16, 28.37. HRMS for $\text{C}_{17}\text{H}_{22}\text{N}_4\text{O}_2\text{Na}$ $[\text{M}+\text{Na}]^+$ calcd. 337.16350, found 337.16360.

**(R)-2,4-Dihydroxy-3,3-dimethyl-N-((5-pentyl-1H-pyrazol-3-yl)methyl)butanamide
(4.1a)**



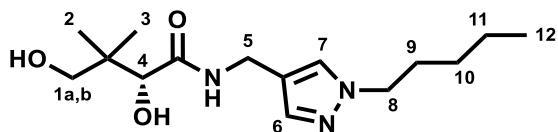
Compound **4.1a** was prepared from **4.3** (0.48 mmol) using general protocol 1. Yield: 31%, $R_f = 0.50$ (10% MeOH in EtOAc). ^1H NMR (500 MHz, CDCl_3) δ 7.55 (m, 1H, -NH), 5.93 (s, 1H, H-6), 4.52 (dd, $J = 15.4, 6.2$ Hz, 1H, H-5a), 4.32 (dd, $J = 15.5, 5.0$ Hz, 1H, H-5b), 4.03 (s, 1H, H-4), 3.47 (m, 2H, H-1), 2.55 (t, $J = 7.7$ Hz, 2H, H-7), 1.58 (m, 2H, H-8), 1.37–1.26 (m, 4H, H-9, H-10), 0.97 (s, 3H, H-2 or H-3), 0.91 (s, 3H, H-2 or H-3), 0.87 (t, $J = 6.7$ Hz, 3H, H-11). ^{13}C NMR (126 MHz, CDCl_3) δ 174.18, 147.71, 147.20, 102.27, 77.28 (based on HSQC and HMBC), 70.51, 39.38, 36.06, 31.40, 28.82, 26.23, 22.36, 21.49, 20.67, 13.96. HRMS for $\text{C}_{15}\text{H}_{27}\text{N}_3\text{O}_3\text{Na}$ $[\text{M}+\text{Na}]^+$ calcd. 320.1945, found 320.1937.

**(R)-2,4-Dihydroxy-3,3-dimethyl-N-((1-pentyl-1H-imidazol-4-yl)methyl)butanamide
(4.1b)**



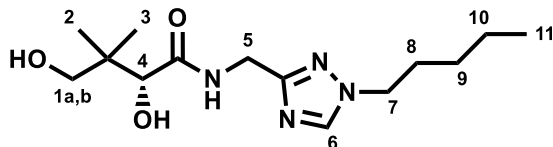
Compound **4.1b** was prepared from **4.4b** (0.95 mmol) using general protocol 6. Yield: 19%, $R_f = 0.24$ (10% MeOH in EtOAc). ^1H NMR (500 MHz, CDCl_3) δ 7.62 (m, 1H, -NH), 7.36 (d, $J = 1.1$ Hz, 1H, H-6 or H-7), 6.83 (s, 1H, H-6 or H-7), 4.40 (dd, $J = 15.0, 6.1$ Hz, 1H, H-5a), 4.32 (dd, $J = 14.9, 5.5$ Hz, 1H, H-5b), 4.05 (s, 1H, H-4), 3.86 (t, $J = 7.2$ Hz, 2H, H-8), 3.49 (d, $J = 11.4$ Hz, 1H, H-1a), 3.46 (d, $J = 11.4$ Hz, 1H, H-1b), 1.75 (m, 2H, H-9), 1.33 (m, 2H, H-10), 1.25 (m, 2H, H-11), 1.05 (s, 3H, H-2 or H-3), 0.93 (s, 3H, H-2 or H-3), 0.89 (t, $J = 7.2$ Hz, 3H, H-12). ^{13}C NMR (126 MHz, CDCl_3) δ 173.55, 138.48, 136.54, 116.36, 77.50, 70.80, 47.31, 39.70, 36.18, 30.57, 28.63, 22.46, 22.12, 20.28, 13.86. HRMS for $\text{C}_{15}\text{H}_{28}\text{N}_3\text{O}_3$ $[\text{M}+\text{H}]^+$ calcd. 298.21252, found 298.21185.

(R)-2,4-Dihydroxy-3,3-dimethyl-N-((1-pentyl-1H-pyrazol-4-yl)methyl)butanamide (4.1c)



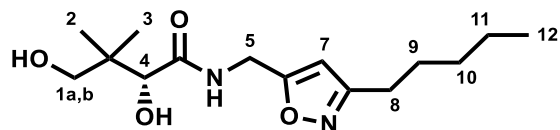
Compound **4.1c** was prepared from **4.4c** (0.95 mmol) using general protocol 6. Yield: 23%, $R_f = 0.59$ (10% MeOH in EtOAc). ^1H NMR (400 MHz, CDCl_3) δ 7.40 (s, 1H, H-6 or H-7), 7.36 (s, 1H, H-6 or H-7), 6.95 (m, 1H, -NH), 4.33 (d, $J = 5.7$ Hz, 2H, H-5), 4.07–4.04 (m, 3H, H-4, H-8), 3.52 (d, $J = 11.2$ Hz, 1H, H-1a), 3.49 (d, $J = 11.2$ Hz, 1H, H-1b), 1.83 (m, 2H, H-9), 1.39–1.20 (m, 4H, H-10, H-11), 1.02 (s, 3H, H-2 or H-3), 0.93–0.86 (m, 6H, H-2 or H-3, H-12). ^{13}C NMR (126 MHz, CDCl_3) δ 172.56, 138.37, 128.30, 117.85, 77.72, 71.42, 52.31, 39.47, 33.55, 30.08, 28.74, 22.21, 21.51, 20.10, 13.92. HRMS for $\text{C}_{15}\text{H}_{27}\text{N}_3\text{O}_3\text{Na}$ $[\text{M}+\text{Na}]^+$ calcd. 320.19446, found 320.19396.

(R)-2,4-Dihydroxy-3,3-dimethyl-N-((1-pentyl-1H-1,2,4-triazol-3-yl)methyl)butanamide (4.1d)



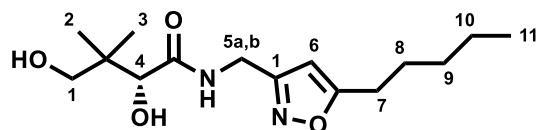
Compound **4.1d** was prepared from **4.4d** (1.14 mmol) using general protocol 6. Yield: 4%, $R_f = 0.62$ (20% MeOH in EtOAc). ^1H NMR (500 MHz, CDCl_3) δ 7.99 (s, 1H, H-6), 7.54 (bs, 1H, -NH), 4.56 (m, 2H, H-5), 4.09–4.05 (m, 3H, H-4, H-7), 3.9 (d, $J = 11.3$ Hz, 1H, H-1a), 3.47 (d, $J = 11.3$ Hz, 1H, H-1b) 1.84 (m, 2H, H-8), 1.37–1.21 (m, 4H, H-9, H-10), 1.03 (s, 3H, H-2 or H-3), 0.95 (s, 3H, H-2 or H-3), 0.88 (t, $J = 7.2$ Hz, 3H, H-11). ^{13}C NMR (126 MHz, CDCl_3) δ 173.72, 160.98, 143.42, 77.64, 70.54, 49.92, 39.51, 36.62, 29.31, 28.55, 22.07, 21.90, 20.78, 13.83. HRMS for $\text{C}_{14}\text{H}_{26}\text{N}_4\text{O}_3\text{Na}$ $[\text{M}+\text{Na}]^+$ calcd. 321.1897, found 321.1895.

(R)-2,4-Dihydroxy-3,3-dimethyl-N-((3-pentylisoxazol-5-yl)methyl)butanamide (4.1e)



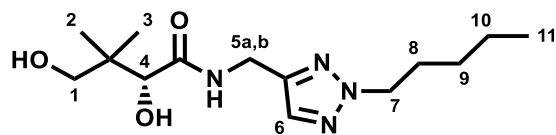
Compound **4.1e** was prepared from **4.10e** (0.35 mmol) using general protocol 1. Yield: 44%, $R_f = 0.39$ (100% EtOAc). ^1H NMR (500 MHz, CDCl_3) δ 7.36 (m, 1H, -NH), 6.04 (s, 1H, H-7), 4.55 (d, $J = 6.1$ Hz, 2H, H-5), 4.09 (s, 1H, H-4), 3.53 (d, $J = 11.1$ Hz, 1H, H-1a), 3.50 (d, $J = 11.1$ Hz, 1H, H-1b), 2.62 (m, 2H, H-8), 1.62 (m, 2H, H-9), 1.38–1.28 (m, 4H, H-10, H-11), 1.02 (s, 3H, H-2 or H-3), 0.92 (s, 3H, H-2 or H-3), 0.89 (t, $J = 7.0$ Hz, 3H, H-12). ^{13}C NMR (126 MHz, CDCl_3) δ 173.19, 168.10, 164.44, 101.92, 77.82, 71.47, 39.32, 34.77, 31.30, 27.86, 25.95, 22.30, 21.13, 20.35, 13.92. HRMS for $\text{C}_{15}\text{H}_{25}\text{N}_2\text{O}_4$ $[\text{M}+\text{H}]^+$ calcd. 297.18198, found 297.18244.

(R)-2,4-Dihydroxy-3,3-dimethyl-N-((5-pentylisoxazol-3-yl)methyl)butanamide (4.1f)



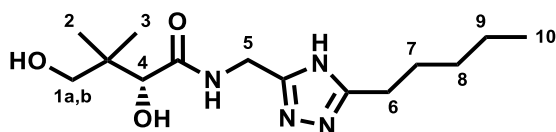
Compound **4.1f** was prepared from **4.10f** (0.43 mmol) using general protocol 1. Yield: 74%, $R_f = 0.50$ (100% EtOAc). ^1H NMR (500 MHz, CDCl_3) δ 7.41 (m, 1H, -NH), 5.95 (s, 1H, H-6), 4.53 (dd, $J = 15.9, 6.1$ Hz, 1H, H-5a), 4.47 (dd, $J = 15.8, 5.9$ Hz, 1H, H-5b), 4.07 (s, 1H, H-4), 3.50 (m, 2H, H-1), 2.69 (t, $J = 7.6$ Hz, 2H, H-7), 1.66 (m, 2H, H-8), 1.37–1.28 (m, 4H, H-9, H-10), 1.01 (s, 3H, H-2 or H-3), 0.94 (s, 3H, H-2 or H-3), 0.89 (t, $J = 7.0$ Hz, 3H, H-11). ^{13}C NMR (126 MHz, CDCl_3) δ 174.67, 173.48, 160.98, 100.01, 77.81, 71.11, 39.38, 35.02, 31.17, 27.10, 26.66, 22.24, 21.39, 20.55, 13.88. HRMS for $\text{C}_{15}\text{H}_{26}\text{N}_2\text{O}_4\text{Na}$ $[\text{M}+\text{Na}]^+$ calcd. 321.17848, found 321.17918.

(R)-2,4-Dihydroxy-3,3-dimethyl-N-((2-pentyl-2H-1,2,3-triazol-4-yl)methyl)butanamide (4.1g)



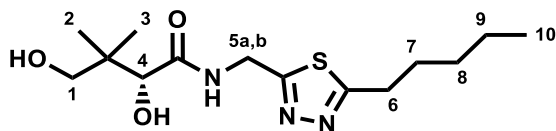
Compound **4.1g** was prepared from **4.12** (0.78 mmol) using general protocol 1. Yield: 45%, $R_f = 0.65$ (10% MeOH in EtOAc). $^1\text{H NMR}$ (500 MHz, CDCl_3) δ 7.50 (s, 1H, H-6), 7.18 (bs, 1H, -NH), 4.59 (dd, $J = 15.4, 6.0$ Hz, 1H, H-5a), 4.51 (dd, $J = 15.4, 5.7$ Hz, 1H, H-5b), 4.36 (t, $J = 7.2$ Hz, 2H, H-7), 4.08 (d, $J = 4.7$ Hz, 1H, H-4), 3.53 (m, 2H, H-1), 1.93 (m, 2H, H-8), 1.39–1.23 (m, 4H, H-9, H-10), 1.04 (s, 3H, H-2 or H-3), 0.94 (s, 3H, H-2 or H-3), 0.89 (t, $J = 7.2$ Hz, 3H, H-11). $^{13}\text{C NMR}$ (126 MHz, CDCl_3) δ 172.75, 144.59, 132.41, 77.91, 71.33, 54.99, 39.47, 34.44, 29.41, 28.62, 22.12, 21.44, 20.38, 13.88. HRMS for $\text{C}_{14}\text{H}_{26}\text{N}_4\text{O}_3\text{Na}$ $[\text{M}+\text{Na}]^+$ calcd. 321.1897, found 321.1899.

(R)-2,4-Dihydroxy-3,3-dimethyl-N-((5-pentyl-4H-1,2,4-triazol-3-yl)methyl)butanamide (4.1h)



Compound **4.1h** was prepared from **4.14** (0.74 mmol) using general protocol 1. Yield: 24%, $R_f = 0.54$ (20% MeOH in EtOAc). $^1\text{H NMR}$ (500 MHz, CD_3OD) δ 4.47 (m, 2H, H-5), 3.96 (s, 1H, H-4), 3.46 (d, $J = 11.0$ Hz, 1H, H-1a), 3.43 (d, $J = 11.0$ Hz, 1H, H-1b), 2.73 (m, 2H, H-6), 1.72 (m, 2H, H-7), 1.41–1.27 (m, 4H, H-8, H-9), 0.95 (s, 3H, H-2 or H-3), 0.94 (s, 3H, H-2 or H-3), 0.91 (t, $J = 7.1$ Hz, 3H, H-10). $^{13}\text{C NMR}$ (126 MHz, CD_3OD) δ 176.20, 161.52, 159.42, 77.43, 70.07, 40.50, 37.10, 32.32, 28.73, 27.06, 23.31, 21.53, 21.00, 14.25. HRMS for $\text{C}_{14}\text{H}_{25}\text{N}_4\text{O}_3$ $[\text{M}-\text{H}]^-$ calcd. 297.19321, found 297.19359.

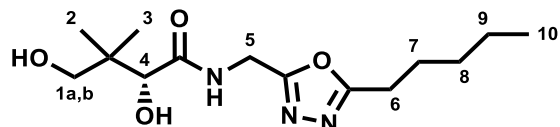
(R)-2,4-Dihydroxy-3,3-dimethyl-N-((5-pentyl-1,3,4-thiadiazol-2-yl)methyl)butanamide (4.1i)



Compound **4.1i** was prepared from **4.16** (0.69 mmol) using general protocol 1. Yield: 41%, $R_f = 0.16$ (100% EtOAc). $^1\text{H NMR}$ (500 MHz, CDCl_3) δ 7.66 (m, 1H, -NH), 4.88 (dd, $J = 15.9, 6.3$ Hz, 1H, H-5a), 4.81 (dd, $J = 15.9, 6.1$ Hz, 1H, H-5b), 4.12 (s, 1H, H-4), 3.54 (m, 2H, H-1), 3.06 (t, $J = 7.6$, 2H, H-6), 1.78 (m, 2H, H-7), 1.42–1.30 (m, 4H, H-8, H-9), 1.04

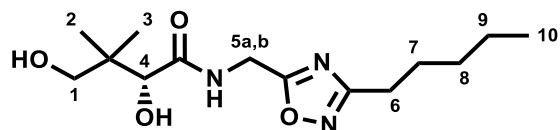
(s, 3H, H-2 or H-3), 0.98 (s, 3H, H-2 or H-3), 0.90 (t, $J = 7.1$ Hz, 3H, H-10). ^{13}C NMR (126 MHz, CDCl_3) δ 173.51, 172.51, 166.77, 78.10, 71.45, 39.59, 38.07, 31.23, 30.21, 29.80, 22.38, 21.40, 20.91, 14.02. HRMS for $\text{C}_{14}\text{H}_{25}\text{N}_3\text{O}_3\text{SNa}$ $[\text{M}+\text{Na}]^+$ calcd. 338.1509, found 338.1509.

(*R*)-2,4-Dihydroxy-3,3-dimethyl-*N*-((5-pentyl-1,3,4-oxadiazol-2-yl)methyl)butanamide (4.1j)



Compound **4.1j** was prepared from **4.17** (0.26 mmol) using general protocol 1. Yield: 39%, $R_f = 0.47$ (10% MeOH in EtOAc). ^1H NMR (500 MHz, CDCl_3) δ 7.73 (t, $J = 5.8$ Hz, 1H, -NH), 4.66 (m, 2H, H-5), 4.11 (s, 1H, H-4), 3.54 (d, $J = 11.1$ Hz, 1H, H-1a), 3.46 (d, $J = 11.1$ Hz, 1H, H-1b), 2.79 (t, $J = 7.6$ Hz, 2H, H-6), 1.75 (m, 2H, H-7), 1.38–1.29 (m, 4H, H-8, H-9), 0.99 (s, 3H, H-2 or H-3), 0.97 (s, 3H, H-2 or H-3), 0.89 (t, $J = 6.9$ Hz, 3H, H-10). ^{13}C NMR (126 MHz, CDCl_3) δ 174.12, 168.05, 163.98, 77.68, 70.91, 39.47, 34.09, 31.18, 26.11, 25.36, 22.25, 21.21, 21.04, 13.93. HRMS for $\text{C}_{14}\text{H}_{25}\text{N}_3\text{O}_4\text{Na}$ $[\text{M}+\text{Na}]^+$ calcd. 322.17373, found 322.17248.

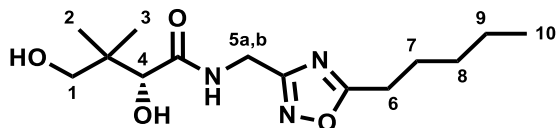
(*R*)-2,4-Dihydroxy-3,3-dimethyl-*N*-((3-pentyl-1,2,4-oxadiazol-5-yl)methyl)butanamide (4.1k)



Compound **4.1k** was prepared from **4.19k** (0.41 mmol) using general protocol 1. Yield: 50%, $R_f = 0.67$ (10% MeOH in EtOAc). ^1H NMR (500 MHz, CDCl_3) δ 7.62 (m, 1H, -NH), 4.75 (dd, $J = 17.3, 6.3$ Hz, 1H, H-5a), 4.63 (dd, $J = 17.3, 5.8$ Hz, 1H, H-5b), 4.10 (s, 1H, H-4), 3.50 (m, 2H, H-1), 2.68 (m, 2H, H-6), 1.71 (m, 2H, H-7), 1.36–1.29 (m, 4H, H-8, H-9), 1.03 (s, 3H, H-2 or H-3), 0.97 (s, 3H, H-2 or H-3), 0.88 (t, $J = 6.9$ Hz, 3H, H-10). ^{13}C NMR (126 MHz, CDCl_3) δ 175.89, 173.90, 170.77, 77.89, 71.07, 39.53, 35.34, 31.30,

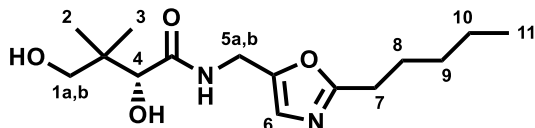
26.61, 25.92, 22.34, 21.28, 20.96, 13.99. HRMS for C₁₄H₂₄N₃O₄ [M-H]⁻ calcd. 298.17723, found 298.17721.

(R)-2,4-Dihydroxy-3,3-dimethyl-N-((5-pentyl-1,2,4-oxadiazol-3-yl)methyl)butanamide (4.1l)



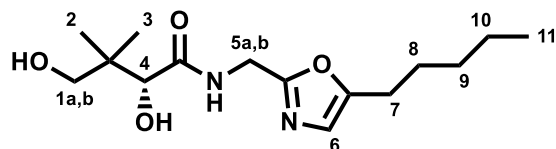
Compound **4.1l** was prepared from **4.19l** (0.82 mmol) using general protocol 1. Yield: 75%, $R_f = 0.62$ (10% MeOH in EtOAc). ¹H NMR (500 MHz, CDCl₃) δ 7.39 (m, 1H, -NH), 4.67 (dd, $J = 16.7, 6.2$ Hz, 1H, H-5a), 4.56 (dd, $J = 16.7, 5.7$ Hz, 1H, H-5b), 4.10 (s, 1H, H-4), 3.55 (m, 2H, H-1), 2.86 (t, $J = 7.6$ Hz, 2H, H-6), 1.80 (m, 2H, H-7), 1.39–1.31 (m, 4H, H-8, H-9), 1.07 (s, 3H, H-2 or H-3), 0.98 (s, 3H, H-2 or H-3), 0.90 (t, $J = 7.1$ Hz, 3H, H-10). ¹³C NMR (126 MHz, CDCl₃) δ 180.97, 173.41, 167.73, 78.12, 71.24, 39.63, 35.18, 31.23, 26.64, 26.30, 22.28, 21.71, 20.81, 13.96. HRMS for C₁₄H₂₅N₃O₄Na [M+Na]⁺ calcd. 322.17373, found 322.17430.

(R)-2,4-Dihydroxy-3,3-dimethyl-N-((2-pentyloxazol-5-yl)methyl)butanamide (4.1m)



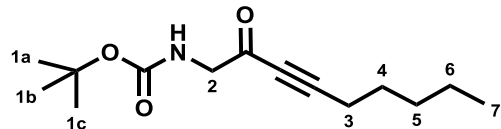
Compound **4.1m** was prepared from **4.20m** (0.34 mmol) using general protocol 1. Yield: 40%, $R_f = 0.50$ (10% MeOH in EtOAc). ¹H NMR (500 MHz, CDCl₃) δ 7.19 (m, 1H, -NH), 6.79 (s, 1H, H-6), 4.50 (dd, $J = 15.8, 6.0$ Hz, 1H, H-5a), 4.44 (dd, $J = 15.8, 5.8$ Hz, 1H, H-5b), 4.07 (s, 1H, H-4), 3.52 (d, $J = 11.1$ Hz, 1H, H-1a), 3.49 (d, $J = 11.1$ Hz, 1H, H-1b), 2.70 (t, $J = 7.6$ Hz, 2H, H-7), 1.72 (m, 2H, H-8), 1.35–1.29 (m, 4H, H-9, H-10), 1.01 (s, 3H, H-2 or H-3), 0.91 (s, 3H, H-2 or H-3), 0.88 (t, $J = 7.0$ Hz, 3H, H-11). ¹³C NMR (126 MHz, CDCl₃) δ 173.14, 165.48, 148.04, 124.00, 77.94, 71.59, 39.42, 33.81, 31.36, 28.23, 26.73, 22.38, 21.26, 20.46, 14.03. HRMS for C₁₅H₂₅N₂O₄ [M-H]⁻ calcd. 297.18198, found 297.18170.

(R)-2,4-Dihydroxy-3,3-dimethyl-N-((5-pentylloxazol-2-yl)methyl)butanamide (4.1n)



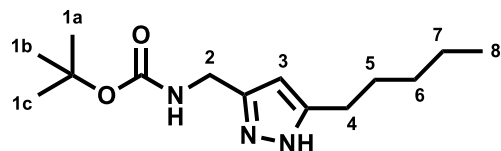
Compound **4.1n** was prepared from **4.20n** (0.25 mmol) using general protocol 1. Yield: 25%, $R_f = 0.50$ (8% MeOH in EtOAc). $^1\text{H NMR}$ (400 MHz, CDCl_3) δ 7.56 (m, 1H, -NH), 6.61 (s, 1H, H-6), 4.63 (dd, $J = 16.8, 6.4$ Hz, 1H, H-5a), 4.48 (dd, $J = 16.8, 5.5$ Hz, 1H, H-5b), 4.07 (s, 1H, H-4), 3.51 (d, $J = 11.2$ Hz, 1H, H-1a), 3.48 (d, $J = 11.2$ Hz, 1H, H-1b), 2.59 (t, $J = 7.6$, 2H, H-7), 1.60 (m, 2H, H-8), 1.36–1.27 (m, 4H, H-9, H-10), 1.04 (s, 3H, H-2 or H-3), 0.99 (s, 3H, H-2 or H-3), 0.89 (t, $J = 6.9$ Hz, 3H, H-11). $^{13}\text{C NMR}$ (101 MHz, CDCl_3) δ 173.87, 159.97, 154.15, 121.75, 78.10, 70.72, 39.63, 36.30, 31.32, 27.24, 25.53, 22.41, 21.99, 21.21, 14.05. HRMS for $\text{C}_{15}\text{H}_{26}\text{N}_2\text{O}_4\text{Na}$ $[\text{M}+\text{Na}]^+$ calcd. 321.1785, found 321.1783.

tert-Butyl (2-oxonon-3-yn-1-yl)carbamate (4.2)



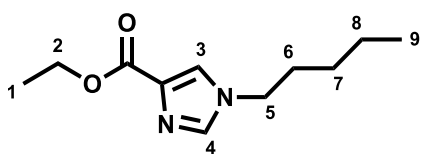
Compound **4.2** was prepared from *N*-(*tert*-butoxycarbonyl)glycine *N'*-methoxy-*N'*-methylamide (2.29 mmol) as described in section 8.1.4.2. Yield: 22%. $R_f = 0.62$ (30% EtOAc in hexanes). $^1\text{H NMR}$ (500 MHz, CDCl_3) δ 5.15 (bs, 1H, -NH), 4.11 (d, $J = 5.0$ Hz, 2H, H-2), 2.38 (t, $J = 7.1$ Hz, 2H, H-3), 1.59 (m, 2H, H-4), 1.45 (s, 9H, H-1a,b,c), 1.42–1.29 (m, 4H, H-5, H-6), 0.91 (t, $J = 7.2$ Hz, 3H, H-7). $^{13}\text{C NMR}$ (126 MHz, CDCl_3) δ 183.10, 155.41, 97.87, 80.01, 78.79, 52.28, 30.96, 28.30, 27.24, 22.07, 19.03, 13.86. HRMS for $\text{C}_{14}\text{H}_{23}\text{NO}_3\text{Na}$ $[\text{M}+\text{Na}]^+$ calcd. 276.1570, found 276.1573.

tert-Butyl ((5-pentyl-1H-pyrazol-3-yl)methyl)carbamate (4.3)



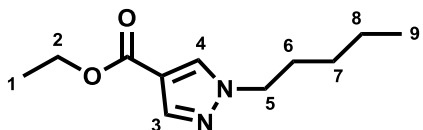
Compound **4.3** was prepared from **4.2** (0.87 mmol) as described in section 8.1.4.3. Yield: 56%. $R_f = 0.23$ (50% EtOAc in hexanes). $^1\text{H NMR}$ (500 MHz, CDCl_3) δ 5.96 (s, 1H, H-3), 5.15 (bs, 1H, -NH), 4.28 (d, $J = 5.7$ Hz, 2H, H-2), 2.60 (t, $J = 7.9$ Hz, 2H, H-4), 1.63 (m, 2H, H-5), 1.45 (s, 9H, H-1a,b,c), 1.35–1.29 (m, 4H, H-6, H-7), 0.89 (t, $J = 6.8$ Hz, 3H, H-8). $^{13}\text{C NMR}$ (126 MHz, CDCl_3) δ 156.19, 147.79, 147.79 (based on HSQC and HMBC), 102.23, 79.62, 37.68, 31.43, 28.89, 28.41, 26.45, 22.40, 13.97. HRMS for $\text{C}_{14}\text{H}_{25}\text{N}_3\text{O}_2\text{Na}$ $[\text{M}+\text{Na}]^+$ calcd. 290.1839, found 290.1843.

Ethyl 1-pentyl-1*H*-imidazole-4-carboxylate (**4.4b**)



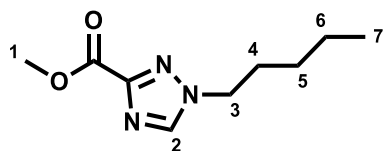
Compound **4.4b** was prepared from ethyl imidazole-4-carboxylate (2.10 mmol) using general protocol 7. Yield: 37%. $R_f = 0.32$ (100% EtOAc). $^1\text{H NMR}$ (500 MHz, CDCl_3) δ 7.59 (s, 1H, H-3 or H-4), 7.46 (s, 1H, H-3 or H-4), 4.35 (q, $J = 7.1$ Hz, 2H, H-2), 3.94 (t, $J = 7.1$ Hz, 2H, H-5), 1.79 (m, 2H, H-6), 1.37 (t, $J = 7.1$ Hz, 3H, H-1), 1.35–1.22 (m, 4H, H-7, H-8), 0.88 (t, $J = 7.2$ Hz, 3H, H-9). $^{13}\text{C NMR}$ (126 MHz, CDCl_3) δ 162.51, 137.81, 134.13, 124.94, 60.50, 47.56, 30.55, 28.52, 22.08, 14.42, 13.82. HRMS for $\text{C}_{11}\text{H}_{18}\text{N}_2\text{O}_2\text{Na}$ $[\text{M}+\text{Na}]^+$ calcd. 233.1260, found 233.1262.

Ethyl 1-pentyl-1*H*-pyrazole-4-carboxylate (**4.4c**)



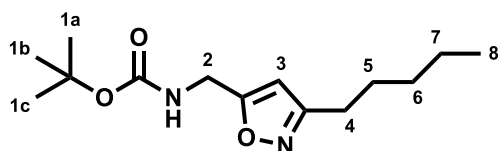
Compound **4.4c** was prepared from ethyl 4-pyrazolecarboxylate (2.10 mmol) using general protocol 7. Yield: 48%, $R_f = 0.55$ (30% EtOAc in hexanes). $^1\text{H NMR}$ (500 MHz, CDCl_3) δ 7.89 (s, 1H, H-3 or H-4), 7.86 (s, 1H, H-3 or H-4), 4.28 (q, $J = 7.1$ Hz, 2H, H-2), 4.11 (t, $J = 7.2$ Hz, 2H, H-5), 1.87 (m, 2H, H-6), 1.37–1.31 (m, 5H, H-1, H-7), 1.26 (m, 2H, H-8), 0.89 (t, $J = 7.2$ Hz, 3H, H-9). $^{13}\text{C NMR}$ (126 MHz, CDCl_3) δ 163.12, 140.89, 132.30, 114.85, 60.11, 52.67, 29.76, 28.61, 22.15, 14.40, 13.87. HRMS for $\text{C}_{11}\text{H}_{18}\text{N}_2\text{O}_2\text{Na}$ $[\text{M}+\text{Na}]^+$ calcd. 233.1260, found 233.1268.

Methyl 1-pentyl-1*H*-1,2,4-triazole-3-carboxylate (4.4d)



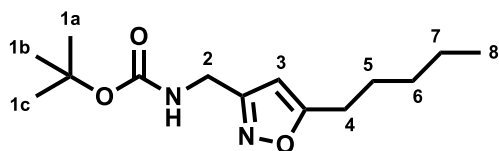
Compound **4.4d** was prepared from methyl 1,2,4-triazole-3-carboxylate (3.93 mmol) using general protocol 7. Yield: 55%, $R_f = 0.15$ (50% EtOAc in hexanes). ^1H NMR (500 MHz, CDCl_3) δ 8.12 (s, 1H, H-2), 4.22 (t, $J = 7.3$ Hz, 2H, H-3), 3.98 (s, 3H, H-1), 1.92 (m, 2H, H-4), 1.39–1.26 (m, 4H, H-5, H-6), 0.88 (t, $J = 7.2$ Hz, 3H, H-7). ^{13}C NMR (126 MHz, CDCl_3) δ 160.20, 154.80, 144.29, 52.74, 50.65, 29.42, 28.49, 22.04, 13.81. HRMS for $\text{C}_9\text{H}_{15}\text{N}_3\text{O}_2\text{Na}$ $[\text{M}+\text{Na}]^+$ calcd. 220.1056, found 220.1059.

tert-Butyl ((3-pentylisoxazol-5-yl)methyl)carbamate (4.10e)



Compound **4.10e** was prepared from **3.3a** (1.29 mmol) using general protocol 8. Yield: 99%, $R_f = 0.32$ (20% EtOAc in hexanes). ^1H NMR (500 MHz, CDCl_3) δ 6.01 (s, 1H, H-3), 4.97 (bs, 1H, -NH), 4.38 (d, $J = 5.6$ Hz, 2H, H-2), 2.62 (t, $J = 7.6$ Hz, 2H, H-4), 1.64 (m, 2H, H-5), 1.45 (s, 9H, H-1a,b,c), 1.36–1.31 (m, 4H, H-6, H-7), 0.90 (t, $J = 7.0$ Hz, 3H, H-8). ^{13}C NMR (126 MHz, CDCl_3) δ 169.08, 164.29, 155.47, 101.45, 80.23, 36.62, 31.33, 28.32, 27.92, 25.97, 22.32, 13.93. HRMS for $\text{C}_{14}\text{H}_{24}\text{N}_2\text{O}_3\text{Na}$ $[\text{M}+\text{Na}]^+$ calcd. 291.1679, found 291.1679.

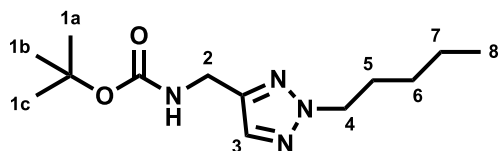
tert-Butyl ((5-pentylisoxazol-3-yl)methyl)carbamate (4.10f)



Compound **4.10f** was prepared from commercial 1-heptyne (0.90 mmol) using general protocol 8. Yield: 23%, $R_f = 0.77$ (50% EtOAc in hexanes). ^1H NMR (500 MHz, CDCl_3) δ 5.96 (s, 1H, H-3), 4.99 (bs, 1H, -NH), 4.34 (d, $J = 5.8$ Hz, 2H, H-2), 2.70 (t, $J = 7.6$ Hz,

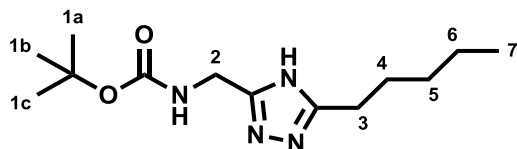
2H, H-4), 1.68 (m, 2H, H-5), 1.46 (s, 9H, H-1a,b,c), 1.35–1.32 (m, 4H, H-6, H-7), 0.90 (t, $J = 7.0$ Hz, 3H, H-8). ^{13}C NMR (126 MHz, CDCl_3) δ 174.30, 161.57, 155.78, 99.86, 79.93, 36.69, 31.20, 28.35, 27.14, 26.68, 22.27, 13.90. HRMS for $\text{C}_{14}\text{H}_{24}\text{N}_2\text{O}_3\text{Na}$ $[\text{M}+\text{Na}]^+$ calcd. 291.16791, found 291.16834.

***tert*-Butyl ((2-pentyl-2*H*-1,2,3-triazol-4-yl)methyl)carbamate (4.12)**



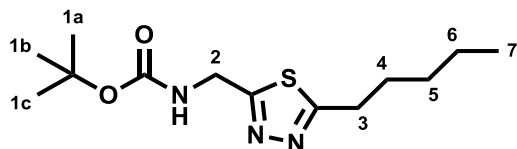
Compound **4.12** was prepared from **3.3a** (1.93 mmol) as described in section 8.1.4.6. Yield: 34%, $R_f = 0.45$ (30% EtOAc in hexanes). ^1H NMR (500 MHz, CDCl_3) δ 7.49 (s, 1H, H-3), 4.94 (bs, 1H, -NH), 4.38–4.34 (m, 4H, H-2, H-4), 1.93 (m, 2H, H-5), 1.45 (s, 9H, H-1a,b,c), 1.38–1.23 (m, 4H, H-6, H-7), 0.89 (t, $J = 7.2$ Hz, 3H, H-8). ^{13}C NMR (126 MHz, CDCl_3) δ 155.71, 145.38, 132.33, 79.74, 54.92, 36.16, 29.43, 28.64, 28.37, 22.13, 13.88. HRMS for $\text{C}_{13}\text{H}_{24}\text{N}_4\text{O}_2\text{Na}$ $[\text{M}+\text{Na}]^+$ calcd. 291.1791, found 291.1799.

***tert*-Butyl ((5-pentyl-4*H*-1,2,4-triazol-3-yl)methyl)carbamate (4.14)**



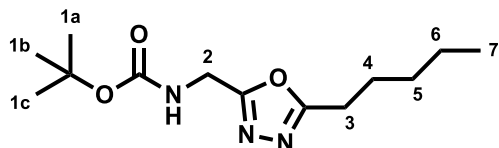
Compound **4.14** was prepared from *N*-Boc-glycinamide (2.18 mmol) as described in section 8.1.4.7. Yield: 52%, $R_f = 0.15$ (60% EtOAc in hexanes). ^1H NMR (500 MHz, CDCl_3) δ 5.42 (bs, 1H, -NH), 4.40 (d, $J = 5.7$ Hz, 2H, H-2), 2.74 (t, $J = 7.7$ Hz, 2H, H-3), 1.75 (m, 2H, H-4), 1.44 (s, 9H, H-1a,b,c), 1.37–1.32 (m, 4H, H-5, H-6), 0.89 (t, $J = 7.1$ Hz, 3H, H-7). ^{13}C NMR (126 MHz, CDCl_3) δ 160.79, 158.20, 156.50, 80.20, 37.67, 31.56, 28.47, 27.88, 27.36, 22.44, 14.05. HRMS for $\text{C}_{13}\text{H}_{25}\text{N}_4\text{O}_2$ $[\text{M}+\text{H}]^+$ calcd. 269.19720, found 269.19651.

***tert*-Butyl ((5-pentyl-1,3,4-thiadiazol-2-yl)methyl)carbamate (4.16)**



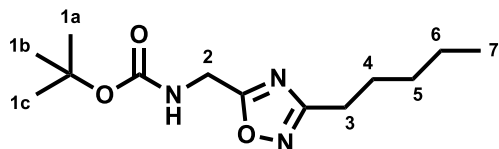
Compound **4.16** was prepared from *N*-Boc glycine (1.14 mmol) as described in section 8.1.4.8. Yield: 60%, $R_f = 0.38$ (50% EtOAc in hexanes). $^1\text{H NMR}$ (500 MHz, CDCl_3) δ 5.27 (bs, 1H, -NH), 4.67 (d, $J = 6.1$ Hz, 2H, H-2), 3.06 (t, $J = 7.6$, 2H, H-3), 1.78 (m, 2H, H-4), 1.46 (s, 9H, H-1a,b,c), 1.41–1.32 (m, 4H, H-5, H-6), 0.90 (t, $J = 7.1$ Hz, 3H, H-7). $^{13}\text{C NMR}$ (126 MHz, CDCl_3) δ 172.11, 167.87, 155.71, 80.65, 39.91, 31.26, 30.24, 29.86, 28.46, 22.39, 14.02. HRMS for $\text{C}_{13}\text{H}_{23}\text{N}_3\text{O}_2\text{SNa}$ $[\text{M}+\text{Na}]^+$ calcd. 308.1403, found 308.1401.

***tert*-Butyl ((5-pentyl-1,3,4-oxadiazol-2-yl)methyl)carbamate (4.17)**



Compound **4.17** was prepared from *N*-Boc glycine (0.88 mmol) as described in section 8.1.4.9. Yield: 31%, $R_f = 0.41$ (50% EtOAc in hexanes). $^1\text{H NMR}$ (500 MHz, CDCl_3) δ 5.10 (bs, 1H, -NH), 4.52 (d, $J = 5.1$ Hz, 2H, H-2), 2.82 (t, $J = 7.6$, 2H, H-3), 1.78 (m, 2H, H-4), 1.46 (s, 9H, H-1a,b,c), 1.39–1.33 (m, 4H, H-5, H-6), 0.90 (t, $J = 7.1$ Hz, 3H, H-7). $^{13}\text{C NMR}$ (126 MHz, CDCl_3) δ 167.89, 163.98, 155.53, 80.70, 36.01, 31.25, 28.43, 26.24, 25.44, 22.31, 13.98. HRMS for $\text{C}_{13}\text{H}_{23}\text{N}_3\text{O}_3\text{Na}$ $[\text{M}+\text{Na}]^+$ calcd. 292.16316, found 292.16219.

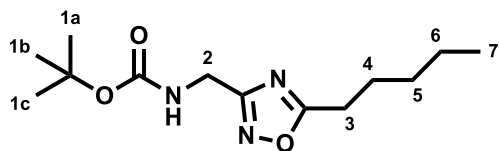
***tert*-Butyl ((3-pentyl-1,2,4-oxadiazol-5-yl)methyl)carbamate (4.19k)**



Compound **4.19k** was prepared from hexanenitrile (2.06 mmol) using general protocol 9. Yield: 36%, $R_f = 0.57$ (40% EtOAc in hexanes). $^1\text{H NMR}$ (500 MHz, CDCl_3) δ 5.13 (bs, 1H, -NH), 4.55 (d, $J = 5.3$ Hz, 2H, H-2), 2.71 (t, $J = 7.7$, 2H, H-3), 1.75 (m, 2H, H-4), 1.46 (s, 9H, H-1a,b,c), 1.37–1.32 (m, 4H, H-5, H-6), 0.90 (t, $J = 7.1$ Hz, 3H, H-7). $^{13}\text{C NMR}$ (126

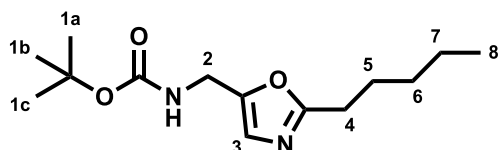
MHz, CDCl₃) δ 176.18, 170.89, 155.50, 80.81, 37.29, 31.39, 28.42, 26.75, 26.04, 22.41, 14.05. HRMS for C₁₃H₂₃N₃O₃Na [M+Na]⁺ calcd. 292.1632, found 292.1639.

***tert*-Butyl ((5-pentyl-1,2,4-oxadiazol-3-yl)methyl)carbamate (4.19l)**



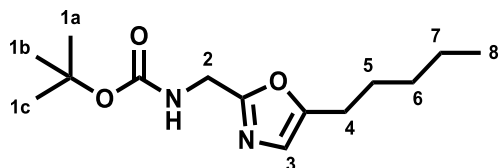
Compound **4.19l** was prepared from *N*-(*tert*-butoxycarbonyl)-2-aminoacetonitrile (1.92 mmol) using general protocol 9. Yield: 45%, *R*_f = 0.70 (50% EtOAc in hexanes). ¹H NMR (500 MHz, CDCl₃) δ 5.12 (bs, 1H, -NH), 4.44 (d, *J* = 5.1 Hz, 2H, H-2), 2.86 (t, *J* = 7.6 Hz, 2H, H-3), 1.80 (m, 2H, H-4), 1.45 (s, 9H, H-1a,b,c), 1.39–1.31 (m, 4H, H-5, H-6), 0.90 (t, *J* = 7.1 Hz, 3H, H-7). ¹³C NMR (126 MHz, CDCl₃) δ 180.72, 168.00, 155.67, 80.27, 37.00, 31.25, 28.46, 26.65, 26.34, 22.28, 13.96. HRMS for C₁₃H₂₃N₃O₃Na [M+Na]⁺ calcd. 292.1632, found 292.1641.

***tert*-Butyl ((2-pentyloxazol-5-yl)methyl)carbamate (4.20m)**



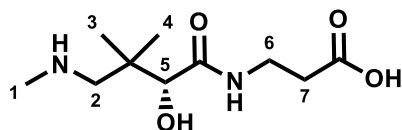
Compound **4.20m** was prepared from **3.3a** (0.38 mmol) using general protocol 10. Yield: 36%, *R*_f = 0.39 (40% EtOAc in hexanes). ¹H NMR (400 MHz, CDCl₃) δ 6.80 (s, 1H, H-3), 4.81 (bs, 1H, -NH), 4.30 (d, *J* = 5.2 Hz, 2H, H-2), 2.71 (t, *J* = 7.6 Hz, 2H, H-4), 1.74 (m, 2H, H-5), 1.45 (s, 9H, H-1a,b,c), 1.37–1.31 (m, 4H, H-6, H-7), 0.89 (t, *J* = 7.0 Hz, 3H, H-8). ¹³C NMR (126 MHz, CDCl₃) δ 165.15, 155.56, 148.55, 123.94, 80.15, 35.70, 31.43, 28.49, 28.30, 26.77, 22.42, 14.06. HRMS for C₁₄H₂₄N₂O₃Na [M+Na]⁺ calcd. 291.1679, found 291.1666.

tert-Butyl ((5-pentylloxazol-2-yl)methyl)carbamate (4.20n)



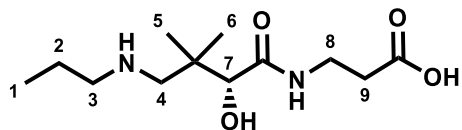
Compound **4.20n** was prepared from 1-heptyne (0.72 mmol) using general protocol 10. Yield: 21%, $R_f = 0.56$ (50% EtOAc in hexanes). $^1\text{H NMR}$ (500 MHz, CDCl_3) δ 6.64 (s, 1H, H-3), 5.11 (bs, 1H, -NH), 4.39 (d, $J = 5.0$ Hz, 2H, H-2), 2.60 (t, $J = 7.4$ Hz, 2H, H-4), 1.61 (m, 2H, H-5), 1.46 (s, 9H, H-1a,b,c), 1.36–1.30 (m, 4H, H-6, H-7), 0.90 (t, $J = 7.0$ Hz, 3H, H-8). $^{13}\text{C NMR}$ (126 MHz, CDCl_3) δ 159.94, 155.70, 153.78, 122.09, 80.15, 38.27, 31.36, 28.47, 27.29, 25.58, 22.44, 14.08. HRMS for $\text{C}_{14}\text{H}_{24}\text{N}_2\text{O}_3\text{Na}$ $[\text{M}+\text{Na}]^+$ calcd. 291.1679, found 291.1669.

(R)-3-(2-Hydroxy-3,3-dimethyl-4-(methylamino)butanamido)propanoic acid (5.1a)



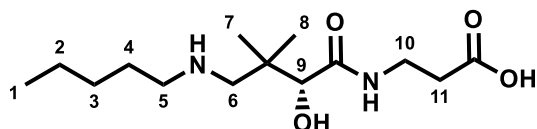
Compound **5.1a** was prepared from compound **5.2a** (0.14 mmol) using the general protocol 11. It was purified twice using reversed-phase HPLC. The first purification was achieved using an isocratic elution with a solution of 90% water in acetonitrile containing 20 mM NH_4HCO_3 on a 9.4 x 250 mm, Zorbax 300 SB-C8 column from Agilent, $R_t = 5.68$ min. The second purification was achieved using an isocratic elution using a 20 mM NH_4HCO_3 aqueous solution on a 10 x 250 mm, Luna 5 μ CN 100 Å column from Phenomenex, $R_t = 9.86$ min. Yield: 29%. $^1\text{H NMR}$ (400 MHz, D_2O) δ 3.95 (s, 1H, H-5), 3.41 (t, $J = 6.5$ Hz, 2H, H-6 or H-7), 3.00 (s, 2H, H-2), 2.67 (s, 3H, H-1), 2.38 (t, $J = 6.4$ Hz, 2H, H-6 or H-7), 1.06 (s, 3H, H-3 or H-4), 0.98 (s, 3H, H-3 or H-4). $^{13}\text{C NMR}$ (126 MHz, D_2O), based on HSQC and HMBC, δ 180.24, 173.68, 77.58, 58.08, 36.17, 36.17, 36.17, 33.89, 22.25, 20.43. HRMS for $\text{C}_{10}\text{H}_{21}\text{N}_2\text{O}_4$ $[\text{M}+\text{H}]^+$ calcd. 233.14958, found 233.14906.

(R)-3-(2-Hydroxy-3,3-dimethyl-4-(propylamino)butanamido)propanoic acid (5.1b)



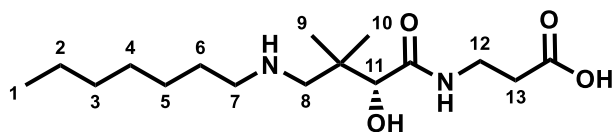
Compound **5.1b** was prepared from compound **5.5** (0.36 mmol) using the general protocols 11, 13 and 14. It was purified twice using reversed-phase HPLC. The first purification was achieved using an isocratic elution with a solution of 90% water in acetonitrile containing 20 mM NH_4HCO_3 on a 9.4 × 250 mm, Zorbax 300 SB-C8 column from Agilent, $R_t = 6.22$ min. The second purification was achieved using an isocratic elution with a solution of 90% water in acetonitrile containing 20 mM NH_4HCO_3 on a 10 × 250 mm, Luna 5 μ CN 100 Å column from Phenomenex, $R_t = 9.08$ min. Yield over four steps: 8%. ^1H NMR (400 MHz, D_2O) δ 4.03 (s, 1H, H-7), 3.47 (t, $J = 6.6$ Hz, 2H, H-8 or H-9), 3.08 (s, 2H, H-4), 3.03 (t, $J = 7.6$ Hz, 2H, H-3), 2.44 (t, $J = 6.6$ Hz, 2H, H-8 or H-9), 1.75 (m, 2H, H-2), 1.12 (s, 3H, H-5 or H-6), 1.05 (s, 3H, H-5 or H-6), 1.00 (t, $J = 7.4$ Hz, 3H, H-1). ^{13}C NMR (126 MHz, D_2O) δ 180.04, 173.63, 77.57, 55.82, 50.10, 36.43, 36.28, 36.10, 22.26, 20.54, 18.63, 10.06. HRMS for $\text{C}_{12}\text{H}_{20}\text{N}_2\text{O}_4\text{Na}$ $[\text{M}+\text{Na}]^+$ calcd. 283.1628, found 283.1636.

(R)-3-(2-Hydroxy-3,3-dimethyl-4-(pentylamino)butanamido)propanoic acid (5.1c)



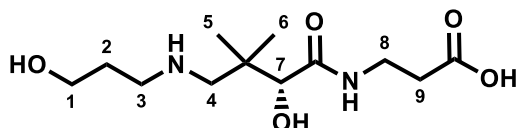
Compound **5.1c** was prepared from compound **5.2c** (0.11 mmol) using the general protocol 11. The purification was achieved using an isocratic elution with a solution of 90% water in acetonitrile containing 20 mM NH_4HCO_3 on a 10 × 250 mm, Luna 5 μ CN 100 Å column from Phenomenex, $R_t = 10.21$ min. Yield: 29%. ^1H NMR (500 MHz, D_2O) δ 4.03 (s, 1H, H-9), 3.47 (t, $J = 6.2$ Hz, 2H, H-10 or H-11), 3.11–3.02 (m, 4H, H-5, H-6), 2.44 (t, $J = 6.2$ Hz, 2H, H-10 or H-11), 1.72 (m, 2H, H-4), 1.43–1.33 (m, 4H, H-2, H-3), 1.12 (s, 3H, H-7 or H-8), 1.05 (s, 3H, H-7 or H-8), 0.91 (t, $J = 6.1$ Hz, 3H, H-1). ^{13}C NMR (126 MHz, D_2O) δ 180.03, 173.61, 77.57, 55.83, 48.56, 36.43, 36.28, 36.09, 27.77, 24.64, 22.28, 21.39, 20.51, 12.96. HRMS for $\text{C}_{14}\text{H}_{29}\text{N}_2\text{O}_4$ $[\text{M}+\text{H}]^+$ calcd. 289.2122, found 289.2125.

(R)-3-(4-(Heptylamino)-2-hydroxy-3,3-dimethylbutanamido)propanoic acid (5.1d)



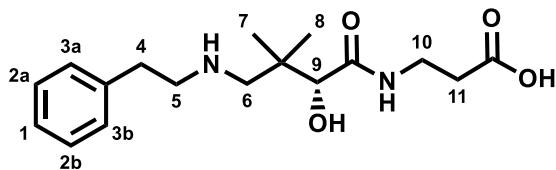
Compound **5.1d** was prepared from compound **5.2d** (0.20 mmol) using general protocol 11. The purification was achieved using an isocratic elution with a solution of 90% water in acetonitrile containing 20 mM NH_4HCO_3 on a 10 x 250 mm, Luna 5 μ CN 100 Å column from Phenomenex, $R_t = 11.83$ min. Yield: 13%. ^1H NMR (500 MHz, D_2O) δ 4.03 (s, 1H, H-11), 3.48 (m, 2H, H-12 or H-13), 3.07–3.04 (m, 4H, H-7, H-8), 2.44 (t, $J = 6.7$ Hz, 2H, H-12 or H-13), 1.71 (m, 2H, H-6), 1.40–1.31 (m, 8H, H-2, H-3, H-4, H-5), 1.12 (s, 3H, H-9 or H-10), 1.05 (s, 3H, H-9 or H-10), 0.89 (t, $J = 7.0$ Hz, 3H, H-1). ^{13}C NMR (126 MHz, D_2O) δ 180.05, 173.62, 77.58, 55.83, 48.59, 36.43, 36.29, 36.09, 30.71, 27.77, 25.55, 24.95, 22.27, 21.78, 20.53, 13.23. HRMS for $\text{C}_{16}\text{H}_{33}\text{N}_2\text{O}_4$ $[\text{M}+\text{H}]^+$ calcd. 317.24348, found 317.24403.

(R)-3-(2-Hydroxy-4-((3-hydroxypropyl)amino)-3,3-dimethylbutanamido)propanoic acid (5.1e)



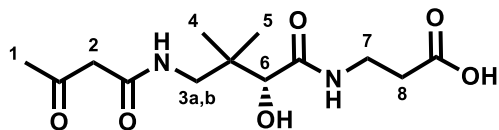
Compound **5.1e** was prepared from compound **5.2e** (0.11 mmol) using the general protocol 11. The purification was achieved using an isocratic elution with a 20 mM aqueous NH_4HCO_3 solution on a 10 x 250 mm, Luna 5 μ CN 100 Å column from Phenomenex, $R_t = 11.35$ min. Yield: 90%. ^1H NMR (500 MHz, D_2O) δ 4.01 (s, 1H, H-7), 3.74 (t, $J = 6.0$ Hz, 2H, H-1), 3.45 (t, $J = 6.6$ Hz, 2H, H-8 or H-9), 3.17 (t, $J = 7.1$ Hz, 2H, H-3), 3.08 (s, 2H, H-4), 2.42 (t, $J = 6.7$ Hz, 2H, H-8 or H-9), 1.95 (m, 2H, H-2), 1.11 (s, 3H, H-5 or H-6), 1.03 (s, 3H, H-5 or H-6). ^{13}C NMR (126 MHz, D_2O) δ 180.07, 173.58, 77.67, 59.32, 56.18, 46.85, 36.45, 36.27, 36.10, 27.32, 22.32, 20.44. HRMS for $\text{C}_{12}\text{H}_{24}\text{N}_2\text{O}_5\text{Na}$ $[\text{M}+\text{Na}]^+$ calcd. 299.1577, found 299.1579.

(R)-3-(2-Hydroxy-3,3-dimethyl-4-(phenethylamino)butanamido)propanoic acid (5.1f)



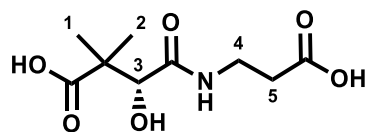
Compound **5.1f** was prepared from compound **5.2f** (0.13 mmol) using the general protocol 11. The purification was achieved using an isocratic elution with a solution of 90% water in acetonitrile containing 20 mM NH_4HCO_3 on a 9.4 × 250 mm, Zorbax ODS column from Agilent, $R_t = 15.82$ min. Yield: 47%. ^1H NMR (500 MHz, D_2O) δ 7.50–7.43 (m, 2H, H-2a,b or H-3a,b), 7.40–7.38 (m, 3H, H-1, H-2a,b or H-3a,b), 3.96 (s, 1H, H-9), 3.45 (m, 2H, H-10 or H-11), 3.34 (m, 2H, H-5), 3.12–3.05 (m, 4H, H-6, H-4), 2.43 (t, $J = 6.7$ Hz, 2H, H-10 or H-11), 1.10 (s, 3H, H-7 or H-8), 1.02 (s, 3H, H-7 or H-8). ^{13}C NMR (126 MHz, D_2O) δ 180.02, 173.47, 147.64, 129.05, 128.76, 127.29, 77.80, 56.25, 49.42, 36.42, 36.22, 35.98, 31.52, 22.31, 20.48. HRMS for $\text{C}_{17}\text{H}_{27}\text{N}_2\text{O}_4$ $[\text{M}+\text{H}]^+$ calcd. 323.1965, found 323.1964.

(R)-3-(2-Hydroxy-3,3-dimethyl-4-(3-oxobutanamido)butanamido)propanoic acid (5.1g)



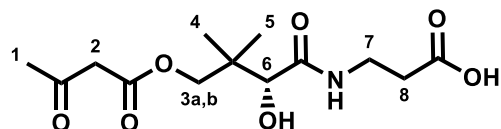
Compound **5.1g** was prepared from compound **5.2g** (0.23 mmol) using the general protocol 11. The purification was achieved on silica gel using a gradient of 0-50% MeOH in EtOAc. Yield: 51%, $R_t = 0.75$ (40% MeOH in DCM). ^1H NMR (400 MHz, D_2O) δ 3.90 (s, 1H, H-6), 3.53 (m, 2H, H-7), 3.36 (s, 1H, due to tautomerism, H-2), 3.35 (d, $J = 13.7$ Hz, 1H, H-3a), 3.13 (d, $J = 13.8$ Hz, 1H, H-3b), 2.64 (t, $J = 6.5$ Hz, 2H, H-8), 2.30 (s, 3H, H-1), 0.96 (s, 3H, H-4 or H-5), 0.92 (s, 3H, H-4 or H-5). ^{13}C NMR (126 MHz, D_2O) δ 207.95, 176.26, 174.56, 169.44, 76.08, 48.83, 46.80, 38.35, 34.81, 33.65, 29.74, 21.33, 20.06. HRMS for $\text{C}_{13}\text{H}_{22}\text{N}_2\text{O}_6\text{Na}$ $[\text{M}+\text{Na}]^+$ calcd. 325.1370, found 325.1376.

(R)-4-((2-Carboxyethyl)amino)-3-hydroxy-2,2-dimethyl-4-oxobutanoic acid (5.1h)



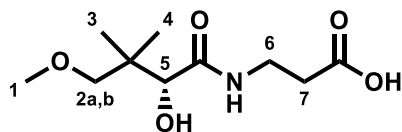
Compound **5.1h** was prepared from compound **5.2h** (0.15 mmol) using the general protocol 11. The first purification was achieved on silica gel using a gradient of 0-100% EtOAc in hexanes (both containing 1% formic acid). The second purification was achieved using an isocratic elution with a 20 mM aqueous NH_4HCO_3 solution on a 10 × 250 mm, Luna 5 μ CN 100 Å column from Phenomenex, $R_t = 4.53$ min. Yield: 71%. ^1H NMR (500 MHz, D_2O) δ 4.29 (s, 1H, H-3), 3.44 (t, $J = 7.0$ Hz, 2H, H-4 or H-5), 2.42 (t, $J = 7.0$ Hz, 2H, H-4 or H-5), 1.13 (s, 3H, H-1 or H-2), 1.09 (s, 3H, H-1 or H-2). ^{13}C NMR (126 MHz, D_2O), based on HSQC and HMBC, δ 182.86, 179.39, 174.22, 76.26, 46.93, 36.46, 35.79, 21.10, 20.70. HRMS for $\text{C}_9\text{H}_{14}\text{NO}_6$ $[\text{M}-\text{H}]^-$ calcd. 232.08266, found 232.08238.

(R)-3-(2-Hydroxy-3,3-dimethyl-4-((3-oxobutanoyl)oxy)butanamido)propanoic acid (5.1i)



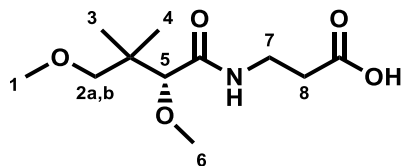
Compound **5.1i** was prepared from compound **5.2i** (0.18 mmol) using the general protocol 11. The purification was achieved on silica gel using a gradient of 0-100% EtOAc in hexanes, followed by 0-50% MeOH in EtOAc. Yield: 30%, $R_t = 0.54$ (20% MeOH in EtOAc). ^1H NMR (500 MHz, CDCl_3) δ 7.35 (s, 1H, -NH), 4.17 (d, $J = 10.9$ Hz, 1H, H-3a), 3.94 (s, 1H, H-6), 3.87 (d, $J = 10.9$ Hz, 1H, H-3b), 3.66–3.38 (m, 4H, H-2, H-7 or H-8), 2.58 (m, 2H, H-7 or H-8), 2.28 (s, 3H, H-1), 1.03 (s, 3H, H-4 or H-5), 0.96 (s, 3H, H-4 or H-5). ^{13}C NMR (126 MHz, CDCl_3) δ 202.13, 172.93, 172.93, 167.30, 74.81, 71.59, 50.15, 38.52, 35.00, 35.00, 30.53, 21.19, 20.34. HRMS for $\text{C}_{13}\text{H}_{20}\text{NO}_7$ $[\text{M}-\text{H}]^-$ calcd. 302.12453, found 302.12491.

(R)-3-(2-Hydroxy-4-methoxy-3,3-dimethylbutanamido)propanoic acid (5.1j)



Compound **5.1j** was prepared from compound **5.2j** (0.09 mmol) using the general protocol 11. The first purification was achieved using a gradient of 0-100% EtOAc in hexanes. The second purification was achieved with a gradient of 99-50% water in acetonitrile (both containing 0.05% trifluoroacetic acid) over 40 min on a reversed-phase 9.4 × 250 mm, Zorbax 300 SB-C8 column from Agilent, $R_t = 15.26$ min. Yield: 14%. The characterization data is in agreement with a previous report.²²¹ ^1H NMR (500 MHz, CD_3OD) δ 3.88 (s, 1H, H-5), 3.47 (m, 2H, H-6), 3.31 (s, 3H, H-1) (based on HSQC), 3.28 (d, $J = 8.8$ Hz, 1H, H-2a), 3.18 (d, $J = 8.8$ Hz, 1H, H-2b), 2.53 (t, $J = 6.6$ Hz, 2H, H-7), 0.95 (s, 3H, H-3 or H-4), 0.92 (s, 3H, H-3 or H-4). ^{13}C NMR (126 MHz, CD_3OD) δ 175.72, 175.42, 80.65, 76.77, 59.41, 39.85, 35.73, 34.68, 22.04, 21.03. HRMS for $\text{C}_{10}\text{H}_{19}\text{NO}_5\text{Na}$ $[\text{M}+\text{Na}]^+$ calcd. 256.1155, found 256.1144.

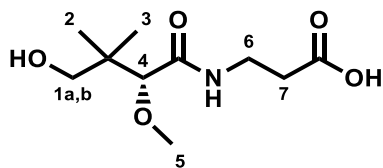
(R)-3-(2,4-Dimethoxy-3,3-dimethylbutanamido)propanoic acid (5.1k)



Compound **5.1k** was prepared from compound **5.2k** (0.15 mmol) using the general protocol 11. The first purification was achieved using a gradient of 0-100% EtOAc in hexanes. The second purification was achieved with a gradient of 99-56% water in acetonitrile (both containing 0.05% trifluoroacetic acid) over 17.5 min on a reversed-phase 9.4 × 250 mm, Zorbax 300 SB-C8 column from Agilent, $R_t = 15.02$ min. Yield: 29%. ^1H NMR (500 MHz, CDCl_3) δ 7.04 (m, 1H, -NH), 3.59 (m, 2H, H-7 or H-8), 3.53 (s, 1H, H-5), 3.34 (s, 3H, H-1 or H-6), 3.32 (s, 3H, H-1 or H-6), 3.21 (d, $J = 8.8$ Hz, 1H, H-2a), 3.14 (d, $J = 8.8$ Hz, 1H, H-2b), 2.63 (m, 2H, H-7 or H-8), 0.95 (s, 3H, H-3 or H-4), 0.90 (s, 3H, H-3 or H-4). ^{13}C NMR (126 MHz, CDCl_3) δ 175.58, 172.03, 86.34, 79.13,

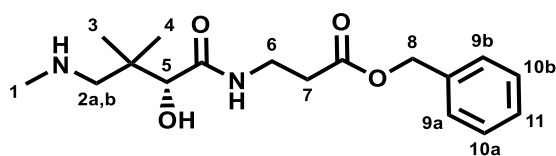
59.42, 59.20, 39.08, 34.43, 34.04, 21.63, 21.01. HRMS for C₁₁H₂₁NO₅Na [M+Na]⁺ calcd. 270.1312, found 270.1304.

(R)-3-(4-Hydroxy-2-methoxy-3,3-dimethylbutanamido)propanoic acid (5.1l)



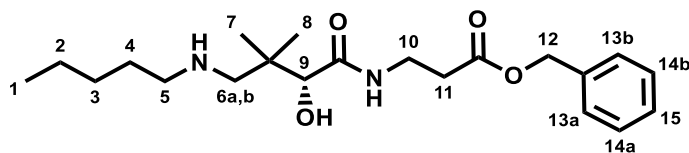
Compound **5.1l** was prepared from compound **5.2l** (0.14 mmol) using the general protocol 11. The purification was achieved using a gradient of 0-100% EtOAc in hexanes. Yield: 48%. The characterization data is in agreement with a previous report.²²¹ ¹H NMR (500 MHz, CDCl₃) δ 7.18 (m, 1H, -NH), 3.59 (m, 2H, H-6), 3.50 (s, 1H, H-4), 3.41 (d, *J* = 11.7 Hz, 1H, H-1a), 3.40 (d, *J* = 11.7 Hz, 1H, H-1b), 3.37 (s, 3H, H-5), 2.61 (t, *J* = 6.0 Hz, 2H, H-7), 1.02 (s, 3H, H-2 or H-3), 0.81 (s, 3H, H-2 or H-3). ¹³C NMR (126 MHz, CDCl₃) δ 175.66, 172.65, 87.99, 70.41, 59.85, 40.08, 34.66, 33.92, 22.63, 19.56. HRMS for C₁₀H₁₉NO₅Na [M+Na]⁺ calcd. 256.1155, found 256.1153.

Benzyl (R)-3-(2-hydroxy-3,3-dimethyl-4-(methylamino)butanamido)propanoate (5.2a)



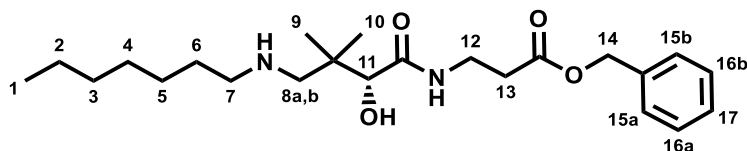
Compound **5.2a** was prepared from compound **5.6a** (0.24 mmol) using the general protocol 12. Yield: 61%, *R*_f = 0.29 (MeOH:EtOAc:TEA = 1:8:1). ¹H NMR (400 MHz, CDCl₃) δ 7.51 (m, 1H, -NH), 7.41–7.29 (m, 5H, H-9a,b, H-10a,b, H-11), 5.14 (m, 2H, H-8), 4.03 (s, 1H, H-5), 3.56 (m, 2H, H-6), 2.72 (d, *J* = 12.3 Hz, 1H, H-2a), 2.62 (t, *J* = 6.3 Hz, 2H, H-7), 2.61 (d, *J* = 12.3 Hz, 1H, H-2b), 2.47 (s, 3H, H-1), 1.09 (s, 3H, H-3 or H-4), 0.93 (s, 3H, H-3 or H-4). ¹³C NMR (126 MHz, CDCl₃) δ 172.75, 172.11, 135.84, 128.74, 128.47, 128.46, 79.50, 66.67, 62.85, 37.01, 36.19, 34.55, 34.45, 24.15, 20.35. HRMS for C₁₇H₂₇N₂O₄ [M+H]⁺ calcd. 323.1965, found 323.1969.

Benzyl (R)-3-(2-hydroxy-3,3-dimethyl-4-(pentylamino)butanamido)propanoate (5.2c)



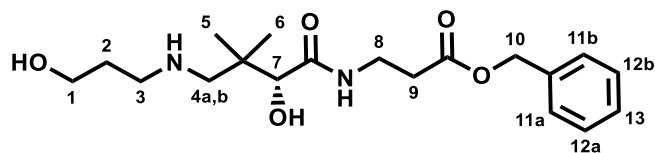
Compound **5.2c** was prepared from compound **5.5** (0.36 mmol) using the general protocols 13 and 14. Yield: 33%, $R_f = 0.05$ (70% EtOAc in hexanes). $^1\text{H NMR}$ (500 MHz, CDCl_3) δ 7.45 (m, 1H, -NH), 7.40–7.31 (m, 5H, H-13a,b, H-14a,b, H-15), 5.12 (m, 2H, H-12), 4.00 (s, 1H, H-9), 3.55 (m, 2H, H-10 or H-11), 2.67 (d, $J = 12.3$ Hz, 1H, H-6a), 2.65–2.52 (m, 5H, H-5, H-6b, H-10 or H-11), 1.49 (m, 2H, H-4), 1.36–1.27 (m, 4H, H-2, H-3), 1.05 (s, 3H, H-7 or H-8), 0.92–0.89 (m, 6H, H-7 or H-8, H-1). $^{13}\text{C NMR}$ (126 MHz, CDCl_3) δ 172.78, 172.16, 135.86, 128.73, 128.44, 128.44, 80.93 (based on HSQC and HMBC), 66.62, 61.78, 50.16, 36.57, 34.51, 34.44, 29.46, 29.30, 24.51, 22.65, 19.60, 14.14. HRMS for $\text{C}_{21}\text{H}_{35}\text{N}_2\text{O}_4$ $[\text{M}+\text{H}]^+$ calcd. 379.2591, found 379.2590.

Benzyl (R)-3-(4-(heptylamino)-2-hydroxy-3,3-dimethylbutanamido)propanoate (5.2d)



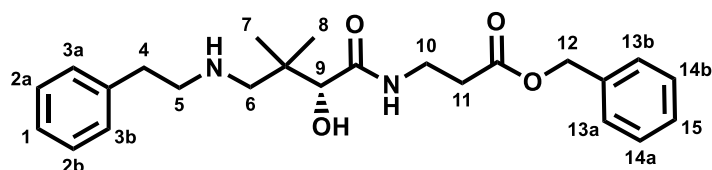
Compound **5.2d** was prepared from compound **5.5** (0.36 mmol) using general protocols 13 and 14. Yield: 61%, $R_f = 0.61$ (10% TEA in EtOAc). $^1\text{H NMR}$ (500 MHz, CDCl_3) δ 7.45 (m, 1H, -NH), 7.38–7.30 (m, 5H, H-15a,b, H-16a,b, H-17), 5.13 (m, 2H, H-14), 4.00 (s, 1H, H-11), 3.63–3.47 (m, 2H, H-12 or H-13), 2.67 (d, $J = 12.3$ Hz, 1H, H-8a), 2.64–2.53 (m, 5H, H-7, H-8b, H-12 or H-13), 1.49 (m, 2H, H-6), 1.35–1.23 (m, 8H, H-2, H-3, H-4, H-5), 1.05 (s, 3H, H-9 or H-10), 0.92–0.86 (m, 6H, H-1, H-9 or H-10). $^{13}\text{C NMR}$ (126 MHz, CDCl_3) δ 172.77, 172.16, 135.86, 128.73, 128.44, 128.44, 80.92, 66.62, 61.80, 50.17, 36.57, 34.51, 34.44, 31.90, 29.65, 29.28, 27.28, 24.52, 22.76, 19.58, 14.23. HRMS for $\text{C}_{23}\text{H}_{39}\text{N}_2\text{O}_4$ $[\text{M}+\text{H}]^+$ calcd. 407.2904, found 407.2904.

Benzyl (R)-3-(2-hydroxy-4-((3-hydroxypropyl)amino)-3,3-dimethylbutanamido)propanoate (5.2e)



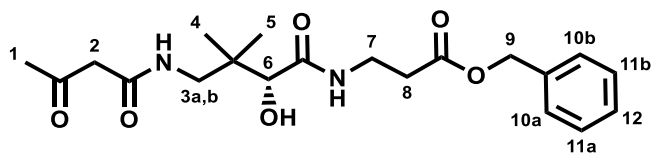
Compound **5.2e** was prepared from compound **5.6e** (0.27 mmol) as in section 8.1.5.4. Yield: 41%, $R_f = 0.26$ (30% MeOH in EtOAc). $^1\text{H NMR}$ (500 MHz, CDCl_3) δ 7.50 (m, 1H, -NH), 7.39–7.30 (m, 5H, H-11a,b, H-12a,b, H-13), 5.10 (m, 2H, H-10), 3.99 (s, 1H, H-7), 3.77 (t, $J = 5.7$ Hz, 2H, H-3), 3.56 (m, 2H, H-8), 2.83 (t, $J = 6.3$ Hz, 2H, H-1), 2.74 (d, $J = 12.2$ Hz, 1H, H-4a), 2.64–2.58 (m, 3H, H-4b, H-9), 1.79 (m, 2H, H-2), 1.06 (s, 3H, H-5 or H-6), 0.93 (s, 3H, H-5 or H-6). $^{13}\text{C NMR}$ (126 MHz, CDCl_3) δ 172.85, 172.30, 135.76, 128.75, 128.49, 128.44, 79.22, 66.72, 61.44, 60.42, 48.03, 36.98, 34.56, 34.39, 30.82, 23.93, 20.68. HRMS for $\text{C}_{19}\text{H}_{31}\text{N}_2\text{O}_5$ $[\text{M}+\text{H}]^+$ calcd. 367.22275, found 367.22185.

Benzyl (R)-3-(2-hydroxy-3,3-dimethyl-4-(phenethylamino)butanamido)propanoate (5.2f)



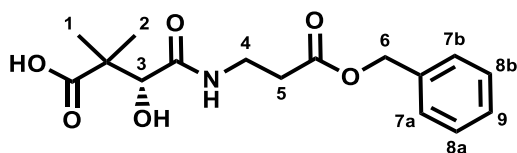
Compound **5.2f** was prepared from compound **5.6f** (0.23 mmol) as in section 8.1.5.5. Yield: 62%, $R_f = 0.27$ (EtOAc:hexanes:TEA = 4:4:1). $^1\text{H NMR}$ (500 MHz, CDCl_3) δ 7.41 (m, 1H, -NH), 7.36–7.19 (m, 10H, H-1, H-2a,b, H-3a,b, H-13a,b, H-14a,b, H-15), 5.07 (m, 2H, H-12), 4.01 (s, 1H, H-9), 3.53 (m, 2H, H-10 or H-11), 2.97–2.86 (m, 4H, H-4, H-5), 2.72–2.56 (m, 4H, H-6, H-10 or H-11), 1.05 (s, 3H, H-7 or H-8), 0.89 (s, 3H, H-7 or H-8). $^{13}\text{C NMR}$ (126 MHz, CDCl_3) δ 172.72, 172.09, 138.42 (based on HMBC), 135.83, 128.87, 128.82, 128.74, 128.46, 128.45, 126.81, 77.36, 66.66, 60.54, 51.15, 36.96, 34.86 (based on HSQC and HMBC), 34.55, 34.42, 24.13, 20.42 (based on HSQC and HMBC). HRMS for $\text{C}_{24}\text{H}_{33}\text{N}_2\text{O}_4$ $[\text{M}+\text{H}]^+$ calcd. 413.24348, found 413.24485.

Benzyl (*R*)-3-(2-hydroxy-3,3-dimethyl-4-(3-oxobutanamido)butanamido)propanoate (5.2g)



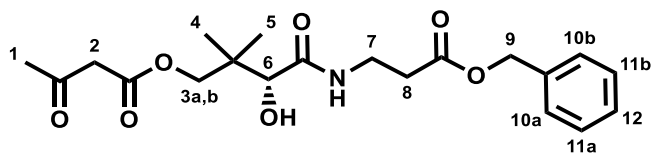
Compound **5.2g** was prepared from compound **5.5** (0.47 mmol) as in section 8.1.5.6. Yield: 50%, $R_f = 0.25$ (72% EtOAc in hexanes). ^1H NMR (400 MHz, CDCl_3) δ 7.66 (m, 1H, -NH), 7.51 (m, 1H, -NH), 7.40–7.28 (m, 5H, H-10a,b, H-11a,b, H-12), 5.13 (s, 2H, H-9), 3.66 (s, 1H, H-6), 3.65–3.53 (m, 3H, H-3a, H-7), 3.46 (s, 2H, H-2), 2.72 (dd, $J = 14.1, 5.7$ Hz, 1H, H-3b), 2.61 (t, $J = 6.3$ Hz, 2H, H-8), 2.27 (s, 3H, H-1), 1.06 (s, 3H, H-4 or H-5), 0.85 (s, 3H, H-4 or H-5). ^{13}C NMR (126 MHz, CDCl_3) δ 204.63, 172.30, 172.01, 167.87, 135.82, 128.73, 128.46, 128.46, 74.19, 66.67, 48.65, 48.56, 39.56, 34.71, 34.39, 31.29, 22.20, 20.45. HRMS for $\text{C}_{20}\text{H}_{28}\text{N}_2\text{O}_6\text{K}$ $[\text{M}+\text{K}]^+$ calcd. 431.1579, found 431.1587.

(*R*)-4-((3-(Benzyloxy)-3-oxopropyl)amino)-3-hydroxy-2,2-dimethyl-4-oxobutanoic acid (5.2h)



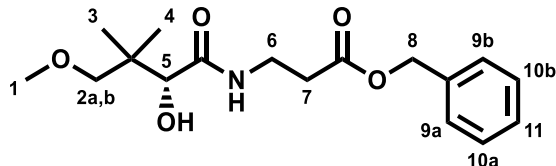
Compound **5.2h** was prepared from compound **5.7** (0.35 mmol) using general protocol 12. Yield: 43%, $R_f = 0.50$ (10% MeOH in EtOAc). ^1H NMR (400 MHz, CD_3OD) δ 7.41–7.26 (m, 5H, H-7a,b, H-8a,b, H-9), 5.13 (s, 2H, H-6), 4.30 (s, 1H, H-3), 3.48 (m, 2H, H-4), 2.60 (t, $J = 6.6$ Hz, 2H, H-5), 1.16 (s, 3H, H-1 or H-2), 1.10 (s, 3H, H-1 or H-2). ^{13}C NMR (126 MHz, CD_3OD) δ 180.40, 174.89, 173.21, 137.44, 129.55, 129.27, 129.23, 76.74, 67.45, 47.48, 35.69, 34.92, 22.29, 20.77. HRMS for $\text{C}_{16}\text{H}_{20}\text{NO}_6$ $[\text{M}-\text{H}]^-$ calcd. 322.12961, found 322.12910.

(*R*)-4-((3-(Benzyloxy)-3-oxopropyl)amino)-3-hydroxy-2,2-dimethyl-4-oxobutyl 3-oxobutanoate (5.2i)



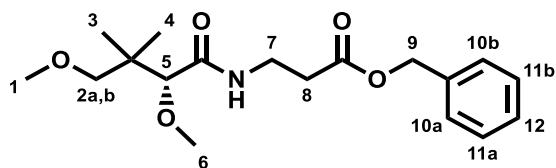
Compound **5.2i** was prepared from compound **5.8** (0.34 mmol) as in section 8.1.5.7. Yield: 56%, $R_f = 0.29$ (70% EtOAc in hexanes). $^1\text{H NMR}$ (500 MHz, CDCl_3) δ 7.39–7.31 (m, 5H, H-10a,b, H-11a,b, H-12), 7.09 (m, 1H, -NH), 5.13 (s, 2H, H-9), 4.20 (d, $J = 11.0$ Hz, 1H, H-3a), 3.89 (s, 1H, H-6), 3.81 (d, $J = 11.0$ Hz, 1H, H-3b), 3.59 (m, 2H, H-7), 3.54 (s, 2H, H-2), 2.62 (t, $J = 6.3$ Hz, 2H, H-8), 2.28 (s, 3H, H-1), 1.03 (s, 3H, H-4 or H-5), 0.93 (s, 3H, H-4 or H-5). $^{13}\text{C NMR}$ (126 MHz, CDCl_3) δ 201.81, 172.08, 171.97, 167.15, 135.78, 128.76, 128.52, 128.47, 74.59, 71.80, 66.73, 50.25, 38.66, 34.93, 34.26, 30.55, 21.17, 20.24. HRMS for $\text{C}_{20}\text{H}_{28}\text{NO}_7$ $[\text{M}+\text{H}]^+$ calcd. 394.18603, found 394.18598.

Benzyl (*R*)-3-(2-hydroxy-4-methoxy-3,3-dimethylbutanamido)propanoate (5.2j)



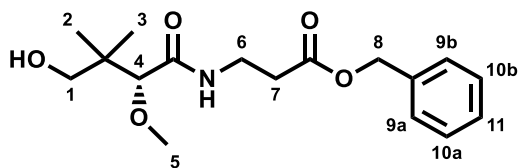
Compound **5.2j** was prepared from compound **5.3** (1.86 mmol) as in section 8.1.5.8. $R_f = 0.37$ (50% EtOAc in hexanes). $^1\text{H NMR}$ (500 MHz, CDCl_3) δ 7.39–7.31 (m, 5H, H-9a,b, H-10a,b, H-11), 7.12 (m, 1H, -NH), 5.14 (s, 2H, H-8), 3.95 (s, 1H, H-5), 3.58 (m, 2H, H-6), 3.34 (s, 3H, H-1), 3.30 (d, $J = 9.2$ Hz, 1H, H-2a), 3.21 (d, $J = 9.1$ Hz, 1H, H-2b), 2.61 (t, $J = 6.1$ Hz, 2H, H-7), 0.98 (s, 3H, H-3 or H-4), 0.97 (s, 3H, H-3 or H-4). $^{13}\text{C NMR}$ (126 MHz, CDCl_3) δ 172.25, 172.21, 135.77, 128.76, 128.52, 128.45, 82.59, 78.72, 66.70, 59.44, 38.43, 34.62, 34.41, 21.98, 20.44. HRMS for $\text{C}_{17}\text{H}_{25}\text{NO}_5\text{Na}$ $[\text{M}+\text{Na}]^+$ calcd. 346.1625, found 346.1626.

Benzyl (*R*)-3-(2,4-dimethoxy-3,3-dimethylbutanamido)propanoate (**5.2k**)



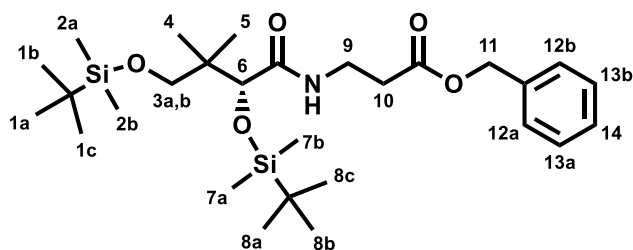
Compound **5.2k** was prepared from compound **5.3** (1.86 mmol) as in section 8.1.5.8. R_f = 0.42 (50% EtOAc in hexanes). $^1\text{H NMR}$ (500 MHz, CDCl_3) δ 7.39–7.30 (m, 5H, H-10a,b, H-11a,b, H-12), 6.94 (m, 1H, -NH), 5.14 (m, 2H, H-9), 3.57 (m, 2H, H-7 or H-8), 3.48 (s, 1H, H-5), 3.31 (s, 3H, H-1 or H-6), 3.26 (s, 3H, H-1 or H-6), 3.19 (d, J = 8.8 Hz, 1H, H-2a), 3.12 (d, J = 8.8 Hz, 1H, H-2b), 2.61 (m, 2H, H-7 or H-8), 0.92 (s, 3H, H-3 or H-4), 0.87 (s, 3H, H-3 or H-4). $^{13}\text{C NMR}$ (126 MHz, CDCl_3) δ 172.26, 171.43, 135.76, 128.76, 128.54, 128.46, 86.31, 79.17, 66.70, 59.28, 59.19, 39.00, 34.46, 34.44, 21.53, 20.92. HRMS for $\text{C}_{18}\text{H}_{27}\text{NO}_5\text{Na}$ $[\text{M}+\text{Na}]^+$ calcd. 360.1781, found 360.1784.

Benzyl (*R*)-3-(4-hydroxy-2-methoxy-3,3-dimethylbutanamido)propanoate (**5.2l**)



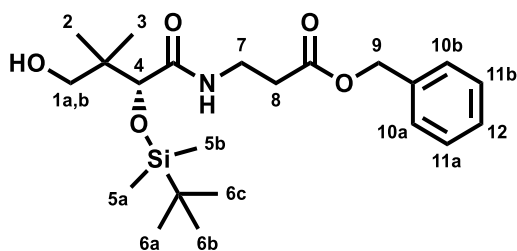
Compound **5.2l** was prepared from compound **5.3** (1.86 mmol) as in section 8.1.5.8. R_f = 0.30 (60% EtOAc in hexanes). $^1\text{H NMR}$ (500 MHz, CDCl_3) δ 7.40–7.31 (m, 5H, H-9a,b, H-10a,b, H-11), 7.05 (m, 1H, -NH), 5.14 (m, 2H, H-8), 3.59 (m, 2H, H-6 or H-7), 3.46 (s, 1H, H-4), 3.42–3.26 (m, 5H, H-1, H-5), 2.63 (m, 2H, H-6 or H-7), 1.01 (s, 3H, H-2 or H-3), 0.76 (s, 3H, H-2 or H-3). $^{13}\text{C NMR}$ (126 MHz, CDCl_3) δ 172.38, 172.12, 135.66, 128.78, 128.61, 128.51, 87.93, 70.72, 66.84, 59.76, 40.18, 34.60, 34.32, 22.78, 19.35. HRMS for $\text{C}_{17}\text{H}_{25}\text{NO}_5\text{Na}$ $[\text{M}+\text{Na}]^+$ calcd. 346.1625, found 346.1633.

Benzyl (R)-3-(2,4-bis((tert-butyl)dimethylsilyloxy)-3,3-dimethylbutanamido)propanoate (5.3)



Compound **5.3** was prepared from D-pantothenic acid hemicalcium salt (2.10 mmol) as in section 8.1.5.9. Yield: 99%, $R_f = 0.15$ (8% EtOAc in hexanes). $^1\text{H NMR}$ (500 MHz, CDCl_3) δ 7.39–7.29 (m, 5H, H-12a,b, H-13a,b, H-14), 6.78 (m, 1H, -NH), 5.14 (m, 2H, H-11), 4.00 (s, 1H, H-6), 3.55 (m, 2H, H-9 or H-10), 3.40 (d, $J = 9.5$ Hz, 1H, H-3a), 3.34 (d, $J = 9.5$ Hz, 1H, H-3b), 2.59 (m, 2H, H-9 or H-10), 0.92 (s, 9H, H-1a,b,c or H-8a,b,c), 0.89 (s, 9H, H-1a,b,c or H-8a,b,c), 0.85 (s, 3H, H-4 or H-5), 0.81 (s, 3H, H-4 or H-5), 0.07 (s, 3H, H-2a or H-2b or H-7a or H-7b), 0.04 (s, 3H, H-2a or H-2b or H-7a or H-7b), 0.02 (s, 3H, H-2a or H-2b or H-7a or H-7b), -0.02 (s, 3H, H-2a or H-2b or H-7a or H-7b). $^{13}\text{C NMR}$ (126 MHz, CDCl_3) δ 172.67, 172.23, 135.72, 128.75, 128.52, 128.46, 76.72, 68.97, 66.70, 40.29, 34.40, 34.22, 26.15, 25.95, 20.97, 20.18, 18.53, 18.14, -4.97, -5.10, -5.20, -5.29. HRMS for $\text{C}_{28}\text{H}_{51}\text{NO}_5\text{Si}_2\text{Na}$ $[\text{M}+\text{Na}]^+$ calcd. 560.3198, found 560.3217.

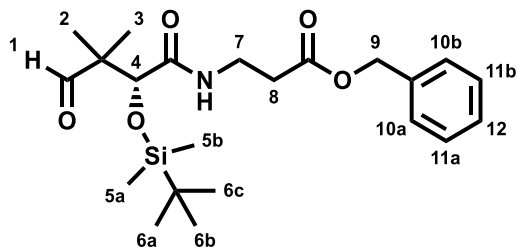
Benzyl (R)-3-(2-((tert-butyl)dimethylsilyloxy)-4-hydroxy-3,3-dimethylbutanamido)propanoate (5.4)



Compound **5.4** was prepared from compound **5.3** (0.36 mmol) as in section 8.1.5.10. Yield: 91%, $R_f = 0.15$ (30% EtOAc in hexanes). $^1\text{H NMR}$ (500 MHz, CDCl_3) δ 7.40–7.30 (m, 5H, H-10a,b, H-11a,b, H-12), 6.95 (m, 1H, -NH), 5.12 (m, 2H, H-9), 4.00 (s, 1H, H-4), 3.55 (m, 2H, H-7 or H-8), 3.39 (d, $J = 11.9$ Hz, 1H, H-1a), 3.36 (d, $J = 11.9$ Hz, 1H, H-1b), 2.61 (m, 2H, H-7 or H-8), 1.00 (s, 3H, H-2 or H-3), 0.94 (s, 9H, H-6a,b,c), 0.75 (s, 3H, H-

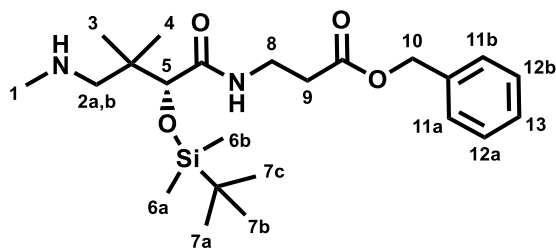
2 or H-3), 0.09 (s, 3H, H-5a or H-5b), -0.02 (s, 3H, H-5a or H-5b). ^{13}C NMR (126 MHz, CDCl_3) δ 173.85, 172.10, 135.61, 128.78, 128.59, 128.51, 78.27, 70.52, 66.83, 40.69, 34.41, 34.20, 25.91, 23.89, 18.81, 18.10, -5.00, -5.12. HRMS for $\text{C}_{22}\text{H}_{38}\text{NO}_5\text{Si}$ $[\text{M}+\text{H}]^+$ calcd. 424.25138, found 424.25030.

Benzyl (R)-3-(2-((*tert*-butyldimethylsilyl)oxy)-3,3-dimethyl-4-oxobutanamido)propanoate (5.5)



Compound **5.5** was prepared from compound **5.4** (1.42 mmol) as in section 8.1.5.11. Yield: 99%, R_f = 0.72 (50% EtOAc in hexanes). ^1H NMR (500 MHz, CDCl_3) δ 9.58 (s, 1H, H-1), 7.42–7.33 (m, 5H, H-10a,b, H-11a,b, H-12), 6.94 (m, 1H, -NH), 5.12 (m, 2H, H-9), 4.25 (s, 1H, H-4), 3.55 (m, 2H, H-7 or H-8), 2.58 (m, 2H, H-7 or H-8), 1.07 (s, 3H, H-2 or H-3), 1.01 (s, 3H, H-2 or H-3), 0.96 (s, 9H, H-6a,b,c), 0.13 (s, 3H, H-5a or H-5b), 0.04 (s, 3H, H-5a or H-5b). ^{13}C NMR (126 MHz, CDCl_3) δ 202.03, 172.16, 171.38, 135.62, 128.76, 128.57, 128.47, 76.34, 66.79, 50.69, 34.35, 34.14, 25.82, 19.05, 18.07, 16.56, -4.89, -4.96. HRMS for $\text{C}_{22}\text{H}_{35}\text{NO}_5\text{SiNa}$ $[\text{M}+\text{Na}]^+$ calcd. 444.2177, found 444.2182.

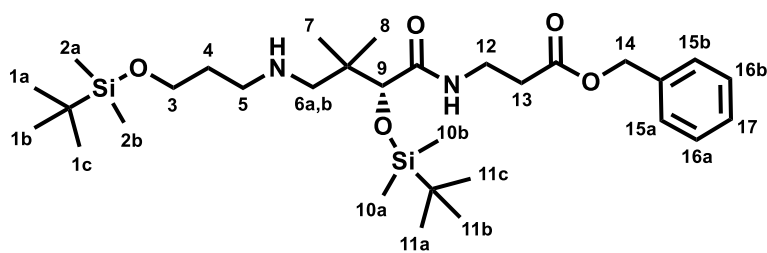
Benzyl (R)-3-(2-((*tert*-butyldimethylsilyl)oxy)-3,3-dimethyl-4-(methylamino)butan-amido)propanoate (5.6a)



Compound **5.6a** was prepared from compound **5.5** (0.36 mmol) using the general protocol 14. Yield: 49%, R_f = 0.42 (EtOAc:hexanes:TEA = 4:5:1). ^1H NMR (500 MHz, CDCl_3) δ 7.40–7.31 (m, 5H, H-11a,b, H-12a,b, H-13), 6.97 (m, 1H, -NH), 5.11 (m, 2H, H-10), 3.95

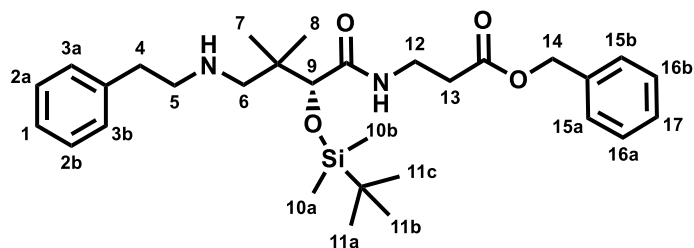
(s, 1H, H-5), 3.55 (m, 2H, H-8 or H-9), 2.59 (m, 2H, H-8 or H-9), 2.51 (d, $J = 11.8$ Hz, 1H, H-2a), 2.41 (s, 3H, H-1), 2.34 (d, $J = 11.8$ Hz, 1H, H-2b), 0.99 (s, 3H, H-3 or H-4), 0.93 (s, 9H, H-7a,b,c), 0.86 (s, 3H, H-3 or H-4), 0.08 (s, 3H, H-6a or H-6b), -0.02 (s, 3H, H-6a or H-6b). ^{13}C NMR (126 MHz, CDCl_3) δ 172.86, 172.17, 135.68, 128.77, 128.56, 128.48, 78.56, 66.77, 60.60, 38.94, 37.18, 34.36, 34.28, 25.94, 23.75, 21.97, 18.12, -5.00, -5.13. HRMS for $\text{C}_{23}\text{H}_{41}\text{N}_2\text{O}_4\text{Si}$ $[\text{M}+\text{H}]^+$ calcd. 437.28301, found 437.28286.

Benzyl (*R*)-11-((*tert*-butyldimethylsilyl)oxy)-2,2,3,3,10,10-hexamethyl-12-oxo-4-oxa-8,13-diaza-3-silahexadecan-16-oate (5.6e)



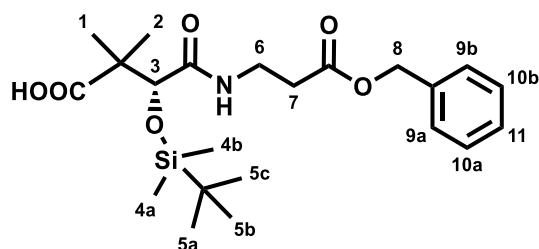
Compound **5.6e** was prepared from compound **5.5** (1.19 mmol) as in section 8.1.5.13. Yield: 25% over three steps, $R_f = 0.31$ (10% MeOH in EtOAc). ^1H NMR (400 MHz, CDCl_3) δ 7.40–7.29 (m, 5H, H-15a,b, H-16a,b, H-17), 7.01 (m, 1H, -NH), 5.12 (m, 2H, H-14), 3.96 (s, 1H, H-9), 3.67 (t, $J = 6.3$ Hz, 2H, H-3), 3.55 (m, 2H, H-12 or H-13), 2.69–2.54 (m, 4H, H-5, H-12 or H-13), 2.50 (d, $J = 11.5$ Hz, 1H, H-6a or H-6b), 2.36 (d, $J = 11.5$ Hz, 1H, H-6a or H-6b), 1.69 (m, 2H, H-4), 0.94 (s, 3H, H-7 or H-8), 0.92 (s, 9H, H-1a,b,c or H-11a,b,c), 0.88 (s, 9H, H-1a,b,c or H-11a,b,c), 0.84 (s, 3H, H-7 or H-8), 0.07 (s, 3H, H-2a or H-2b or H-10a or H-10b), 0.04 (s, 6H, 2 of H-2a/H-2b/H-10a/H-10b), -0.03 (s, 3H, H-2a or H-2b or H-10a or H-10b). ^{13}C NMR (126 MHz, CDCl_3) δ 172.91, 172.15, 135.70, 128.75, 128.53, 128.47, 78.55, 66.71, 61.75, 58.23, 47.91, 38.98, 34.33, 34.30, 32.99, 26.12, 25.94, 23.24, 22.09, 18.50, 18.12, -4.99, -5.16. HRMS for $\text{C}_{31}\text{H}_{59}\text{N}_2\text{O}_5\text{Si}_2$ $[\text{M}+\text{H}]^+$ calcd. 595.39570, found 595.39611.

Benzyl (R)-3-(2-((tert-butyldimethylsilyl)oxy)-3,3-dimethyl-4-(phenethylamino)-butanamido)propanoate (5.6f)



Compound **5.6f** was prepared from compound **5.5** (0.47 mmol) using the general protocol 14. Yield: 49%, $R_f = 0.08$ (EtOAc:hexanes:TEA = 4:9:0.1). ^1H NMR (500 MHz, CDCl_3) δ 7.41–7.18 (m, 10H, H-1, H-2a,b, H-3a,b, H-15a,b, H-16a,b, H-17), 7.03 (m, 1H, -NH), 5.14 (s, 2H, H-14), 3.99 (s, 1H, H-9), 3.56 (m, 2H, H-12 or H-13), 2.96–2.74 (m, 4H, H-4, H-5), 2.65–2.37 (m, 4H, H-6, H-12 or H-13), 0.98–0.93 (m, 12H, H-7 or H-8, H-11a,b,c), 0.88 (s, 3H, H-7 or H-8), 0.10 (s, 3H, H-10a or H-10b), 0.00 (s, 3H, H-10a or H-10b). ^{13}C NMR (126 MHz, CDCl_3) δ 172.95, 172.15, 140.63 (based on HMBC), 135.70, 128.90, 128.76, 128.55, 128.47, 128.47, 126.23, 78.58, 66.74, 57.90, 52.29, 38.96, 36.49 (based on HSQC), 34.35, 34.29, 25.95, 23.06 (based on HSQC), 22.13, 18.13, -4.98, -5.14. HRMS for $\text{C}_{30}\text{H}_{47}\text{N}_2\text{O}_4\text{Si}$ $[\text{M}+\text{H}]^+$ calcd. 527.32996, found 527.33145.

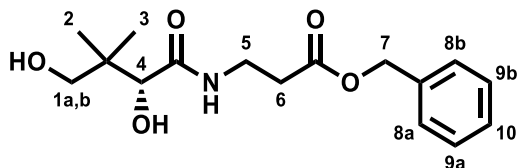
(R)-4-((3-(Benzyloxy)-3-oxopropyl)amino)-3-((tert-butyldimethylsilyl)oxy)-2,2-dimethyl-4-oxobutanoic acid (5.7)



Compound **5.7** was prepared from compound **5.5** (0.47 mmol) as in section 8.1.5.14. Yield: 74%, $R_f = 0.15$ (50% EtOAc in hexanes). ^1H NMR (500 MHz, CDCl_3) δ 7.39–7.29 (m, 5H, H-9a,b, H-10a,b, H-11), 6.95 (m, 1H, -NH), 5.12 (m, 2H, H-8), 4.39 (s, 1H, H-3), 3.56 (m, 2H, H-7), 2.58 (td, $J = 5.5, 1.7$ Hz, 2H, H-6), 1.17 (s, 3H, H-1 or H-2), 1.13 (s, 3H, H-1 or H-2), 0.92 (s, 9H, H-5a,b,c), 0.10 (s, 3H, H-4a or H-4b), 0.01 (s, 3H, H-4a or H-4b). ^{13}C NMR (126 MHz, CDCl_3) δ 180.13, 172.21, 171.69, 135.67, 128.75, 128.54,

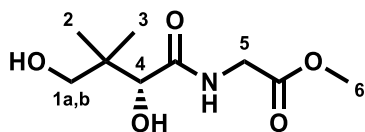
128.47, 77.41 (based on HSQC and HMBC), 66.76, 47.32, 34.41, 34.13, 25.85, 21.82, 20.20, 18.09, -4.85, -5.10. HRMS for $C_{22}H_{34}NO_6Si$ $[M-H]^-$ calcd. 436.21609, found 436.21652.

Benzyl (*R*)-3-(2,4-dihydroxy-3,3-dimethylbutanamido)-propanoate (**5.8**)



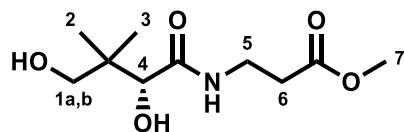
Compound **5.8** was prepared from β -alanine benzyl ester 4-toluenesulfonate salt (1.42 mmol) as in section 8.1.5.15. Yield: 73%, $R_f = 0.16$ (70% EtOAc in hexanes). 1H NMR (400 MHz, $CDCl_3$) δ 7.42–7.32 (m, 5H, H-8a,b, H-9a,b, H-10), 7.11 (m, 1H, -NH), 5.14 (s, 2H, H-7), 3.98 (s, 1H, H-4), 3.59 (m, 2H, H-5), 3.48 (d, $J = 11.2$ Hz, 1H, H-1a), 3.46 (d, $J = 11.2$ Hz, 1H, H-1b), 2.62 (t, $J = 6.0$ Hz, 2H, H-6), 1.00 (s, 3H, H-2 or H-3), 0.88 (s, 3H, H-2 or H-3). ^{13}C NMR (126 MHz, $CDCl_3$) δ 172.89, 172.29, 135.72, 128.80, 128.61, 128.54, 77.82, 71.40, 66.82, 39.48, 34.80, 34.28, 21.59, 20.29. HRMS for $C_{16}H_{24}NO_5$ $[M+H]^+$ calcd. 310.16490, found 310.16479.

Methyl (*R*)-(2,4-dihydroxy-3,3-dimethylbutanoyl)glycinate (**5.9a**)



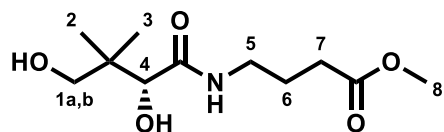
Compound **5.9a** was prepared from D-pantolactone (3.1 mmol) as in section 8.1.5.16. Yield: 25%, $R_f = 0.53$ (10% MeOH in EtOAc). 1H NMR (500 MHz, $CDCl_3$) δ 4.14–4.03 (m, 3H, H-4, H-5), 3.76 (s, 3H, H-6), 3.57 (d, $J = 11.1$ Hz, 1H, H-1a), 3.54 (d, $J = 11.1$ Hz, 1H, H-1b), 1.07 (s, 3H, H-2 or H-3), 0.96 (s, 3H, H-2 or H-3). ^{13}C NMR (126 MHz, $CDCl_3$) δ 173.49, 170.50, 77.94, 71.40, 52.58, 40.85, 39.57, 21.50, 20.53. HRMS for $C_9H_{17}NO_5Na$ $[M+Na]^+$ calcd. 242.0999, found 242.0996.

Methyl (*R*)-3-(2,4-dihydroxy-3,3-dimethylbutanamido)propanoate (**5.9b**)



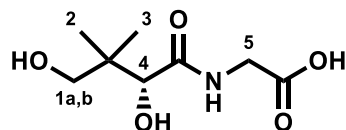
Compound **5.9b** was prepared from commercial D-pantolactone (1.54 mmol, 1.0 eq) and β -alanine methyl ester hydrochloride (1.69 mmol, 1.1 eq) using the general protocol 15. Yield: 74%, $R_f = 0.23$ (100% EtOAc). The characterization data is in agreement with a previous report.²²² ^1H NMR (500 MHz, CDCl_3) δ 7.18 (bs, 1H, -NH), 4.02 (s, 1H, H-4), 3.70 (s, 3H, H-7), 3.58 (m, 2H, H-5), 3.52 (d, $J = 11.2$ Hz, 1H, H-1a), 3.50 (d, $J = 11.2$ Hz, 1H, H-1b), 2.58 (t, $J = 6.1$ Hz, 2H, H-6), 1.02 (s, 3H, H-2 or H-3), 0.91 (s, 3H, H-2 or H-3).

Methyl (*R*)-4-(2,4-dihydroxy-3,3-dimethylbutanamido)-butanoate (**5.9c**)



Compound **5.9c** was prepared from D-pantolactone (3.1 mmol) as in section 8.1.5.18. Yield: 27%, $R_f = 0.42$ (10% MeOH in EtOAc). ^1H NMR (500 MHz, CDCl_3) δ 4.04 (s, 1H, H-4), 3.69 (s, 3H, H-8), 3.56 (d, $J = 11.2$ Hz, 1H, H-1a), 3.50 (d, $J = 11.3$ Hz, 1H, H-1b), 3.36 (m, 2H, H-5), 2.39 (t, $J = 7.2$ Hz, 2H, H-7), 1.88 (m, 2H, H-6), 1.04 (s, 3H, H-2 or H-3), 0.92 (s, 3H, H-2 or H-3). ^{13}C NMR (126 MHz, CDCl_3) δ 173.11 (based on HMBC), 172.70 (based on HMBC), 77.97, 71.54, 51.94, 39.54, 38.72, 31.64, 24.82, 21.67, 20.25. HRMS for $\text{C}_{11}\text{H}_{21}\text{NO}_5\text{Na}$ $[\text{M}+\text{Na}]^+$ calcd. 270.13119, found 270.13124.

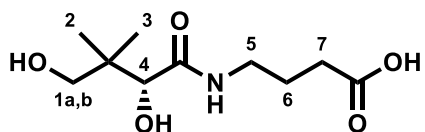
(*R*)-(2,4-Dihydroxy-3,3-dimethylbutanoyl)glycine (**5.9d**)



Compound **5.9d** was prepared from **5.9a** (0.43 mmol) using the general protocol 16. Yield: 48%, $R_f = 0.48$ (50% MeOH in EtOAc). The characterization data is in agreement with a previous report.²²¹ ^1H NMR (500 MHz, D_2O) δ 4.03 (s, 1H, H-4), 4.00 (s, 2H, H-5), 3.51 (d, $J = 11.3$ Hz, 1H, H-1a), 3.39 (d, $J = 11.3$ Hz, 1H, H-1b), 0.93 (s, 3H, H-2 or H-3), 0.91

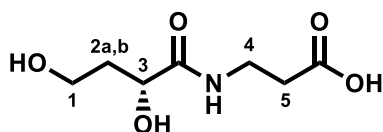
(s, 3H, H-2 or H-3). ^{13}C NMR (126 MHz, D_2O) δ 176.50, 173.90, 76.32, 68.92, 41.30, 39.37, 21.00, 19.68. HRMS for $\text{C}_8\text{H}_{14}\text{NO}_5$ $[\text{M}-\text{H}]^-$ calcd. 204.08775, found 204.08706.

(R)-4-(2,4-Dihydroxy-3,3-dimethylbutanamido)butanoic acid (5.9e)



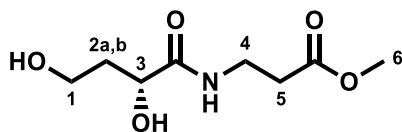
Compound **5.9e** was prepared from **5.9c** (0.80 mmol) using the general protocol 16. Yield: 40%, $R_f = 0.75$ (50% MeOH in EtOAc). The characterization data is in agreement with a previous report.²²¹ ^1H NMR (500 MHz, D_2O) δ 3.99 (s, 1H, H-4), 3.52 (d, $J = 11.2$ Hz, 1H, H-1a), 3.40 (d, $J = 11.2$ Hz, 1H, H-1b), 3.29 (t, $J = 6.9$ Hz, 2H, H-5), 2.43 (t, $J = 7.4$ Hz, 2H, H-7), 1.83 (m, 2H, H-6), 0.94 (s, 3H, H-2 or H-3), 0.91 (s, 3H, H-2 or H-3).

(R)-3-(2,4-Dihydroxybutanamido)propanoic acid (5.9f)



Compound **5.9f** was prepared from compound **5.10** (0.49 mmol) as in section 8.1.5.20. Yield: 81%. The characterization data is in agreement with a previous report.²²¹ ^1H NMR (500 MHz, D_2O) δ 4.24 (dd, $J = 8.8, 3.8$ Hz, 1H, H-3), 3.73 (dd, $J = 7.4, 5.7$ Hz, 2H, H-1), 3.45 (t, $J = 6.8$ Hz, 2H, H-4), 2.42 (t, $J = 6.8$ Hz, 2H, H-5), 2.03 (m, 1H, H-2a), 1.80 (m, 1H, H-2b). ^{13}C NMR (126 MHz, D_2O) δ 180.26, 176.33, 68.69, 57.73, 36.56, 36.18, 35.69.

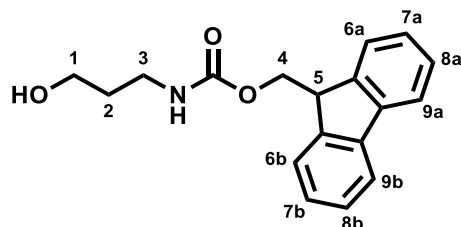
Methyl (R)-3-(2,4-dihydroxybutanamido)propanoate (5.10)



Compound **5.10** was prepared from commercial (*R*)-(+)- α -hydroxy- γ -butyrolactone (0.98 mmol, 1.0 eq) and β -alanine methyl ester hydrochloride (1.08 mmol, 1.1 eq) using the general protocol 15. Yield: 97%, $R_f = 0.32$ (10% MeOH in EtOAc). ^1H NMR (500 MHz, CDCl_3) δ 4.31 (dd, $J = 7.6, 3.9$ Hz, 1H, H-3), 3.94 (m, 2H, H-1), 3.71 (s, 3H, H-6), 3.58

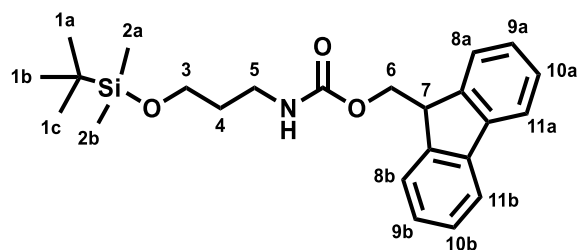
(m, 2H, H-4), 2.58 (dd, $J = 6.9, 5.5$ Hz, 2H, H-5), 2.14 (m, 1H, H-2a), 1.94 (m, 1H, H-2b). ^{13}C NMR (126 MHz, CDCl_3) δ 173.67, 172.93, 72.83, 61.86, 52.05, 35.59, 34.75, 34.06. HRMS for $\text{C}_8\text{H}_{15}\text{NO}_5\text{Na}$ $[\text{M}+\text{Na}]^+$ calcd. 228.0842, found 228.0842.

(9H-Fluoren-9-yl)methyl (3-hydroxypropyl)carbamate (5.12)



Compound **5.12** was prepared from 3-amino-1-propanol (13.31 mmol) as in section 8.1.5.21. Yield: 99%, $R_f = 0.30$ (80% EtOAc in hexanes). The characterization data is in agreement with a previous report. 223 ^1H NMR (500 MHz, CDCl_3) δ 7.77 (d, $J = 7.5$ Hz, 2H, H-6a,b or H-9a,b), 7.59 (d, $J = 7.5$ Hz, 2H, H-6a,b or H-9a,b), 7.40 (t, $J = 7.5$ Hz, 2H, H-7a,b or H-8a,b), 7.32 (t, $J = 7.4$ Hz, 2H, H-7a,b or H-8a,b), 5.00 (bs, 1H, -NH), 4.44 (d, $J = 6.7$ Hz, 2H, H-4), 4.22 (t, $J = 6.7$ Hz, 1H, H-5), 3.65 (m, 2H, H-1), 3.36 (m, 2H, H-3), 1.70 (m, 2H, H-2).

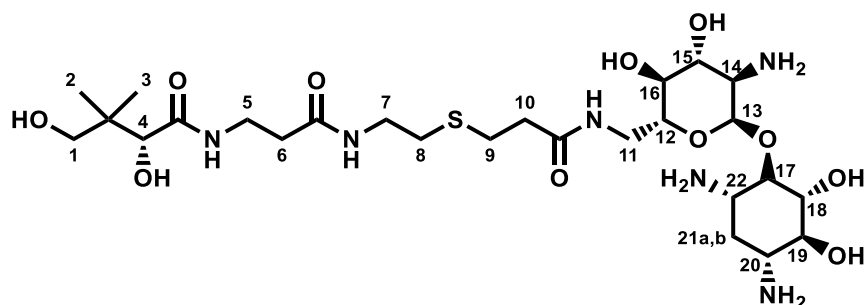
(9H-Fluoren-9-yl)methyl (3-((tert-butyl)dimethylsilyloxy)propyl)carbamate (5.13)



Compound **5.13** was prepared from compound **5.12** (13.31 mmol) as in section 8.1.5.22. Yield: 99%, $R_f = 0.43$ (20% EtOAc in hexanes). ^1H NMR (500 MHz, CDCl_3) δ 7.76 (d, $J = 7.5$ Hz, 2H, H-8a,b or H-11a,b), 7.60 (d, $J = 7.5$, 2H, H-8a,b or H-11a,b), 7.40 (t, $J = 7.4$ Hz, 2H, H-9a,b or H-10a,b), 7.31 (t, $J = 7.5$, 2H, H-9a,b or H-10a,b), 5.39 (bs, 1H, -NH), 4.38 (d, $J = 7.0$ Hz, 2H, H-6), 4.21 (t, $J = 6.9$ Hz, 1H, H-7), 3.74 (t, $J = 5.5$ Hz, 2H, H-3), 3.35 (m, 2H, H-5), 1.74 (m, 2H, H-4), 0.91 (s, 9H, H-1a,b,c), 0.10 (s, 3H, H-2a or H-2b), 0.07 (s, 3H, H-2a or H-2b). ^{13}C NMR (126 MHz, CDCl_3) δ 156.53, 144.25, 141.45, 127.75,

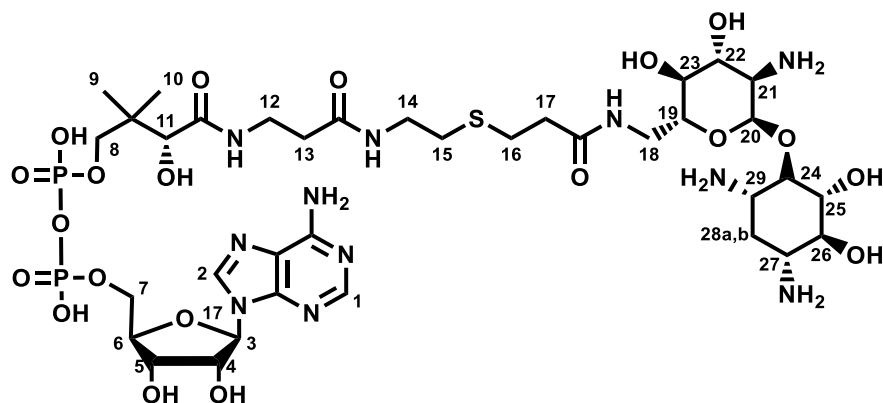
127.13, 125.23, 120.08, 66.66, 62.46, 47.48, 40.00, 31.95, 26.05, 18.35, -3.42, -5.30.
HRMS for C₂₄H₃₄NO₃Si [M+H]⁺ calcd. 412.23025, found 412.23105.

Compound P-1b



Compound **P-1b** was prepared from neamine (1.80 mmol, 1.0 eq) as described in section 8.1.6.1. Yield: 23%. The characterization data is in agreement with a previous report.¹³² ¹H NMR (500 MHz, D₂O) δ 5.73 (d, *J* = 4.0 Hz, 1H, H-13), 3.99 (s, 1H, H-4), 3.96–3.84 (m, 3H), 3.72–3.63 (m, 2H), 3.62–3.45 (m, 7H), 3.43–3.38 (m, 3H), 3.38–3.25 (m, 2H), 2.85 (t, *J* = 6.9 Hz, 2H, H-9), 2.72 (t, *J* = 6.6 Hz, 2H, H-8), 2.61 (t, *J* = 6.8 Hz, 2H, H-10), 2.55–2.50 (m, 3H, H-6, H-21a), 1.92–1.84 (m, 1H, H-21b), 0.93 (s, 3H, H-2 or H-3), 0.89 (s, 3H, H-2 or H-3).

Compound 6.3b



Compound **6.3b** was prepared from **P-1b** as described in section 8.1.6.2. Yield: 64%. Purity is 85%, *R*_t = 8.11 min with method A and *R*_t = 19.76 min with method B (Table 8.2). ¹H NMR (800 MHz, D₂O) δ 8.52 (s, 1H, H-1), 8.27 (s, 1H, H-2), 6.15 (d, *J* = 5.7 Hz, 1H, H-3), 5.51 (bs, 1H, H-20), 4.78 (m, 1H, H-4), 4.54 (dd, *J* = 5.2, 3.9 Hz, 1H, H-5), 4.41 (m,

1H, H-6), 4.25 (m, 2H, H-7), 4.02 (s, 1H, H-11), 3.90–3.80 (m, 4H, H-8, 2H of H-19/H-22/H-23/H-24/H-25/H-26), 3.62–3.50 (m, 5H, H-18, 3H of H-19/H-22/H-23/H-24/H-25/H-26), 3.48 (t, $J = 6.4$ Hz, 2H, H-12), 3.41 (m, 1H, 1H of H-19/H-22/H-23/H-24/H-25/H-26), 3.36 (t, $J = 6.8$ Hz, 2H, H-14), 3.25 (m, 1H, H-21 or H-27 or H-29), 3.20 (m, 1H, H-21 or H-27 or H-29), 3.09 (m, 1H, H-21 or H-27 or H-29), 2.81 (t, $J = 7.0$ Hz, 2H, H-16), 2.67 (t, $J = 6.8$ Hz, 2H, H-15), 2.57 (m, 2H, H-17), 2.47 (t, $J = 6.4$ Hz, 2H, H-13), 2.30 (m, 1H, H-28a), 1.61 (m, 1H, H-28b), 0.91 (s, 3H, H-9 or H-10), 0.80 (s, 3H, H-9 or H-10). ^{13}C NMR (201 MHz, D_2O), based on HSQC and HMBC, δ 174.80, 174.61, 173.99, 155.74, 152.87, 149.17, 139.91, 118.69, 97.79, 86.93, 83.78, 83.74, 75.30, 74.22, 74.14, 73.19, 71.83, 71.76, 71.42, 70.77, 70.22, 70.10, 65.18, 54.36, 50.30, 48.91, 38.54, 38.37, 35.54, 35.39, 35.38, 31.18, 30.36, 26.81, 20.84, 18.36. HRMS for $\text{C}_{36}\text{H}_{64}\text{N}_{11}\text{O}_{20}\text{P}_2\text{S}$ $[\text{M}+\text{H}]^+$ calcd. 1064.35195, found 1064.35209.

8.3 Biology

8.3.1 Materials

The bacterial strains that were used for antibacterial activity measurements include *Escherichia coli* ATCC 25922, *Enterococcus faecium* ATCC 19434, *Staphylococcus aureus* ATCC 29213 and *Pseudomonas aeruginosa* ATCC 27853, which were all purchased from Cedarlane, Canada. Unless otherwise mentioned, *E. coli* ATCC 25922, *S. aureus* ATCC 29213 and *P. aeruginosa* ATCC 27853 were cultured in Difco™ Tryptic Soy Broth, and *E. faecium* ATCC 19434 was cultured in Difco™ Brain Heart Infusion Broth. The *E. coli* BL21 and the constructed *E. coli* BL21-AAC(6')-li strains were grown in minimal medium (M9 growth medium + 0.2% glycerol). All the reagents used were obtained from Fisher Scientific Canada, VWR Canada, Chem Impex International Inc. or Sigma-Aldrich Canada. MilliQ-quality water was used whenever water is mentioned. The Ni-NTA agarose chromatography resin was acquired from Qiagen, Netherlands. The Superdex 75 prep grade size exclusion chromatography resin was purchased from GE Healthcare. Unless otherwise mentioned, a SpectraMax i3x microtiter plate reader from Molecular Devices, United States, was used for UV-Vis absorption measurements, including those of MIC and kinetic studies. Rosetta™(DE3) cells were obtained from

Novagen, Canada. BL21 competent *E. coli* cells were a gift from the Thibodeaux lab at McGill University. An UltiMate 3000 UHPLC System from Thermo Fisher Scientific coupled to a MaXis Impact HD Mass Spectrometer from Bruker were used for metabolomics studies, unless otherwise mentioned.

8.3.2 Measurement of antibacterial activity

The antibacterial activity of compounds **2.10**, **3.1**, **3.7a,b,d**, **3.13a**, **5.1a-l**, **5.9a-f**, **5.11**, **P-1b**, tobramycin and ribostamycin was determined using the broth microdilution method.²²⁴ Briefly, bacteria were cultured at 37°C in their corresponding medium for 5-10 hours, before dilution to 10⁷ CFU/mL and inoculation (10 µL) of the wells of a 96-well plate containing fresh growth medium (180 µL) supplemented with different concentrations of the desired compound (10 µL). The *E. faecium* ATCC 19434 concentration (CFU/mL) was determined using the calibration-derived equation $OD_{600} = 3 \cdot 10^{-10}x + 0.0285$, the *E. coli* ATCC 25922 concentration (CFU/mL) was determined using the calibration-derived equation $OD_{600} = 10^{-10}x + 0.0647$, the *S. aureus* ATCC 29213 concentration (CFU/mL) was determined using the calibration-derived equation $OD_{600} = 3 \cdot 10^{-10}x + 0.2324$, the *P. aeruginosa* ATCC 27853 concentration (CFU/mL) was determined using the calibration-derived equation $OD_{600} = 7 \cdot 10^{-11}x - 0.0428$, and the *E. coli* BL21 and *E. coli* BL21-AAC(6')-II concentration (CFU/mL) was determined using the calibration-derived equation $OD_{600} = 10^{-10}x$, where x is the bacterial concentration (CFU/mL) and OD₆₀₀ is the optical density at 600 nm when the cell path length is 1 cm. After 16 hours of incubation at 37°C, the OD₆₀₀ of the cell suspension in each well was measured. The optical density measured for the well without any tested compound was taken as 100% growth. All experiments were performed at least in duplicates.

8.3.3 Protein expression and purification

8.3.3.1 *P. aeruginosa* pantothenate kinase

For PaPanK expression, the plasmid pET28a(+)/PanK, which was generously provided by Dr. Suzanne Jackowski at St. Jude Children's Research Hospital, was transformed into *E. coli* Rosetta™(DE3) cells. The cells were cultured at 37°C in 50 mL LB medium supplemented with 50 µg/mL kanamycin for 15 hours. The cell culture (10 mL) was next

transferred into 1 L of LB medium supplemented with 50 $\mu\text{g}/\text{mL}$ kanamycin. The cells were cultured at 37°C to an OC_{600} of 0.5-0.6, before induction of protein expression with 1 mM isopropyl β -D-1-thiogalactopyranoside (IPTG) and further growing at 37°C for another 3 hours. The cell culture was centrifuged at 4°C, 5000 $\times g$ for 15 minutes. The resultant cell pellet was washed with PBS buffer (50 mL) and collected at 4°C, 5000 $\times g$ for 15 minutes.

To purify PaPank, the cell pellet was resuspended in Tris-HCl buffer (20 mM, pH = 7.9, 30 mL) containing 0.5 M NaCl, 1 mM PMSF, 1 mg/mL lysozyme, 5 mM β -mercaptoethanol and 5 mM imidazole. The mixture was incubated on ice for 30 minutes, and then sonicated on ice for 8 cycles (sonicating 15 s, waiting for 105 s) at 85% cycle duty, power 8 with a Branson Sonifier 450. The cell debris were removed by centrifugation at 4°C, 10,000 $\times g$ for 1 hour. The supernatant was applied onto a Ni-NTA column (6 mL slurry) at a flow rate of 0.5-0.8 mL/min (the column had been pre-equilibrated in the loading buffer: 20 mM, pH = 7.9 Tris-HCl containing 0.5 M NaCl, 5 mM β -mercaptoethanol and 5 mM imidazole,). The column was next washed with Tris-HCl buffer (20 mM, pH = 7.9, 100 mL) containing 0.5 M NaCl and 5 mM β -mercaptoethanol, before slowly increasing the imidazole concentration (5-250 mM). The flow rate was kept between 0.5-2 mL/min. The pure protein (based on sodium dodecyl sulfate polyacrylamide gel electrophoresis) was pooled, dialyzed three times against Tris-HCl buffer (50 mM, pH = 7.5, 4 L) containing 1 mM dithiothreitol and 1 mM EDTA. Finally, the protein was aliquoted, flashed-frozen in liquid nitrogen and stored at -80°C.

8.3.3.2 *E. faecium* aminoglycoside 6'-N-acetyltransferase type li

For AAC(6')-li expression, the plasmid pET22b(+)/AAC(6')-li, which was generously provided by Dr. Gerard D. Wright at McMaster University, was transformed into *E. coli* BL21 cells. The cells were cultured in 10 mL LB medium containing 100 $\mu\text{g}/\text{mL}$ ampicillin for 9 hours at 37°C. The culture (10 mL) was next transferred into 1 L of LB medium containing 100 $\mu\text{g}/\text{mL}$ ampicillin, and allowed to grow at 37°C. Once the OD_{600} reached 0.7, protein expression was induced with 1 mM IPTG before further growth at 37°C for another 3 hours. The cell culture was centrifuged at 4°C, 5000 $\times g$ for 15 minutes. The

cell pellets were washed with PBS buffer (50 mL) and collected again at 4°C, 5000 × *g* for 15 minutes.

The purification of the AAC(6′)-li protein followed a previously reported procedure with modifications.²²⁵ To purify the AAC(6′)-li protein, the cell pellets were suspended in HEPES buffer (25 mM, pH = 7.5, 60 mL) containing 2 mM EDTA, 1 mM PMSF, 1 mM bestatin, 1 μg/mL aprotinin, 1 mg/mL leupeptin, and 1 mg/mL lysozyme (10 mg per gram of bacterial pellet). The mixture was incubated on ice for 30 minutes, and then sonicated on ice for 8 cycles (sonicating 15 s, waiting for 45 s) at 85% cycle duty, power 8 with a Branson Sonifier 450. The cell debris was removed by centrifugation at 4°C, 18,000 × *g* for 15 minutes. The supernatant was next applied onto a Superdex 75 PG size-exclusion column (2 × 115 cm) at a flow rate of 0.5-0.8 mL/min (the column had been pre-equilibrated in the loading buffer: 25 mM, pH = 7.5 HEPES containing 2 mM EDTA). The column was washed with HEPES buffer (25 mM, pH = 7.5, 500 mL) containing 2 mM EDTA (flow rate between 0.5-2 mL/min). The purest protein (based on sodium dodecyl sulfate polyacrylamide gel electrophoresis) was aliquoted, flashed-frozen in liquid nitrogen, and stored at -80°C.

8.3.4 Enzymatic assays

8.3.4.1 Statistical analysis

Initial velocities were calculated by linear regression of the readings made over the first 40 s period, using the raw kinetic data. For each experiment, the three readings representing the same conditions were averaged and reported with the standard error of the mean (SEM).

8.3.4.2 *E. coli* pantothenate kinase assay

The enzyme assay which couples the production of adenosine diphosphate by PanK to the consumption of nicotinamide adenine dinucleotide (NADH) through the activity of pyruvate kinase (PK) and lactic dehydrogenase (LDH) was monitored by the decrease in A₃₄₀. An extinction coefficient of 6,220 M⁻¹·cm⁻¹ was used for NADH. The enzyme concentration was determined using the Bradford protein assay with bovine serum albumin as a standard. All experiments were performed in triplicates.

The *EcPanK* assay followed the previously described protocol with small modifications.¹⁴³ For inhibitory study, the reaction mixture (200 μL) contained the desired pantothenate analogue (200 μM), ATP (60 μM), pantothenate (25 μM), *EcPanK* (0.40 μM), NADH (0.3 mM), phospho(enol)pyruvate (2 mM), MgCl_2 (10 mM), KCl (20 mM) and PK/LDH enzymes from rabbit muscle (10 μL) in Tris-HCl buffer (50 mM, pH = 7.6) in each well of a 96-well microtiter plate. The reaction was initiated with the addition of ATP at 37°C.

For substrate study, the reaction mixture (200 μL) contained the desired pantothenate analogue (0-4 mM), ATP (1.5 mM), *EcPanK* (0.20 μM), NADH (0.3 mM), phospho(enol)pyruvate (2 mM), MgCl_2 (10 mM), KCl (20 mM) and PK/LDH enzymes from rabbit muscle (10 μL) in Tris-HCl buffer (50 mM, pH = 7.6) in each well of a 96-well microtiter plate. The reaction was initiated with the addition of ATP at 25°C. The kinetic parameters were determined by fitting the data to Michaelis-Menten equation.

8.3.4.3 *P. aeruginosa* pantothenate kinase assay

The enzyme assay which coupled the production of adenosine diphosphate to the consumption of NADH through the activity of PK and LDH was monitored by the decrease in A_{340} . An extinction coefficient of $6,220 \text{ M}^{-1}\cdot\text{cm}^{-1}$ was used for NADH. The enzyme concentration was determined using the Bradford protein assay with bovine serum albumin as a standard. All experiments were performed in triplicates.

For the *PaPanK* inhibitory assay, the reaction mixture (200 μL) contained the desired pantothenate analogue (200 μM), ATP (7.5 mM), pantothenate (30 μM), *PaPanK* (0.34 μM), NADH (0.3 mM), phospho(enol)pyruvate (2 mM), MgCl_2 (10 mM), NH_4Cl (60 mM) and PK/LDH enzymes from rabbit muscle (10 μL) in HEPES buffer (100 mM, pH = 7.5) in each well of a 96-well microtiter plate. The reaction was initiated with the addition of ATP at 37°C.

For the *PaPanK* substrate assay, the reaction mixture (200 μL) contained the desired pantothenate analogue (0-4 mM), ATP (1.5 mM), *PaPanK* (0.92 μM), NADH (0.3 mM), phospho(enol)pyruvate (2 mM), MgCl_2 (10 mM), NH_4Cl (60 mM) and PK/LDH enzymes from rabbit muscle (10 μL) in HEPES buffer (100 mM, pH = 7.5) in each well of a 96-well

microtiter plate. The reaction was initiated with the addition of ATP at 37°C. The kinetic parameters were determined by fitting the data to Michaelis-Menten equation.

8.3.4.4 *E. faecium* aminoglycoside 6'-N-acetyltransferase type Ii inhibition assay

The enzyme assay which couples the production of CoA to the consumption of 5,5'-dithio-bis-[2-nitrobenzoic acid] (Ellman's reagent) was monitored by the increase in A₄₁₂ with a Synergy™ H4 hybrid multi-mode microplate reader from BioTek. An extinction coefficient of 14,150 M⁻¹·cm⁻¹ was used to quantify the produced 2-nitro-5-thiobenzoate. The enzyme concentration was determined using the k_{cat}/K_m data obtained with acetyl-CoA, where 0.18 nmol protein gives $k_{cat}/K_m = 0.017 \mu\text{M}^{-1}\cdot\text{s}^{-1}$.²²⁵ All experiments were performed at least in triplicates. The assay was performed as previously reported with small modifications.¹⁶⁸ The reaction mixture (200 μL) contained kanamycin A (200 μM), 5,5'-dithiobis-(2-nitrobenzoic acid) (2 mM), AAC(6')-Ii (0.90 μM), acetyl-CoA (12.50 μM) and different concentration of **6.3b** (0, 0.25, 0.50 or 1.00 μM) in HEPES buffer (25 mM, pH = 7.5) in each well of a 96-well microtiter plate. The reaction was initiated with the addition of kanamycin A at 37°C. The initial reaction velocities at different concentrations of **6.3b** were obtained. Similarly, the initial reaction velocities were also measured when increasing the acetyl-CoA concentration to 18.75, 25, 37.5 and 50 μM respectively.

To determine the K_i of **6.3b**, the obtained initial reaction velocities at different concentrations of acetyl-CoA and **6.3b** were fitted to Equation 1 for competitive inhibition, Equation 2 for noncompetitive inhibition, and Equation 3 for uncompetitive inhibition, where v is the initial reaction velocity, $[S]$ is the concentration of acetyl-CoA, K_m is the Michaelis-Menten constant, V_{max} is the maximal velocity, $[I]$ is the concentration of **6.3b** and K_i is the inhibition constant.

$$v = \frac{V_{max}[S]}{[S] + K_m(1 + \frac{[I]}{K_i})} \quad (1)$$

$$v = \frac{V_{max}[S]}{([S] + K_m)(1 + \frac{[I]}{K_i})} \quad (2)$$

$$v = \frac{V_{\max}[S]}{K_m + [S](1 + \frac{[I]}{K_i})} \quad (3)$$

As previously reported for the nanomolar inhibitor **I-1b**,¹⁸³ the obtained K_i values from Equation 1, 2 and 3 are all in the same range as the concentration of AAC(6')-Ii, which suggests tight binding inhibition. Therefore, the apparent K_i^{app} at each concentration of acetyl-CoA was determined by fitting the initial reaction velocities and concentrations of **6.3b** to the Morrison equation (Equation 4), where $[E]$ is the enzyme concentration, v_i is the initial velocity in the presence of inhibitor at concentration $[I]$ and v_0 is the initial velocity in the absence of inhibitor. Next, the obtained K_i^{app} at different concentrations of acetyl-CoA were fitted to Equation 5 for tight binding competitive inhibition, Equation 6 for tight binding noncompetitive inhibition, or Equation 7 for tight binding uncompetitive inhibition, where $[S]$ is the concentration of acetyl-CoA, K_i is the inhibition constant.

$$\frac{v_i}{v_0} = 1 - \frac{([E] + [I] + K_i^{\text{app}}) - \sqrt{([E] + [I] + K_i^{\text{app}})^2 - 4[E][I]}}{2[E]} \quad (4)$$

$$K_i^{\text{app}} = K_i \left(1 + \frac{[S]}{K_m}\right) \quad (5)$$

$$K_i^{\text{app}} = K_i \quad (6)$$

$$K_i^{\text{app}} = K_i \left(1 + \frac{K_m}{[S]}\right) \quad (7)$$

The experimental data fit Equation 5 better than 6 or 7, confirming that the **6.3b** is a tight binding competitive inhibitor for acetyl-CoA.

8.3.5 Checkerboard assays

8.3.5.1 Checkerboard assay with *E. faecium* to determine the MIC of tobramycin

The potentiation of tobramycin by **P-1b** was determined by a broth microdilution method.²²⁴ Briefly, the *E. faecium* ATCC 19434 cells were cultured at 37°C for 9 hours, before dilution to 2×10^6 CFU/mL and inoculation (10 μ L) of each well of a 96-well plate

containing brain heart infusion broth (150 μ L) supplemented with different concentrations of **P-1b** (20 μ L) and tobramycin (20 μ L). The *E. faecium* ATCC 19434 concentration (CFU/mL) was determined using the calibration-derived equation $OD_{600} = 3 \cdot 10^{-10}x + 0.0285$, where x is the bacterial concentration (CFU/mL), and OD_{600} is the optical density at 600 nm when the cell path length is 1 cm. After 16 hours of incubation at 37°C, the OD_{600} of the cell suspension in each well was measured. The optical density measured in the well without any tobramycin nor **P-1b** was taken as 100% growth. All experiments were performed in triplicates. The data points shown are averages and plotted with the SEM.

8.3.5.2 Checkerboard assay with AAC(6')-li-expressing *E. coli* to determine the MIC of ribostamycin

The potentiation of ribostamycin by **P-1b** was determined by a broth microdilution method.²²⁴ Firstly, an aminoglycoside-resistant *E. coli* strain was generated by transforming the plasmid pET22b(+)/AAC(6')-li into *E. coli* BL21. Next, the BL21 cells were cultured at 37°C in minimal medium (M9 growth medium + 0.2% glycerol) for 9 hours, before dilution to 10^7 CFU/mL and inoculation (10 μ L) of each well of a 96-well plate containing minimal medium (160 μ L) supplemented with **P-1b** (10 μ L, final concentration is 512 μ g/mL) and different concentrations of ribostamycin (20 μ L). The *E. coli* BL21-AAC(6')-li concentration (CFU/mL) was determined using the calibration-derived equation $OD_{600} = 10^{-10}x$, where x is the bacterial concentration (CFU/mL), and OD_{600} is the optical density at 600 nm when the cell path length is 1 cm. Ribostamycin was prepared as a stock concentration of 20480 μ g/mL and serially diluted down to 10 μ g/mL, so that the final concentration in each well was adjusted to 0-2048 μ g/mL. After 16 hours of incubation at 37°C, the OD_{600} of the cell suspension in each well was measured. The optical density measured in the well without any ribostamycin nor **P-1b** was taken as 100% growth. All experiments were performed at least in triplicates. The data points shown are averages and plotted with the SEM.

8.3.5.3 Checkerboard assay with AAC(6')-li-expressing *E. coli* to verify that P-1b competes with pantothenate for the same pathway

To confirm that **P-1b** is in competition with pantothenate *in cellulose*, a similar checkerboard assay was performed.²²⁴ Briefly, *E. coli* BL21-AAC(6')-li cells were cultured at 37°C in minimal medium (M9 growth medium + 0.2% glycerol) for 9 hours, before dilution to 2×10^6 CFU/mL and inoculation (10 μ L) of the well of a 96-well plate containing minimal medium (150 μ L) supplemented with pantothenate (10 μ L, final concentration is 100 μ M), **P-1b** (10 μ L, final concentration is 512 μ g/mL) and different concentrations of ribostamycin (20 μ L). The cell concentration (CFU/mL) was determined using the calibration-derived equation $OD_{600} = 10^{-10}x$, where x is the bacterial concentration (CFU/mL), and OD_{600} is the optical density at 600 nm when the cell path length is 1 cm. Ribostamycin was prepared at stock concentrations of 0, 1280, 1760, 2240, 2560, 3151, 3840, 4480, 5120, 10240 and 13653 μ g/mL respectively, so that the final concentration in each well was adjusted to 0-1365 μ g/mL. After 16 hours of incubation at 37°C, the OD_{600} of the cell suspension in each well was measured. The optical density measured in the well without any ribostamycin nor **P-1b** was taken as 100% growth. All experiments were performed in triplicates. The data points shown are averages and plotted with the SEM.

8.3.6 Time-kill assays

The time-kill assay was performed following a previously reported procedure with modifications.²²⁶ *E. faecium* ATCC 19434 was cultured at 37°C in brain heart infusion broth for 5-12 hours. The bacterial culture was then diluted sequentially to ca. 10^5 CFU/mL, aliquoted and added with different concentrations of tobramycin and **P-1b**. The inoculum (CFU/mL) was confirmed at time 0, and measured again at 1, 2, 4, 6, 8, 10 and 12 hours respectively. Sampling for colony counts was done by removing 0.1 mL samples of culture at the specified times. Each sample was diluted with sterile PBS buffer to produce 10-fold, 100-fold and 1000-fold dilutions. Next, pipetting out 100 μ L of each dilution and spreading evenly on brain heart infusion agar plates. Colonies were counted after incubation of these agar plates at 37°C for 18 hours. Based on the counted colonies and the dilutions mentioned above, cell concentration (CFU/mL) for each time point was

determined. All procedures were performed in triplicates. The data points shown are averages and plotted with the SEM.

8.3.7 Metabolomics studies

8.3.7.1 Studying the fate of P-1b in *E. faecium* over time

E. faecium ATCC 19434 was cultured at 37°C in brain heart infusion broth for 5-12 hours. The culture was next diluted to a concentration of 10^9 CFU/mL, to which 384 μ g/mL **P-1b** was added. Next, at 1, 2, 3, 4, 5 and 6 hours respectively, sample of cell culture, each containing 17×10^9 *E. faecium* ATCC 19434 colonies were collected. The *E. faecium* ATCC 19434 concentration (CFU/mL) was determined using the calibration-derived equation $OD_{600} = 3 \times 10^{-10}x + 0.0285$, where x is the bacterial concentration (CFU/mL), and OD_{600} is the optical density at 600 nm when the cell path length is 1 cm. The collected cell culture sample was centrifuged at $4,000 \times g$ for 5 minutes at 4°C. The supernatant was discarded. The cell pellet was washed by resuspending in ammonium formate (4°C, 150 mM, pH = 7.4, 1 mL). The washing buffer was separated by centrifugation at $4,000 \times g$ for 5 minutes and discarded. To break the cell membranes, the cell pellet was resuspended in an emulsion of 4°C water (1 mL) and -20°C DCM containing 0.1 M formic acid (1 mL). The mixture was heavily vortexed for 45 seconds, and then rested on ice for 45 seconds. The process was repeated four times. To make sure that the cell membranes were fully broken, the mixture was left on ice for another 5 minutes. The mixture was next centrifuged at 4°C, $14,000 \times g$ for 2 minutes, to separate the aqueous and DCM phases. The aqueous phase (930 μ L) was collected, and mixed with 500 μ L of an aqueous 0.4 M NH_4HCO_3 solution at 4°C to neutralize the previously introduced formic acid. The resulting sample was filtered, frozen quickly in an acetone/dry ice bath, and then left to lyophilize for 6-12 hours to fully remove the water. Finally, the solid residue was redissolved in 0.1% aqueous formic acid and analyzed by LCMS following the condition listed in Table 8.3. The four compounds of interest (**P-1b**, **6.2b**, **6.3b** and **I-1b**) were quantified by monitoring their corresponding MS signals: **P-1b** (655.3343 ± 0.01 ; $R_t = 1.1$ min), **6.2b** (735.2998 ± 0.01 ; 368.1530 ± 0.01 ; $R_t = 1.1$ min), and **6.3b** (532.6815 ± 0.01 ; 1064.3530 ± 0.01 ; $R_t = 3.2$ min). No **I-1b** (expected $m/z = 572.6638 \pm 0.02$ and 1144.3190 ± 0.02 ; expected $R_t =$

3.8 min) was detected in the bacterial samples. All procedures were performed in triplicates. The data points shown are averages and plotted with the SEM.

Table 8.3. LCMS method for studying the four compounds of interest (**P-1b**, **6.2b**, **6.3b**, **I-1b**).

Flow rate: 0.2 mL/min

Column: Luna 3 μm C18(2) 100 Å 50 x 2.00 mm 3 micron from Phenomenex

Time (min)	Water with 0.1% formic acid additive (%)	Methanol (%)
0	95	5
1	95	5
8	60	40
10	0	100
12	0	100
12.5	95	5

8.3.7.2 Use of spiked standards to confirm the nature of the P-1b metabolites

A standard solution of all four compounds of interest (**P-1b**, **6.2b**, **6.3b** and **I-1b**) was prepared by enzymatic transformation with purified enzymes. Briefly, to a mixture of ATP (1 mM), **P-1b** (1 mM), dithiothreitol (1 mM), MgCl_2 (10 mM) and KCl (20 mM) dissolved in Tris-HCl buffer (50 mM, pH = 7.6, 940 μL), was added the purified *E. coli* PanK (0.0004 μmol , 20 μL), PPAT (0.0015 μmol , 20 μL) and DPCK (0.0010 μmol , 20 μL). The reaction was incubated for 3 hours at 37°C, before quenching with 1 mL of -20°C DCM containing 0.1 M formic acid for 5 minutes. The precipitated protein was removed by centrifugation (14,000 $\times g$) for 2 minutes. The collected supernatant containing the four compounds of interest was next used to prepare the spiked standard solution. To this end, *E. faecium* ATCC 19434 cell pellets prepared in advance were resuspended into the collected supernatant mentioned above, to which 1 mL of -20 °C DCM containing 0.1 M formic acid was added. The mixture was heavily vortexed for 45 seconds, and then rested on ice for 45 seconds. The process was repeated four times. To make sure that the cell membranes were fully broken, the mixture was left on ice for another 5 minutes. The mixture was next centrifuged at 4°C, 14,000 $\times g$ for 2 minutes, to separate the aqueous from the DCM phase. The aqueous phase (930 μL) was collected, and mixed with 500 μL of an aqueous

0.4 M NH_4HCO_3 solution at 4°C to neutralize the previously introduced formic acid. The resulting sample was filtered, frozen quickly using an acetone/dry ice bath, and then left to lyophilize for 6-12 hours to fully remove the water. Finally, the solid residue was redissolved in 0.1% aqueous formic acid and analyzed by LCMS using the condition listed in Table 8.3. The retention times are: 1.1 min for **P-1b**, 1.1 min for **6.2b**, 3.2 min for **6.3b**, and 3.8 min for **I-1b**. All are consistent for both the standard and the bacterial samples.

8.3.7.3 Calibration curves

To determine the concentration of the four compounds of interest (**P-1b**, **6.2b**, **6.3b** and **I-1b**), calibration curves were prepared for each compound.

Pure **P-1b** was synthesized as in section 8.1.6.1. In order to prepare the calibration curve for LCMS quantification of **P-1b**, 0.038, 0.076, 0.153, 0.305, 0.458, 0.611, 0.916 nmol of **P-1b** were injected into the LCMS system (UltiMate 3000 UHPLC System from Thermo Fisher Scientific coupled with a MaXis Impact HD Mass Spectrometer from Bruker). The LCMS condition used is shown in Table 8.3. The area of the selected ion peak monitored for **P-1b** (655.3343 ± 0.01 ; $R_t = 1.1$ min) was integrated after each injection. The calibration curve for quantifying **P-1b** by LCMS using selected ion monitoring (SIM) is shown in Figure 8.1. All procedures were performed at least in duplicates. The data points are averages and plotted with the SEM.

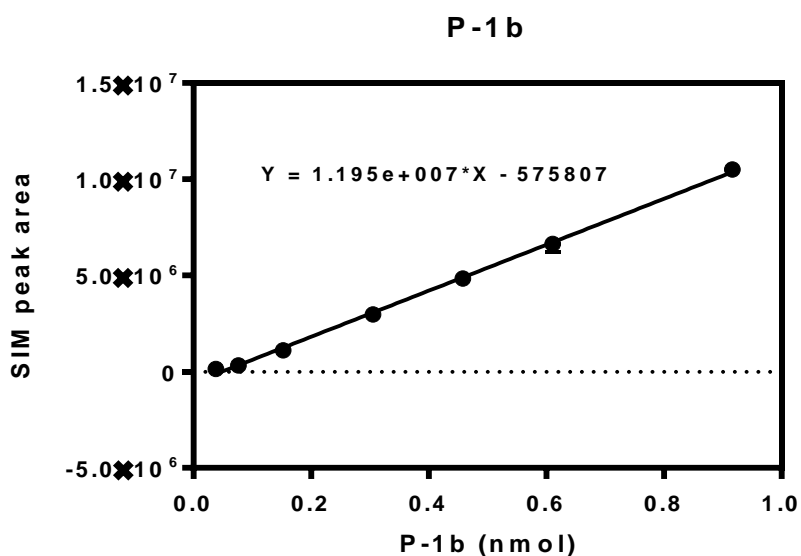


Figure 8.1. Calibration curve for quantification of **P-1b** by LCMS using SIM detection at $m/z = 655.3343 \pm 0.01$.

Compound **6.2b** was prepared enzymatically. To a mixture of ATP (1 mM), **P-1b** (1 mM), dithiothreitol (1 mM), $MgCl_2$ (10 mM) and KCl (20 mM) dissolved in Tris-HCl buffer (50 mM, pH = 7.6, 460 μ L), was added the purified *E. coli* PanK (0.0008 μ mol, 40 μ L). The reaction mixture was incubated for 3 hours at 37°C, before quenching with 1 mL of -20 °C DCM containing 0.1 M formic acid for 5 minutes. The precipitated protein was removed by centrifugation (14,000 \times g) for 2 minutes, and the supernatant was collected. The **6.2b** concentration in the supernatant was quantified by HPLC-UV using the molar absorptivity of **P-1b**. To do this, several dilutions of the supernatant and of pure **P-1b** were injected into the HPLC-UV system (Agilent 6120 Quadrupole LCMS) separately. The HPLC-UV conditions are shown in Table 8.4. The area of the **P-1b** peak at 214 nm ($R_t = 21.52$ min) was integrated after each injection. The calibration curve for quantifying **P-1b** by HPLC-UV is shown in Figure 8.2A. It is assumed that **P-1b** and **6.2b** have the same molar absorptivity at 214 nm. Therefore, based on the calibration curve of **P-1b** at 214 nm and the area of the **6.2b** peak at 214 nm ($R_t = 13.47$ min), the concentration of **6.2b** in the supernatant was determined.

Table 8.4. HPLC methods for A) generating **P-1b** calibration curve (UV detection at 214 nm), and B) determining the concentration of **6.2b** in the supernatant (UV detection at 214 nm).

A.

Flow rate: 0.5 mL/min; wavelength: 214 nm

Column: SYNERGI 4 μ Hydro-RP 80 Å from Phenomenex

Time (min)	Water with 20 mM NH ₄ HCO ₃ additive (%)	Acetonitrile (%)
0	99	1
3	99	1
5	90	10
10	80	20
20	60	40
23	60	40
25	99	1

B.

Flow rate: 0.5 mL/min; wavelength: 214 nm

Column: SYNERGI 4 μ Hydro-RP 80 Å from Phenomenex

Time (min)	Water with 20 mM NH ₄ HCO ₃ additive (%)	Acetonitrile (%)
0	99	1
3	99	1
5	90	10
10	80	20
40	60	40
45	60	40
50	99	1

Once the concentration of **6.2b** in the supernatant was determined, 0.13, 0.26, 0.52, 1.03, 2.58 pmol **6.2b** was injected into the LCMS system (UltiMate 3000 UHPLC System from Thermo Fisher Scientific coupled with a MaXis Impact HD Mass Spectrometer from Bruker). The LCMS condition used is shown in Table 8.3. The area of the selected ion peak monitored for **6.2b** (735.2998 \pm 0.01; 368.1530 \pm 0.01; R_t = 1.1 min) was integrated after each injection. The calibration curve for quantifying **6.2b** by LCMS using SIM is shown in Figure 8.2B. All procedures were performed in triplicates. The data points are averages and plotted with the SEM.

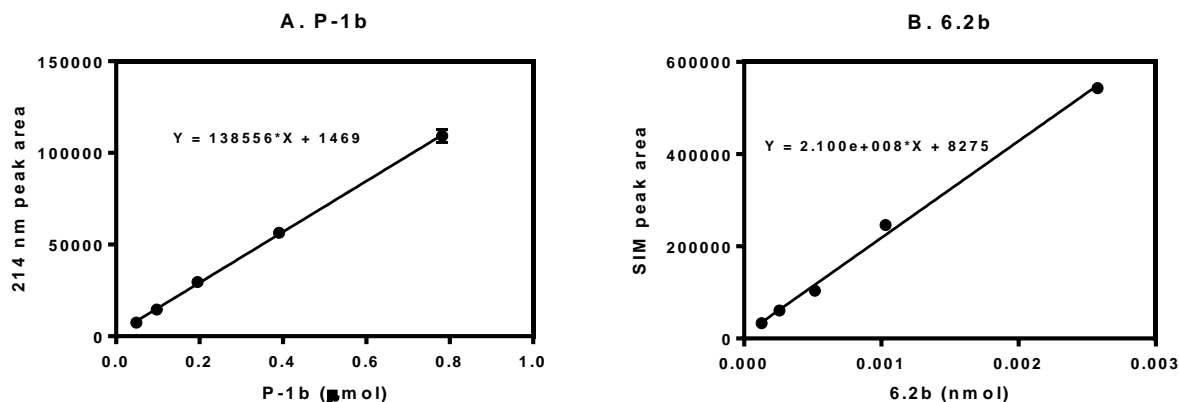


Figure 8.2. Calibration curves A) for **P-1b** as determined by HPLC with UV detection at 214 nm, and B) for **6.2b** as determined by LCMS using SIM detection at $m/z = 735.2998 \pm 0.01$ and 368.1530 ± 0.01 .

Compounds **6.3b** and **I-1b** were also prepared enzymatically. To a mixture of ATP (1 mM), **P-1b** (1 mM), dithiothreitol (1 mM), $MgCl_2$ (10 mM) and KCl (20 mM) dissolved in Tris-HCl buffer (50 mM, pH = 7.6, 440 μ L), was added the purified *E. coli* PanK (0.0004 μ mol, 20 μ L), PPAT (0.0015 μ mol, 20 μ L), and DPCK (0.0010 μ mol, 20 μ L). The reaction was incubated for 3 hours at 37°C, before quenching with 1 mL of -20 °C DCM containing 0.1 M formic acid for 5 minutes. The precipitated protein was removed by centrifugation (14,000 \times g) for 2 minutes, and the supernatant was collected. The concentrations of **6.3b** and **I-1b** in the supernatant were quantified by HPLC-UV using the molar absorptivity of CoA. To do this, several dilutions of the supernatant and pure CoA were injected into the HPLC-UV system (Agilent 6120 Quadrupole LCMS) separately. The HPLC-UV condition used for CoA calibration curve is shown in Table 8.5, and HPLC-UV condition used for concentration determination of **6.3b** and **I-1b** is shown in method B of Table 8.2. The area of the CoA peak at 260 nm ($R_t = 4.85$ min) was integrated after each injection. The calibration curve for quantifying CoA by HPLC-UV is shown in Figure 8.3A. It assumed that compounds **6.3b** and **I-1b** have the same molar absorptivity as CoA at 260 nm. Therefore, based on the calibration curve of CoA at 260 nm and the areas of **6.3b** ($R_t = 21.41$ min) and **I-1b** at 260 nm ($R_t = 16.56$ min), the concentrations of **6.3b** and **I-1b** in the supernatant were determined.

Once the concentration of **6.3b** in the supernatant was determined, 0.25, 0.51, 1.02, 2.03, 5.08, 10.15 and 20.30 pmol of **6.3b** were injected into the LCMS system (UltiMate 3000 UHPLC System from Thermo Fisher Scientific coupled with a MaXis Impact HD Mass Spectrometer from Bruker). The LCMS condition used is shown in Table 8.3. The area of the selected ion peak monitored for **6.3b** (532.6815 ± 0.01 ; 1064.3530 ± 0.01 ; $R_t = 3.2$ min) was integrated after each injection. The calibration curve for quantifying **6.3b** by LCMS using SIM is shown in Figure 8.3B. Similarly, 0.053, 0.11, 0.21, 0.53, 1.06, 2.11 pmol of **I-1b** were injected into the LCMS system (UltiMate 3000 UHPLC System from Thermo Fisher Scientific coupled with a MaXis Impact HD Mass Spectrometer from Bruker). The LCMS condition used is shown in Table 8.3. The area of the selected ion peak monitored for **I-1b** (572.6638 ± 0.02 ; 1144.3190 ± 0.02 ; $R_t = 3.8$ min) was integrated after each injection. The calibration curve for quantifying **I-1b** by LCMS using SIM is shown in Figure 8.3C. All procedures were performed in triplicates. The data points are averages and plotted with the SEM.

Table 8.5. HPLC method used to generate the CoA calibration curve (UV detection at 260 nm).

Flow rate: 0.5 mL/min; wavelength: 260 nm

Column: SYNERGI 4 μ Hydro-RP 80 Å from Phenomenex

Time (min)	Water with 20 mM NH_4HCO_3 additive (%)	Acetonitrile (%)
0	99	1
3	99	1
5	90	10
10	80	20
12	60	40
15	99	1

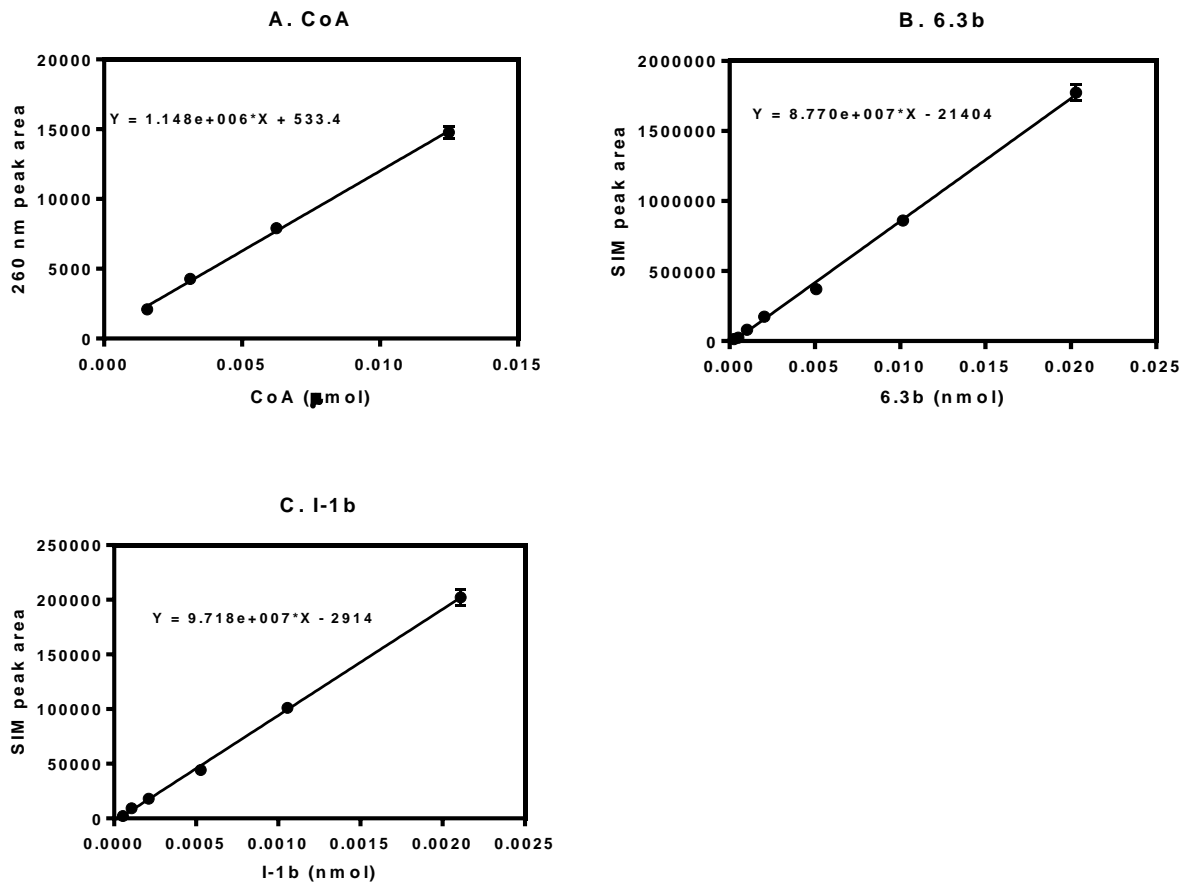


Figure 8.3. Calibration curves A) for quantifying CoA by HPLC with UV detection at 260 nm, B) for quantifying **6.3b** by LCMS using SIM detection at $m/z = 532.6815 \pm 0.01$ and 1064.3530 ± 0.01 , and C) for quantifying **I-1b** by LCMS using SIM detection at $m/z = 572.6638 \pm 0.02$ and 1144.3190 ± 0.02 .

References

1. Cox, F. E. G., History of human parasitology. *Clinical Microbiology Reviews* **2002**, 15, 595-612.
2. Aminov, R. I., A brief history of the antibiotic era: lessons learned and challenges for the future. *Frontiers in Microbiology* **2010**, 1: 134.
3. Blevins, S. M.; Bronze, M. S., Robert Koch and the 'golden age' of bacteriology. *International Journal of Infectious Diseases* **2010**, 14, e744-751.
4. Kaufmann, S. H. E., Paul Ehrlich: founder of chemotherapy. *Nature Reviews Drug Discovery* **2008**, 7, 373.
5. Lloyd, N. C.; Morgan, H. W.; Nicholson, B. K.; Ronimus, R. S., The composition of Ehrlich's salvarsan: resolution of a century-old debate. *Angewandte Chemie International Edition* **2005**, 44, 941-944.
6. Aminov, R., History of antimicrobial drug discovery: major classes and health impact. *Biochemical Pharmacology* **2017**, 133, 4-19.
7. World Health Organization, Critically important antimicrobials for human medicine – 5th rev. **2017**.
8. O'Neill, J., Tackling drug-resistant infections globally: final report and recommendations. *Review on Antimicrobial Resistance* **2016**.
9. Sodeik, B.; Griffiths, G.; Ericsson, M.; Moss, B.; Doms, R. W., Assembly of vaccinia virus: effects of rifampin on the intracellular distribution of viral protein p65. *Journal of Virology* **1994**, 68, 1103-1114.
10. De Clercq, E., Molecular targets for antiviral agents. *The Journal of Pharmacology and Experimental Therapeutics* **2001**, 297, 1-10.
11. Menendez-Arias, L.; Gago, F., Antiviral agents: structural basis of action and rational design. *Subcellular Biochemistry* **2013**, 68, 599-630.
12. Patel, M. C.; Shirey, K. A.; Pletneva, L. M.; Boukhvalova, M. S.; Garzino-Demo, A.; Vogel, S. N.; Blanco, J. C. G., Novel drugs targeting Toll-like receptors for antiviral therapy. *Future Virology* **2014**, 9, 811-829.
13. Goldman, E.; Green, L. H., Practical handbook of microbiology, 3rd Edition. CRC Press, Taylor & Francis Group, Boca Raton. **2015**.

14. O'Neill, J., Antimicrobial resistance: tackling a crisis for the health and wealth of nations. *Review on Antimicrobial Resistance* **2014**.
15. World Health Organization, Global action plan on antimicrobial resistance. **2015**.
16. World Health Organization, World malaria report 2017. **2017**.
17. Fair, R. J.; Tor, Y., Antibiotics and bacterial resistance in the 21st century. *Perspectives in Medicinal Chemistry* **2014**, 6, 25-64.
18. Rolain, J. M.; Abat, C.; Jimeno, M. T.; Fournier, P. E.; Raoult, D., Do we need new antibiotics? *Clinical Microbiology and Infection* **2016**, 22, 408-415.
19. World Health Organization, World health day 2011: policy briefs. **2011**.
20. Ouellette, M., Biochemical and molecular mechanisms of drug resistance in parasites. *Tropical Medicine & International Health* **2001**, 6, 874-882.
21. McKeegan, K. S.; Borges-Walmsley, M. I.; Walmsley, A. R., Microbial and viral drug resistance mechanisms. *Trends in Microbiology* **2002**, 10, S8-14.
22. Mulvey, M. R.; Simor, A. E., Antimicrobial resistance in hospitals: how concerned should we be? *CMAJ* **2009**, 180, 408-415.
23. Blair, J. M.; Webber, M. A.; Baylay, A. J.; Ogbolu, D. O.; Piddock, L. J. V., Molecular mechanisms of antibiotic resistance. *Nature Reviews Microbiology* **2015**, 13, 42-51.
24. Lipmann, F., Development of the acetylation problem, a personal account. *Science* **1954**, 120, 855-865.
25. Theodoulou, F. L.; Sibon, O. C. M.; Jackowski, S.; Gout, I., Coenzyme A and its derivatives: renaissance of a textbook classic. *Biochemical Society Transactions* **2014**, 42, 1025-1032.
26. Brown, G. M.; Reynolds, J. J., Biogenesis of the water-soluble vitamins. *Annual Review of Biochemistry* **1963**, 32, 419-462.
27. Strauss, E., Coenzyme A biosynthesis and enzymology, in *Comprehensive Natural Products II*, first edition. Elsevier Science. **2010**.
28. Takagi, M.; Tamaki, H.; Miyamoto, Y.; Leonardi, R.; Hanada, S.; Jackowski, S.; Chohnan, S., Pantothenate kinase from the thermoacidophilic archaeon *Picrophilus torridus*. *Journal of Bacteriology* **2010**, 192, 233-241.

29. Brand, L. A.; Strauss, E., Characterization of a new pantothenate kinase isoform from *Helicobacter pylori*. *Journal of Biological Chemistry* **2005**, 280, 20185-20188.
30. Song, W. J.; Jackowski, S., Cloning, sequencing, and expression of the pantothenate kinase (coaA) gene of *Escherichia coli*. *Journal of Bacteriology* **1992**, 174, 6411-6417.
31. Song, W. J.; Jackowski, S., Kinetics and regulation of pantothenate kinase from *Escherichia coli*. *Journal of Biological Chemistry* **1994**, 269, 27051-27058.
32. Das, S.; Kumar, P.; Bhor, V.; Surolia, A.; Vijayan, M., Invariance and variability in bacterial PanK: a study based on the crystal structure of *Mycobacterium tuberculosis* PanK. *Acta Crystallographica Section D Biological Crystallography* **2006**, 62, 628-638.
33. Franklin, M. C.; Cheung, J.; Rudolph, M. J.; Burshteyn, F.; Cassidy, M.; Gary, E.; Hillerich, B.; Yao, Z. K.; Carlier, P. R.; Totrov, M.; Love, J. D., Structural genomics for drug design against the pathogen *Coxiella burnetii*. *Proteins* **2015**, 83, 2124-2136.
34. Strauss, E.; de Villiers, M.; Rootman, I., Biocatalytic production of coenzyme A analogues. *ChemCatChem* **2010**, 2, 929-937.
35. Van Dijk, A. A.; Badenhorst, C. P. S., Synthesis of acyl-pantetheine derivatives and their use in the enzymatic synthesis of acyl-coenzyme A derivatives. WO2012017400A1. **2012**.
36. Balibar, C. J.; Hollis-Symynkywicz, M. F.; Tao, J., Pantethine rescues phosphopantothenoylecysteine synthetase and phosphopantothenoylecysteine decarboxylase deficiency in *Escherichia coli* but not in *Pseudomonas aeruginosa*. *Journal of Bacteriology* **2011**, 193, 3304-3312.
37. Hong, B. S.; Yun, M. K.; Zhang, Y. M.; Chohnan, S.; Rock, C. O.; White, S. W.; Jackowski, S.; Park, H. W.; Leonardi, R., Prokaryotic type II and type III pantothenate kinases: the same monomer fold creates dimers with distinct catalytic properties. *Structure* **2006**, 14, 1251-1261.
38. Hong, B. S.; Senisterra, G.; Rabeh, W. M.; Vedadi, M.; Leonardi, R.; Zhang, Y. M.; Rock, C. O.; Jackowski, S.; Park, H. W., Crystal structures of human pantothenate kinases. Insights into allosteric regulation and mutations linked to a neurodegeneration disorder. *Journal of Biological Chemistry* **2007**, 282, 27984-27993.

39. Subramanian, C.; Yun, M. K.; Yao, J.; Sharma, L. K.; Lee, R. E.; White, S. W.; Jackowski, S.; Rock, C. O., Allosteric regulation of mammalian pantothenate kinase. *Journal of Biological Chemistry* **2016**, 291, 22302-22314.
40. Abiko, Y., Investigations on pantothenic acid and its related compounds. IX. Biochemical studies. 4. Separation and substrate specificity of pantothenate kinase and phosphopantothenoylecysteine synthetase. *The Journal of Biochemistry* **1967**, 61, 290-299.
41. Abiko, Y.; Ashida, S. I.; Shimizu, M., Purification and properties of D-pantothenate kinase from rat liver. *Biochim et Biophysica Acta* **1972**, 268, 364-372.
42. Calder, R. B.; Williams, R. S. B.; Ramaswamy, G.; Rock, C. O.; Campbell, E.; Unkles, S. E.; Kinghorn, J. R.; Jackowski, S., Cloning and characterization of a eukaryotic pantothenate kinase gene (*panK*) from *Aspergillus nidulans*. *Journal of Biological Chemistry* **1999**, 274, 2014-2020.
43. Rock, C. O.; Karim, M. A.; Zhang, Y. M.; Jackowski, S., The murine pantothenate kinase (*Pank1*) gene encodes two differentially regulated pantothenate kinase isozymes. *Gene* **2002**, 291, 35-43.
44. Zhang, Y. M.; Rock, C. O.; Jackowski, S., Feedback regulation of murine pantothenate kinase 3 by coenzyme A and coenzyme A thioesters. *Journal of Biological Chemistry* **2005**, 280, 32594-32601.
45. Miller, J. R.; Ohren, J.; Sarver, R. W.; Mueller, W. T.; de Dreu, P.; Case, H.; Thanabal, V., Phosphopantetheine adenylyltransferase from *Escherichia coli*: investigation of the kinetic mechanism and role in regulation of coenzyme A biosynthesis. *Journal of Bacteriology* **2007**, 189, 8196-8205.
46. Leonardi, R.; Chohnan, S.; Zhang, Y. M.; Virga, K. G.; Lee, R. E.; Rock, C. O.; Jackowski, S., A pantothenate kinase from *Staphylococcus aureus* refractory to feedback regulation by coenzyme A. *Journal of Biological Chemistry* **2005**, 280, 3314-3322.
47. Yang, K.; Eyobo, Y.; Brand, L. A.; Martynowski, D.; Tomchick, D.; Strauss, E.; Zhang, H., Crystal structure of a type III pantothenate kinase: insight into the mechanism of an essential coenzyme A biosynthetic enzyme universally distributed in bacteria. *Journal of Bacteriology* **2006**, 188, 5532-5540.

48. Nicely, N. I.; Parsonage, D.; Paige, C.; Newton, G. L.; Fahey, R. C.; Leonardi, R.; Jackowski, S.; Mallett, T. C.; Claiborne, A., Structure of the type III pantothenate kinase from *Bacillus anthracis* at 2.0 Å resolution: implications for coenzyme A-dependent redox biology. *Biochemistry* **2007**, 46, 3234-3245.
49. Yang, K.; Strauss, E.; Huerta, C.; Zhang, H., Structural basis for substrate binding and the catalytic mechanism of type III pantothenate kinase. *Biochemistry* **2008**, 47, 1369-1380.
50. Shimosaka, T.; Tomita, H.; Atomi, H., Regulation of coenzyme A biosynthesis in the hyperthermophilic bacterium *Thermotoga maritima*. *Journal of Bacteriology* **2016**, 198, 1993-2000.
51. Strauss, E.; Kinsland, C.; Ge, Y.; McLafferty, F. W.; Begley, T. P., Phosphopantothenoylcysteine synthetase from *Escherichia coli*. Identification and characterization of the last unidentified coenzyme A biosynthetic enzyme in bacteria. *Journal of Biological Chemistry* **2001**, 276, 13513-13516.
52. Kupke, T., Molecular characterization of the 4'-phosphopantothenoylcysteine synthetase domain of bacterial Dfp flavoproteins. *Journal of Biological Chemistry* **2002**, 277, 36137-36145.
53. Osterman, A.; Overbeek, R., Missing genes in metabolic pathways: a comparative genomics approach. *Current Opinion in Chemical Biology* **2003**, 7, 238-251.
54. Stanitzek, S.; Augustin, M. A.; Huber, R.; Kupke, T.; Steinbacher, S., Structural basis of CTP-dependent peptide bond formation in coenzyme A biosynthesis catalyzed by *Escherichia coli* PPC synthetase. *Structure* **2004**, 12, 1977-1988.
55. Kupke, T., Active-site residues and amino acid specificity of the bacterial 4'-phosphopantothenoylcysteine synthetase CoaB. *European Journal of Biochemistry* **2004**, 271, 163-172.
56. Kupke, T.; Schwarz, W., 4'-Phosphopantetheine biosynthesis in archaea. *Journal of Biological Chemistry* **2006**, 281, 5435-5444.
57. Yao, J.; Patrone, J. D.; Dotson, G. D., Characterization and kinetics of phosphopantothenoylcysteine synthetase from *Enterococcus faecalis*. *Biochemistry* **2009**, 48, 2799-2806.

58. Daugherty, M.; Polanuyer, B.; Farrell, M.; Scholle, M.; Lykidis, A.; de Crecy-Lagard, V.; Osterman, A., Complete reconstitution of the human coenzyme A biosynthetic pathway via comparative genomics. *Journal of Biological Chemistry* **2002**, *277*, 21431-21439.
59. Manoj, N.; Strauss, E.; Begley, T. P.; Ealick, S. E., Structure of human phosphopantothienoylcysteine synthetase at 2.3 Å resolution. *Structure* **2003**, *11*, 927-936.
60. Kupke, T.; Hernandez-Acosta, P.; Cullianez-Macia, F. A., 4'-Phosphopantetheine and coenzyme A biosynthesis in plants. *Journal of Biological Chemistry* **2003**, *278*, 38229-38237.
61. Yao, J.; Dotson, G. D., Kinetic characterization of human phosphopantothienoylcysteine synthetase. *Biochim et Biophysica Acta* **2009**, *1794*, 1743-1750.
62. Geerlof, A.; Lewendon, A.; Shaw, W. V., Purification and characterization of phosphopantetheine adenylyltransferase from *Escherichia coli*. *Journal of Biological Chemistry* **1999**, *274*, 27105-27111.
63. Armengaud, J.; Fernandez, B.; Chaumont, V.; Rollin-Genetet, F.; Finet, S.; Marchetti, C.; Myllykallio, H.; Vidaud, C.; Pellequer, J. L.; Gribaldo, S.; Forterre, P.; Gans, P., Identification, purification, and characterization of an eukaryotic-like phosphopantetheine adenylyltransferase (coenzyme A biosynthetic pathway) in the hyperthermophilic archaeon *Pyrococcus abyssi*. *Journal of Biological Chemistry* **2003**, *278*, 31078-31087.
64. Rubio, S.; Whitehead, L.; Larson, T. R.; Graham, I. A.; Rodriguez, P. L., The coenzyme A biosynthetic enzyme phosphopantetheine adenylyltransferase plays a crucial role in plant growth, salt/osmotic stress resistance, and seed lipid storage. *Plant Physiology* **2008**, *148*, 546-556.
65. Breus, O.; Panasyuk, G.; Gout, I. T.; Filonenko, V.; Nemazanyy, I., CoA Synthase is phosphorylated on tyrosines in mammalian cells, interacts with and is dephosphorylated by Shp₂PTP. *Molecular and Cellular Biochemistry* **2010**, *335*, 195-202.

66. Chatterjee, R.; Mondal, A.; Basu, A.; Datta, S., Transition of phosphopantetheine adenyltransferase from catalytic to allosteric state is characterized by ternary complex formation in *Pseudomonas aeruginosa*. *Biochim et Biophysica Acta* **2016**, 1864, 773-786.
67. Izard, T.; Geerlof, A., The crystal structure of a novel bacterial adenyltransferase reveals half of sites reactivity. *EMBO Journal* **1999**, 18, 2021-2030.
68. Suzuki, T.; Abiko, Y.; Shimizu, M, Investigations on pantothenic acid and its related compounds XII. Biochemical studies (7). Dephospho-CoA pyrophosphorylase and dephospho-CoA kinase as a possible bifunctional enzyme complex. *The Journal of Biochemistry* **1967**, 62, 642-649.
69. Skrede, S.; Halvorsen, O., Mitochondrial pantetheinephosphate adenyltransferase and dephospho-CoA kinase. *European Journal of Biochemistry* **1983**, 131, 57-63.
70. Worrall, D. M.; Tubbs, P. K., A bifunctional enzyme complex in coenzyme A biosynthesis: purification of pantetheine phosphate adenyltransferase and dephospho-CoA kinase. *Biochemical Journal* **1983**, 215, 153-157.
71. Aghajanian, S.; Worrall, D. M., Identification and characterization of the gene encoding the human phosphopantetheine adenyltransferase and dephospho-CoA kinase bifunctional enzyme (CoA synthase). *Biochemical Journal* **2002**, 365, 13-18.
72. Zhyvoloup, A.; Nemazanyy, I.; Panasyuk, G.; Valovka, T.; Fenton, T.; Rebholz, H.; Wang, M. L.; Foxon, R.; Lyzogubov, V.; Usenko, V.; Kyyamova, R.; Gorbenko, O.; Matsuka, G.; Filonenko, V.; Gout, I. T., Subcellular localization and regulation of coenzyme A synthase. *Journal of Biological Chemistry* **2003**, 278, 50316-50321.
73. Martin, D. P.; Drueckhammer, D. G., Separate enzymes catalyze the final two steps of coenzyme A biosynthesis in *Brevibacterium ammoniagenes*: purification of pantetheine phosphate adenyltransferase. *Biochemical and Biophysical Research Communications* **1993**, 192, 1155-1161.
74. Eom, S. J.; Ahn, H. J.; Kim, H. W.; Baek, S. H.; Suh, S. W., Crystallization and preliminary X-ray crystallographic studies of phosphopantetheine adenyltransferase from *Helicobacter pylori*. *Acta Crystallographica Section D Biological Crystallography* **2003**, 59, 561-562.

75. Izard, T., A novel adenylate binding site confers phosphopantetheine adenylyltransferase interactions with coenzyme A. *Journal of Bacteriology* **2003**, 185, 4074-4080.
76. Takahashi, H.; Inagaki, E.; Fujimoto, Y.; Kuroishi, C.; Nodake, Y.; Nakamura, Y.; Arisaka, F.; Yutani, K.; Kuramitsu, S.; Yokoyama, S.; Yamamoto, M.; Miyano, M.; Tahirov, T. H., Structure and implications for the thermal stability of phosphopantetheine adenylyltransferase from *Thermus thermophilus*. *Acta Crystallographica Section D Biological Crystallography* **2004**, 60, 97-104.
77. Brown, K. L.; Morris, V. K.; Izard, T., Rhombohedral crystals of *Mycobacterium tuberculosis* phosphopantetheine adenylyltransferase. *Acta Crystallographica Section D Biological Crystallography* **2004**, 60, 195-196.
78. Kang, J. Y.; Lee, H. H.; Yoon, H. J.; Kim, H. S.; Suh, S. W., Overexpression, crystallization and preliminary X-ray crystallographic analysis of phosphopantetheine adenylyltransferase from *Enterococcus faecalis*. *Acta Crystallographica Section F Structural Biology Communications* **2006**, 62, 1131-1133.
79. Lee, H. H.; Yoon, H. J.; Kang, J. Y.; Park, J. H.; Kim, D. J.; Choi, K. H.; Lee, S. K.; Song, J.; Kim, H. J.; Suh, S. W., The structure of *Staphylococcus aureus* phosphopantetheine adenylyltransferase in complex with 3'-phosphoadenosine 5'-phosphosulfate reveals a new ligand-binding mode. *Acta Crystallographica Section F Structural Biology Communications* **2009**, 65, 987-991.
80. Wubben, T. J.; Mesecar, A. D., Kinetic, thermodynamic, and structural insight into the mechanism of phosphopantetheine adenylyltransferase from *Mycobacterium tuberculosis*. *Journal of Molecular Biology* **2010**, 404, 202-219.
81. Wubben, T.; Mesecar, A. D., Structure of *Mycobacterium tuberculosis* phosphopantetheine adenylyltransferase in complex with the feedback inhibitor CoA reveals only one active-site conformation. *Acta Crystallographica Section F Structural Biology Communications* **2011**, 67, 541-545.
82. Cheng, C. S.; Chen, C. H.; Luo, Y. C.; Chen, W. T.; Chang, S. Y.; Lyu, P. C.; Kao, M. C.; Yin, H. S., Crystal structure and biophysical characterisation of *Helicobacter pylori* phosphopantetheine adenylyltransferase. *Biochemical and Biophysical Research Communications* **2011**, 408, 356-361.

83. Edwards, T. E.; Leibly, D. J.; Bhandari, J.; Statnekov, J. B.; Phan, I.; Dieterich, S. H.; Abendroth, J.; Staker, B. L.; Van Voorhis, W. C.; Myler, P. J.; Stewart, L. J., Structures of phosphopantetheine adenylyltransferase from *Burkholderia pseudomallei*. *Acta Crystallographica Section F Structural Biology Communications* **2011**, 67, 1032-1037.
84. Yoon, H. J.; Kang, J. Y.; Mikami, B.; Lee, H. H.; Suh, S. W., Crystal structure of phosphopantetheine adenylyltransferase from *Enterococcus faecalis* in the ligand-unbound state and in complex with ATP and pantetheine. *Molecules and Cells* **2011**, 32, 431-435.
85. Olzhausen, J.; Moritz, T.; Neetz, T.; Schuller, H. J., Molecular characterization of the heteromeric coenzyme A-synthesizing protein complex (CoA-SPC) in the yeast *Saccharomyces cerevisiae*. *FEMS Yeast Research* **2013**, 13, 565-573.
86. Gudkova, D.; Panasyuk, G.; Nemazanyy, I.; Zhyvoloup, A.; Monteil, P.; Filonenko, V.; Gout, I., EDC4 interacts with and regulates the dephospho-CoA kinase activity of CoA synthase. *FEBS Letters* **2012**, 586, 3590-3595.
87. Spry, C.; Kirk, K.; Saliba, K. J., Coenzyme A biosynthesis: an antimicrobial drug target. *FEMS Microbiology Reviews* **2008**, 32, 56-106.
88. Moolman, W. J.; de Villiers, M.; Strauss, E., Recent advances in targeting coenzyme A biosynthesis and utilization for antimicrobial drug development. *Biochemical Society Transactions* **2014**, 42, 1080-1086.
89. Venkatraman, J.; Bhat, J.; Solapure, S. M.; Sandesh, J.; Sarkar, D.; Aishwarya, S.; Mukherjee, K.; Datta, S.; Malolanarasimhan, K.; Bandodkar, B.; Das, K. S., Screening, identification, and characterization of mechanistically diverse inhibitors of the *Mycobacterium tuberculosis* enzyme, pantothenate kinase (CoaA). *Journal of Biomolecular Screening* **2012**, 17, 293-302.
90. Bjorkelid, C.; Bergfors, T.; Raichurkar, A. K.; Mukherjee, K.; Malolanarasimhan, K.; Bandodkar, B.; Jones, T. A., Structural and biochemical characterization of compounds inhibiting *Mycobacterium tuberculosis* pantothenate kinase. *Journal of Biological Chemistry* **2013**, 288, 18260-18270.
91. Reddy, B. K. K.; Landge, S.; Ravishankar, S.; Patil, V.; Shinde, V.; Tantry, S.; Kale, M.; Raichurkar, A.; Menasinakai, S.; Mudugal, N. V.; Ambady, A.; Ghosh, A.; Tunduguru, R.; Kaur, P.; Singh, R.; Kumar, N.; Bharath, S.; Sundaram, A.; Bhat, J.; Sambandamurthy,

- V. K.; Bjorkelid, C.; Jones, T. A.; Das, K.; Bandodkar, B.; Malolanarasimhan, K.; Mukherjee, K.; Ramachandran, V., Assessment of *Mycobacterium tuberculosis* pantothenate kinase vulnerability through target knockdown and mechanistically diverse inhibitors. *Antimicrobial Agents and Chemotherapy* **2014**, 58, 3312-3326.
92. Clifton, G.; Bryant, S. R.; Skinner, C. G., *N'*-(substituted) pantothenamides, antimetabolites of pantothenic acid. *Archives of Biochemistry and Biophysics* **1970**, 137, 523-528.
93. Choudhry, A. E.; Mandichak, T. L.; Broskey, J. P.; Egolf, R. W.; Kinsland, C.; Begley, T. P.; Seefeld, M. A.; Ku, T. W.; Brown, J. R.; Zalacain, M.; Ratnam, K., Inhibitors of pantothenate kinase: novel antibiotics for staphylococcal infections. *Antimicrobial Agents and Chemotherapy* **2003**, 47, 2051-2055.
94. Akinnusi, T. O.; Vong, K.; Auclair, K., Geminal dialkyl derivatives of *N*-substituted pantothenamides: synthesis and antibacterial activity. *Bioorganic & Medicinal Chemistry* **2011**, 19, 2696-2706.
95. de Villiers, M.; Barnard, L.; Koekemoer, L.; Snoep, J. L.; Strauss, E., Variation in pantothenate kinase type determines the pantothenamide mode of action and impacts on coenzyme A salvage biosynthesis. *FEBS Journal* **2014**, 281, 4731-4753.
96. Hermkens, P. H. H.; Schalkwijk, J.; Jansen, P. A. M.; Botman, P., Pantothenamide analogues. WO 2016/072854 A2. **2016**.
97. Barnard, L.; Mostert, K. J.; van Otterlo, W. A. L.; Strauss, E., Developing pantetheinase-resistant pantothenamide antibacterials: structural modification impacts on PanK interaction and mode of action. *ACS Infectious Diseases* **2018**, 4, 736-743.
98. Hughes, S. J.; Antoshchenko, T.; Kim, K. P.; Smil, D.; Park, H. W., Structural characterization of a new *N*-substituted pantothenamide bound to pantothenate kinases from *Klebsiella pneumoniae* and *Staphylococcus aureus*. *Proteins* **2014**, 82, 1542-1548.
99. Hughes, S. J.; Barnard, L.; Mottaghi, K.; Tempel, W.; Antoshchenko, T.; Hong, B. S.; Allali-Hassani, A.; Smil, D.; Vedadi, M.; Strauss, E.; Park, H. W., Discovery of potent pantothenamide inhibitors of *Staphylococcus aureus* pantothenate kinase through a minimal SAR study: inhibition is due to trapping of the product. *ACS Infectious Diseases* **2016**, 2, 627-641.

100. Spry, C.; Chai, C. L.; Kirk, K.; Saliba, K. J., A class of pantothenic acid analogs inhibits *Plasmodium falciparum* pantothenate kinase and represses the proliferation of malaria parasites. *Antimicrobial Agents and Chemotherapy* **2005**, 49, 4649-4657.
101. Rowan, A. S.; Nicely, N. I.; Cochrane, N.; Wlassoff, W. A.; Claiborne, A.; Hamilton, C. J., Nucleoside triphosphate mimicry: a sugar triazolyl nucleoside as an ATP-competitive inhibitor of *B. anthracis* pantothenate kinase. *Organic & Biomolecular Chemistry* **2009**, 7, 4029-4036.
102. Strauss, E.; Begley, T. P., The antibiotic activity of *N*-pentylpantothenamide results from its conversion to ethyldethia-coenzyme A, a coenzyme A antimetabolite. *Journal of Biological Chemistry* **2002**, 277, 48205-48209.
103. Zhang, Y. M.; Frank, M. W.; Virga, K. G.; Lee, R. E.; Rock, C. O.; Jackowski, S., Acyl carrier protein is a cellular target for the antibacterial action of the pantothenamide class of pantothenate antimetabolites. *Journal of Biological Chemistry* **2004**, 279, 50969-50975.
104. Thomas, J.; Cronan, J. E., Antibacterial activity of *N*-pentylpantothenamide is due to inhibition of coenzyme A synthesis. *Antimicrobial Agents and Chemotherapy* **2010**, 54, 1374-1377.
105. Arnott, Z. L. P.; Nozaki, S.; Monteiro, D. C. F.; Morgan, H. E.; Pearson, A. R.; Niki, H.; Webb, M. E., The mechanism of regulation of pantothenate biosynthesis by the PanD-PanZ·AcCoA complex reveals an additional mode of action for the antimetabolite *N*-pentyl pantothenamide (N5-Pan). *Biochemistry* **2017**, 56, 4931-4939.
106. de Villiers, M.; Spry, C.; Macuamule, C. J.; Barnard, L.; Wells, G.; Saliba, K. J.; Strauss, E., Antiplasmodial mode of action of pantothenamides: pantothenate kinase serves as a metabolic activator not as a target. *ACS Infectious Diseases* **2017**, 3, 527-541.
107. Tjhin, E. T.; Spry, C.; Sewell, A. L.; Hoegl, A.; Barnard, L.; Sexton, A. E.; Siddiqui, G.; Howieson, V. M.; Maier, A. G.; Creek, D. J.; Strauss, E.; Marquez, R.; Auclair, K.; Saliba, K. J., Mutations in the pantothenate kinase of *Plasmodium falciparum* confer diverse sensitivity profiles to antiplasmodial pantothenate analogues. *PLoS Pathogens* **2018**, 14: e1006918.

108. Chiu, J. E.; Thekkiniath, J.; Choi, J. Y.; Perrin, B. A.; Lawres, L.; Plummer, M.; Virji, A. Z.; Abraham, A.; Toh, J. Y.; Zandt, M. V.; Aly, A. S. I.; Voelker, D. R.; Mamoun, C. B., The antimalarial activity of the pantothenamide α -PanAm is via inhibition of pantothenate phosphorylation. *Scientific Reports* **2017**, 7: 14234.
109. Schalkwijk, J.; Allman, E. L.; Jansen, P. A. M.; de Vries, L. E.; Jackowski, S.; Botman, P. N. M.; Beuckens-Schortinghuis, C. A.; Koolen, K. M.; Bolscher, J. M.; Vos, M. W.; Miller, K.; Reeves, S.; Pett, H.; Trevitt, G.; Wittlin, S.; Scheurer, C.; Sax, S.; Fischli, C.; Josling, G.; Kooij, T. W. A.; Bonnert, R.; Campo, B.; Blaauw, R. H.; Rutjes, F. P. J. T.; Sauerwein, R.; Llinas, M.; Hermkens, P. H. H.; Dechering, K. J., Antimalarial pantothenamide metabolites target acetyl-CoA synthesis in *Plasmodium falciparum*. *BioRxiv* **2018**, <https://doi.org/10.1101/256669>.
110. Sugie, Y.; Dekker, K. A.; Hirai, H.; Ichiba, T.; Ishiguro, M.; Shiomi, Y.; Sugiura, A.; Brennan, L.; Duignan, J.; Huang, L. H.; Sutcliffe, J.; Kojima, Y., CJ-15,801, a novel antibiotic from a fungus, *Seimatosporium* sp. *The Journal of Antibiotics (Tokyo)* **2001**, 54, 1060-1065.
111. van der Westhuyzen, R.; Hammons, J. C.; Meier, J. L.; Dahesh, S.; Moolman, W. J. A.; Pelly, S. C.; Nizet, V.; Burkart, M. D.; Strauss, E., The antibiotic CJ-15,801 is an antimetabolite that hijacks and then inhibits CoA biosynthesis. *Chemistry & Biology* **2012**, 19, 559-571.
112. Saliba, K. J.; Kirk, K., CJ-15,801, a fungal natural product, inhibits the intraerythrocytic stage of *Plasmodium falciparum* in vitro via an effect on pantothenic acid utilisation. *Molecular and Biochemical Parasitology* **2005**, 141, 129-131.
113. Spry, C.; Sewell, A. L.; Hering, Y.; Villa, M. V. J.; Weber, J.; Hobson, S. J.; Harnor, S. J.; Gul, S.; Marquez, R.; Saliba, K. J., Structure-activity analysis of CJ-15,801 analogues that interact with *Plasmodium falciparum* pantothenate kinase and inhibit parasite proliferation. *European Journal of Medicinal Chemistry* **2018**, 143, 1139-1147.
114. Patrone, J. D.; Yao, J.; Scott, N. E.; Dotson, G. D., Selective inhibitors of bacterial phosphopantothenoylcysteine synthetase. *Journal of the American Chemical Society* **2009**, 131, 16340-16341.

115. Snell, E. E.; Shive, W., Growth inhibition by analogues of pantothenic acid. Pantothenyl alcohol and related compounds. *Journal of Biological Chemistry* **1945**, 158, 551-559.
116. Saliba, K. J.; Ferru, I.; Kirk, K., Provitamin B5 (pantothenol) inhibits growth of the intraerythrocytic malaria parasite. *Antimicrobial Agents and Chemotherapy* **2005**, 49, 632-637.
117. Kumar, P.; Chhibber, M.; Surolia, A., How pantothenol intervenes in coenzyme-A biosynthesis of *Mycobacterium tuberculosis*. *Biochemical and Biophysical Research Communications* **2007**, 361, 903-909.
118. Chohnan, S.; Murase, M.; Kurikawa, K.; Higashi, K.; Ogata, Y., Antimicrobial activity of pantothenol against *Staphylococci* possessing a prokaryotic type II pantothenate kinase. *Microbes and Environments* **2014**, 29, 224-226.
119. Fletcher, S.; Avery, V. M., A novel approach for the discovery of chemically diverse anti-malarial compounds targeting the *Plasmodium falciparum* coenzyme A synthesis pathway. *Malaria Journal* **2014**, 13: 343.
120. Fletcher, S.; Lucantoni, L.; Sykes, M. L.; Jones, A. J.; Holleran, J. P.; Saliba, K. J.; Avery, V. M., Biological characterization of chemically diverse compounds targeting the *Plasmodium falciparum* coenzyme A synthesis pathway. *Parasites & Vectors* **2016**, 9: 589.
121. Zhao, L.; Allanson, N. M.; Thomson, S. P.; Maclean, J. K. F.; Barker, J. J.; Primrose, W. U.; Tyler, P. D.; Lewendon, A., Inhibitors of phosphopantetheine adenylyltransferase. *European Journal of Medicinal Chemistry* **2003**, 38, 345-349.
122. Miller, J. R.; Thanabal, V.; Melnick, M. M.; Lall, M.; Donovan, C.; Sarver, R. W.; Lee, D. Y.; Ohren, J.; Emerson, D., The use of biochemical and biophysical tools for triage of high-throughput screening hits - a case study with *Escherichia coli* phosphopantetheine adenylyltransferase. *Chemistry Biology & Drug Design* **2010**, 75, 444-454.
123. Cheng, C. S.; Jia, K. F.; Chen, T.; Chang, S. Y.; Lin, M. S.; Yin, H. S., Experimentally validated novel inhibitors of *Helicobacter pylori* phosphopantetheine adenylyltransferase discovered by virtual high-throughput screening. *PLoS One* **2013**, 8: e74271.

124. de Jonge, B. L. M.; Walkup, G. K.; Lahiri, S. D.; Huynh, H.; Neckermann, G.; Utley, L.; Nash, T. J.; Brock, J.; San Martin, M.; Kutschke, A.; Johnstone, M.; Laganas, V.; Hajec, L.; Gu, R. F.; Ni, H.; Chen, B.; Hutchings, K.; Holt, E.; McKinney, D.; Gao, N.; Livchak, S.; Thresher, J., Discovery of inhibitors of 4'-phosphopantetheine adenylyltransferase (PPAT) to validate PPAT as a target for antibacterial therapy. *Antimicrobial Agents and Chemotherapy* **2013**, 57, 6005-6015.
125. Williams, R. J.; Lyman, C. M.; Goodyear, G. H.; Truesdail, J. H.; Holaday, D., "Pantothenic acid," a growth determinant of universal biological occurrence. *Journal of the American Chemical Society* **1933**, 55, 2912-2927.
126. Williams, R. J.; Weinstock, H. H.; Rohrmann, E.; Truesdail, J. H.; Mitchell, H. K.; Meyer, C. E., Pantothenic acid. III. Analysis and determination of constituent groups. *Journal of the American Chemical Society* **1939**, 61, 454-457.
127. Snell, E. E., A specific growth inhibition reversed by pantothenic acid. *Journal of Biological Chemistry* **1941**, 139, 975-976.
128. Winterbottom, R.; Clapp, J. W.; Miller, W. H.; English, J. P.; Roblin, R. O., Studies in chemotherapy. XV. Amides of pantooyltaurine. *Journal of the American Chemical Society* **1947**, 69, 1393-1401.
129. Woolley, D. W.; Collyer, M. L., Phenyl pantothenone, an antagonist of pantothenic acid. *Journal of Biological Chemistry* **1945**, 159, 263-271.
130. McIlwain, H., Bacterial inhibition by metabolite analogues: analogues of pantothenic acid. *Biochemical Journal* **1942**, 36, 417-427.
131. Drell, W.; Dunn, M. S., Inhibition of lactic acid bacteria by analogs of pantothenic acid. *Journal of the American Chemical Society* **1948**, 70, 2057-2063.
132. Vong, K.; Tam, I. S.; Yan, X.; Auclair, K., Inhibitors of aminoglycoside resistance activated in cells. *ACS Chemical Biology* **2012**, 7, 470-475.
133. Vong, K., Prodrug inhibitors of the aminoglycoside resistance-causing enzyme aminoglycoside N-6'-acetyltransferase. McGill University, **2013**.
134. Hammerer, F.; Chang, J. H.; Duncan, D.; Castaneda Ruiz, A.; Auclair, K., Small molecule restores itaconate sensitivity in *Salmonella enterica*: a potential new approach to treating bacterial infections. *ChemBioChem* **2016**, 17, 1513-1517.

135. Brown, E. D.; Wright, G. D., Antibacterial drug discovery in the resistance era. *Nature* **2016**, 529, 336-343.
136. Pogue, J. M.; Marchaim, D.; Kaye, D.; Kaye, K. S., Revisiting "older" antimicrobials in the era of multidrug resistance. *Pharmacotherapy* **2011**, 31, 912-921.
137. Wright, G. D., Something old, something new: revisiting natural products in antibiotic drug discovery. *Canadian Journal of Microbiology* **2014**, 60, 147-154.
138. Spry, C.; Macuamule, C.; Lin, Z.; Virga, K. G.; Lee, R. E.; Strauss, E.; Saliba, K. J., Pantothenamides are potent, on-target inhibitors of *Plasmodium falciparum* growth when serum pantetheinase is inactivated. *PLoS One* **2013**, 8: e54974.
139. Saliba, K. J.; Spry, C., Exploiting the coenzyme A biosynthesis pathway for the identification of new antimalarial agents: the case for pantothenamides. *Biochemical Society Transactions* **2014**, 42, 1087-1093.
140. Jansen, P. A. M.; Hermkens, P. H. H.; Zeeuwen, P. L. J. M.; Botman, P. N. M.; Blaauw, R. H.; Burghout, P.; van Galen, P. M.; Mouton, J. W.; Rutjes, F. P. J. T.; Schalkwijk, J., Combination of pantothenamides with vanin inhibitors as a novel antibiotic strategy against gram-positive bacteria. *Antimicrobial Agents and Chemotherapy* **2013**, 57, 4794-4800.
141. Pett, H. E.; Jansen, P. A. M.; Hermkens, P. H. H.; Botman, P. N. M.; Beuckens-Schortinghuis, C. A.; Blaauw, R. H.; Graumans, W.; van de Vegte-Bolmer, M.; Koolen, K. M. J.; Rutjes, F. P. J. T.; Dechering, K. J.; Sauerwein, R. W.; Schalkwijk, J., Novel pantothenate derivatives for anti-malarial chemotherapy. *Malaria Journal* **2015**, 14: 169.
142. de Villiers, M.; Macuamule, C.; Spry, C.; Hyun, Y. M.; Strauss, E.; Saliba, K. J., Structural modification of pantothenamides counteracts degradation by pantetheinase and improves antiplasmodial activity. *ACS Medicinal Chemistry Letters* **2013**, 4, 784-789.
143. Awuah, E.; Ma, E.; Hoegl, A.; Vong, K.; Habib, E.; Auclair, K., Exploring structural motifs necessary for substrate binding in the active site of *Escherichia coli* pantothenate kinase. *Bioorganic & Medicinal Chemistry* **2014**, 22, 3083-3090.
144. Hoegl, A.; Darabi, H.; Tran, E.; Awuah, E.; Kerdo, E. S.; Habib, E.; Saliba, K. J.; Auclair, K., Stereochemical modification of geminal dialkyl substituents on pantothenamides alters antimicrobial activity. *Bioorganic & Medicinal Chemistry* **2014**, 24, 3274-3277.

145. Macuamule, C. J.; Tjhin, E. T.; Jana, C. E.; Barnard, L.; Koekemoer, L.; de Villiers, M.; Saliba, K. J.; Strauss, E., A pantetheinase-resistant pantothenamide with potent, on-target, and selective antiplasmodial activity. *Antimicrobial Agents and Chemotherapy* **2015**, 59, 3666-3668.
146. Howieson, V. M.; Tran, E.; Hoegl, A.; Fam, H. L.; Fu, J.; Sivonen, K.; Li, X. X.; Auclair, K.; Saliba, K. J., Triazole substitution of a labile amide bond stabilizes pantothenamides and improves their antiplasmodial potency. *Antimicrobial Agents and Chemotherapy* **2016**, 60, 7146-7152.
147. Chatterjee, A. K.; Choi, T. L.; Sanders, D. P.; Grubbs, R. H., A general model for selectivity in olefin cross metathesis. *Journal of the American Chemical Society* **2003**, 125, 11360-11370.
148. Hachey, M., Modifying the pantooyl moiety of *N*-alkylpantothenamides through stereoselective alkylations and olefin cross-metathesis. McGill University, **2013**.
149. Dess, D. B.; Martin, J. C., Readily accessible 12-I-5 oxidant for the conversion of primary and secondary alcohols to aldehydes and ketones. *The Journal of Organic Chemistry* **1983**, 48, 4155-4156.
150. Lindgren, B. O.; Nilsson, T., Preparation of carboxylic acids from aldehydes (including hydroxylated benzaldehydes) by oxidation with chlorite. *Acta Chemica Scandinavica* **1973**, 27, 888-890.
151. Kraus, G. A.; Roth, B., Synthetic studies toward verrucarol. 2. Synthesis of the AB ring system. *The Journal of Organic Chemistry* **1980**, 45, 4825-4830.
152. Kraus, G. A.; Taschner, M. J., Model studies for the synthesis of quassinoids. 1. Construction of the BCE ring system. *The Journal of Organic Chemistry* **1980**, 45, 1175-1176.
153. Bal, B. S.; Childers, W. E.; Pinnick, H. W., Oxidation of α,β -unsaturated aldehydes. *Tetrahedron* **1981**, 37, 2091-2096.
154. Verlinden, B. K.; Louw, A.; Birkholtz, L. M., Resisting resistance: is there a solution for malaria? *Expert Opinion on Drug Discovery* **2016**, 11, 395-406.
155. World Health Organization, Status report on artemisinin and ACT resistance. **2017**.
156. Wells, T. N. C.; Hooft van Huijsduijnen, R.; Van Voorhis, W. C., Malaria medicines: a glass half full? *Nature Reviews Drug Discovery* **2015**, 14, 424-442.

157. Tron, G. C.; Pirali, T.; Billington, R. A.; Canonico, P. L.; Sorba, G.; Genazzani, A. A., Click chemistry reactions in medicinal chemistry: applications of the 1,3-dipolar cycloaddition between azides and alkynes. *Medicinal Research Reviews* **2008**, 28, 278-308.
158. Bonandi, E.; Christodoulou, M. S.; Fumagalli, G.; Perdicchia, D.; Rastelli, G.; Passarella, D., The 1,2,3-triazole ring as a bioisostere in medicinal chemistry. *Drug Discov Today* **2017**, 22, 1572-1581.
159. Boren, B. C.; Narayan, S.; Rasmussen, L. K.; Zhang, L.; Zhao, H.; Lin, Z.; Jia, G.; Fokin, V. V., Ruthenium-catalyzed azide-alkyne cycloaddition: scope and mechanism. *Journal of the American Chemical Society* **2008**, 130, 8923-8930.
160. Himo, F.; Lovell, T.; Hilgraf, R.; Rostovtsev, V. V.; Noodleman, L.; Sharpless, K. B.; Fokin, V. V., Copper(I)-catalyzed synthesis of azoles. DFT study predicts unprecedented reactivity and intermediates. *Journal of the American Chemical Society* **2005**, 127, 210-216.
161. Müller, S.; Liepold, B.; Roth, G. J.; Bestmann, H. J., An improved one-pot procedure for the synthesis of alkynes from aldehydes. *Synlett* **1996**, 1996, 521-522.
162. Pryde, D. C.; Maw, G. N.; Planken, S.; Platts, M. Y.; Sanderson, V.; Corless, M.; Stobie, A.; Barber, C. G.; Russell, R.; Foster, L.; Barker, L.; Wayman, C.; Van Der Graaf, P.; Stacey, P.; Morren, D.; Kohl, C.; Beaumont, K.; Coggon, S.; Tute, M., Novel selective inhibitors of neutral endopeptidase for the treatment of female sexual arousal disorder. Synthesis and activity of functionalized glutaramides. *Journal of Medicinal Chemistry* **2006**, 49, 4409-4424.
163. He, W.; Li, C.; Zhang, L., An efficient [2 + 2 + 1] synthesis of 2,5-disubstituted oxazoles via gold-catalyzed intermolecular alkyne oxidation. *Journal of the American Chemical Society* **2011**, 133, 8482-8485.
164. Hu, Y.; Li, C. Y.; Wang, X. M.; Yang, Y. H.; Zhu, H. L., 1,3,4-Thiadiazole: synthesis, reactions, and applications in medicinal, agricultural, and materials chemistry. *Chemical Reviews* **2014**, 114, 5572-5610.
165. Beno, B. R.; Yeung, K. S.; Bartberger, M. D.; Pennington, L. D.; Meanwell, N. A., A survey of the role of noncovalent sulfur interactions in drug design. *Journal of Medicinal Chemistry* **2015**, 58, 4383-4438.

166. Taylor, R. D.; MacCoss, M.; Lawson, A. D. G., Rings in drugs. *Journal of Medicinal Chemistry* **2014**, 57, 5845-5859.
167. World Health Organization, Global antimicrobial resistance surveillance system. **2015**.
168. Gao, F.; Yan, X.; Shakya, T.; Baettig, O. M.; Ait-Mohand-Brunet, S.; Berghuis, A. M.; Wright, G. D.; Auclair, K., Synthesis and structure-activity relationships of truncated bisubstrate inhibitors of aminoglycoside 6'-N-acetyltransferases. *Journal of Medicinal Chemistry* **2006**, 49, 5273-5281.
169. Ivey, R. A.; Zhang, Y. M.; Virga, K. G.; Hevener, K.; Lee, R. E.; Rock, C. O.; Jackowski, S.; Park, H. W., The structure of the pantothenate kinase·ADP·pantothenate ternary complex reveals the relationship between the binding sites for substrate, allosteric regulator, and antimetabolites. *Journal of Biological Chemistry* **2004**, 279, 35622-35629.
170. Virga, K. G.; Zhang, Y. M.; Leonardi, R.; Ivey, R. A.; Hevener, K.; Park, H. W.; Jackowski, S.; Rock, C. O.; Lee, R. E., Structure-activity relationships and enzyme inhibition of pantothenamide-type pantothenate kinase inhibitors. *Bioorganic & Medicinal Chemistry* **2006**, 14, 1007-1020.
171. Zhang, Y. M.; Chohnan, S.; Virga, K. G.; Stevens, R. D.; Ilkayeva, O. R.; Wenner, B. R.; Bain, J. R.; Newgard, C. B.; Lee, R. E.; Rock, C. O.; Jackowski, S., Chemical knockout of pantothenate kinase reveals the metabolic and genetic program responsible for hepatic coenzyme A homeostasis. *Chemistry & Biology* **2007**, 14, 291-302.
172. Bull, M. J.; Plummer, N. T., Part 1: The human gut microbiome in health and disease. *Integrative Medicine (Encinitas)* **2014**, 13, 17-22.
173. Bouza, E., Consequences of *Clostridium difficile* infection: understanding the healthcare burden. *Clinical Microbiology and Infection* **2012**, 18, 5-12.
174. Langdon, A.; Crook, N.; Dantas, G., The effects of antibiotics on the microbiome throughout development and alternative approaches for therapeutic modulation. *Genome Medicine* **2016**, 8: 39.
175. Schatz, A.; Bugle, E.; Waksman, S. A., Streptomycin, a substance exhibiting antibiotic activity against gram-positive and gram-negative bacteria. *Experimental Biology and Medicine* **1944**, 55, 66-69.

176. Takahashi, Y.; Igarashi, M., Destination of aminoglycoside antibiotics in the 'post-antibiotic era'. *The Journal of Antibiotics (Tokyo)* **2018**, 71, 4-14.
177. Becker, B.; Cooper, M. A., Aminoglycoside antibiotics in the 21st century. *ACS Chemical Biology* **2013**, 8, 105-115.
178. Zarate, S. G.; De la Cruz Claire, M. L.; Benito-Arenas, R.; Revuelta, J.; Santana, A. G.; Bastida, A., Overcoming aminoglycoside enzymatic resistance: design of novel antibiotics and inhibitors. *Molecules* **2018**, 23: 284.
179. Ramirez, M. S.; Tolmasky, M. E., Aminoglycoside modifying enzymes. *Drug Resistance Updates* **2010**, 13, 151-171.
180. Labby, K. J.; Garneau-Tsodikova, S., Strategies to overcome the action of aminoglycoside-modifying enzymes for treating resistant bacterial infections. *Future Medicinal Chemistry* **2013**, 5, 1285-1309.
181. Chow, J. W., Aminoglycoside resistance in *Enterococci*. *Clinical Infectious Diseases* **2000**, 31 (2), 586-589.
182. Ramirez, M. S.; Tolmasky, M. E., Amikacin: uses, resistance, and prospects for inhibition. *Molecules* **2017**, 22: 2267.
183. Gao, F.; Yan, X.; Baettig, O. M.; Berghuis, A. M.; Auclair, K., Regio- and chemoselective 6'-N-derivatization of aminoglycosides: bisubstrate inhibitors as probes to study aminoglycoside 6'-N-acetyltransferases. *Angewandte Chemie International Edition* **2005**, 44, 6859-6862.
184. Yan, X.; Gao, F.; Yotphan, S.; Bakirtzian, P.; Auclair, K., The use of aminoglycoside derivatives to study the mechanism of aminoglycoside 6'-N-acetyltransferase and the role of 6'-NH₂ in antibacterial activity. *Bioorganic & Medicinal Chemistry* **2007**, 15, 2944-2951.
185. Magalhaes, M. L.; Vetting, M. W.; Gao, F.; Freiburger, L.; Auclair, K.; Blanchard, J. S., Kinetic and structural analysis of bisubstrate inhibition of the *Salmonella enterica* aminoglycoside 6'-N-acetyltransferase. *Biochemistry* **2008**, 47, 579-584.
186. Gao, F.; Yan, X.; Zahr, O.; Larsen, A.; Vong, K.; Auclair, K., Synthesis and use of sulfonamide-, sulfoxide-, or sulfone-containing aminoglycoside-CoA bisubstrates as mechanistic probes for aminoglycoside N-6'-acetyltransferase. *Bioorganic & Medicinal Chemistry* **2008**, 18, 5518-5522.

187. Gao, F.; Yan, X.; Auclair, K., Synthesis of a phosphonate-linked aminoglycoside-coenzyme A bisubstrate and use in mechanistic studies of an enzyme involved in aminoglycoside resistance. *Chemistry* **2009**, 15, 2064-2070.
188. Yan, X.; Akinnusi, T. O.; Larsen, A. T.; Auclair, K., Synthesis of 4'-aminopantetheine and derivatives to probe aminoglycoside *N*-6'-acetyltransferase. *Organic & Biomolecular Chemistry* **2011**, 9, 1538-1546.
189. Szychowski, J.; Kondo, J.; Zahr, O.; Auclair, K.; Westhof, E.; Hanessian, S.; Keillor, J. W., Inhibition of aminoglycoside-deactivating enzymes APH(3')-IIIa and AAC(6')-II by amphiphilic paromomycin O^{2'}-ether analogues. *ChemMedChem* **2011**, 6, 1961-1966.
190. Kashuba, A. D. M.; Bertino, J. S.; Nafziger, A. N., Dosing of aminoglycosides to rapidly attain pharmacodynamic goals and hasten therapeutic response by using individualized pharmacokinetic monitoring of patients with pneumonia caused by gram-negative organisms. *Antimicrobial Agents and Chemotherapy* **1998**, 42, 1842-1844.
191. Prayle, A.; Watson, A.; Fortnum, H.; Smyth, A., Side effects of aminoglycosides on the kidney, ear and balance in cystic fibrosis. *Thorax* **2010**, 65, 654-658.
192. Pagkalis, S.; Mantadakis, E.; Mavros, M. N.; Ammari, C.; Falagas, M. E., Pharmacological considerations for the proper clinical use of aminoglycosides. *Drugs* **2011**, 71, 2277-2294.
193. Hyams, P. J.; Simberkoff, M. S.; Rahal, J. J., In vitro bactericidal effectiveness of four aminoglycoside antibiotics. *Antimicrobial Agents and Chemotherapy* **1973**, 3, 87-94.
194. Lacy, M. K.; Nicolau, D. P.; Nightingale, C. H.; Quintiliani, R., The pharmacodynamics of aminoglycosides. *Clinical Infectious Diseases* **1998**, 27, 23-27.
195. Pankey, G. A.; Sabath, L. D., Clinical relevance of bacteriostatic versus bactericidal mechanisms of action in the treatment of gram-positive bacterial infections. *Clinical Infectious Diseases* **2004**, 38, 864-870.
196. Ventola, C. L., The antibiotic resistance crisis: part 1: causes and threats. *Pharmacy and Therapeutics* **2015**, 40, 277-283.
197. Gonzalez-Bello, C., Antibiotic adjuvants - a strategy to unlock bacterial resistance to antibiotics. *Bioorganic & Medicinal Chemistry* **2017**, 27, 4221-4228.
198. Fraser, S. L.; Donskey, C. J.; Salata, R. A., Enterococcal infections. *Medscape, Drugs & Diseases* **2017**.

199. Krenk, O.; Kratochvíl, J.; Špulák, M.; Buchta, V.; Kuneš, J.; Nováková, L.; Ghavre, M.; Pour, M., Methodology for synthesis of enantiopure 3,5-disubstituted pyrrol-2-ones. *European Journal of Organic Chemistry* **2015**, 2015, 5414-5423.
200. Buchstaller, H. P.; Dorsch, D., Imidazopyrazinone derivatives. US20170002010A1. **2017**.
201. Chu, S. S.; Alegria, L. A.; Bleckman, T. M.; Chong, W. K. M.; Duvadie, R. K.; Li, L.; Reich, S. H.; Romines, W. H.; Wallace, M. B.; Yang, Y., Thiazole benzamide derivatives and pharmaceutical compositions for inhibiting cell proliferation, and methods for their use. WO2003004467A2. **2003**.
202. Raminelli, C.; Gargalaka, J.; Silveira, C. C.; Comasseto, J. V., The coupling of butylvinyltellurides with organometallic reagents catalysed by nickel complexes. *Tetrahedron* **2007**, 63, 8801-8809.
203. Grewal, G.; Hennessy, E.; Kamhi, V.; Li, D.; Oza, V.; Saeh, J. C.; Su, Q., Sulfonamide compounds useful as edg receptor modulators. WO2007129019A1. **2007**.
204. Glinka, T.; Rodny, O.; Bostian, K. A.; Wallace, D. M.; Higuchi, R. I.; Chow, C.; Mak, C. C.; Hirst, G.; Eastman, B., Polybasic bacterial efflux pump inhibitors and therapeutic uses thereof. US20100152098A1. **2010**.
205. Ohkanda, J.; Buckner, F. S.; Lockman, J. W.; Yokoyama, K.; Carrico, D.; Eastman, R.; de Luca-Fradley, K.; Davies, W.; Croft, S. L.; Van Voorhis, W. C.; Gelb, M. H.; Sebti, S. M.; Hamilton, A. D., Design and synthesis of peptidomimetic protein farnesyltransferase inhibitors as anti-*Trypanosoma brucei* agents. *Journal of Medicinal Chemistry* **2004**, 47, 432-445.
206. Sekirnik née Measures, A. R.; Hewings, D. S.; Theodoulou, N. H.; Jursins, L.; Lewendon, K. R.; Jennings, L. E.; Rooney, T. P. C.; Heightman, T. D.; Conway, S. J., Isoxazole-derived amino acids are bromodomain-binding acetyl-lysine mimics: incorporation into histone H4 peptides and histone H3. *Angewandte Chemie International Edition* **2016**, 55, 8353-8357.
207. Aulakh, V. S.; Casarez, A.; Lin, X.; Lindvall, M.; McEnroe, G.; Moser, H. E.; Reck, F.; Tjandra, M.; Simmons, R. L.; Yifu, A.; Zhu, Q., Monobactam organic compounds for the treatment of bacterial infections. US20150266867A1. **2015**.

208. Bergeron, R. J.; McManis, J. S.; Dionis, J.; Garlich, J. R., An efficient total synthesis of agrobactin and its gallium(III) chelate. *The Journal of Organic Chemistry* **1985**, 50, 2780-2782.
209. Videnov, G.; Kaiser, D.; Kempter, C.; Jung, G., Synthesis of naturally occurring, conformationally restricted oxazole- and thiazole-containing di- and tripeptide mimetics. *Angewandte Chemie International Edition* **1996**, 35, 1503-1506.
210. Khomenko, D. M.; Doroschuk, R. O.; Trachevskii, V. V.; Shova, S.; Lampeka, R. D., Facile synthesis of hexahydropyrazino[2,3-e]pyrazines from 3-aminomethyl-1,2,4-triazoles. *Tetrahedron Letters* **2016**, 57, 990-992.
211. Rajapakse, H. A.; Zhu, H.; Young, M. B.; Mott, B. T., A mild and efficient one pot synthesis of 1,3,4-oxadiazoles from carboxylic acids and acyl hydrazides. *Tetrahedron Letters* **2006**, 47, 4827-4830.
212. Boehm, M. F.; Martinborough, E.; Moorjani, M.; Tamiya, J.; Huang, L.; Yeager, A. R.; Brahmachary, E.; Fowler, T.; Novak, A.; Meghani, P.; Knaggs, M.; Glynn, D.; Mills, M., Glp-1 receptor modulators. WO2016094729A1. **2016**.
213. Engers, D. W.; Blobaum, A. L.; Gogliotti, R. D.; Cheung, Y. Y.; Salovich, J. M.; Garcia-Barrantes, P. M.; Daniels, J. S.; Morrison, R.; Jones, C. K.; Soars, M. G.; Zhuo, X.; Hurley, J.; Macor, J. E.; Bronson, J. J.; Conn, P. J.; Lindsley, C. W.; Niswender, C. M.; Hopkins, C. R., Discovery, synthesis, and preclinical characterization of *N*-(3-Chloro-4-fluorophenyl)-1*H*-pyrazolo[4,3-*b*]pyridin-3-amine (VU0418506), a novel positive allosteric modulator of the metabotropic glutamate receptor 4 (mGlu₄). *ACS Chemical Neuroscience* **2016**, 7, 1192-1200.
214. Dickson, H. D.; Smith, S. C.; Hinkle, K. W., A convenient scalable one-pot conversion of esters and Weinreb amides to terminal alkynes. *Tetrahedron Letters* **2004**, 45, 5597-5599.
215. Li, M.; Dixon, D. J., Stereoselective spirolactam synthesis via palladium catalyzed arylation allene carbocyclization cascades. *Organic Letters* **2010**, 12, 3784-3787.
216. Di Pietro, O.; Alencar, N.; Esteban, G.; Viayna, E.; Szalaj, N.; Vazquez, J.; Juarez-Jimenez, J.; Sola, I.; Perez, B.; Sole, M.; Unzeta, M.; Munoz-Torrero, D.; Luque, F. J., Design, synthesis and biological evaluation of *N*-methyl-*N*-[(1,2,3-triazol-4-

yl)alkyl]propargylamines as novel monoamine oxidase B inhibitors. *Bioorganic & Medicinal Chemistry* **2016**, 24, 4835-4854.

217. Ijsselstijn, M., Synthesis of conformationally restricted beta-turn mimics. Radboud University, **2006**.

218. Vescovi, A.; Knoll, A.; Koert, U., Synthesis and functional studies of THF-gramicidin hybrid ion channels. *Organic & Biomolecular Chemistry* **2003**, 1, 2983-2997.

219. Rajagopal, B.; Chen, Y. Y.; Chen, C. C.; Liu, X. Y.; Wang, H. R.; Lin, P. C., Cu(I)-catalyzed synthesis of dihydropyrimidin-4-ones toward the preparation of beta- and beta³-amino acid analogues. *The Journal of Organic Chemistry* **2014**, 79, 1254-1264.

220. Reginato, G.; Mordini, A.; Messina, F.; Degl'Innocenti, A.; Poli, G., A new stereoselective synthesis of chiral γ -functionalized (*E*)-allylic amines. *Tetrahedron* **1996**, 52, 10985-10996.

221. Chirapu, S. R.; Rotter, C. J.; Miller, E. L.; Varma, M. V.; Dow, R. L.; Finn, M. G., High specificity in response of the sodium-dependent multivitamin transporter to derivatives of pantothenic acid. *Current Topics in Medicinal Chemistry* **2013**, 13, 837-842.

222. Martin, D. P.; Bibart, R. T.; Drueckhammer, D. G., Synthesis of novel analogs of acetyl coenzyme A: mimics of enzyme reaction intermediates. *Journal of the American Chemical Society* **1994**, 116, 4660-4668.

223. Lin, P. K. T., The synthesis of oxa-analogues and homologues of naturally occurring polyamines. *Synthesis* **1998**, 1998, 859-866.

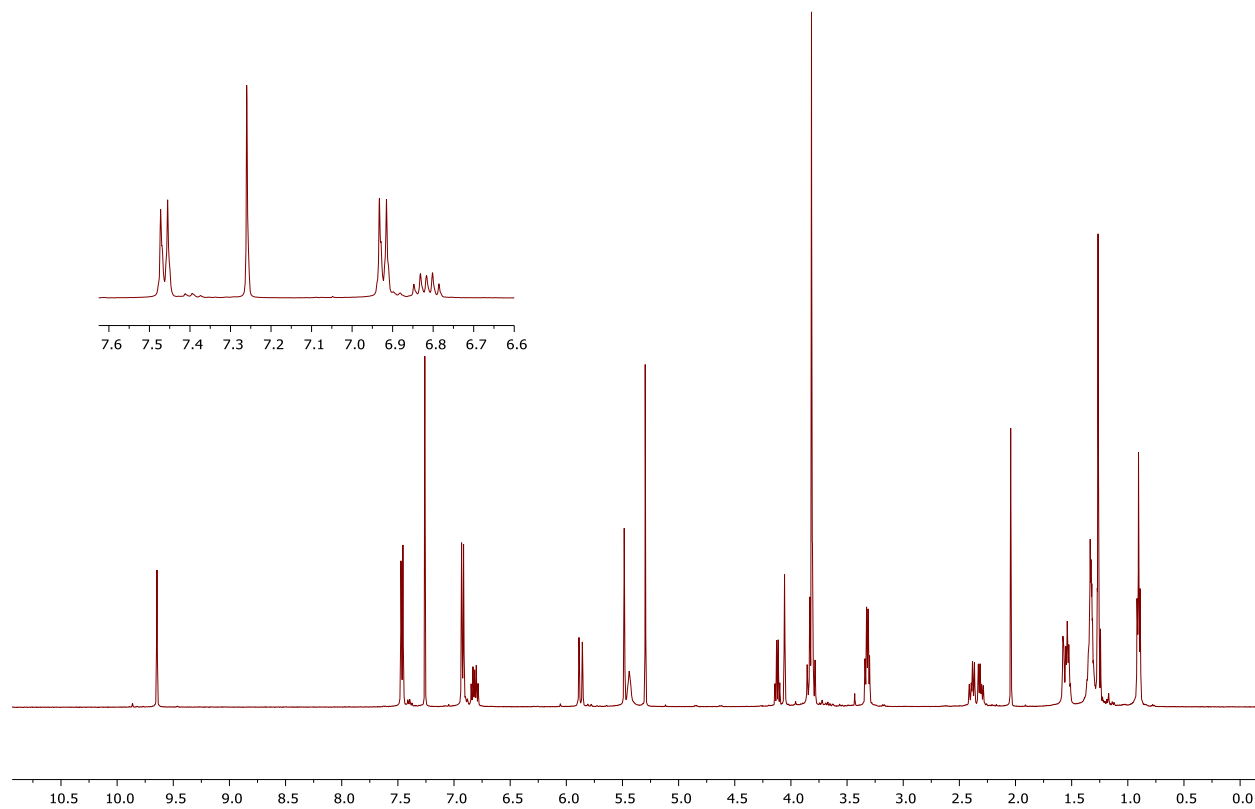
224. NCCLS, Performance standards for antimicrobial susceptibility testing (approved standard, NCCLS document M100-S14). **2004**.

225. Wright, G. D.; Ladak, P., Overexpression and characterization of the chromosomal aminoglycoside 6'-*N*-acetyltransferase from *Enterococcus faecium*. *Antimicrobial Agents and Chemotherapy* **1997**, 41, 956-960.

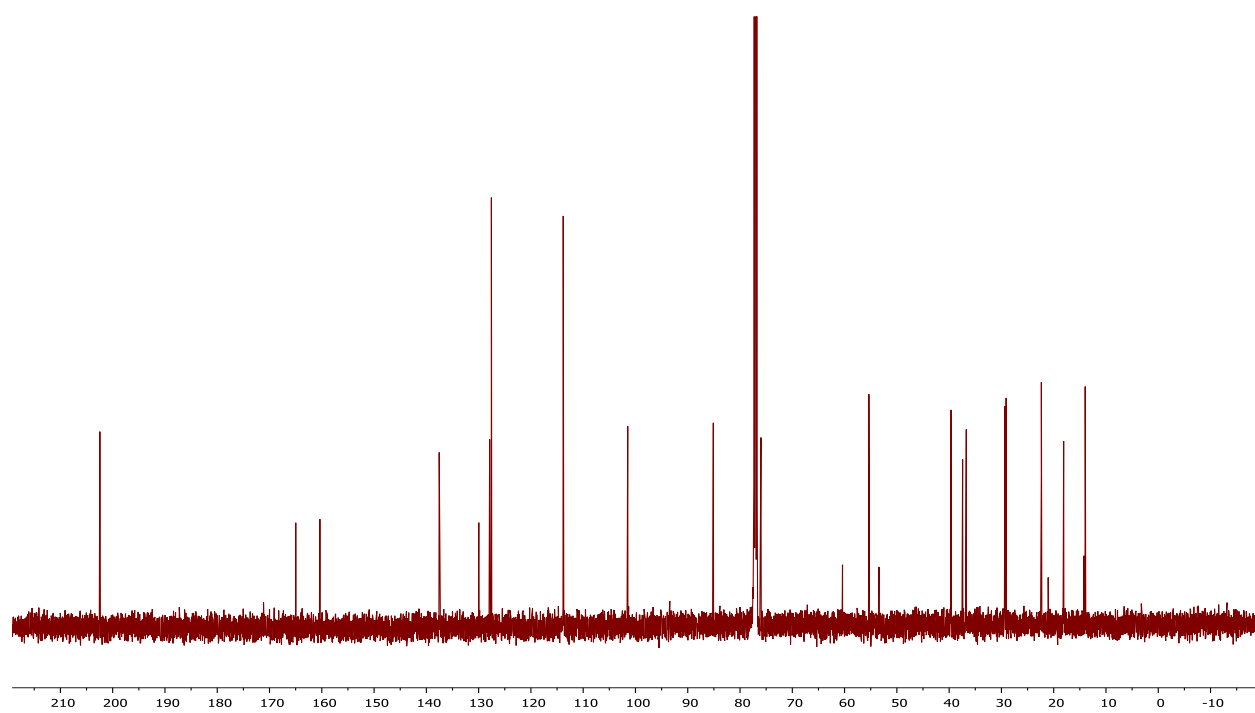
226. Pendland, S. L.; Diaz-Linares, M.; Garey, K. W.; Woodward, J. G.; Ryu, S.; Danziger, L. H., Bactericidal activity and postantibiotic effect of levofloxacin against anaerobes. *Antimicrobial Agents and Chemotherapy* **1999**, 43, 2547-2549.

Appendix

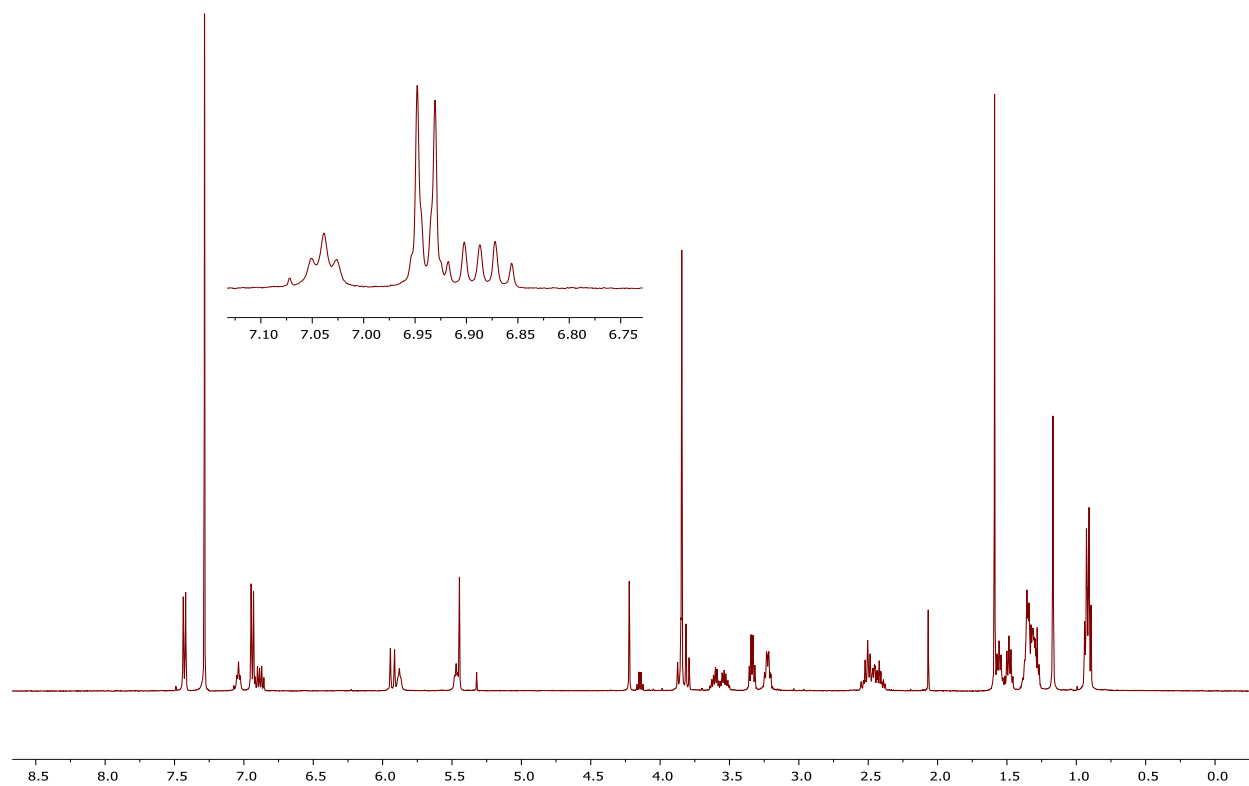
¹H NMR of compound 2.15



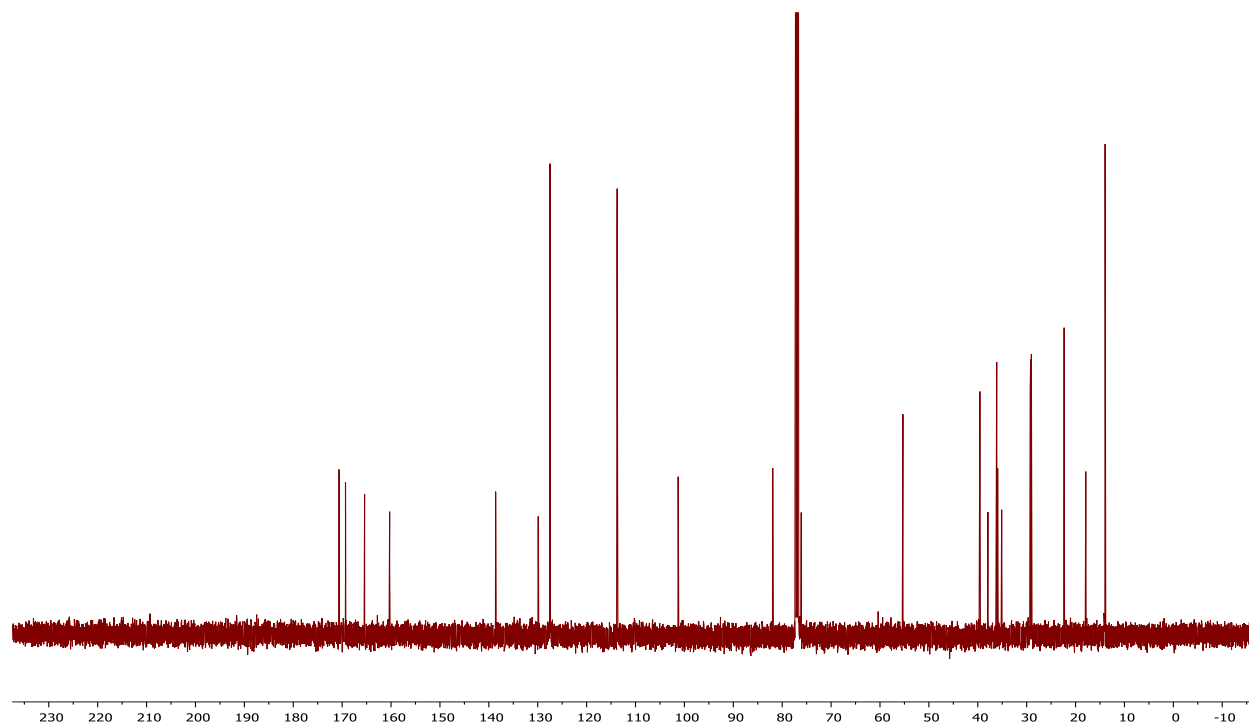
¹³C NMR of compound 2.15



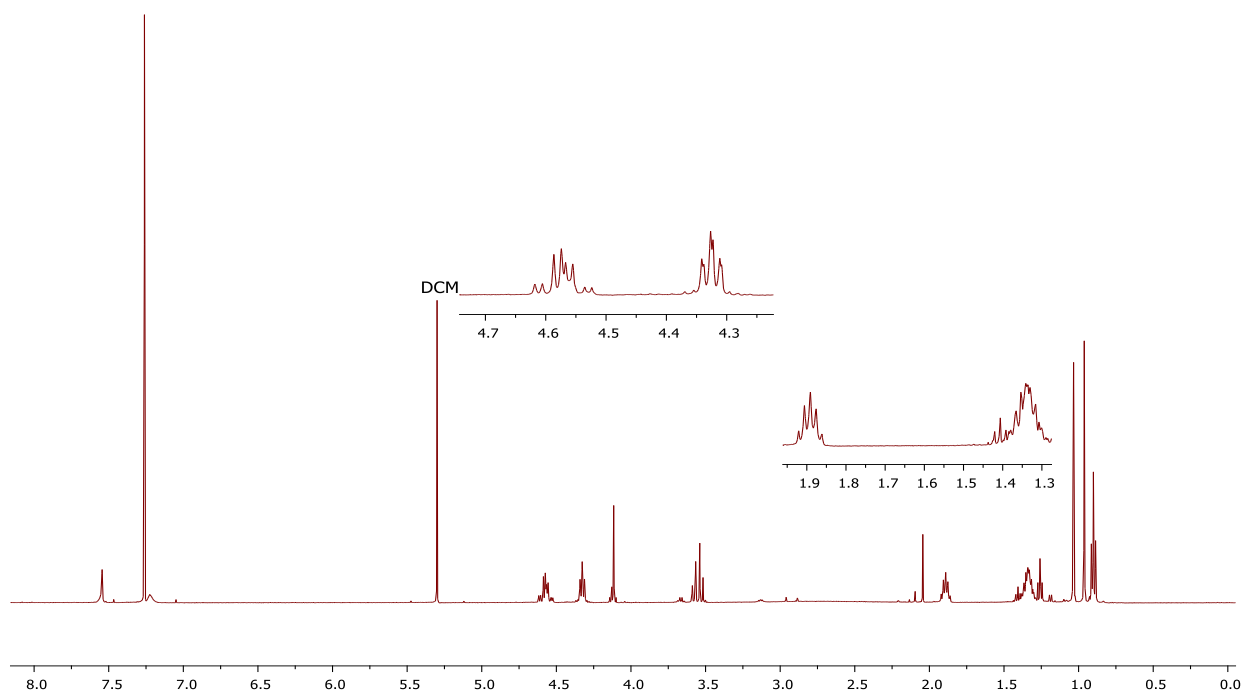
¹H NMR of compound 2.18



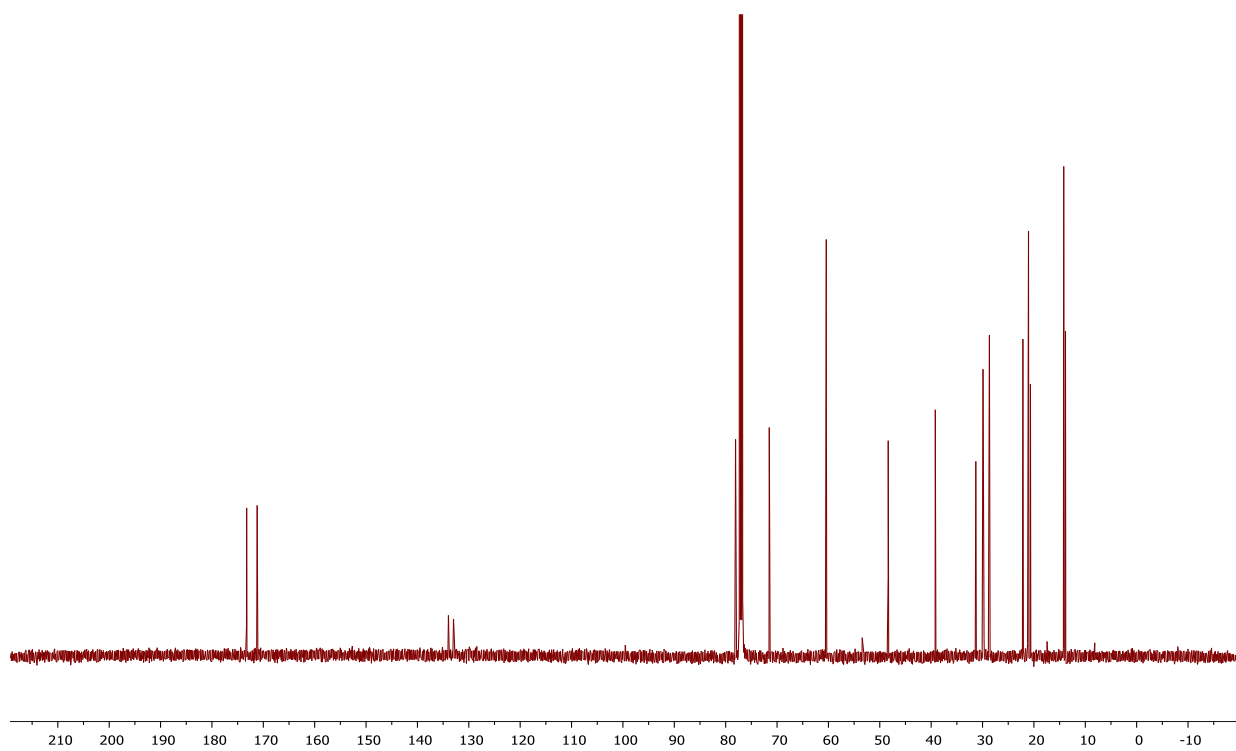
¹³C NMR of compound 2.18



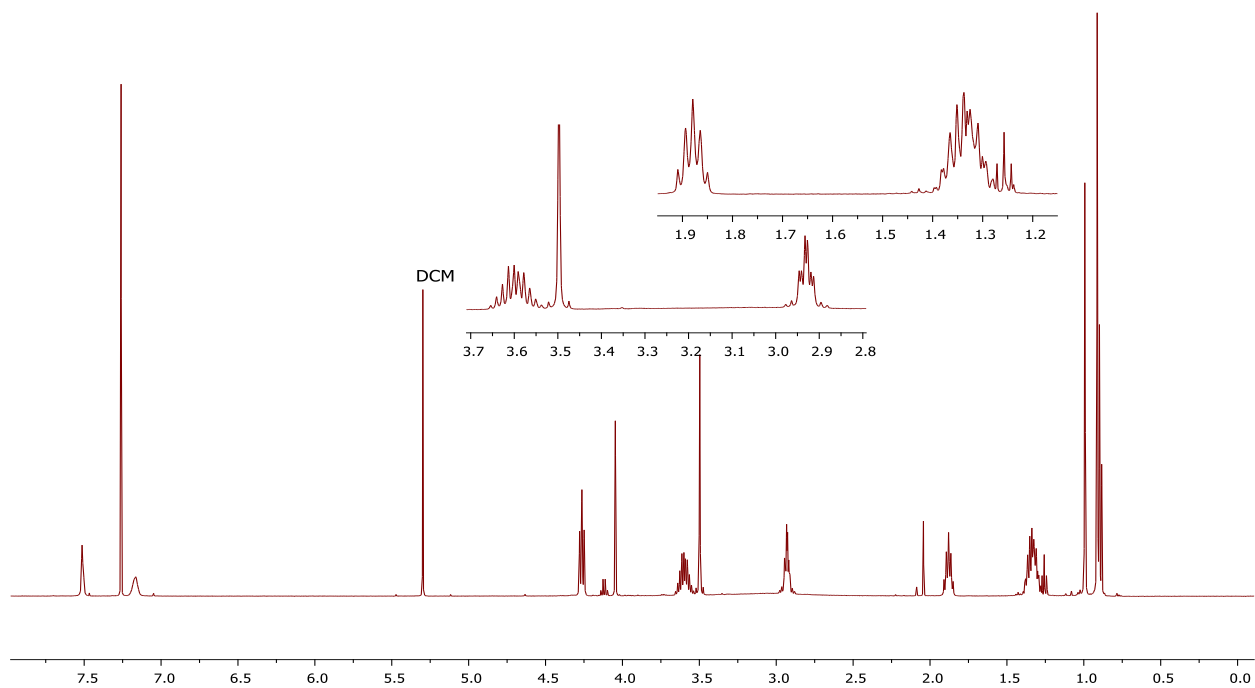
¹H NMR of compound 3.2a



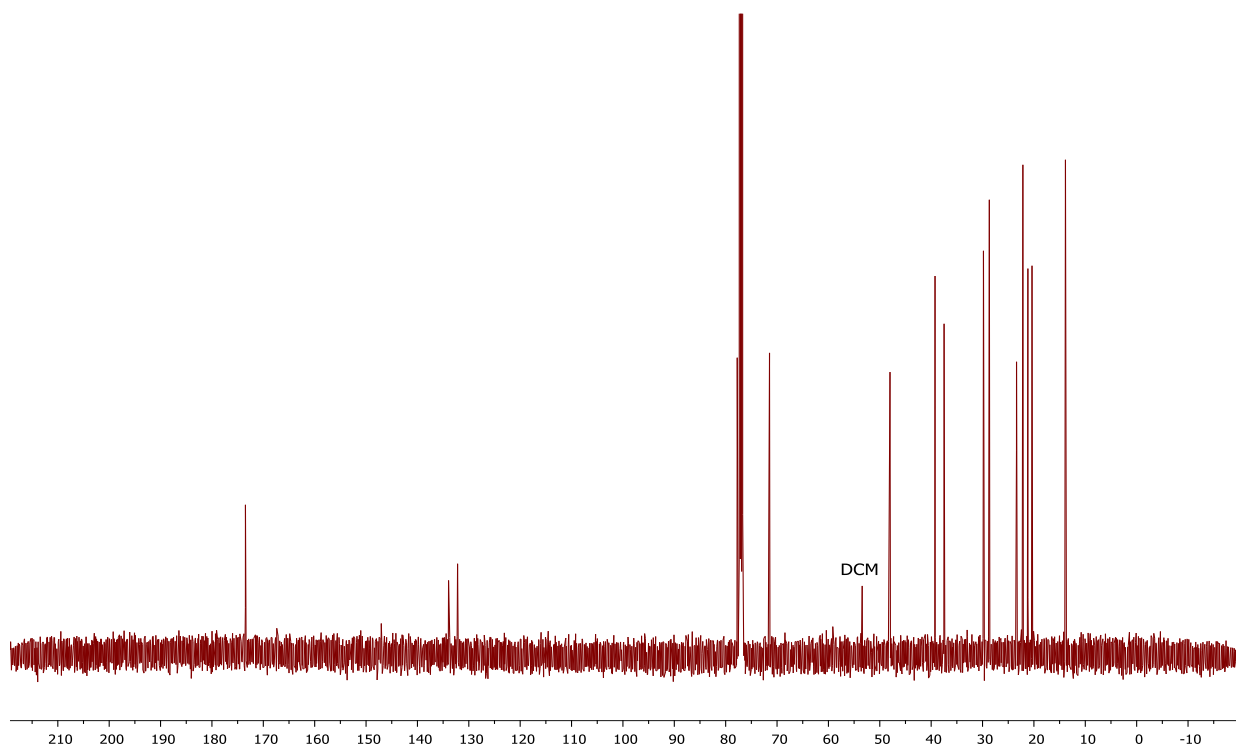
¹³C NMR of compound 3.2a



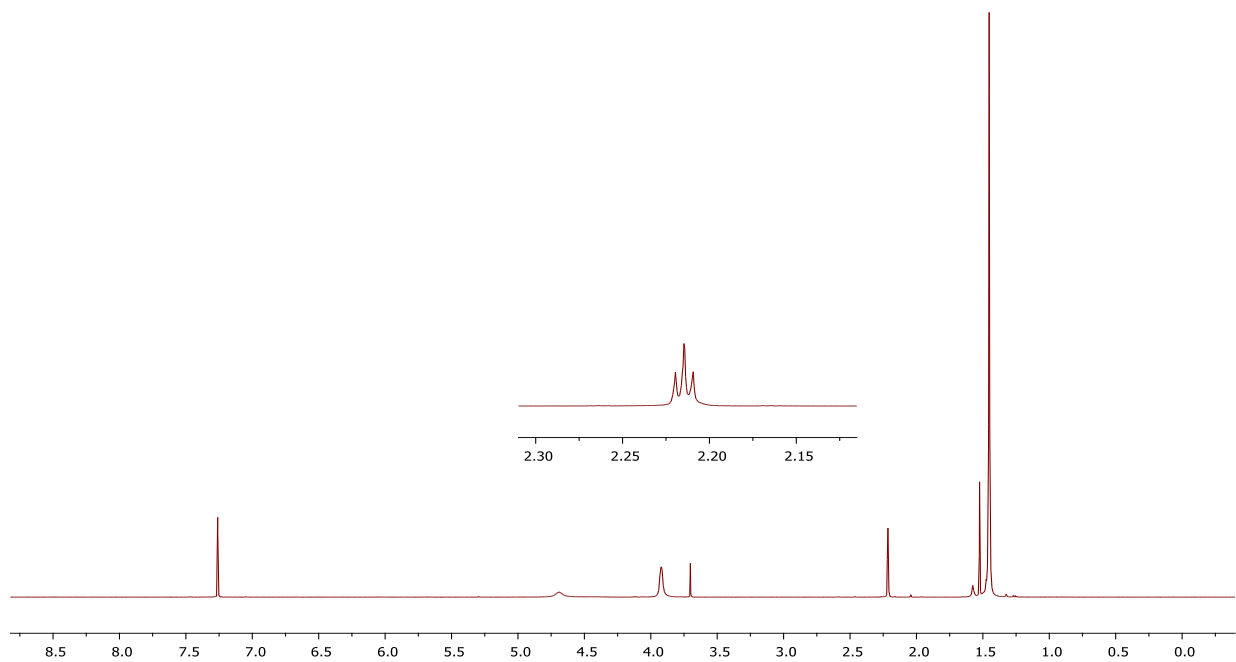
¹H NMR of compound 3.2b



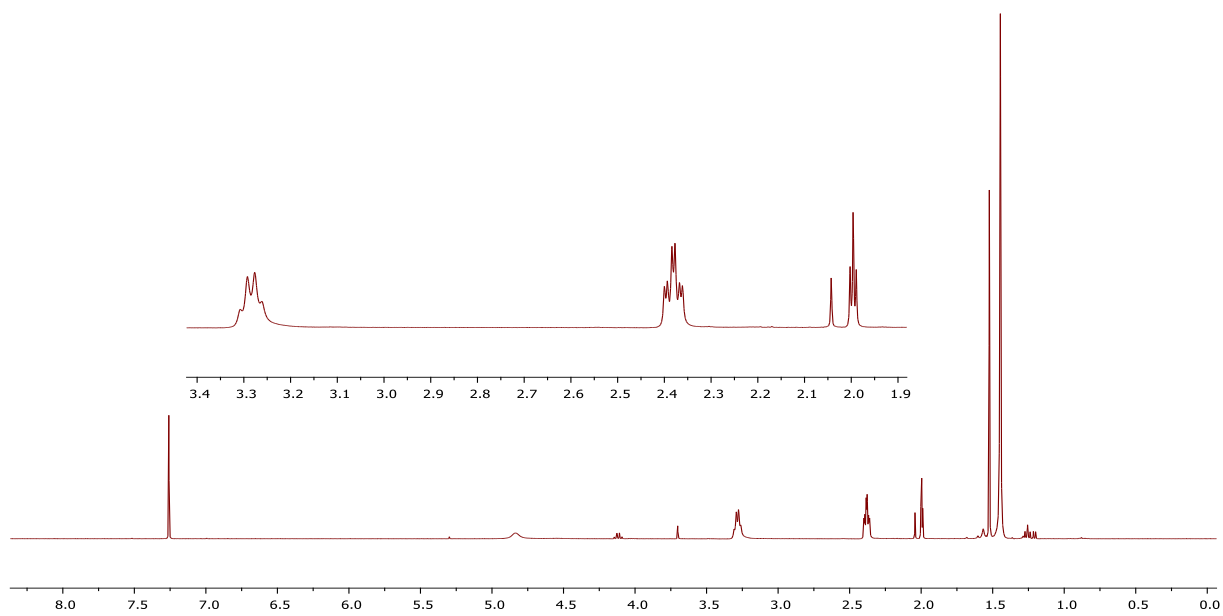
¹³C NMR of compound 3.2b



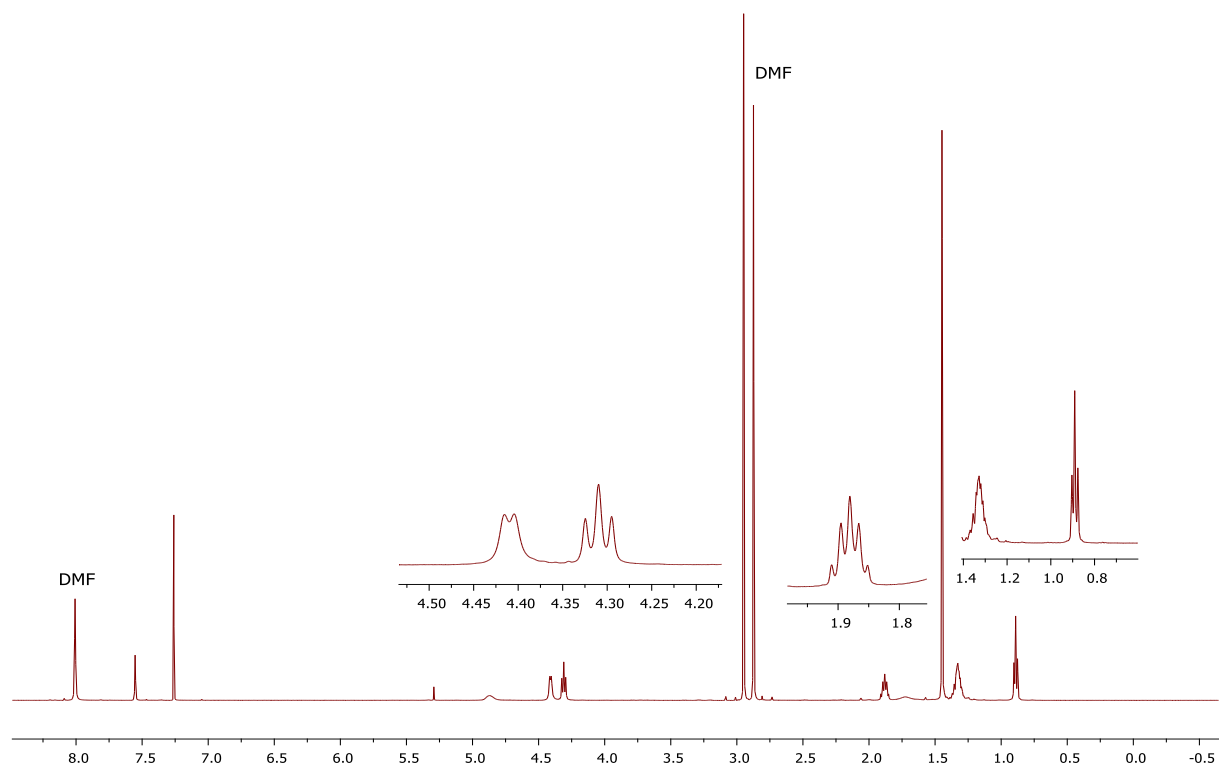
¹H NMR of compound 3.3a



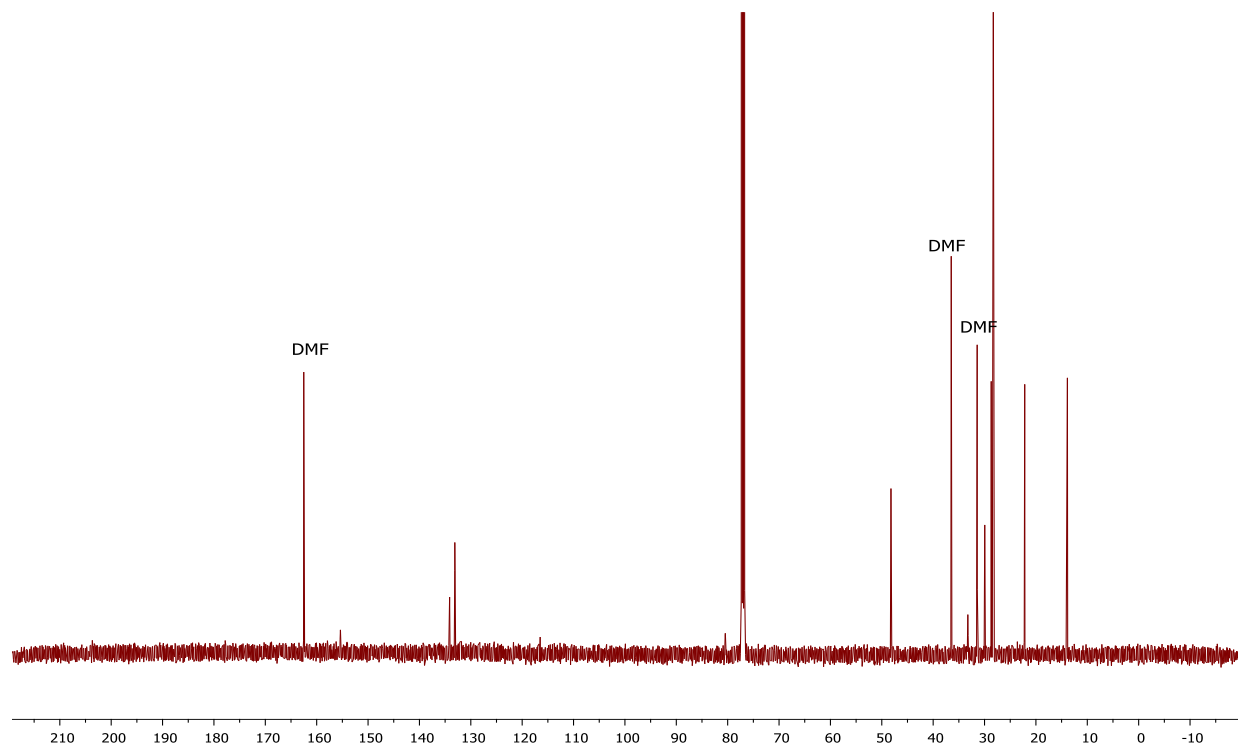
¹H NMR of compound 3.3b



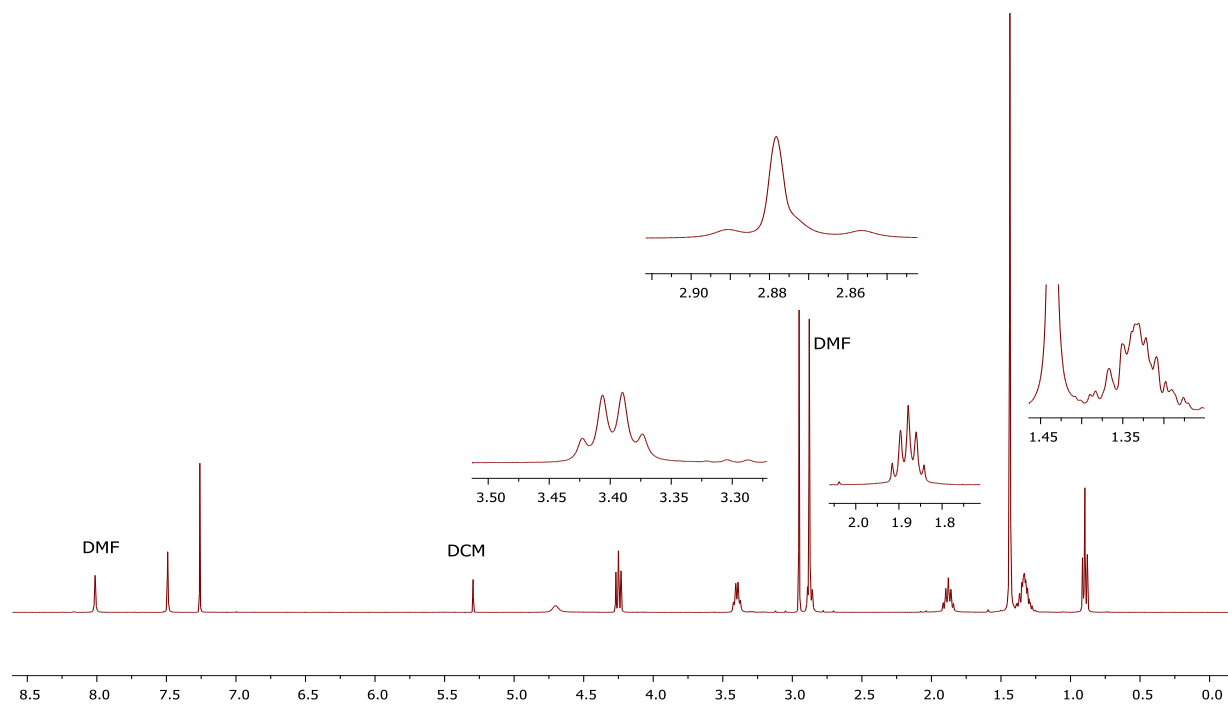
¹H NMR of compound 3.5a



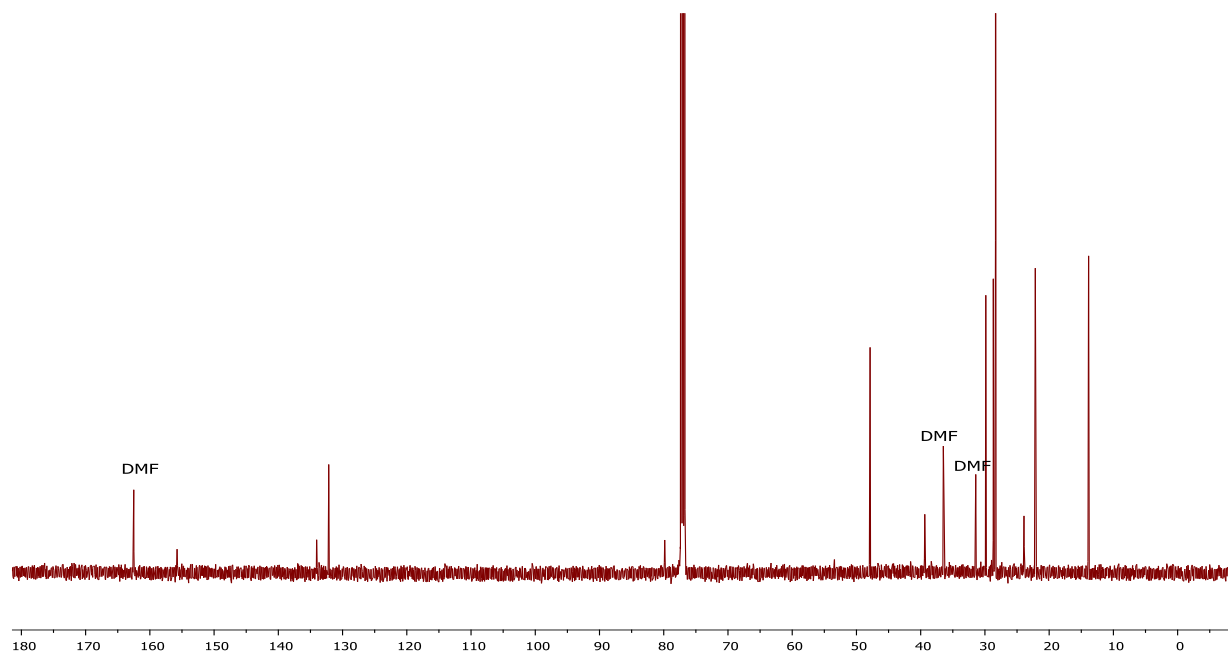
¹³C NMR of compound 3.5a



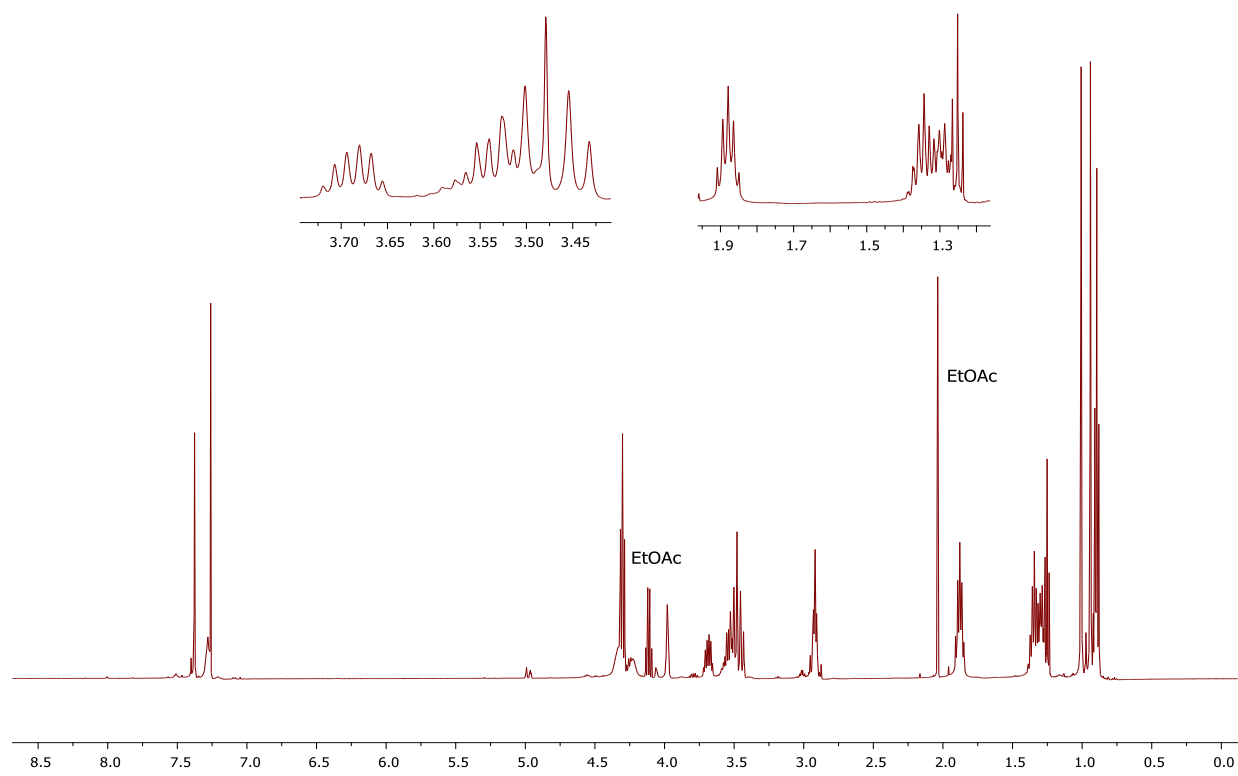
¹H NMR of compound 3.5b



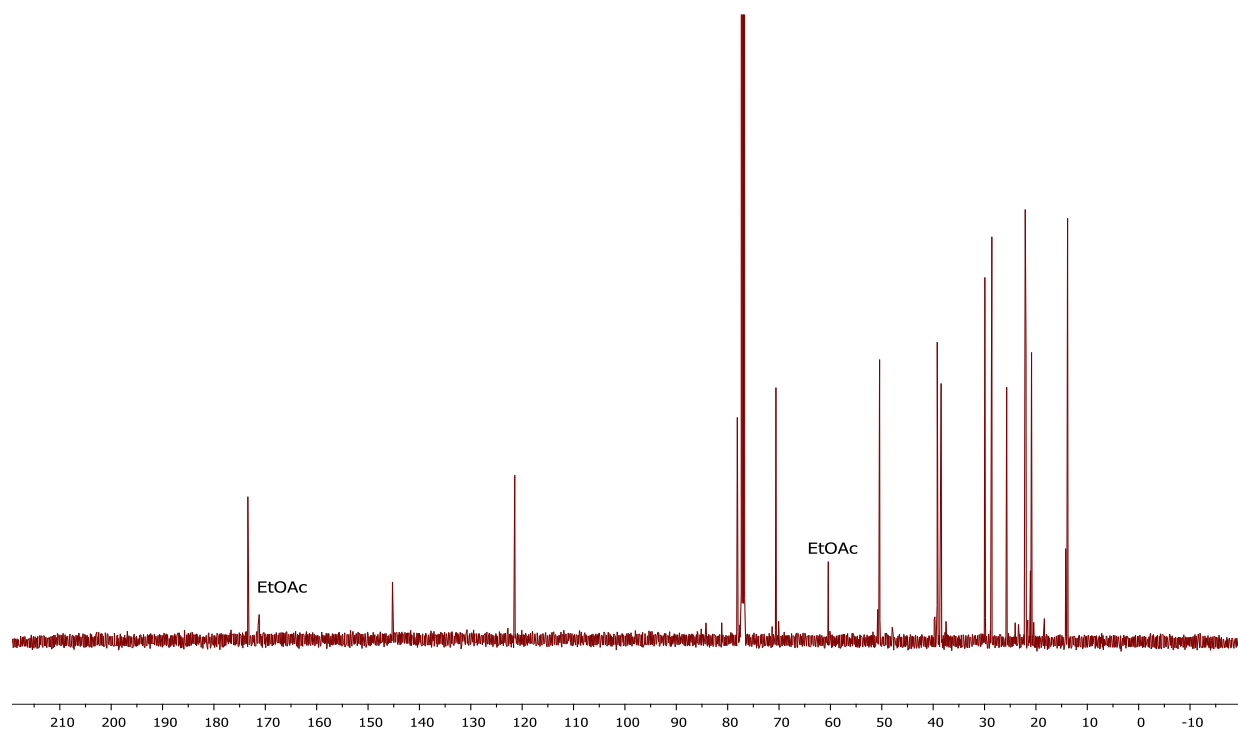
¹³C NMR of compound 3.5b



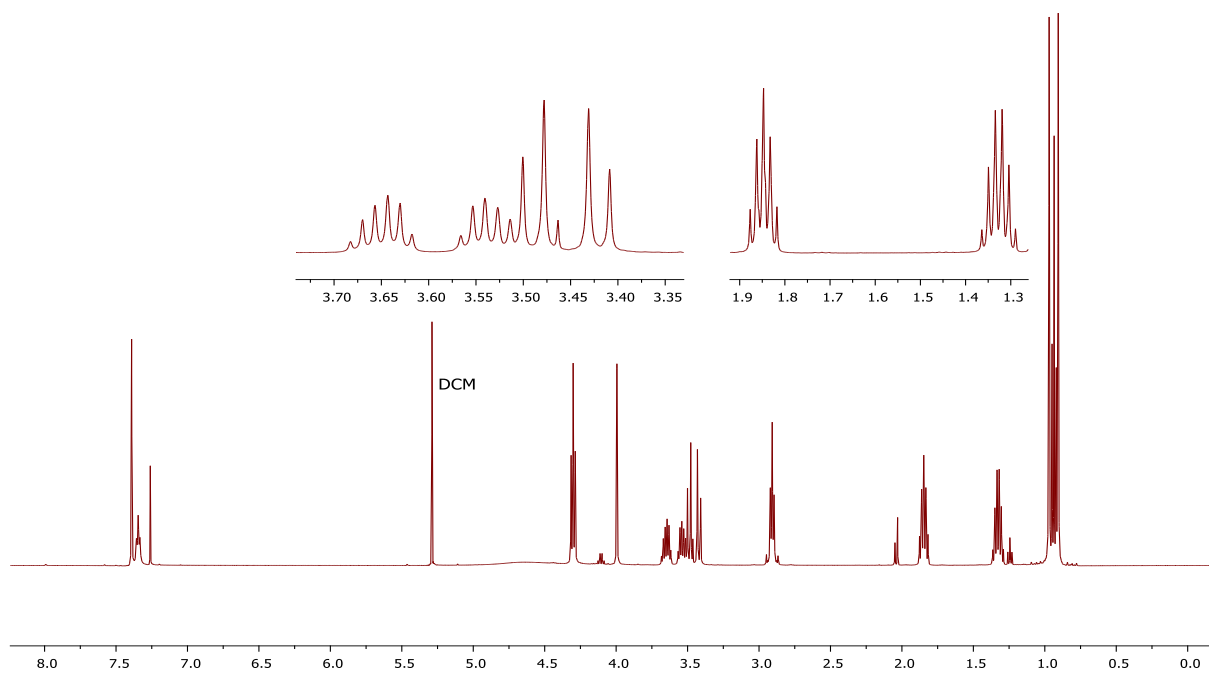
¹H NMR of compound 3.7a



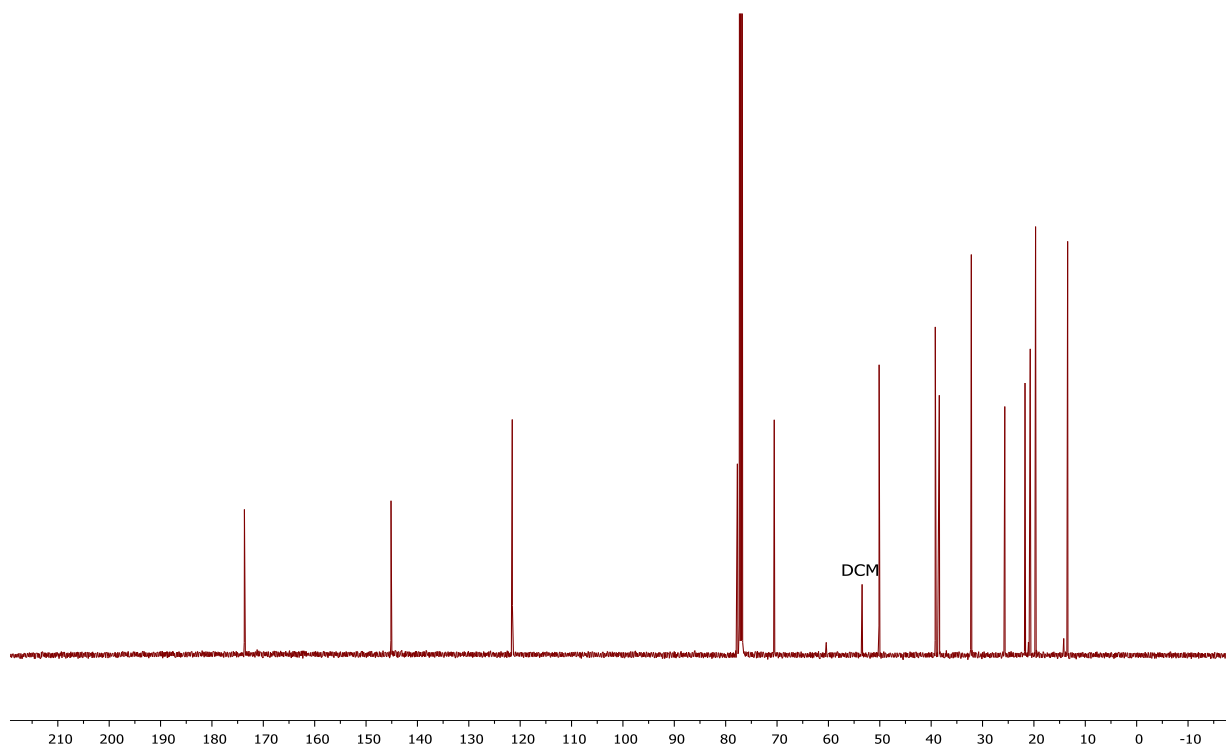
¹³C NMR of compound 3.7a



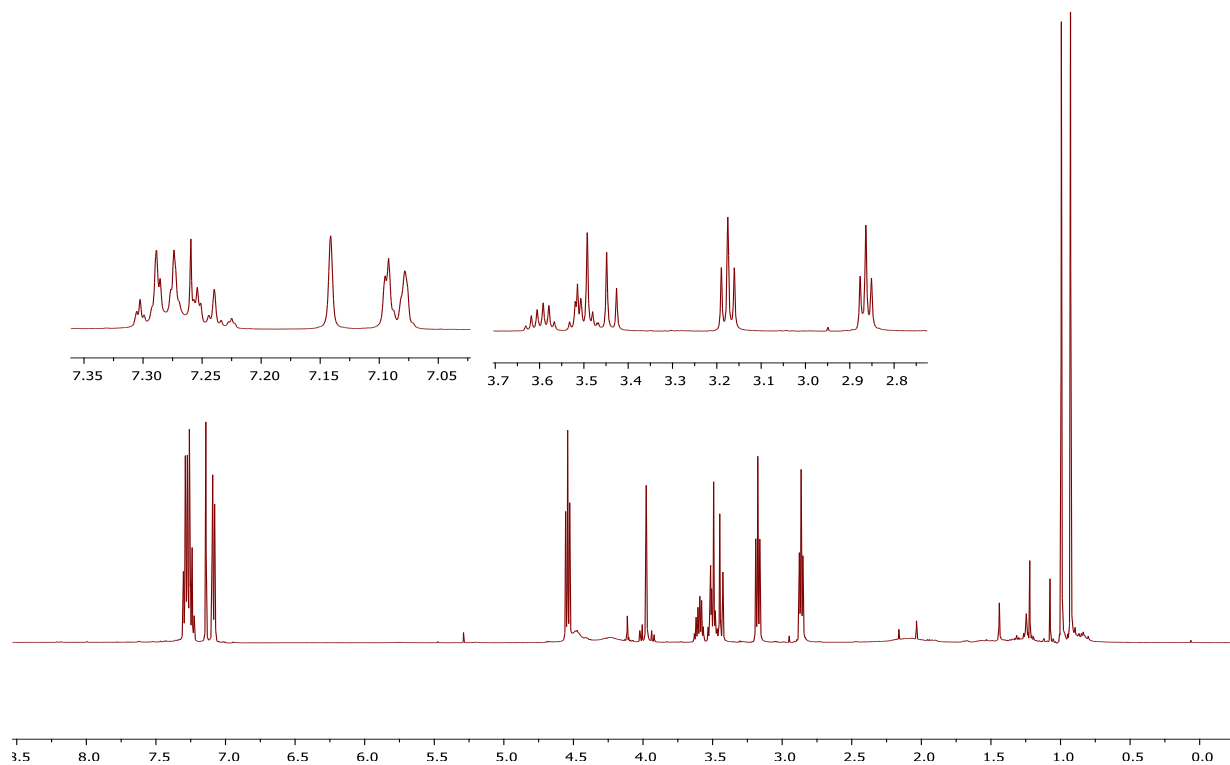
¹H NMR of compound 3.7b



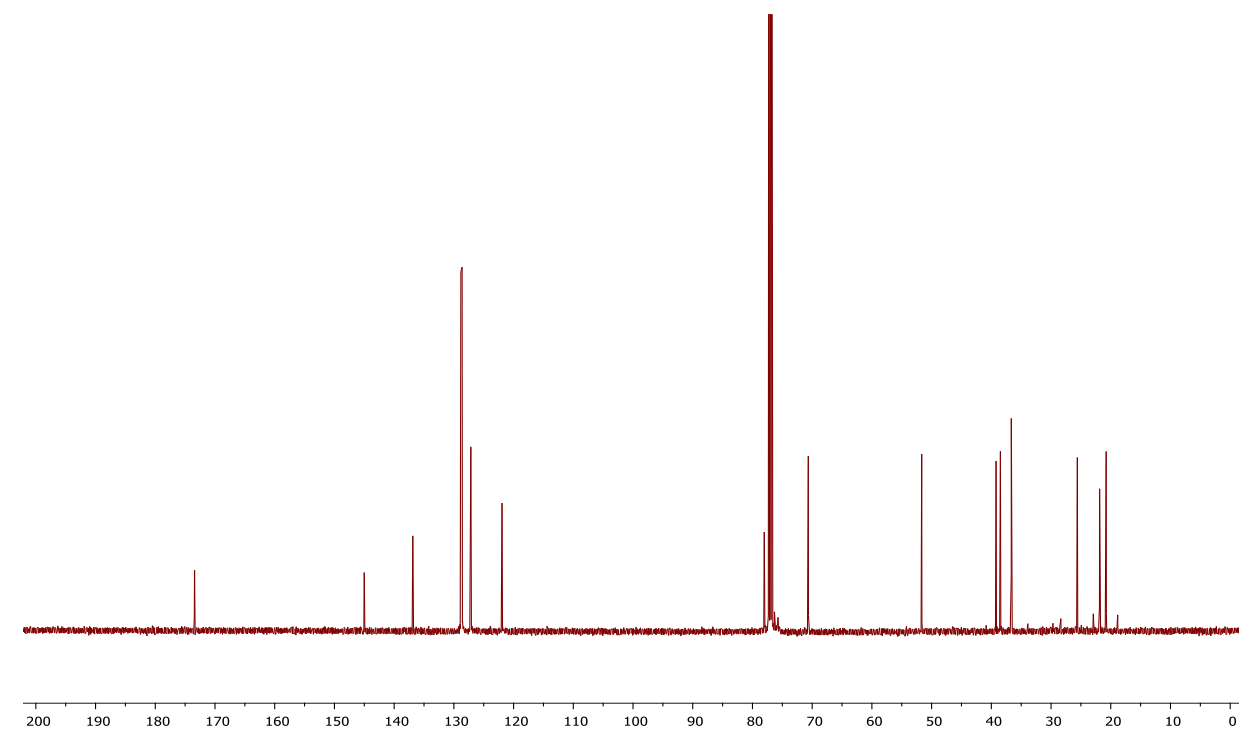
¹³C NMR of compound 3.7b



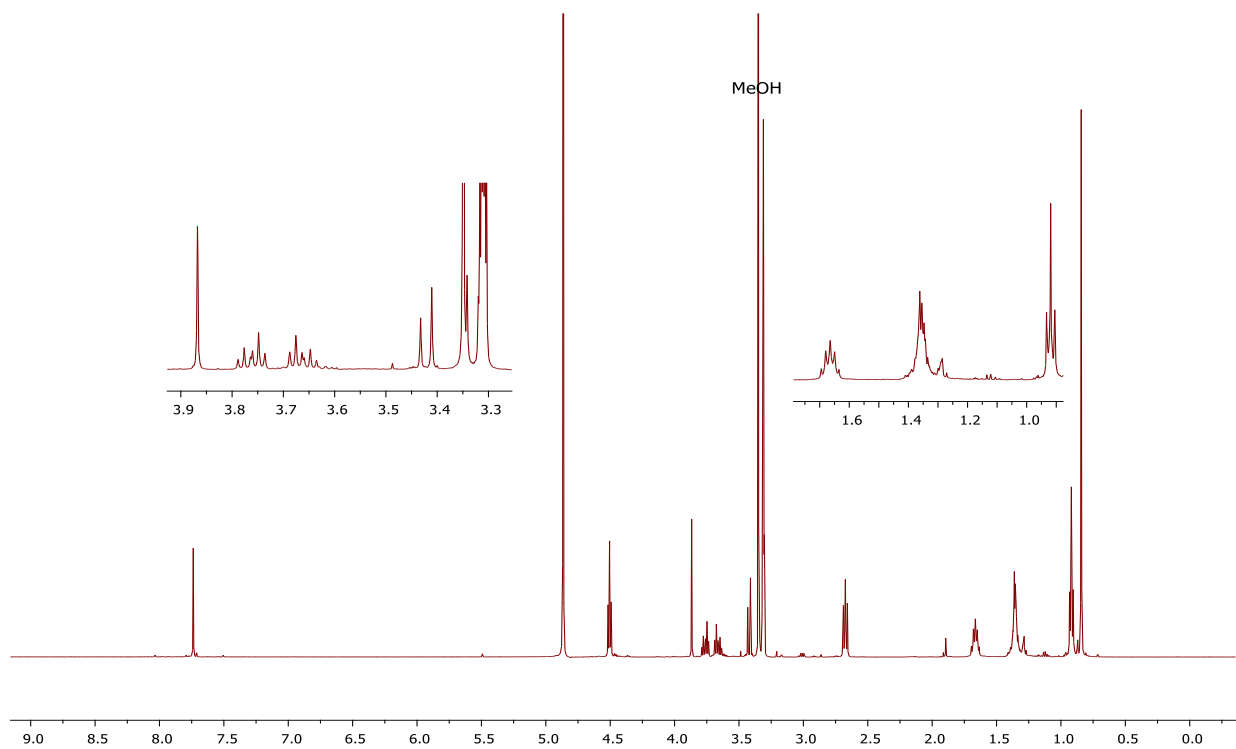
¹H NMR of compound 3.7c



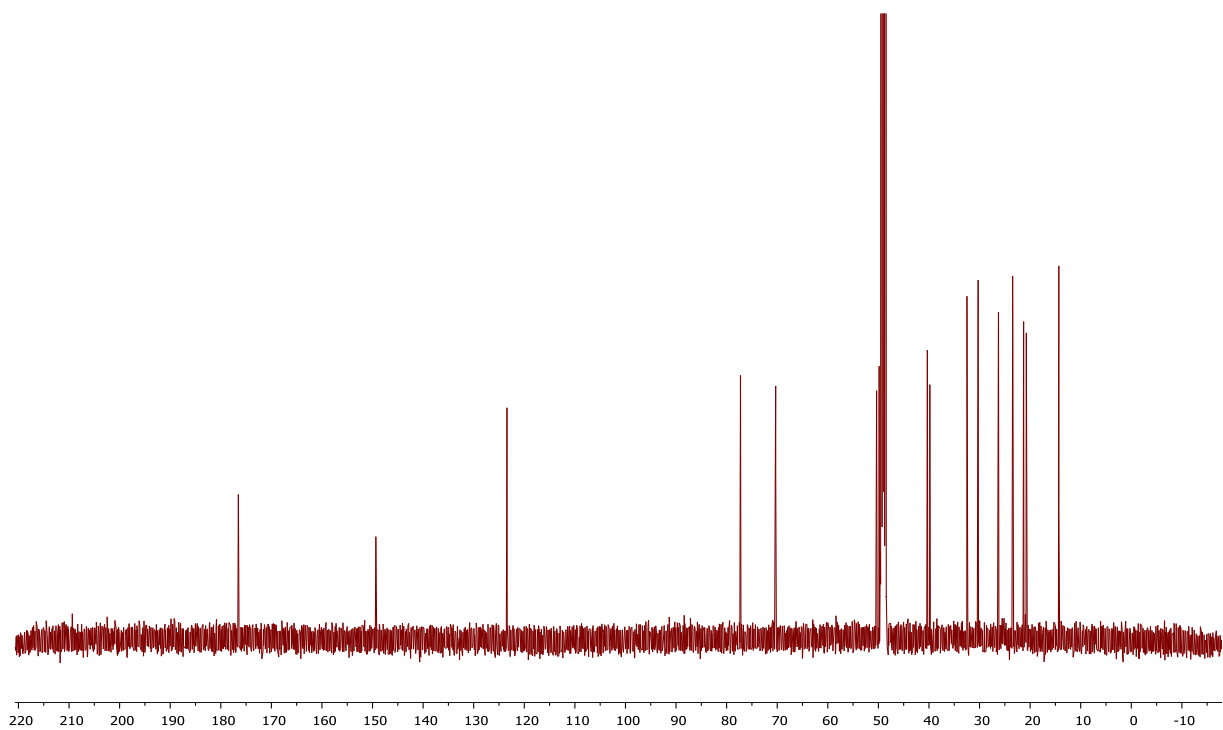
¹³C NMR of compound 3.7c



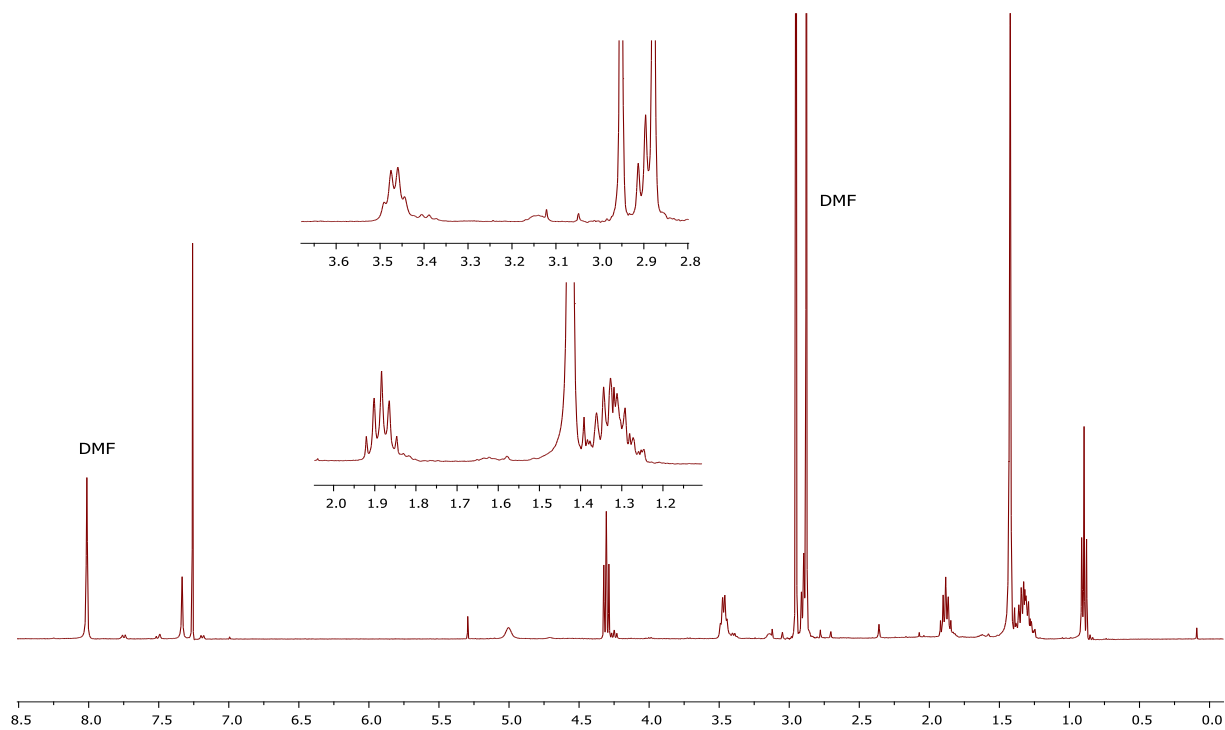
¹H NMR of compound 3.7d



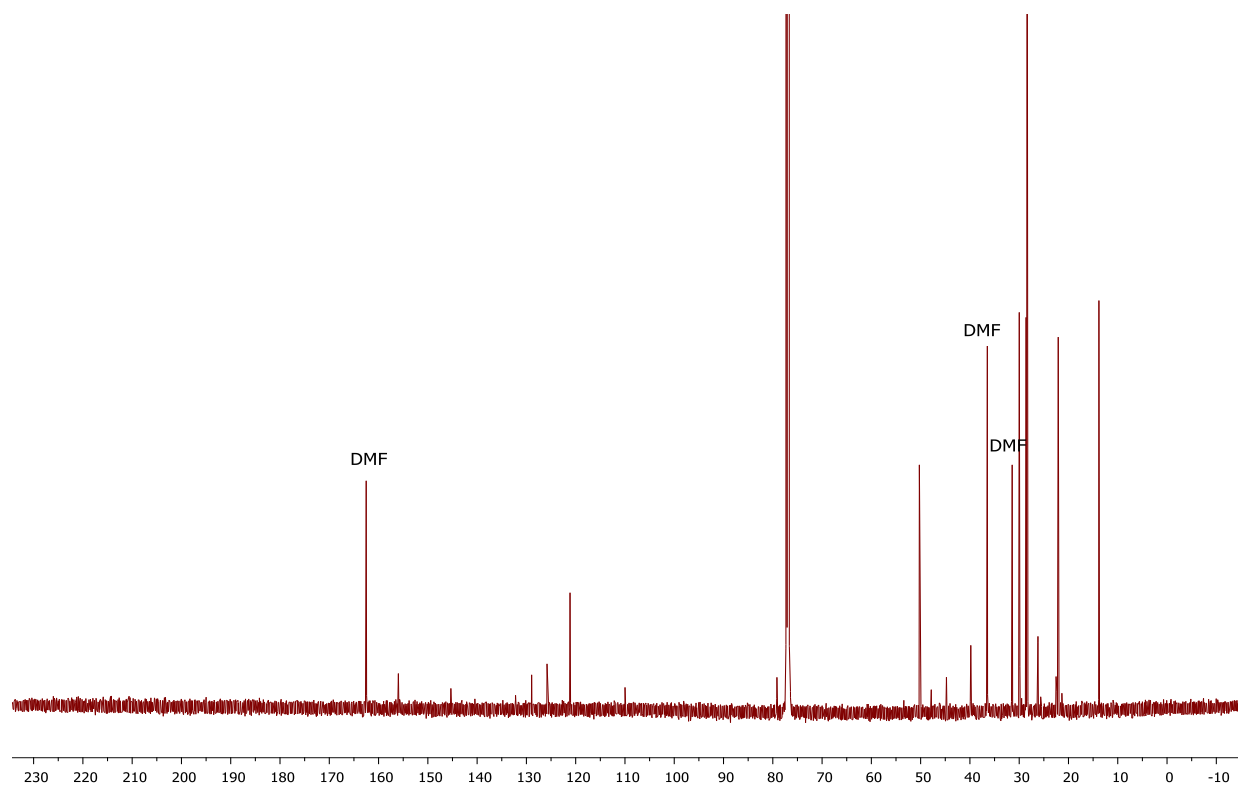
¹³C NMR of compound 3.7d



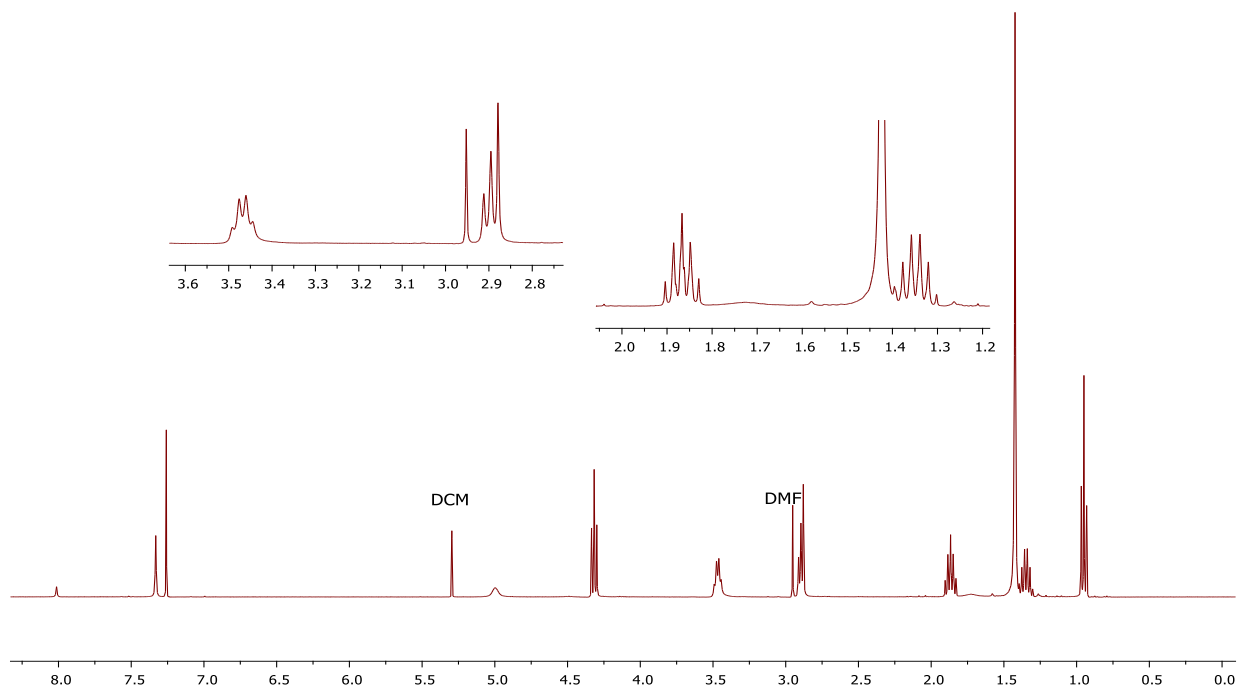
¹H NMR of compound 3.8a



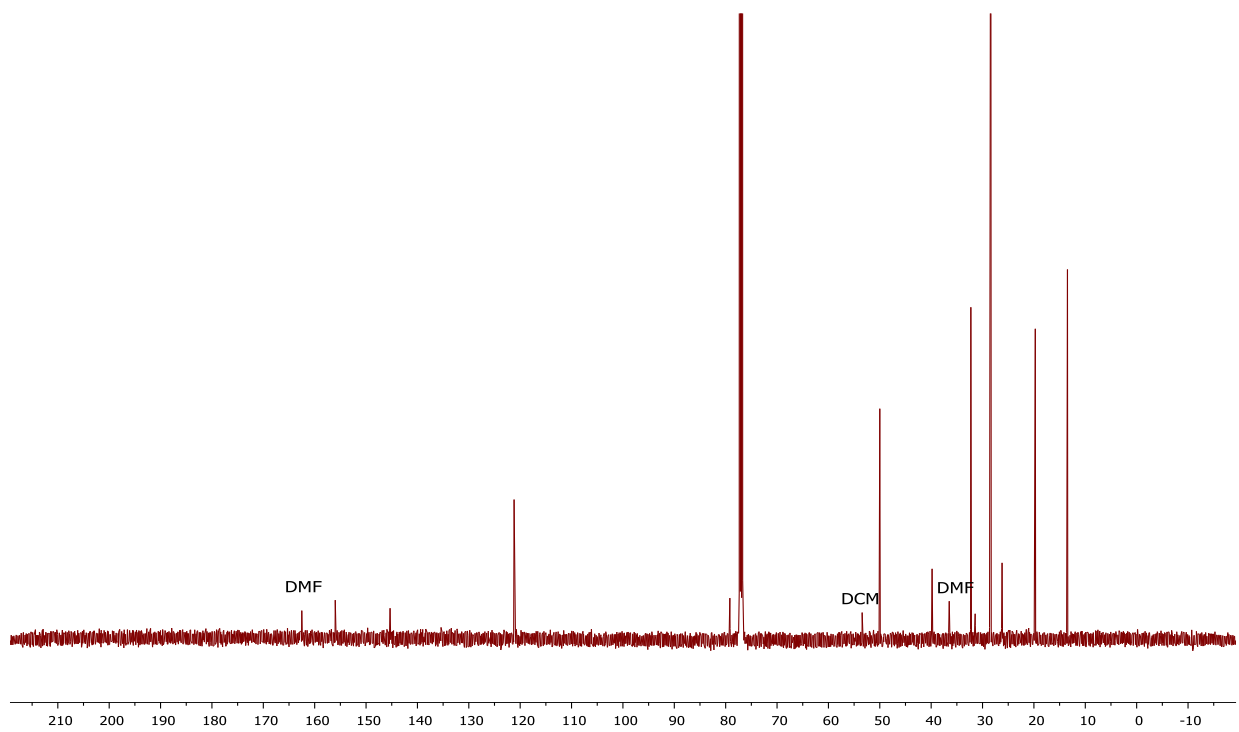
¹³C NMR of compound 3.8a



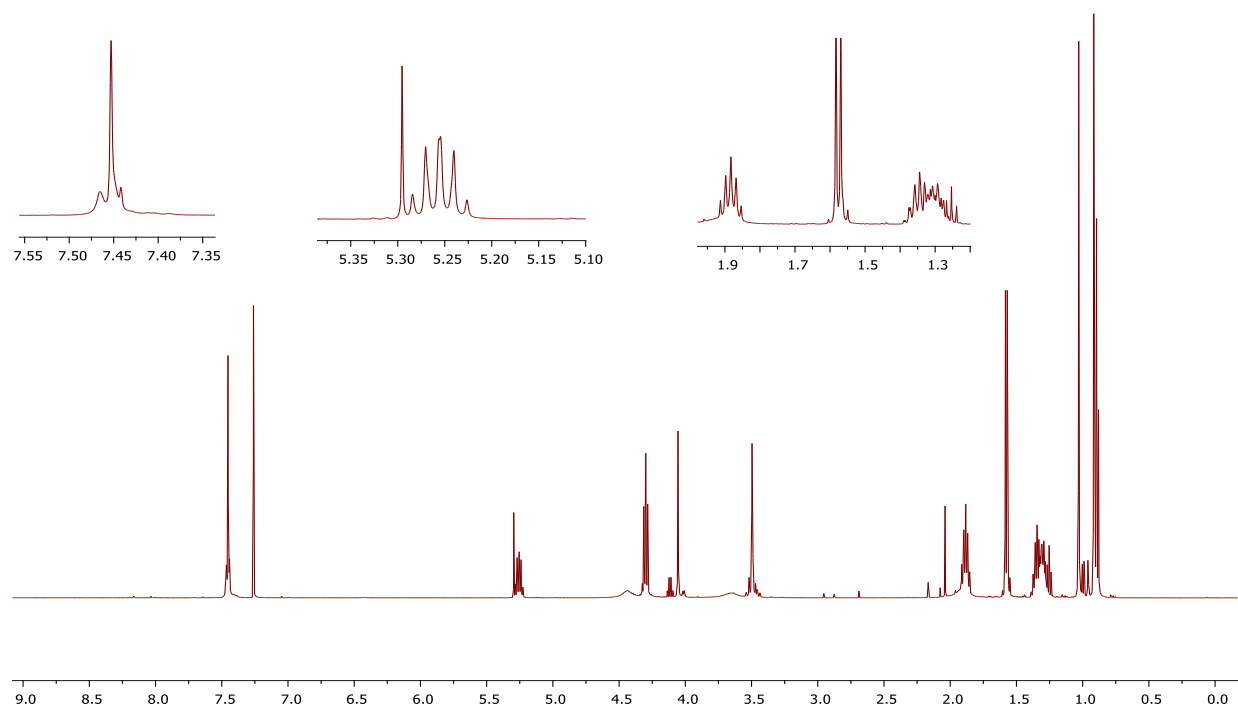
¹H NMR of compound 3.8b



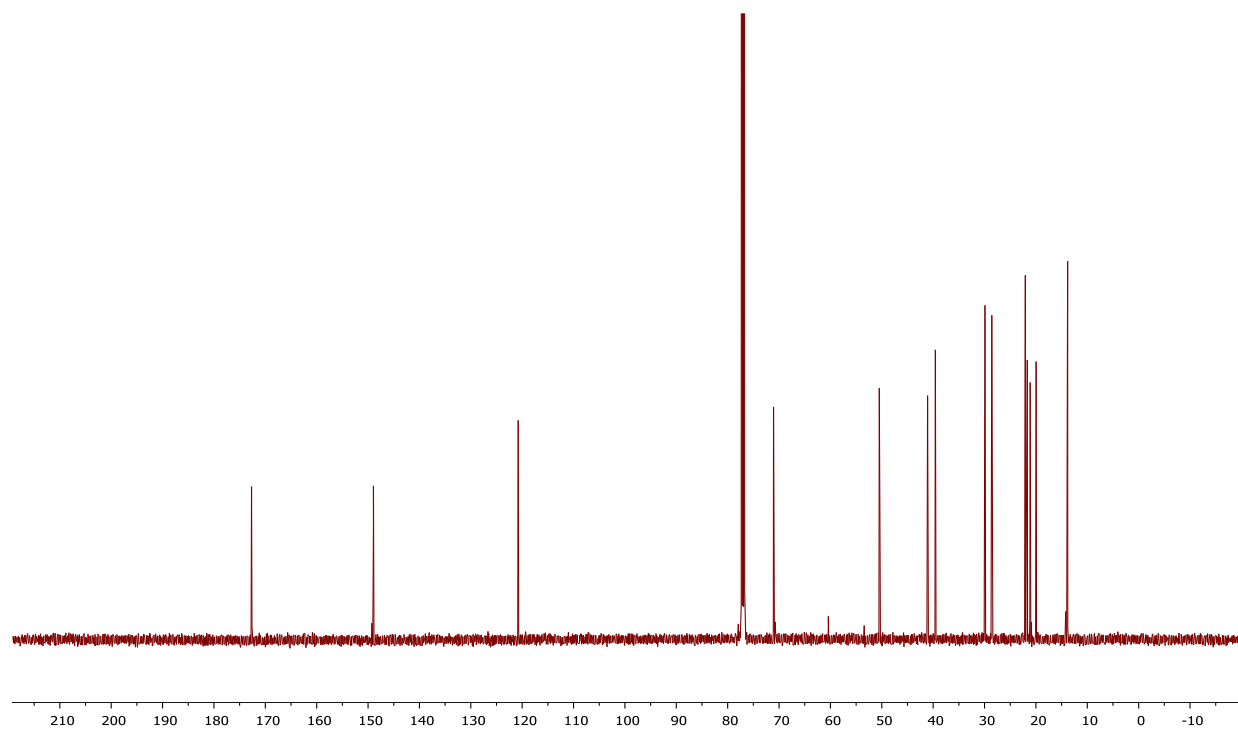
¹³C NMR of compound 3.8b



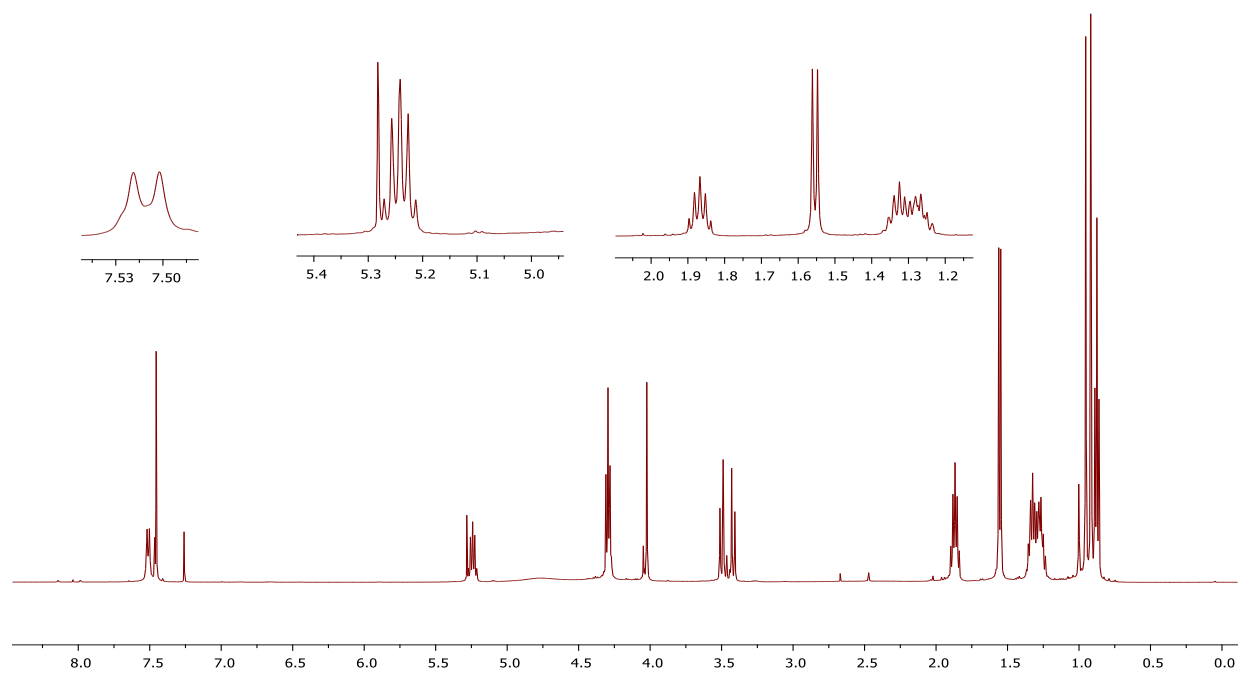
¹H NMR of compound 3.9a



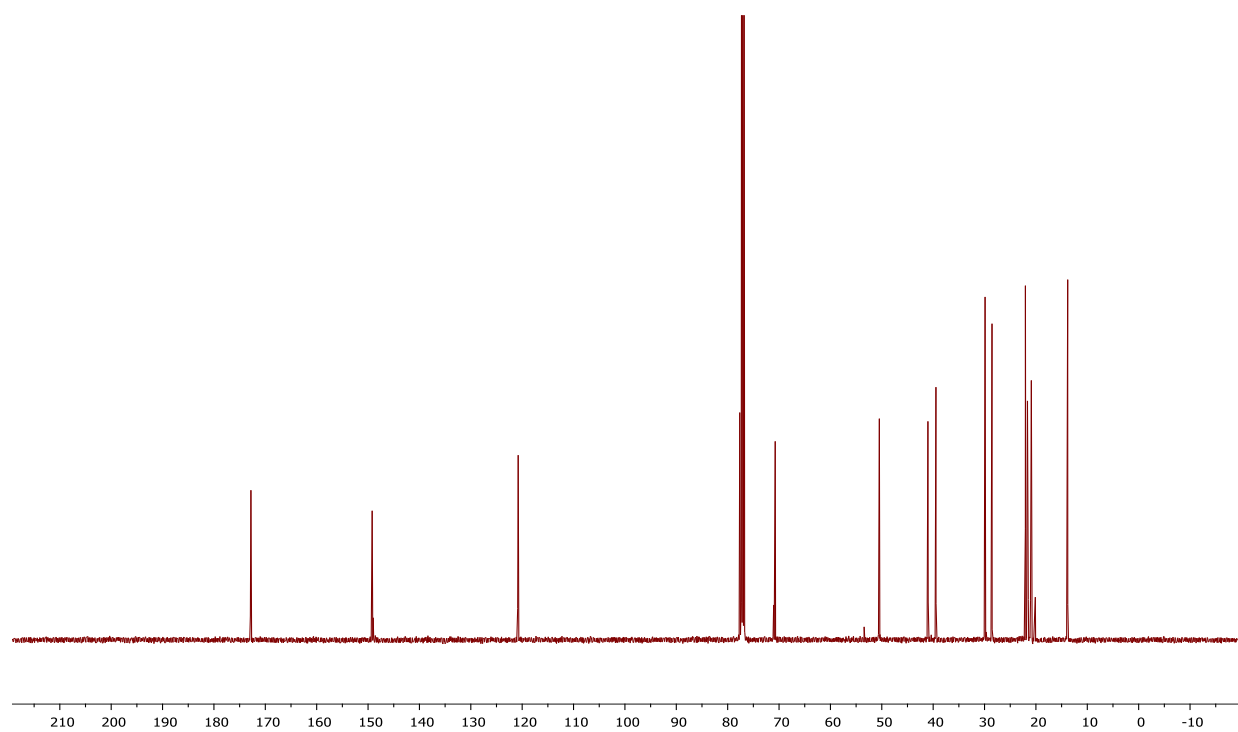
¹³C NMR of compound 3.9a



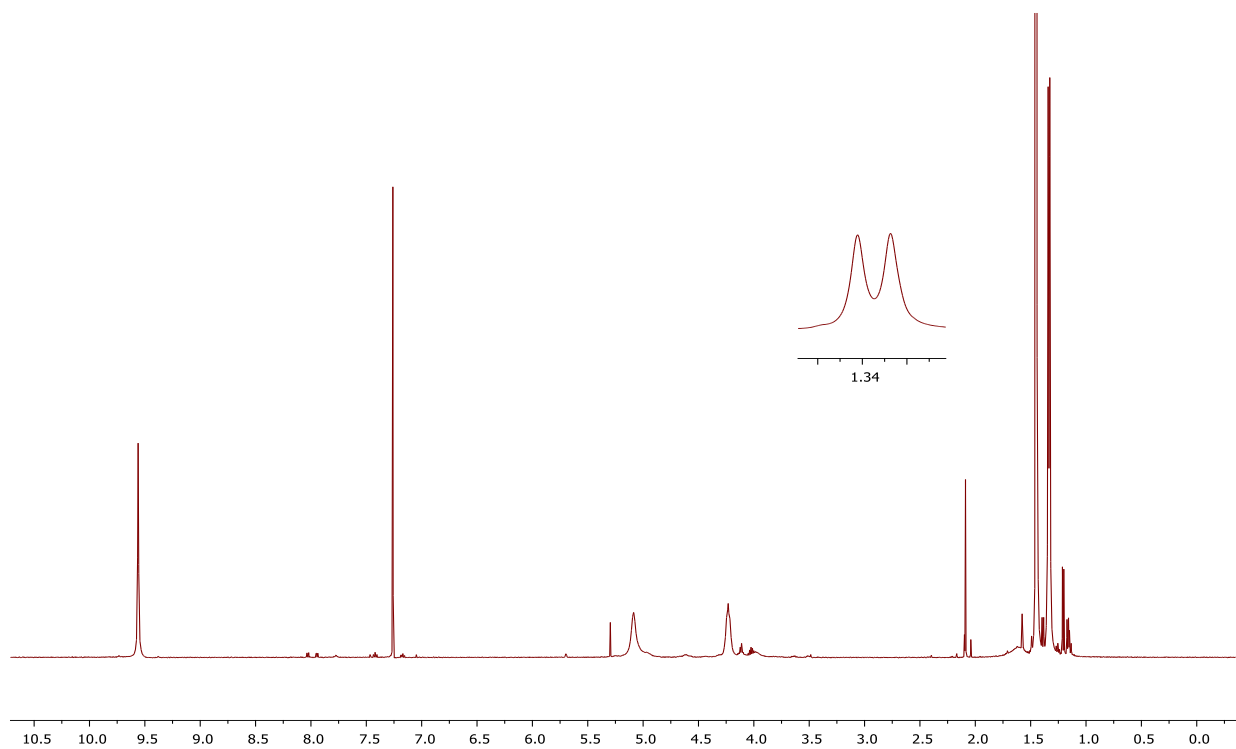
¹H NMR of compound 3.9b



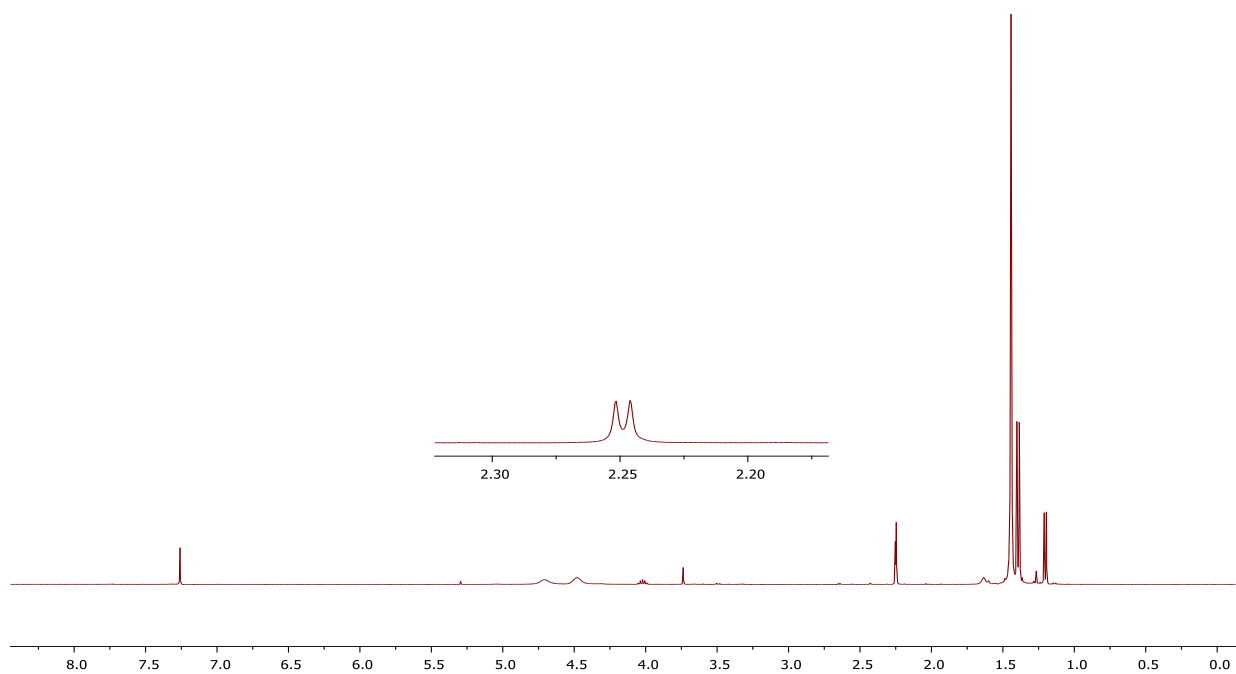
¹³C NMR of compound 3.9b



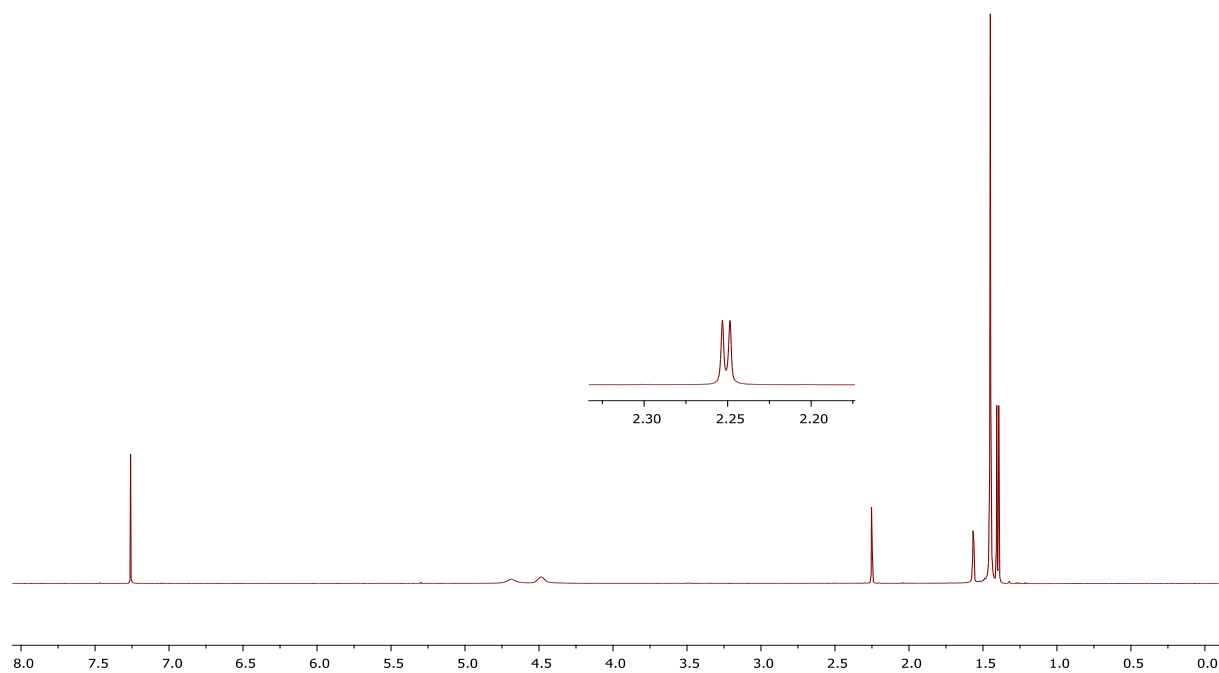
¹H NMR of compound 3.10a



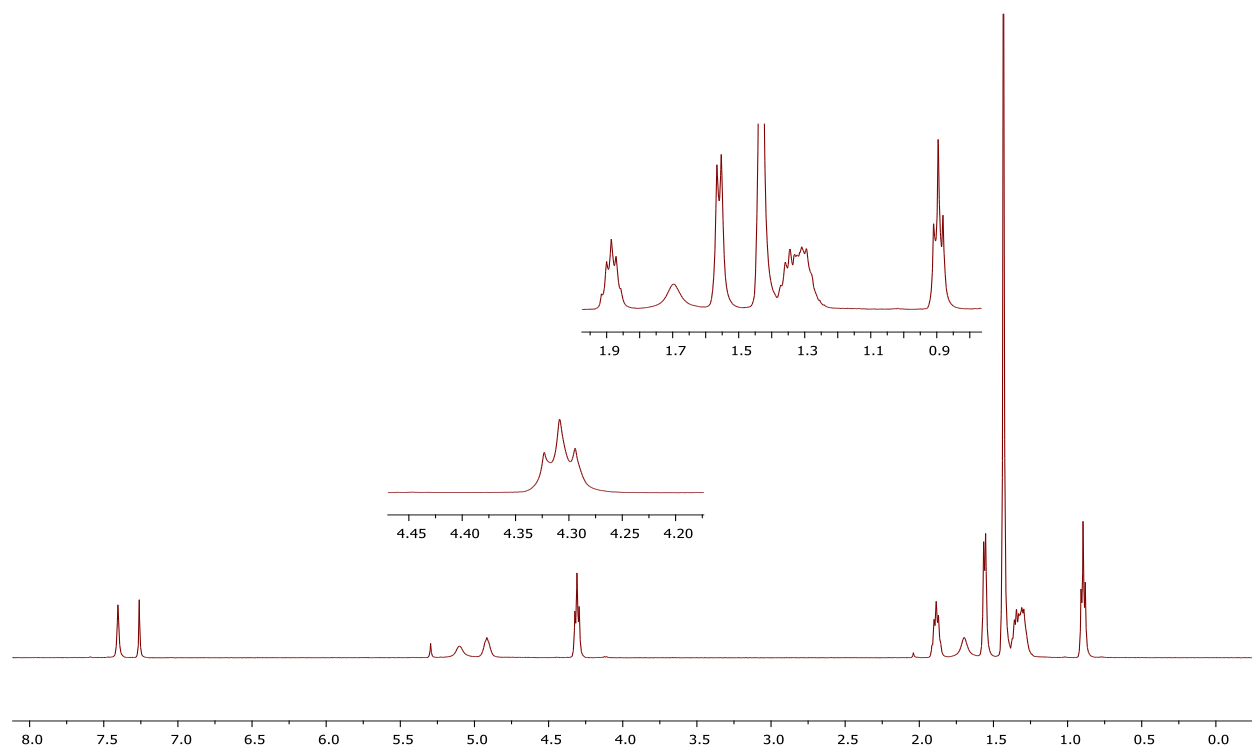
¹H NMR of compound 3.11a



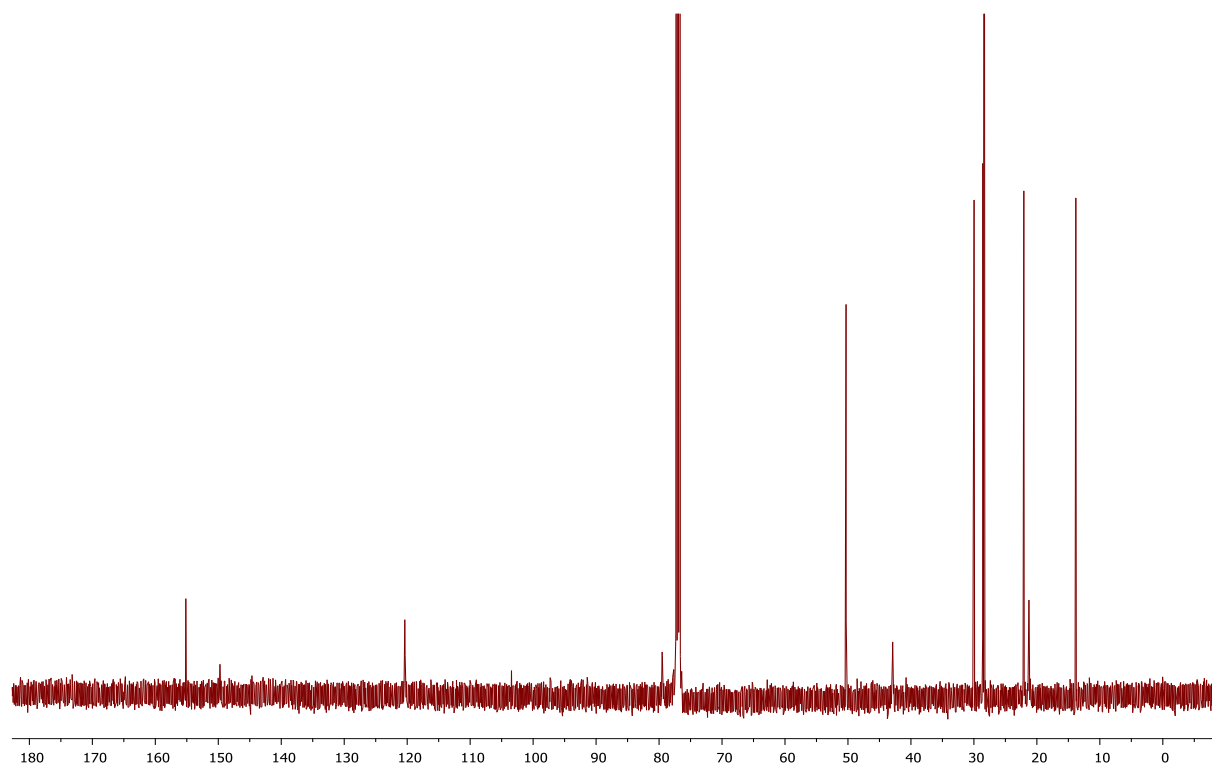
^1H NMR of compound 3.11b



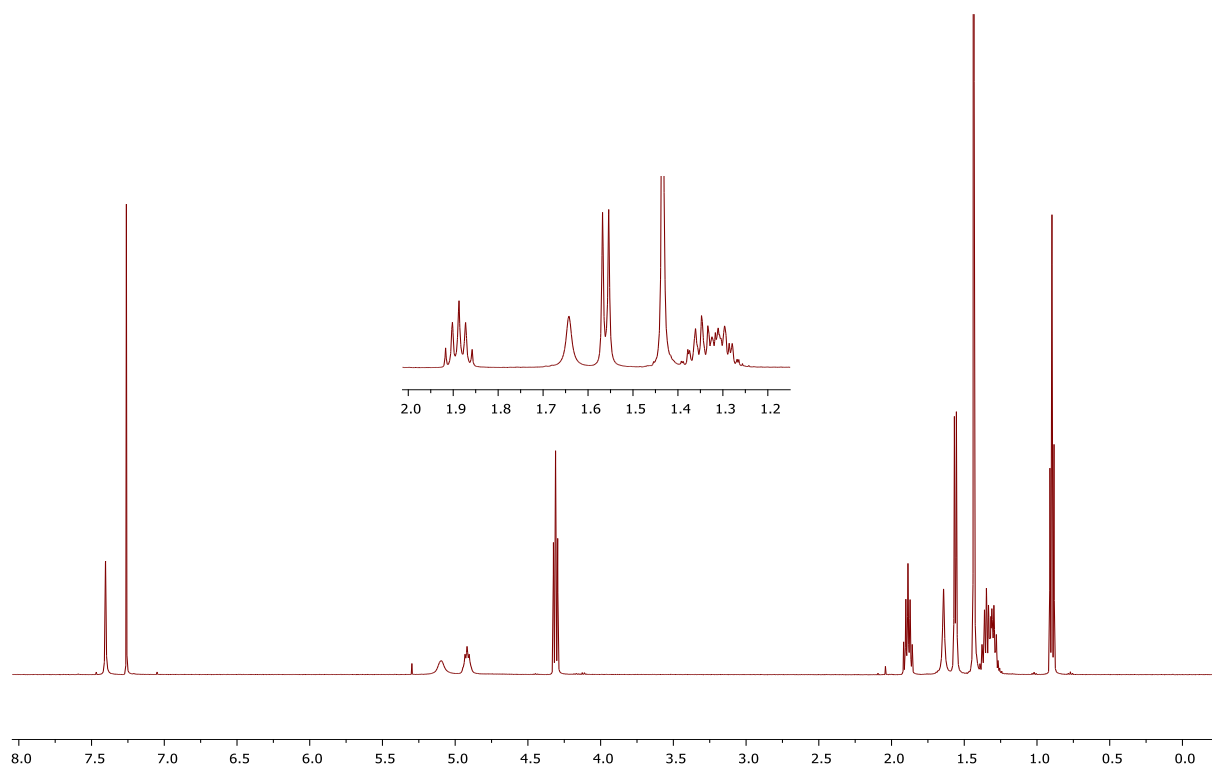
^1H NMR of compound 3.12a



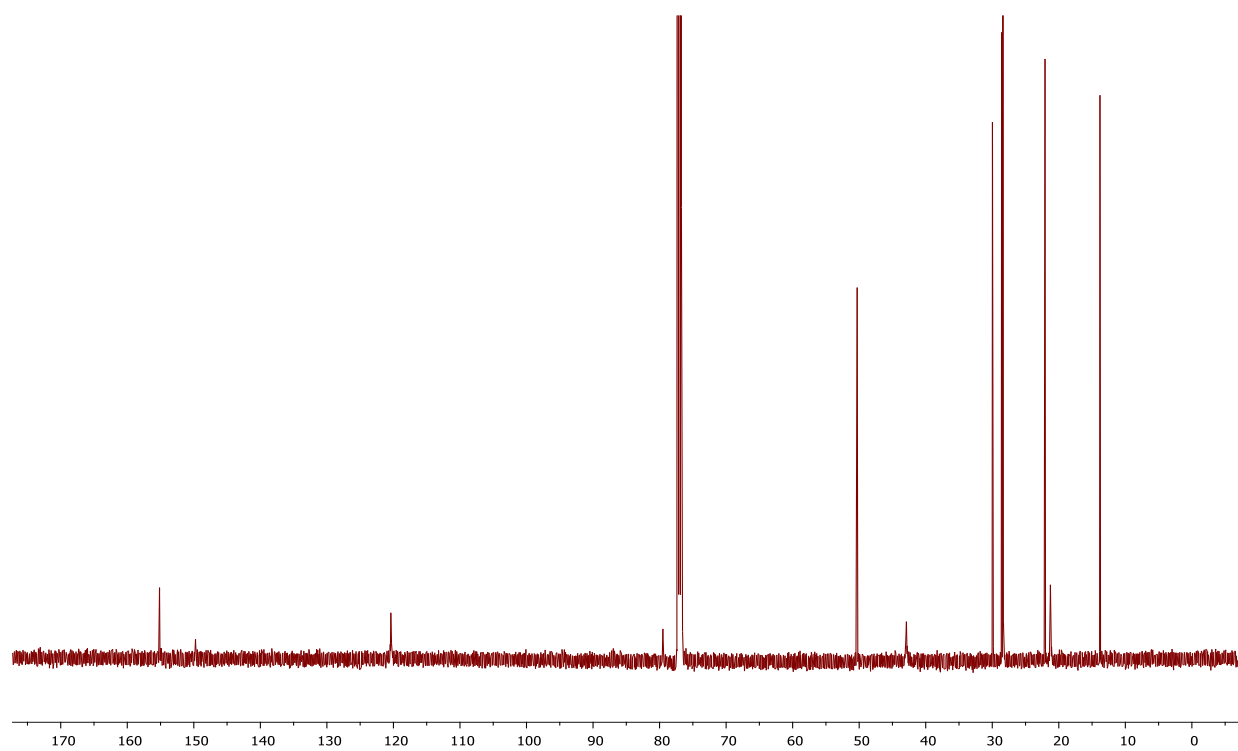
¹³C NMR of compound 3.12a



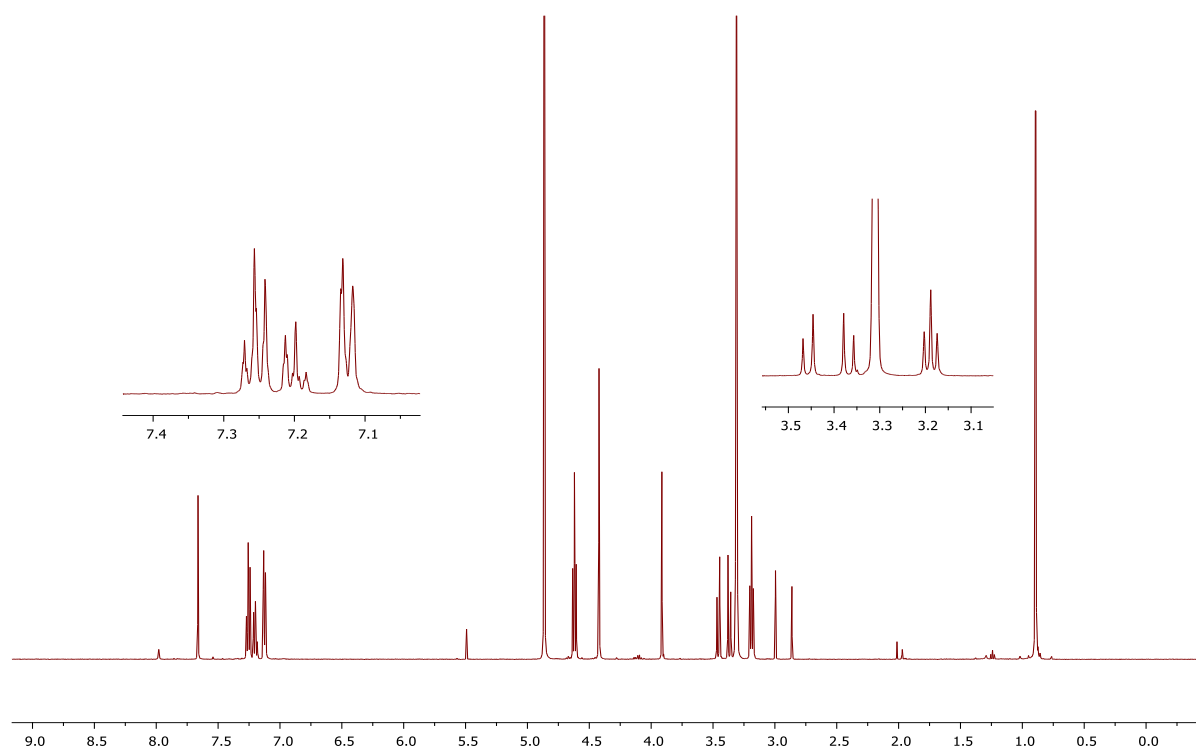
¹H NMR of compound 3.12b



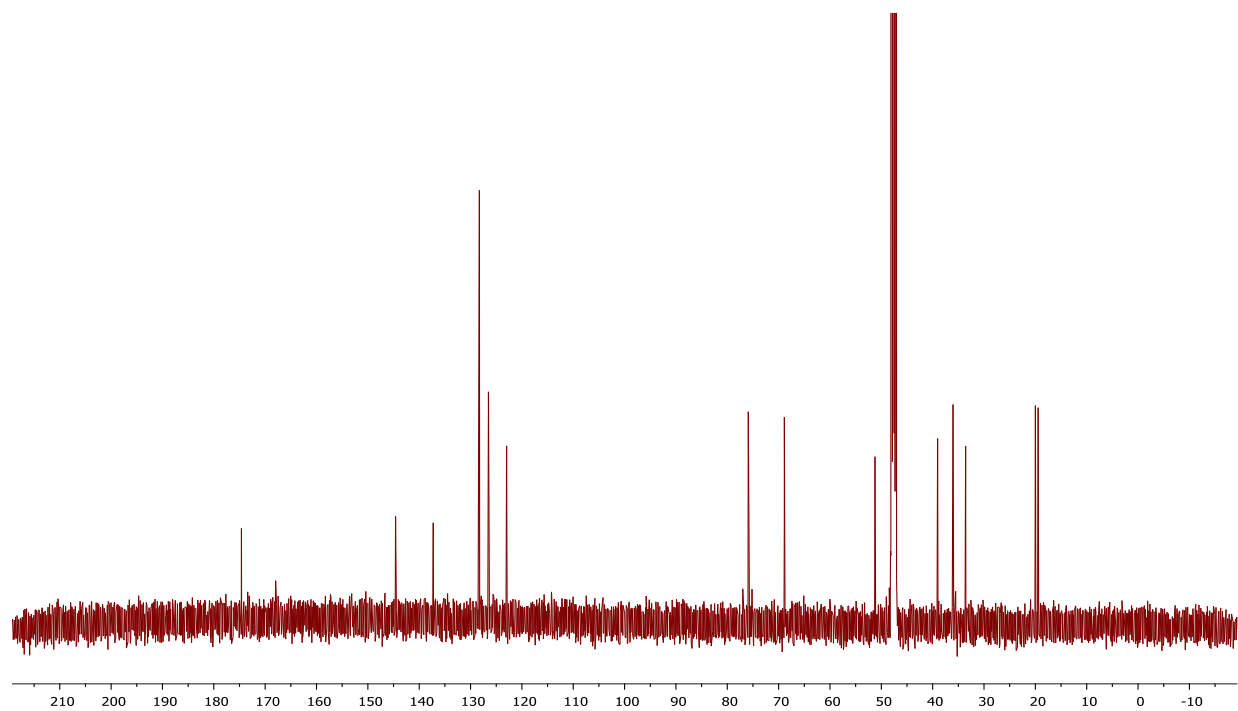
¹³C NMR of compound 3.12b



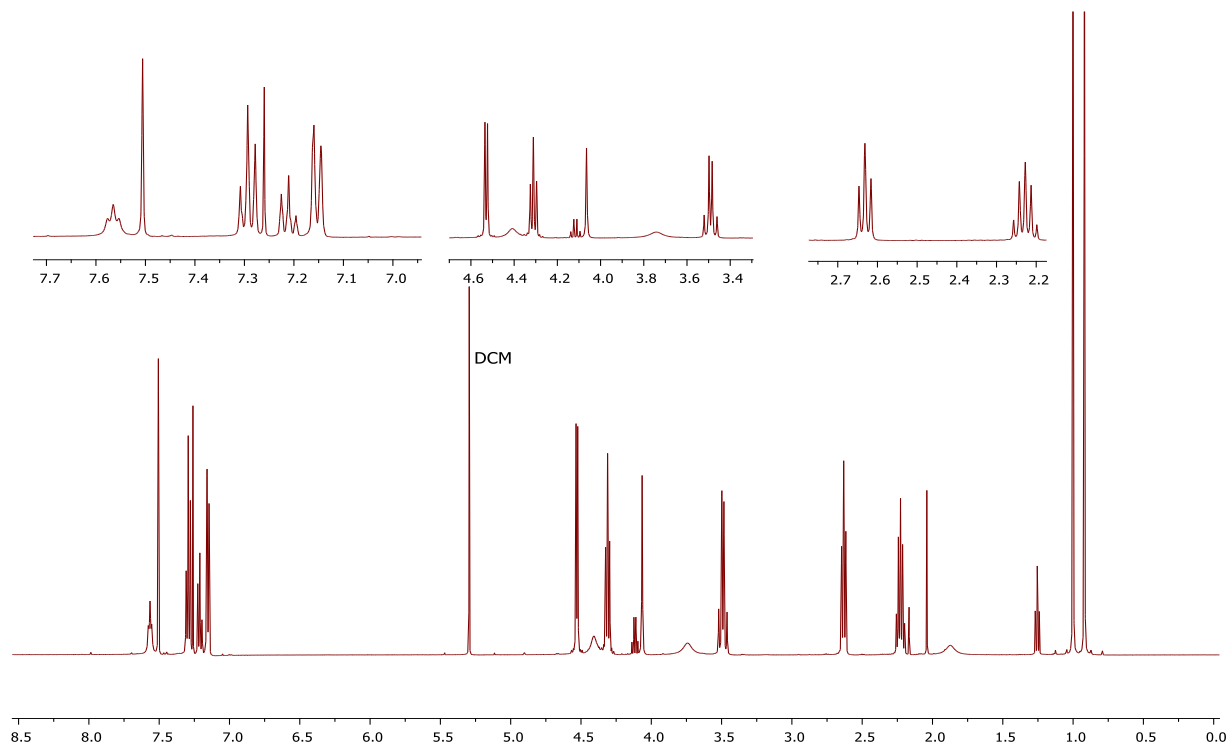
¹H NMR of compound 3.13a



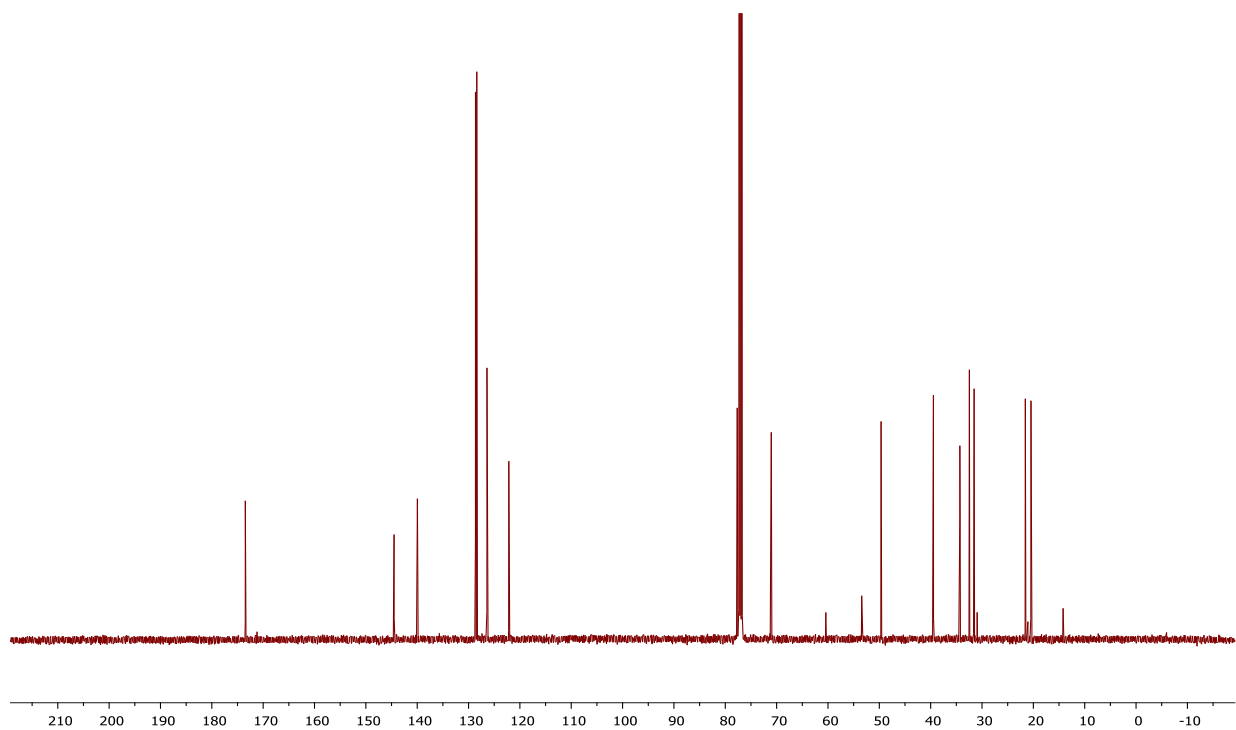
^{13}C NMR of compound 3.13a



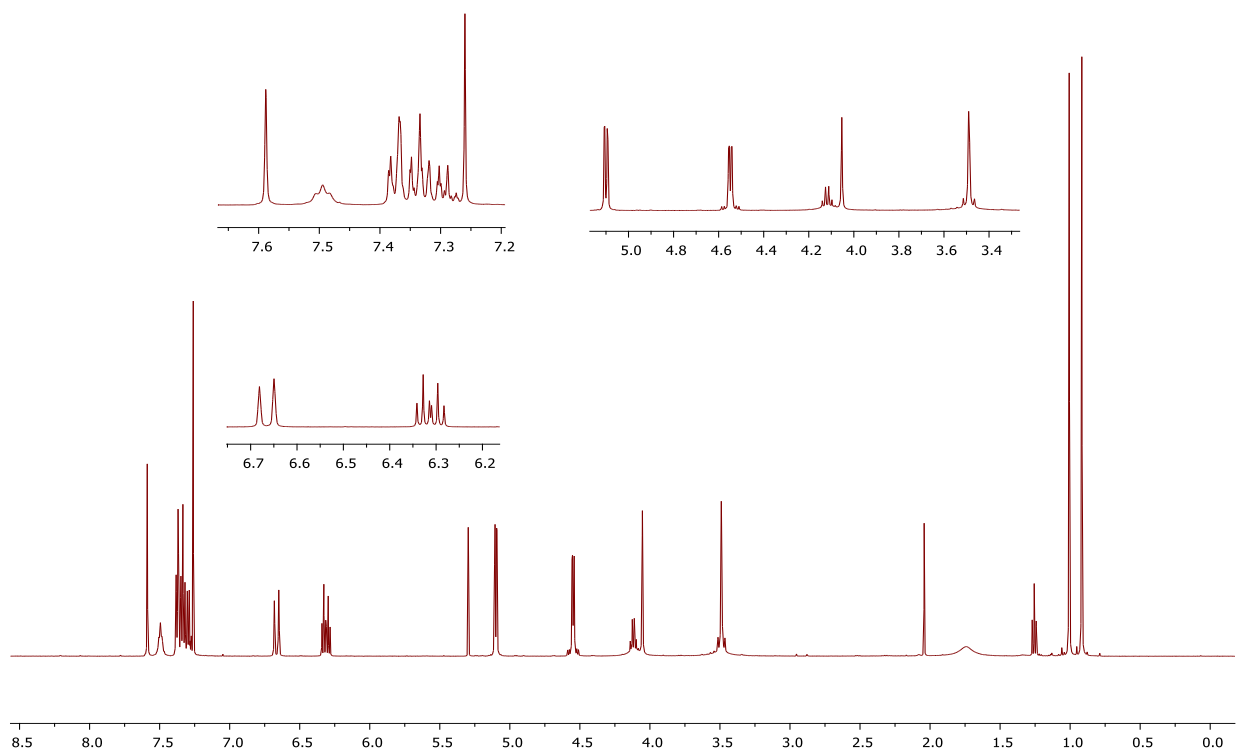
^1H NMR of compound 3.13b



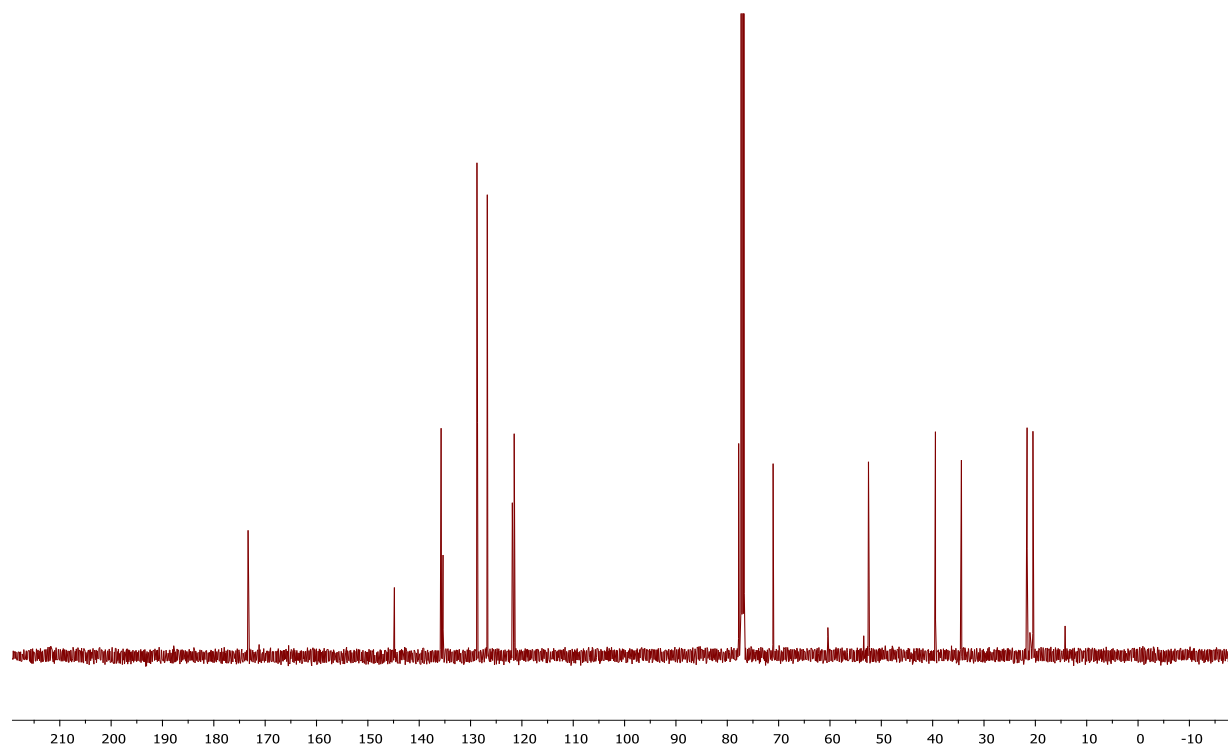
^{13}C NMR of compound 3.13b



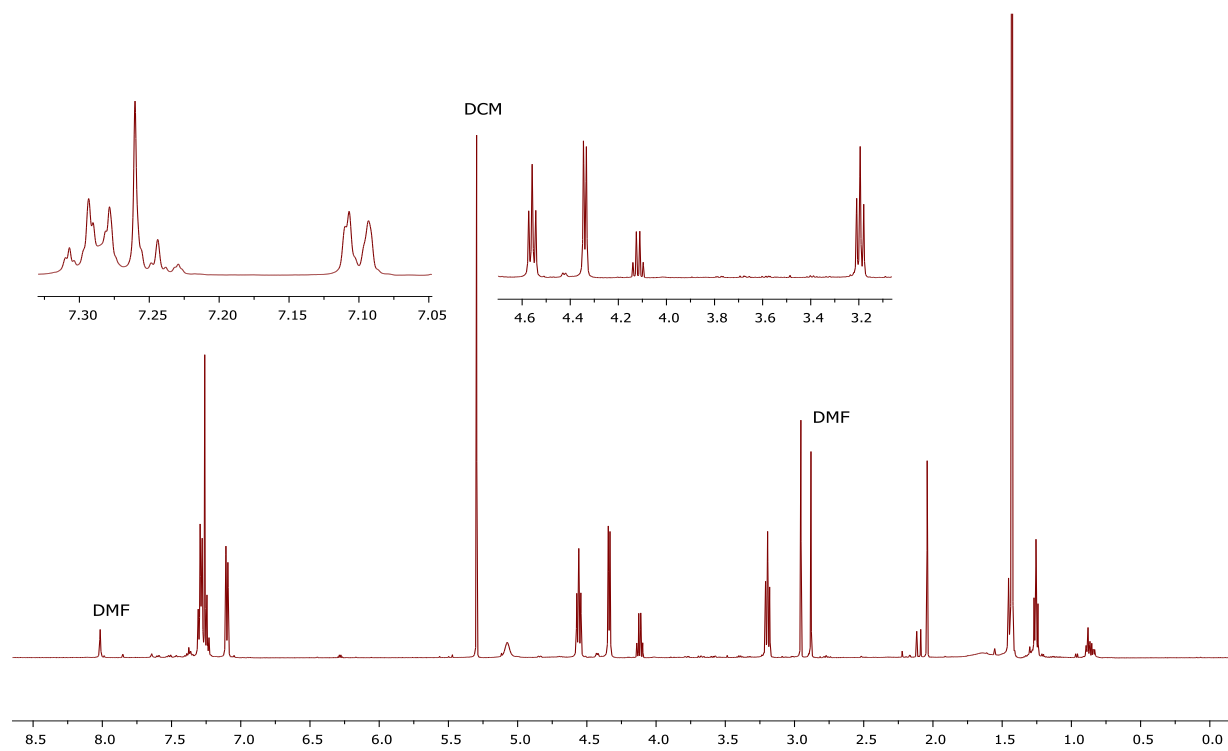
^1H NMR of compound 3.13c



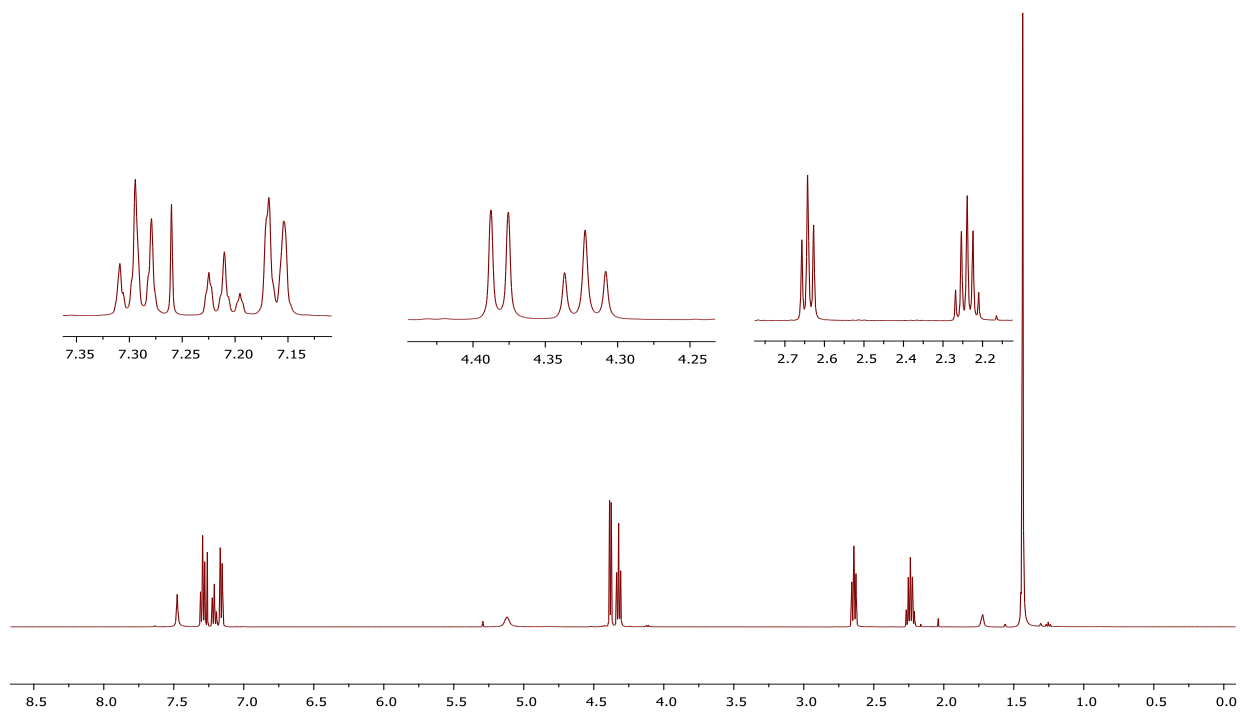
¹³C NMR of compound 3.13c



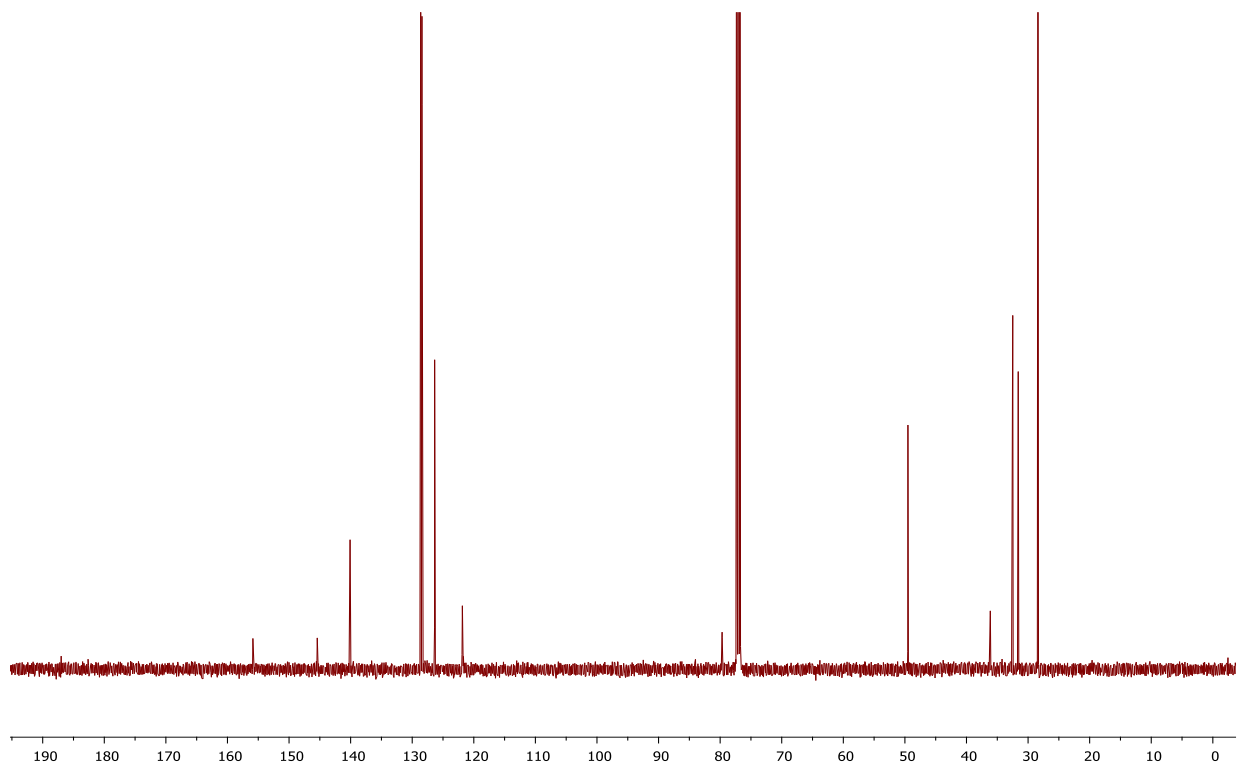
¹H NMR of compound 3.14a



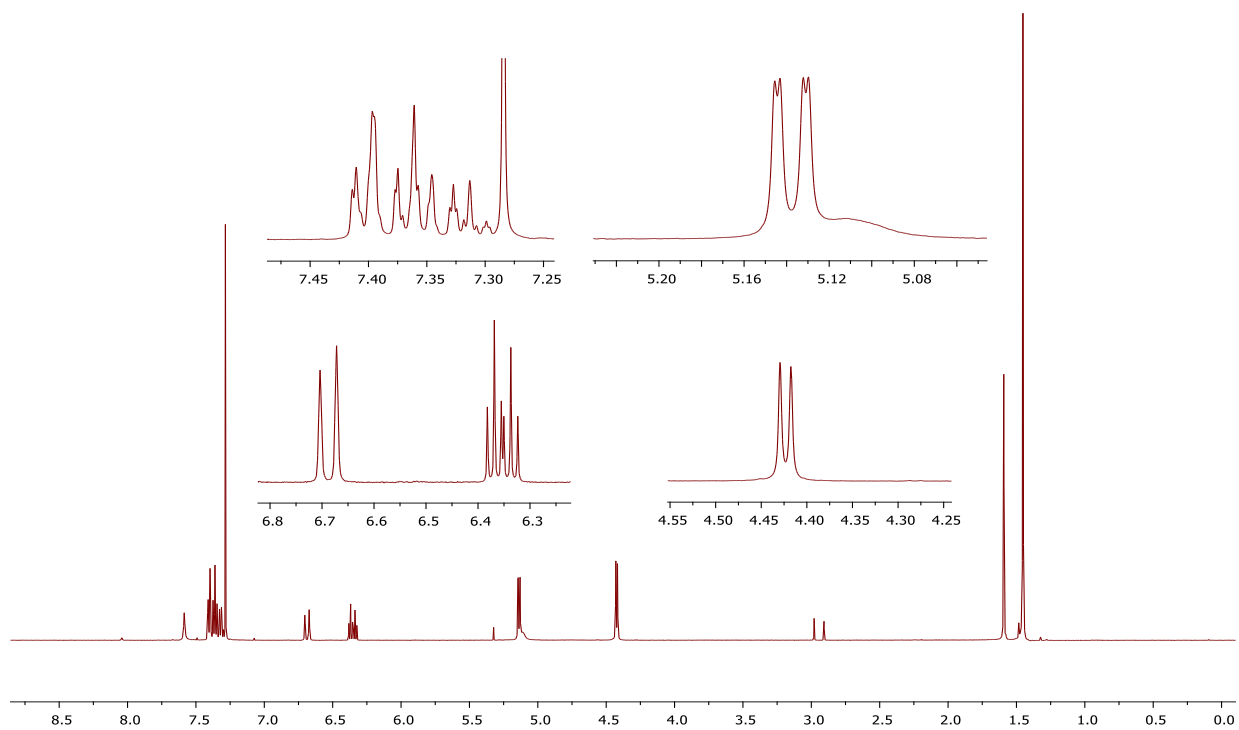
¹H NMR of compound 3.14b



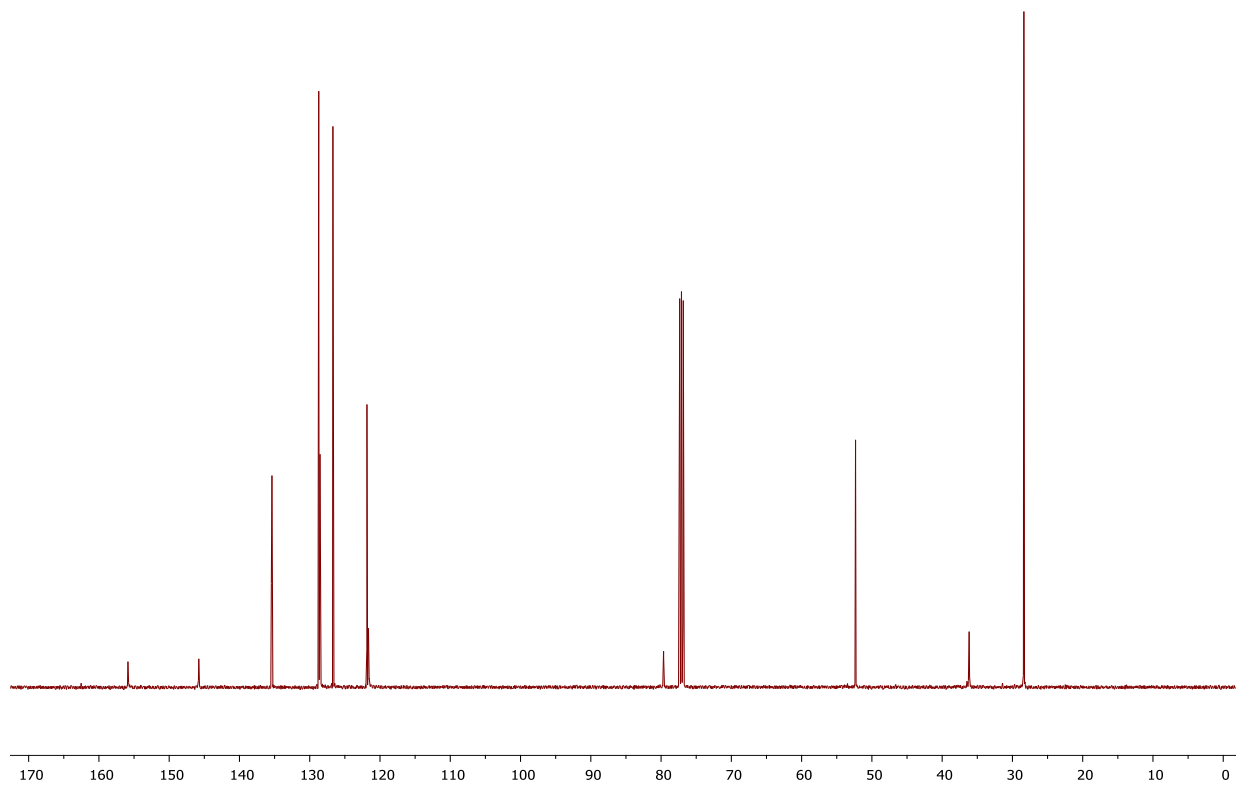
¹³C NMR of compound 3.14b



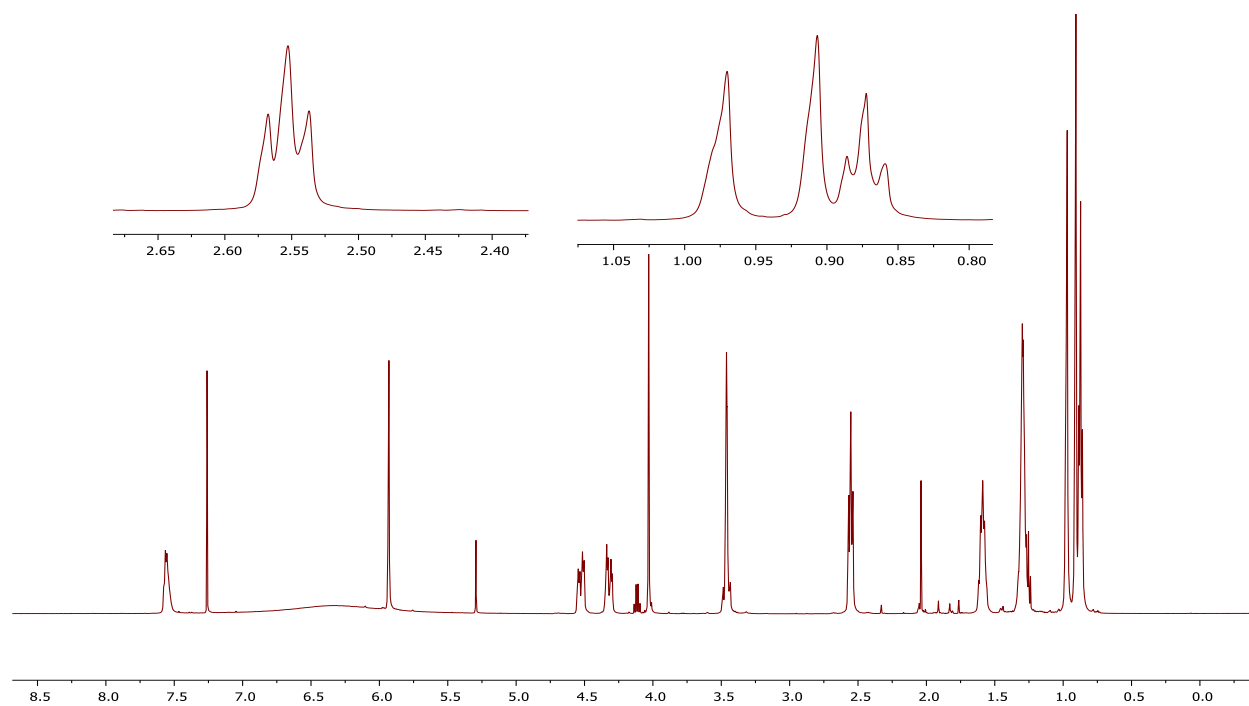
¹H NMR of compound 3.14c



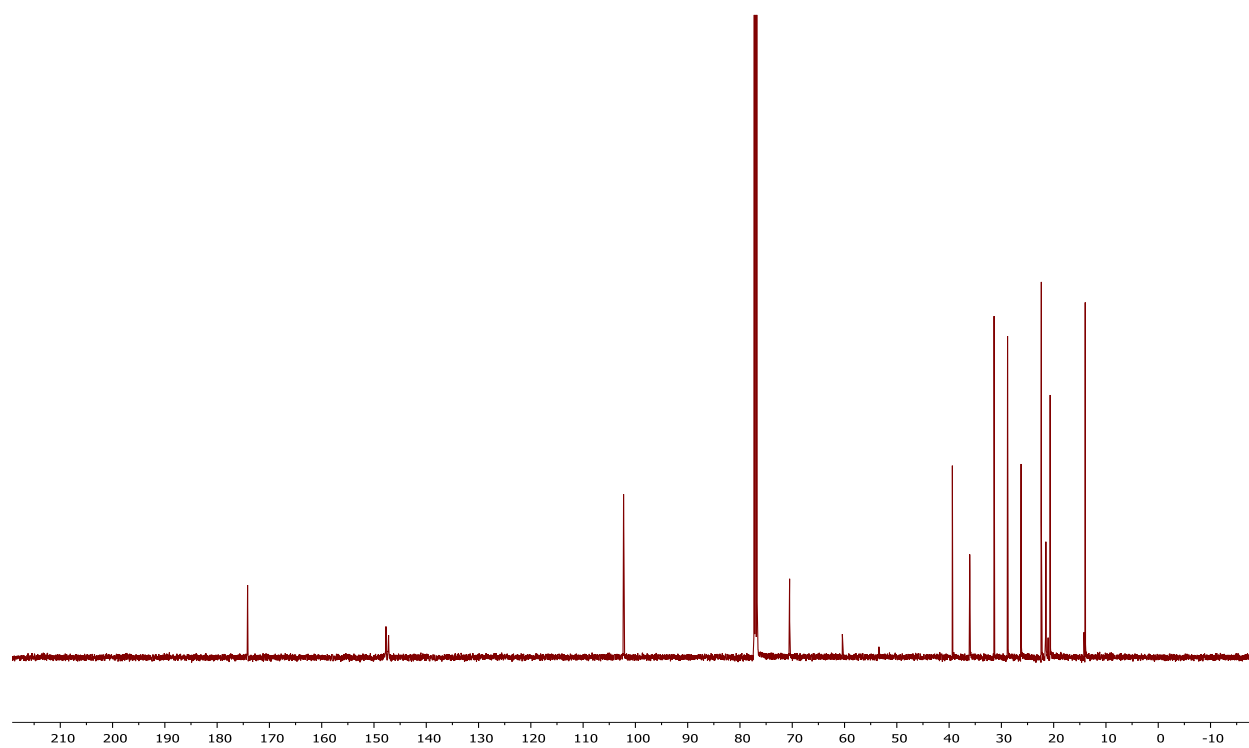
¹³C NMR of compound 3.14c



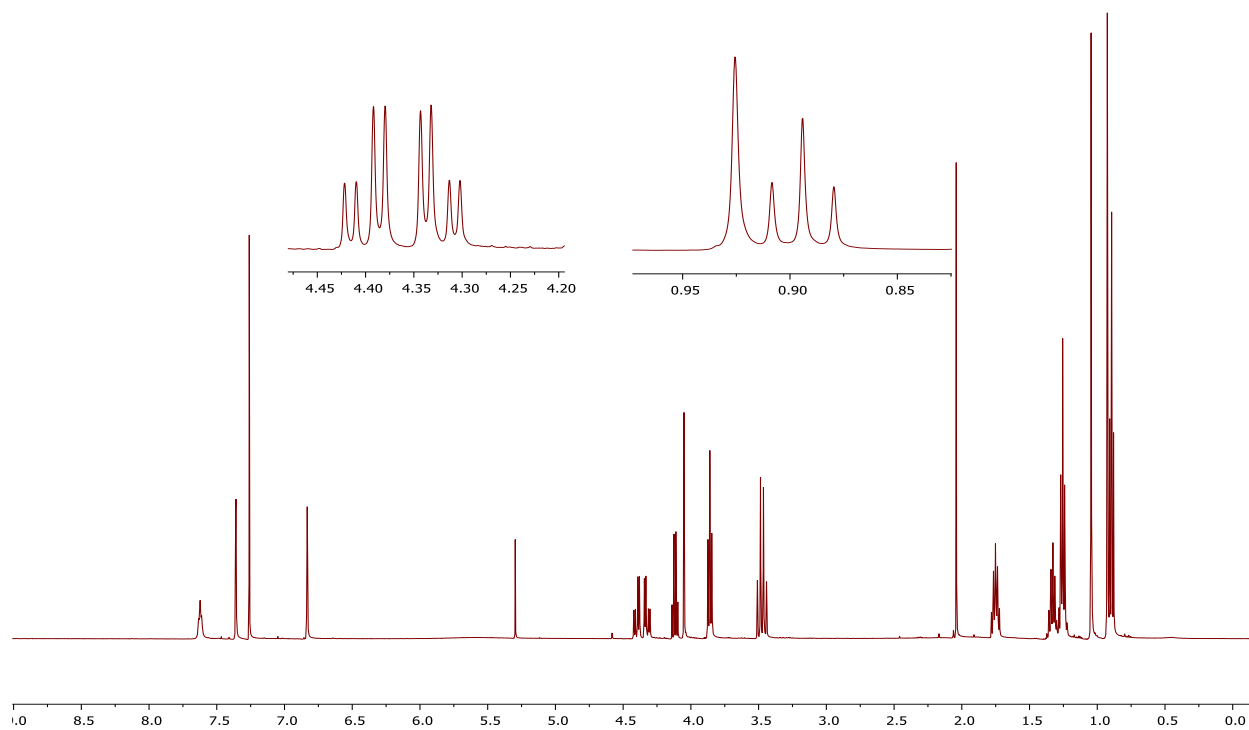
¹H NMR of compound 4.1a



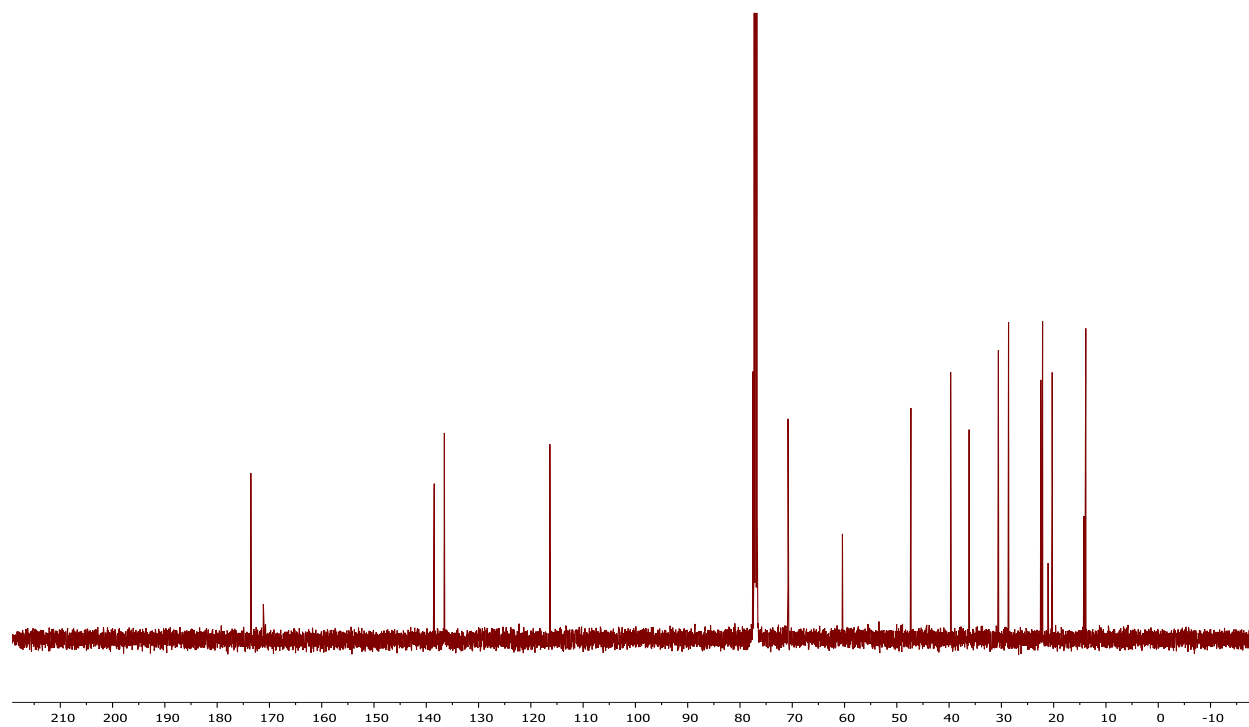
¹³C NMR of compound 4.1a



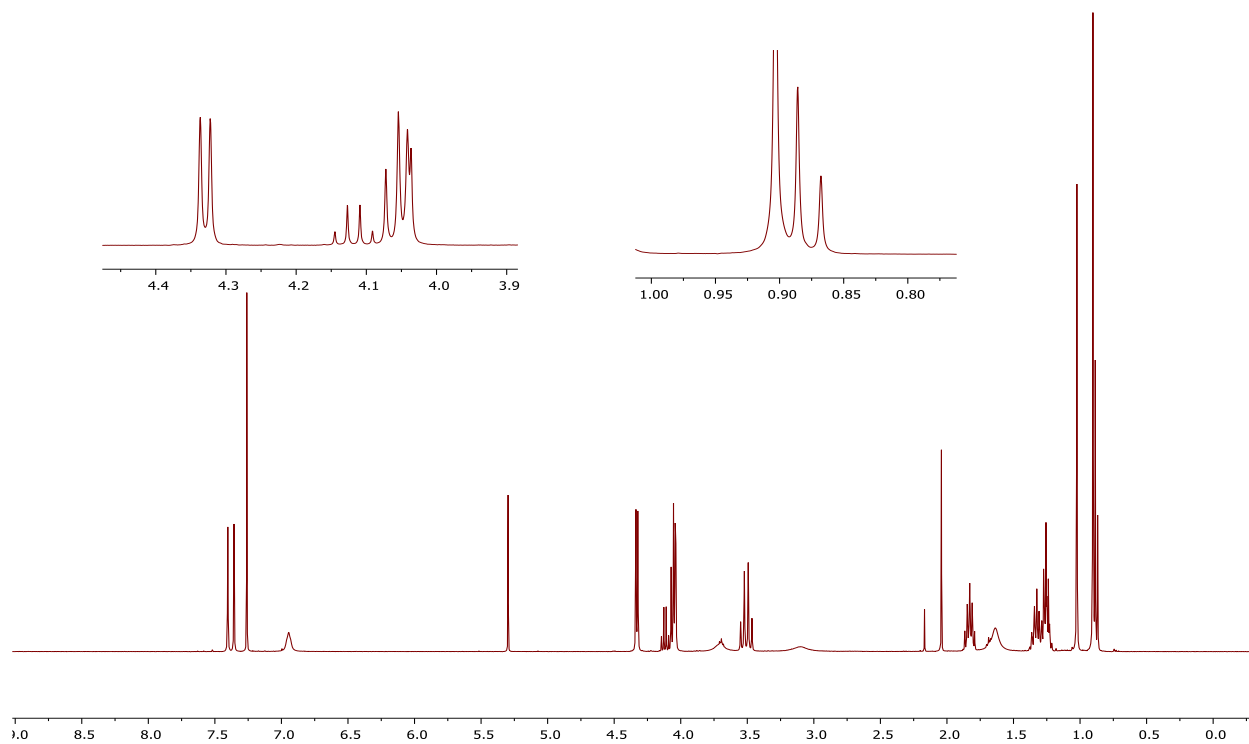
¹H NMR of compound 4.1b



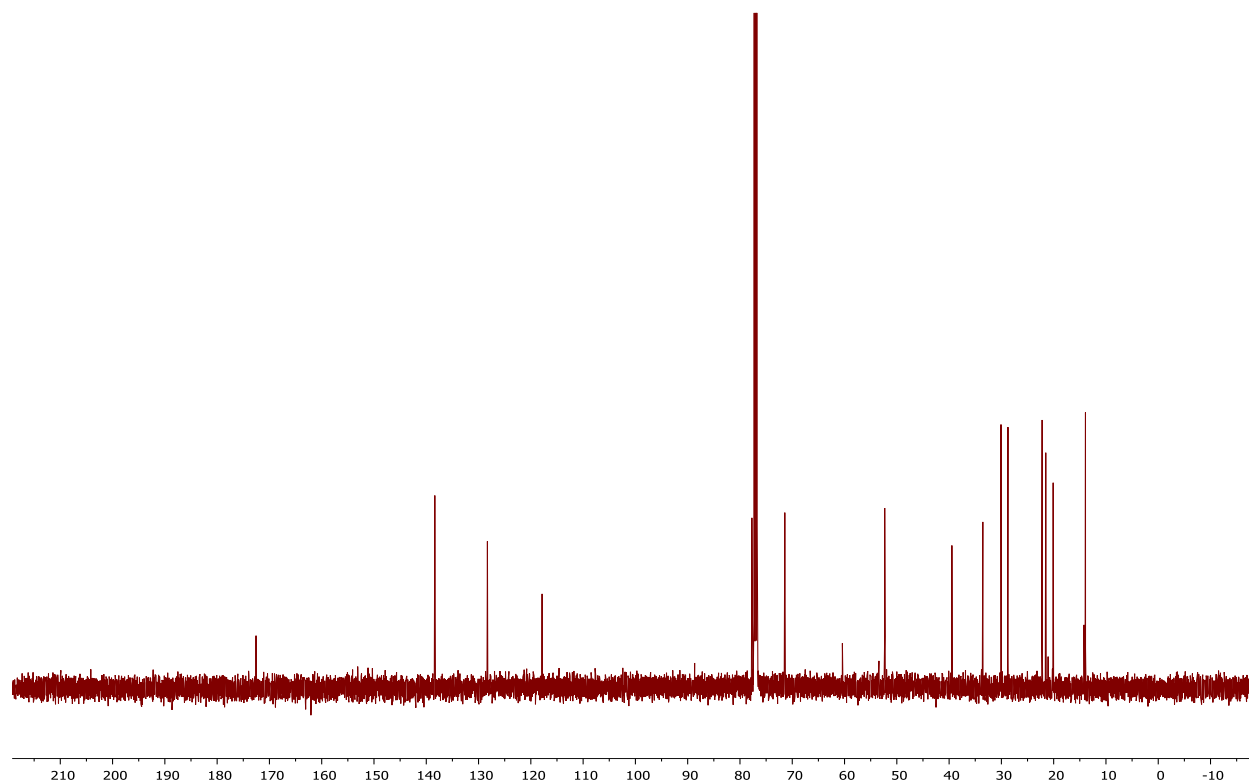
¹³C NMR of compound 4.1b



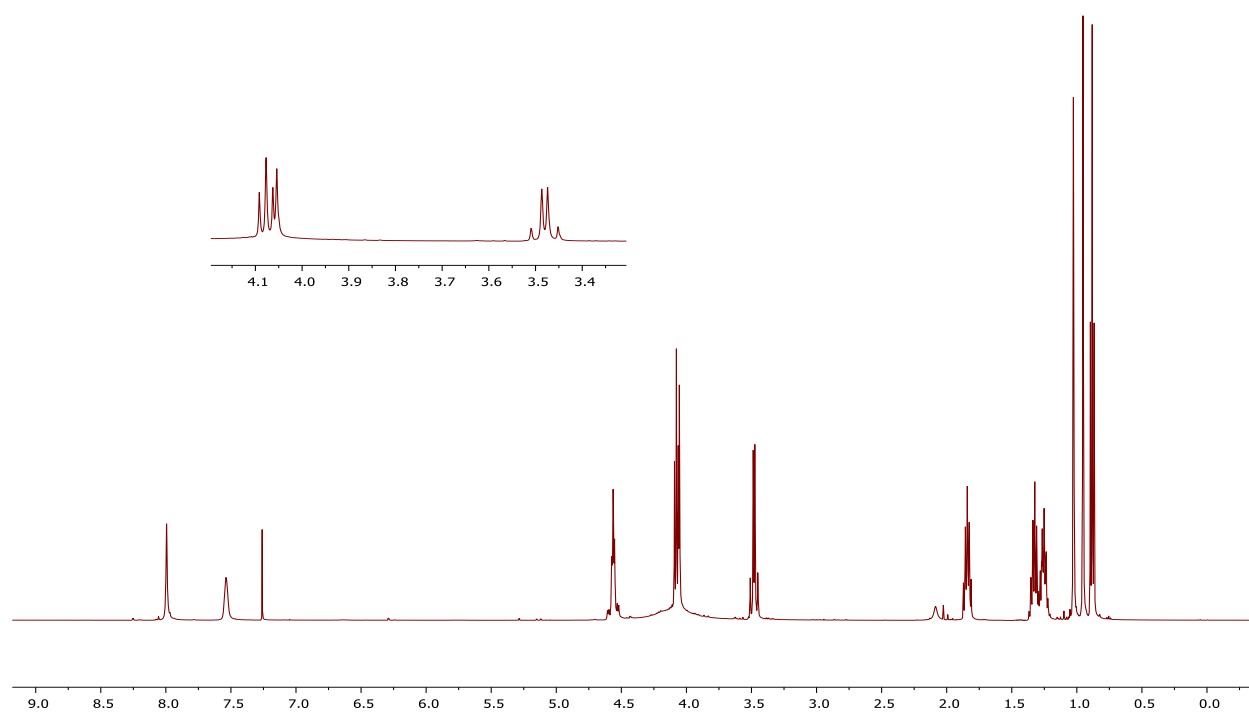
¹H NMR of compound 4.1c



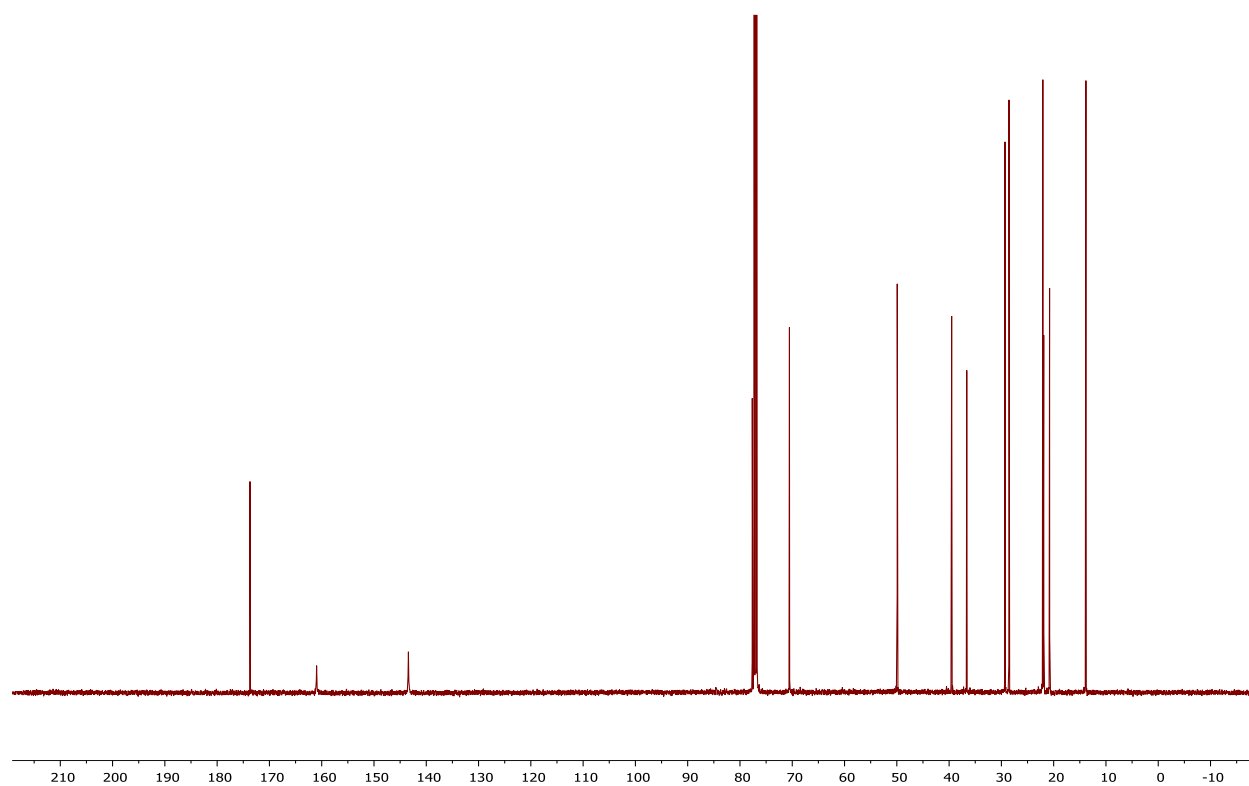
¹³C NMR of compound 4.1c



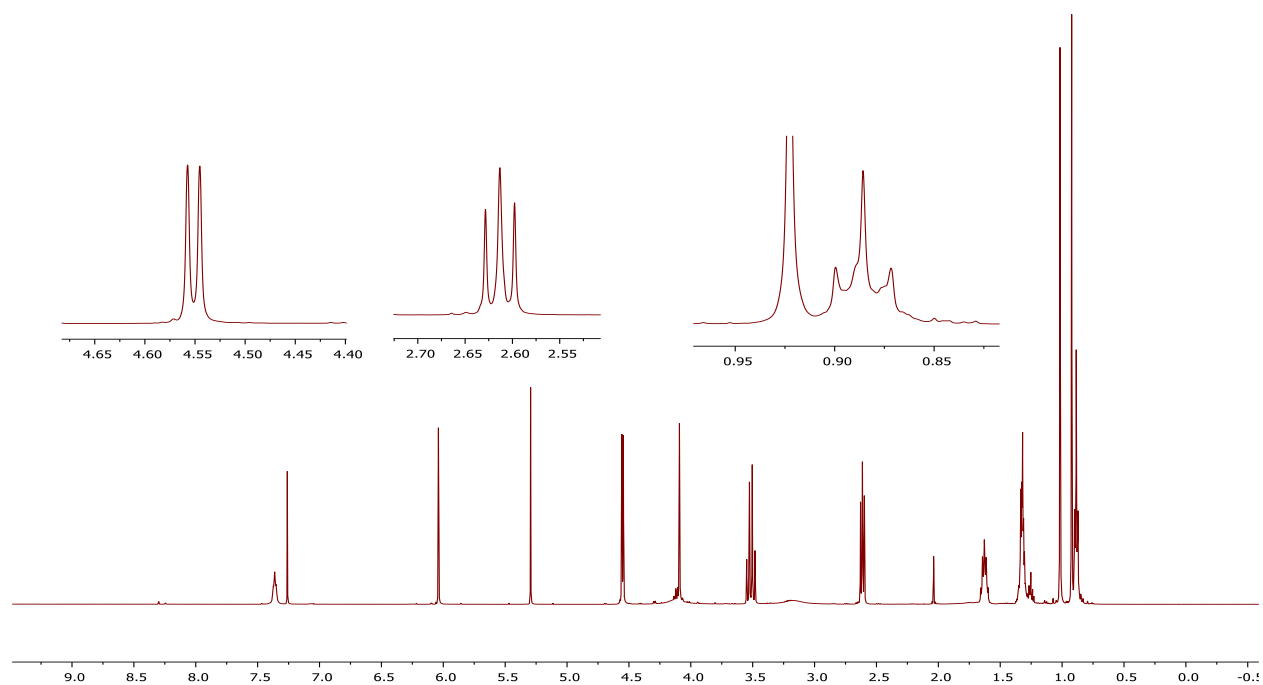
¹H NMR of compound 4.1d



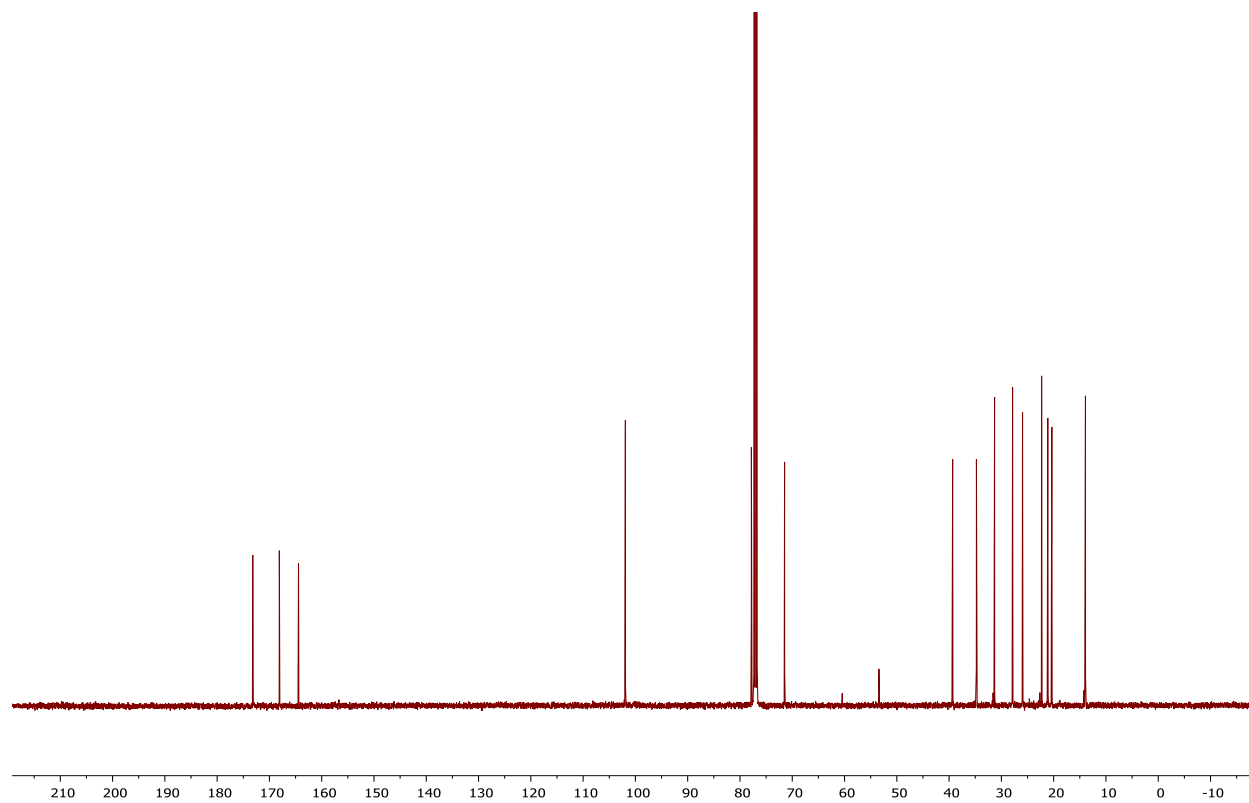
¹³C NMR of compound 4.1d



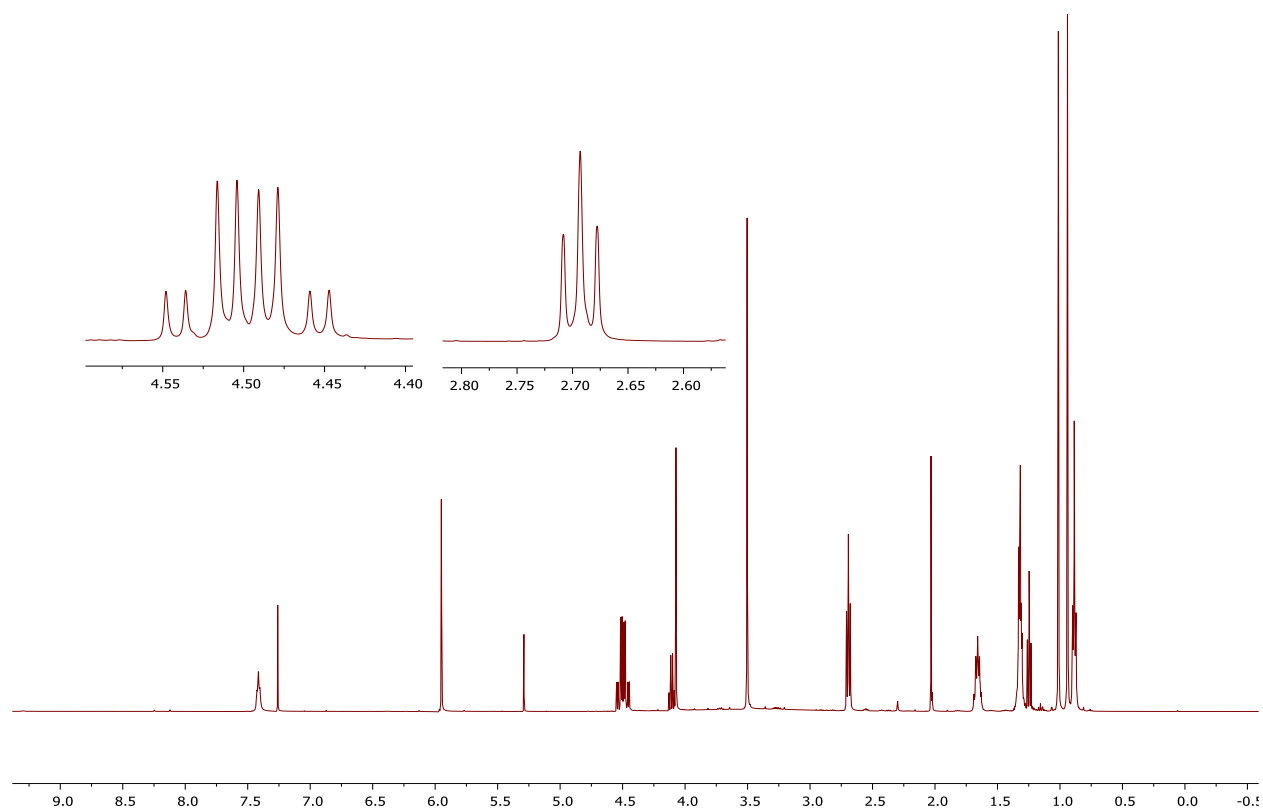
¹H NMR of compound 4.1e



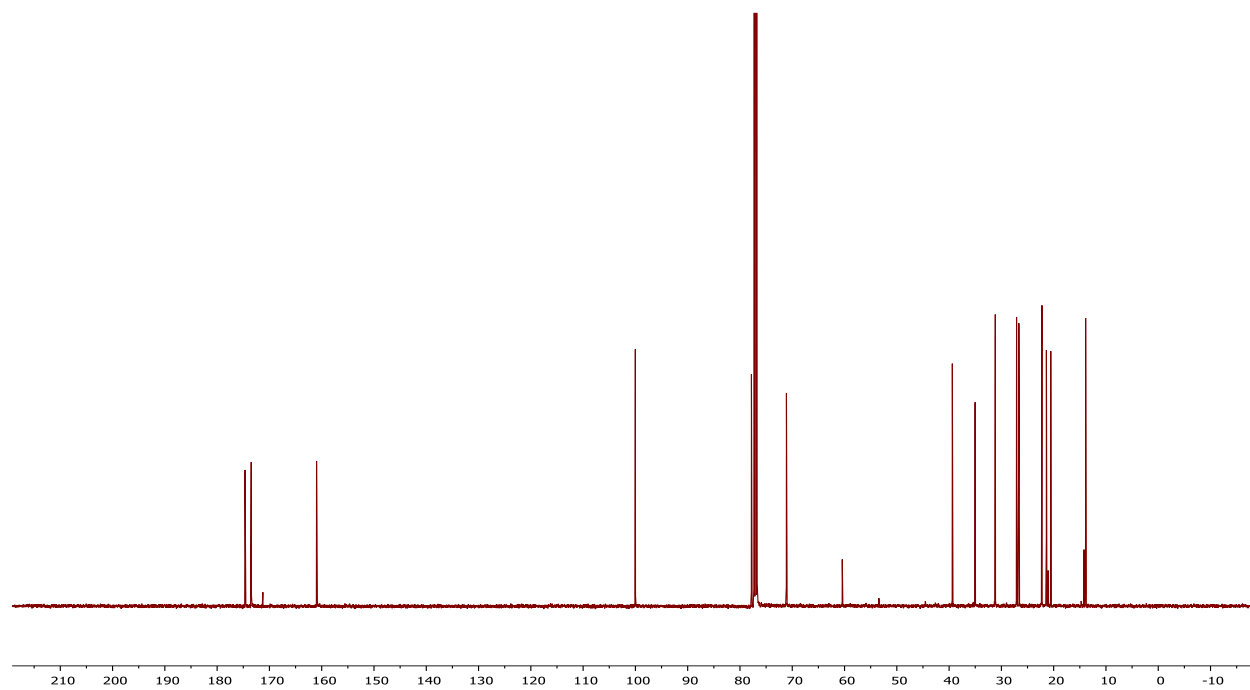
¹³C NMR of compound 4.1e



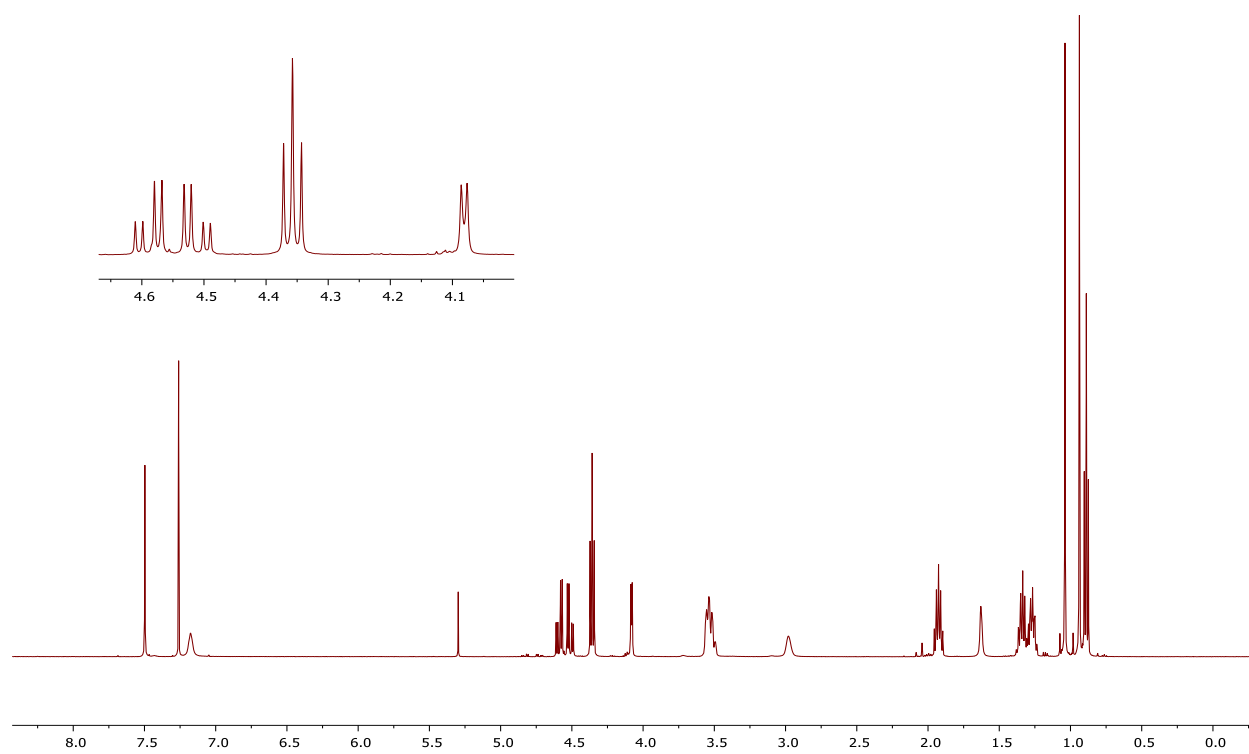
¹H NMR of compound 4.1f



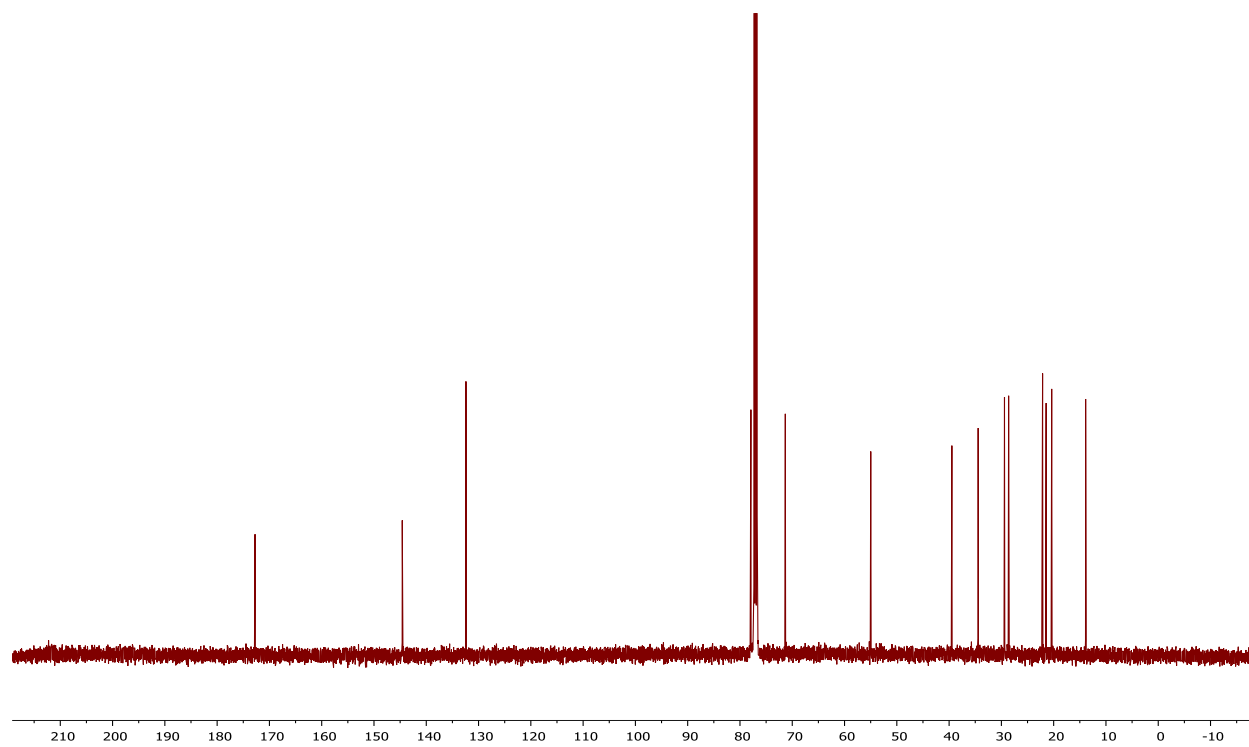
¹³C NMR of compound 4.1f



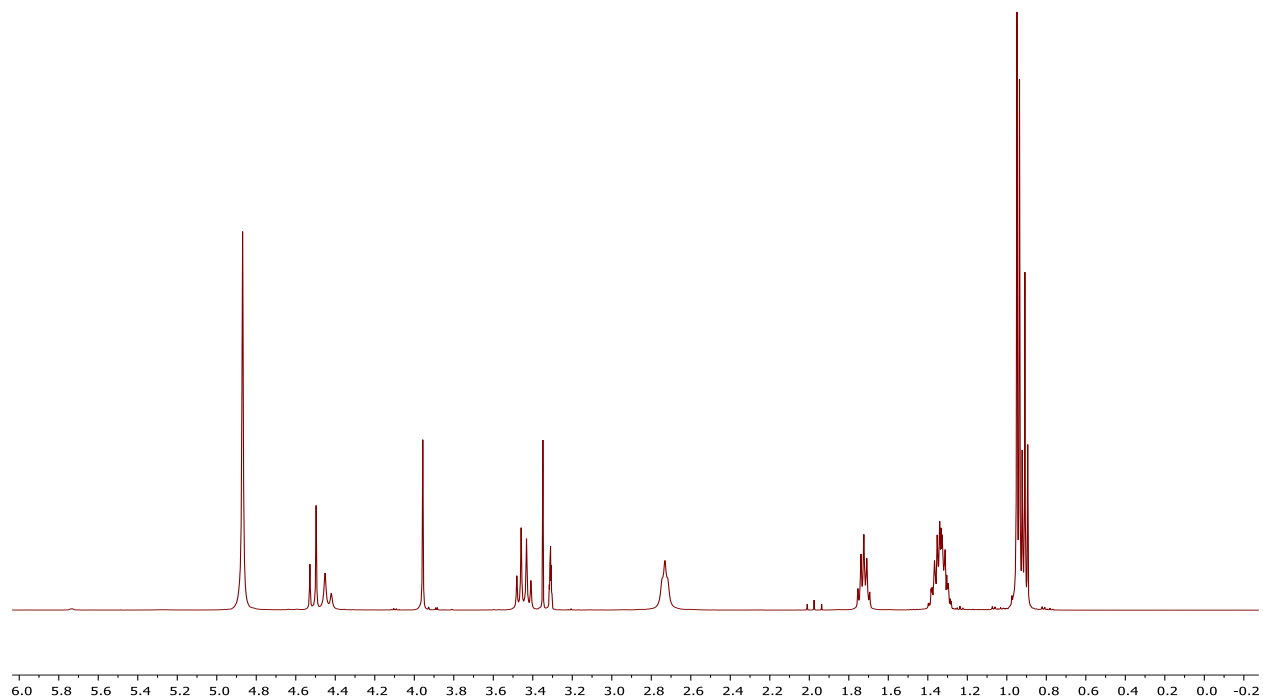
¹H NMR of compound 4.1g



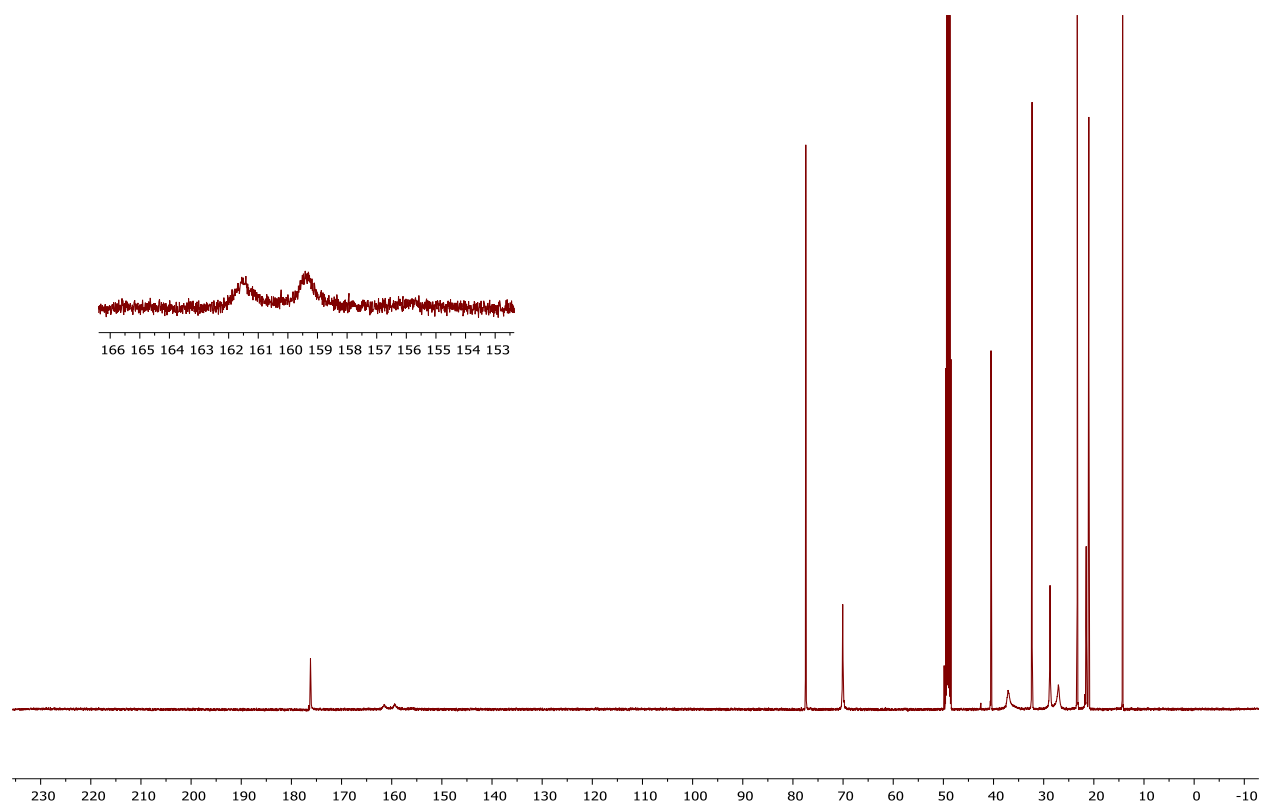
¹³C NMR of compound 4.1g



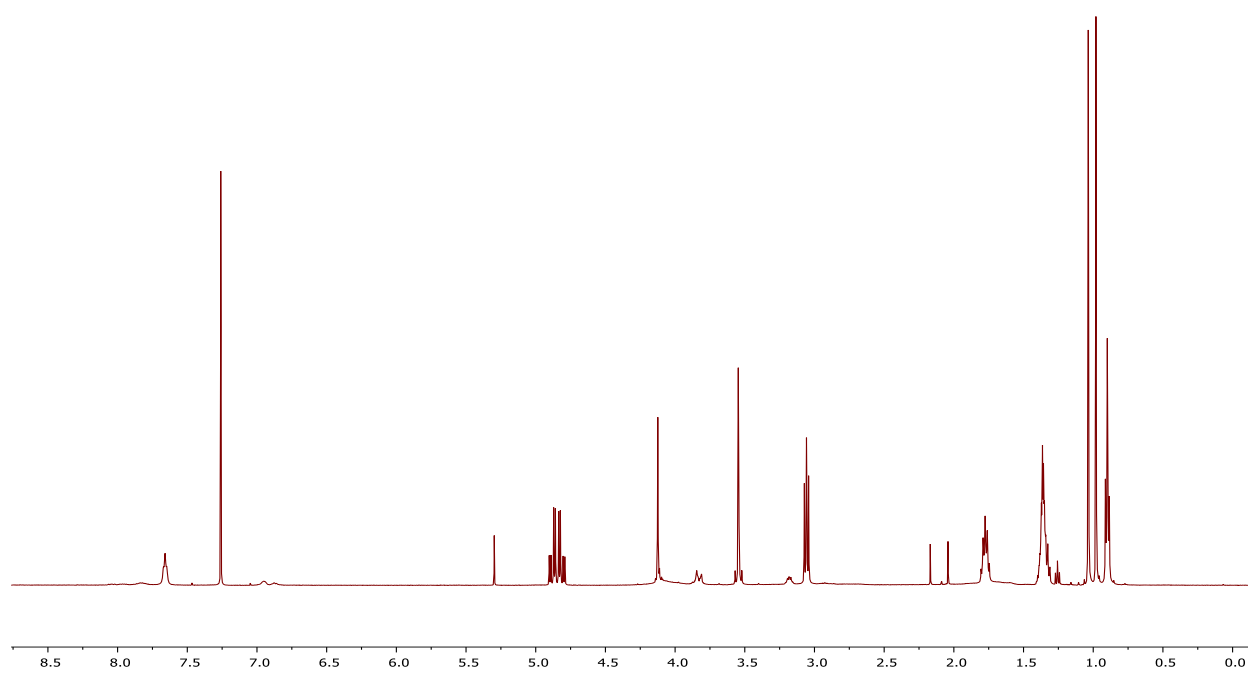
¹H NMR of compound 4.1h



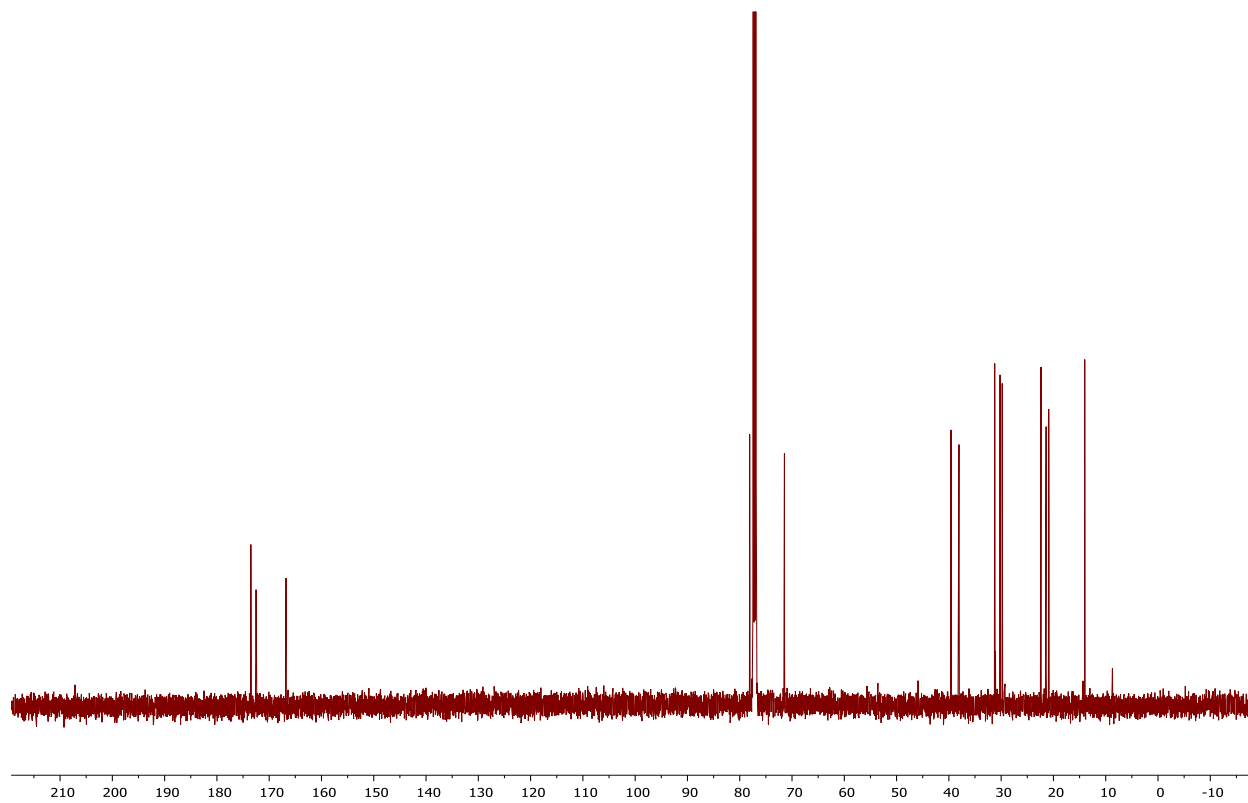
¹³C NMR of compound 4.1h



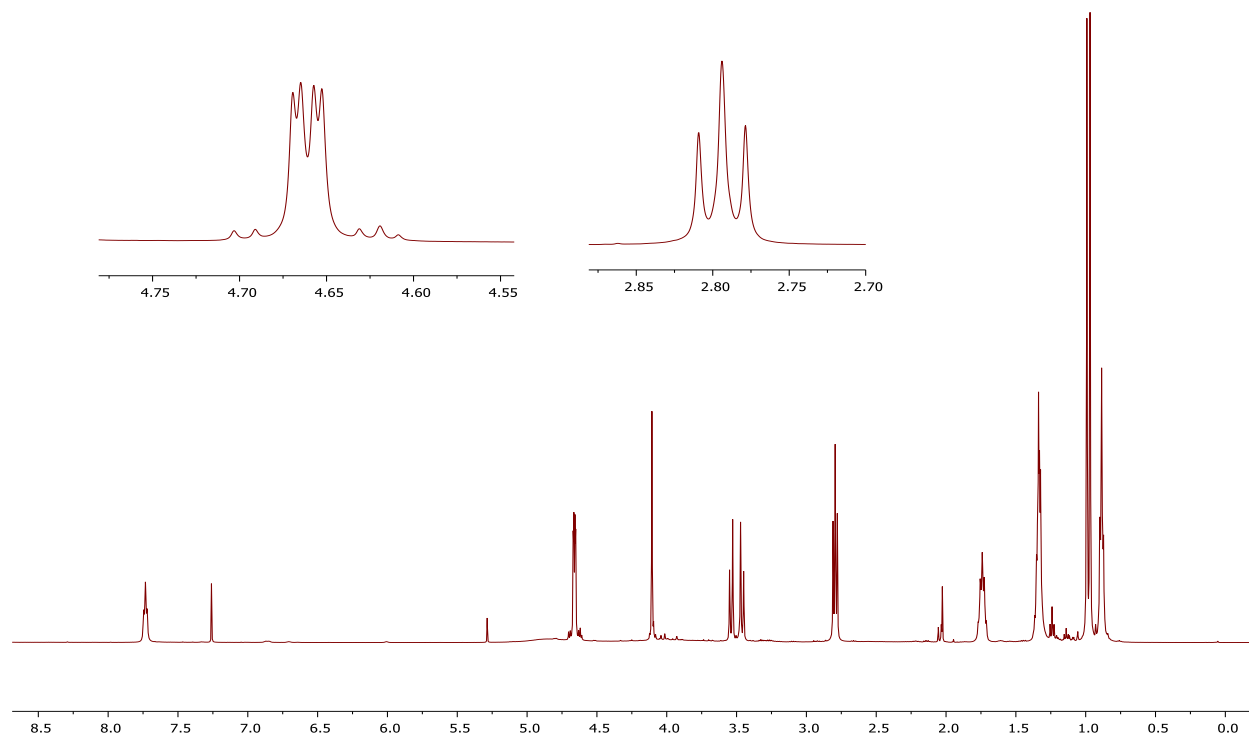
¹H NMR of compound 4.1i



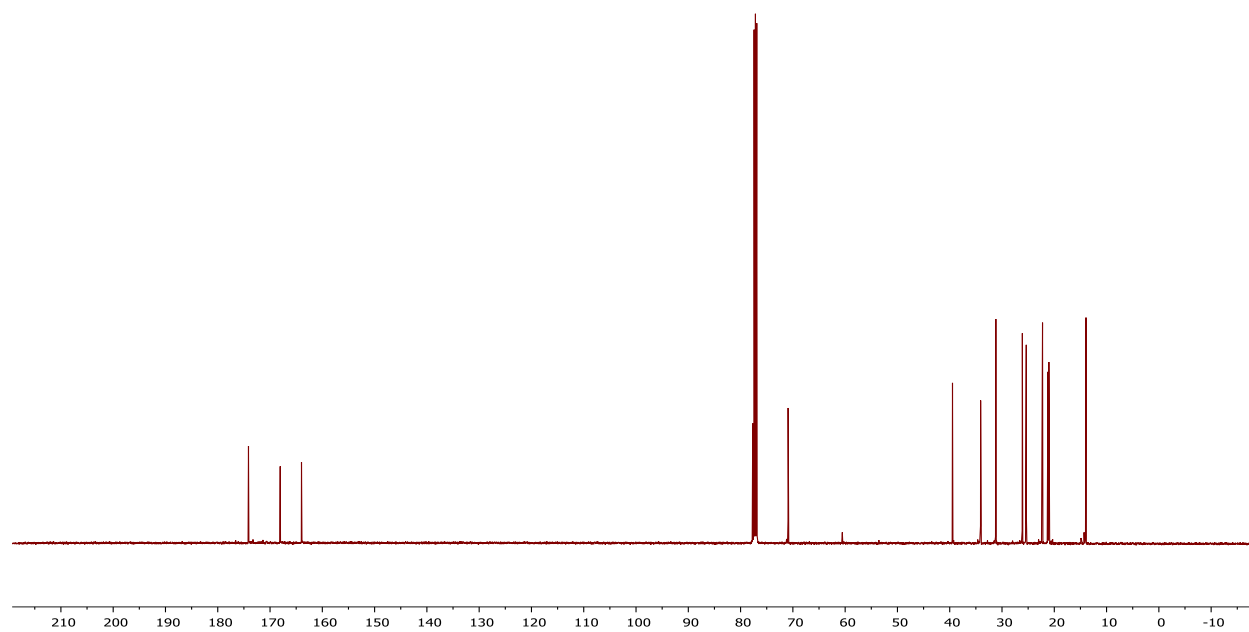
¹³C NMR of compound 4.1i



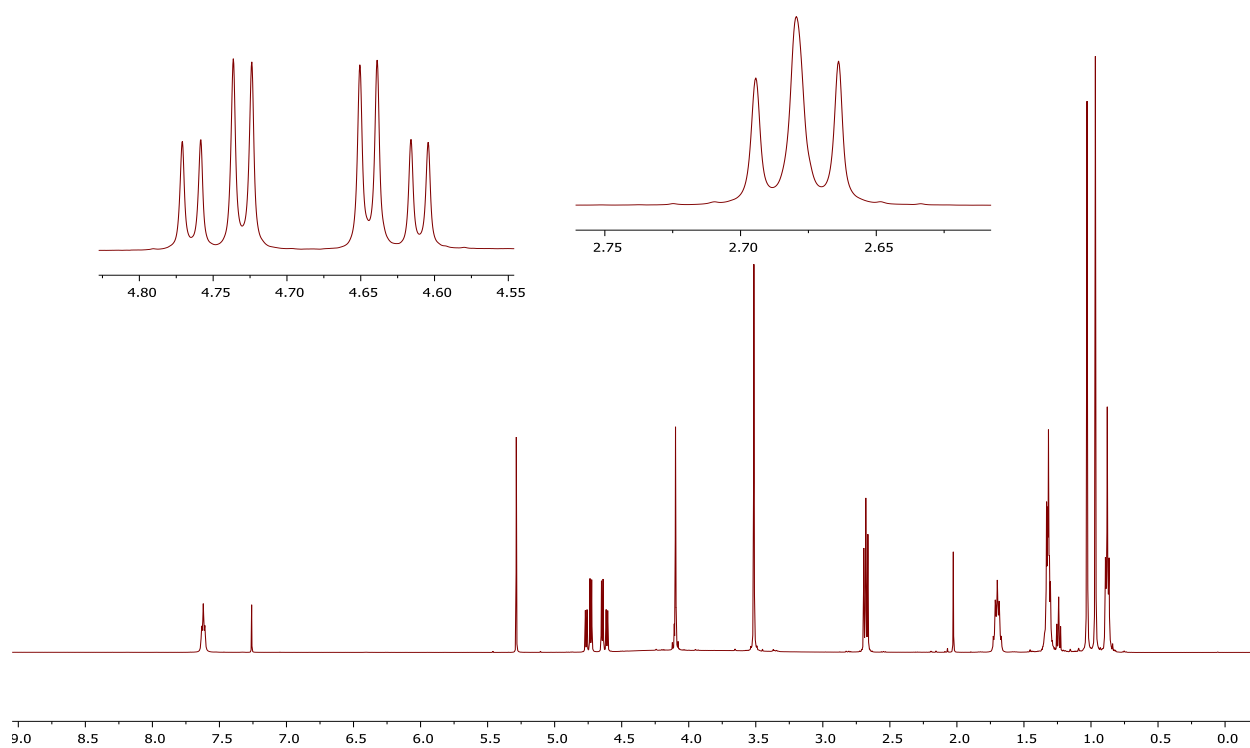
¹H NMR of compound 4.1j



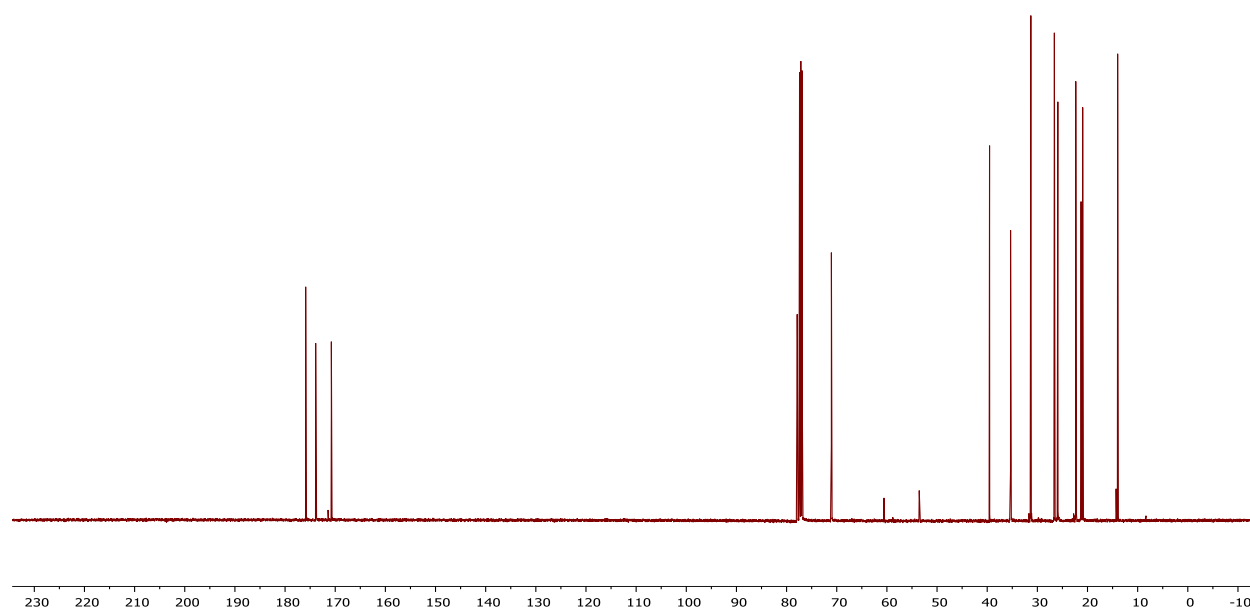
¹³C NMR of compound 4.1j



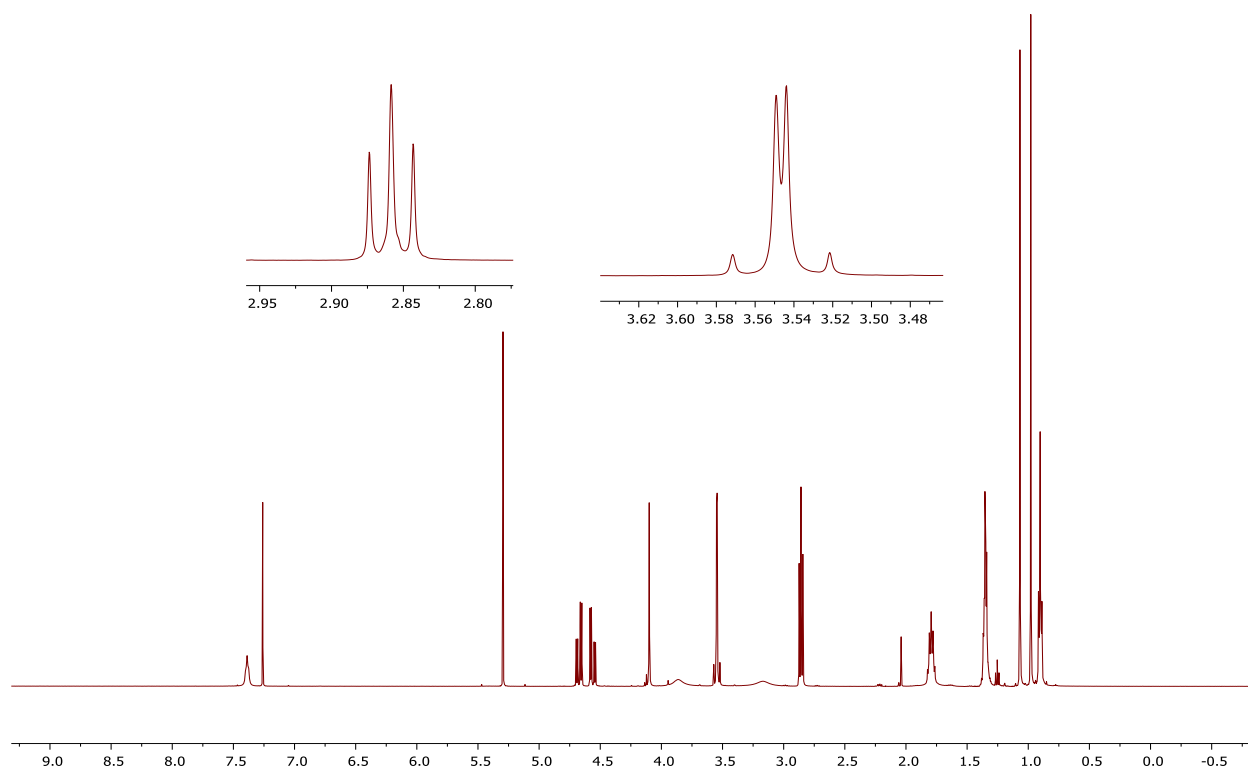
¹H NMR of compound 4.1k



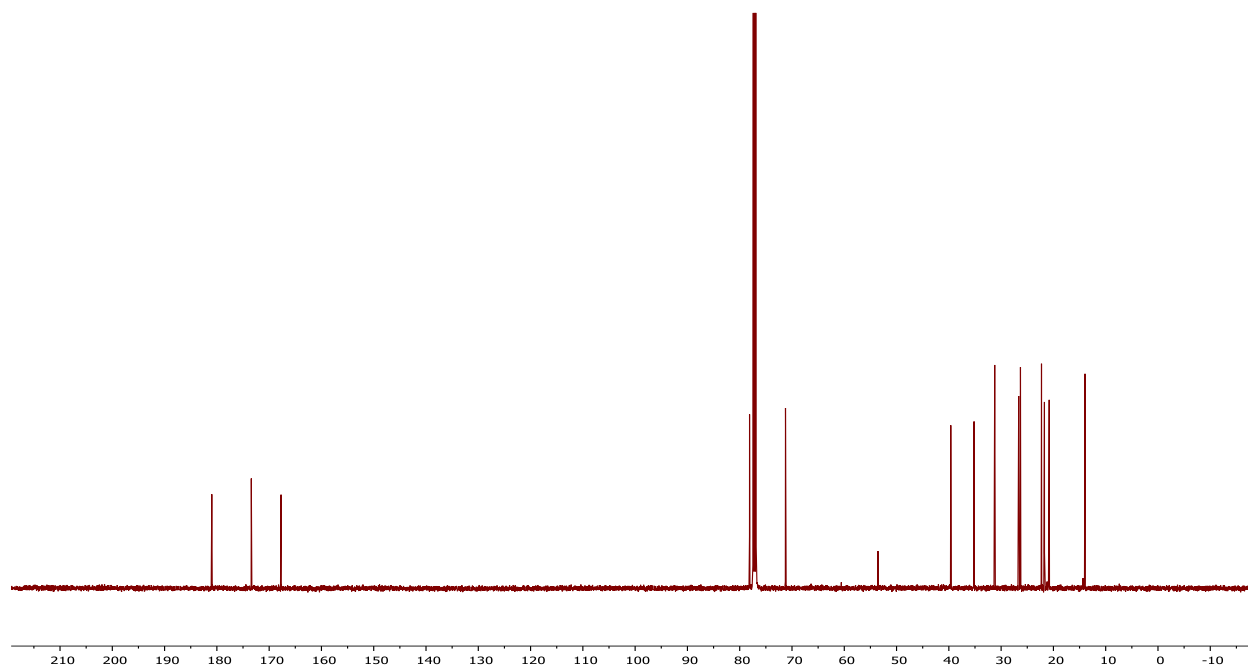
¹³C NMR of compound 4.1k



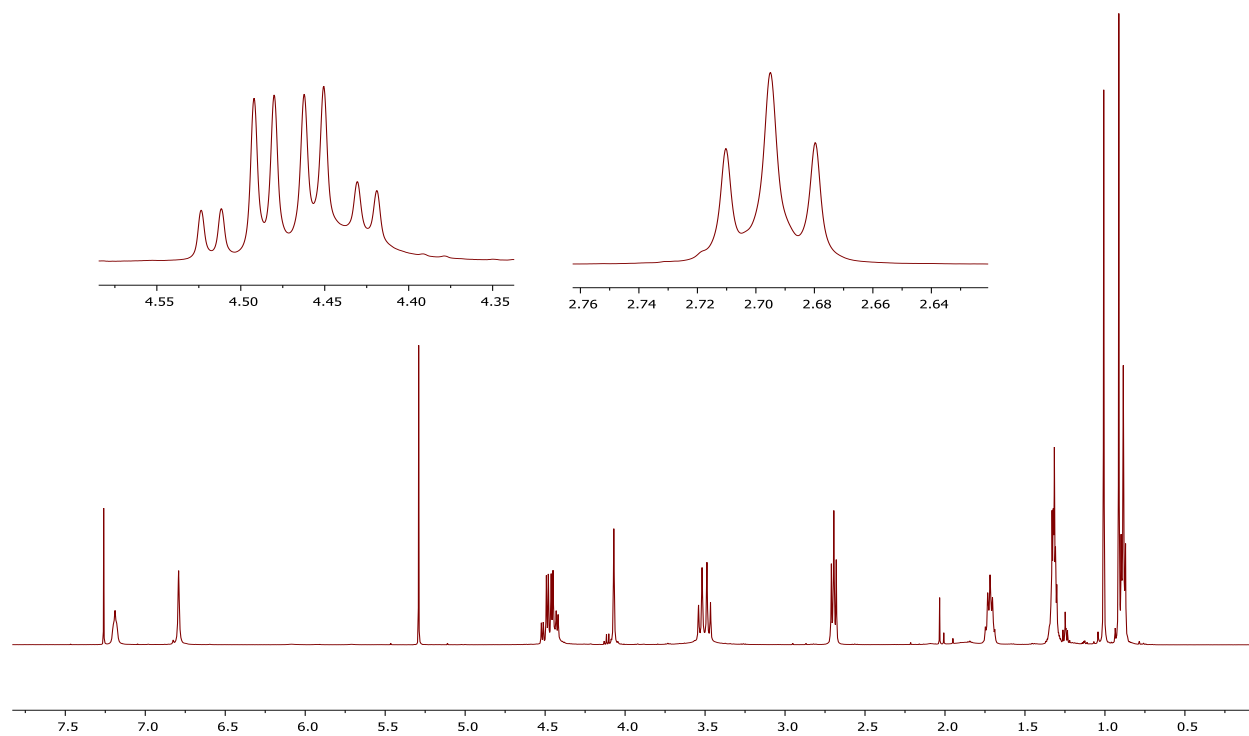
¹H NMR of compound 4.11



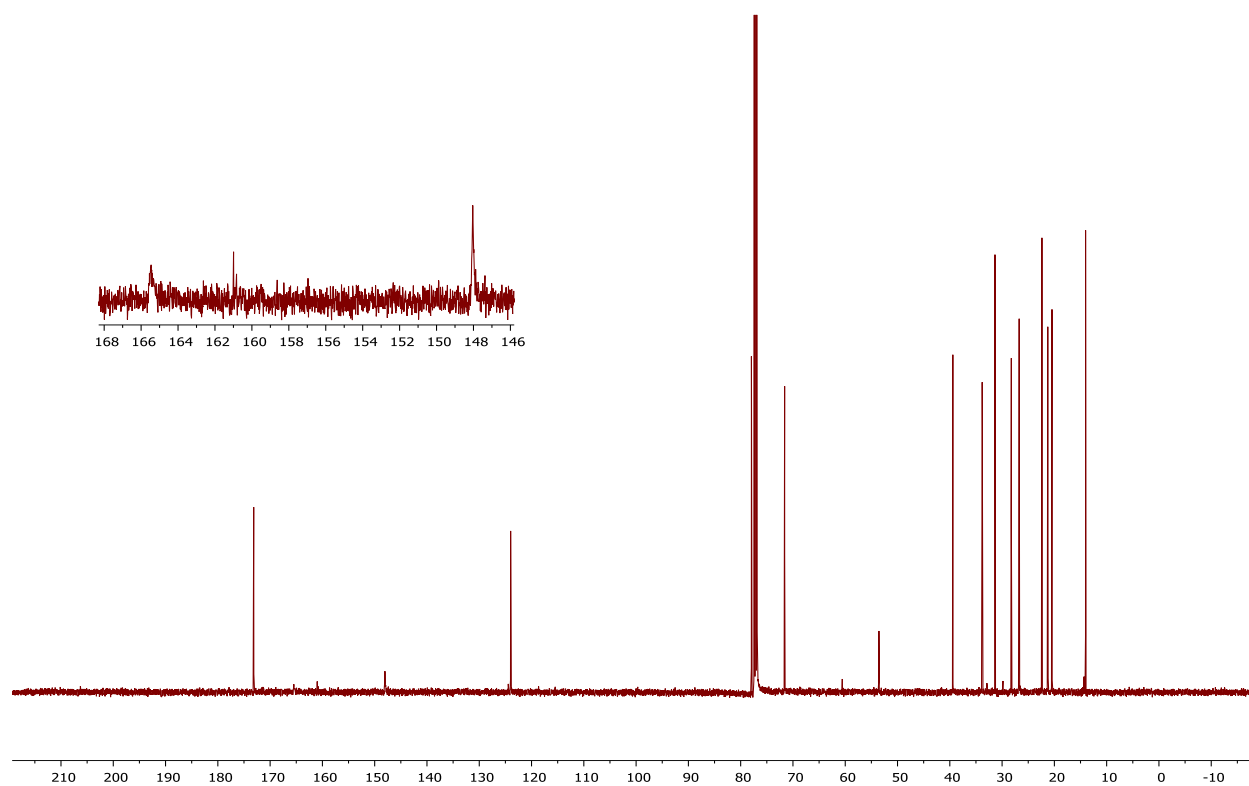
¹³C NMR of compound 4.11



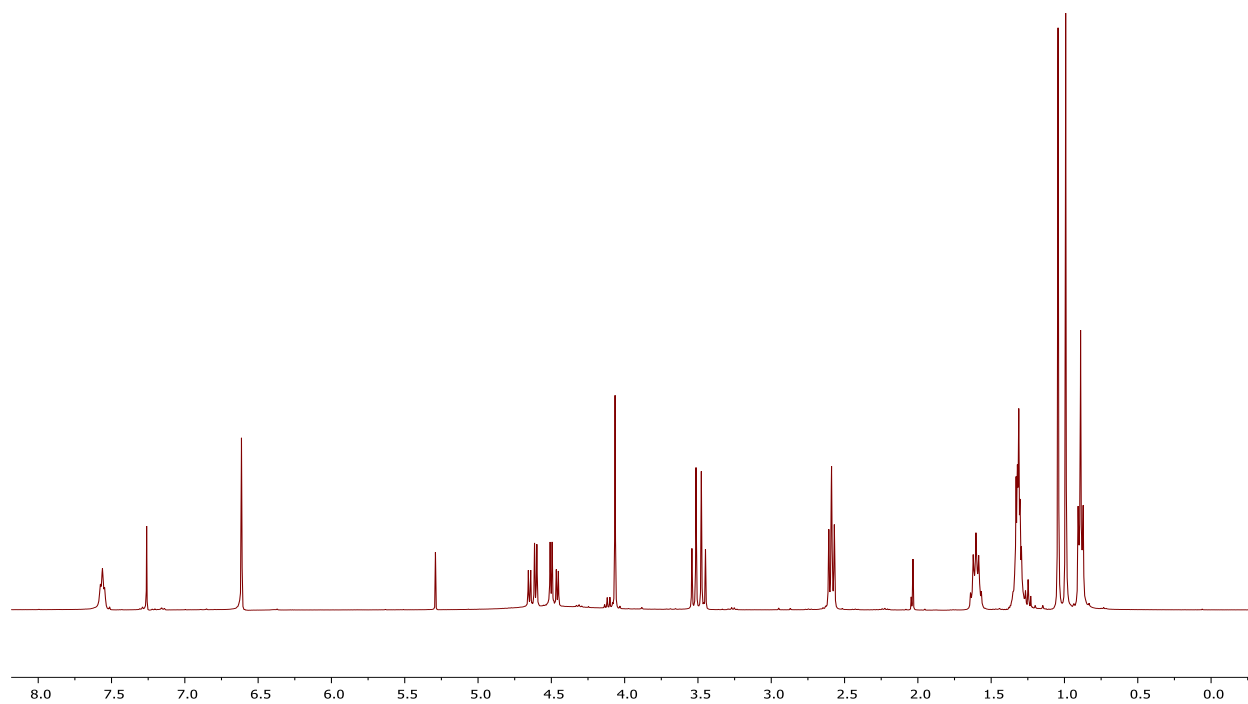
¹H NMR of compound 4.1m



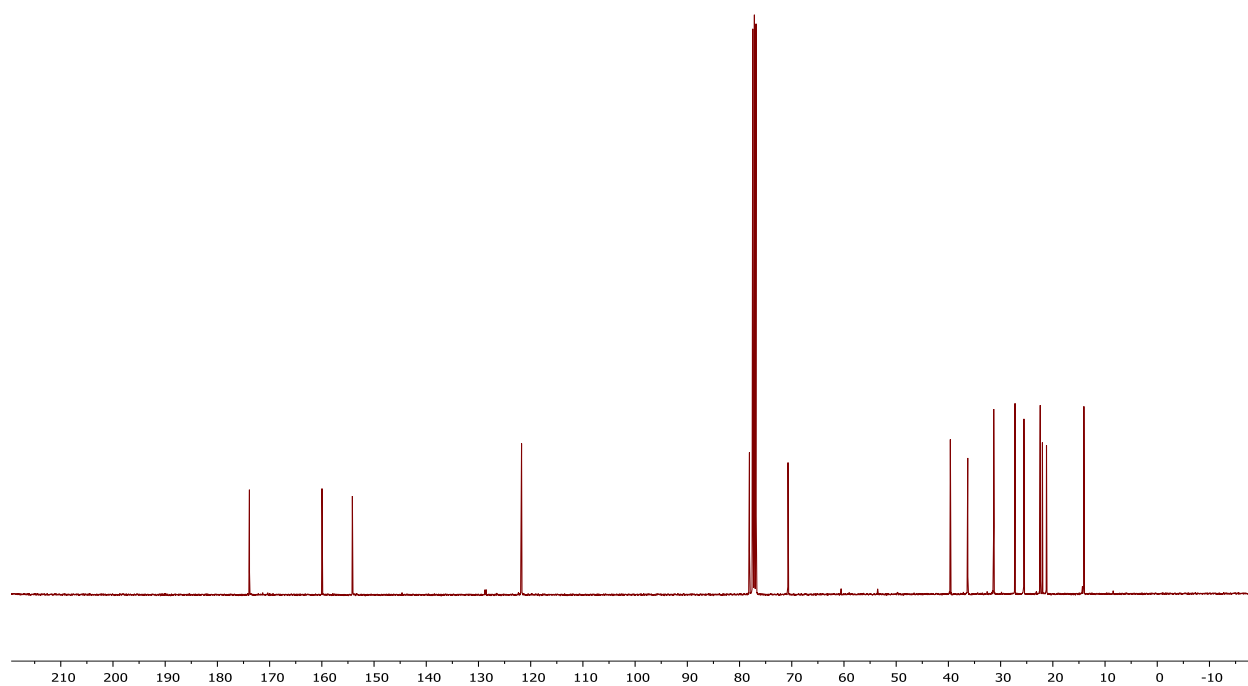
¹³C NMR of compound 4.1m



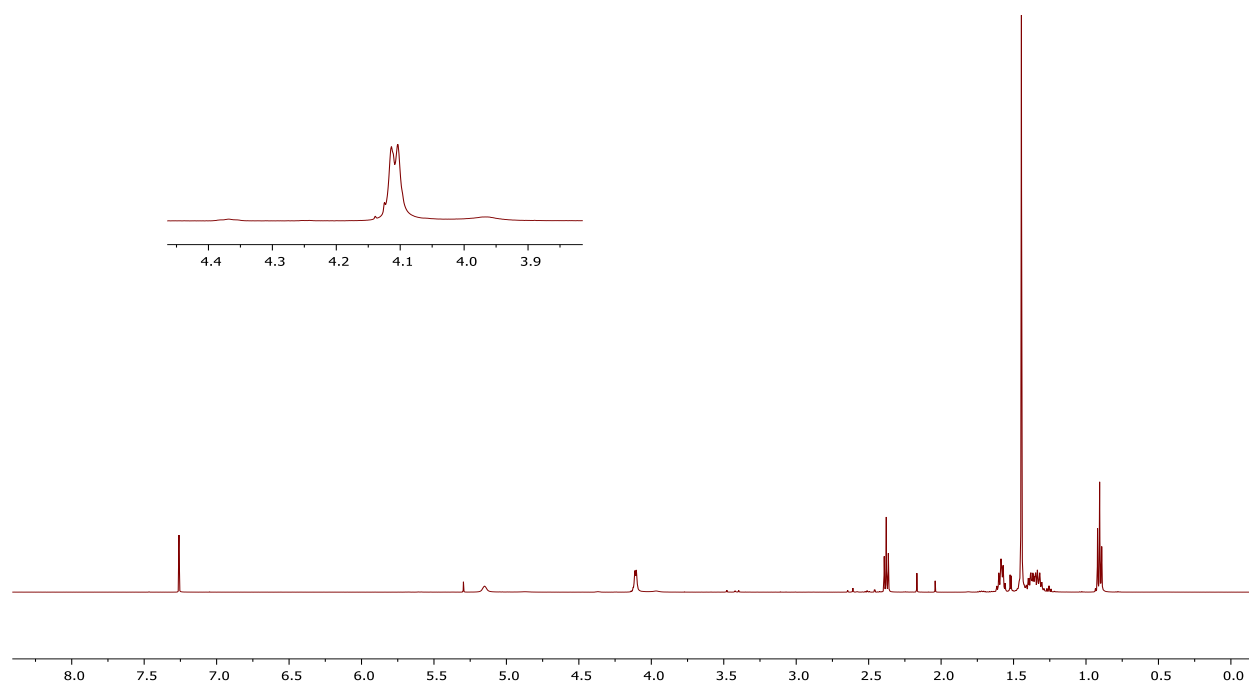
¹H NMR of compound 4.1n



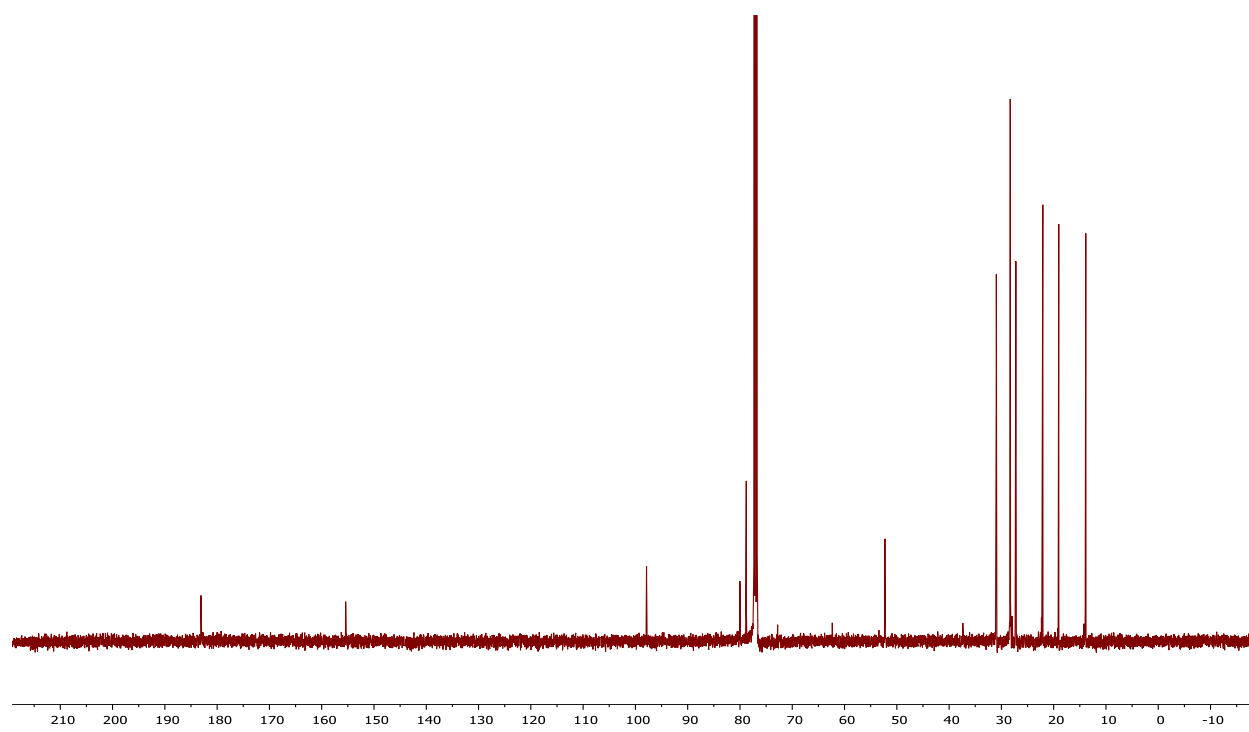
¹³C NMR of compound 4.1n



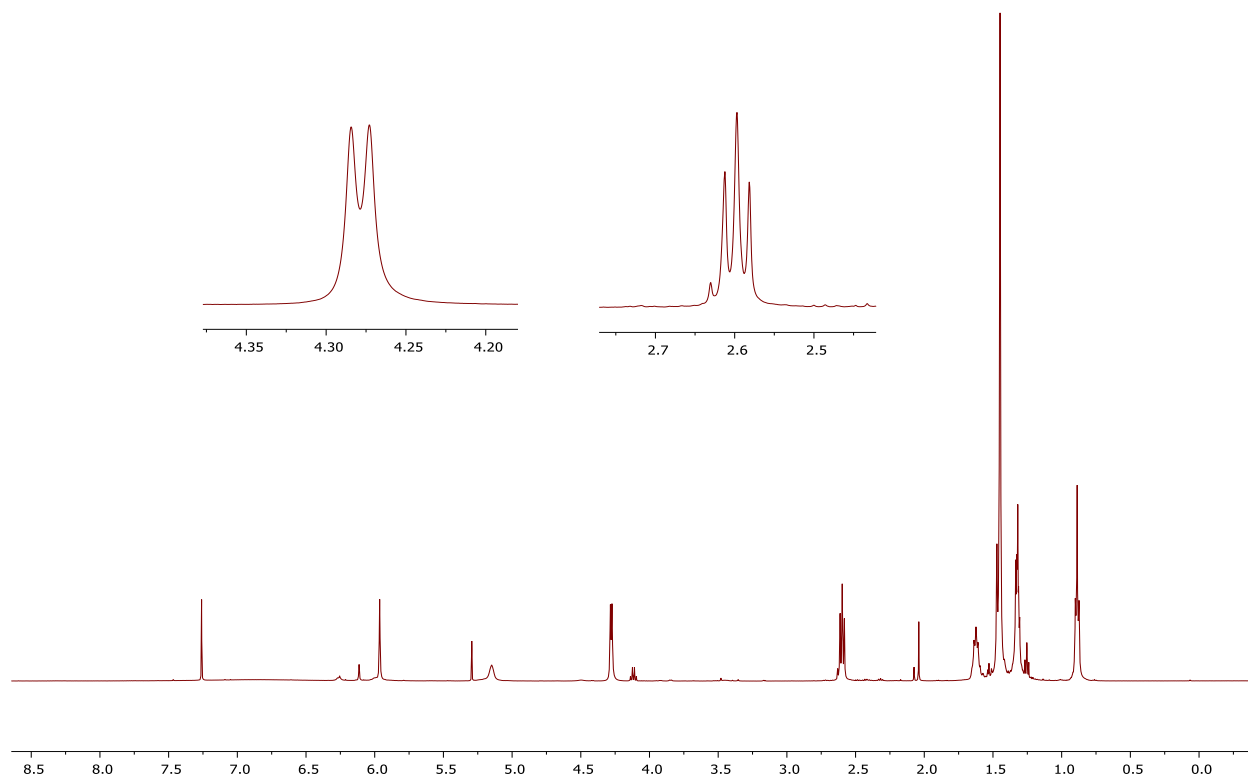
^1H NMR of compound 4.2



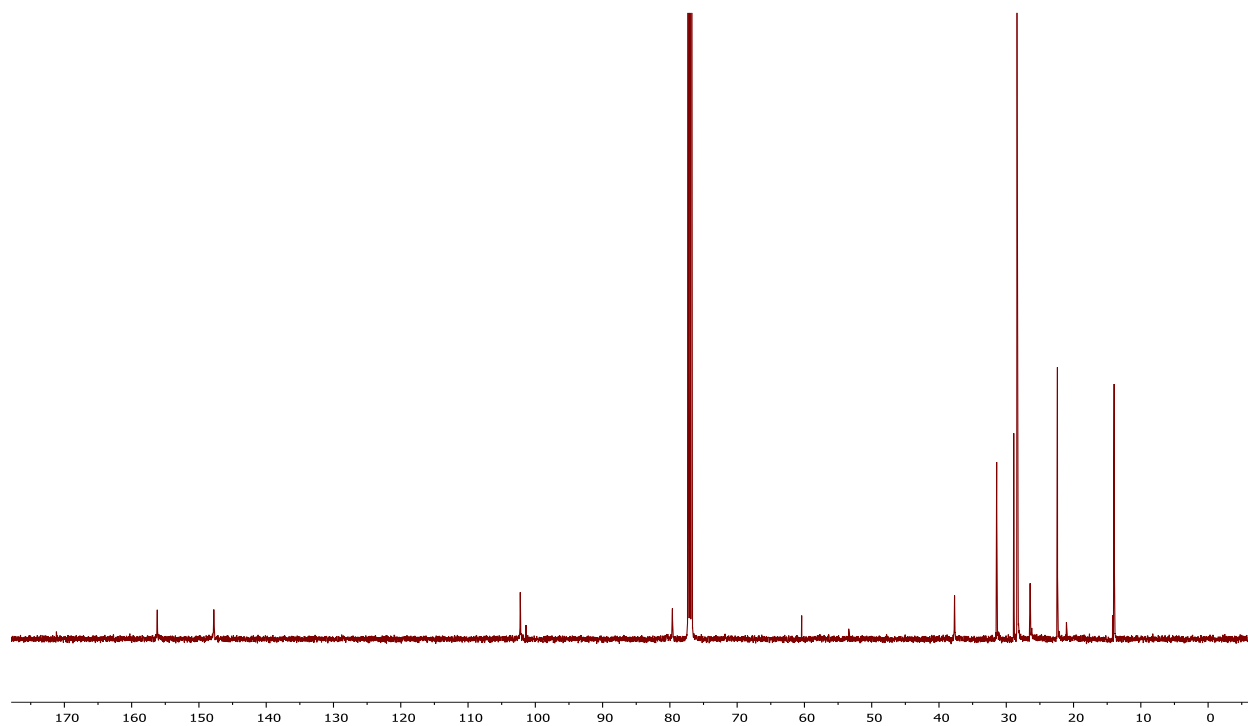
^{13}C NMR of compound 4.2



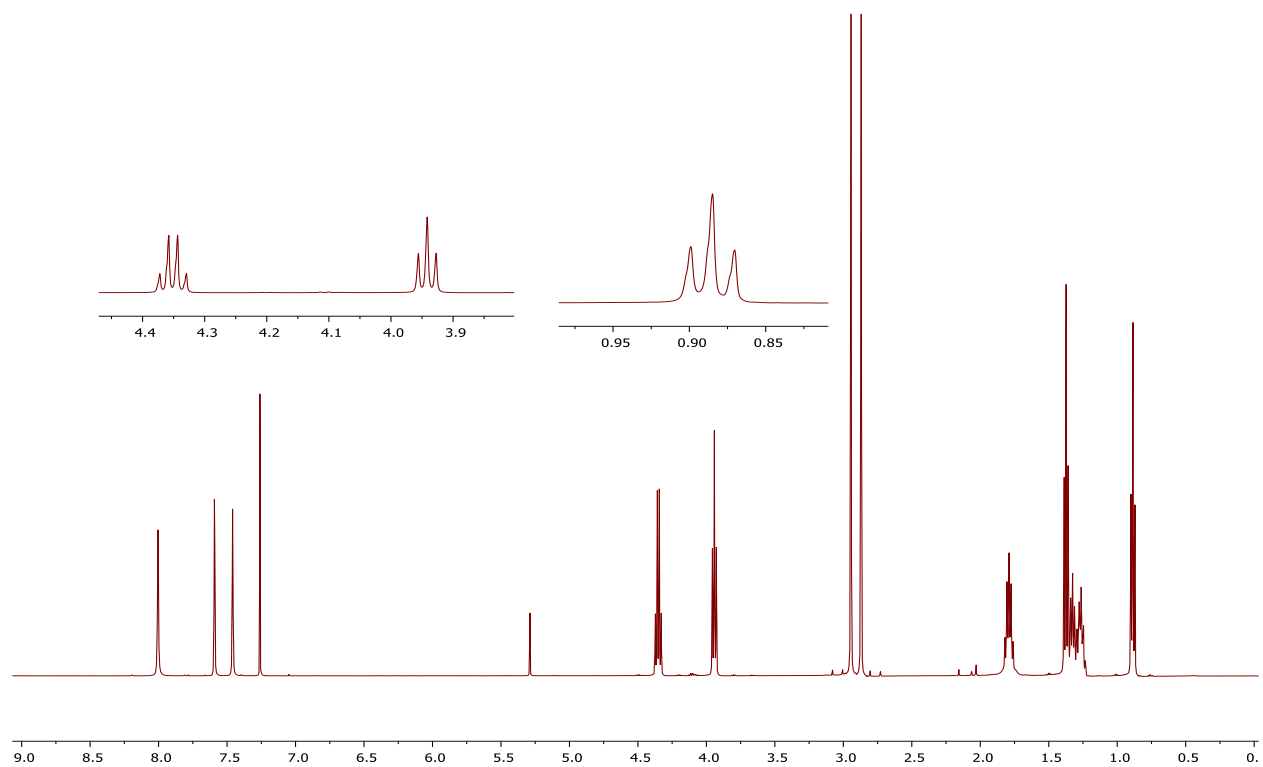
¹H NMR of compound 4.3



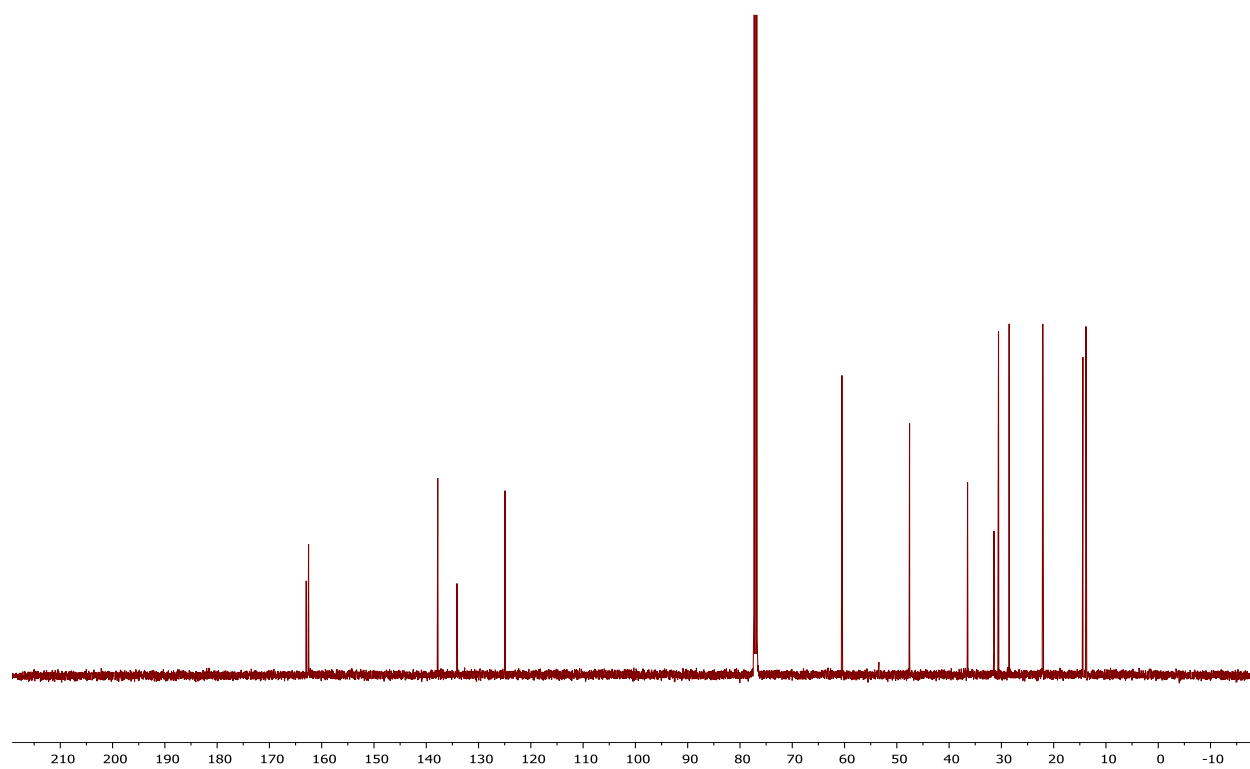
¹³C NMR of compound 4.3



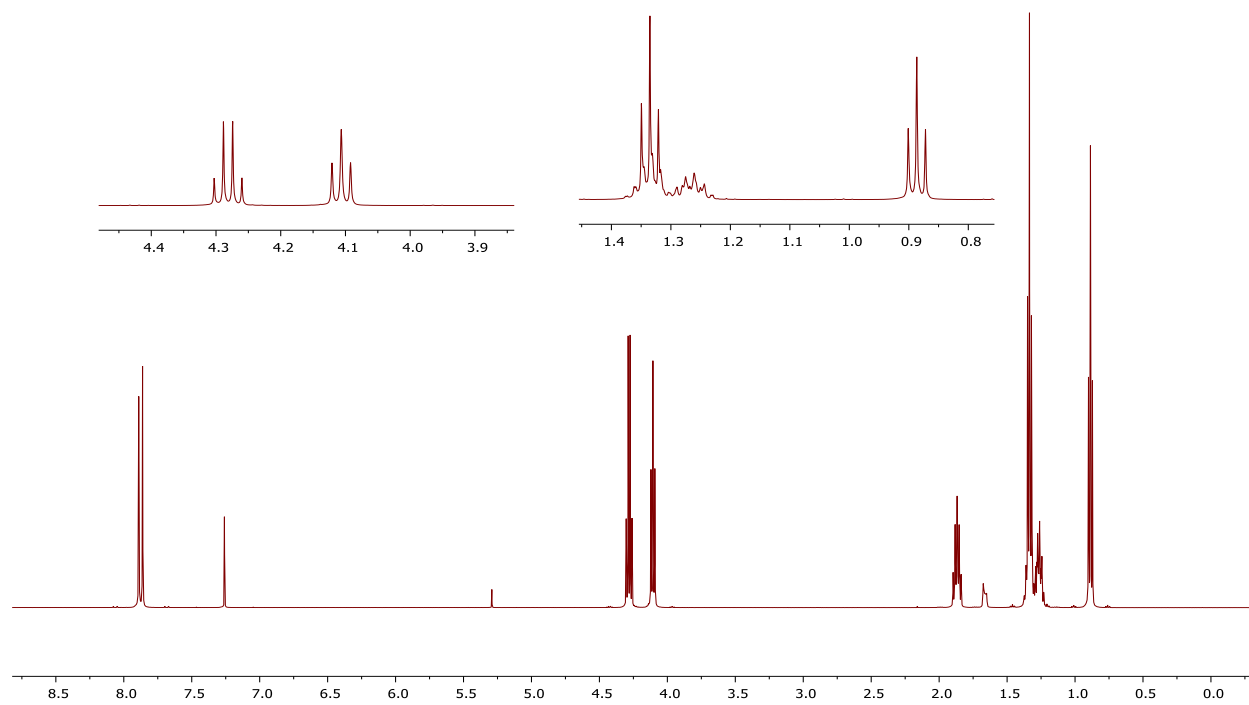
¹H NMR of compound 4.4b



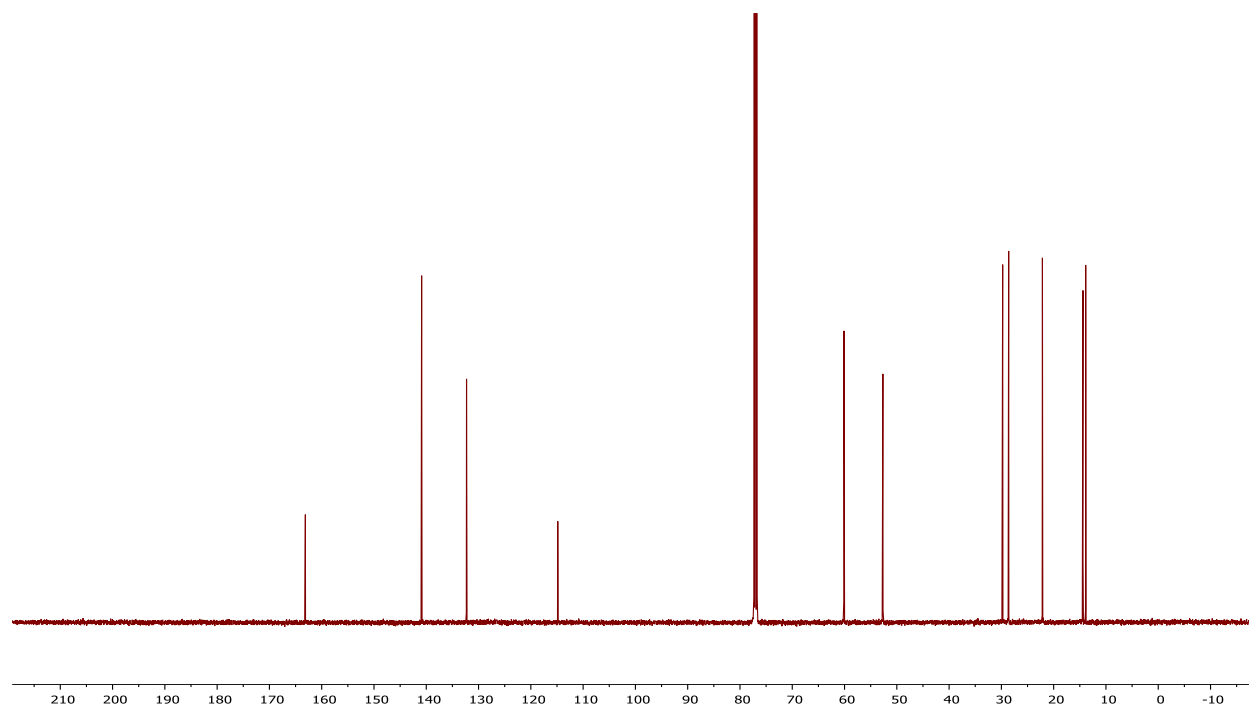
¹³C NMR of compound 4.4b



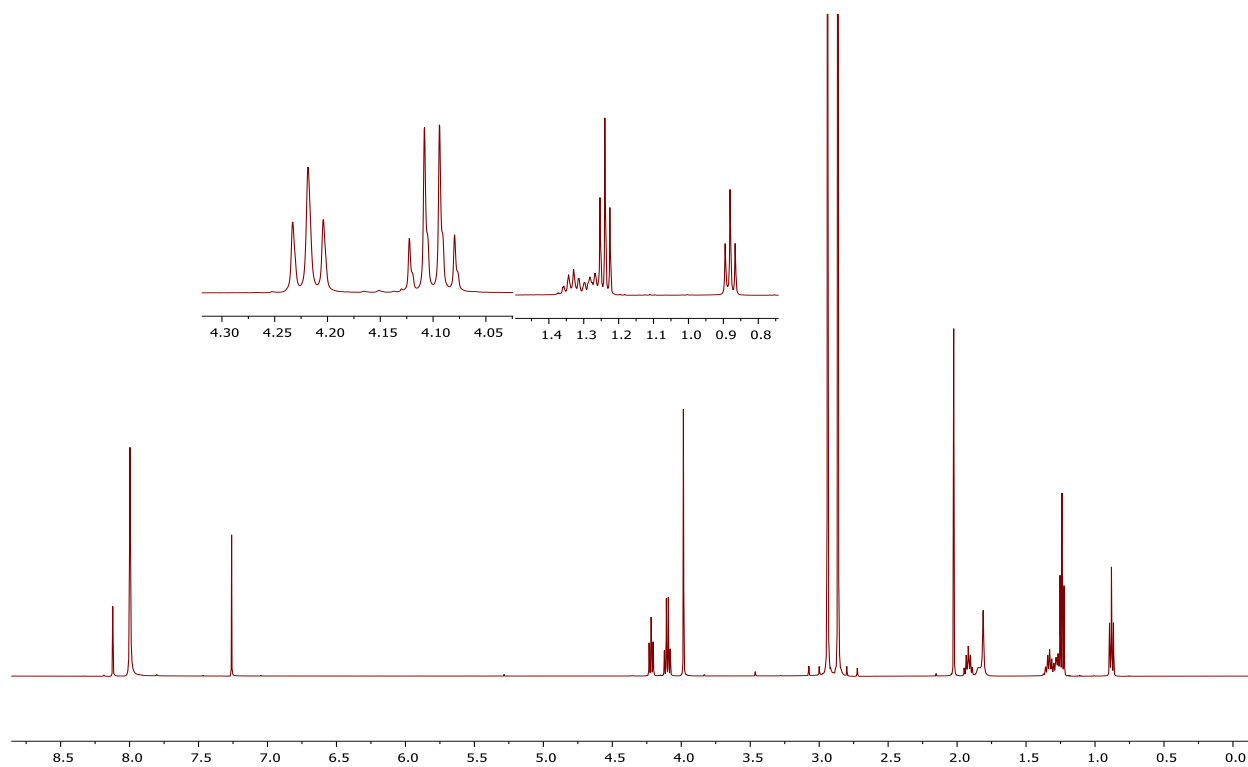
¹H NMR of compound 4.4c



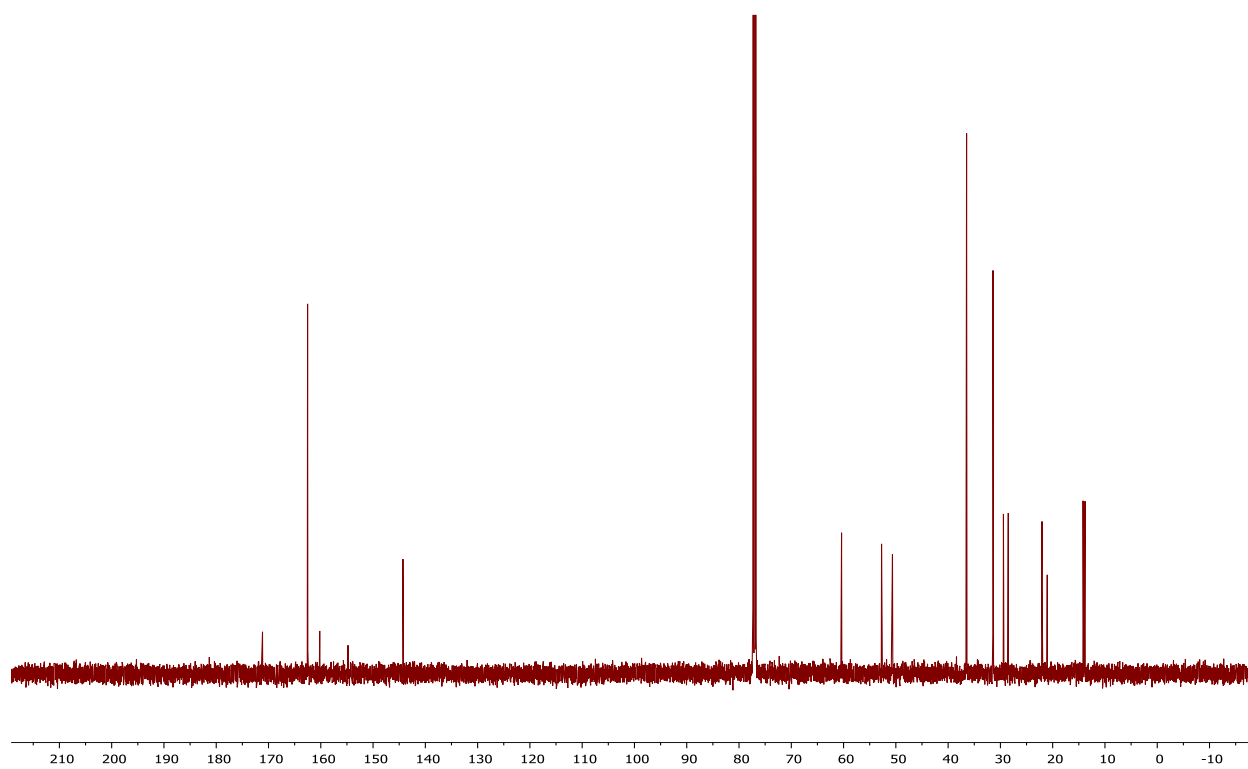
¹³C NMR of compound 4.4c



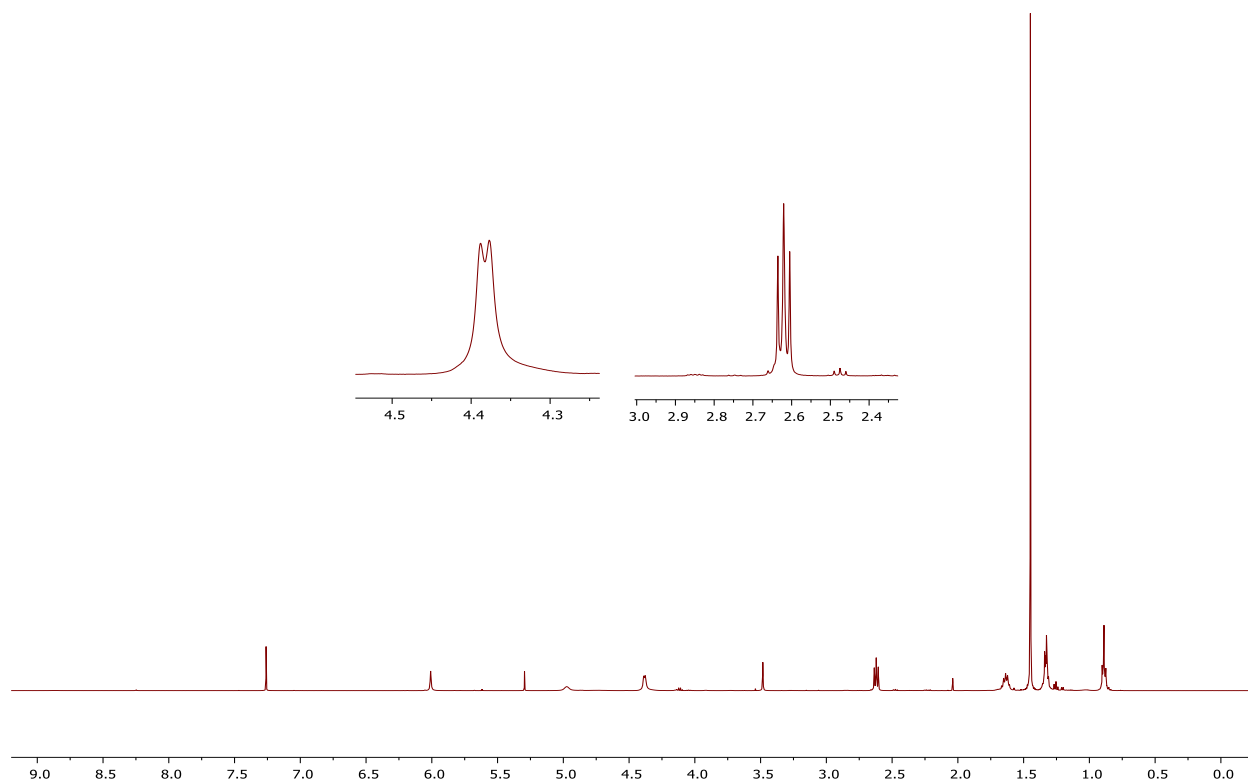
¹H NMR of compound 4.4d



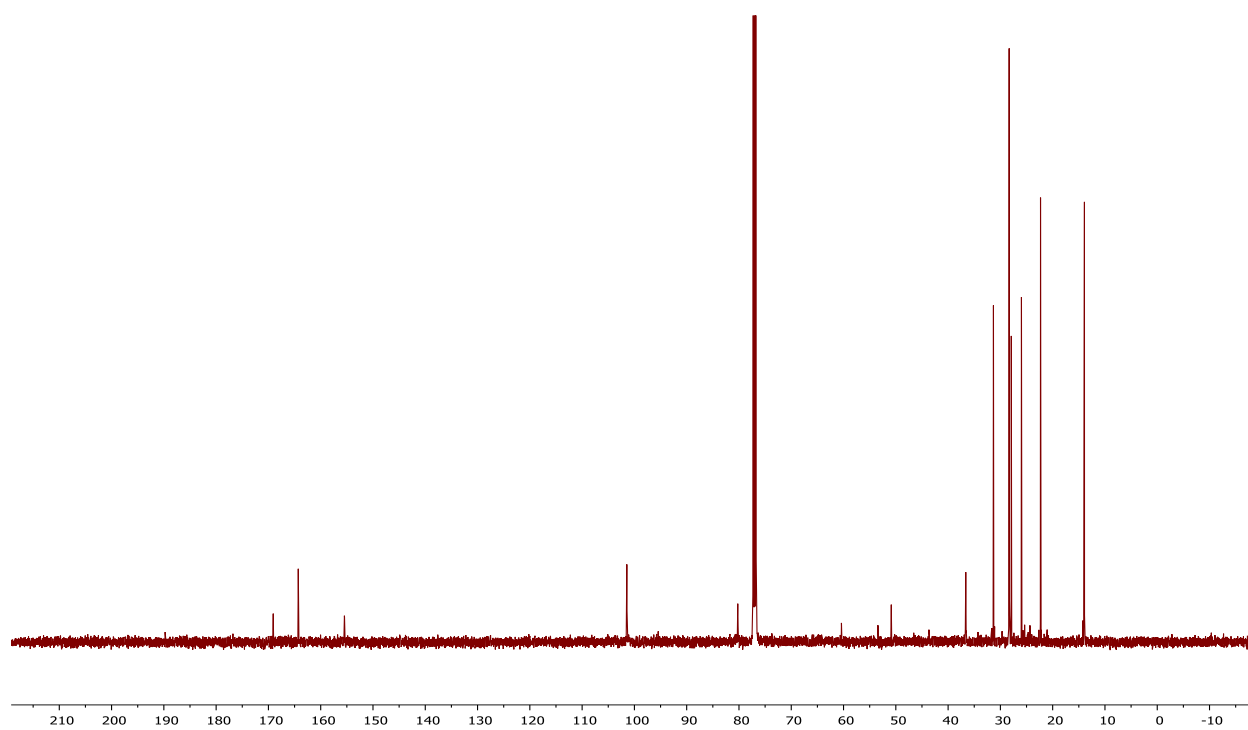
¹³C NMR of compound 4.4d



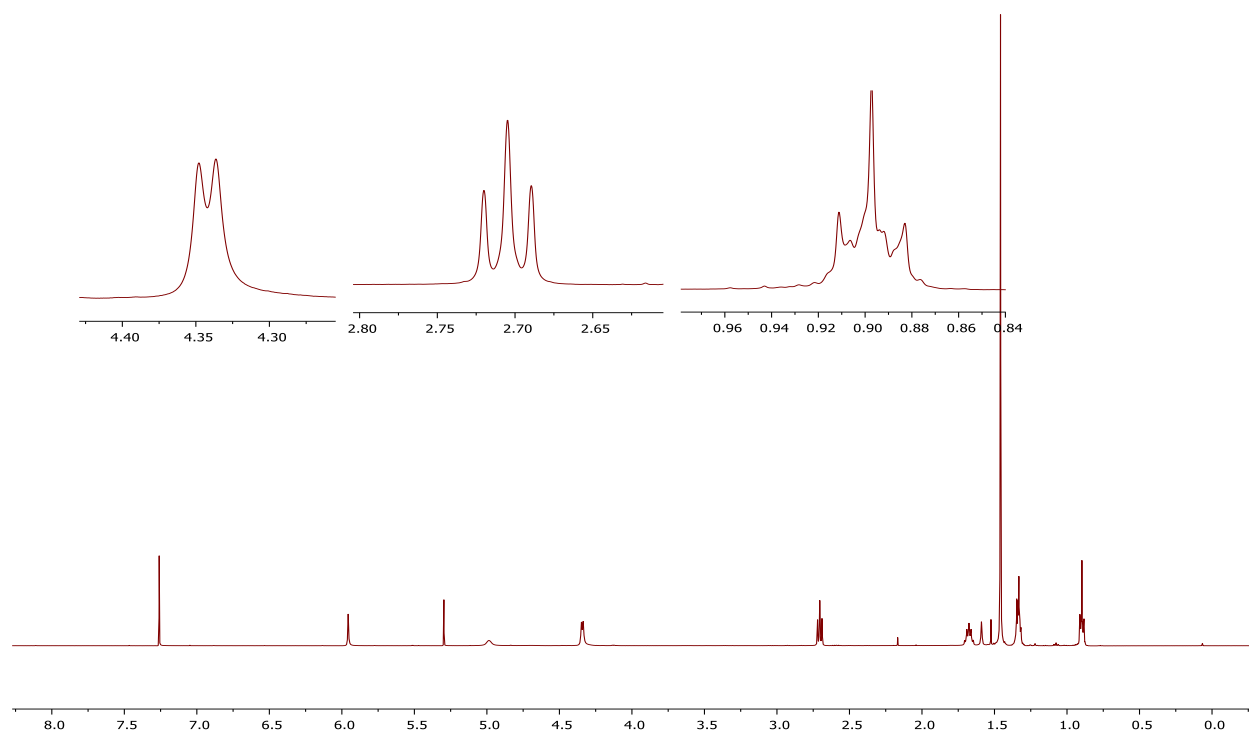
¹H NMR of compound 4.10e



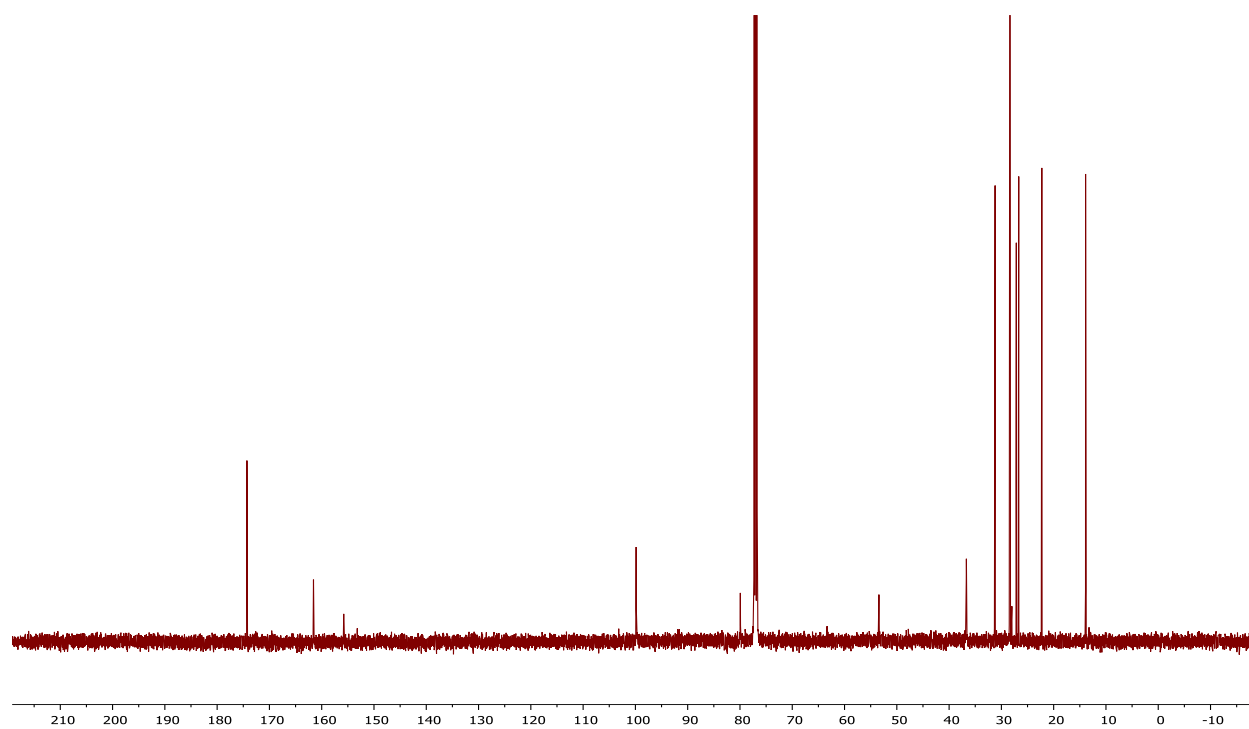
¹³C NMR of compound 4.10e



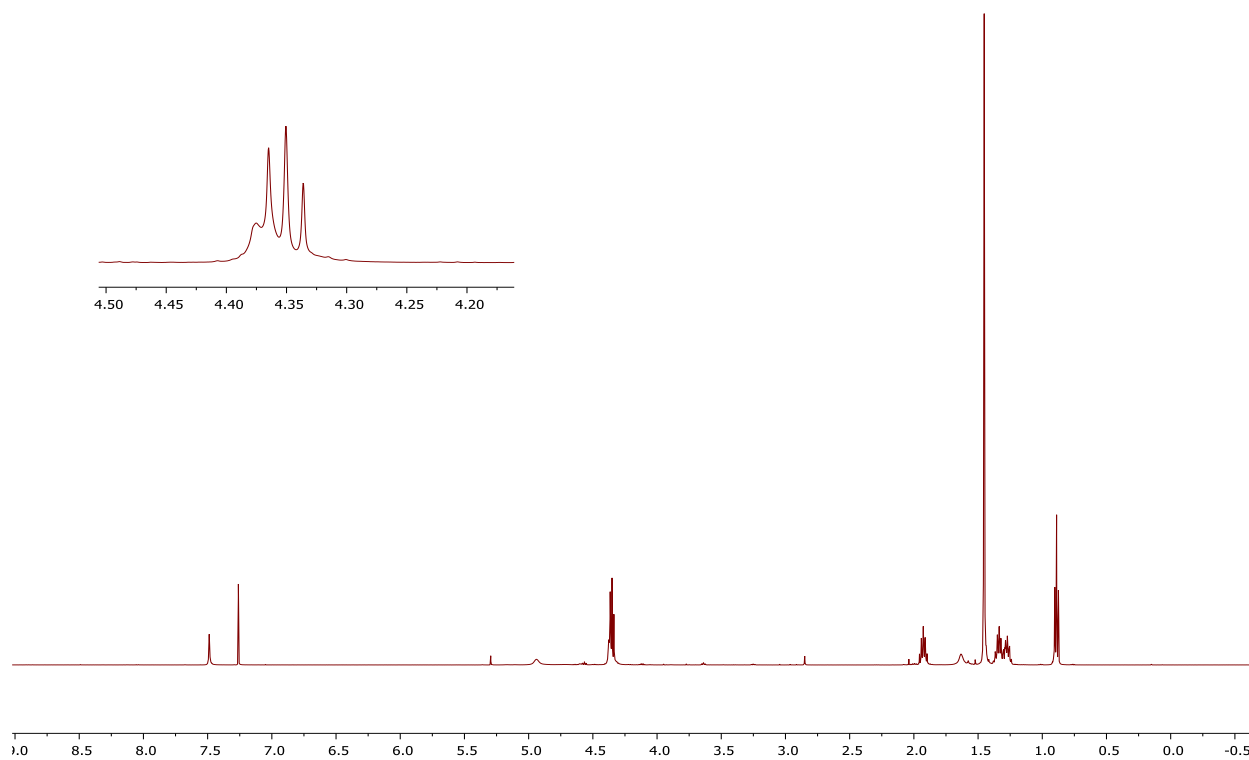
¹H NMR of compound 4.10f



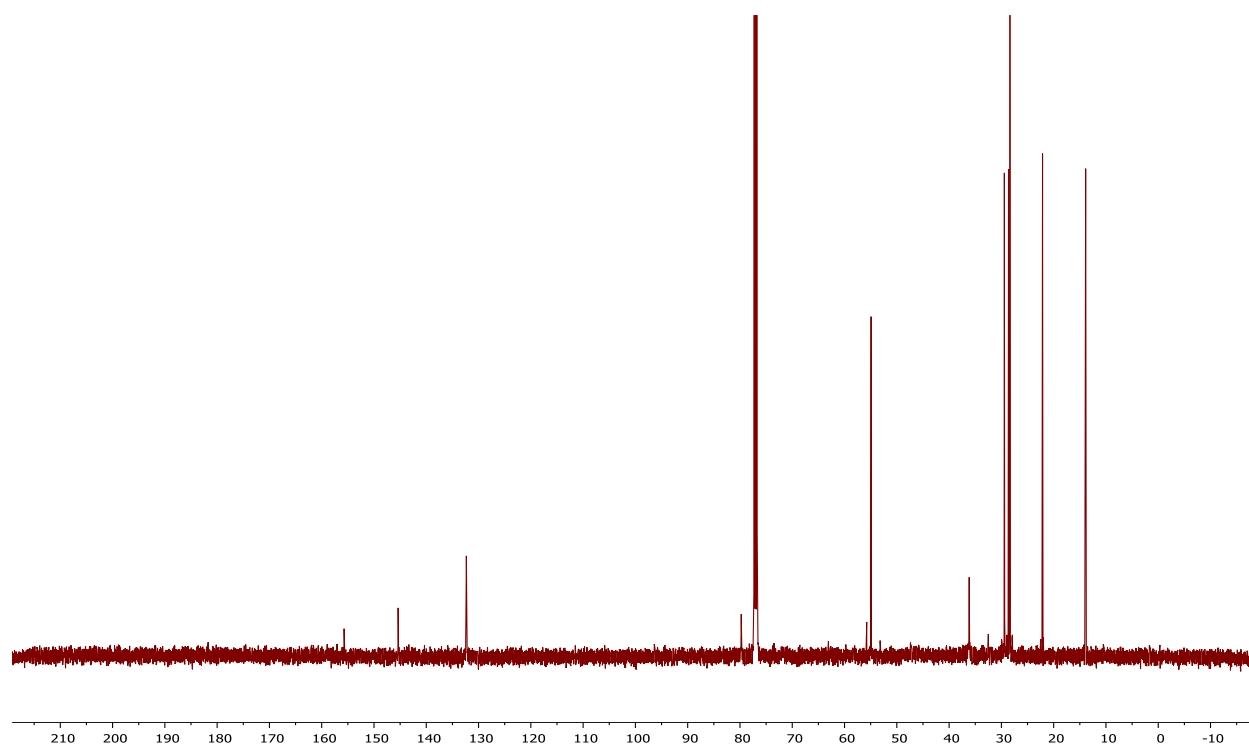
¹³C NMR of compound 4.10f



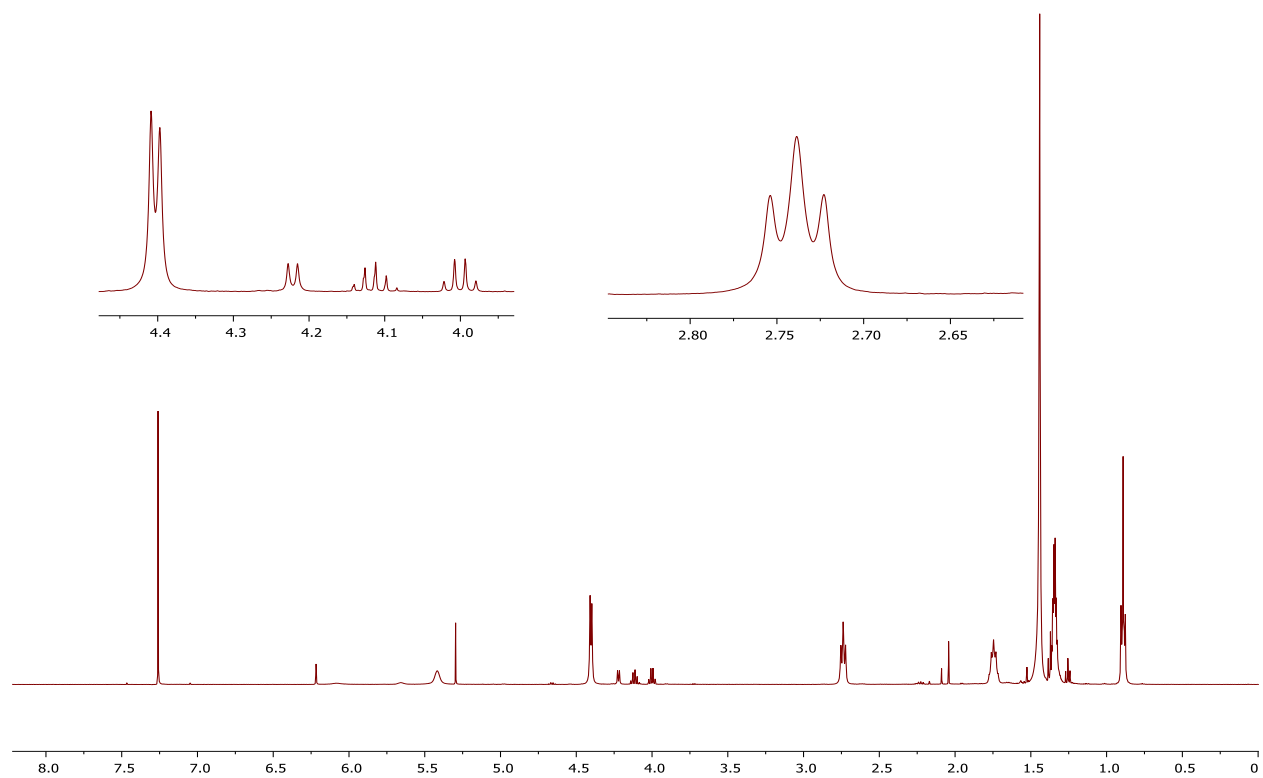
¹H NMR of compound 4.12



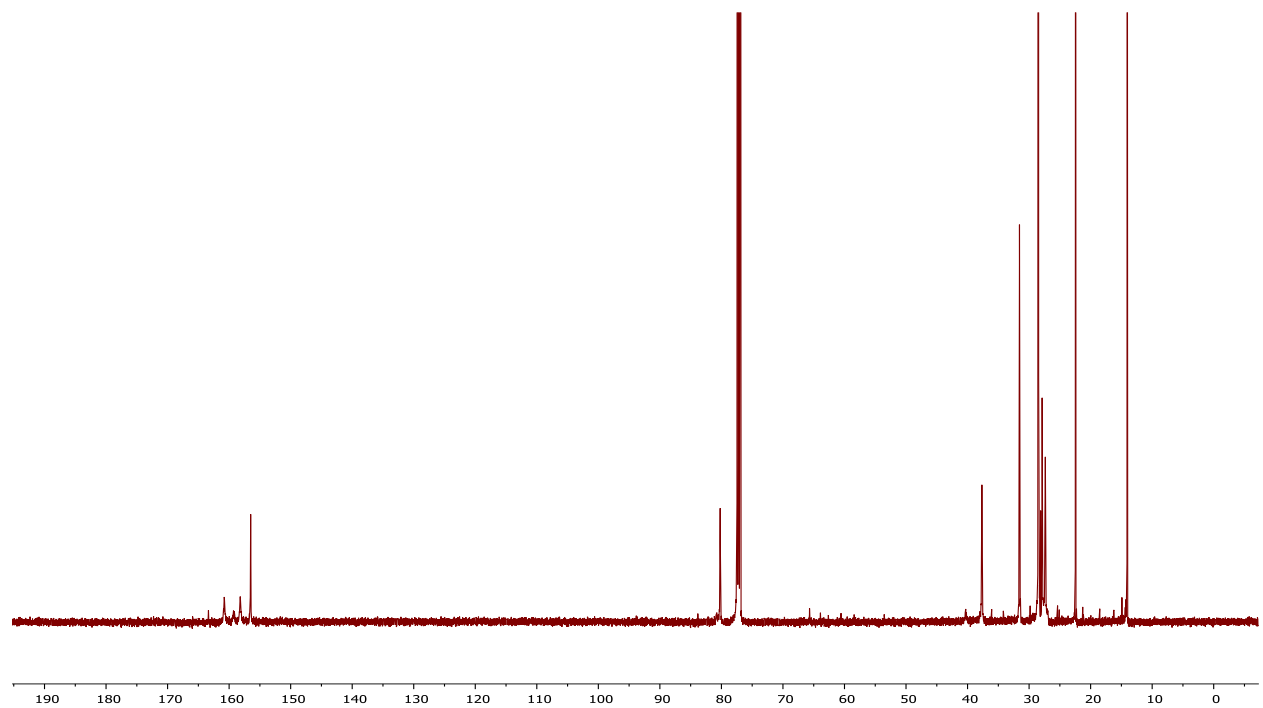
¹³C NMR of compound 4.12



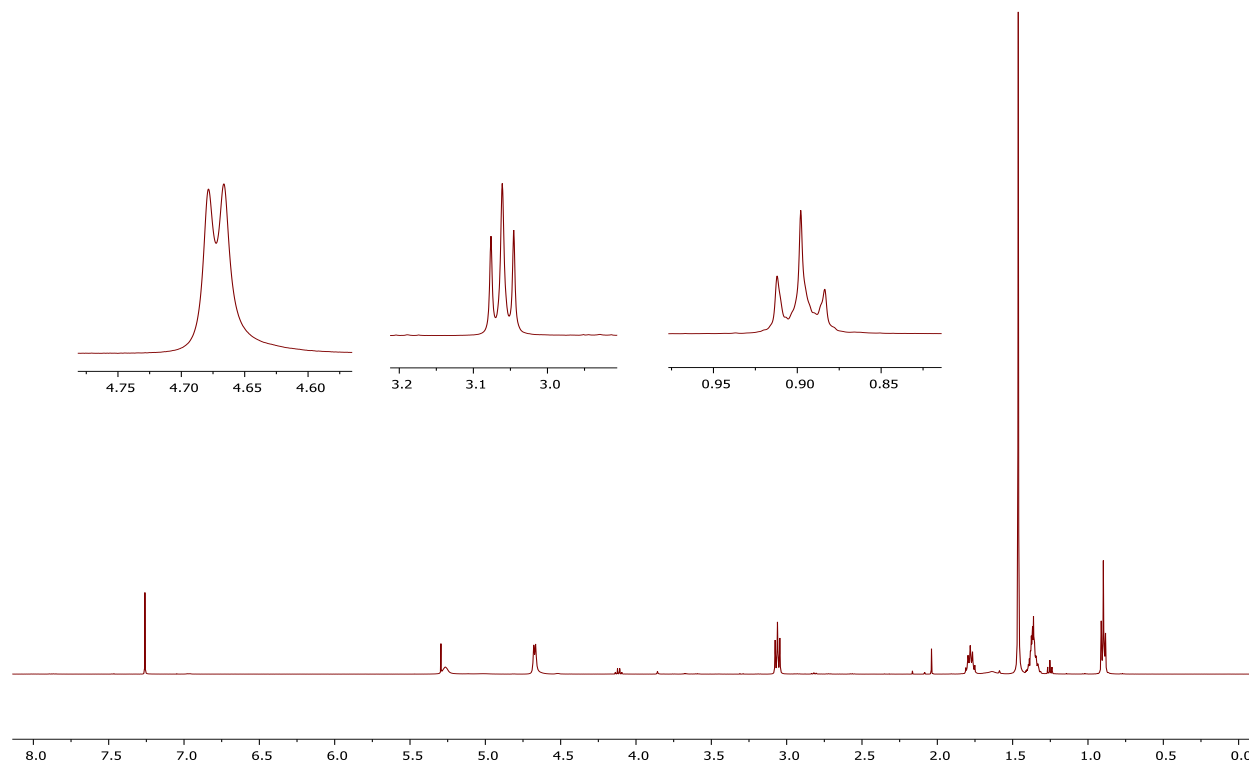
¹H NMR of compound 4.14



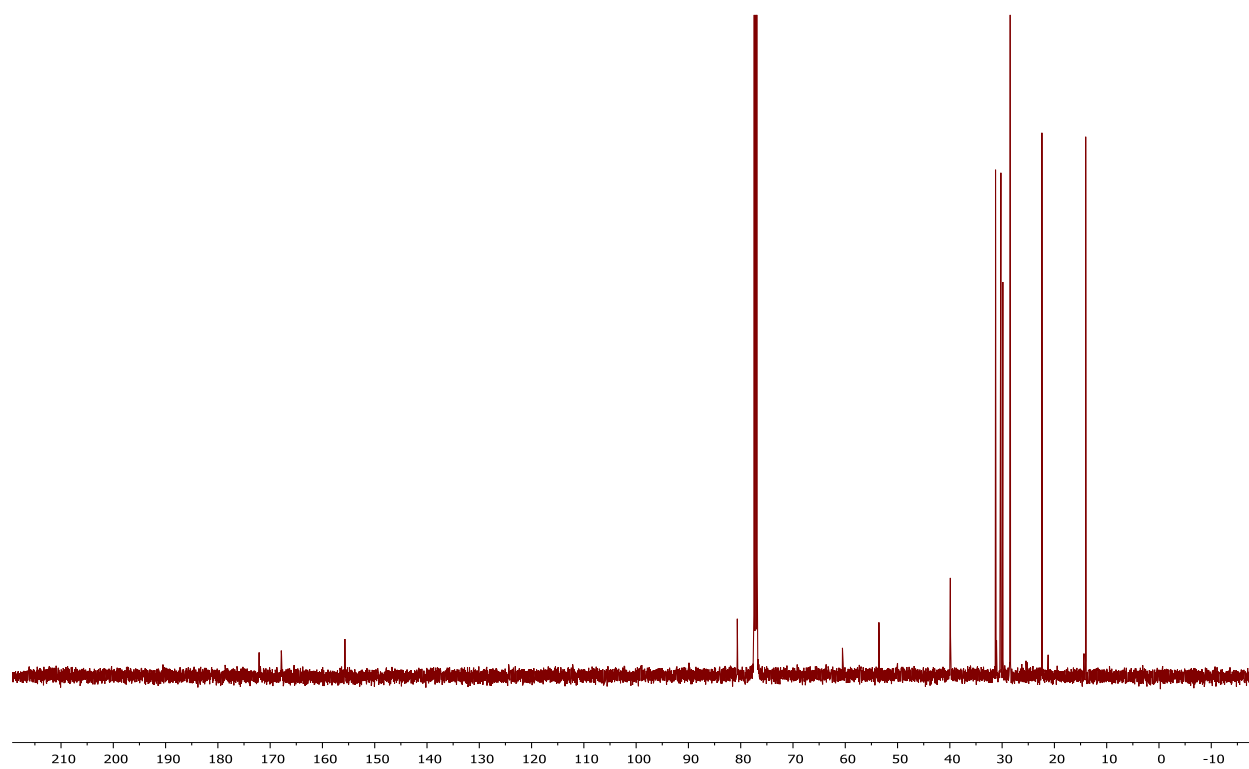
¹³C NMR of compound 4.14



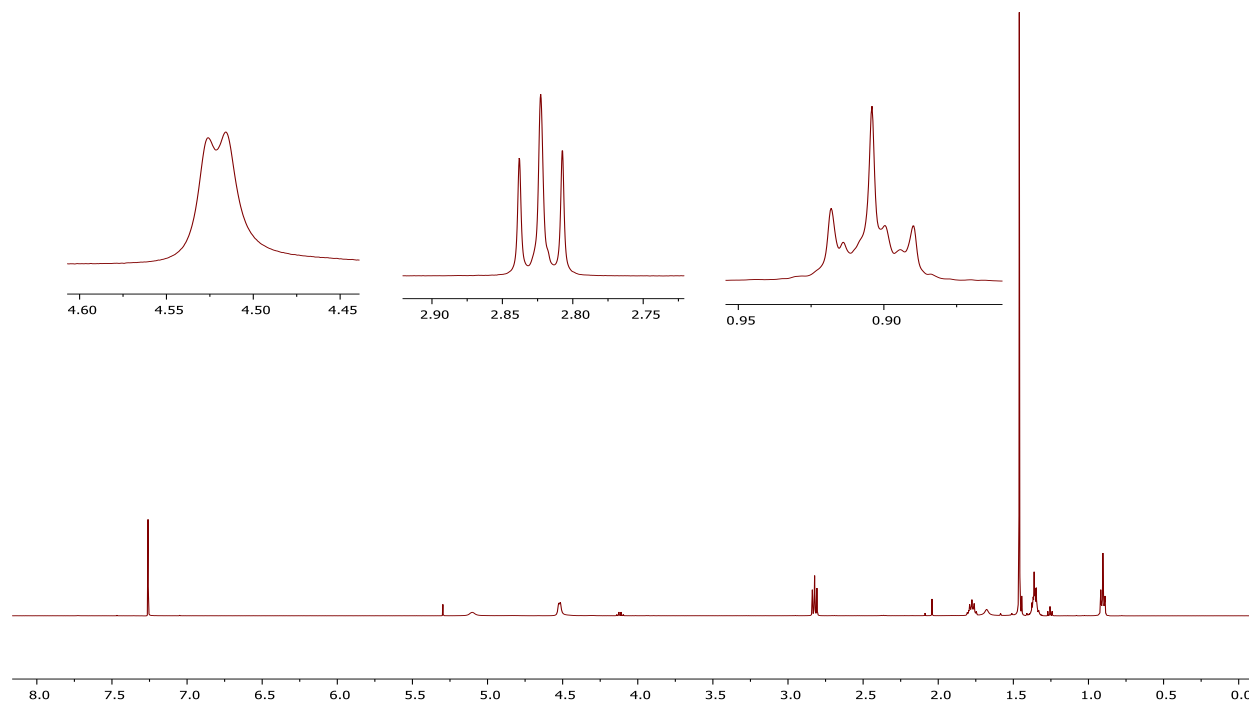
¹H NMR of compound 4.16



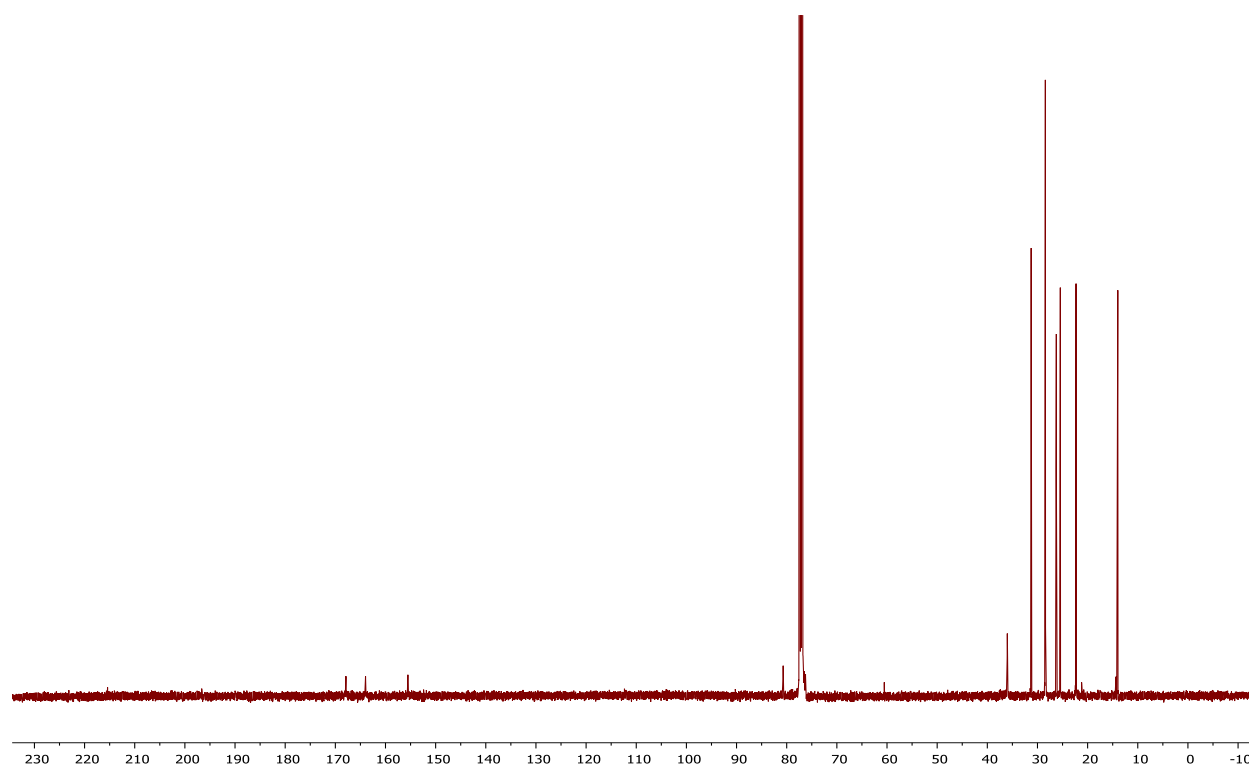
¹³C NMR of compound 4.16



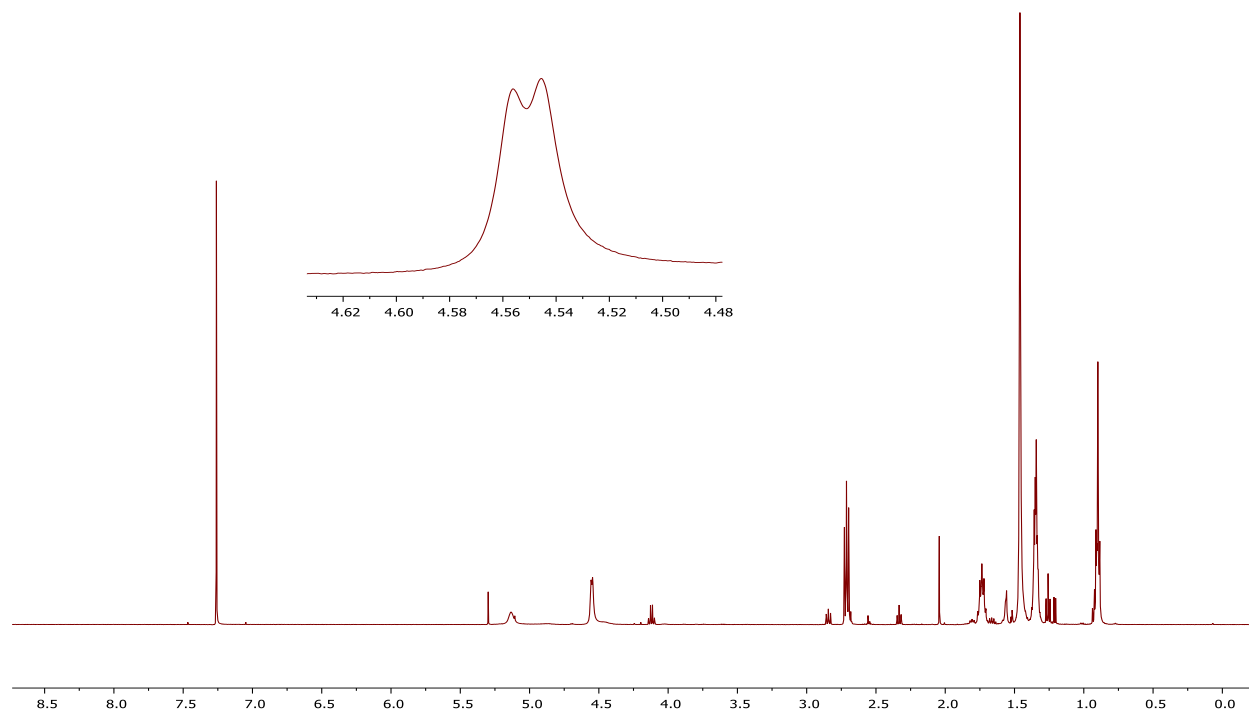
¹H NMR of compound 4.18



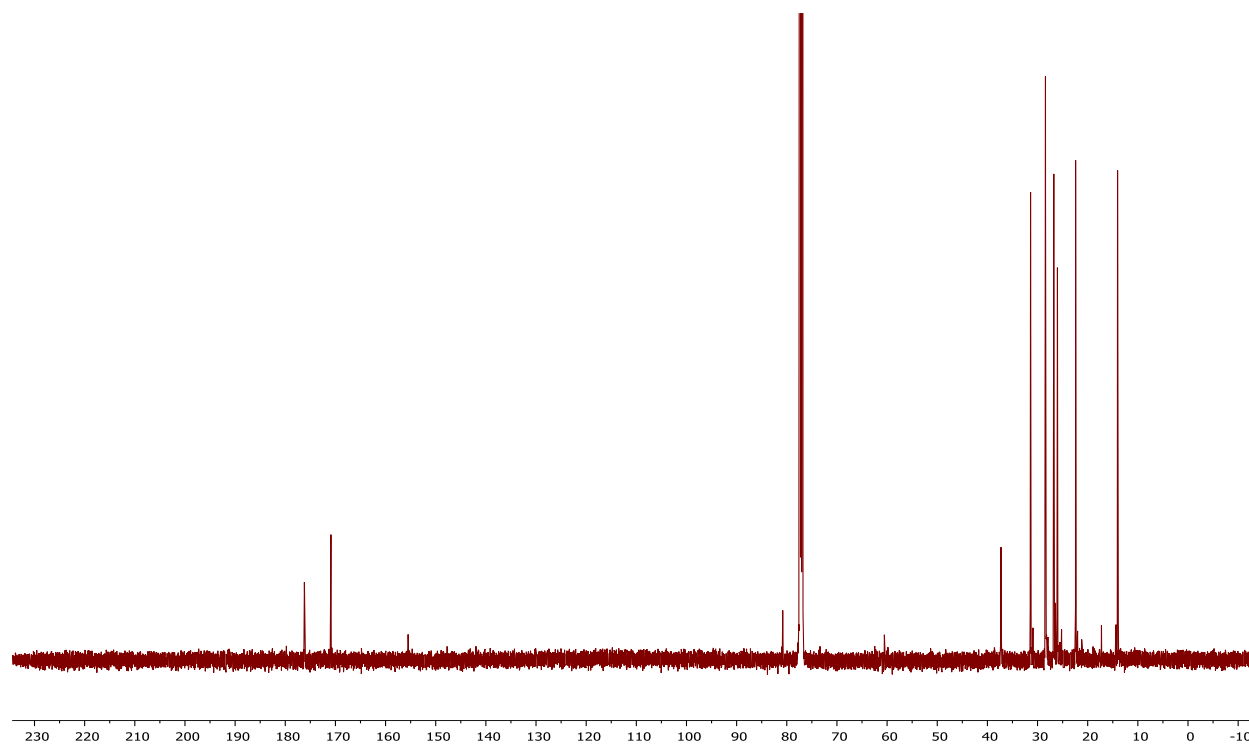
¹³C NMR of compound 4.18



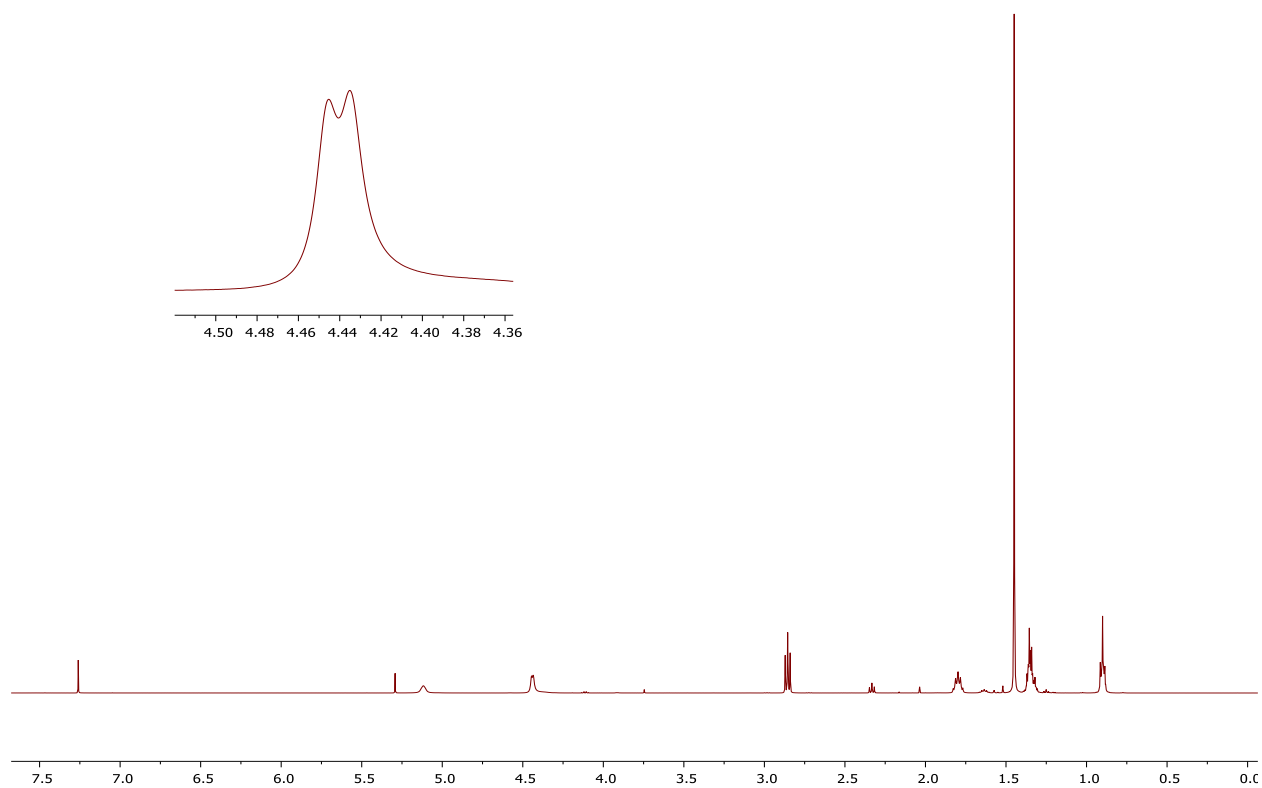
¹H NMR of compound 4.20k



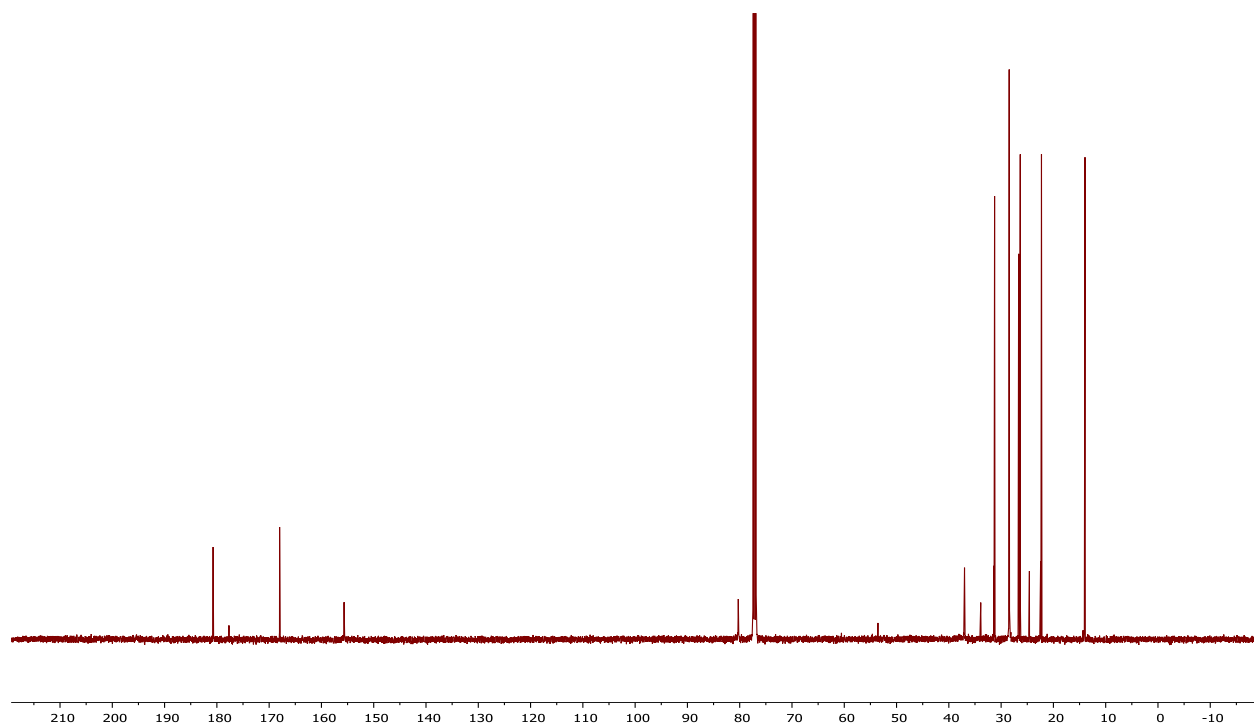
¹³C NMR of compound 4.20k



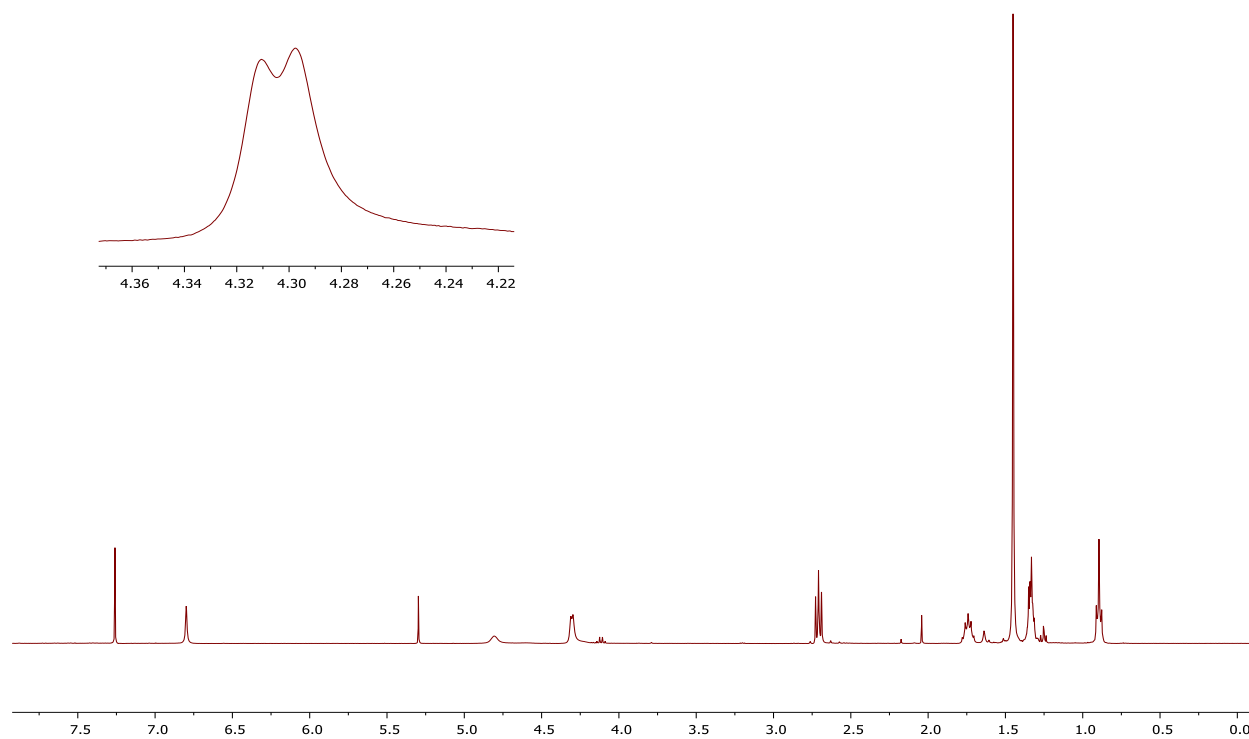
¹H NMR of compound 4.20I



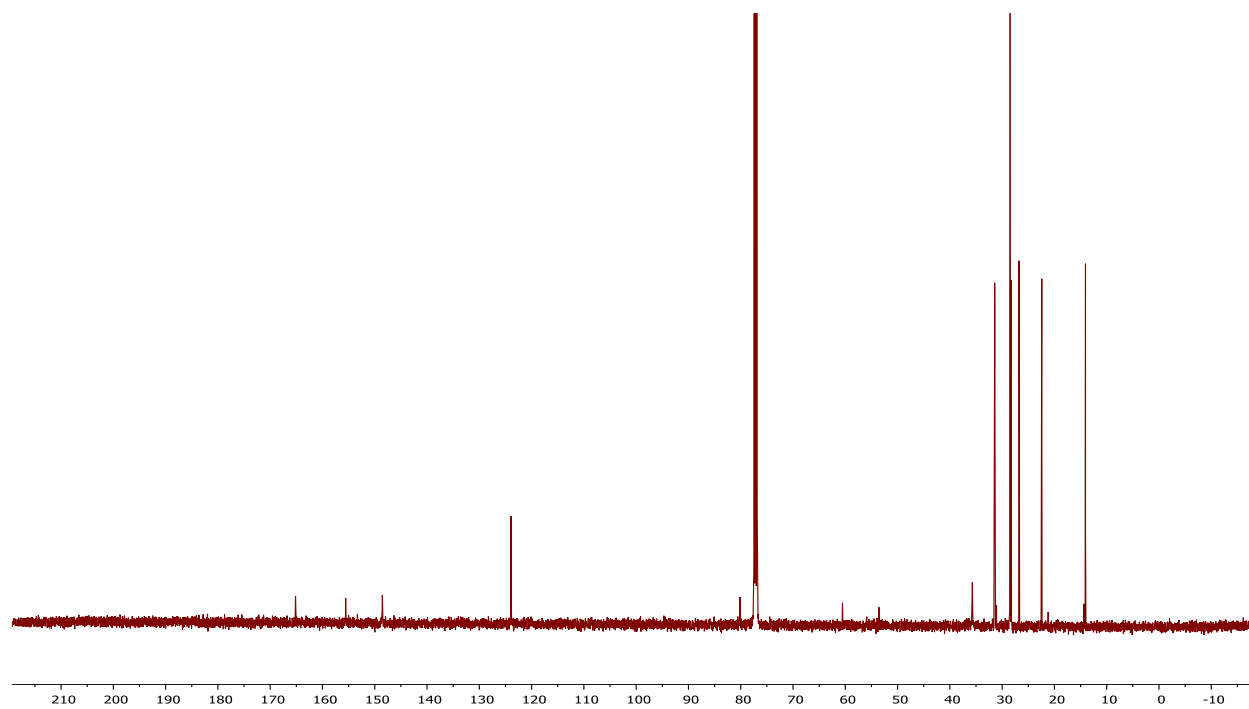
¹³C NMR of compound 4.20I



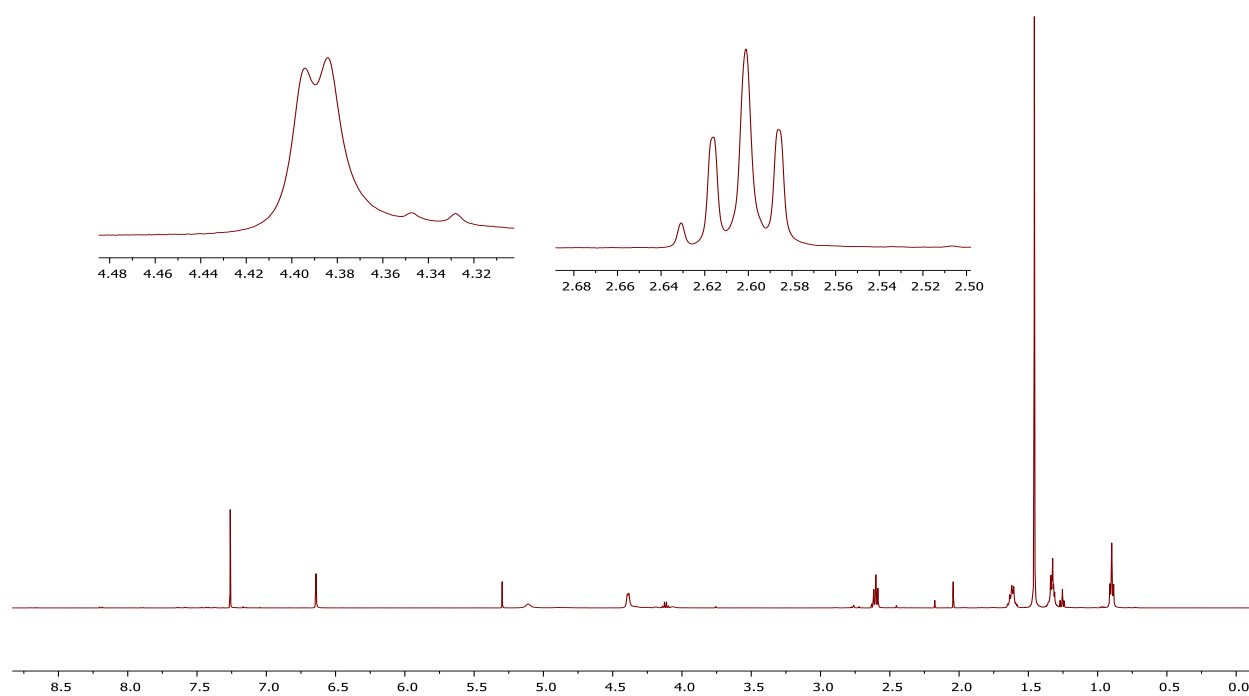
¹H NMR of compound 4.21m



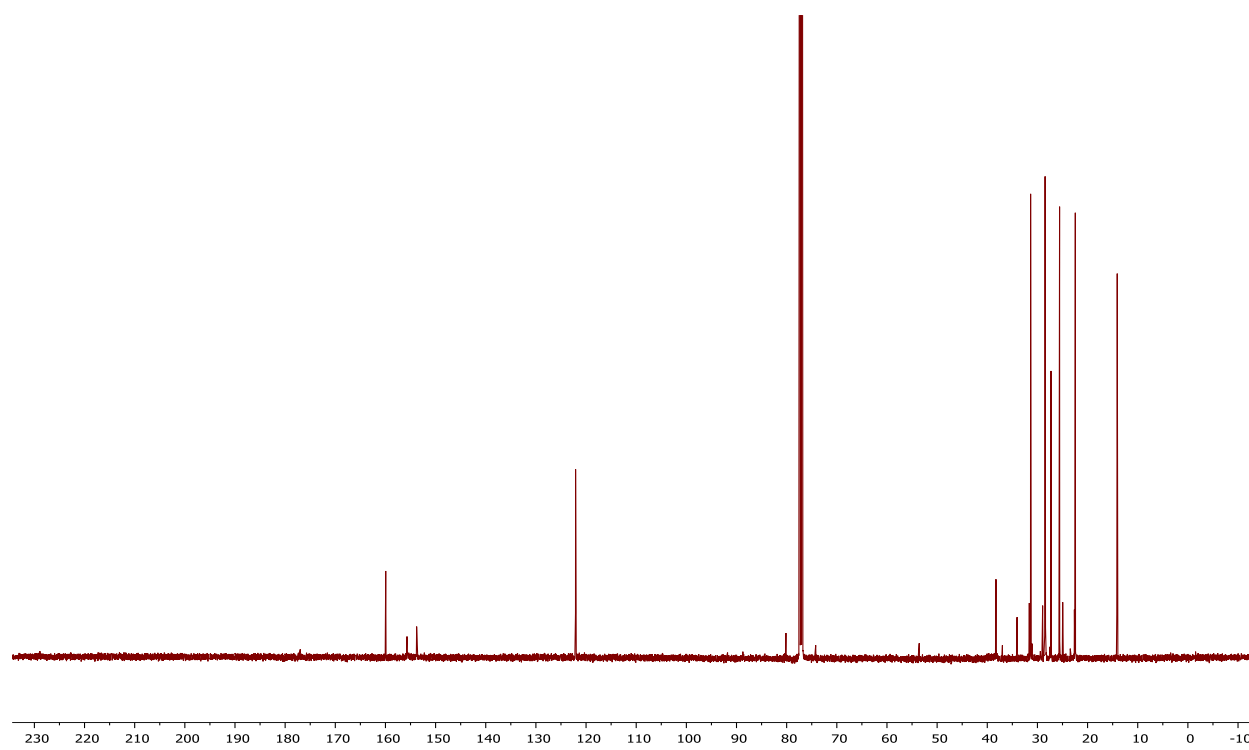
¹³C NMR of compound 4.21m



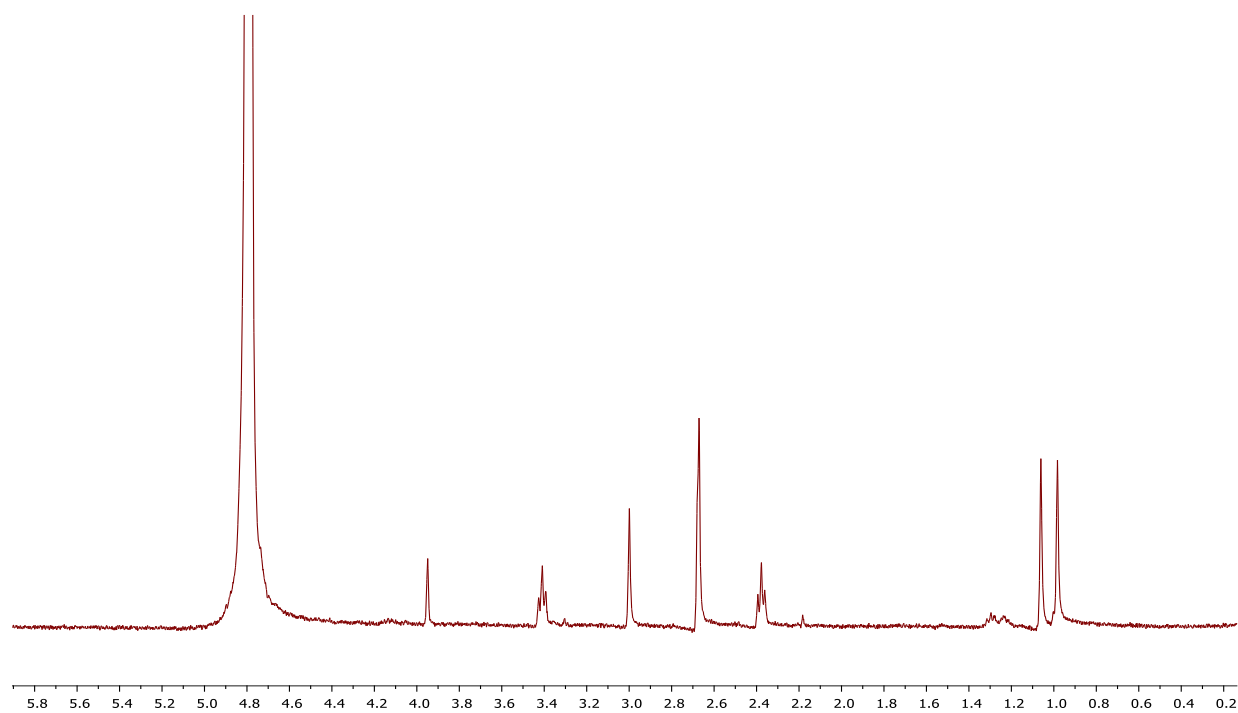
¹H NMR of compound 4.21n



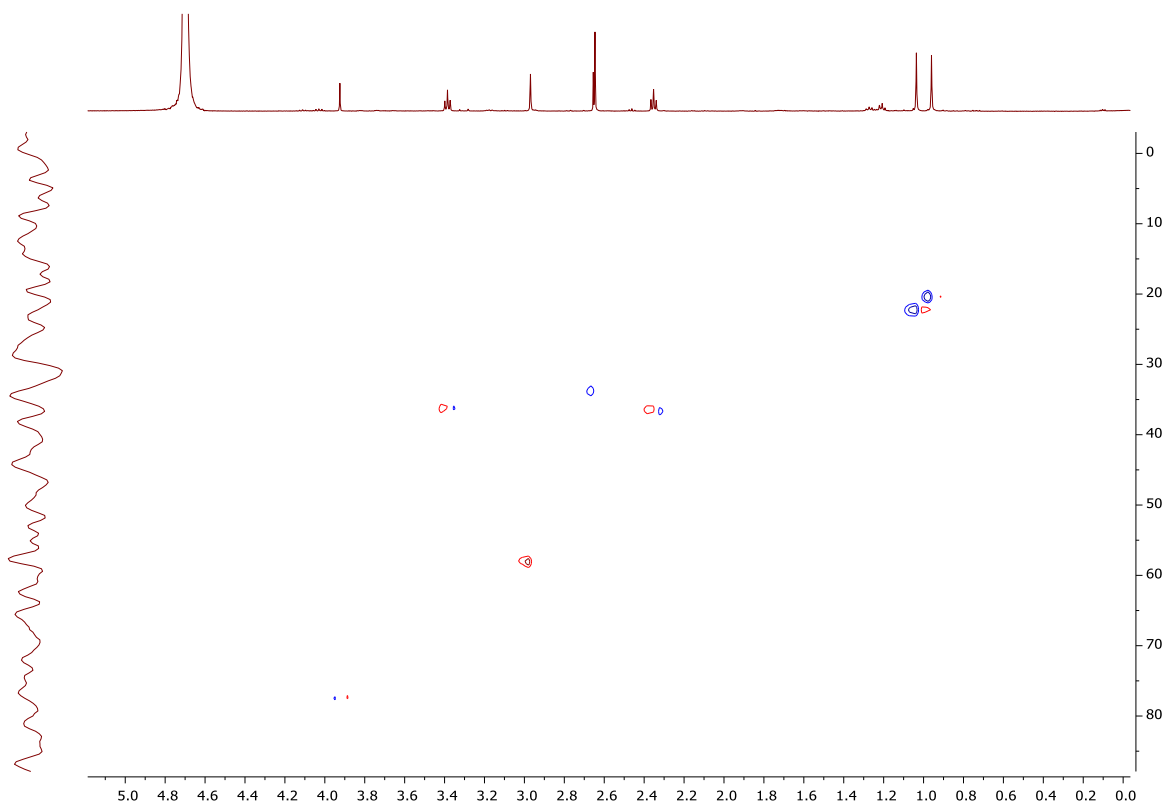
¹³C NMR of compound 4.21n



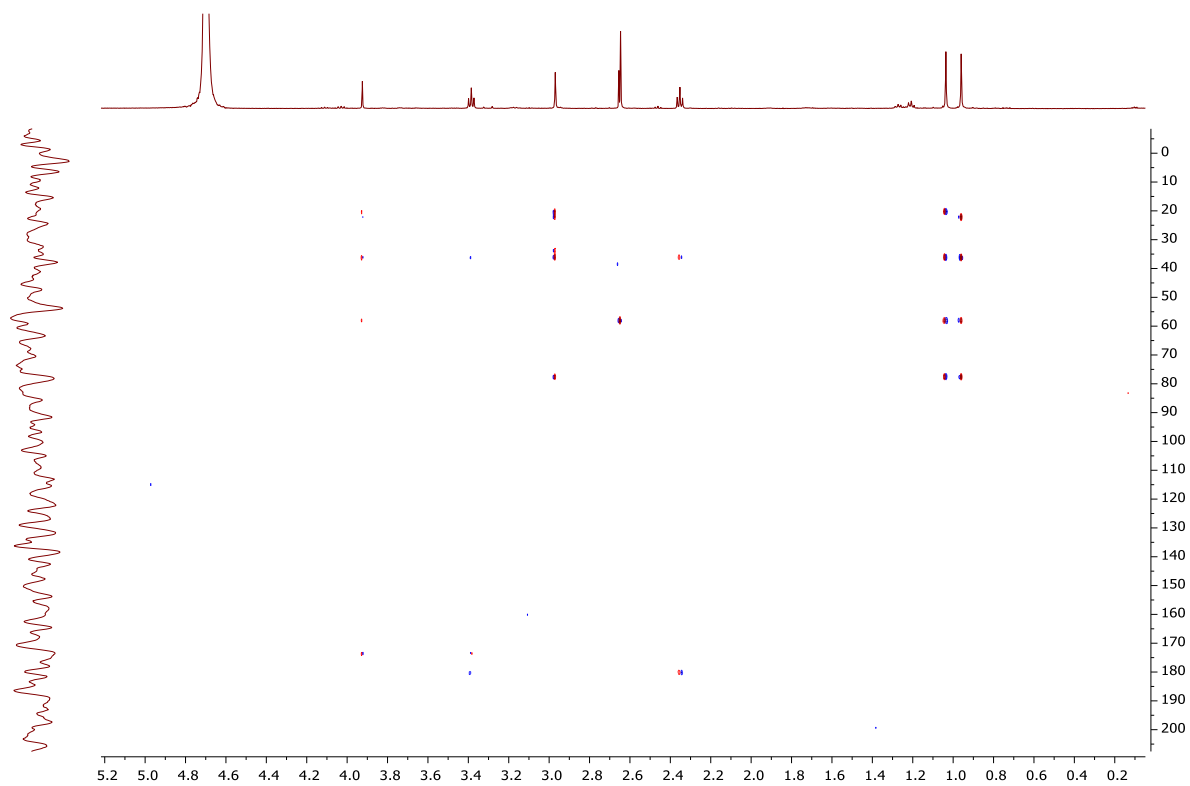
¹H NMR of compound 5.1a



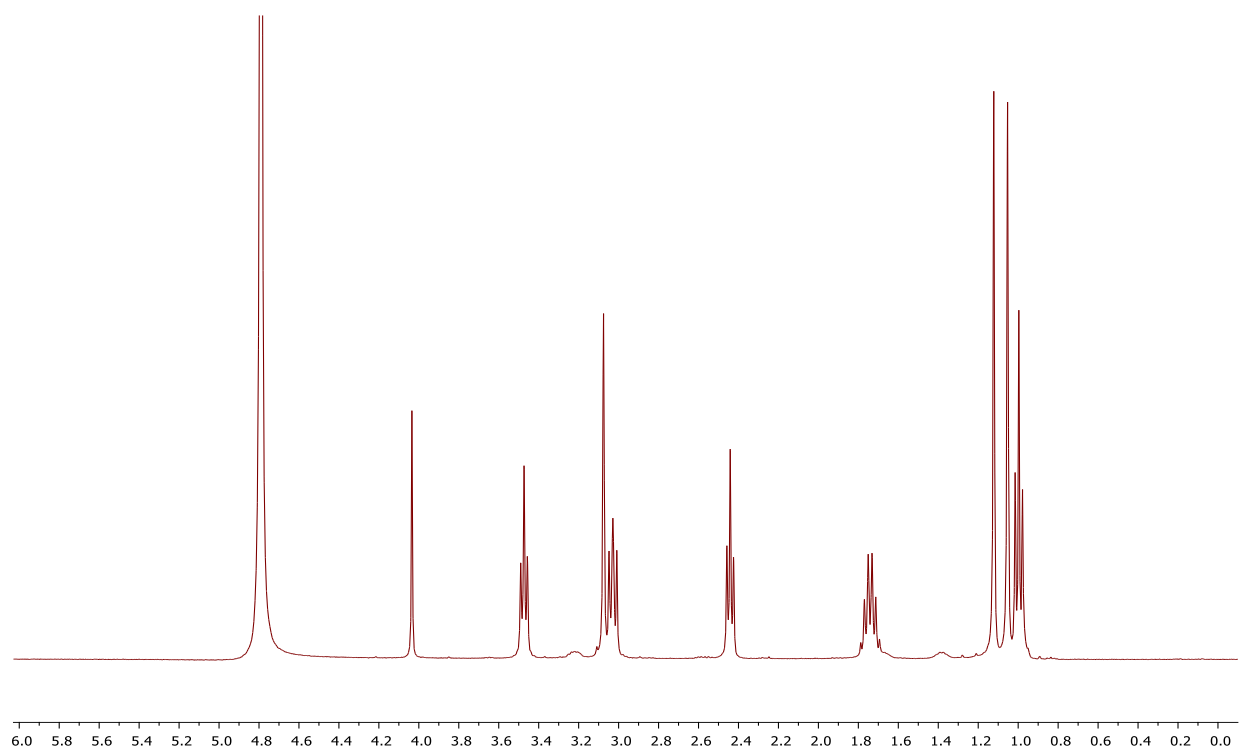
HSQC of compound 5.1a



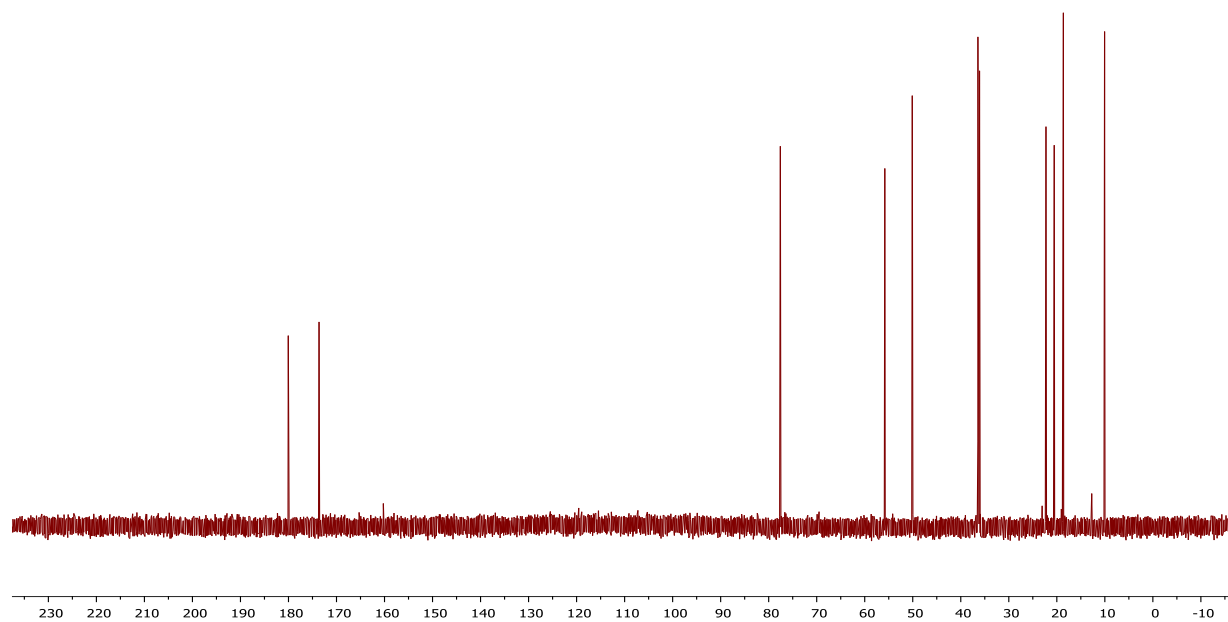
HMBC of compound 5.1a



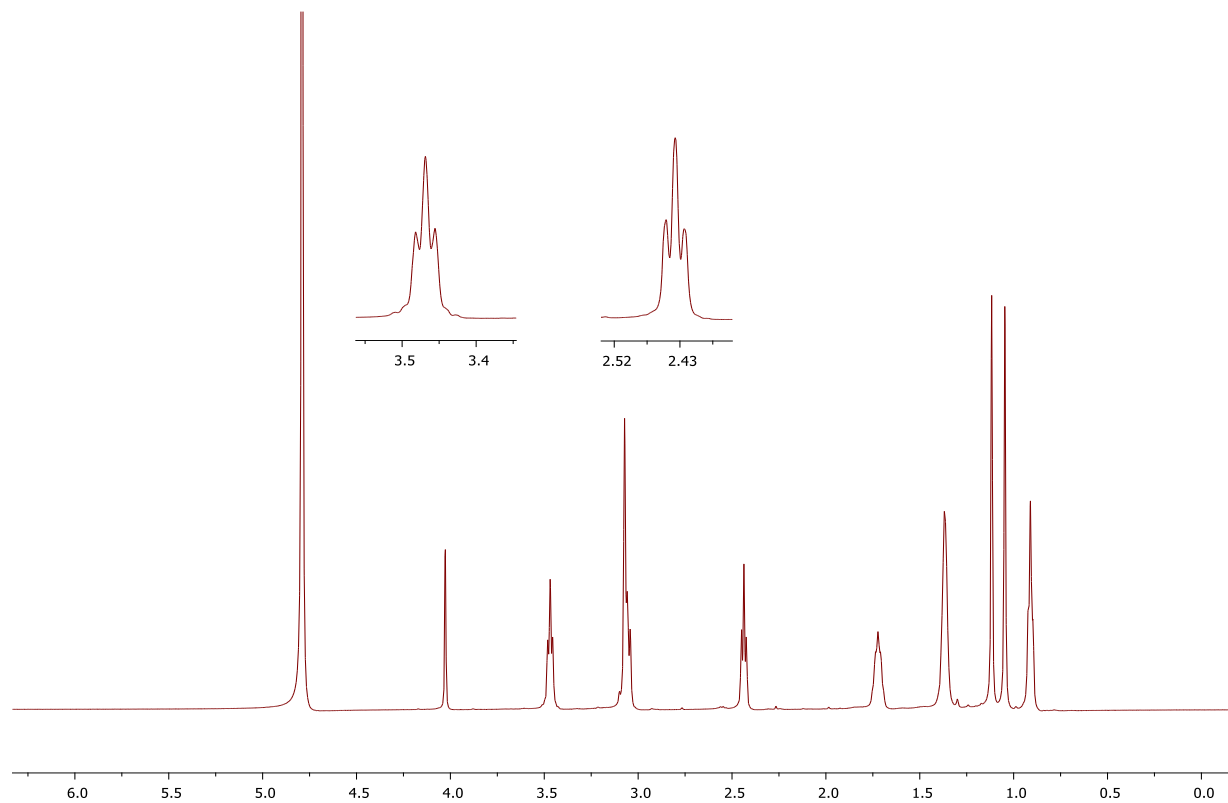
^1H NMR of compound 5.1b



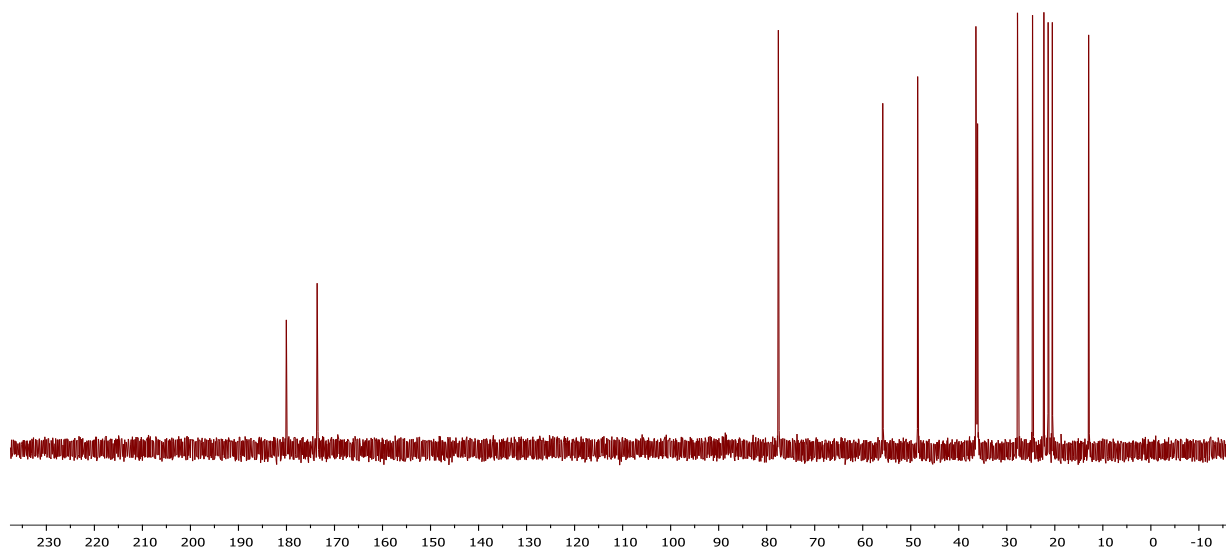
¹³C NMR of compound 5.1b



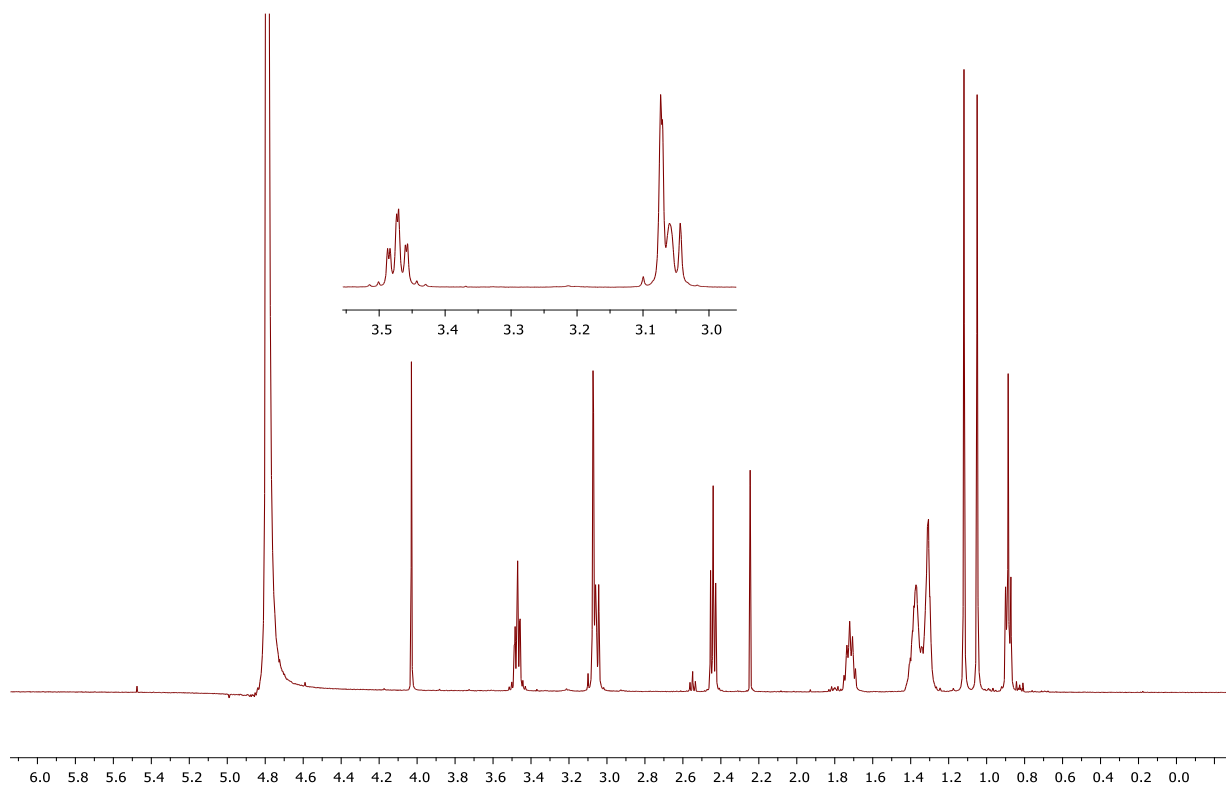
¹H NMR of compound 5.1c



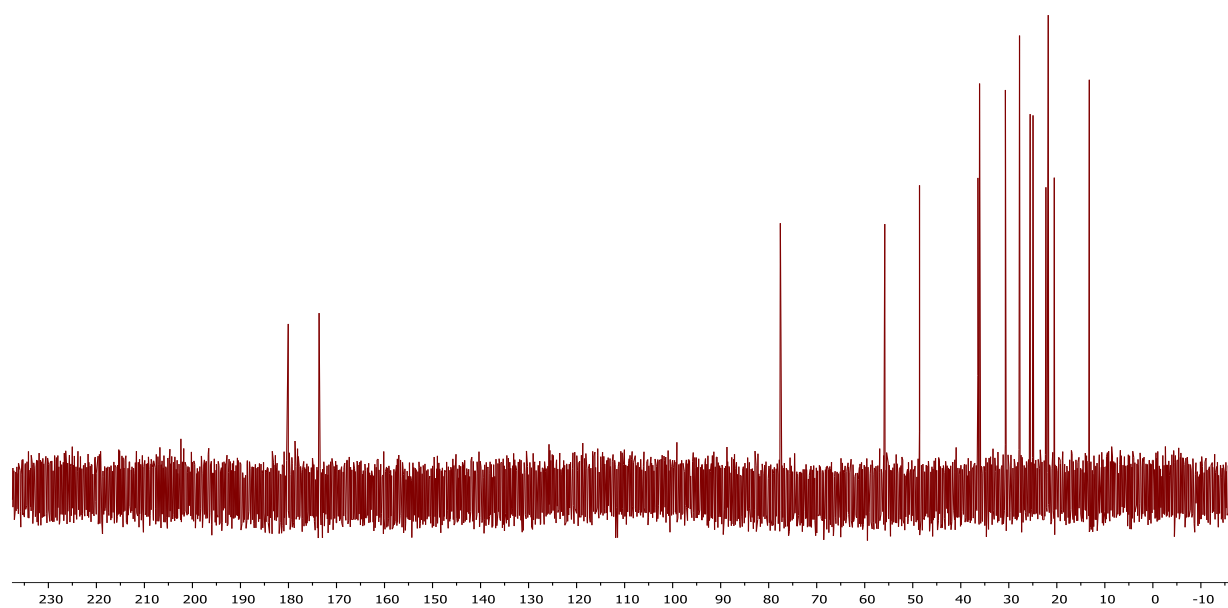
¹³C NMR of compound 5.1c



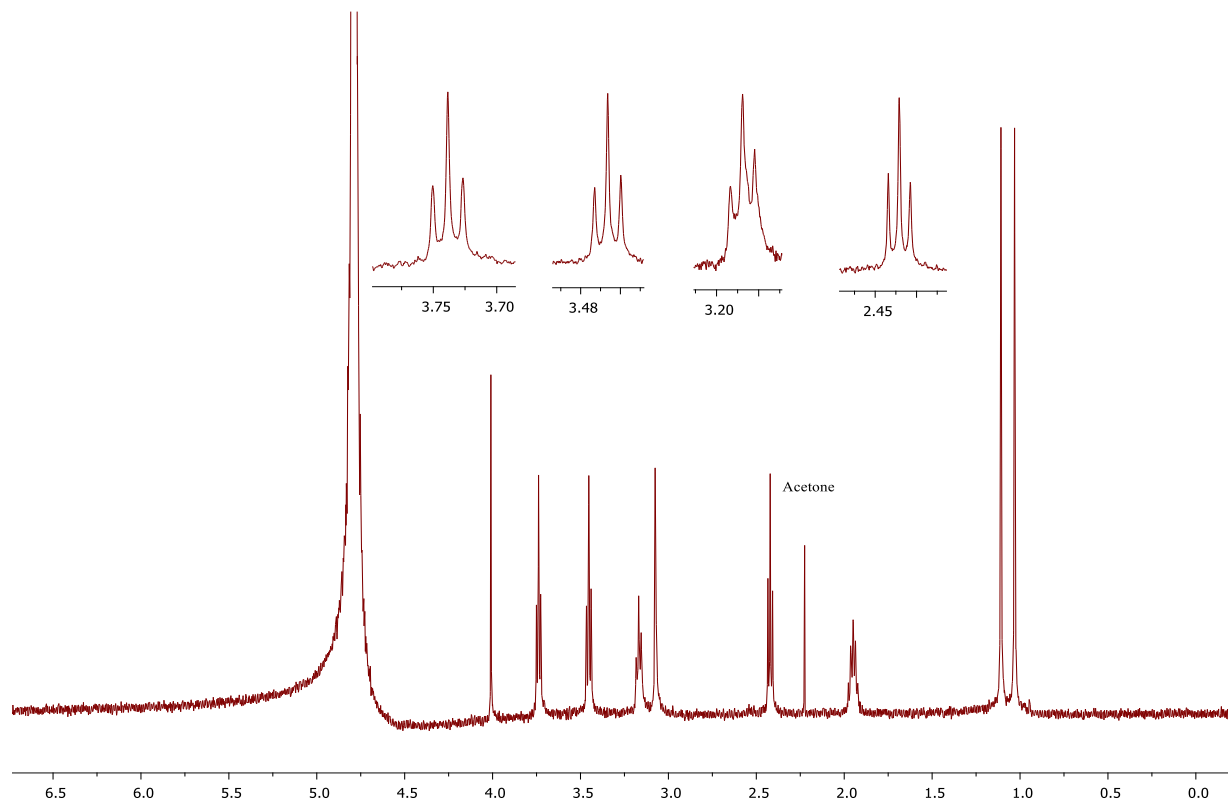
¹H NMR of compound 5.1d



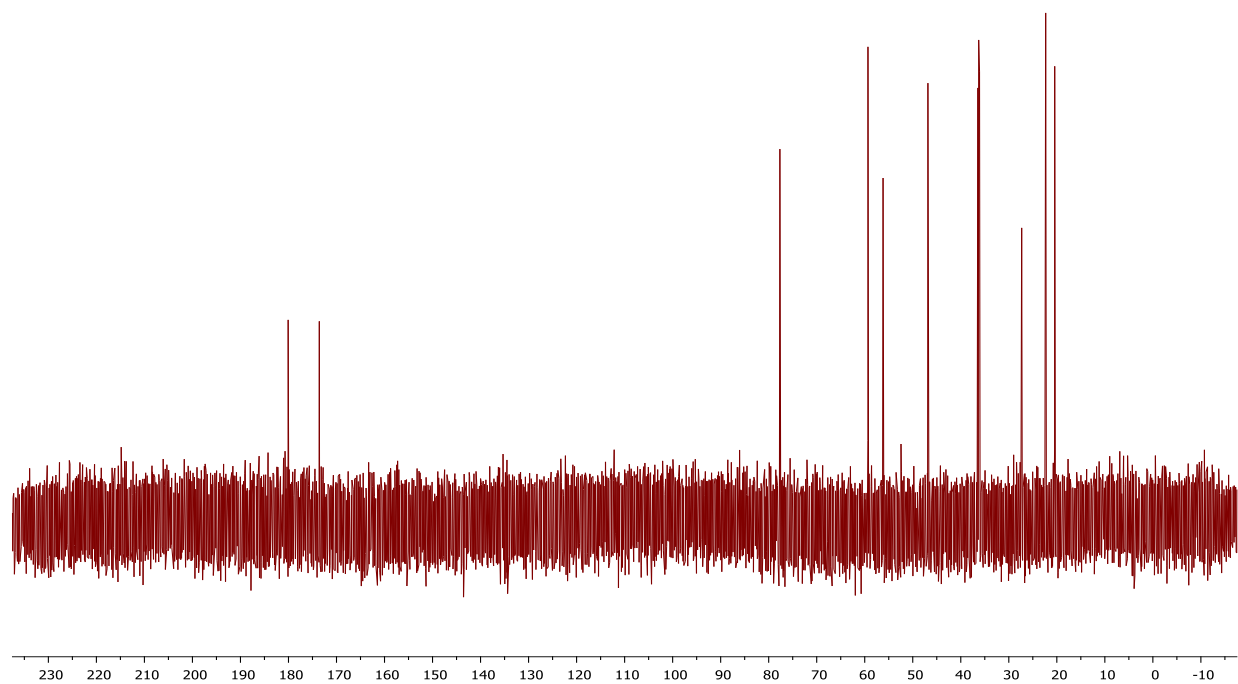
¹³C NMR of compound 5.1d



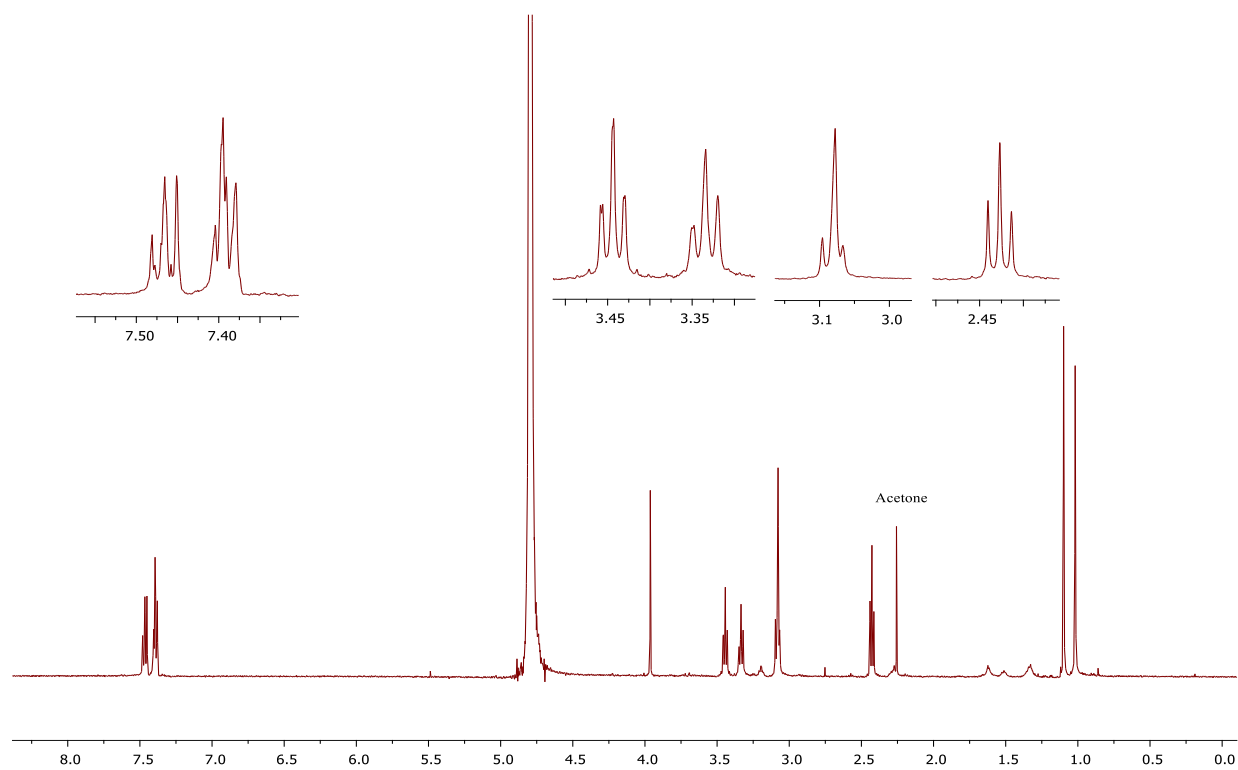
¹H NMR of compound 5.1e



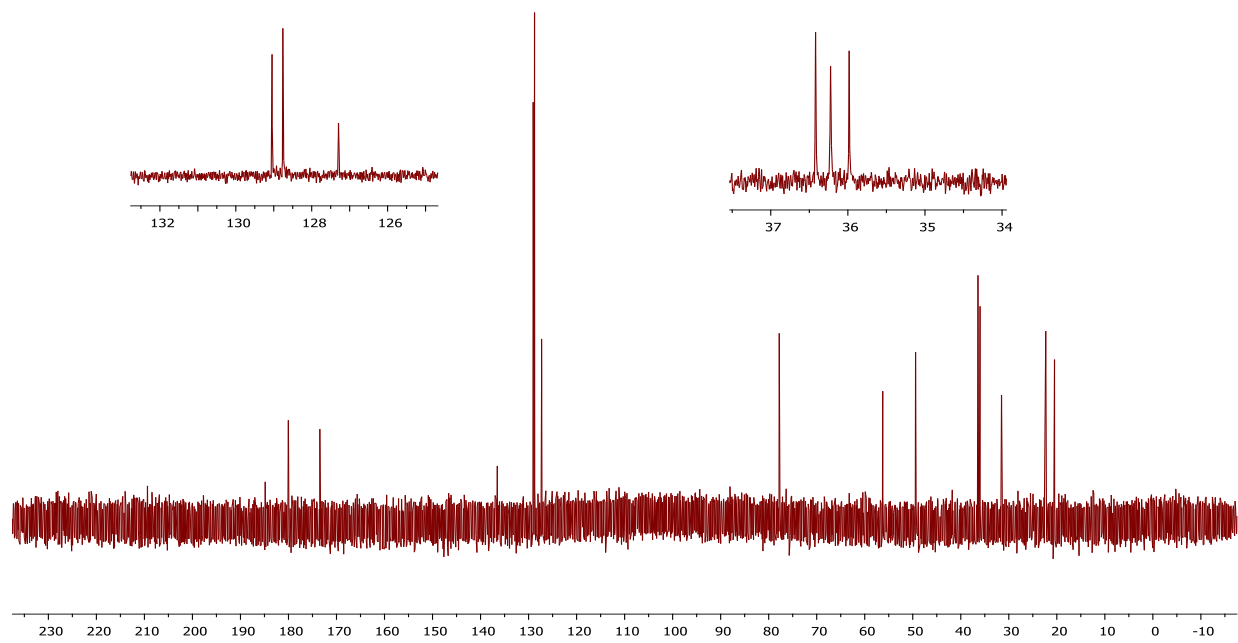
^{13}C NMR of compound 5.1e



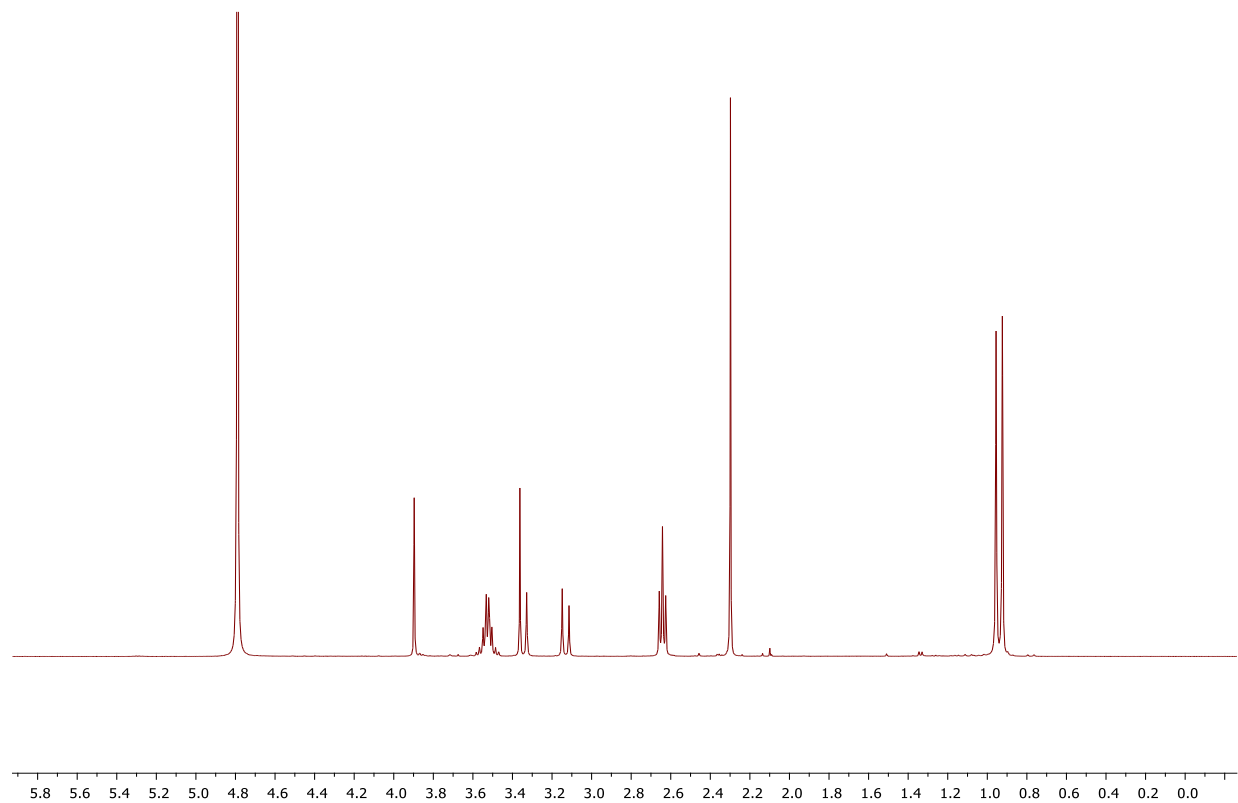
^1H NMR of compound 5.1f



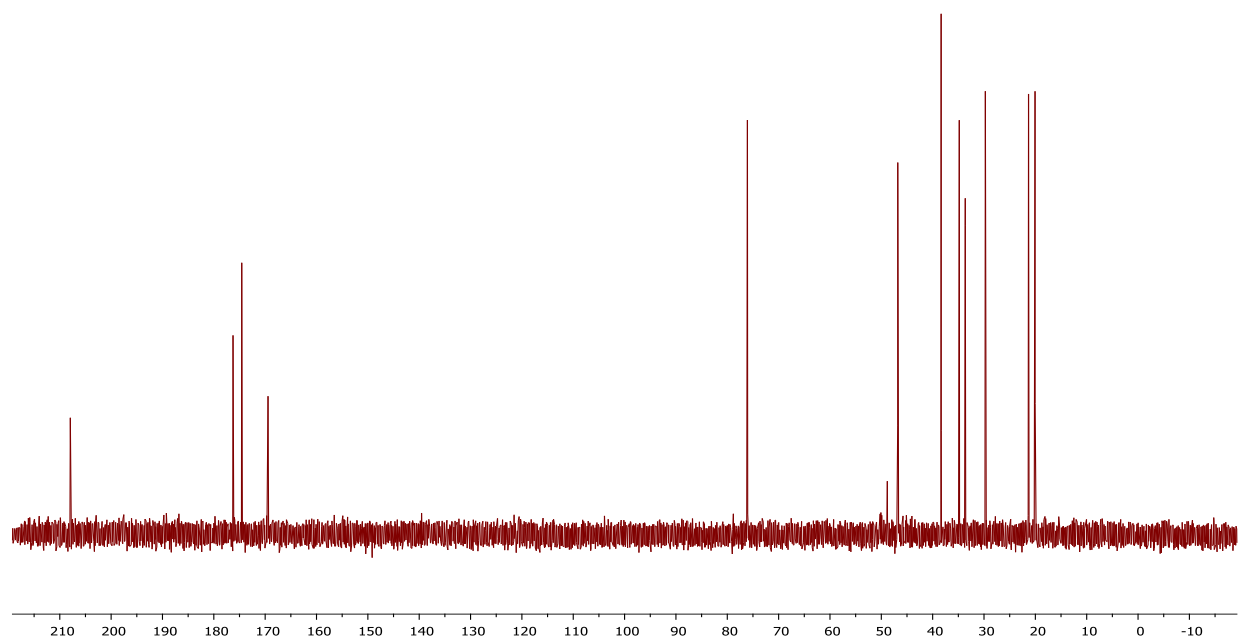
¹³C NMR of compound 5.1f



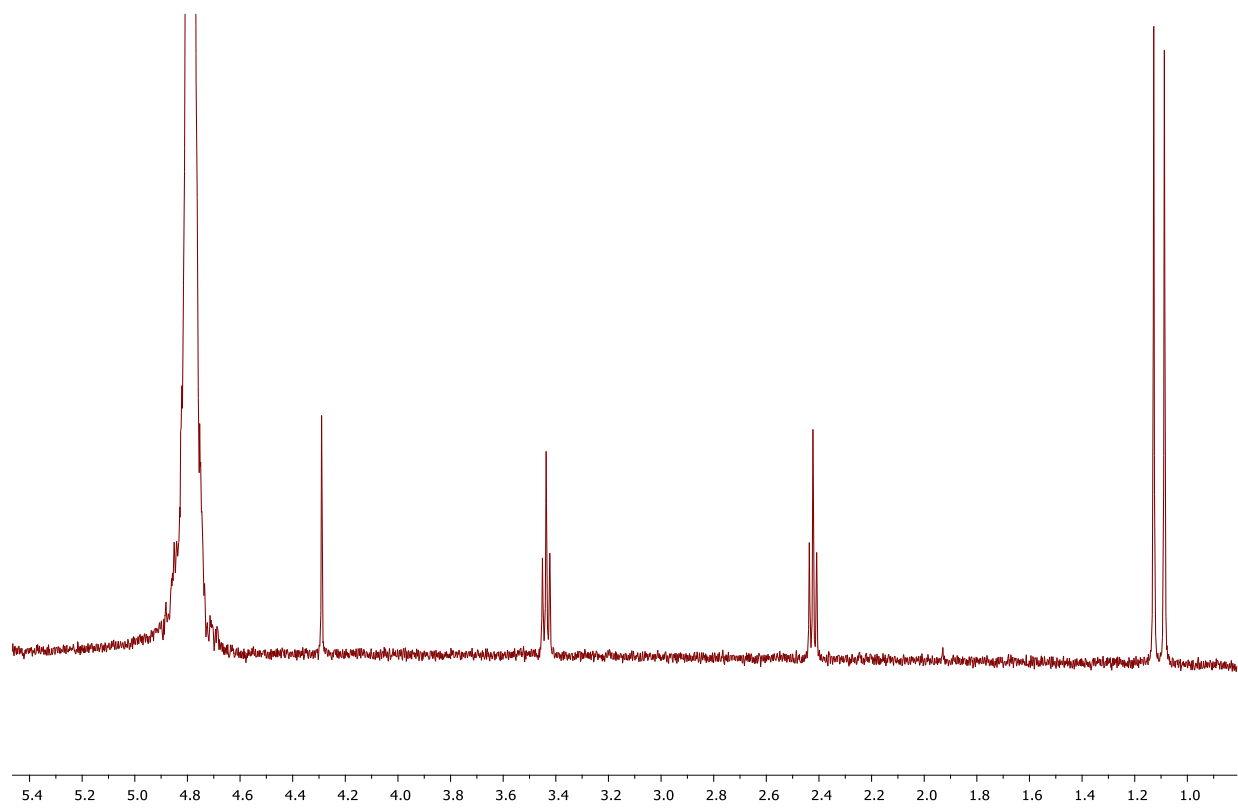
¹H NMR of compound 5.1g



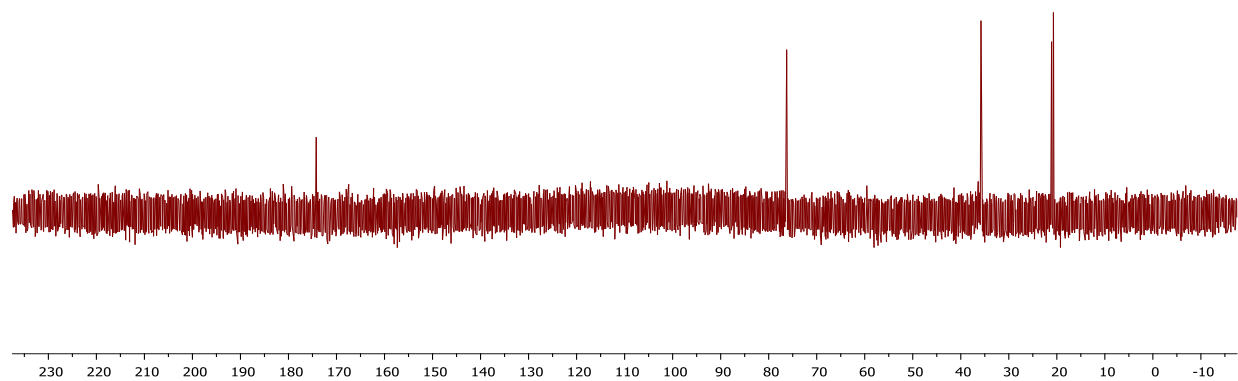
¹³C NMR of compound 5.1g



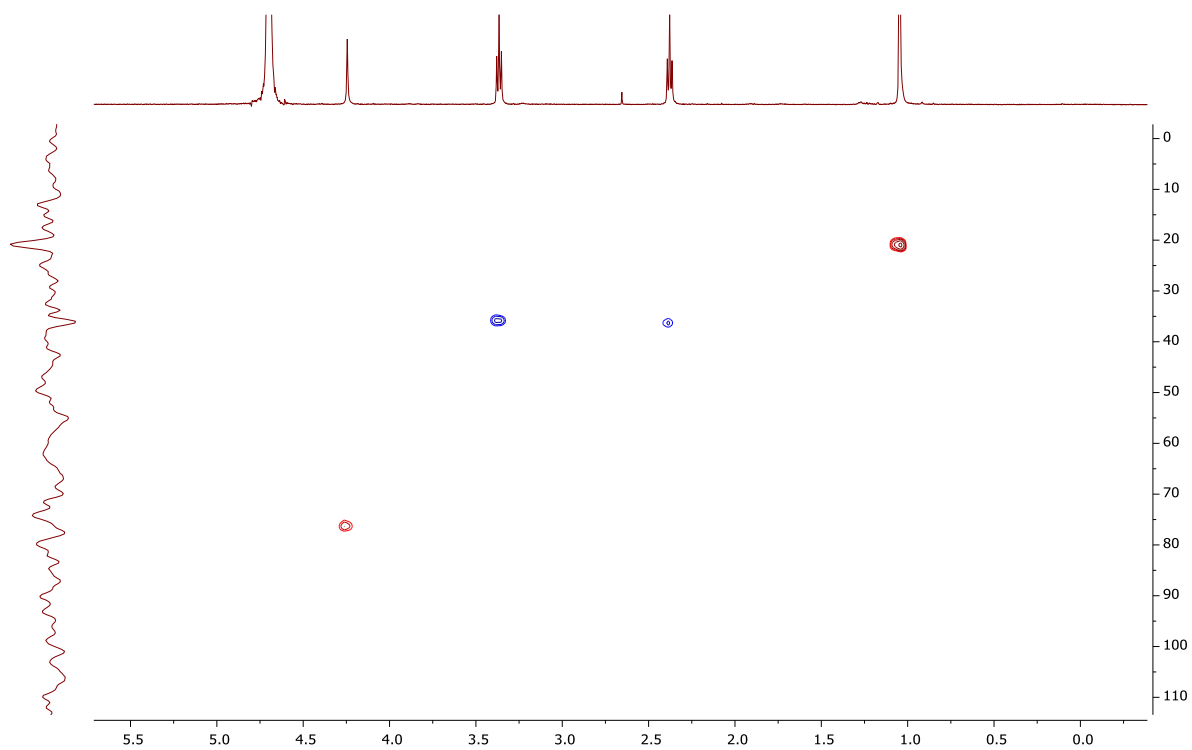
¹H NMR of compound 5.1h



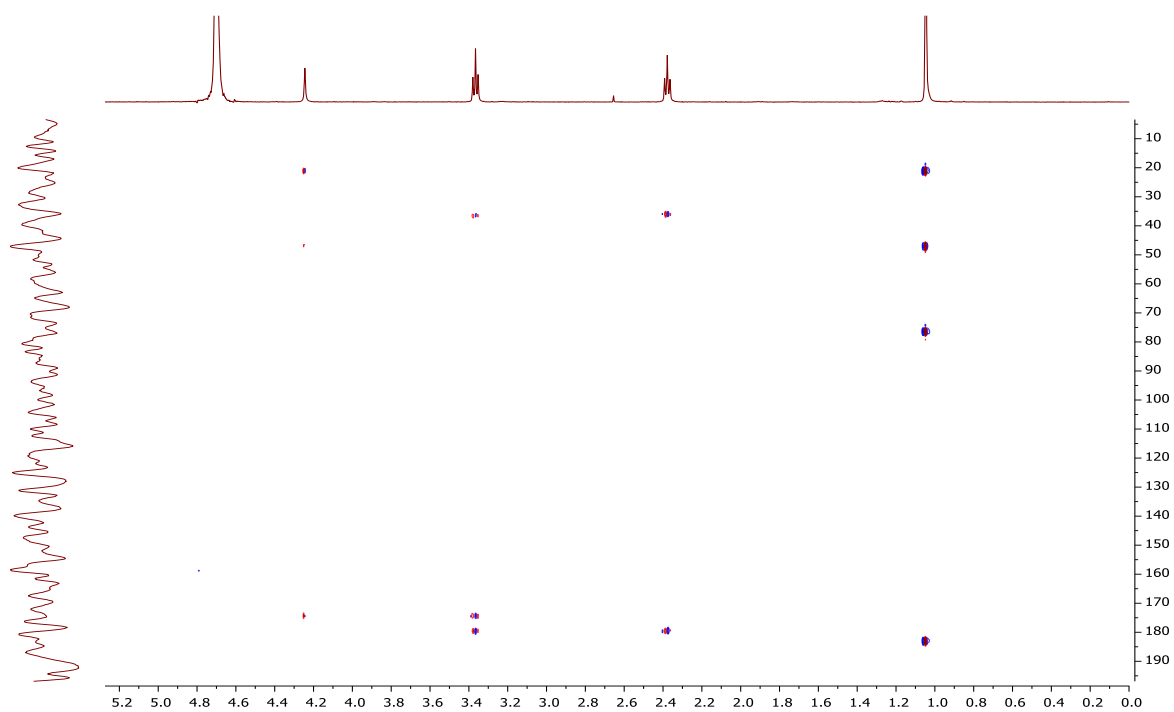
^{13}C NMR of compound 5.1h



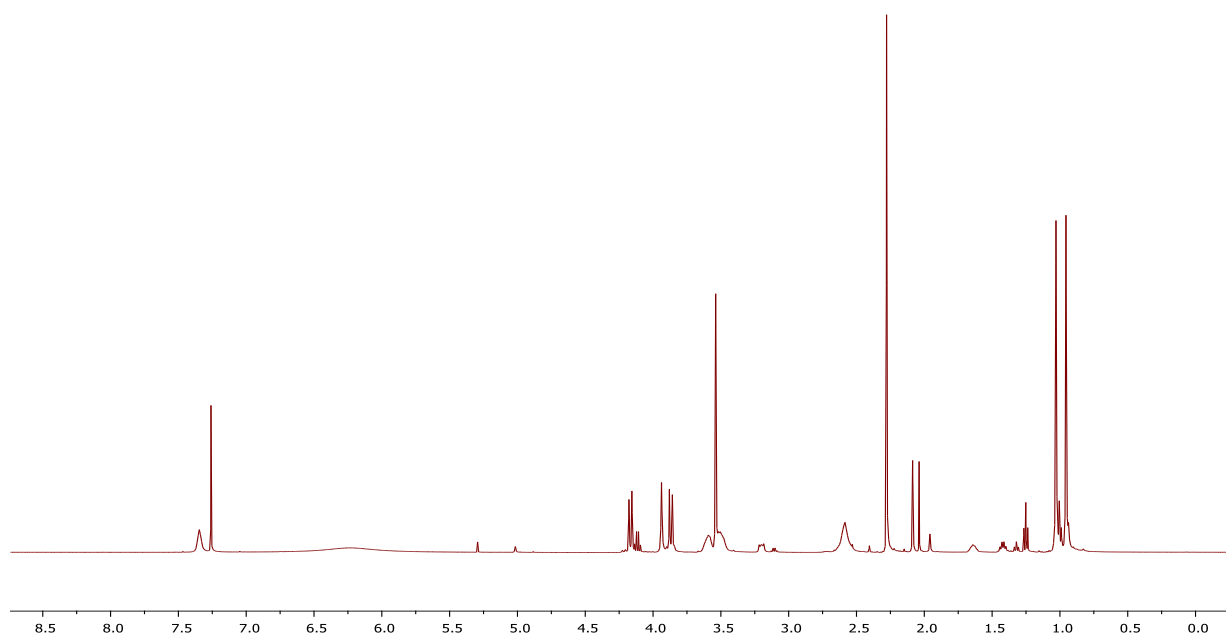
HSQC of compound 5.1h



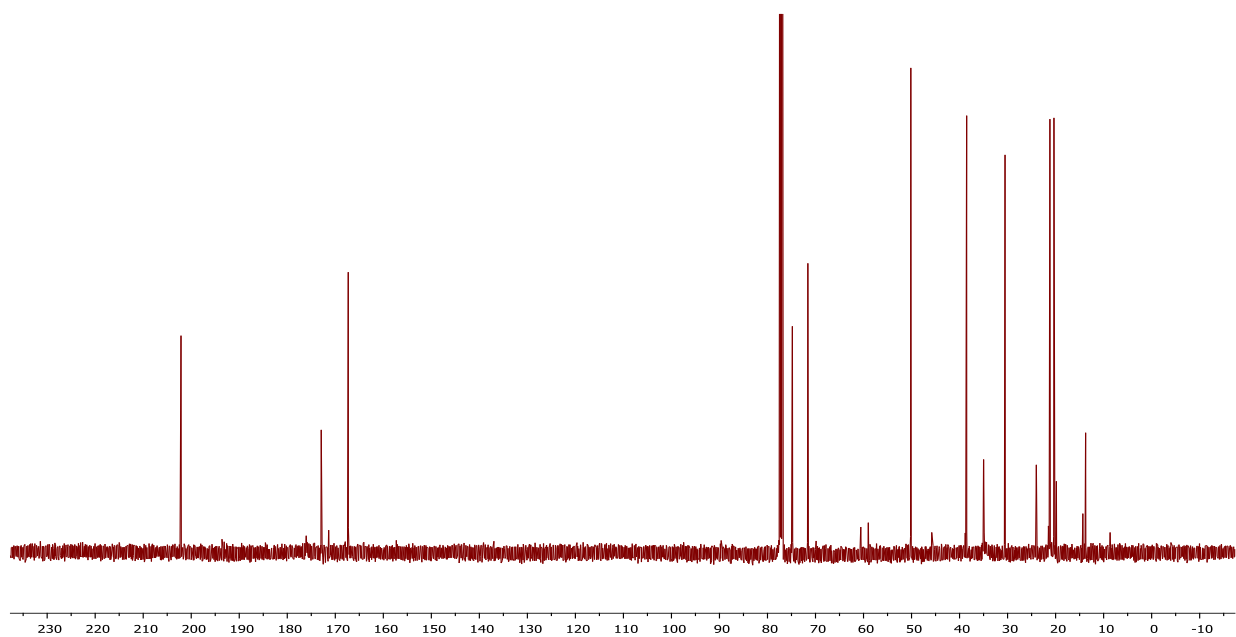
HMBC of compound 5.1h



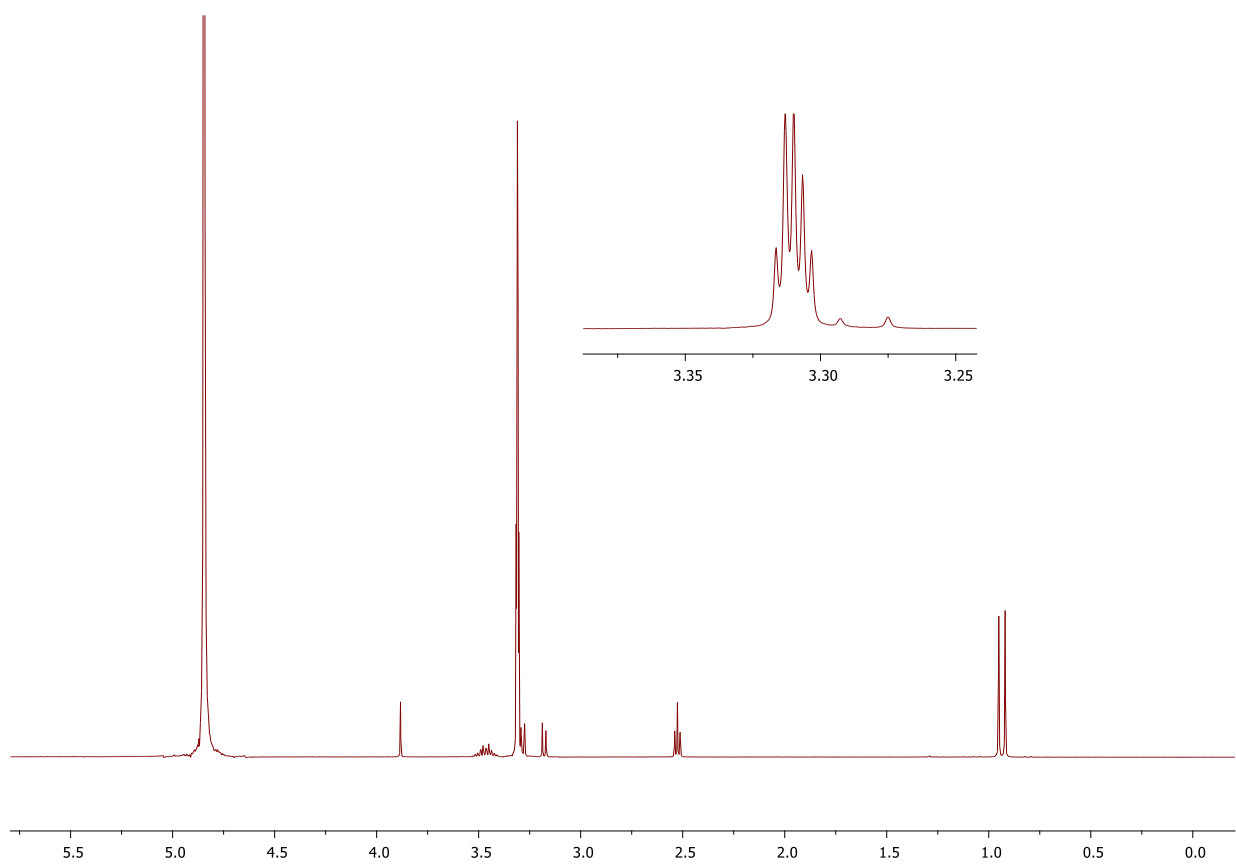
^1H NMR of compound 5.1i



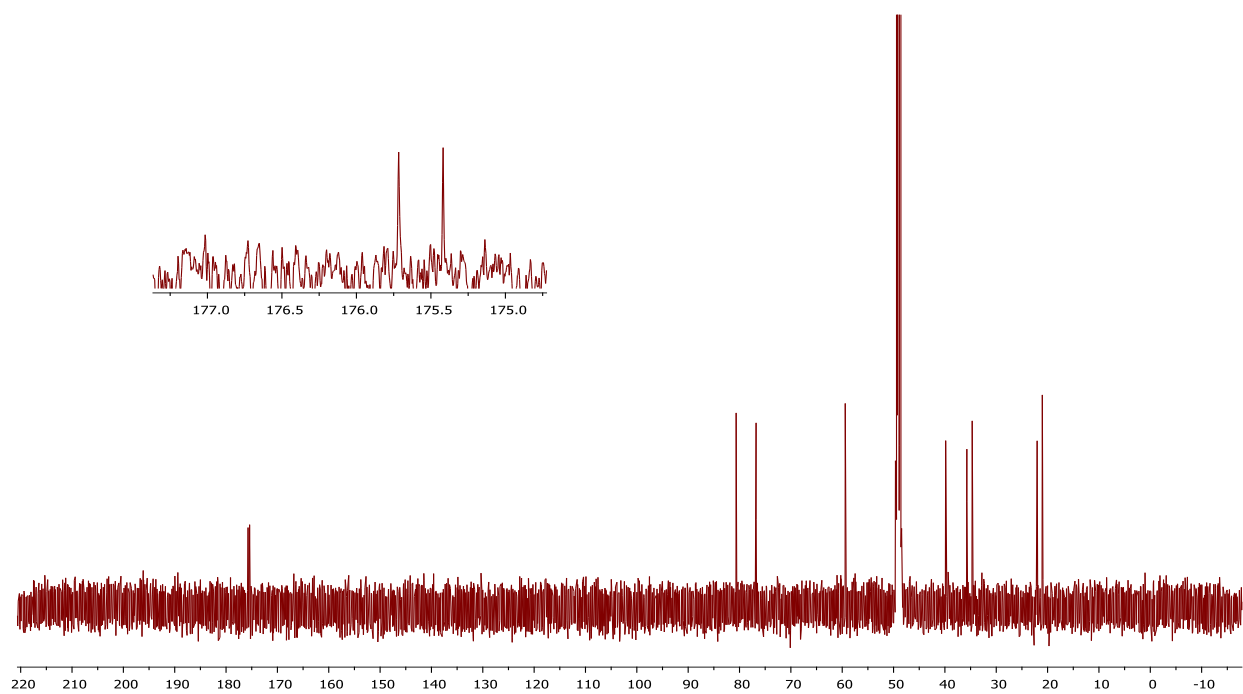
¹³C NMR of compound 5.1i



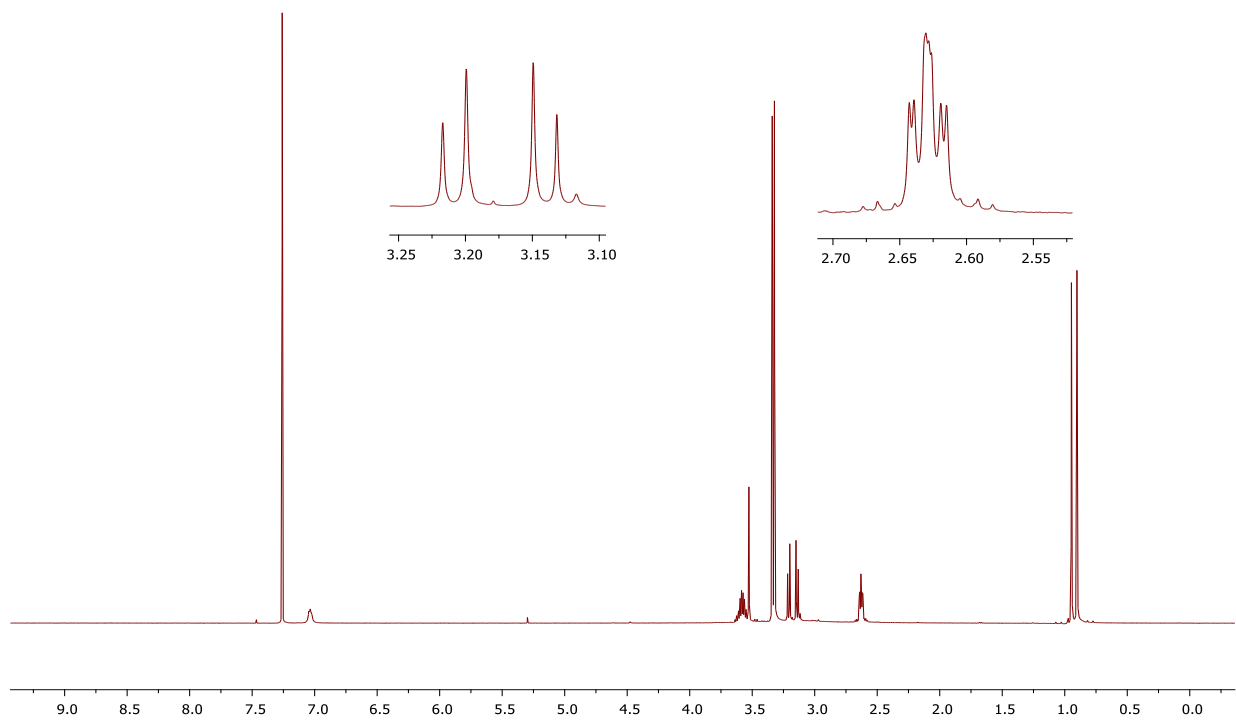
¹H NMR of compound 5.1j



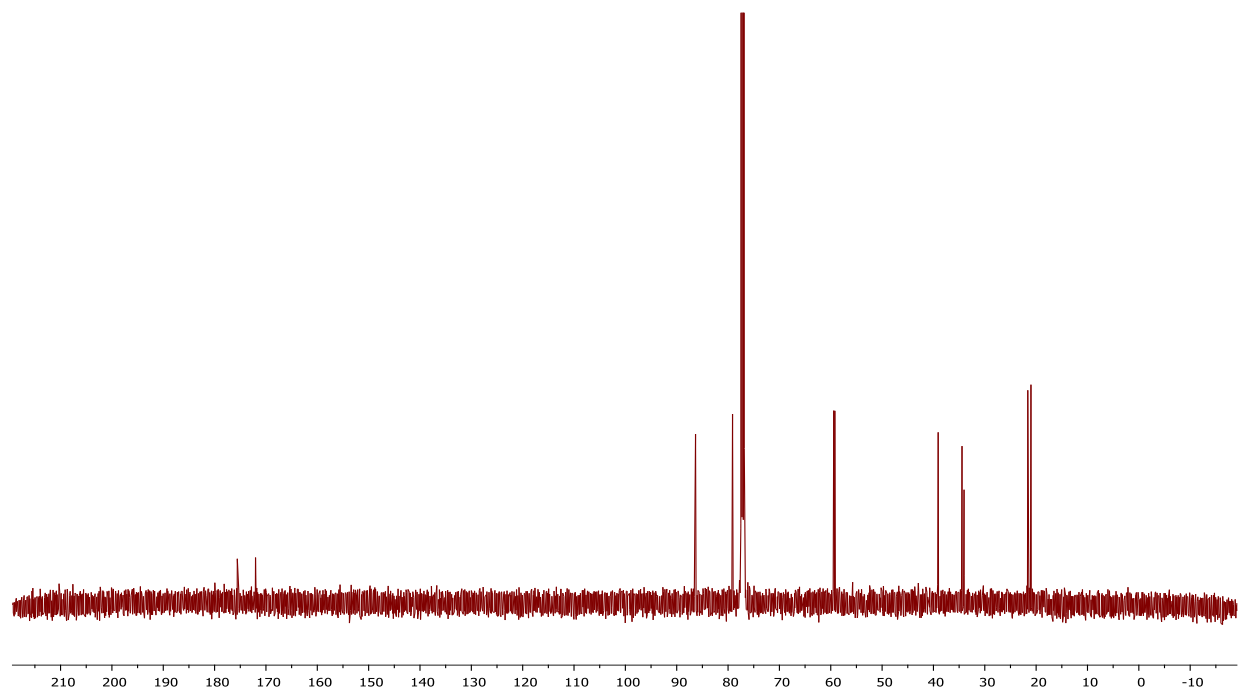
¹³C NMR of compound 5.1j



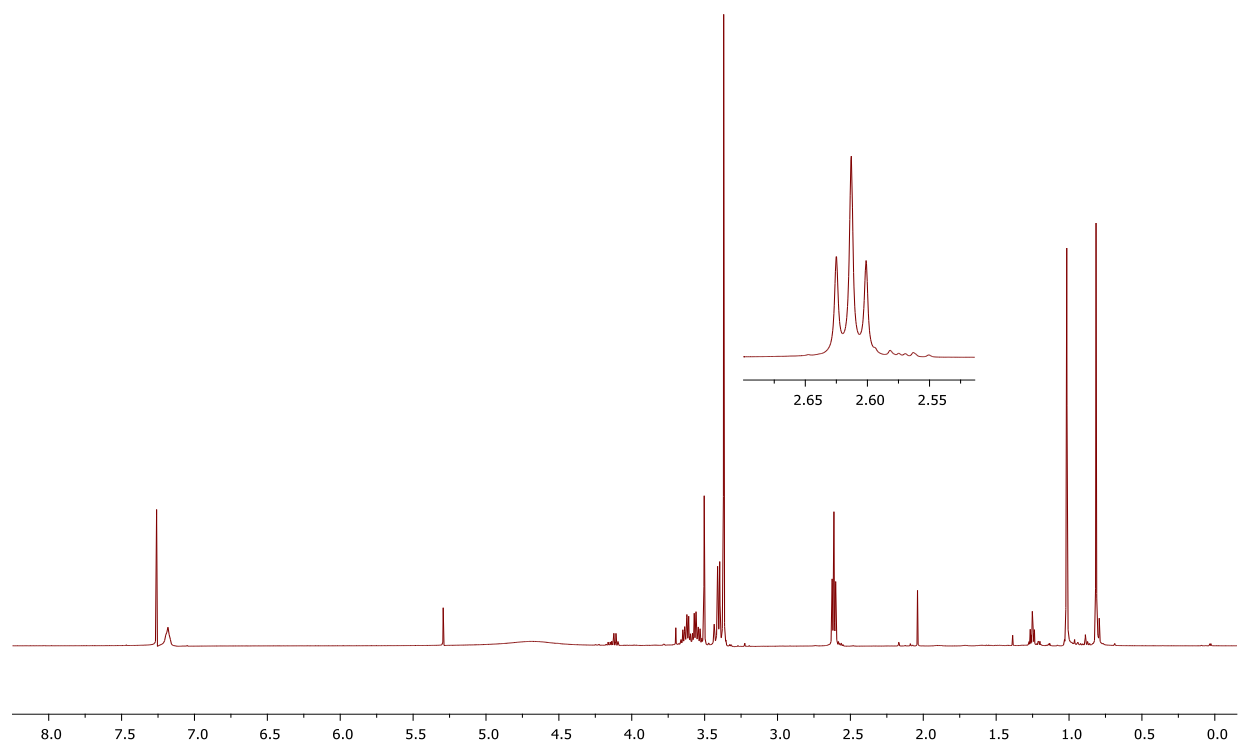
¹H NMR of compound 5.1k



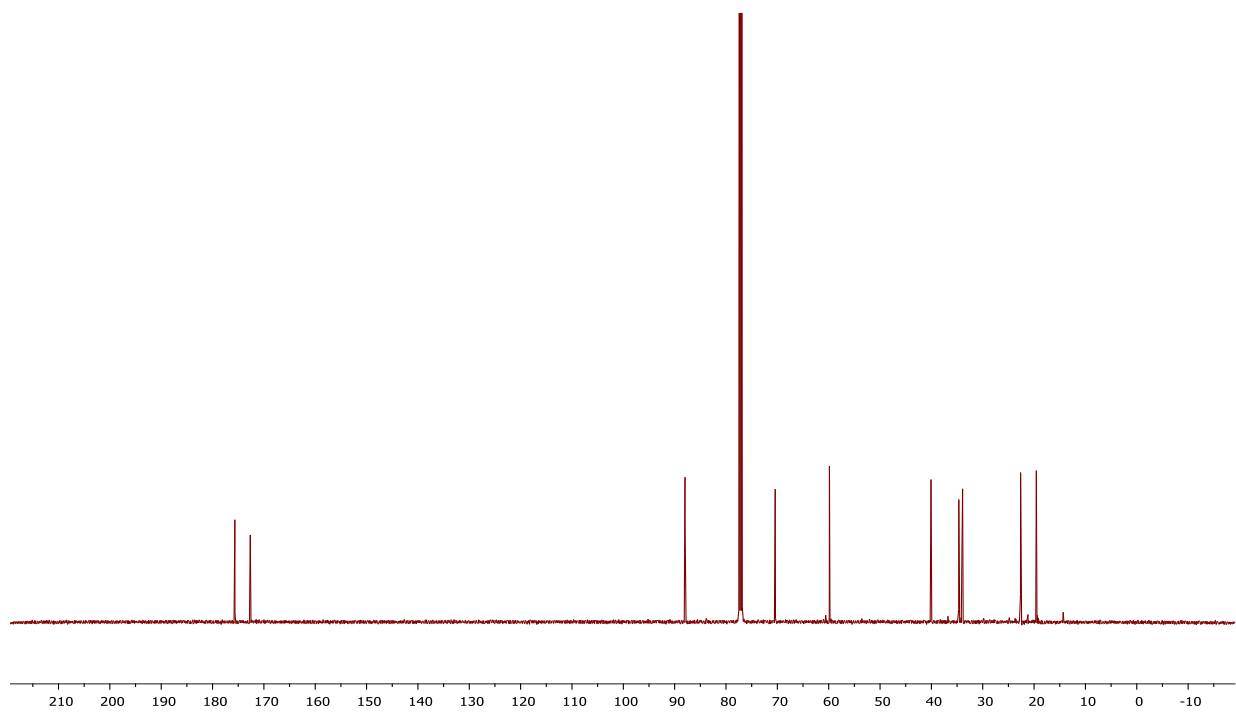
^{13}C NMR of compound 5.1k



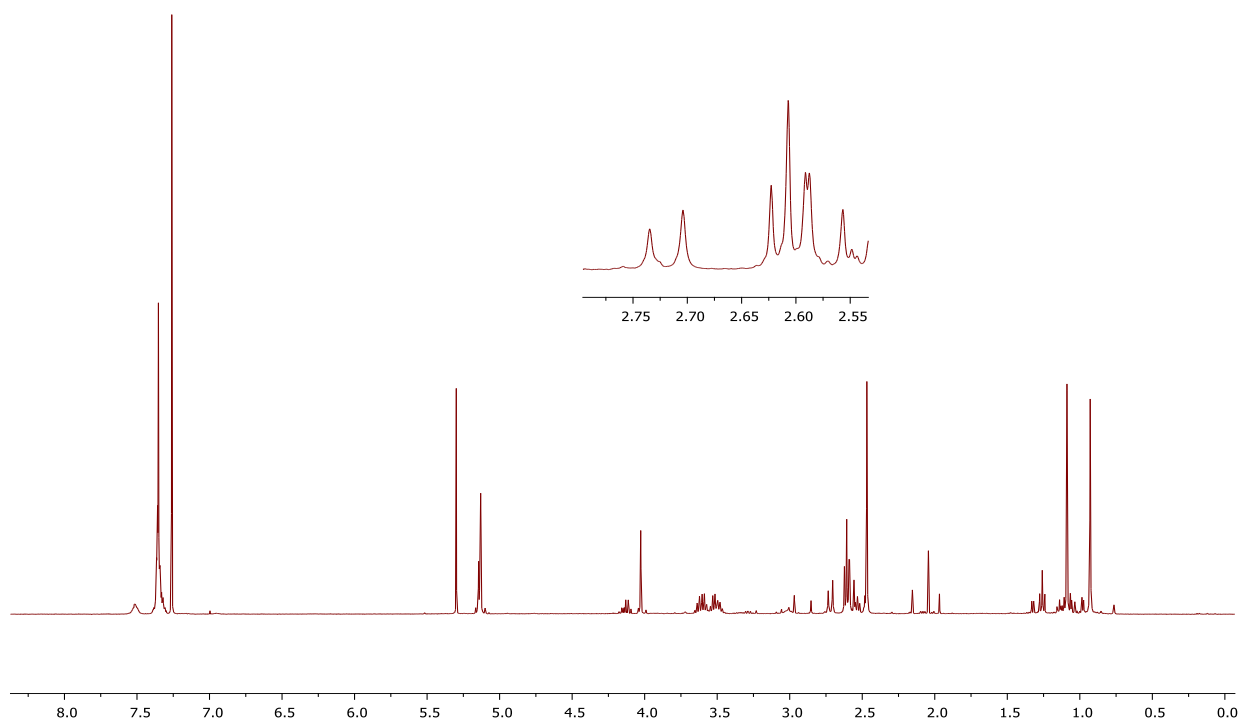
^1H NMR of compound 5.1l



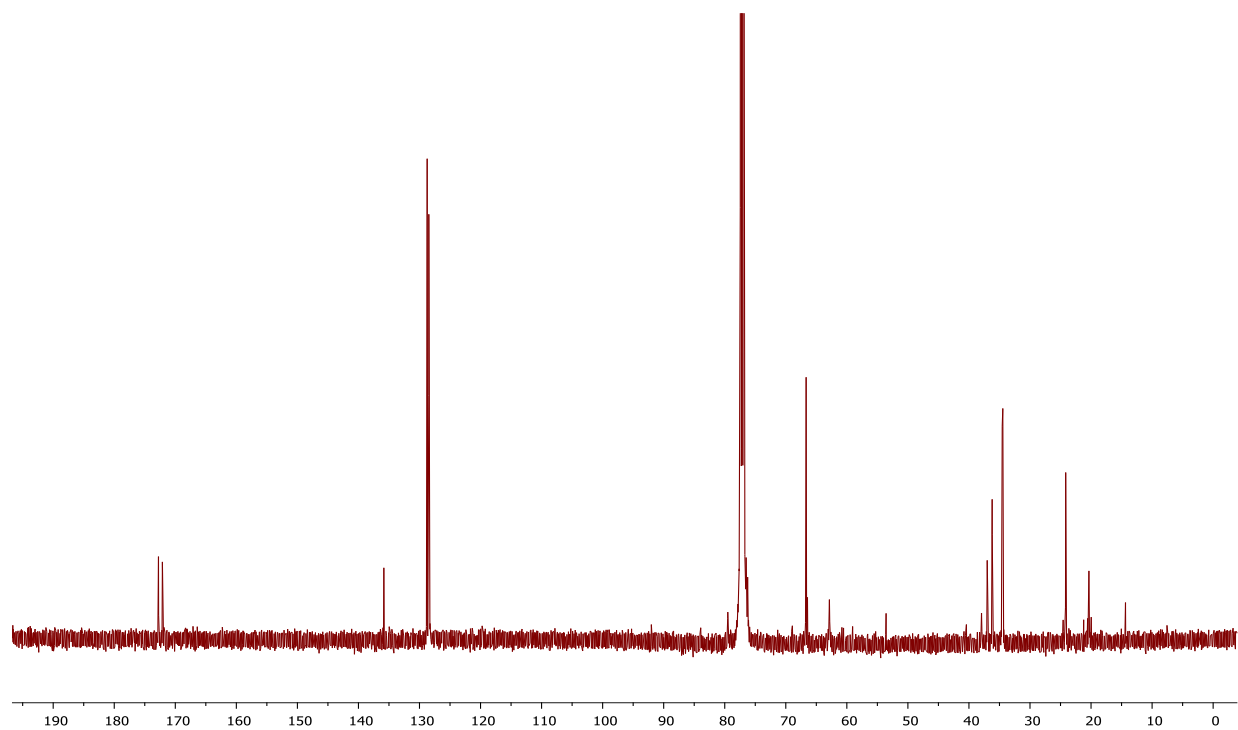
^{13}C NMR of compound 5.1l



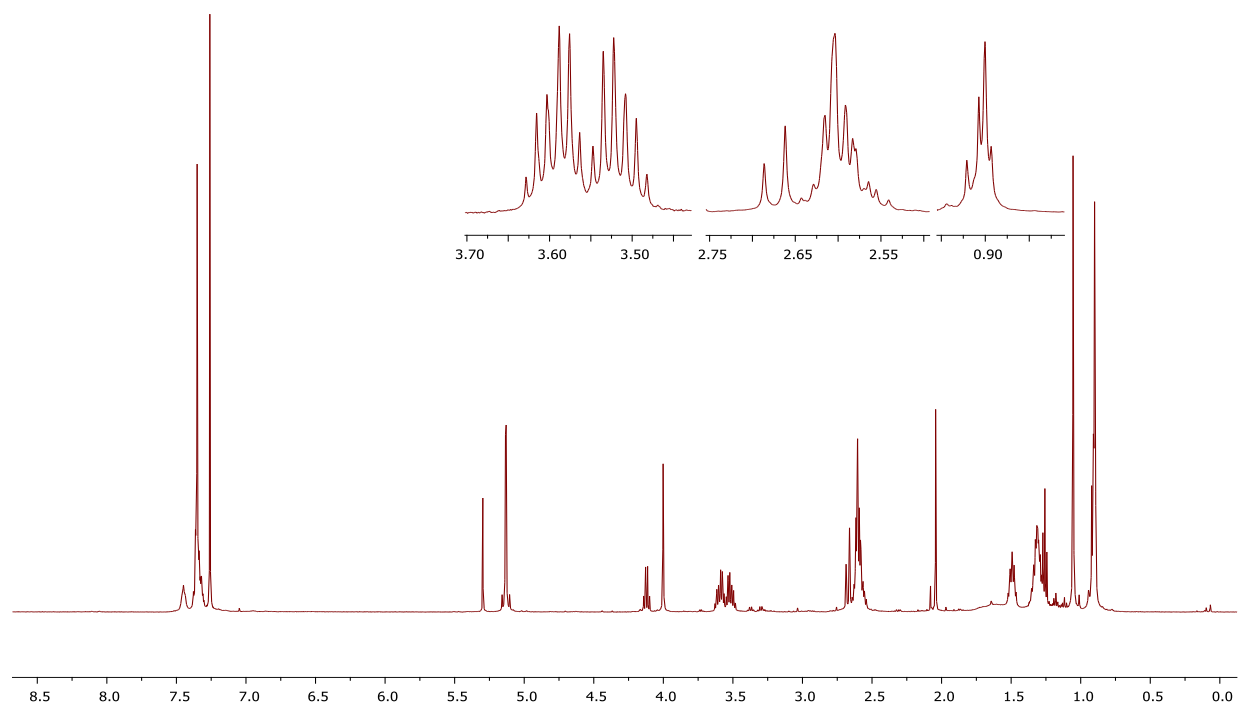
^1H NMR of compound 5.2a



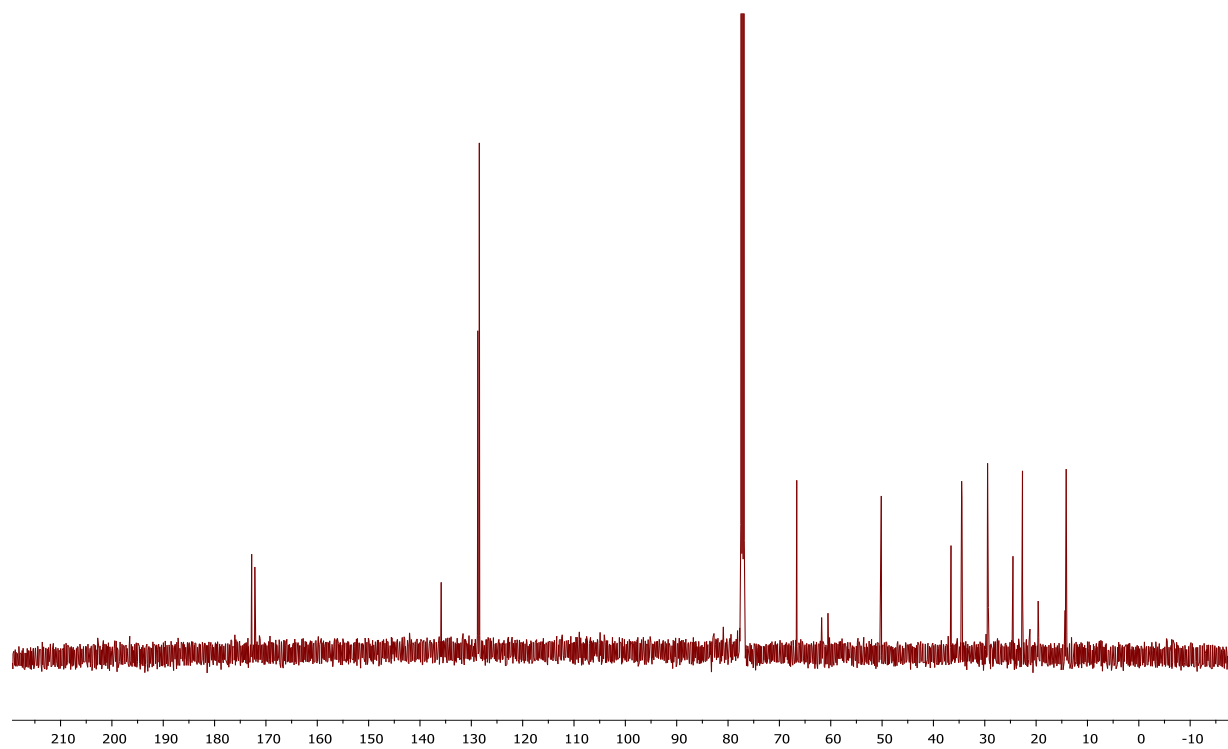
¹³C NMR of compound 5.2a



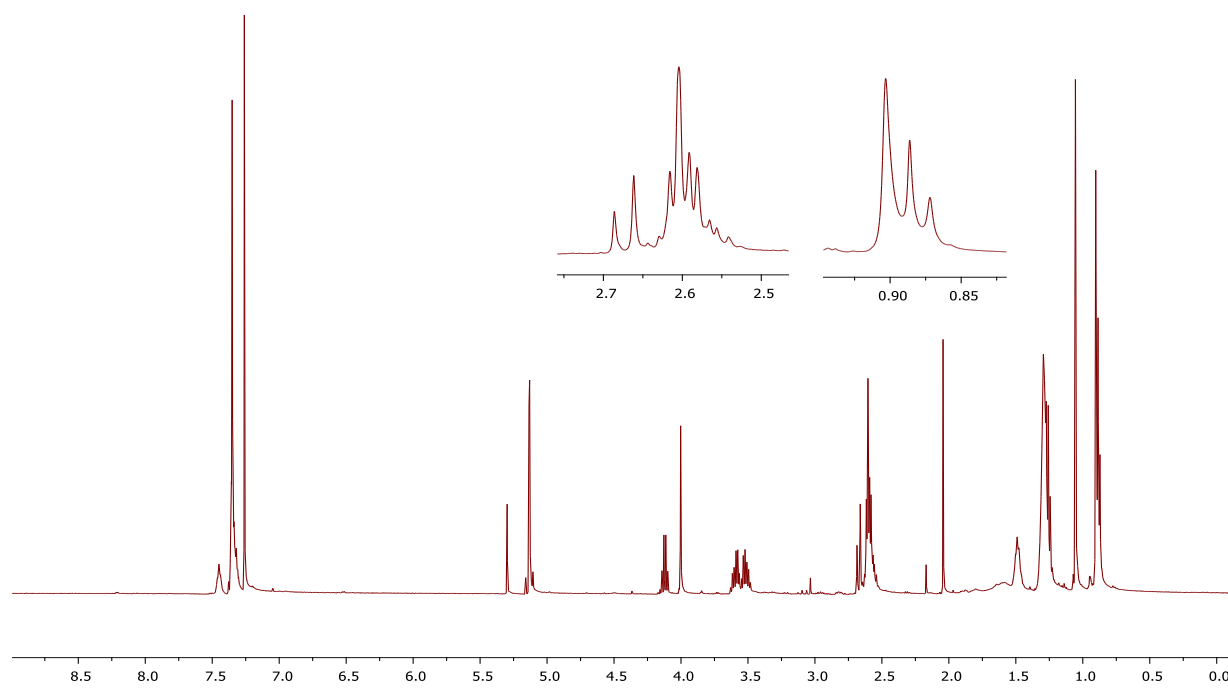
¹H NMR of compound 5.2c



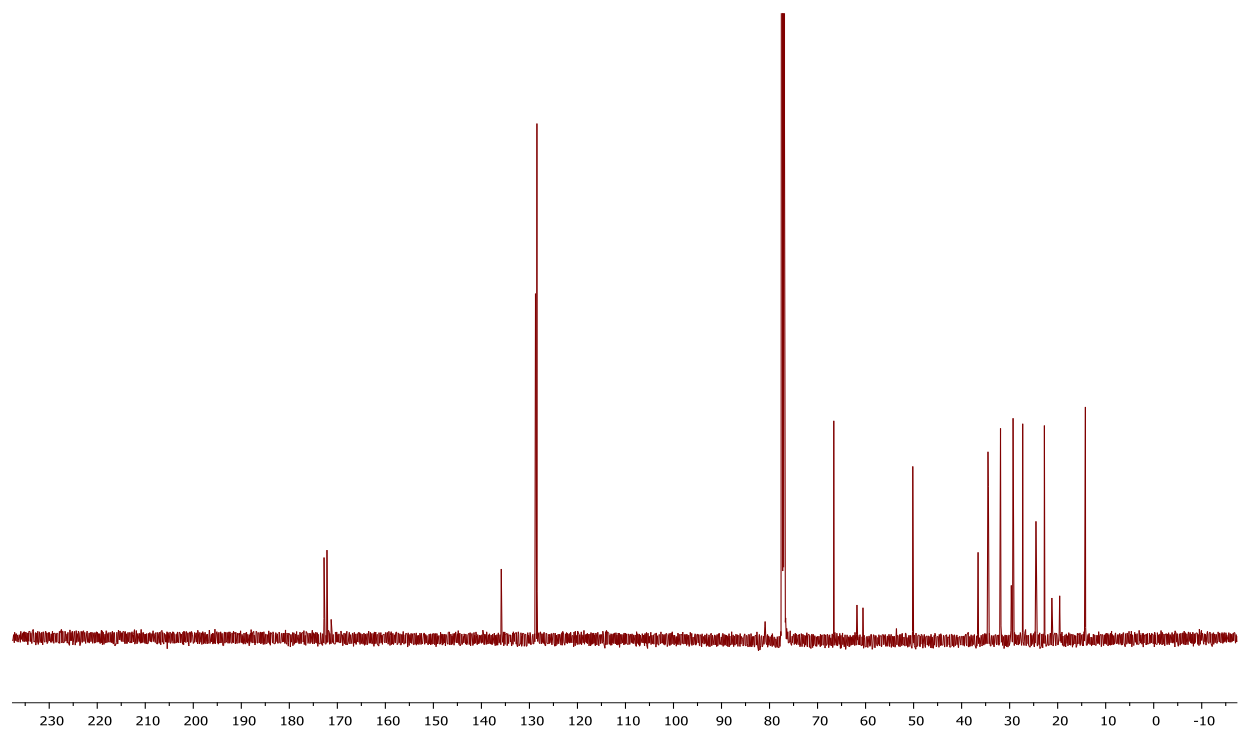
¹³C NMR of compound 5.2c



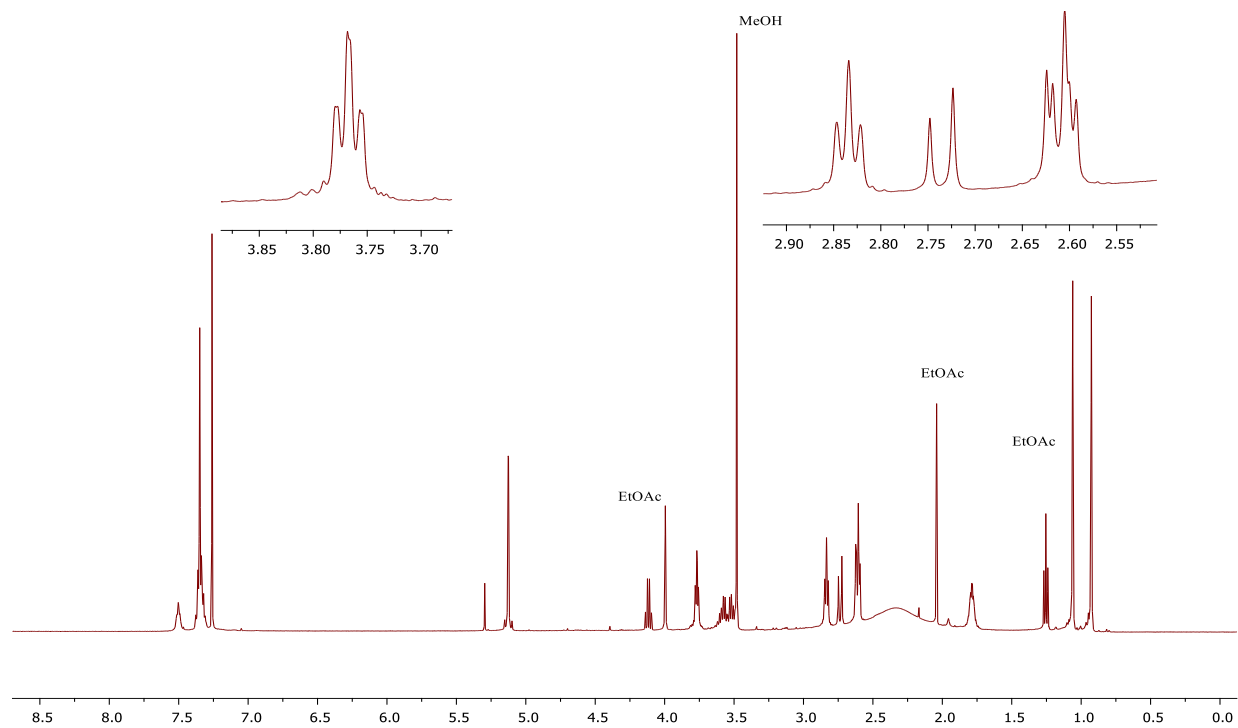
¹H NMR of compound 5.2d



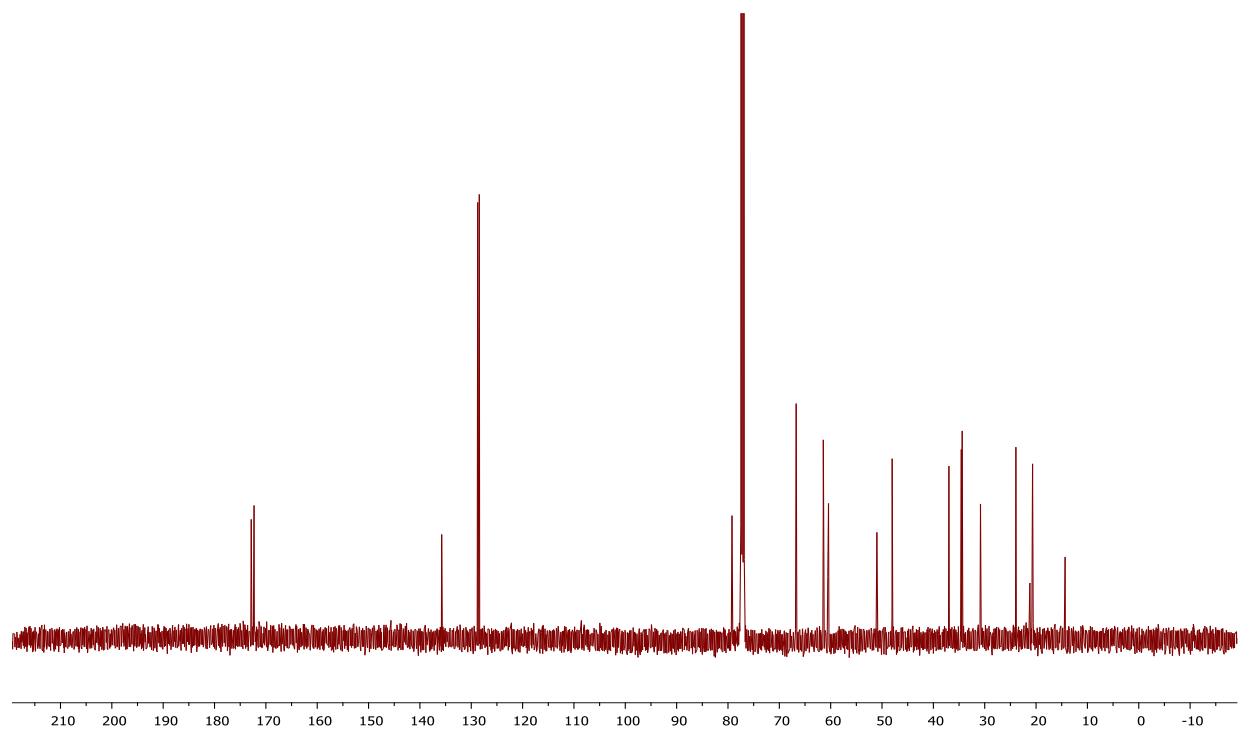
¹³C NMR of compound 5.2d



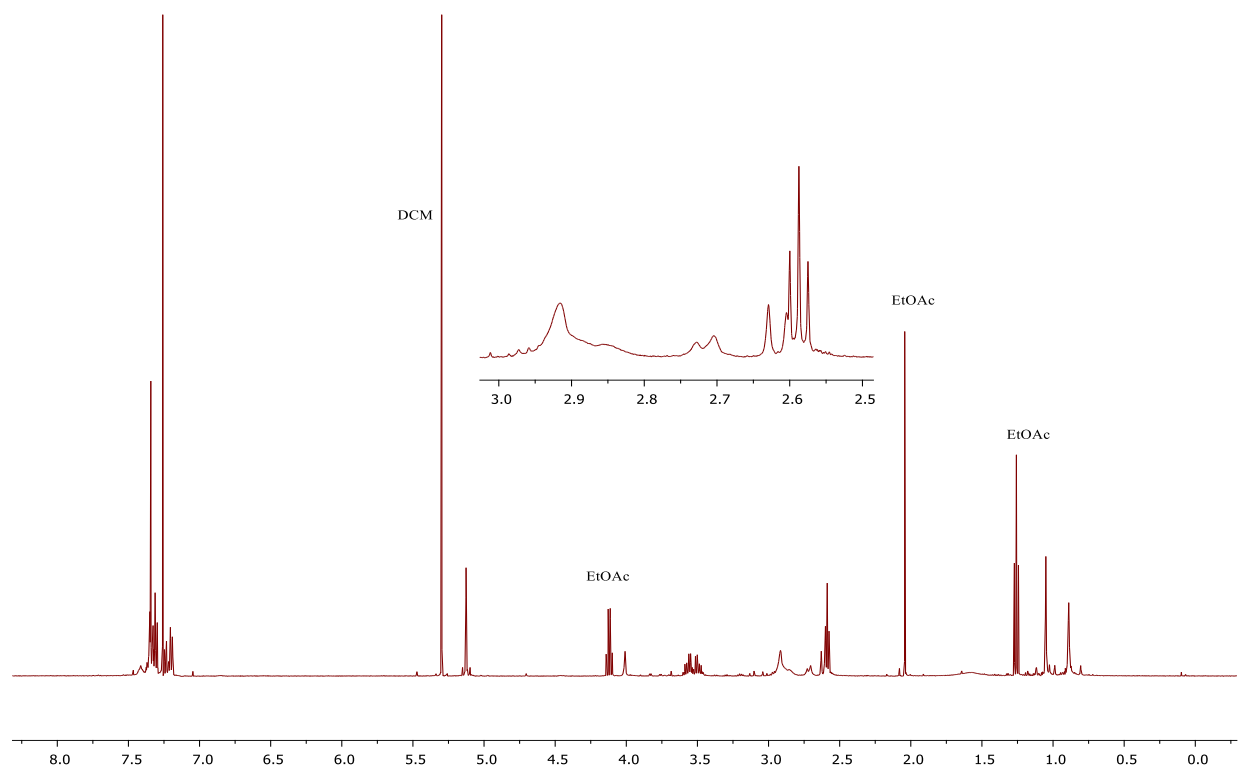
¹H NMR of compound 5.2e



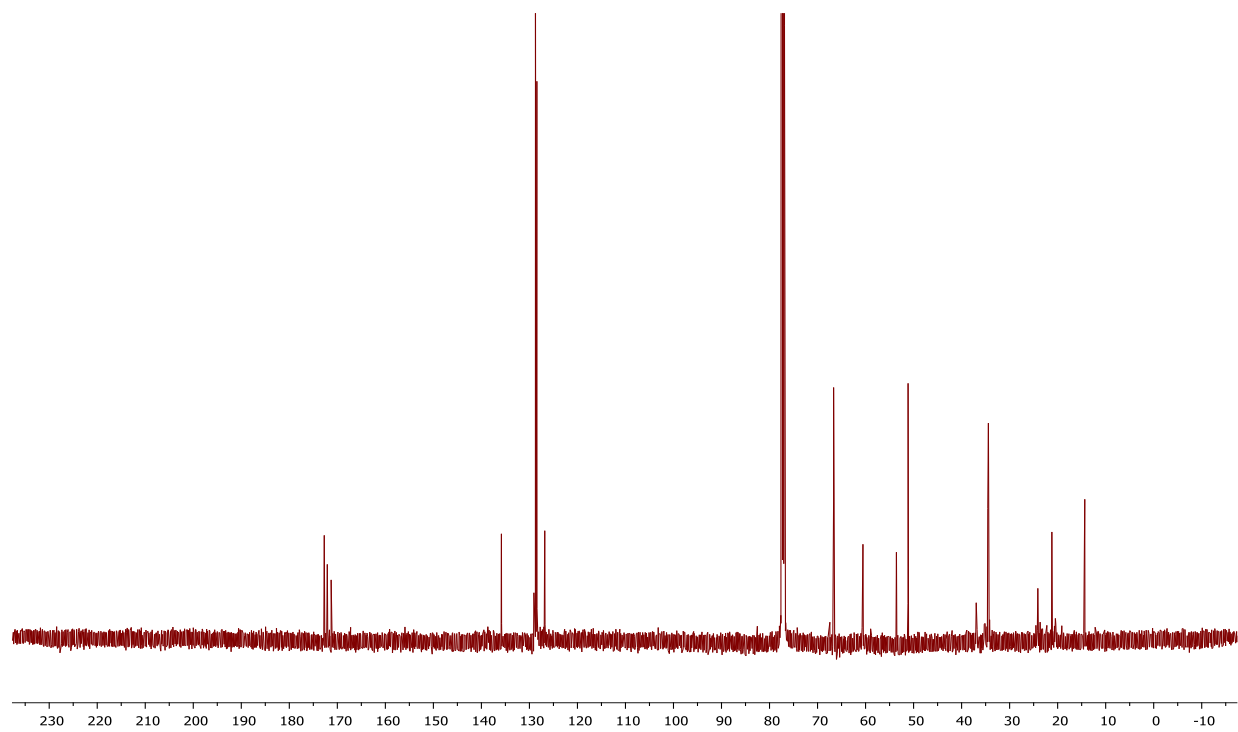
^{13}C NMR of compound 5.2e



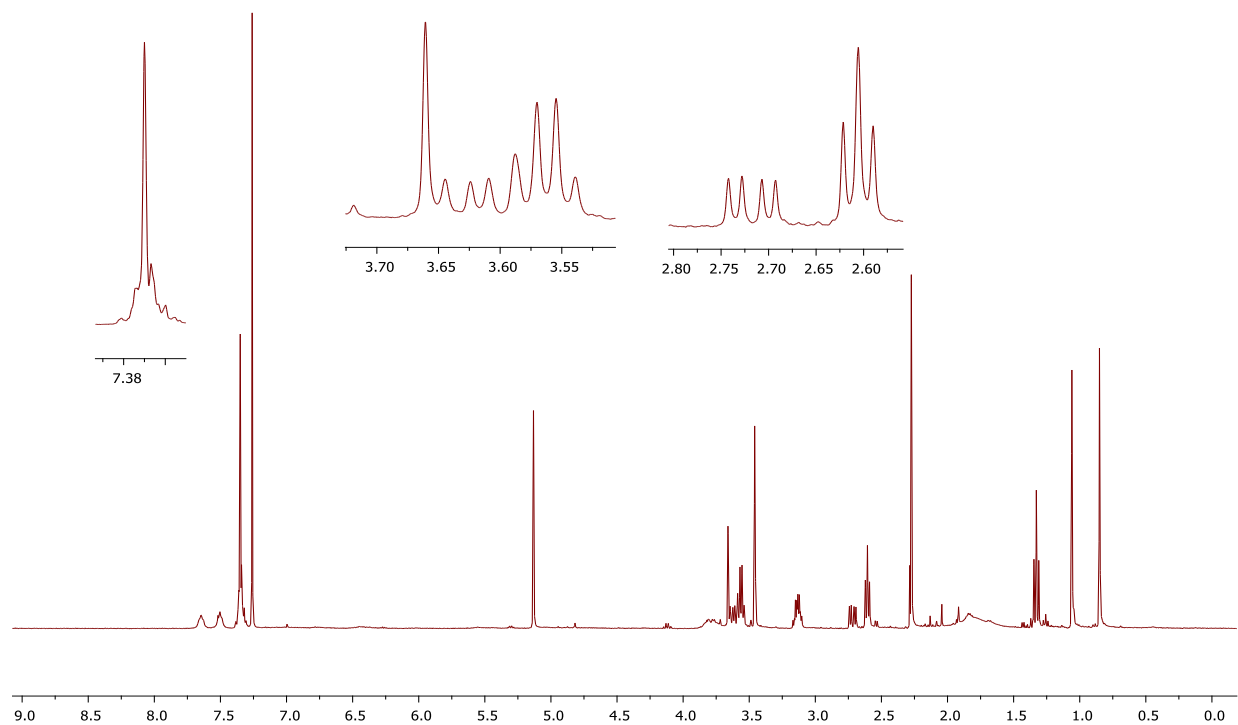
^1H NMR of compound 5.2f



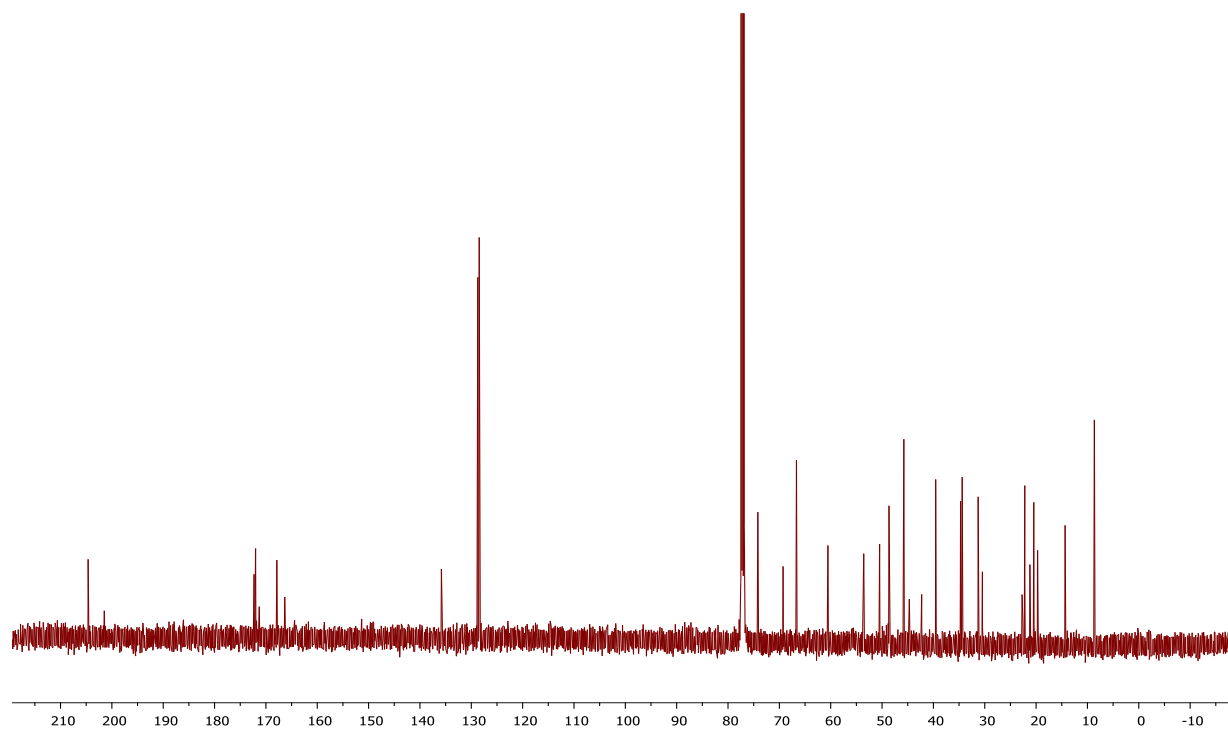
¹³C NMR of compound 5.2f



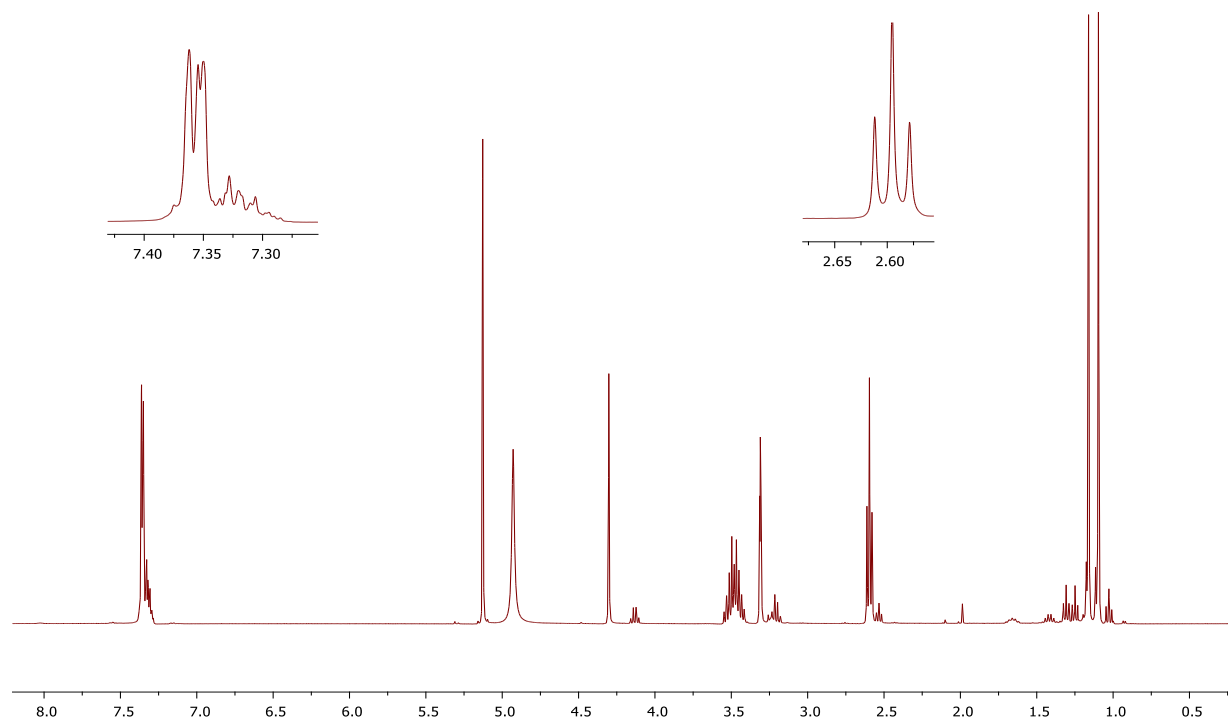
¹H NMR of compound 5.2g



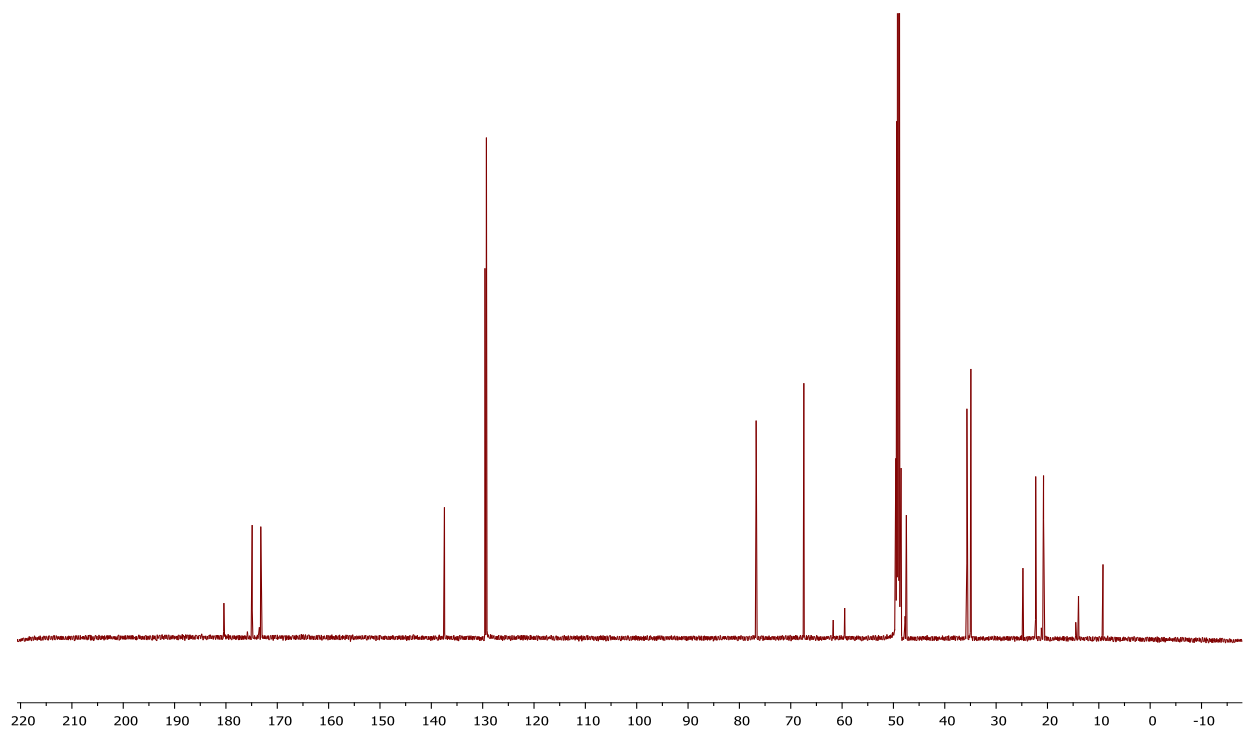
^{13}C NMR of compound 5.2g



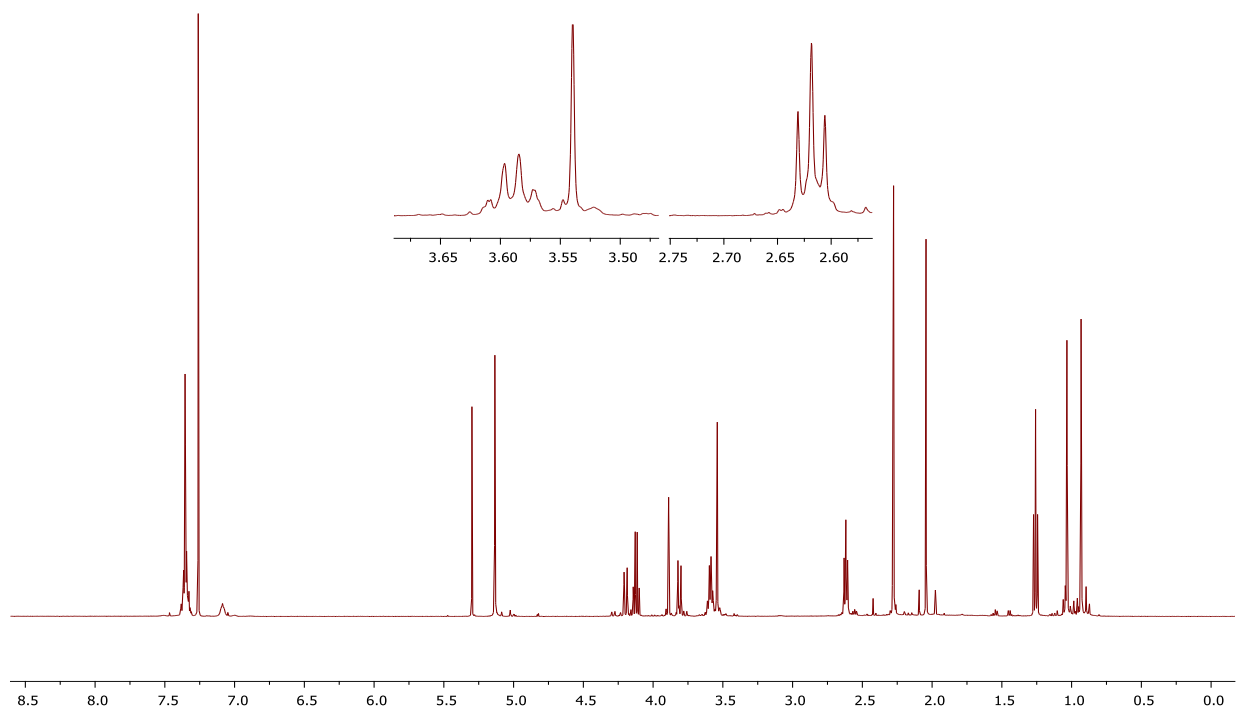
^1H NMR of compound 5.2h



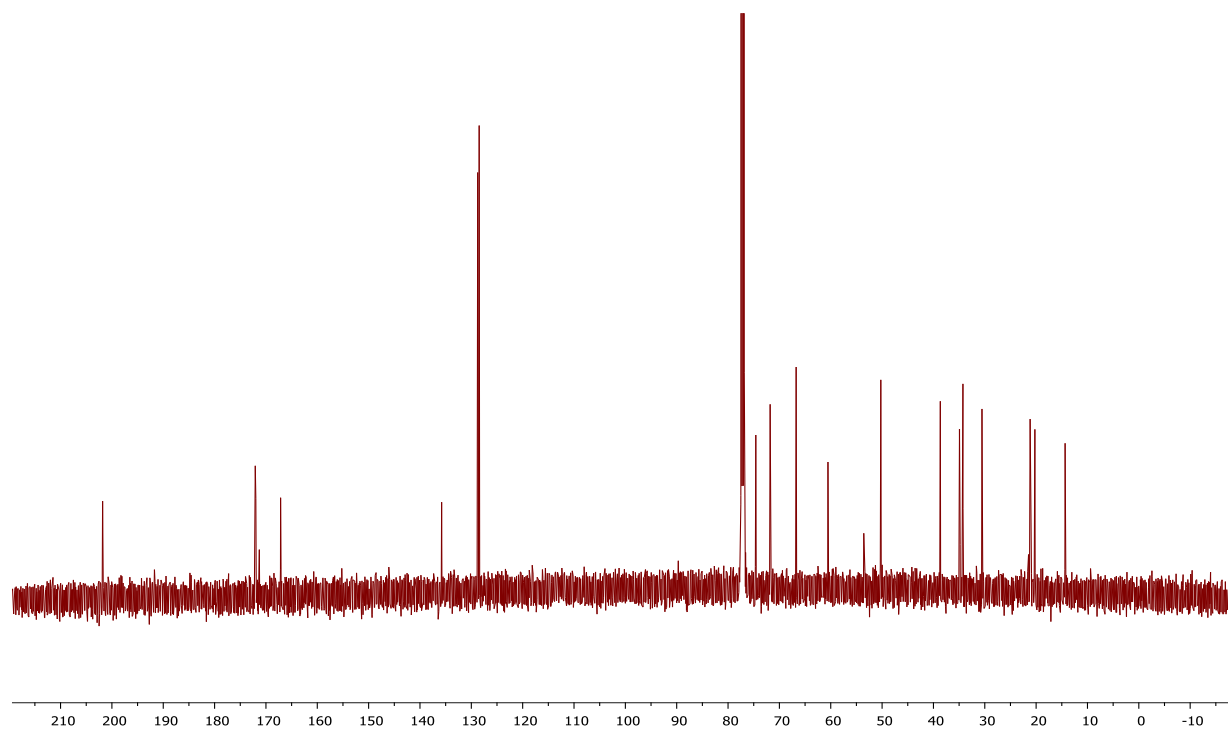
¹³C NMR of compound 5.2h



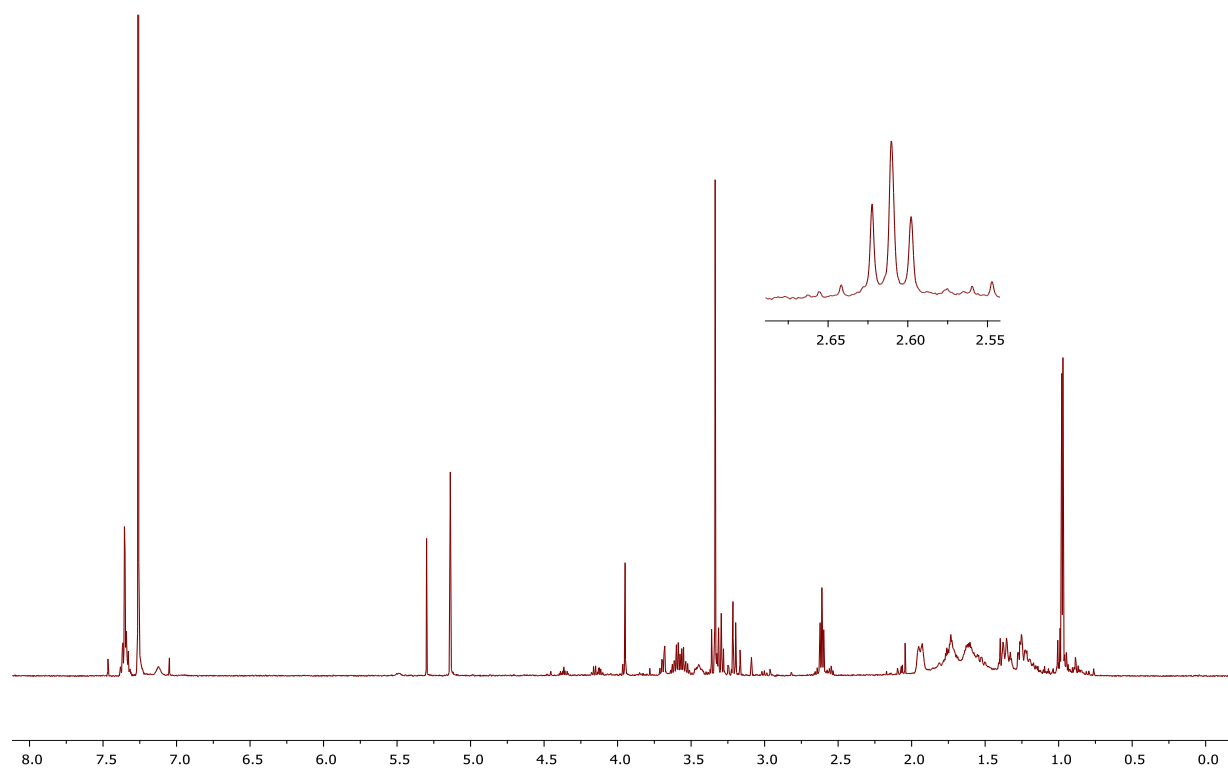
¹H NMR of compound 5.2i



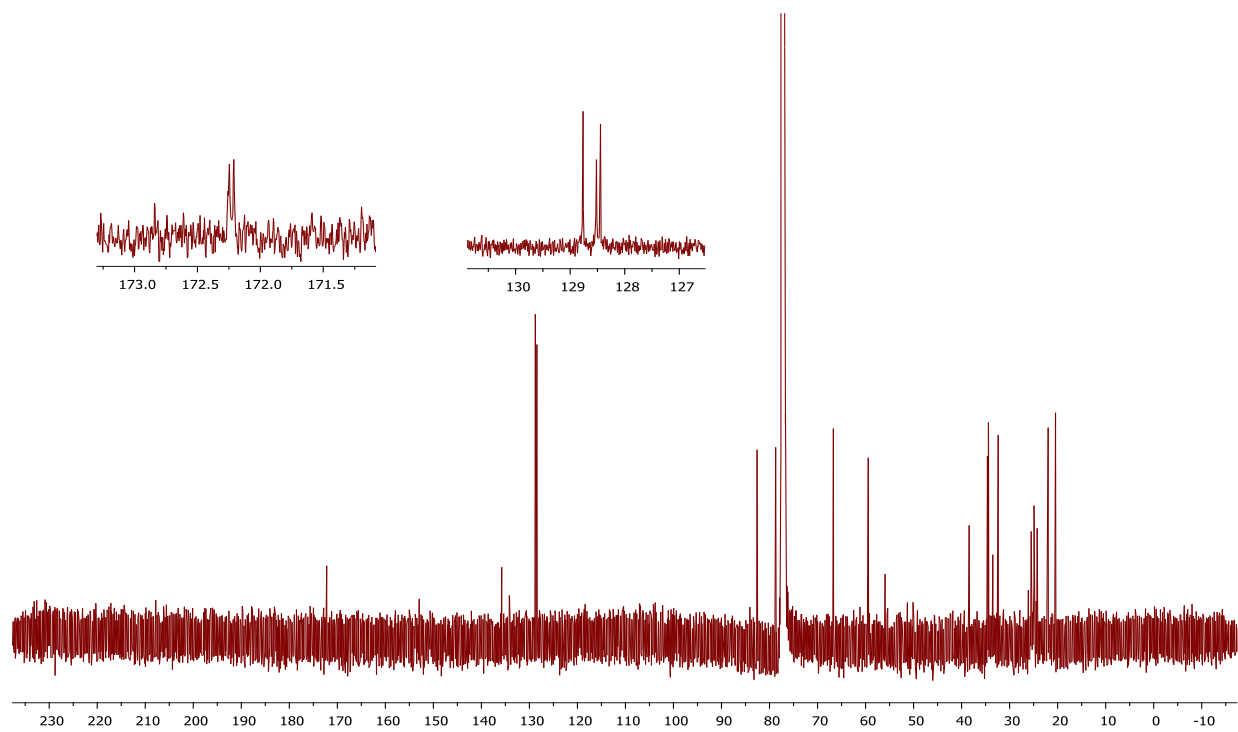
^{13}C NMR of compound 5.2i



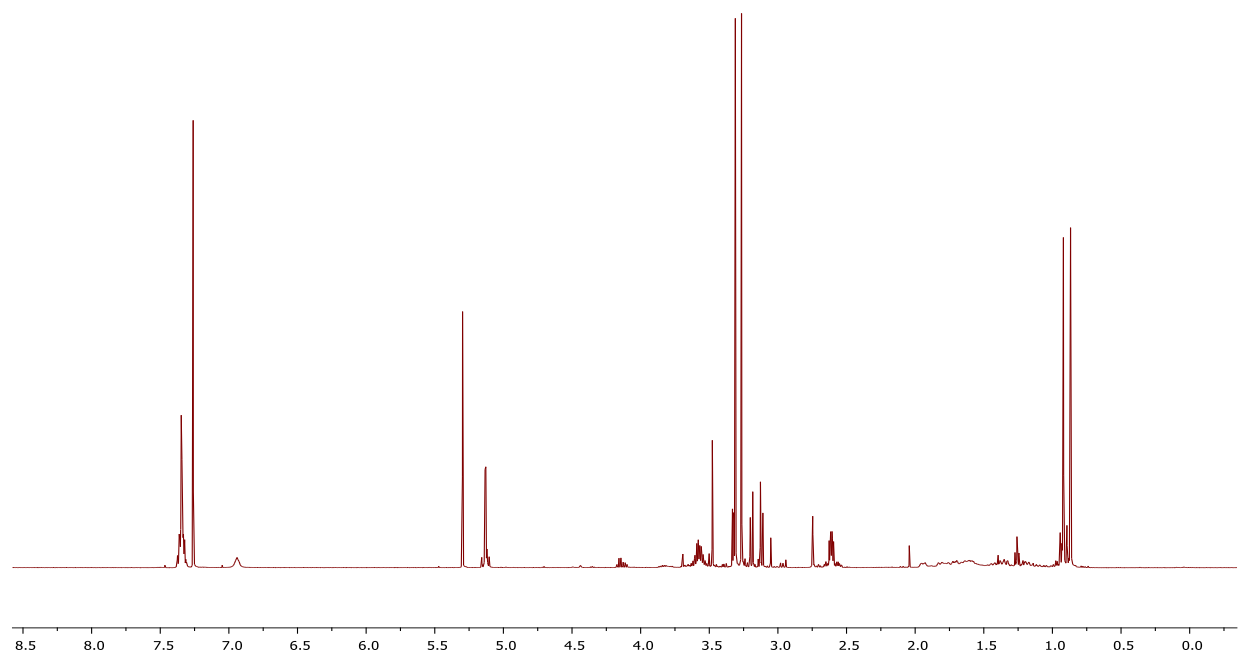
^1H NMR of compound 5.2j



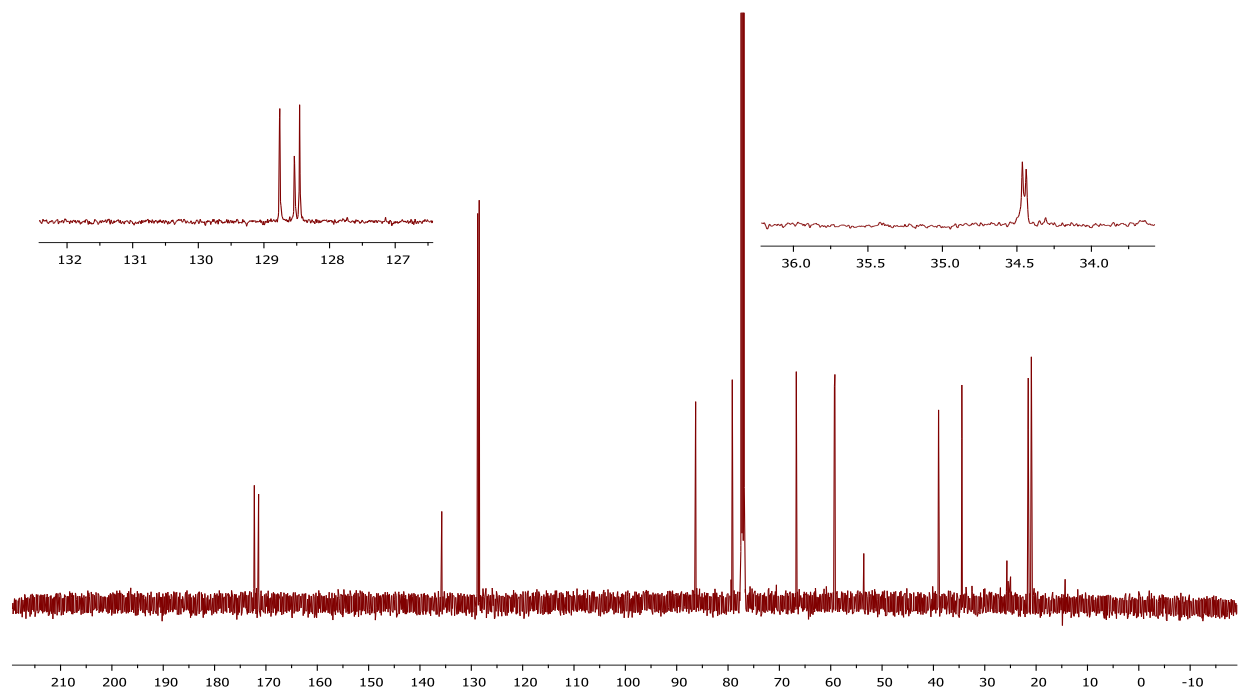
¹³C NMR of compound 5.2j



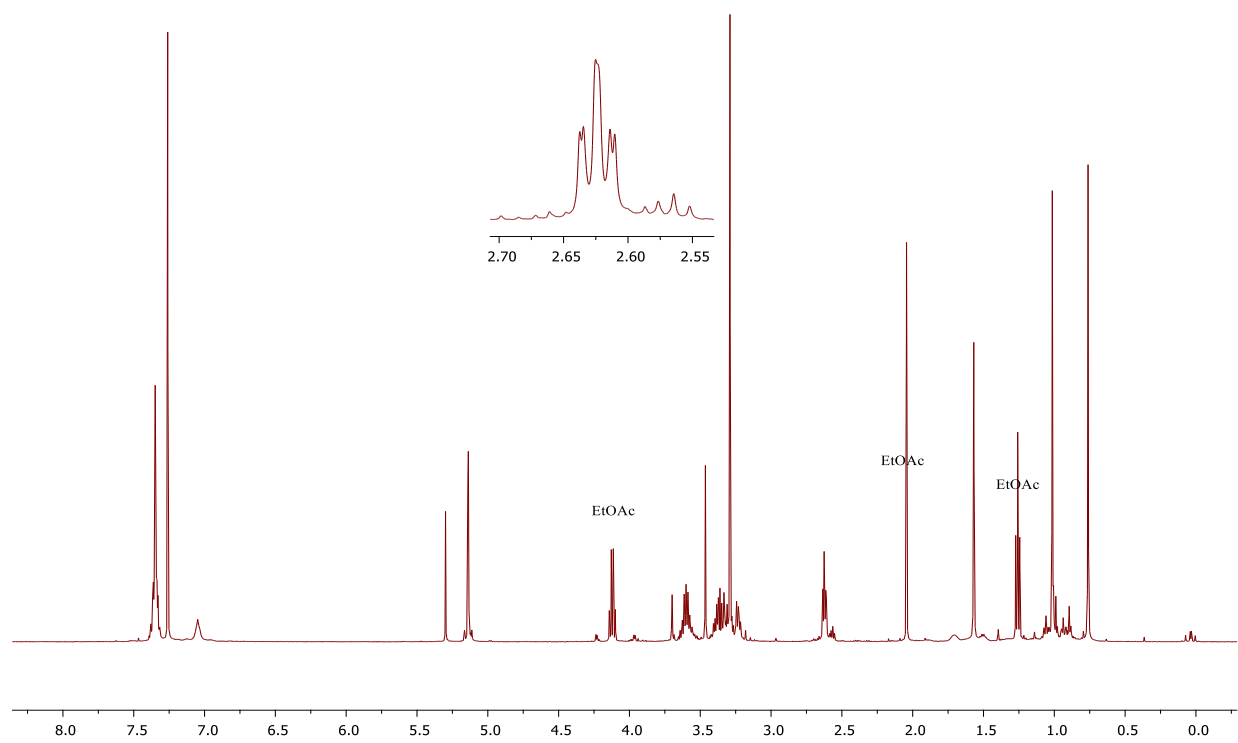
¹H NMR of compound 5.2k



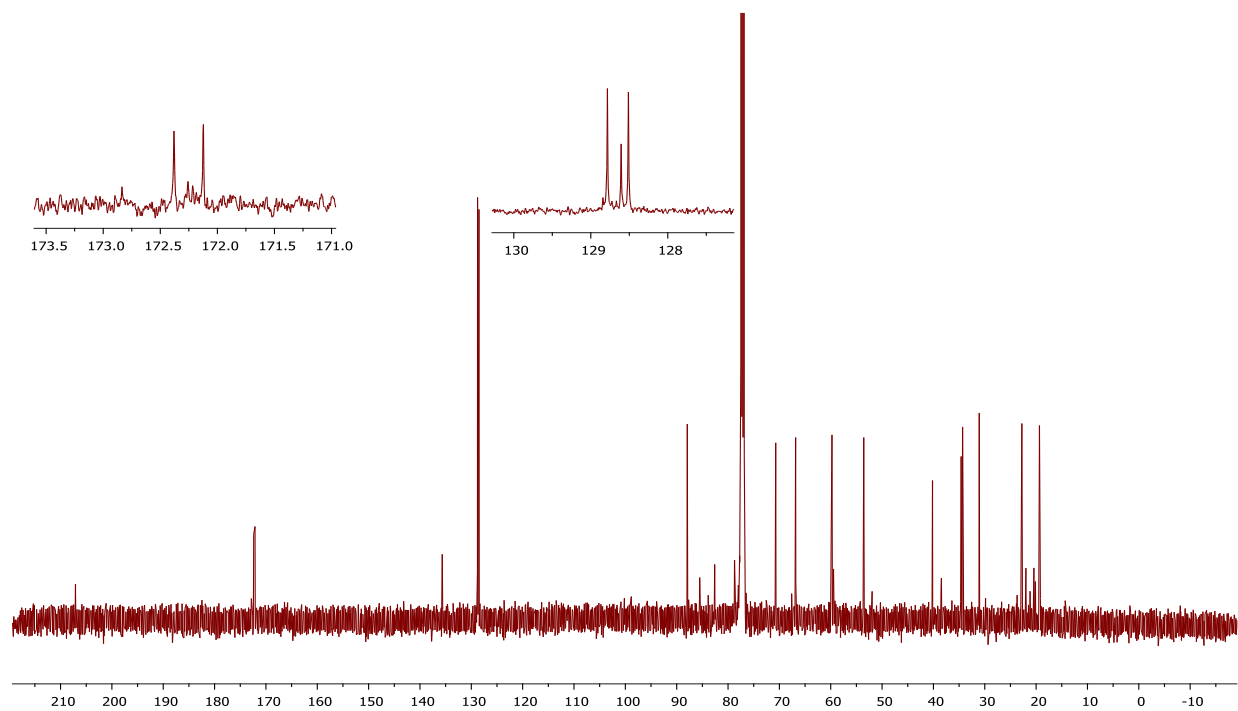
^{13}C NMR of compound 5.2k



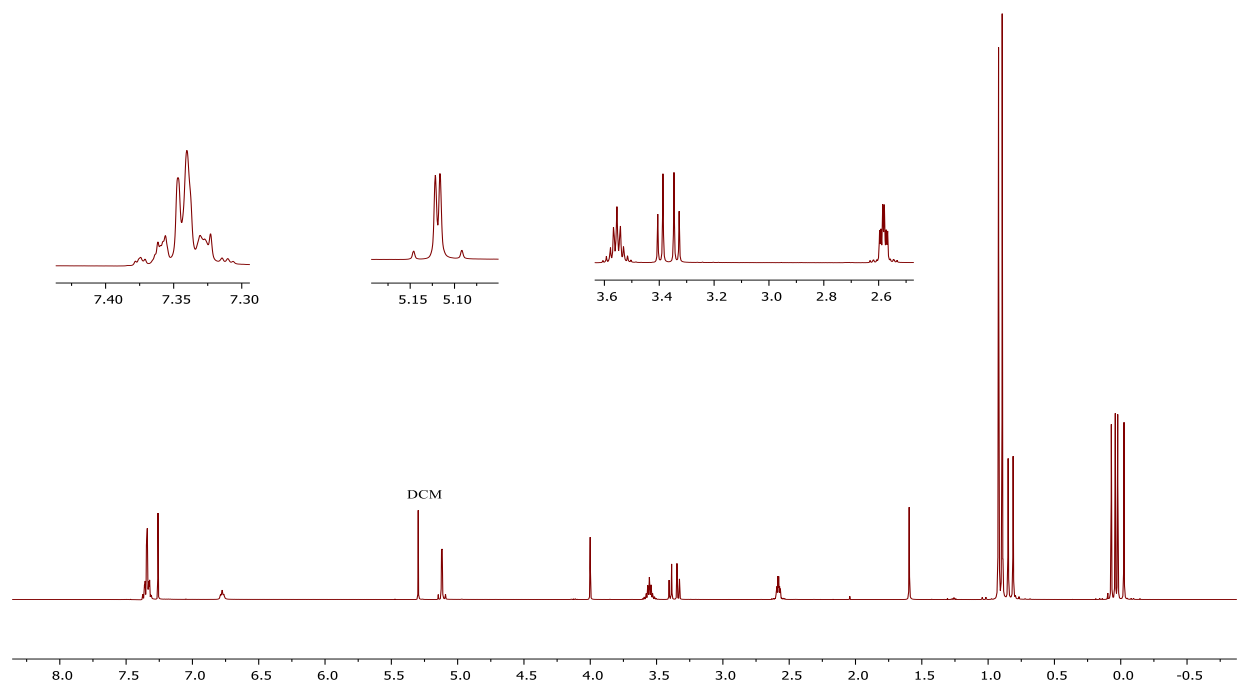
^1H NMR of compound 5.2l



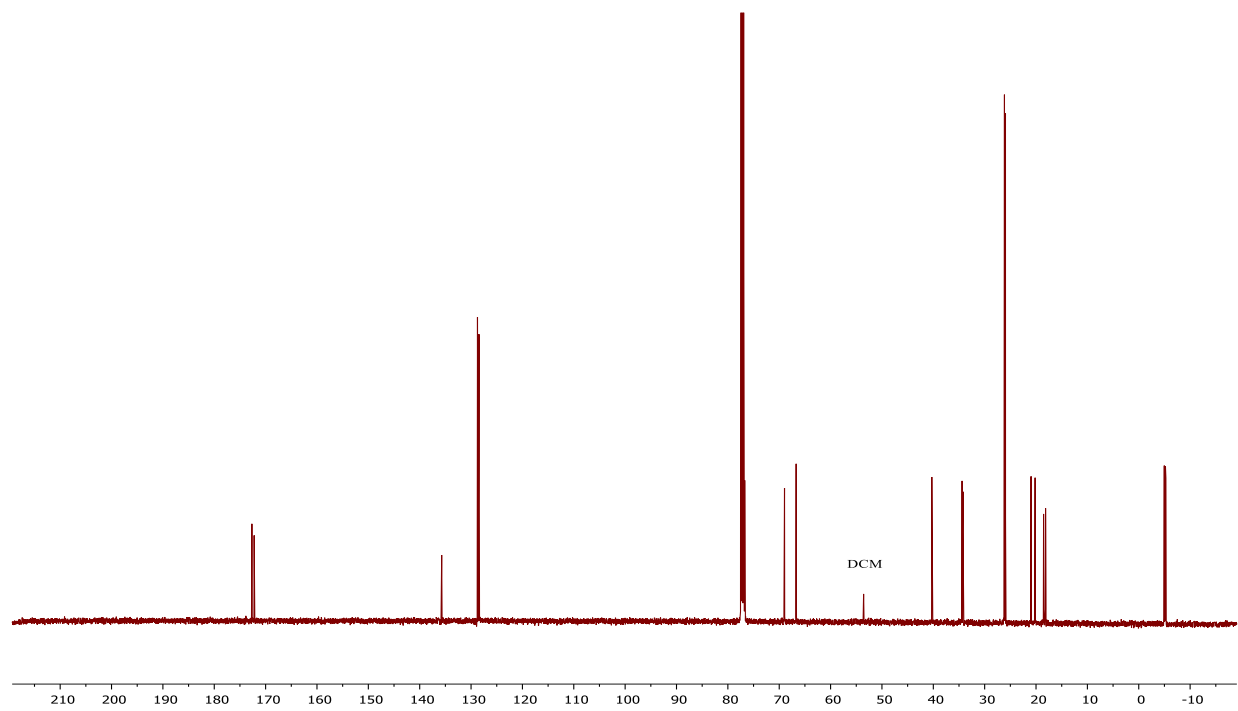
^{13}C NMR of compound 5.21



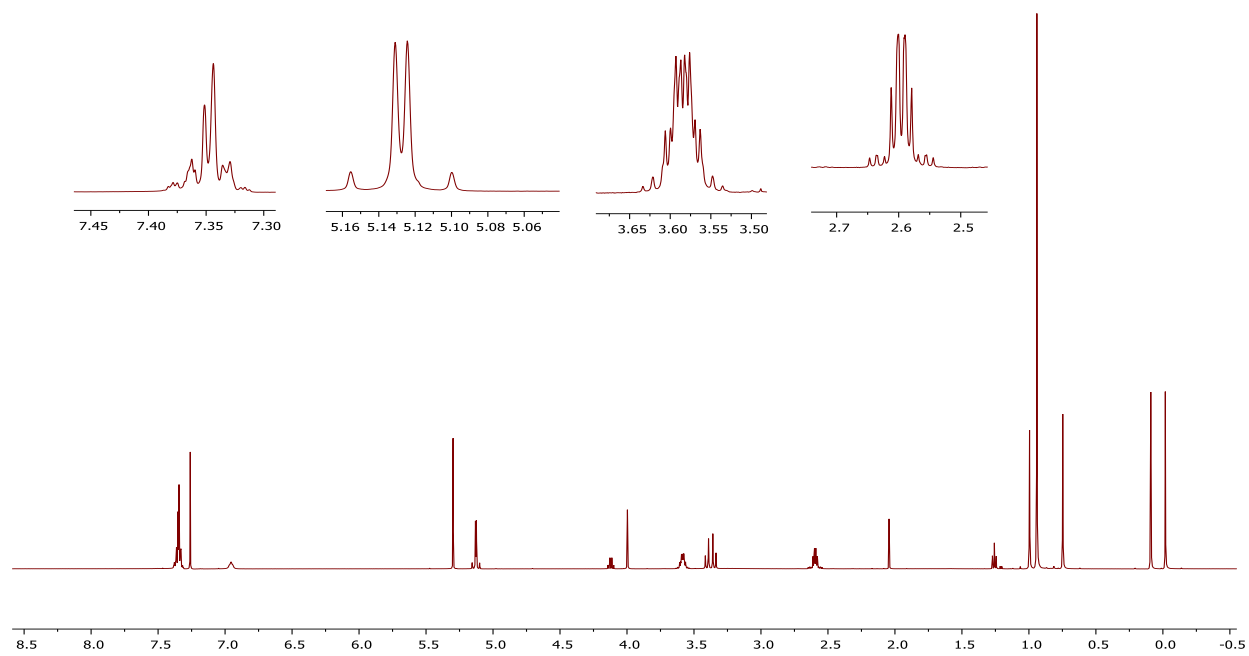
^1H NMR of compound 5.3



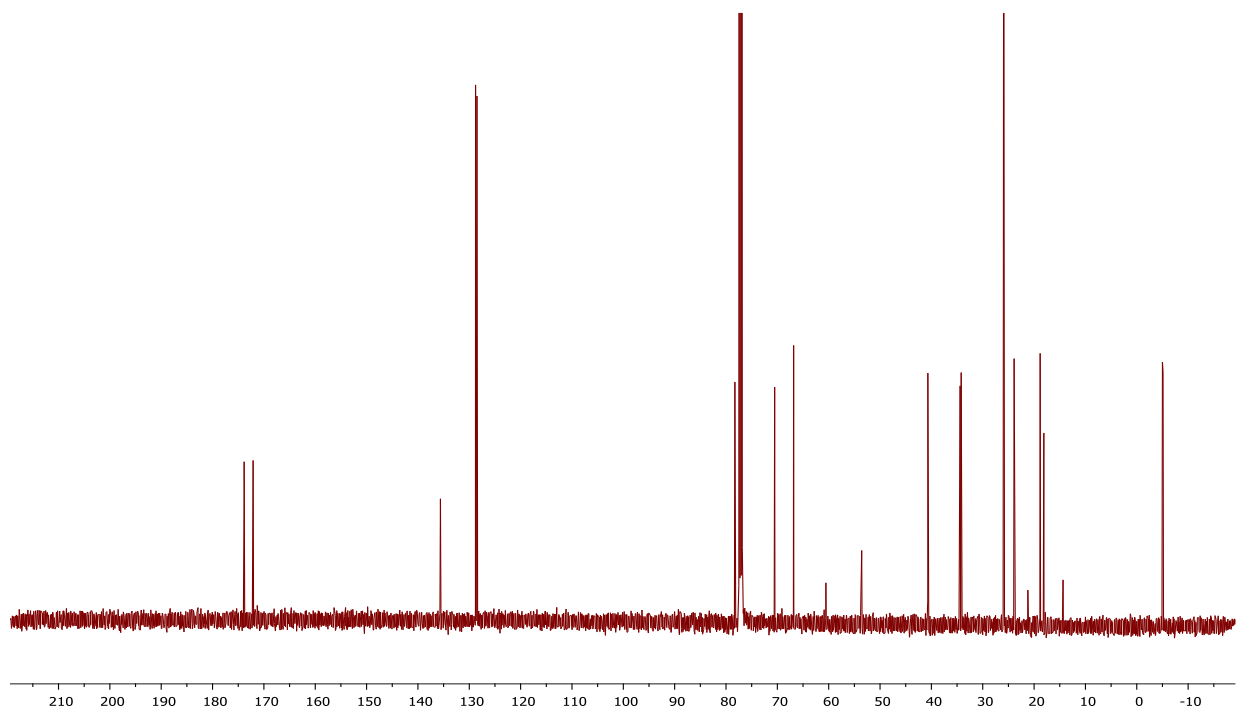
^{13}C NMR of compound 5.3



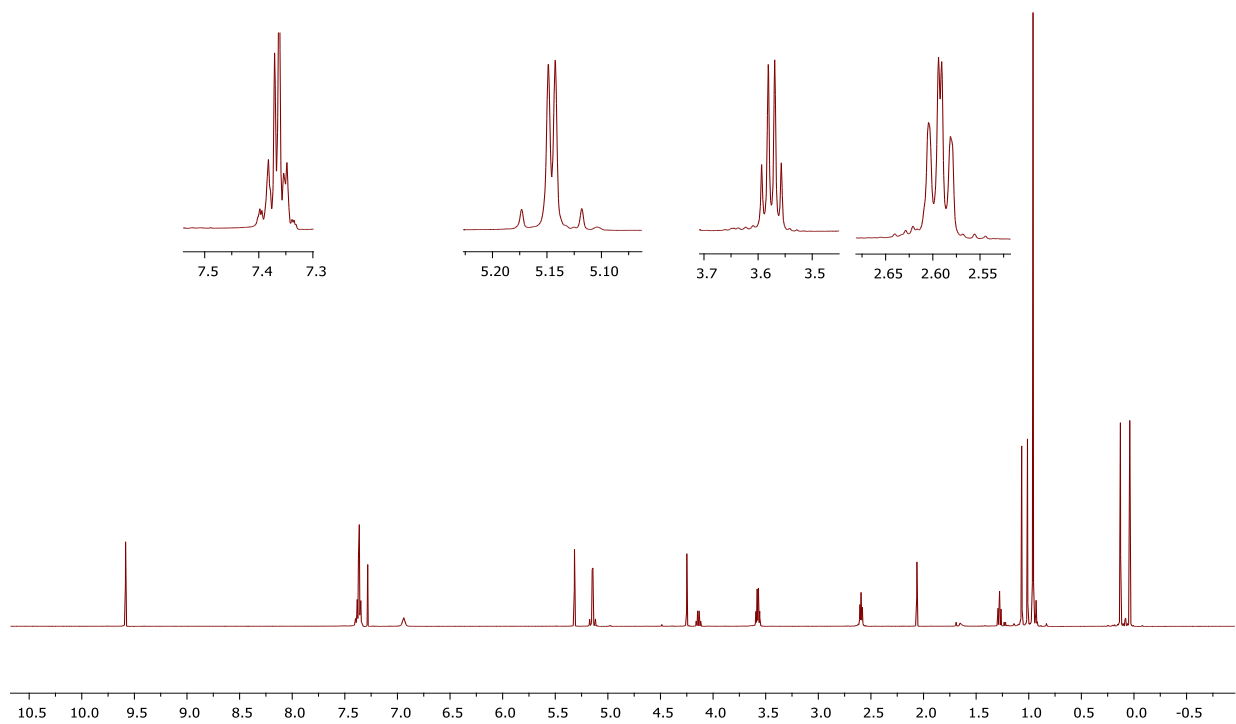
^1H NMR of compound 5.4



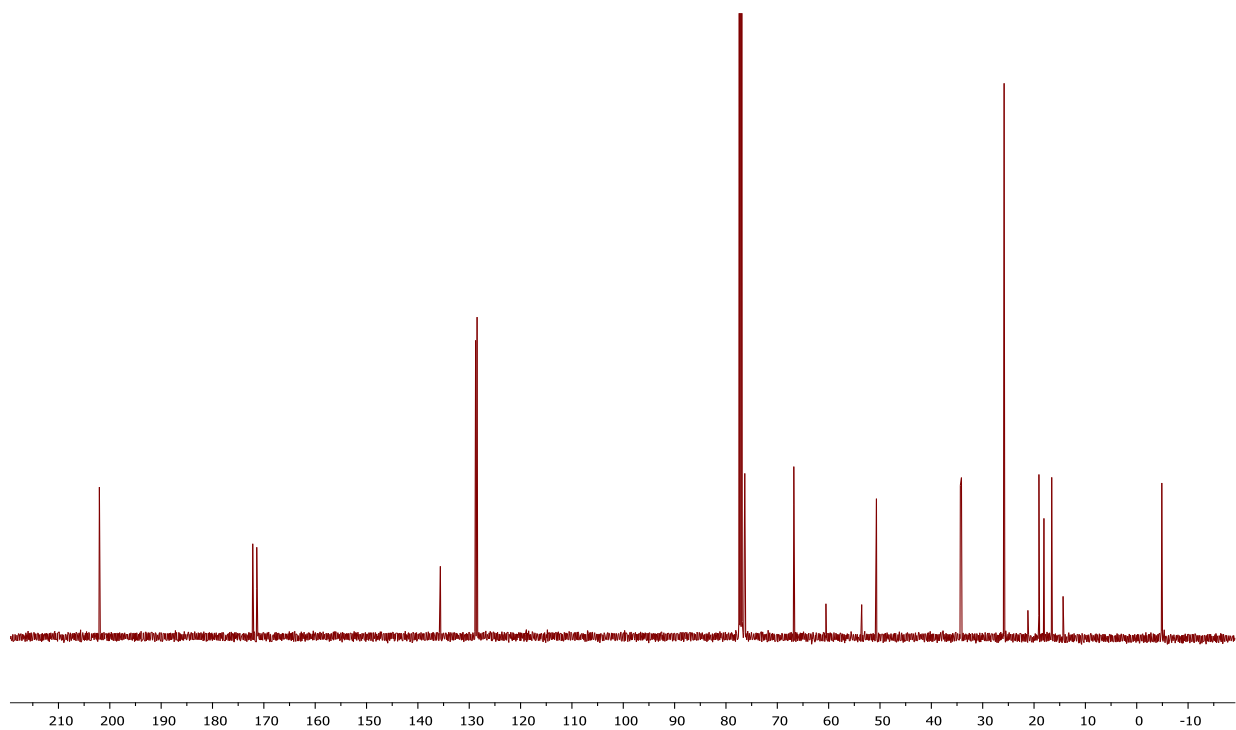
^{13}C NMR of compound 5.4



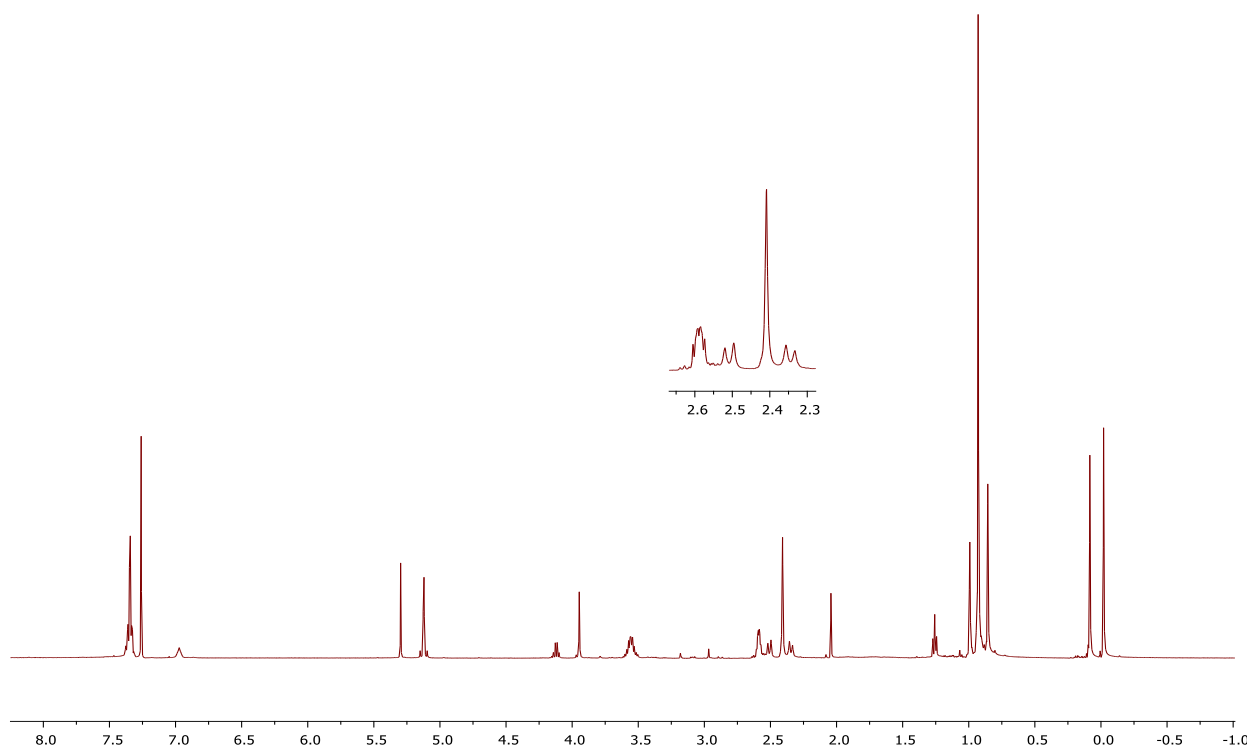
^1H NMR of compound 5.5



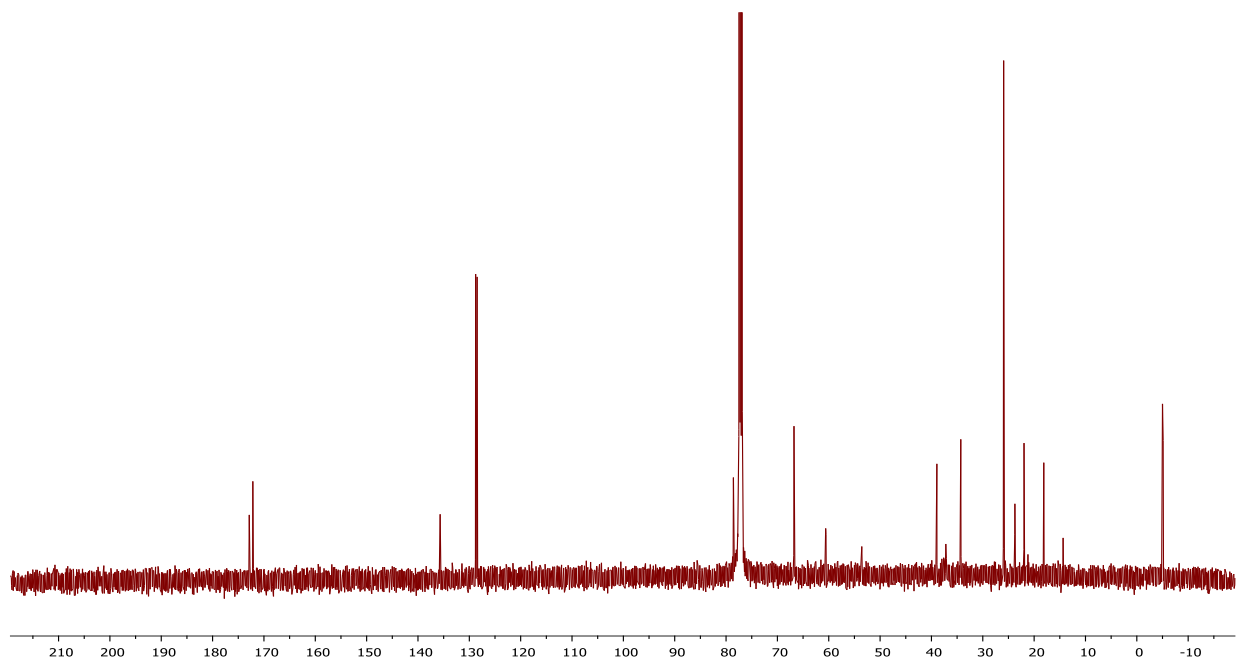
^{13}C NMR of compound 5.5



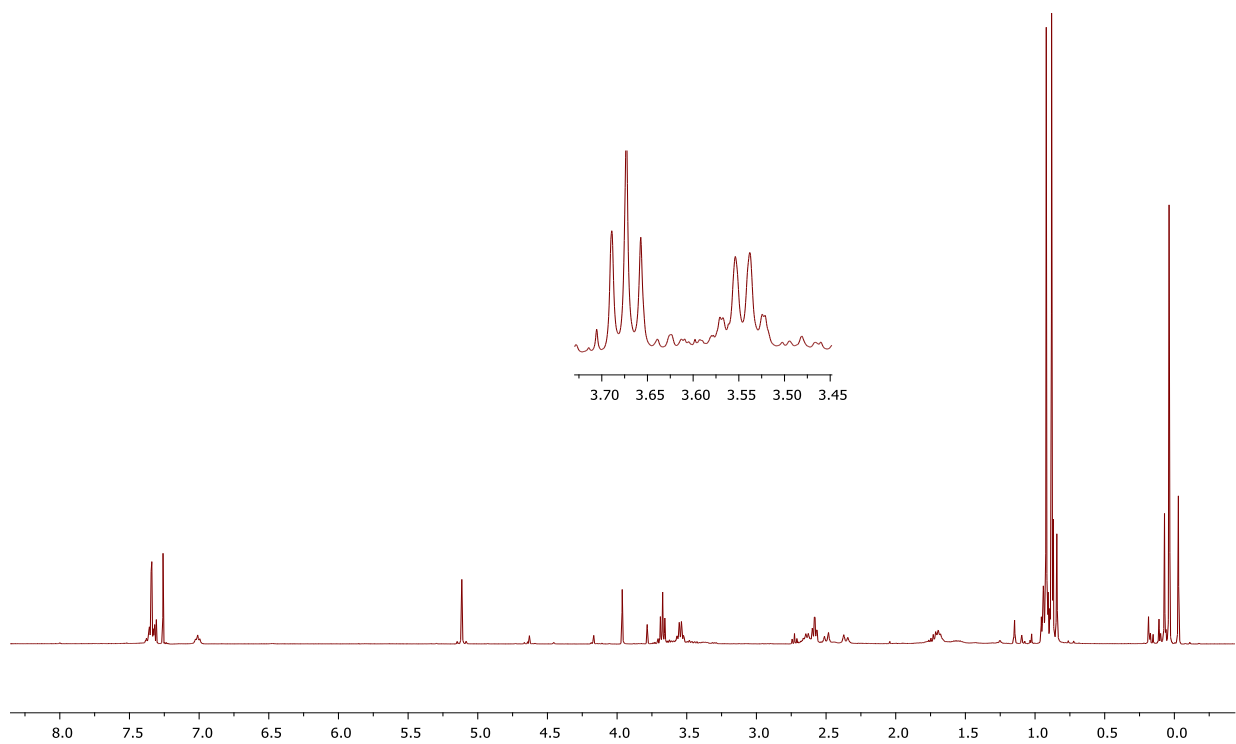
^1H NMR of compound 5.6a



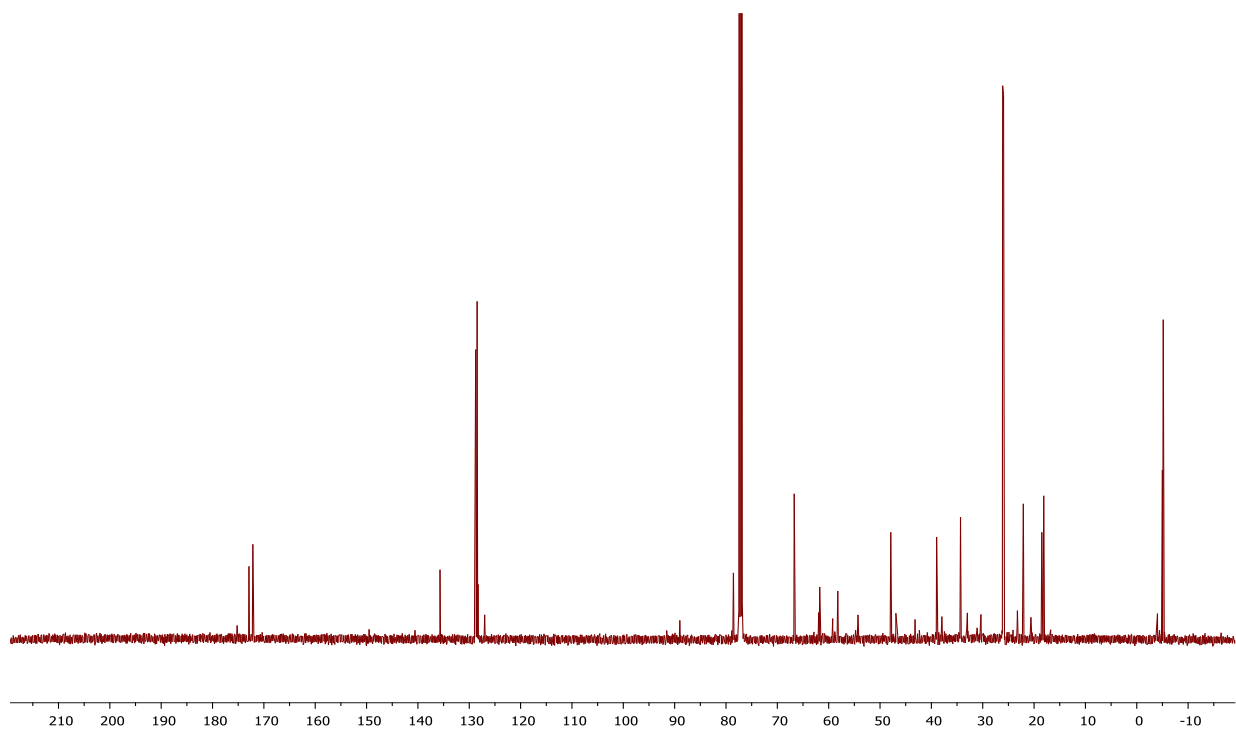
¹³C NMR of compound 5.6a



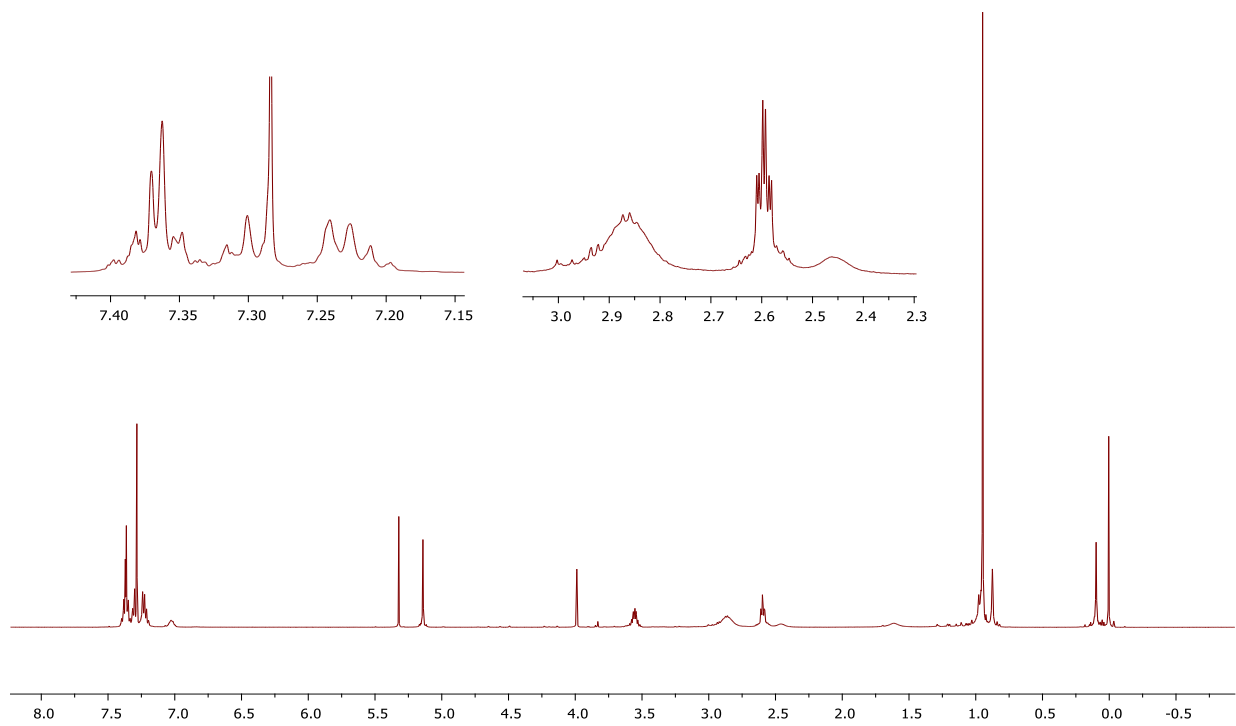
¹H NMR of compound 5.6e



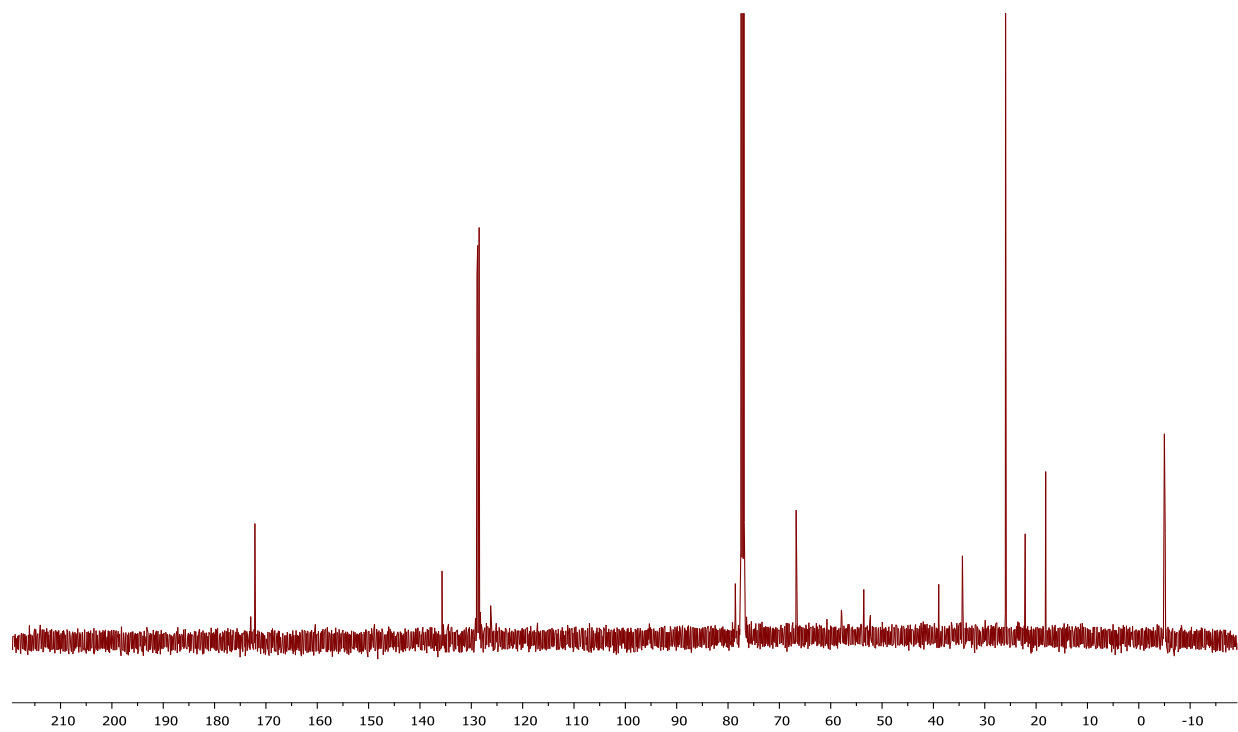
^{13}C NMR of compound 5.6e



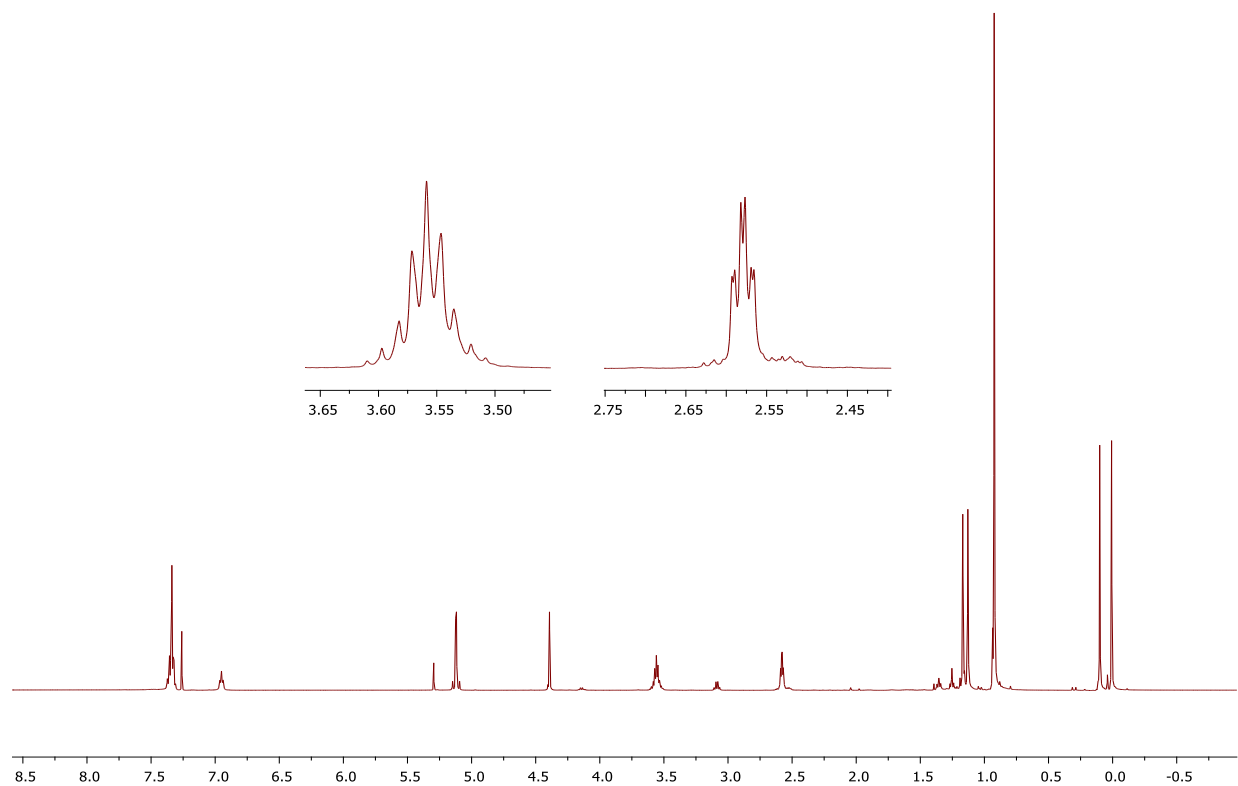
^1H NMR of compound 5.6f



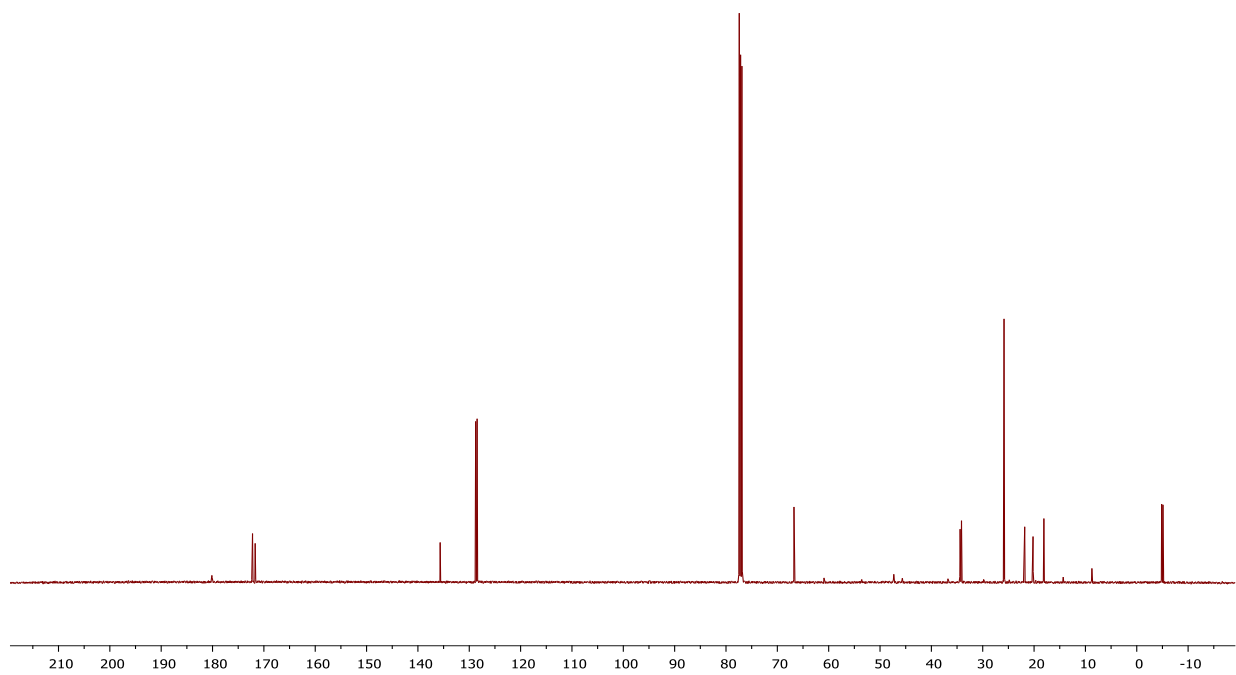
^{13}C NMR of compound 5.6f



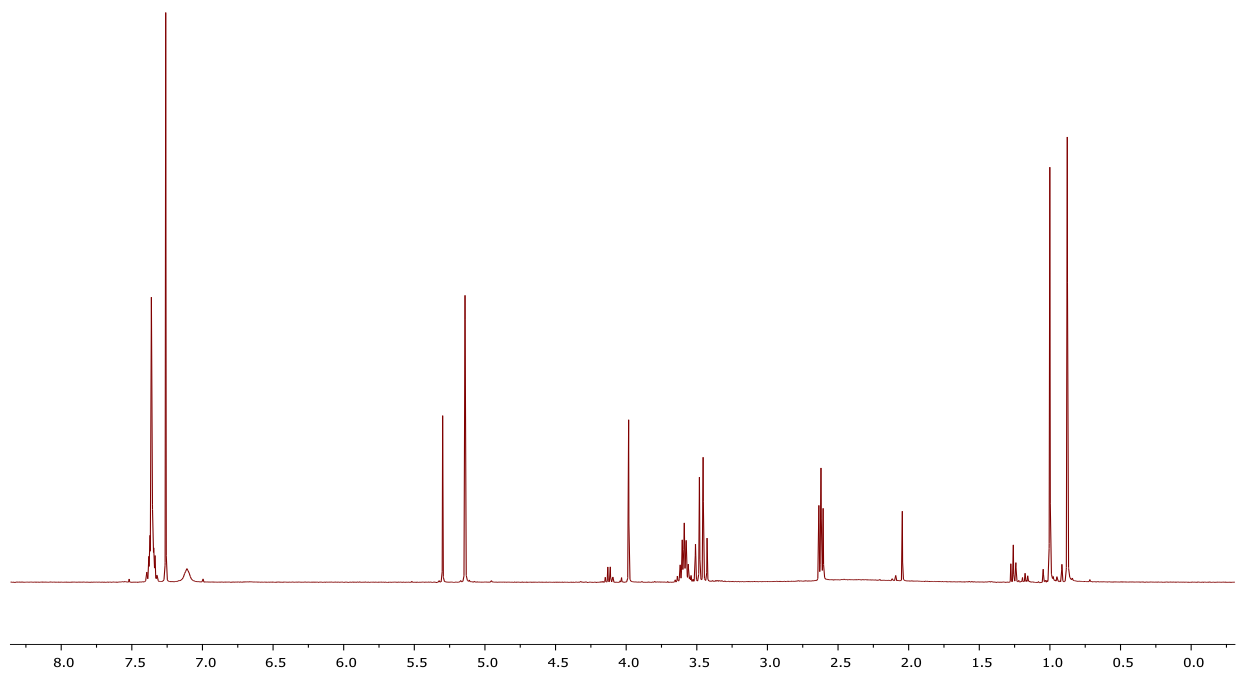
^1H NMR of compound 5.7



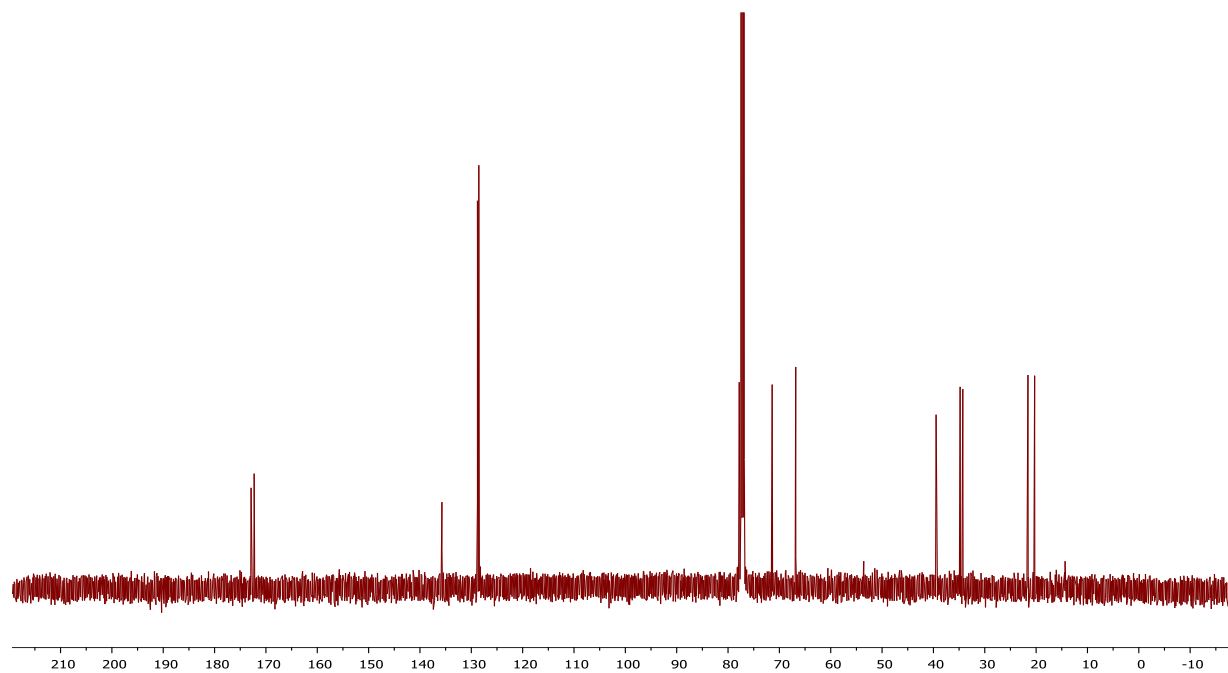
^{13}C NMR of compound 5.7



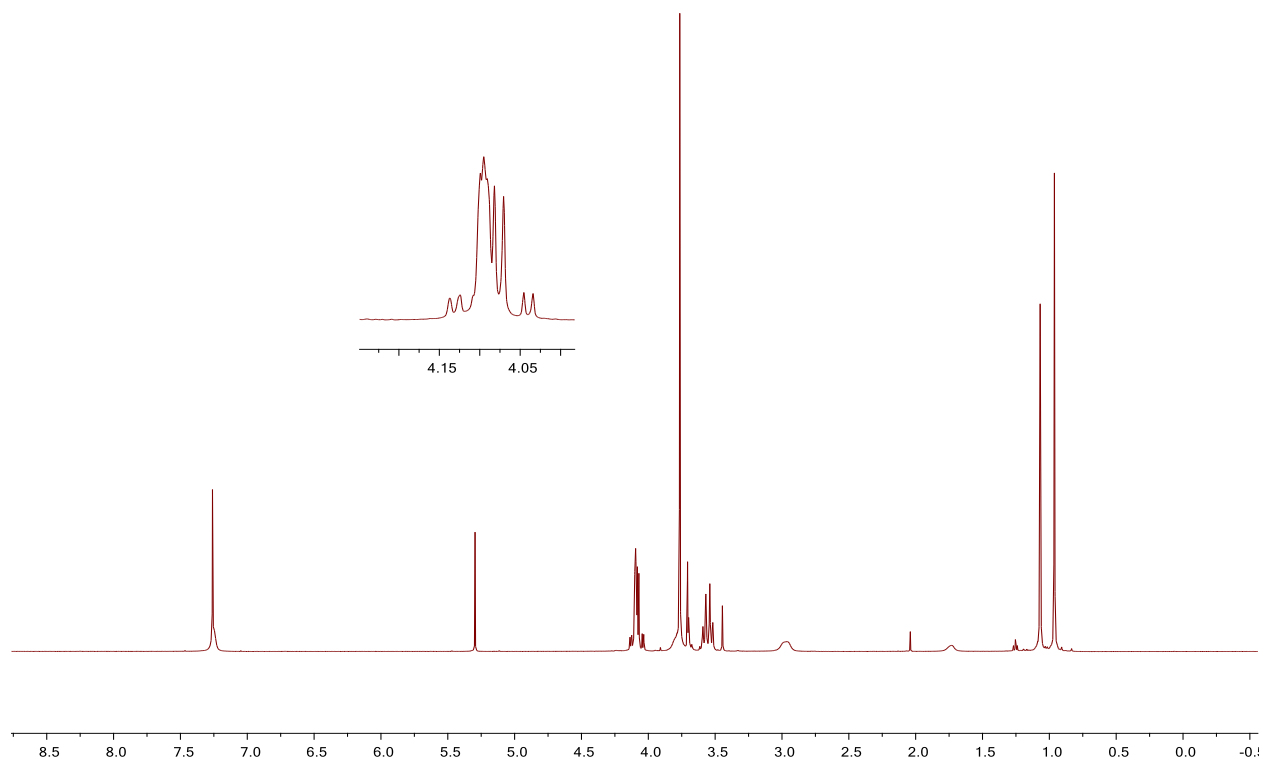
^1H NMR of compound 5.8



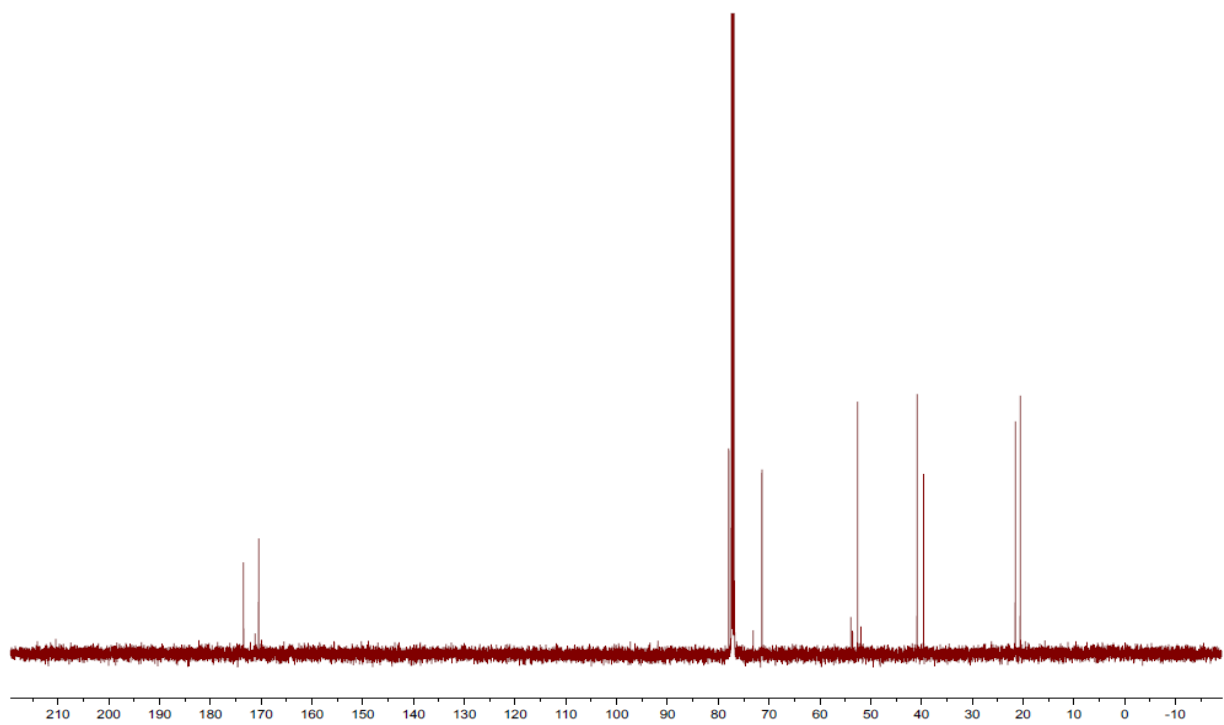
¹³C NMR of compound 5.8



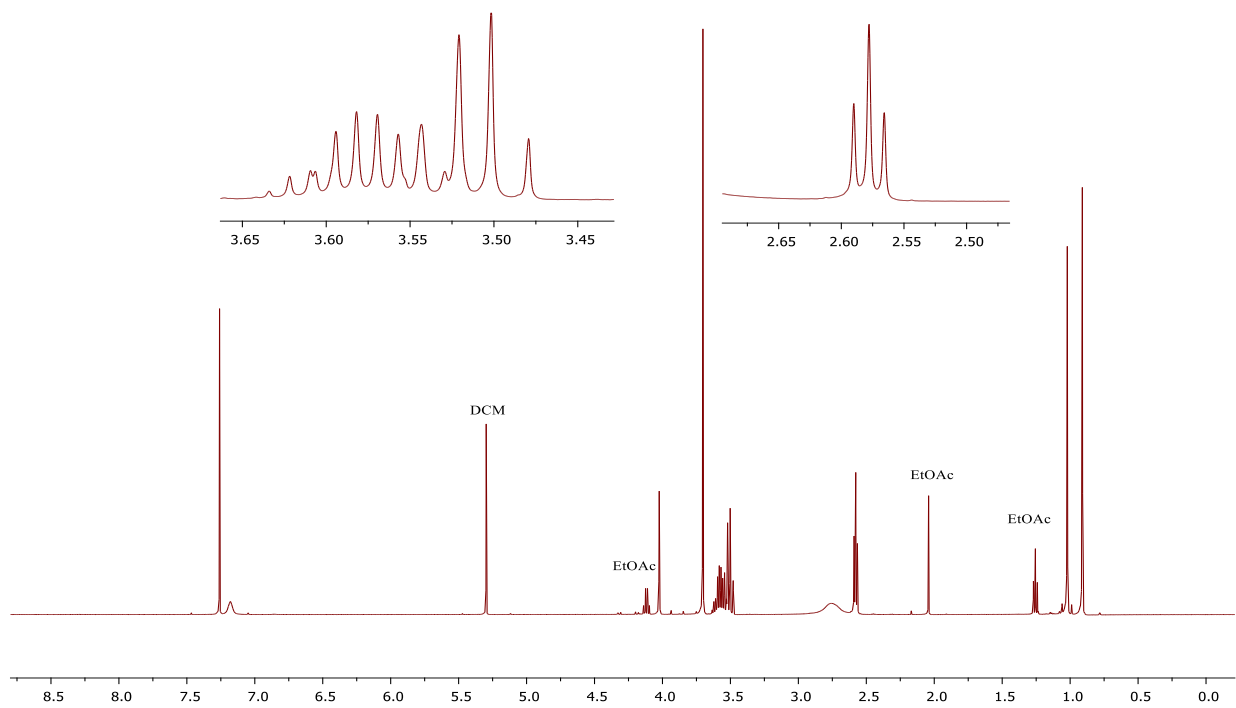
¹H NMR of compound 5.9a



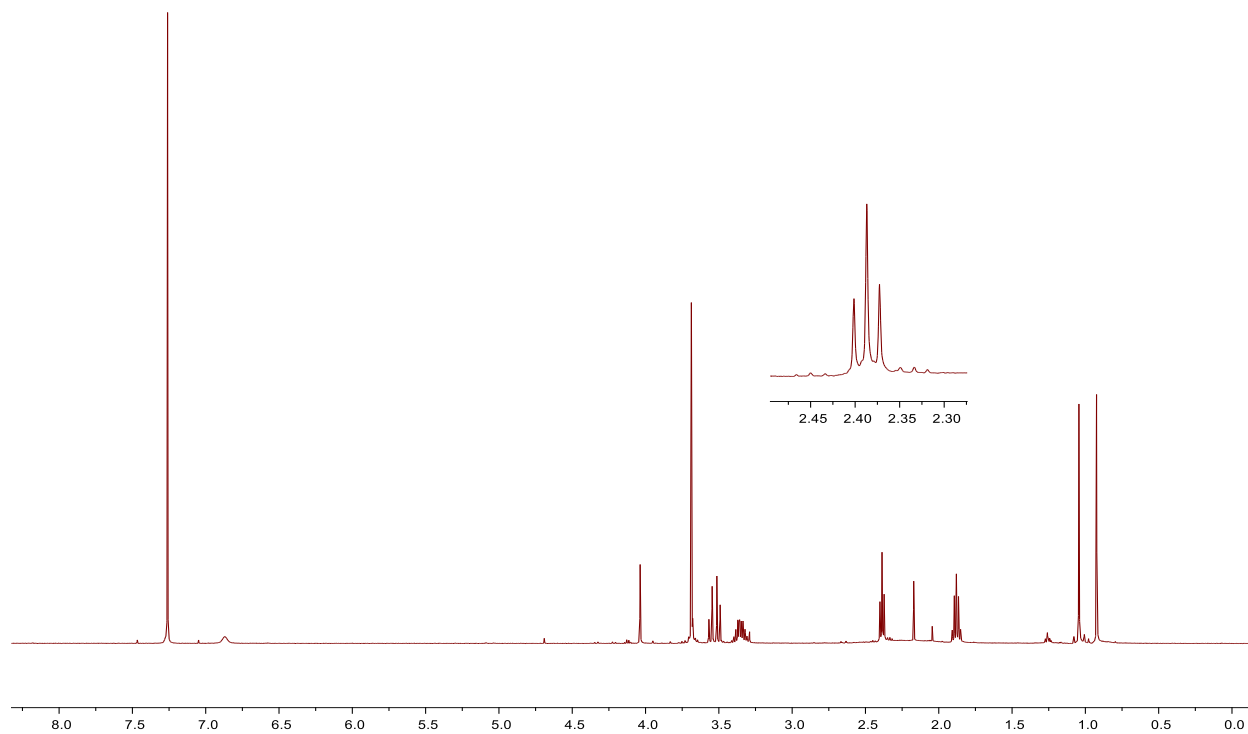
^{13}C NMR of compound 5.9a



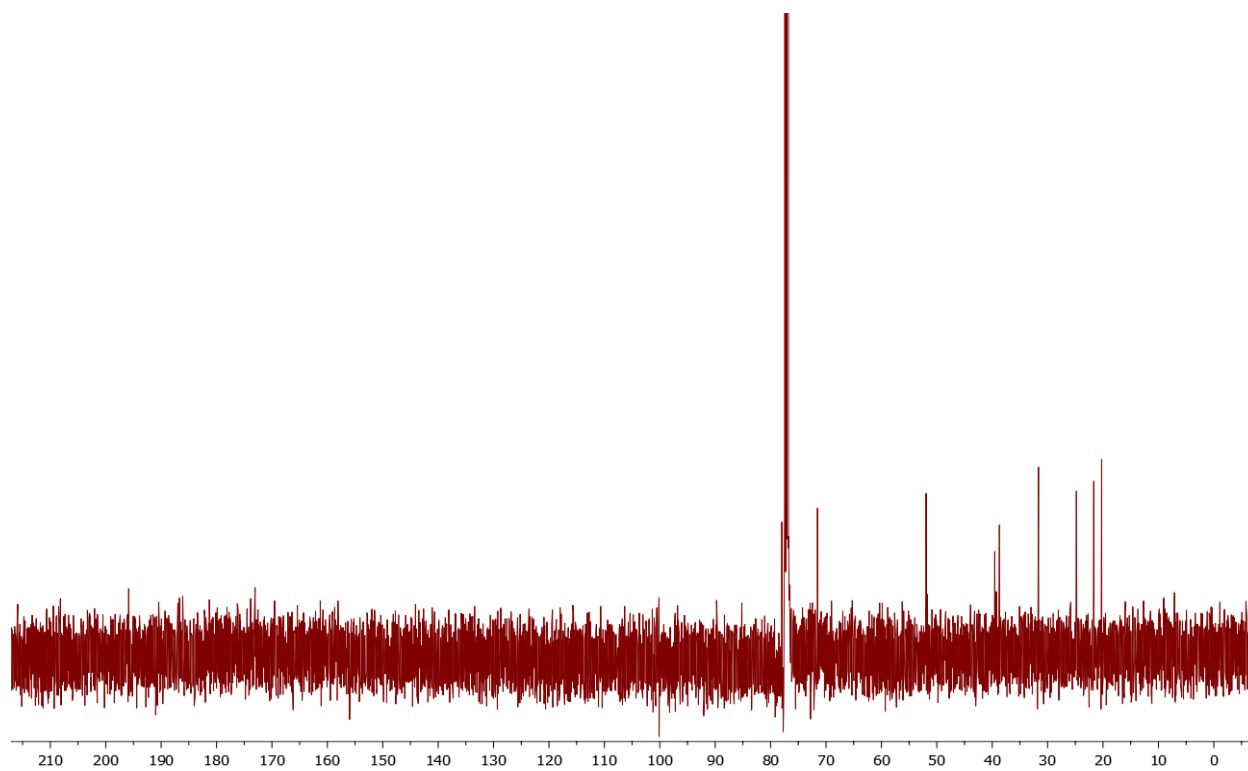
^1H NMR of compound 5.9b



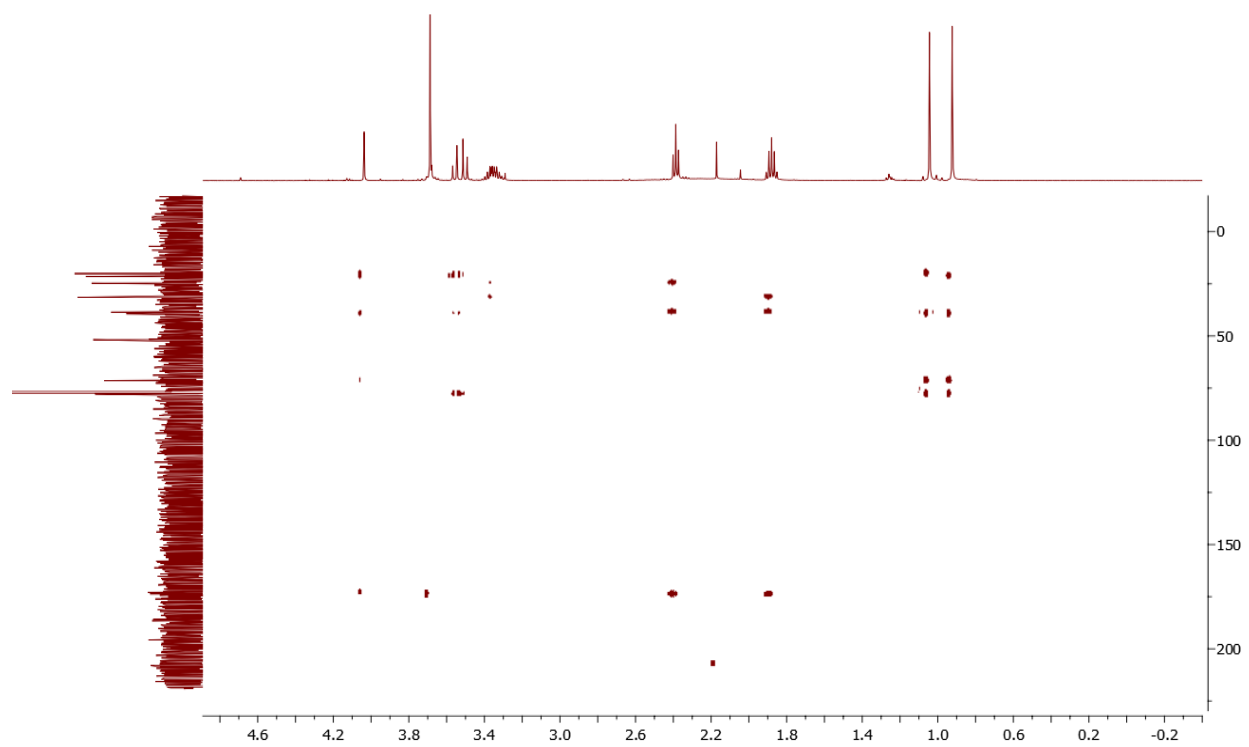
¹H NMR of compound 5.9c



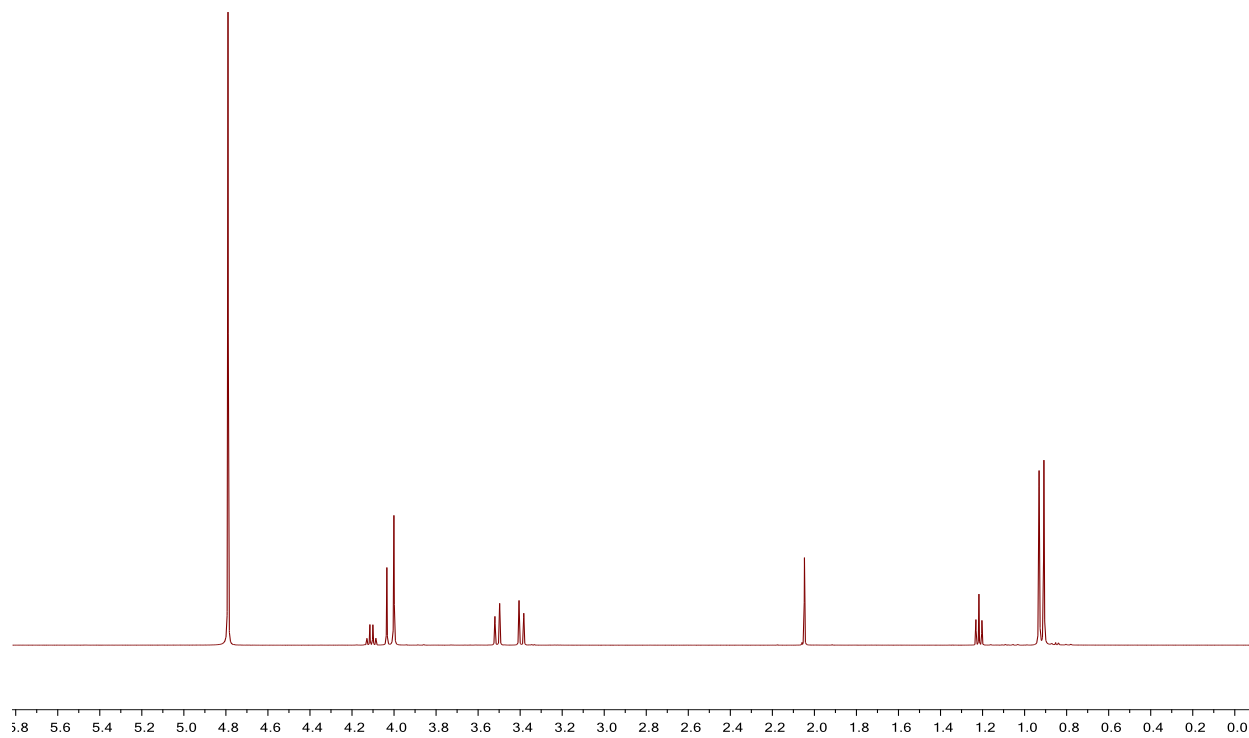
¹³C NMR of compound 5.9c



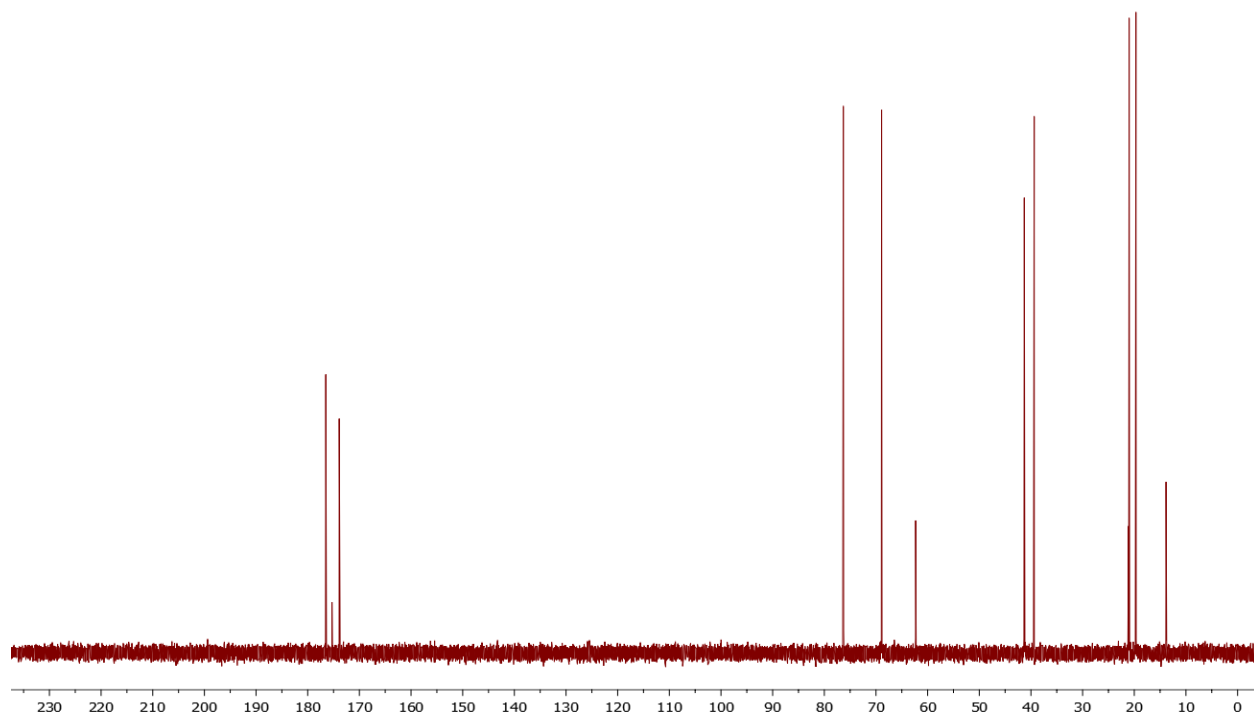
HMBC of compound 5.9c



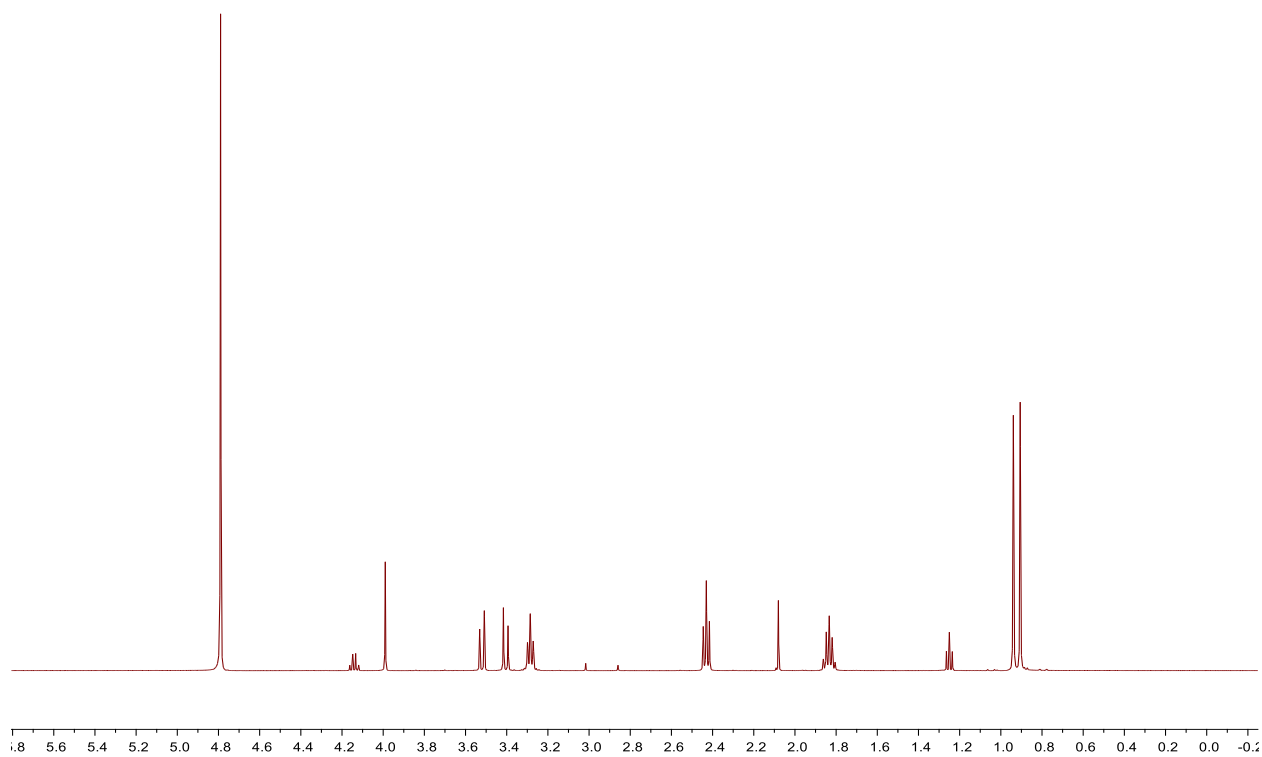
^1H NMR of compound 5.9d



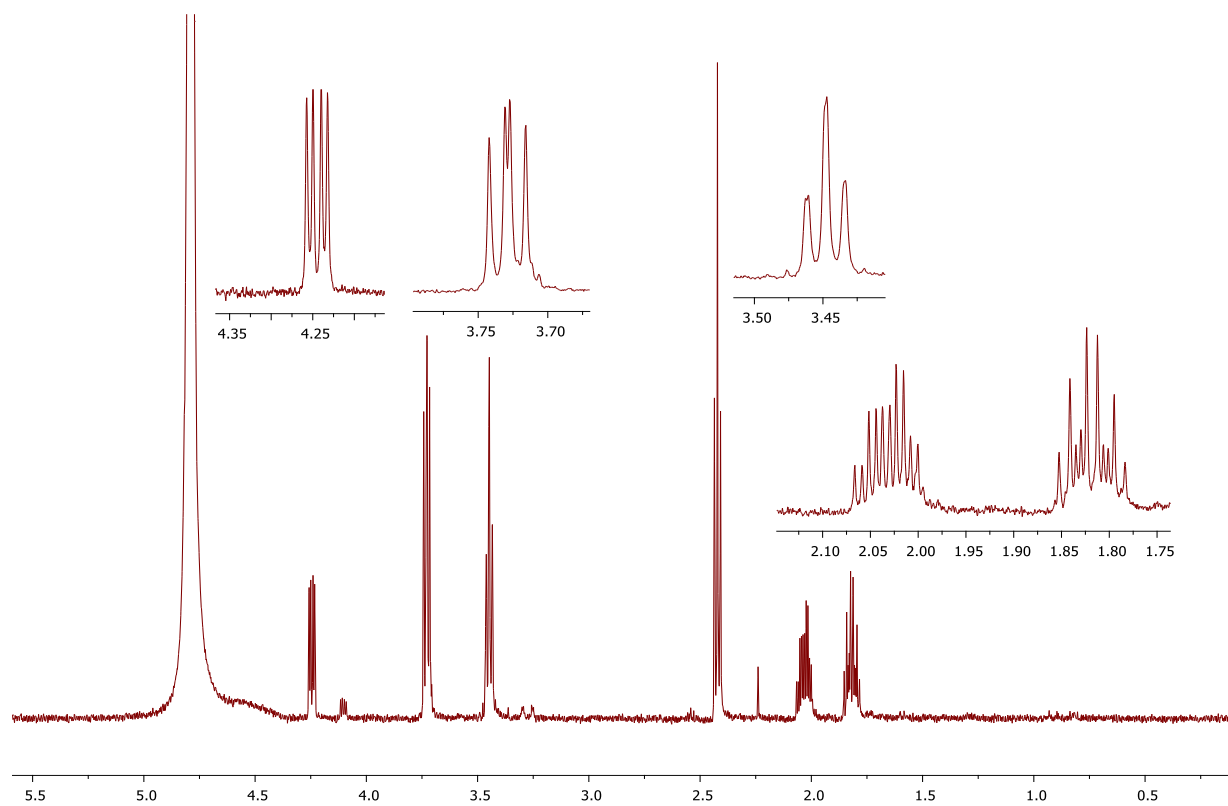
^{13}C NMR of compound 5.9d



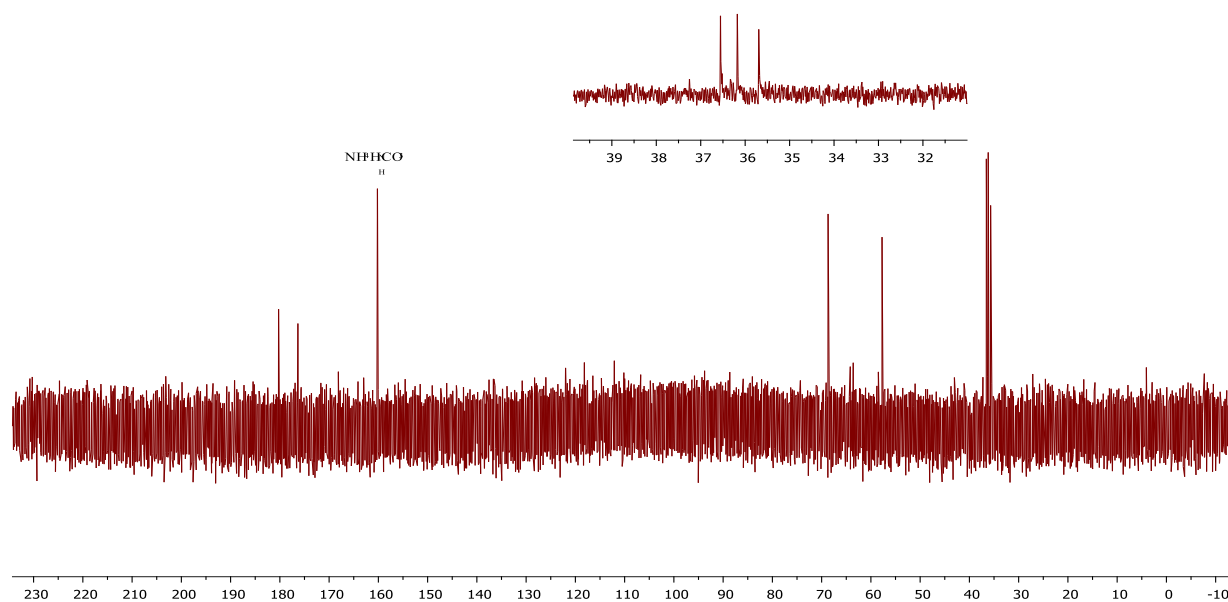
^1H NMR of compound 5.9e



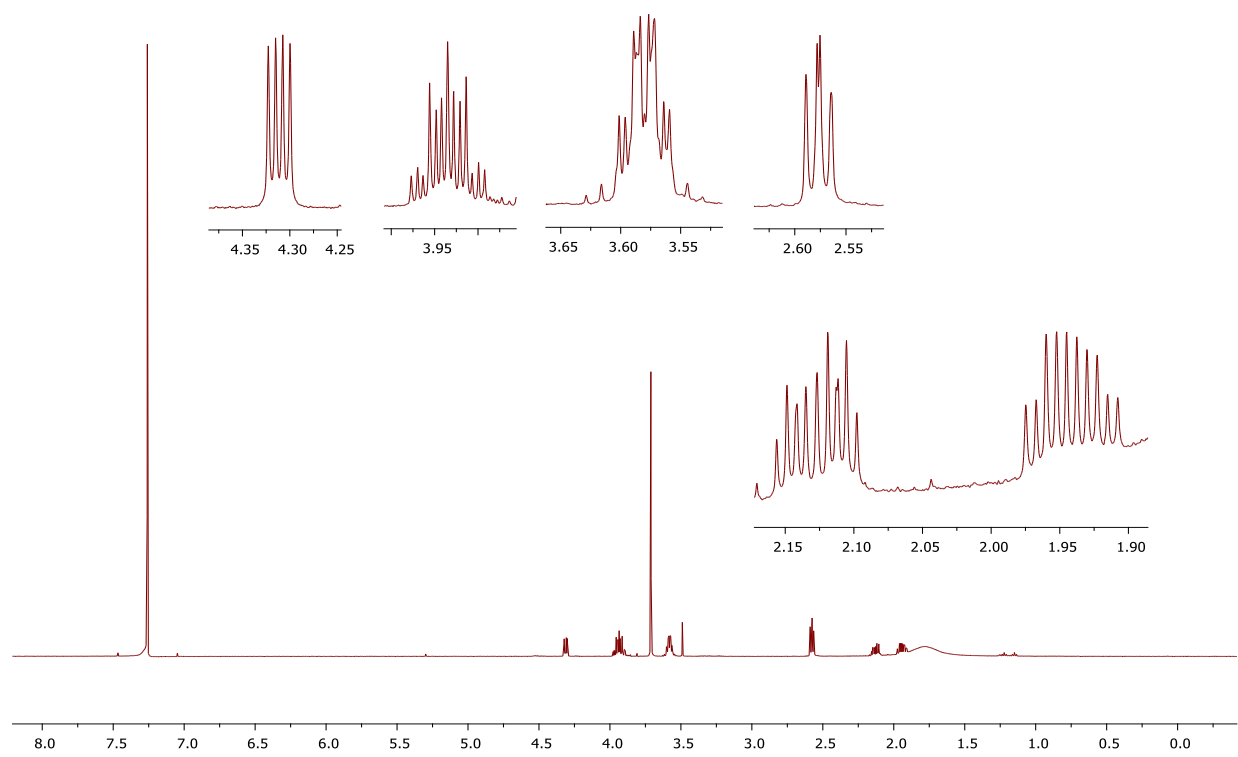
¹H NMR of compound 5.9f



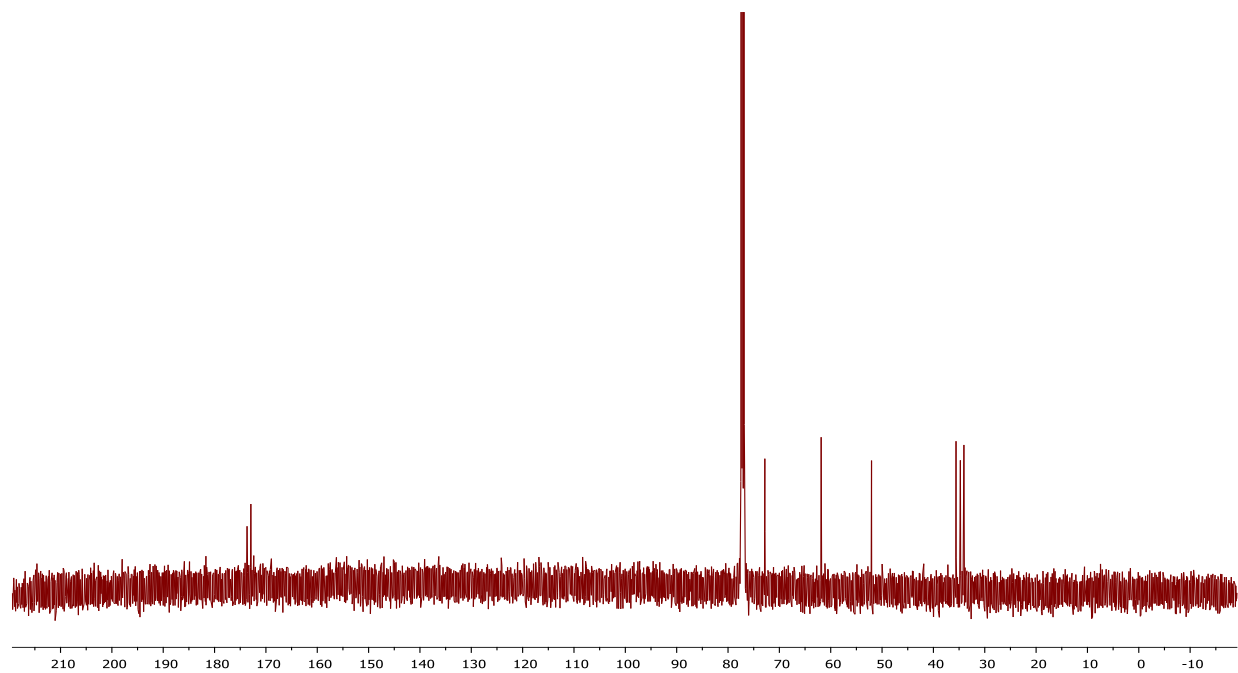
¹³C NMR of compound 5.9f



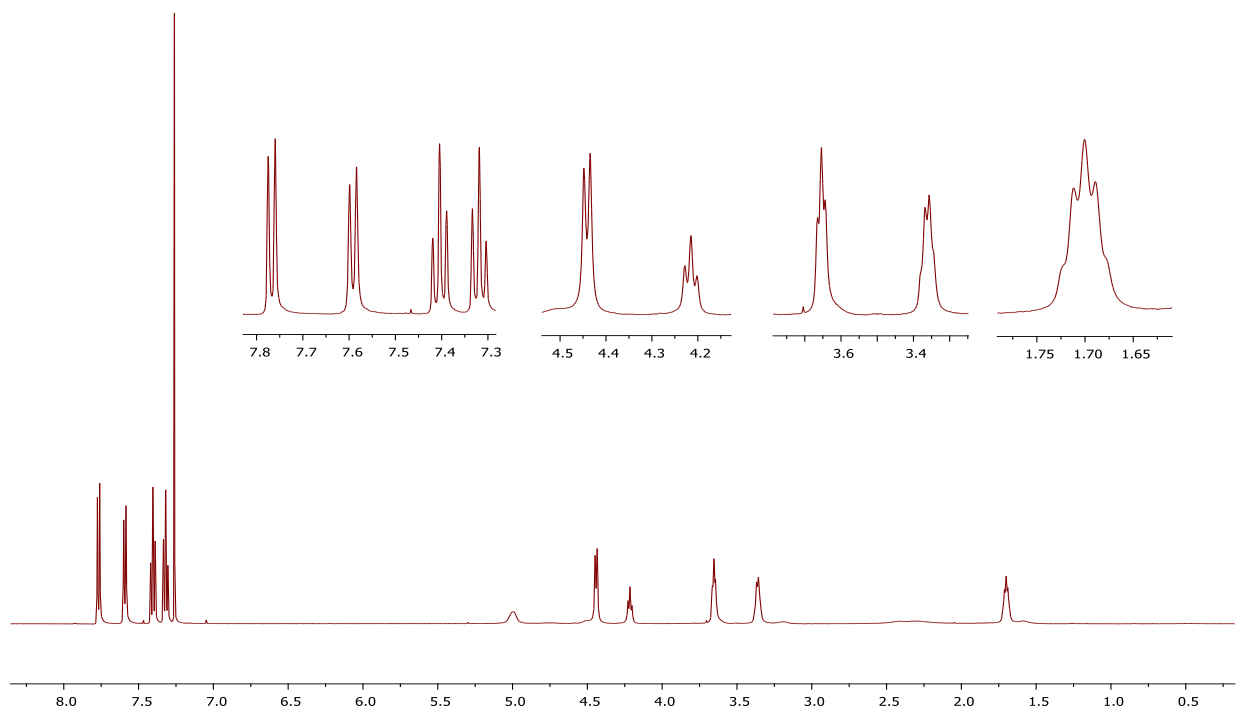
^1H NMR of compound 5.10



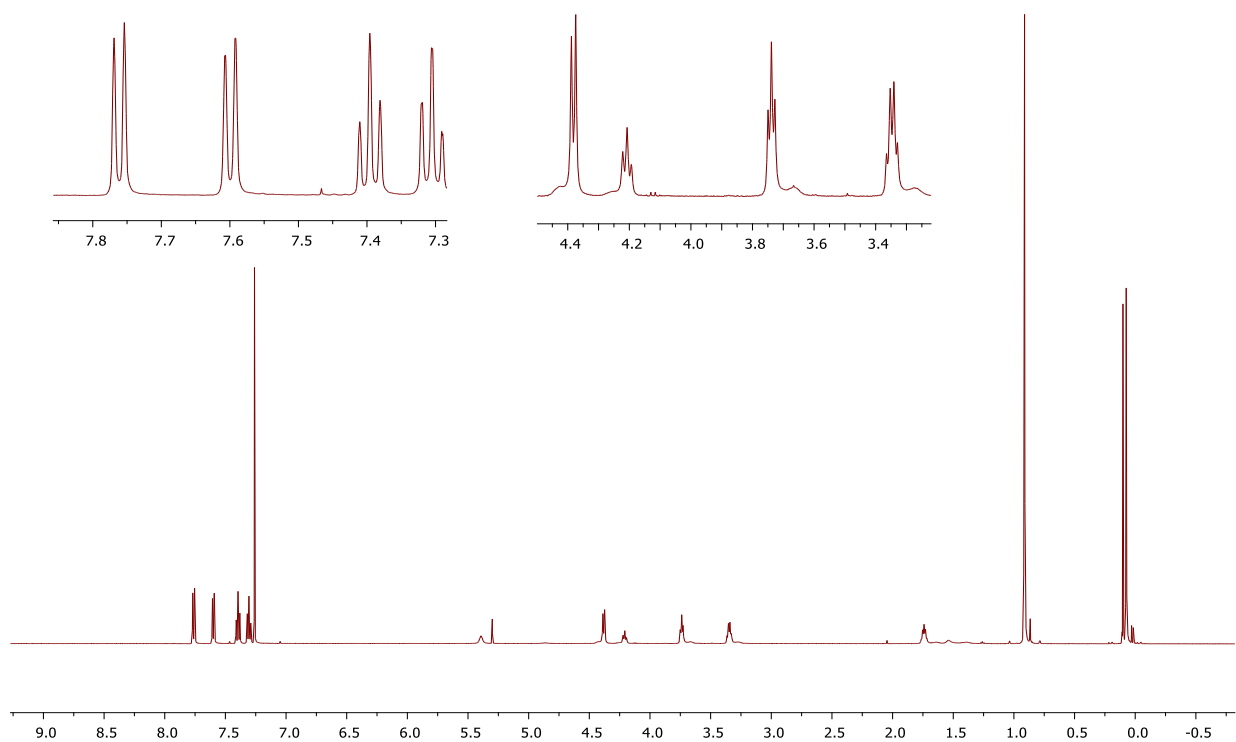
^{13}C NMR of compound 5.10



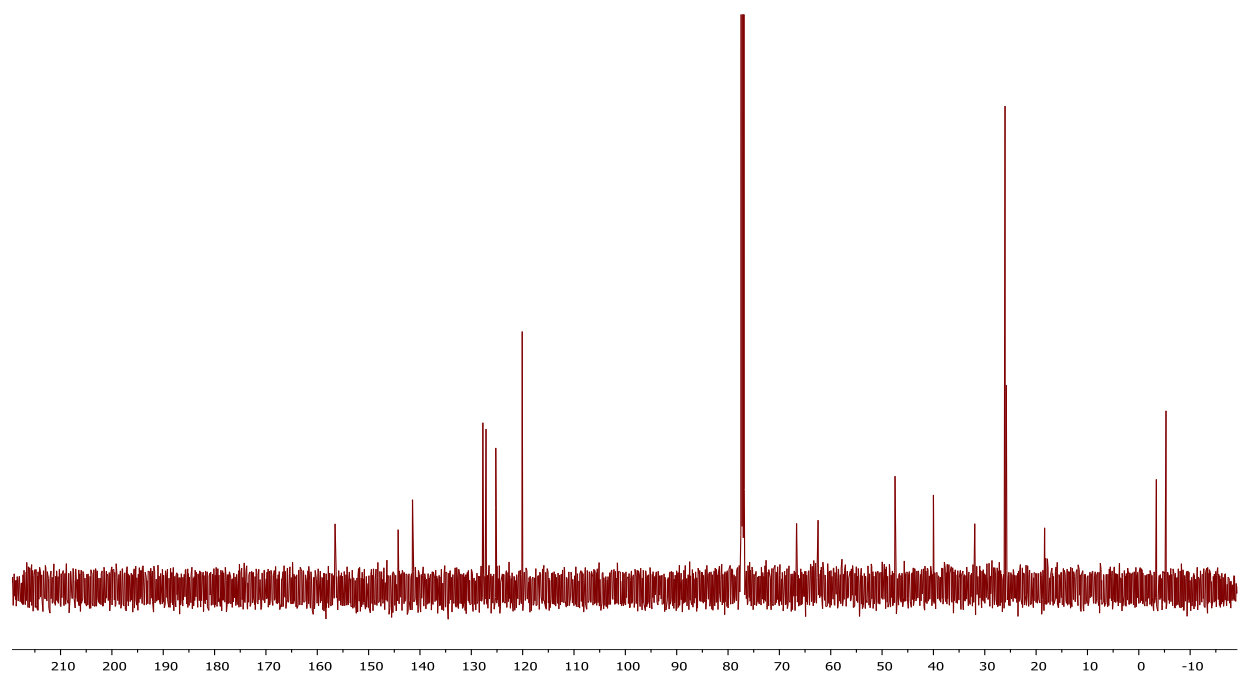
¹H NMR of compound 5.12



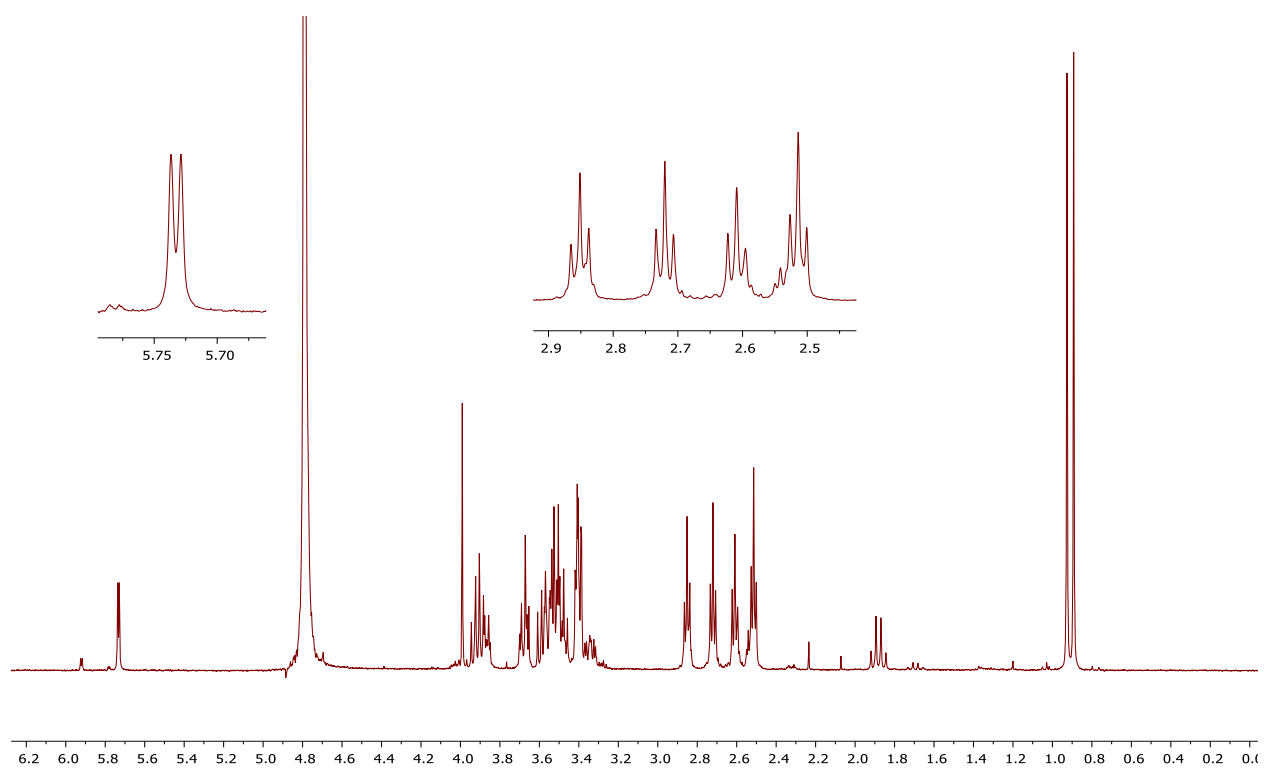
¹H NMR of compound 5.13



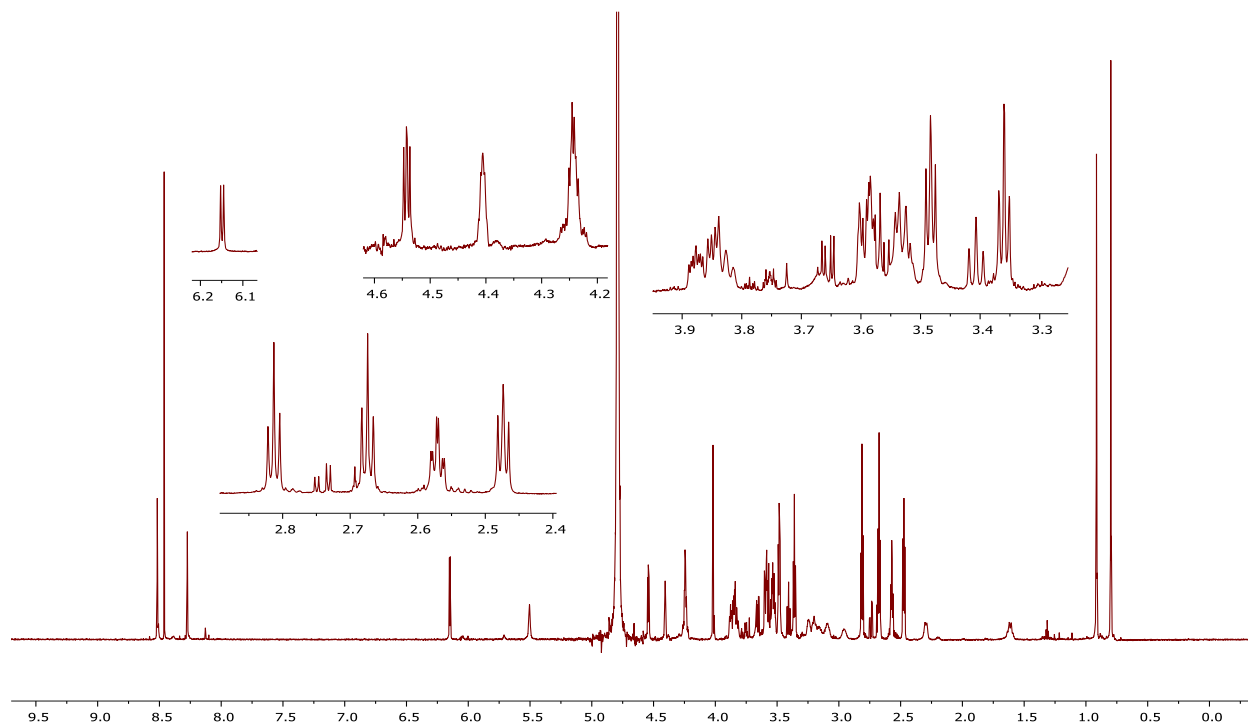
^{13}C NMR of compound 5.13



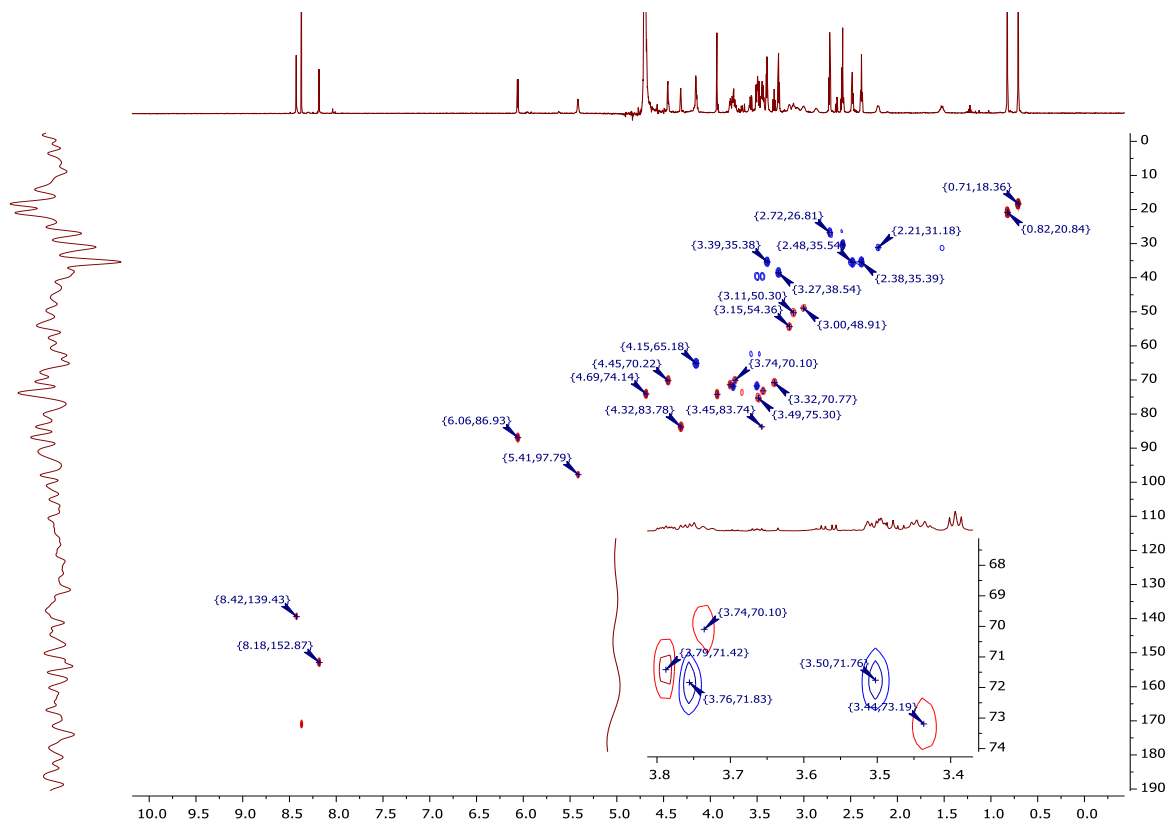
^1H NMR of P-1b



¹H NMR of 6.3b



HSQC of 6.3b



HMBC of 6.3b

